Application for Certificate of Compliance for the Traveller PWR Fuel Shipping Package

NRC Certificate of Compliance
USA/9297/AF-96
Docket 71-9297

Westinghouse

RECORD OF REVISIONS

Rev. No.	Date	Description of Revision
0	March 2004	Original application. (Ref: NMS-NRC-04-004)
1	November 2004	Response to NRC request for additional information. (Ref: NMS-NRC-04-009, NMS-NRC-04-011)
2	February 2005	Response to NRC request for additional information. (Ref: NMS-NRC-05-002)
3	March 2005	Response to NRC request for additional information. Correct one error, revise certain tables to make the SAR parameter tables consistent with those that will be published in the CoC, clarify the results of the rod container analysis, and clarify the maintenance requirements for the shock mounts. (Ref: NMS-NRC-05-003)
4	March 2005	Response to NRC request for additional information. Correct entries in various tables that list the Traveller design weights. Clarify in Sections 2 and 3 that the shock mounts were intact following the drop and fire tests. Provide justification in Section 2 for establishing payload weights that are higher than fuel assembly weights used in actual testing. (Ref: NMS-NRC-05-004)
5	March 2006	Information about loose rod pipe packaging in license drawings and revision to Safety Analysis Report to describe this new loose rod pipe packaging. (Ref: UAM-NRC-06-005)
6	September 2006	A packaging component used to secure these non-Westinghouse fuel assembly types in the Traveller was designed after approval of the Traveller. Information about packaging components used to secure the contents. (Ref: UAM-NRC-06-011)
7	October 2007	Response to NRC request for additional information. Added sketch of package in Chapter 1 and revised Section 1.1 Revised Sections 2.6.3 and 2.6.4 to delete reference to calculations because the package is not sealed against pressure. Revised Section 2.7.1.2 regarding test sequence justification. Revised Section 8.2.3.3 to clarify shock mount inspection frequency. Revised Section 8.2.5 to clarify BORAL plate inspection frequency. Administrative change to Table 6-21, showing the correct number of fuel and non-fuel rods in a 15x15 STD/OFA fuel assembly. (Ref: LCPT-10-6)
8	May 2010	Add CE16NGF and CE16VA fuel assemblies to criticality safety evaluation. (Ref: LCPT-10-14)

RECORD OF REVISIONS (cont.)

Rev. No.	Date	Description of Revision
9	November 2010	Style and Composition An appendix is added to each section of the application as recommended in Regulatory Guide 7.9 to provide a list of documents that are referenced in the text of that section. The addition of this first appendix may result in renumbering of headings and pages where other appendices already existed for that section. Typographical changes have also been made. Section 1 – General Information 1.2.1.2 Outerpack Added description of vibration and shock dampening system. 1.2.1.3 Clamshell Revised to provide more detailed description of clamshell features, including a design change for an alternate top end plate. Figures were revised to show typical configurations for the axial restraint and axial spacer. 1.2.1.4 Rod Container Removed rod box as an option. 1.2.3 Contents Revised description to add more detailed description of fuel assembly and components that may be transported in the fuel assembly. Added a Figure 1-8 showing a typical PWR fuel assembly. Added wording to describe the number of rods per pipe and how the rods are loaded. 1.4 Appendices Added Appendix 1.4.1, References. Renamed Appendix 1.4.2, Engineering Drawings for Packaging The engineering drawings for packaging Drawing No. 10004E58 Safety Related Items, Traveller XL and STD was revised to show modifications to the clamshell top end plate and changes to the outer pack such as silicone rubber weather gasket, tie down chain tray gussets, new swing bolts, and clamshell cam lock wave washer. Section 2 – Structural Evaluation 2.12.3.2.4.1 Internal/External Pressure Added silicone foam rubber seal and removed description of seal function as providing thermal protection. 2.12 Appendices Added Appendix 2.12.1, References Added Appendix 2.12.6, Supplement to Drop Analysis for the Traveller XL Shipping Package – Clamshell Axial Spacer Structural Evaluation. Added Appendix 2.12.7, Supplement to Drop Analysis for the Traveller XL Shipping Package – Clamshell Removable Top Plate Structural Evaluation.

RECORD OF REVISIONS (cont.)

Rev. No.	Date	Description of Revision
9 (cont.)		Section 3 – Thermal Evaluation Revised introduction to clarify that there is no heat generating material. Tables 3-2 and 3-3 and bullets in the text were revised to be consistent with ASME Code 3.1.3 Description of maximum temperatures Added silicone rubber gasket to Table 3-1, Summary Table of Temperatures for Traveller Materials 3.1.4 Description of maximum pressures Added silicone rubber gasket. 3.4 Thermal Evaluation Under Normal Conditions of Transport Revised to clarify that there is no heat generating material. 3.5.3 Maximum Temperatures and Pressures Revised description of the purpose for seals used around the Outerpack door. Added silicone foam rubber as an acceptable seal material. Added Figure 3-8A to show location of weather seal gaskets. Section 4 – Containment Added Section 4.3, Appendices, and 4.3.1 References. No references are cited. Section 5 – Shielding Evaluation Added Section 5.1, Appendices, and 5.1.1 References. No references are cited. Section 6 – Criticality Evaluation Section 6.2, Fissile Material Contents Added statement that reactor control cluster (RCC) assemblies, secondary source assemblies, and solid stainless steel rods that may be placed in the PWR fuel assembly are non-fissile material. 6.2.1 PWR Fuel Assemblies Added justification for allowing RCC, secondary source rods, or stainless steel rods in fuel assembly contents. 6.2.2 PWR and BWR Rods Revise limit for wrapping or sleeving in Table 6-5 Fuel Rod Parameters 6.3.1.1 Contents Models Removed rod box as an option. 6.10.2 PWR Fuel Assembly Parameters Revised dimensions for guide tube and pellet in Table 6-22 Parameters for 16X16 Fuel Assemblies 6.10 Appendices Added Appendix 6.10.1, References Section 7 – Package Operations Revised all sections to incorporate operating experience and more accurately represent the current package operations. Added Section 7.4, Appendices, and 7.4.1 References. No references are cited.

RECORD OF REVISIONS (cont.)

Rev. No.	Date	Description of Revision
9 (cont.)		Section 8 – Acceptance tests and Maintenance Program Replace "poison plate" with term "neutron absorber plate", and replace "neutronics testing" with term "neutron absorber testing" to standardize reference to BORAL neutron absorber material. Add criteria for visual inspection of neutron absorber plates to Section 8.2.5. 8.1.5.1.4 Thermal Properties Thermal properties is revised to show the thermal conductivity for FR-3706, FR-3610, and FR-3620.
10	September 2013	Style and Composition A number of typographical errors throughout the entire document have been corrected in this revision. A side result of the typographical corrections has been the addition of several pages, in order to accommodate paragraphs or figures which no longer had room to fit on the pages they previously occupied. Section 1 – General Information 1.2.1.1 Package Types Revised weights of packages where required. 1.2.1.4 Rod Pipe Further corrections added to clarify that the Rod Pipe will be the only rod container moving forward. 1.4.2 Engineering Drawings for Packaging Included the most recent revisions to the licensing drawings Section 2 – Structural Evaluation Updated equations and weights throughout the Section. 2.11.1 Rod Pipe Further corrections added to clarify that the Rod Pipe will be the only rod container moving forward. 2.12 Appendices Revised the appendices to provide an updated structural analysis which accounts for the revised weight of the Traveller package. 2.12.3.2.2 Lifting Provided additional information on Traveller STD four-point lift. Tables 2-7, 2-8, and 2-9 Removed, as the information was either already present or was consolidated elsewhere. Section 6 – Criticality 6.1.2, and 6.1.3 Corrections added to clarify that the Rod Pipe will be the only rod container moving forward. Figure 6-17 Replaced with the correct figure.

RECORD OF REVISIONS (cont.)

Rev. No.	Date	Description of Revision
10 (cont.)		Section 7 – Package Operations 7.1.1.3 Clarification and consolidation of information. 7.1.2, 7.12.1, and 7.2.2 Added tolerances for Torque figures. Section 8 – Acceptance Tests and Maintenance Program Clarification and consolidation of information.

TABLE OF CONTENTS

TRAVELLER SAFETY ANALYSIS REPORT
LIST OF EFFECTIVE PAGES

Page	Rev.	Date
i	8	5/2010
ii	9	11/2010
iii	9	11/2010
iv	10	9/2013
v	10	9/2013
vi	0	3/2004
1-i	10	9/2013
1-ii	9	11/2010
1-iii	10	9/2013
1-iv	9	11/2010
1-1	10	9/2013
1-2	10	9/2013
1-3	10	9/2013
1-4	10	9/2013
1-5	9	11/2010
1-5A	9	11/2010
1-5B	9	11/2010
1-5C	9	11/2010
1-5D	9	11/2010
1-5E	9	11/2010
1-5F	10	9/2013
1-6	10	9/2013
1-6A	10	9/2013
1-6B	7	10/2009
1-7	9	11/2010
1-7A	10	9/2013
1-7B	9	11/2010
1-7C	10	9/2013
1-7D	9	11/2010
1-8	10	9/2013
10004E58	8	
10006E58	5	
2-i	4	3/2005
2-ii	10	9/2013
2-iii	9	11/2010
2-iv	10	9/2013
2-v	10	9/2013
2-vi	10	9/2013
2-vii	1	11/2004
2-viii	2	2/2005
2-ix	1	11/2004
2-x	1	11/2004
2-xi	2	2/2005
2-xii	9	11/2010
2-1	10	9/2013
2-1A	1	11/2004
2-1B	1	11/2004
2-2	0	3/2004
2-3	9	11/2010
2-4	10	9/2013
2-5	10	9/2013
2-6	9	11/2010
2-7	0	3/2004
2-8	9	11/2010
2-9	10	9/2013
2-10	9	11/2010
2-11	10	9/2013
2-12	9	11/2010
2-13	10	9/2013
2-14	10	9/2013
2-14A	10	9/2013
2-14B	1	11/2004
2-15	9	11/2010
2-16	10	9/2013
2-17	2	2/2005
2-18	2	2/2005
2-19	0	3/2004
2-20	0	3/2004
2-21	0	3/2004
2-22	1	11/2004
2-22A	1	11/2004
2-22B	1	11/2004
2-22C	1	11/2004
2-22D	1	11/2004
2-23	10	9/2013
2-24	10	9/2013
2-24A	10	9/2013
2-24B	9	11/2010
2-25	10	9/2013
2-26	9	11/2010
2-27	9	11/2010
2-28	0	3/2004
2-29	0	3/2004
2-30	0	3/2004
2-31	0	3/2004
2-32	10	9/2013
2-32A	10	9/2013
2-32B	1	11/2004
2-33	9	11/2010
2-34	10	9/2013
2-35	0	3/2004
2-36	10	9/2013
2-37	0	3/2004
2-38	10	9/2013
2-39	10	9/2013
2-40	10	9/2013
2-41	10	9/2013
2-42	10	9/2013
2-43	10	9/2013
2-44	10	9/2013
2-45	10	9/2013
2-46	10	9/2013
2-47	10	9/2013
2-48	10	9/2013
2-49	10	9/2013
2-49A	10	9/2013
2-50	10	9/2013
2-50A	10	9/2013
2-50B	10	9/2013
2-50C	10	9/2013
2-51	10	9/2013
2-52	0	3/2004
2-53	0	3/2004
2-54	0	3/2004
2-55	0	3/2004
2-56	1	11/2004
2-57	10	9/2013
2-58	10	9/2013
2-59	10	9/2013
2-60	10	9/2013
2-61	0	3/2004
2-62	0	3/2004
2-63	10	9/2013
2-64	10	9/2013
2-65	10	9/2013
2-66	10	9/2013
2-67	9	11/2010
2-67A	9	11/2010
2-67B	2	2/2005
2-68	9	11/2010
2-69	0	3/2004
2-70	0	3/2004
2-71	0	3/2004
2-72	9	11/2010
2-73	0	3/2004
2-74	0	3/2004
2-75	0	3/2004
2-76	0	3/2004
2-77	0	3/2004
2-78	0	3/2004
2-79	0	3/2004

TRAVELLER SAFETY ANALYSIS REPORT
LIST OF EFFECTIVE PAGES (cont.)

Page	Rev.	Date	Page	Rev.	Date	Page	Rev.	Date
2-80	0	3/2004	2-126	2	2/2005	2-162	0	3/2004
2-81	0	3/2004	2-127	1	11/2004	2-163	0	3/2004
2-82	0	3/2004	2-128	9	11/2010	2-164	0	3/2004
2-83	0	3/2004	2-129	9	11/2010	2-165	0	3/2004
2-84	0	3/2004	2-130	1	11/2004	2-166	0	3/2004
2-85	0	3/2004	2-131	1	11/2004	2-167	9	11/2010
2-86	9	11/2010	2-132	0	3/2004	2-168	1	11/2004
2-87	0	3/2004	2-133	9	11/2010	2-169	0	3/2004
2-88	0	3/2004	2-134	9	11/2010	2-170	0	3/2004
2-89	1	11/2004	2-134A	1	11/2004	2-171	0	3/2004
2-90	0	3/2004	2-134B	1	11/2004	2-172	2	2/2005
2-91	0	3/2004	2-134C	1	11/2004	2-173	0	3/2004
2-92	0	3/2004	2-134D	1	11/2004	2-174	0	3/2004
2-93	0	3/2004	2-135	1	11/2004	2-175	9	11/2010
2-94	0	3/2004	2-135A	9	11/2010	2-176	0	3/2004
2-95	0	3/2004	2-135B	1	11/2004	2-177	1	11/2004
2-96	0	3/2004	2-135C	9	11/2010	2-178	0	3/2004
2-97	10	9/2013	2-135D	1	11/2004	2-179	0	3/2004
2-98	9	11/2010	2-136	9	11/2010	2-180	0	3/2004
2-99	10	9/2013	2-137	0	3/2004	2-181	0	3/2004
2-100	0	3/2004	2-138	9	11/2010	2-182	0	3/2004
2-101	1	11/2004	2-139	1	11/2004	2-183	9	11/2010
2-102	0	3/2004	2-139A	1	11/2004	2-184	0	3/2004
2-103	1	11/2004	2-139B	1	11/2004	2-185	0	3/2004
2-104	9	11/2010	2-140	0	3/2004	2-186	0	3/2004
2-105	2	2/2005	2-141	1	11/2004	2-187	0	3/2004
2-106	1	11/2004	2-142	0	3/2004	2-188	0	3/2004
2-106A	9	11/2010	2-143	9	11/2010	2-189	0	3/2004
2-106B	1	11/2004	2-144	9	11/2010	2-190	4	3/2005
2-107	0	3/2004	2-145	1	11/2004	2-191	0	3/2004
2-108	0	3/2004	2-146	0	3/2004	2-192	9	11/2010
2-109	0	3/2004	2-147	0	3/2004	2-192A	4	3/2005
2-110	0	3/2004	2-148	9	11/2010	2-192B	4	3/2005
2-111	0	3/2004	2-149	0	3/2004	2-192C	9	11/2010
2-112	0	3/2004	2-150	0	3/2004	2-192D	4	3/2005
2-113	0	3/2004	2-151	0	3/2004	2-193	0	3/2004
2-114	0	3/2004	2-152	0	3/2004	2-194	0	3/2004
2-115	0	3/2004	2-153	0	3/2004	2-195	0	3/2004
2-116	9	11/2010	2-154	0	3/2004	2-196	0	3/2004
2-117	0	3/2004	2-155	1	11/2004	2-197	0	3/2004
2-118	9	11/2010	2-155A	1	11/2004	2-198	0	3/2004
2-119	0	3/2004	2-155B	1	11/2004	2-199	0	3/2004
2-120	0	3/2004	2-156	2	2/2005	2-200	0	3/2004
2-121	0	3/2004	2-157	2	2/2005	2-201	10	9/2013
2-122	0	3/2004	2-158	1	11/2004	2-202	10	9/2013
2-123	0	3/2004	2-159	0	3/2004	2-203	10	9/2013
2-124	0	3/2004	2-160	0	3/2004	2-204	9	11/2010
2-125	9	11/2010	2-161	0	3/2004	2-205	9	11/2010

TRAVELLER SAFETY ANALYSIS REPORT
LIST OF EFFECTIVE PAGES (cont.)

Page	Rev.	Date
2-206	9	11/2010
2-207	9	11/2010
2-208	9	11/2010
2-209	9	11/2010
2-210	10	9/2013
2-211	9	11/2010
2-212	10	9/2013
2-213	9	11/2010
2-214	10	9/2013
2-215	9	11/2010
2-216	9	11/2010
2-217	9	11/2010
2-218	9	11/2010
3-i	9	11/2010
3-ii	1	11/2004
3-iii	9	11/2010
3-iv	9	11/2010
3-1	10	9/2013
3-2	9	11/2010
3-3	10	9/2013
3-4	9	11/2010
3-5	10	9/2013
3-6	0	3/2004
3-7	0	3/2004
3-8	0	3/2004
3-9	0	3/2004
3-10	10	9/2013
3-11	0	3/2004
3-12	0	3/2004
3-13	10	9/2013
3-14	10	9/2013
3-14A	9	11/2010
3-14B	9	11/2010
3-15	9	11/2010
3-15A	9	11/2010
3-15B	9	11/2010
3-16	10	9/2013
3-17	0	3/2004
3-18	1	11/2004
3-19	9	11/2010
3-20	0	3/2004
3-21	10	9/2013
3-22	0	3/2004
3-23	0	3/2004
3-24	0	3/2004
3-25	9	11/2010
3-26	10	9/2013
3-27	0	3/2004
3-28	9	11/2010
3-29	0	3/2004
3-30	0	3/2004
3-31	9	11/2010
3-32	0	3/2004
3-33	9	11/2010
3-34	0	3/2004
3-35	10	9/2013
3-35A	1	11/2004
3-35B	10	9/2013
3-36	0	3/2004
3-37	0	3/2004
3-38	1	11/2004
3-39	0	3/2004
3-40	10	9/2013
3-41	0	3/2004
3-42	1	11/2004
3-42A	1	11/2004
3-42B	1	11/2004
3-43	0	3/2004
3-44	0	3/2004
3-45	0	3/2004
3-46	10	9/2013
3-46A	1	11/2004
3-46B	1	11/2004
3-47	0	3/2004
3-48	0	3/2004
3-49	10	9/2013
3-50	1	11/2004
4-i	9	11/2010
4-ii	9	11/2010
4-1	9	11/2010
5-i	9	11/2010
5-ii	9	11/2010
5-1	9	11/2010
6-i	1	11/2004
6-ii	9	11/2010
6-iii	9	11/2010
6-iv	8	5/2010
6-v	8	5/2010
6-vi	2	2/2005
6-vii	10	9/2013
6-viii	9	11/2010
6-1	10	9/2013
6-2	0	3/2004
6-3	2	2/2005
6-4	2	2/2005
6-5	0	3/2004
6-6	1	11/2004
6-7	1	11/2004
6-7A	1	11/2004
6-7B	1	11/2004
6-8	0	3/2004
6-9	10	9/2013
6-10	10	9/2013
6-11	10	9/2013
6-12	10	9/2013
6-13	10	9/2013
6-14	9	11/2010
6-15	9	11/2010
6-16	1	11/2004
6-17	10	9/2013
6-18	1	11/2004
6-19	2	2/2005
6-20	2	2/2005
6-21	2	2/2005
6-22	2	2/2005
6-23	2	2/2005
6-24	1	11/2004
6-25	10	9/2013
6-26	1	11/2004
6-27	1	11/2004
6-27A	10	9/2013
6-27B	1	11/2004
6-28	1	11/2004
6-29	1	11/2004
6-30	1	11/2004
6-31	1	11/2004
6-32	2	2/2005
6-33	1	11/2004
6-34	1	11/2004
6-35	1	11/2004
6-36	1	11/2004
6-37	1	11/2004
6-38	1	11/2004
6-39	1	11/2004
6-40	2	2/2005
6-41	10	9/2013
6-42	1	11/2004
6-42A	1	11/2004
6-42B	1	11/2004
6-43	1	11/2004

TRAVELLER SAFETY ANALYSIS REPORT
LIST OF EFFECTIVE PAGES (cont.)

Page	Rev.	Date	Page	Rev.	Date	Page	Rev.	Date
6-44	10	9/2013	6-67	1	11/2004	6-107L	2	2/2005
6-45	1	11/2004	6-68	0	3/2004	6-107M	3	3/2005
6-46	1	11/2004	6-69	9	11/2010	6-107N	2	2/2005
6-46A	1	11/2004	6-70	1	11/2004	6-107O	2	2/2005
6-46B	1	11/2004	6-71	1	11/2004	6-107P	2	2/2005
6-47	10	9/2013	6-72 – 6-76	1	11/2004	6-107Q	2	2/2005
6-47A	2	2/2005	6-77	1	11/2004	6-107R	2	2/2005
6-47B	1	11/2004	6-78	1	11/2004	6-107S	2	2/2005
6-48	2	2/2005	6-79	1	11/2004	6-107T	2	2/2005
6-48A	1	11/2004	6-80	1	11/2004	6-107U	2	2/2005
6-48B	10	9/2013	6-81	1	11/2004	6-107V	2	2/2005
6-48C	2	2/2005	6-82	1	11/2004	6-107W	2	2/2005
6-48D	2	2/2005	6-82A	1	11/2004	6-107X	2	2/2005
6-49	0	3/2004	6-82B	1	11/2004	6-107Y	2	2/2005
6-50	10	9/2013	6-82C	1	11/2004	6-107Z	2	2/2005
6-51	10	9/2013	6-82D	1	11/2004	6-107AA	2	2/2005
6-51A	10	9/2013	6-83	9	11/2010	6-107BB	3	3/2005
6-52	10	9/2013	6-84	1	11/2004	6-107CC	3	3/2005
6-52A	9	11/2010	6-85	1	11/2004	6-107DD	3	3/2005
6-52B	9	11/2010	6-86	1	11/2004	6-107EE	3	3/2005
6-53	9	11/2010	6-87 – 6-91	1	11/2004	6-107FF	3	3/2005
6-54	3	3/2005	6-92	1	11/2004	6-107GG	3	3/2005
6-54A	1	11/2004	6-93	1	11/2004	6-107HH	3	3/2005
6-54B	1	11/2004	6-94	1	11/2004	6-108	10	9/2013
6-55	7	10/2009	6-95	1	11/2004	6-109	1	11/2004
6-56	9	11/2010	6-96	1	11/2004	6-110	1	11/2004
6-56A	8	5/2010	6-97	1	11/2004	6-111	1	11/2004
6-56B	9	11/2010	6-97A	1	11/2004	6-112	1	11/2004
6-57	10	9/2013	6-97B	1	11/2004	6-113	1	11/2004
6-57A	8	5/2010	6-98	1	11/2004	6-114	1	11/2004
6-57B	9	11/2010	6-99 – 6-103	1	11/2004	6-115	1	11/2004
6-58	10	9/2013	6-104	9	11/2010	6-116	1	11/2004
6-58A	10	9/2013	6-104A	10	9/2013	6-117	1	11/2004
6-58B	10	9/2013	6-104B	1	11/2004	6-118	1	11/2004
6-58C	10	9/2013	6-105	2	2/2005	6-119	1	11/2004
6-58D	10	9/2013	6-106	2	2/2005	6-120	1	11/2004
6-58E	10	9/2013	6-107	3	3/2005	6-121	1	11/2004
6-58F	10	9/2013	6-107A	3	3/2005	6-122	1	11/2004
6-59	0	3/2004	6-107B	2	2/2005	6-123	1	11/2004
6-60	9	11/2010	6-107C	2	2/2005	6-124	1	11/2004
6-61	9	11/2010	6-107D	2	2/2005	6-125	1	11/2004
6-62	0	3/2004	6-107E	2	2/2005	6-126	1	11/2004
6-63	9	11/2010	6-107F	2	2/2005	6-127	1	11/2004
6-64	1	11/2004	6-107G	2	2/2005	6-128	1	11/2004
6-64A	1	11/2004	6-107H	2	2/2005	6-129	9	11/2010
6-64B	1	11/2004	6-107I	2	2/2005	6-130	1	11/2004
6-65	2	2/2005	6-107J	2	2/2005	6-131	1	11/2004
6-66	10	9/2013	6-107K	2	2/2005	6-132	1	11/2004

TRAVELLER SAFETY ANALYSIS REPORT
LIST OF EFFECTIVE PAGES (cont.)

Page	Rev.	Date
6-133	1	11/2004
6-134	1	11/2004
6-135	1	11/2004
6-136	1	11/2004
6-137	1	11/2004
6-138	1	11/2004
6-139	9	11/2010
6-140	1	11/2004
6-141	1	11/2004
6-142	1	11/2004
6-143	1	11/2004
6-144	1	11/2004
6-145	1	11/2004
6-146	1	11/2004
6-147	1	11/2004
6-148	1	11/2004
6-149	1	11/2004
6-150	1	11/2004
6-151	1	11/2004
6-152	1	11/2004
6-153	1	11/2004
6-154	1	11/2004
6-155	1	11/2004
6-156	1	11/2004
6-157	1	11/2004
6-158	1	11/2004
6-159	9	11/2010
6-160	1	11/2004
6-160A	2	2/2005
6-160B	2	2/2005
6-160C	2	2/2005
6-160D	2	2/2005
6-160E	2	2/2005
6-160F	2	2/2005
6-160G	2	2/2005
6-160H	2	2/2005
6-160I	2	2/2005
6-160J	2	2/2005
6-161	9	11/2010
6-162	0	3/2004
6-163	0	3/2004
6-164	1	11/2004
6-165	0	3/2004
6-166	10	9/2013
9/2013		

Page	Rev.	Date
7-i	9	11/2010
7-ii	9	11/2010
7-1	10	9/2013
7-2	10	9/2013
7-3	10	9/2013
7-4	10	9/2013
7-5	9	11/2010
8-i	10	9/2013
8-ii	9	11/2010
8-1	10	9/2013
8-2	0	3/2004
8-3	0	3/2004
8-4	9	11/2010
8-5	9	11/2010
8-5A	2	2/2005
8-5B	9	11/2010
8-5C	9	11/2010
8-5D	1	11/2004
8-5E	9	11/2010
8-6	9	11/2010
8-7	2	2/2005
8-8	10	9/2013
8-8A	10	9/2013
8-8B	1	11/2004

Page	Rev.	Date

This page intentionally left blank.

TABLE OF CONTENTS

LIST OF TABLES

LIST OF FIGURES

This page intentionally left blank.

1.0 GENERAL INFORMATION

1.1 INTRODUCTION

The Traveller[1] is a shipping package designed to transport non-irradiated uranium fuel assemblies or rods with enrichments up to 5.0 weight percent. It will carry several types of PWR fuel assemblies as well as either BWR- or PWR rods. This is described further in Section 6. The proposed Criticality Safety Index (CSI) for the Traveller is 0.7 when transporting fuel assemblies and 0.0 when transporting loose rods. The following sections describe the package design and testing program in detail. Drawings are presented in Section 1.4.1. A generic sketch of the Traveller representing the package as prepared for transport is provided in Figure 1-7.

1.2 PACKAGE DESCRIPTION

1.2.1 Packaging

The Traveller package is designed to carry one (1) fuel assembly or one (1) pipe for loose rods. It is made up of three basic components: 1) an Outerpack, 2) a Clamshell, and 3) a Fuel Assembly or Rod Pipe. The Outerpack and Clamshell are connected together with a suspension system that reduces the forces applied to the fuel assembly during transport. The Rod Pipe is secured inside the Clamshell during transport of loose rods.

1.2.1.1 Package Types

There are two types of packagings in the Traveller family.

1.2.1.1.1 Traveller Standard (Traveller STD)

- Gross Weight = 4,500 pounds (2041 kg)
- Tare Weight = 2,850 pounds (1293 kg)
- Outer Dimensions = 197.0" length x 27.0" width x 39.3" height
  (5004 mm x 688 mm x 998 mm)

1. Traveller is a Westinghouse trademark.

1.2.1.1.2 Traveller XL

- Gross Weight = 5,230 pounds (2,372 kg)
- Tare Weight = 3,255 pounds (1,476 kg)
- Outer Dimensions = 226.0" length x 27.1" width and 39.3" height (5740 mm x 688 mm x 998 mm)

1.2.1.2 Outerpack

The Outerpack is a structural component that serves as the primary impact and thermal protection for the Fuel Assembly. It also provides for lifting, stacking, and tie down during transportation. The Outerpack is a long tubular design consisting of a top and bottom half as shown in Figure 1-1. Each half consists of a stainless steel outer shell, a layer of rigid polyurethane foam, and an inner stainless steel shell. The stainless steel provides structural strength and acts as a protective covering to the foam. A typical cross-section showing key elements of the package is depicted in Figure 1-2.

The outerpack is comprised of independent impact limiters at the top end and lower end. Each end impact limiter is a system containing a pillow sub-assembly adjacent to 20 pcf polyurethane foam. The 20 pcf foam is encased by the package outerpack stainless steel skins. The top pillow sub-assembly consists of 6 pcf foam encased between two stainless steel plates to allow mating with the upper outerpack. A detail of the top pillow assembly is shown on 10004E58, sheet 6. The lower pillow assembly consists of 6 pcf foam encased in a stainless steel circular housing which allows mating with the lower outerpack. A detail of the lower pillow assembly is also shown on 10004E58, sheet 6.

The foam is a rigid, closed cell polyurethane that is an excellent impact absorber and thermal insulator and has well defined characteristics that make it ideal for this application. The steel-foam-steel “sandwich” is the primary fire protection, and is described in more detail in Section 3.

The inside of the Outerpack is lined with blocks of Ultra High Molecular Weight (UHMW) polyethylene. The polyethylene has a dual purpose. It provides a conformal cavity for the Clamshell and fuel assembly to fall into during low-angle drops. The clamshell is fastened to the lower Outerpack using shock absorbing rubber mounts. Polyethylene foam sheeting may be positioned between the clamshell and lower Outerpack to augment the shock absorbing characteristics for routine transport. A weather gasket between the mating surfaces of the upper and lower Outerpack provides a seal to prevent rain and water spray from entering the package.

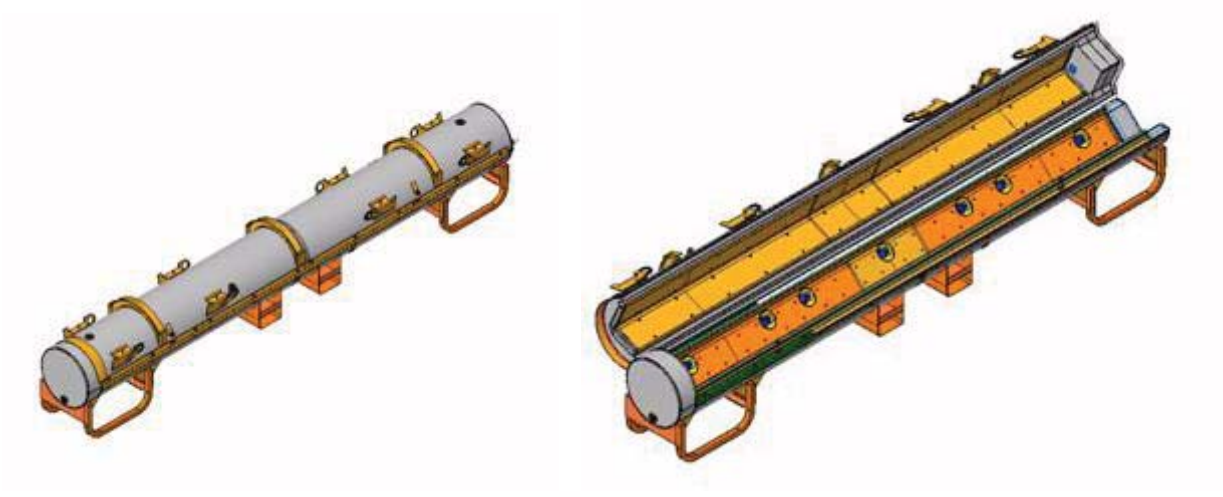

Figure 1-1 Outerpack Closed Position (left) and Opened Position (right)

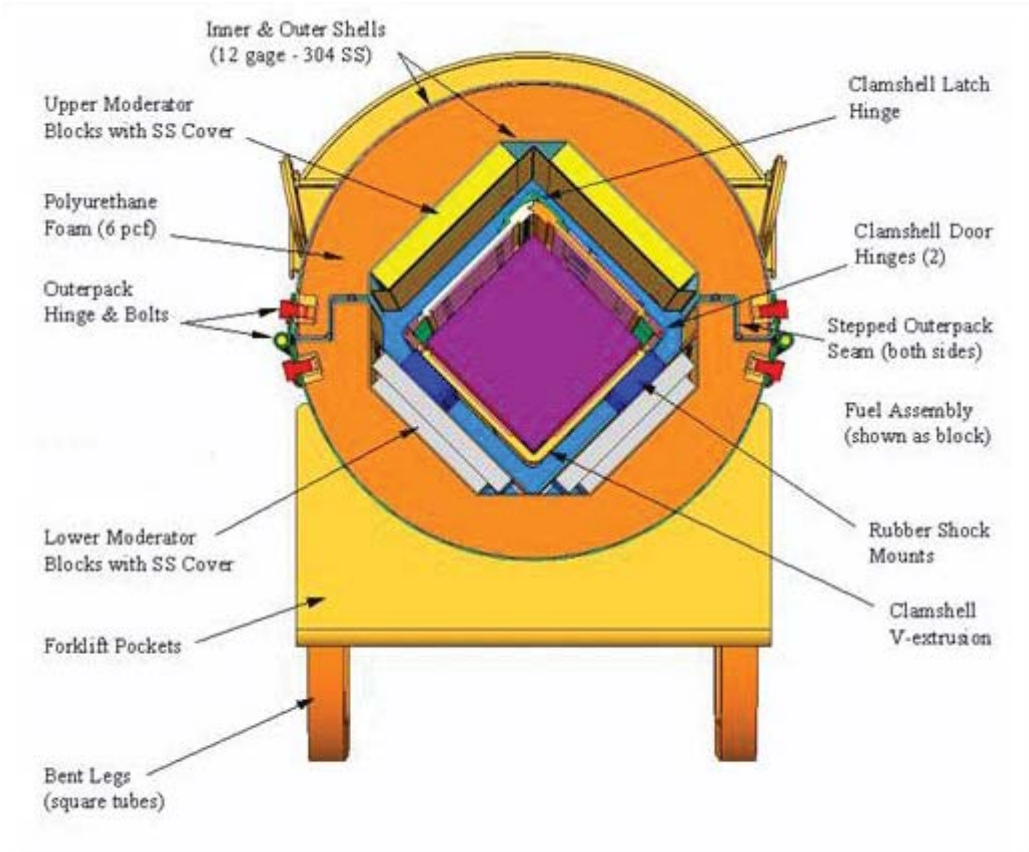

Figure 1-2 Outerpack Cross-Section View (typical) Clamshell

1.2.1.3 Clamshell

The purpose of the Clamshell is to protect the contents during routine handling and limit rearrangement of the contents in the event of a transport accident. During routine handling, the Clamshell doors open to load the contents and are secured with multi-point cammed latches and hinge pins. The Clamshell is a part of the confinement system that protects and restrains the fuel assembly or fuel rod tube contents during all transport conditions. During accident transport conditions the clamshell remains closed and the structure limits rearrangement of the fuel assembly. Neutron absorber plates are installed on the inside surface of the clamshell along the full length of each side.

The Clamshell structural components consist of an aluminum "V" strong back, two aluminum panel doors, a small top "V" access door, bottom and top end plates, and a multi-point cammed latch closure mechanism. Piano type hinges (continuous hinges) connect each panel door and the small top "V" access door to the "V" strong back. The neutron absorber plates are secured to the clamshell with threaded fasteners. The absorber plates do not provide any structural strength to the clamshell. The "V" strong back and bottom plate are lined with a cork rubber pad to cushion the contents and prevent damage during normal handling and routine transport conditions.

The top plate of the clamshell has two configurations in order to accommodate different fuel types. Each uses a combination of flat head cap screws and tongue and groove joints to fasten securely to the clamshell. The Fixed Top Plate (FTP), shown in Figure 1-3, is secured directly to the top access door with cap screws. It has a tongue edge that fits into grooved shear bars that are attached directly to both faces of the clamshell base with cap screws. The Removable Top Plate (RTP), shown in Figure 1-4, has grooved edges all around, and mates with shear bars that are fastened to all four faces of the clamshell. The bottom plate is secured to the clamshell base with cap screws. Closure is provided by tongue and groove joining with the clamshell doors.

The panel doors are secured by multi-point cammed latches that are spaced along the length of the clamshell. These mechanical fasteners consist of a cam latch on the right main door that engages a keeper on the left main door. The cam latch is rotated a quarter-turn to engage the keeper as shown in Figure 1-5. A wave spring washer prevents inadvertent movement of the cam latch. There are 9 cam latches on the Traveller STD clamshell and 11 cam latches on the Traveller XL clamshell. The top access door is secured with a short hinge pin inserted into the hinge knuckles when the small top access door is closed.

Clamping mechanisms that interface with the contents provide axial and lateral restraint during all transport conditions. An adjustable, threaded rod clamping device provides axial restraint at the top of the fuel assembly or rod tube. The design of the top axial restraint components, as shown in Figures 1-5A, 1-5B, and 1-5C) depends on the clamshell top plate configuration (FTP or RTP) and the fuel assembly type. An additional restraint may be added to secure core components (reactor core control components or secondary source rods) when shipped within the fuel assembly. Rubber pads are positioned at axial locations along the inside of the clamshell doors to restrain lateral movement. These restraints, referred to as grid pads, are positioned to match the mid-grid locations for each fuel assembly type.

Traveller XL clamshell dimensions accommodate both the longer fuel designs and fuel designs with a larger cross section dimensions. The longer length may be adapted for shorter fuel assembly designs that are normally shipped in the Traveller STD by adding an aluminum spacer component as shown in Figure 1-5D. The spacer is placed on the bottom end plate to elevate the fuel assembly in the longer clamshell so it can be secured with the axial restraints at the top of the clamshell. The larger cross section dimension may be adapted for fuel assemblies with smaller cross sections by adding fuel spacer assemblies in the aluminum "V" strong back. as shown in Figure 1-5E.

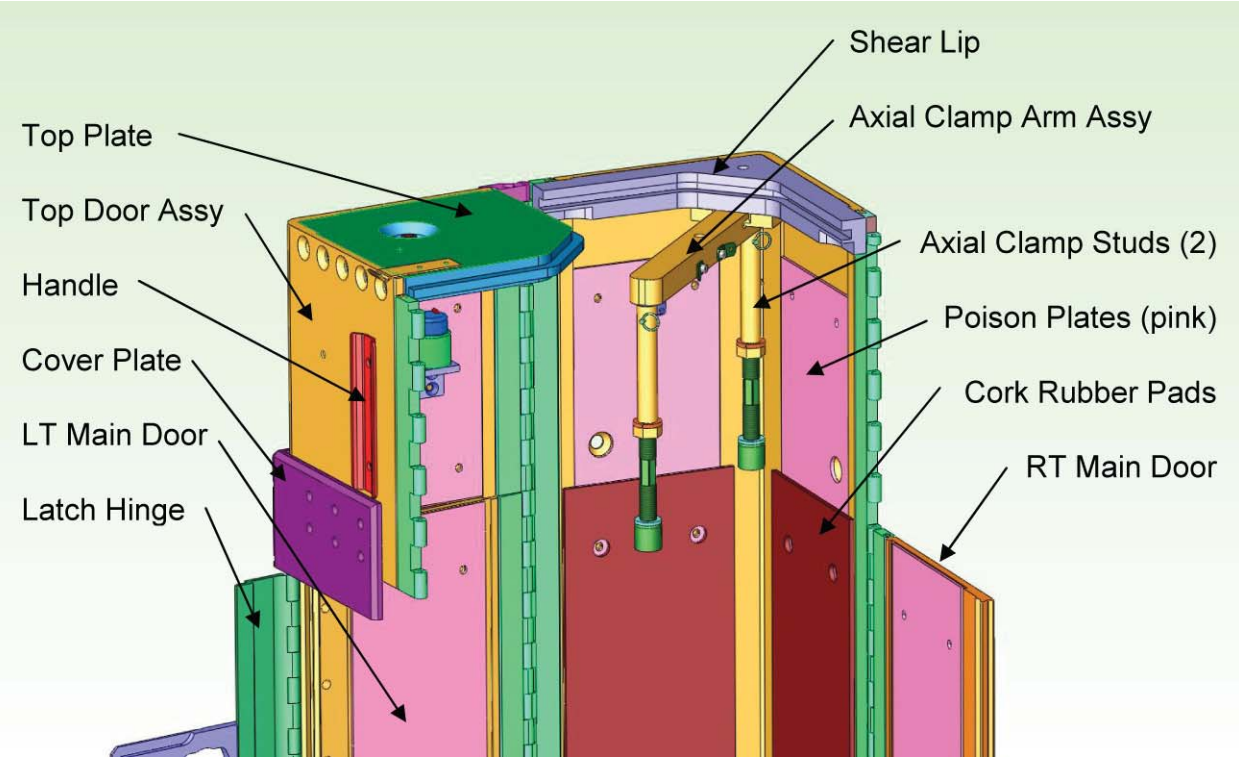

Figure 1-3 Clamshell with Fixed Top Plate (FTP)

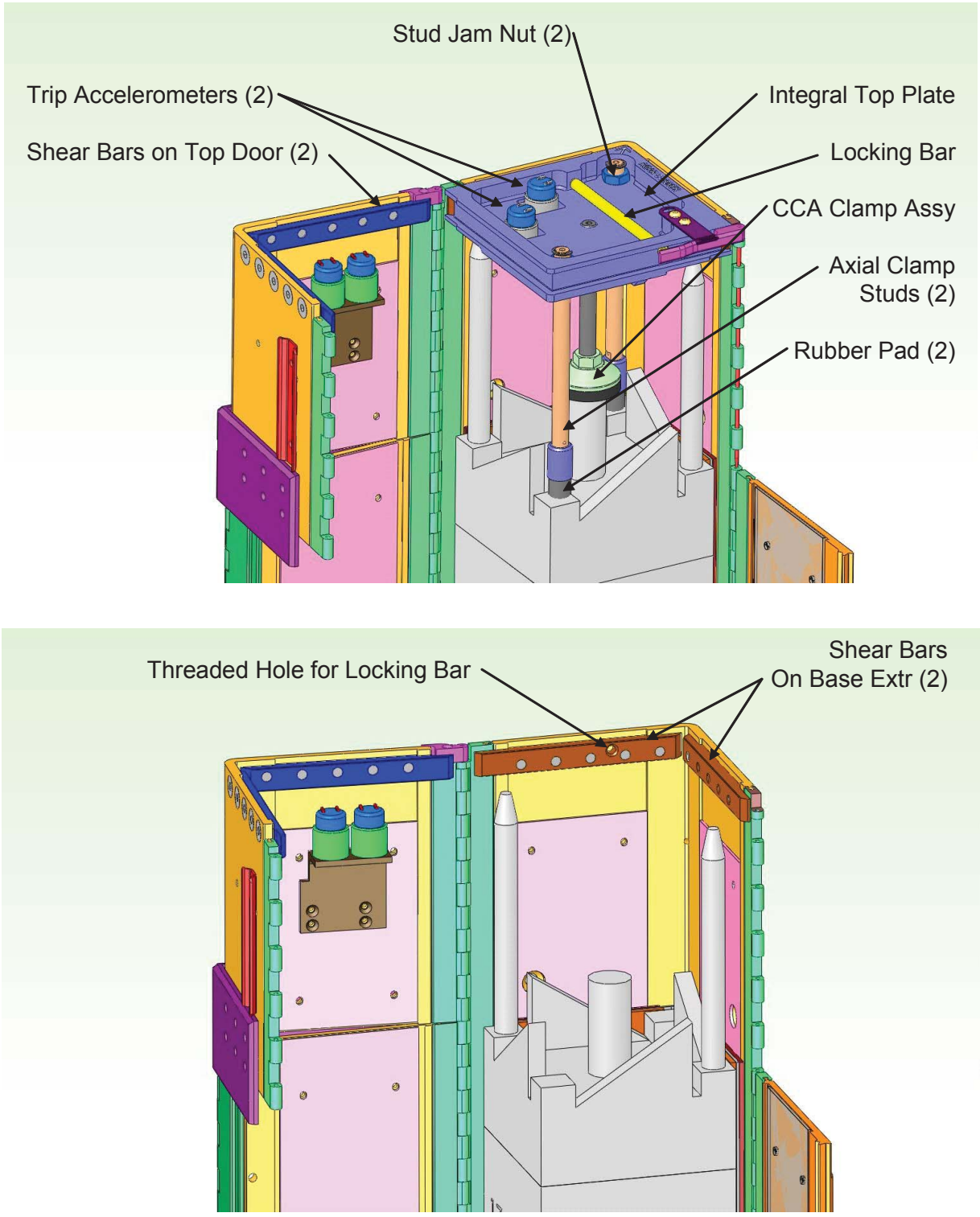

Figure 1-4 Clamshell with Removable Top Plate (RTP)

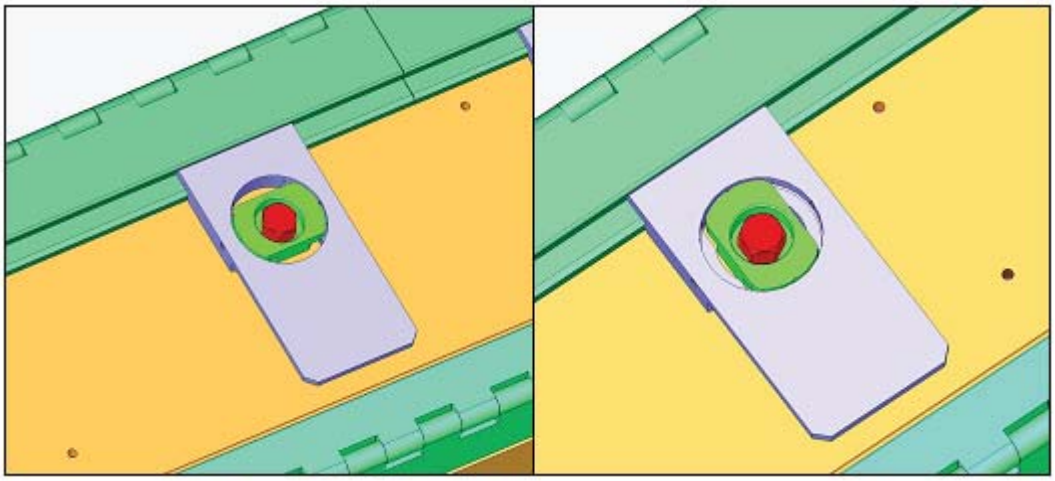

Figure 1-5 Clamshell Latch Locked Position (left) and Open Position (right)

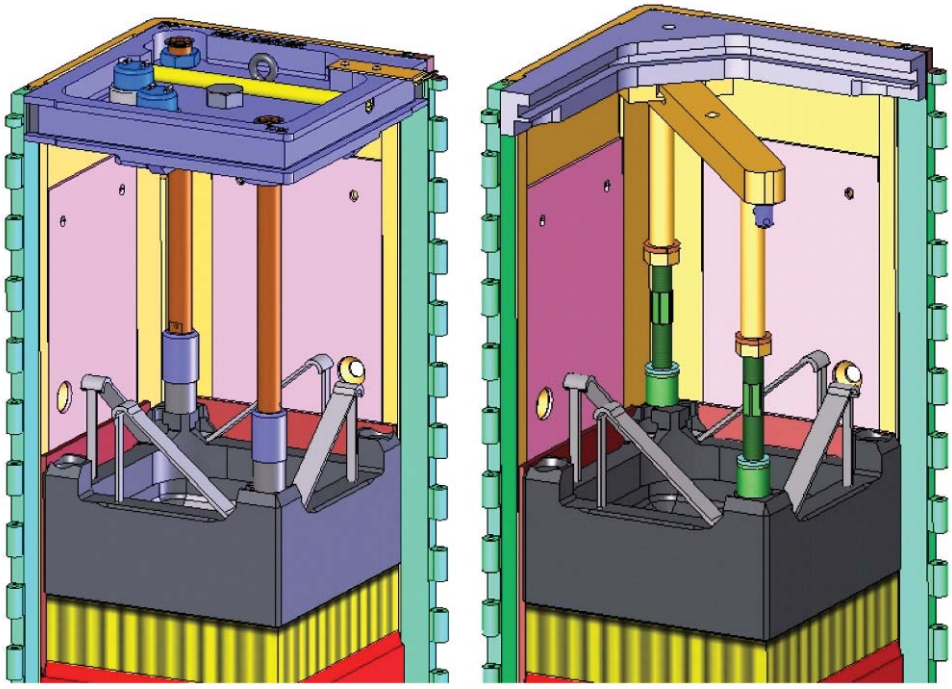

Fuel Assembly

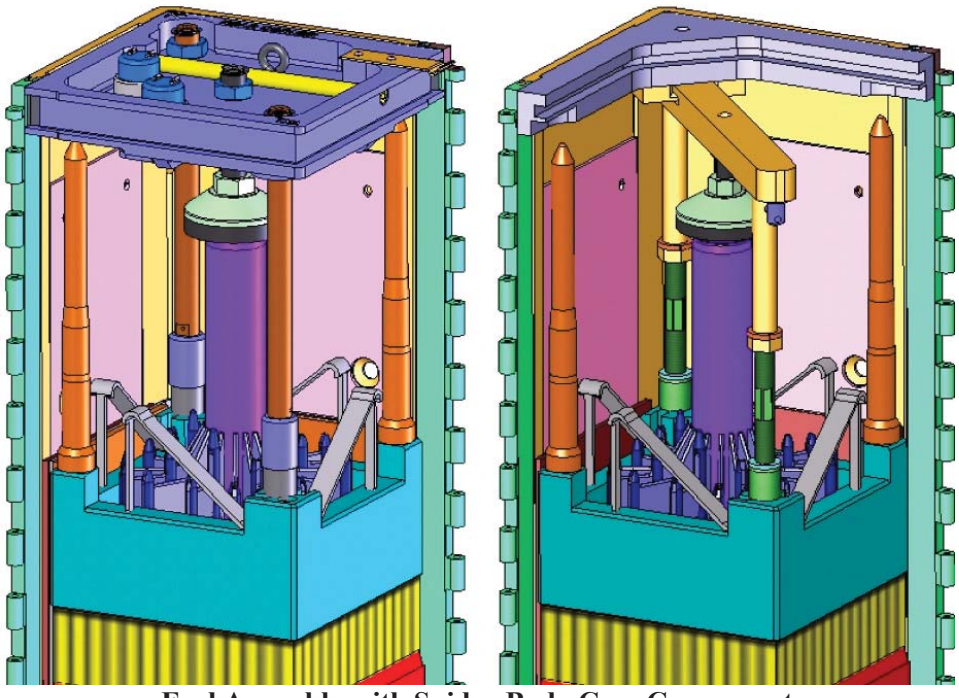

Fuel Assembly with Spider-Body Core Component

Figure 1-5A Corner Post Axial Restraint – Removable Top Plate (left), Fixed Top Plate (right)

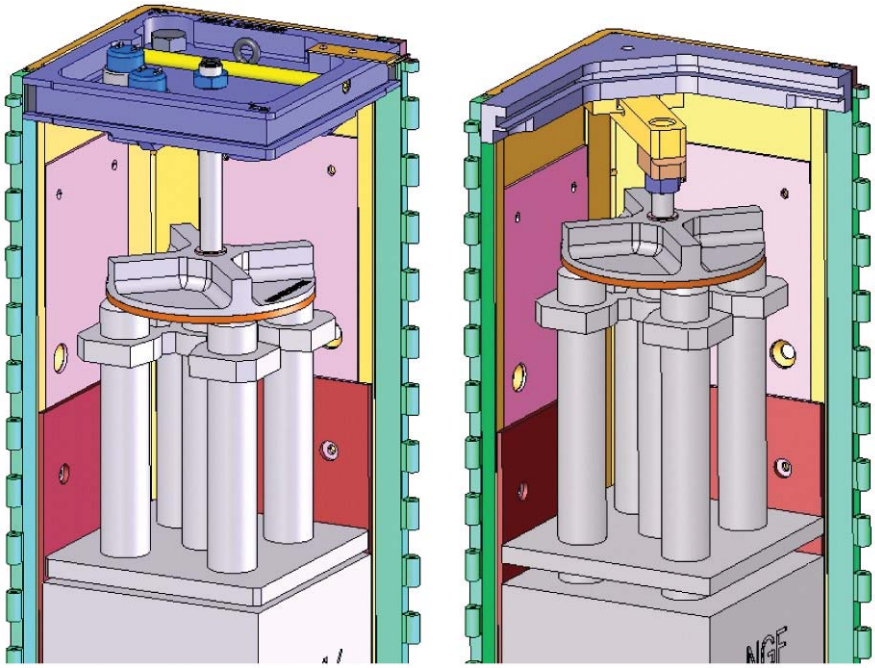

Figure 1-5B Center Plate Axial Restraint – Removable Top Plate (left), Fixed Top Plate (right)

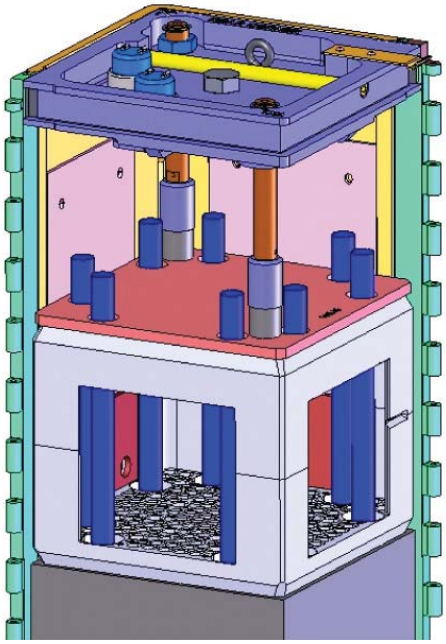

Figure 1-5C ATOM Corner Post Axial Restraint

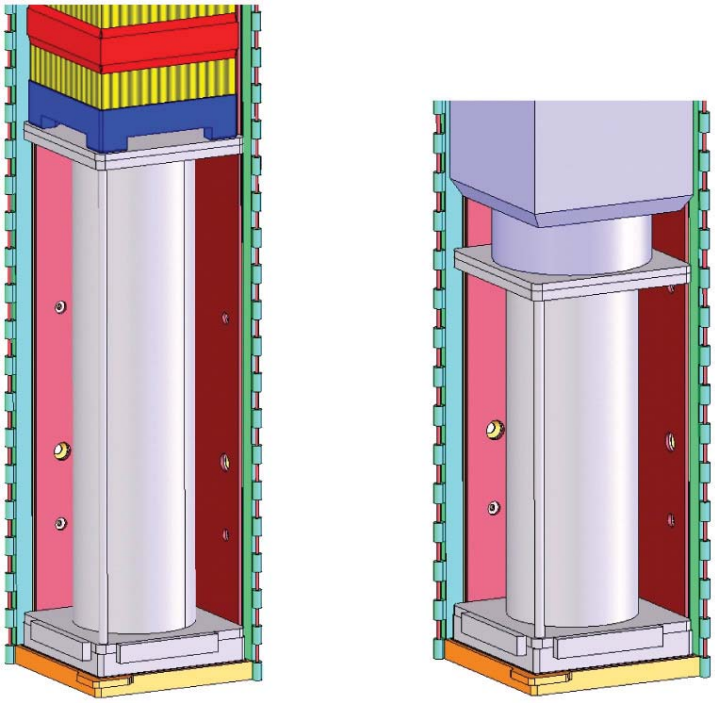

Figure 1-5D Axial Spacer Assembly (length depends on fuel assembly type)

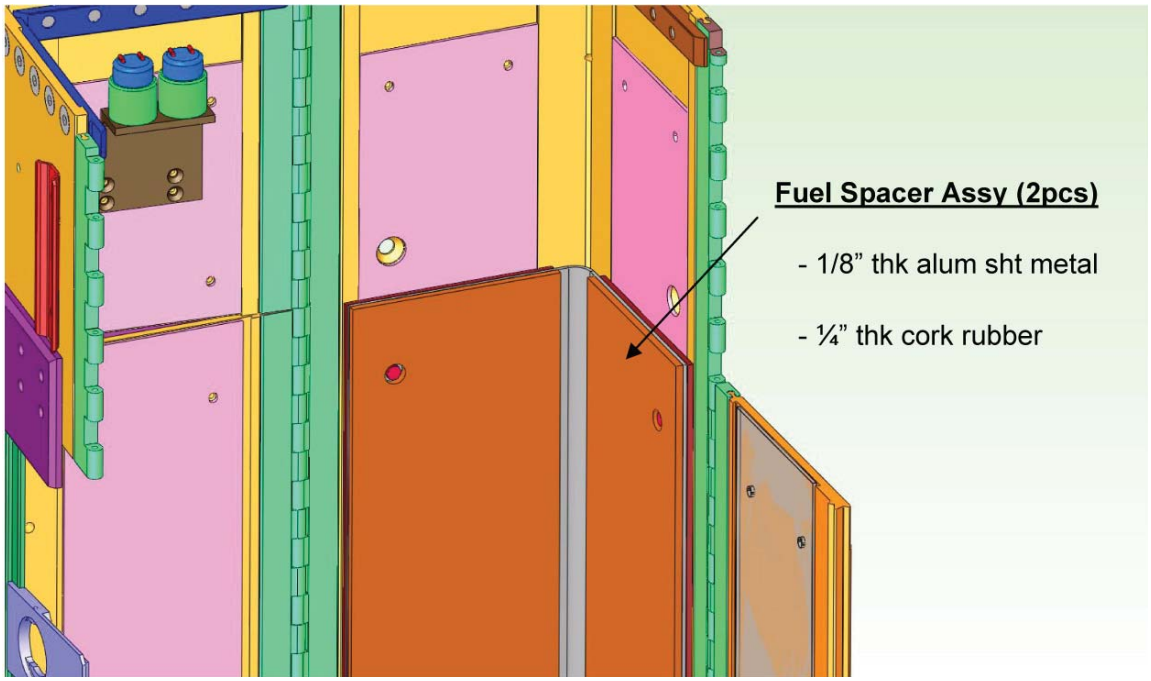

Figure 1-5E XL Clamshell Fuel Spacer Assembly

This page intentionally left blank.

1.2.1.4 Rod Pipe

The Traveller is designed to carry loose rods using the rod pipe shown in Figure 1-6. The rod pipe consists of a 6" (15.24 cm) standard 304 stainless steel, Schedule 40 pipe, and standard 304 stainless steel closures at each end. The closure is a 0.25 inch (6.35 mm) thick cover secured with Type 304 stainless steel hardware to a flange fabricated from 0.25 inch (6.35 mm) thick plate.

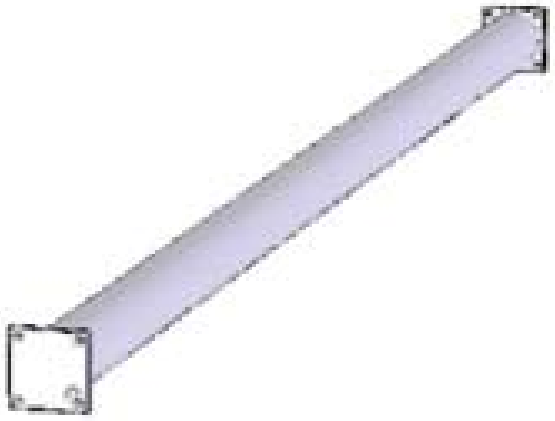

Figure 1-6 Rod Pipe

The rod pipe is held in place by clamshell restraining devices. Axial restraint is provided by the axial clamp assembly shown on Sheet 7 of 9 of drawing 10004E58. The axial clamp arm is bolted into the top shear lip and contact the fuel rod pipe is performed by an adjustable jack screw. Lateral and vertical restraint is accomplished through the use of removal rubber pads located inside the clamshell door lip in conjunction with the latch assemblies on the clamshell doors. The rubber pads are of varying thickness to accommodate the loose rod shipping pipes. The rod pipe design has a maximum loaded weight of 1650lb (748kg).

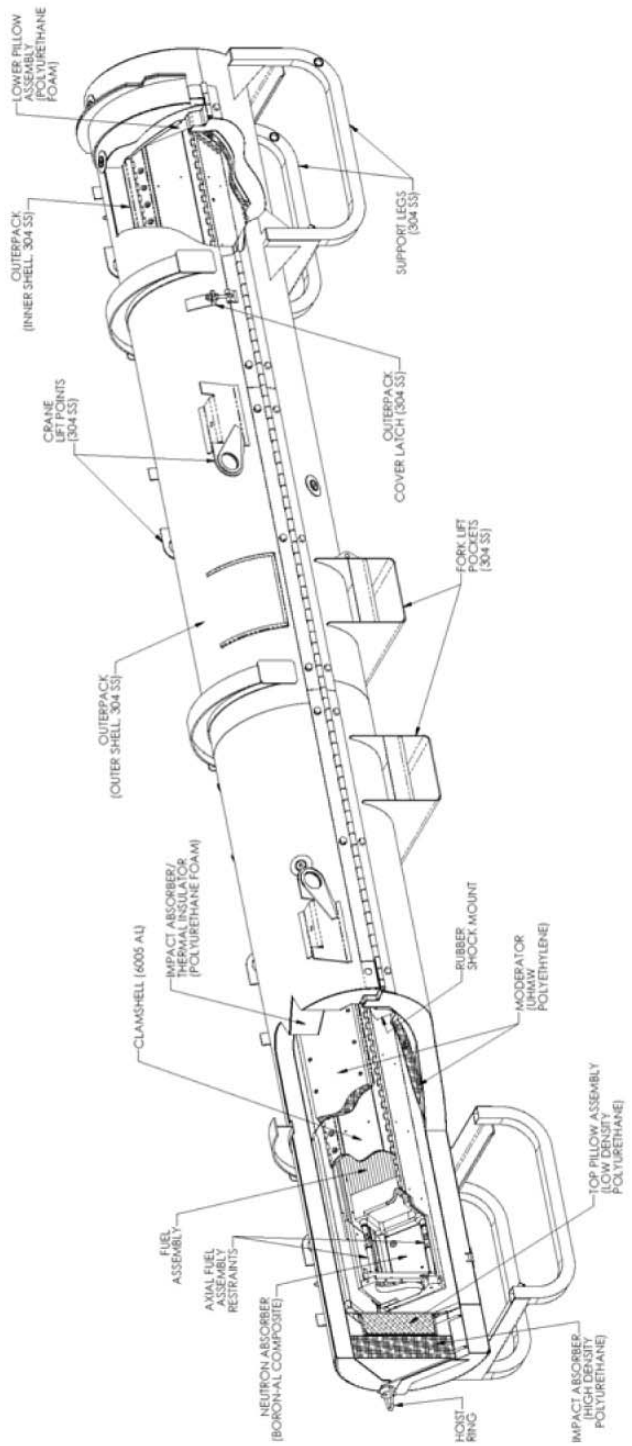

Figure 1-7 Generic Sketch of Traveller Representing the Package as Prepared for Transport

1.2.2 Containment System

The Containment System is described in both IAEA Regulations for the Safe Transport of Radioactive Material, Safety Standard Series No. TS-R-1 (213) and the Code of Federal Regulations, Title 10, Part 71.4 as, "the assembly of components of the packaging intended to retain the radioactive material during transport." The Containment System for the Traveller is the fuel rod. Containment is described in greater detail in Section 6.

1.2.3 Contents

Westinghouse Electric Company provides fuel assembly designs that are transported in the Traveller for use in pressurized water reactors (PWR). The general configuration and dimensions of the PWR fuel assembly designs are similar, but there are unique features in some of the components of the fuel assembly. A typical PWR fuel assembly is shown in Figure 1-8.

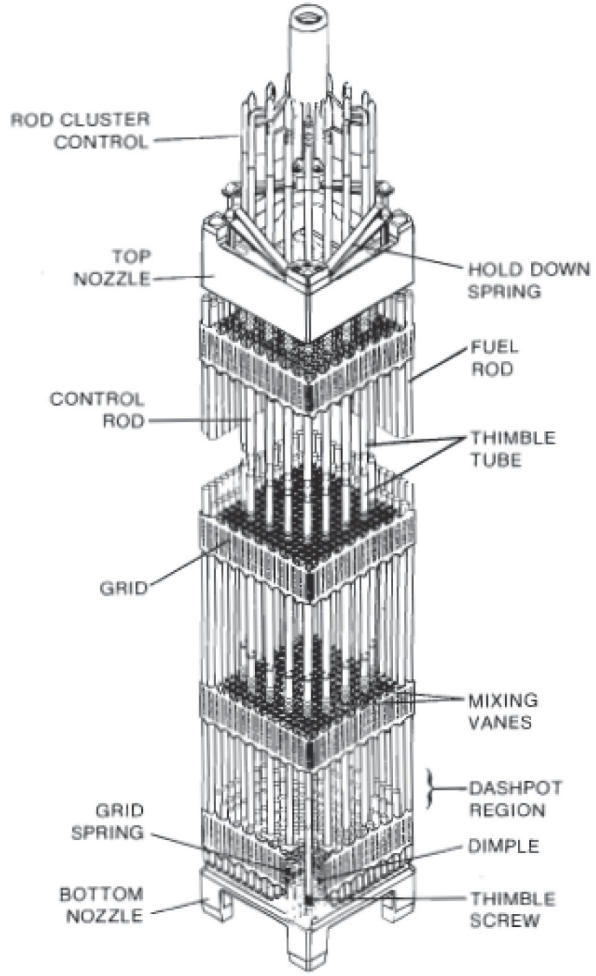

Figure 1-8 Cutaway of 17x17 Optimized Fuel Assembly with RCC

1.2.3.1 Type and Form

The contents is a single PWR fuel assembly and fuel rods. Fuel rods are transported in a fuel rod pipe. Any number of fuel rods may be transported in a fuel rod pipe. Fuel rods include designs for both pressurized water reactors (PWR) and boiling water reactors (BWR). For the range of fuel rod diameters (0.37 – 0.45 inch) the maximum number of fuel rods that fit inside the rod pipe is 250 to 170 fuel rods. The actual number of fuel rods placed in a rod pipe is less than this because some space is required to accommodate the packaging materials and allow for handling fuel rods. The PWR fuel assembly may be transported with reactor core components A single fuel assembly with non-fissile base-plate mounted core components or spider-body core components, or a single fuel rod pipe is transported in a package. The core components include rod cluster control (RCC) assemblies and secondary source rods that are not radioactive material. In addition, any of the fuel rods is a fuel assembly may be replaced by a solid stainless steel rod. The maximum contents weight is 748 kg (1,650 lbs) for a Traveller STD, and 894 kg (1,971 lbs) for a Traveller XL.

1.2.3.1.1 Fuel Pellets

The fuel pellet is composed of enriched uranium dioxide powder that is compacted by cold pressing and then sintered to attain the required density. The sintered uranium dioxide is chemically inert at reactor temperatures and pressures. Slightly dished ends of each pellet permit axial expansion at the center of the pellets.

1.2.3.1.2 Fuel Rod

Uranium dioxide pellets are inserted into a zirconium alloy tube, and each end of the tube is sealed by welding on an end plug to form a fuel rod. The pellets are prevented form shifting during handling and shipment by a compression spring located between the top of the fuel pellet stack and the top end plug.

The fuel rod is designed as a pressure vessel. Fuel rod pre-pressurization which reduces fuel and cladding mechanical interaction significantly reduces the number and extent of cyclic stresses experienced by the cladding. The result is a marked extension of the fatigue life margin of cladding with enhanced cladding reliability. A representative nominal internal pressure of fuel rods at room temperature conditions is 2.62 MPa (380 psig). There is no pressure relief device that would allow radioactive contents to escape.

The ASME Boiler and Pressure Vessel Code, Section III, is used as a guide in the mechanical design and stress analysis of the fuel rod. The rod is designed to withstand the applied loads, both external and internal. The fuel pellet is sized to provide sufficient volume within the fuel tube to accommodate differential expansion between fuel and cladding. Welds of the fuel rods are verified for integrity by such means as X-ray inspection, ultrasonic testing, or process control.

1.2.3.1.3 Fuel Assembly

A square or hexagonal array of fuel rods that are structurally bound together in a skeleton constitutes a fuel assembly. The skeleton consists of thimble tubes, spring clip grids, a top nozzle, bottom nozzle and other

hardware (i.e., springs, nuts, etc.). Control rod thimbles replace fuel rods at selected spaces in the array and are fastened to the top and bottom nozzles of the assembly. Spring clip grid assemblies are fastened to the guide thimbles along the height of the fuel assembly to provide support for the fuel rods. The fuel rods are contained and supported, and the rod-to-rod centerline spacing is maintained within this skeletal framework.

The bottom nozzle of the fuel assembly controls flow distribution in the reactor core and also serves as the bottom structural element. The top nozzle functions as the fuel assembly upper structural element and forms a plenum space where the heated reactor coolant is mixed and directed toward the flow holes in the upper core plate.

The spring clip grids provide support for the fuel rods in two perpendicular directions. Each rod is supported as six points in each cell of the grid. Four support points are fixed: two on onside of the grid strap, and two similarly located on the adjacent side. Two more support points are provided by spring straps located opposite the fixed points. Each spring strap exerts a force on the fuel rod such that lateral fuel rod vibration is restrained. Because the fuel rods are not physically bound to the support points, they are free to expand axially to accommodate thermal and radiation growth.

All fuel assemblies employ the same basic mechanical design. While all assemblies are capable of accepting control rod clusters, these are not used in every fuel assembly. Selected fuel assemblies have neutron sources or burnable absorber rods installed in the control rod guides thimbles. Fuel assemblies not containing either control rod clusters, source assemblies, or burnable absorbers rods, are fitted with plugs in the upper nozzle to restrict the flow through the vacant control rod guide thimbles. Fuel assemblies may be shipped with any of these core components, except for primary neutron source rods which contain Californium-252 that requires a package with radiation shielding features.

The fuel assembly design provides optimum core performance by minimizing neutron absorption in the structural materials and maximizing heat transfer capabilities. Mixing vane grids increase the heat transfer capability of the fuel rods. High fuel utilization is achieved by minimizing the parasitic absorption of neutrons in the core. The only structural materials in the fuel region are the spring clip grids, control rod guide thimbles, and fuel cladding. Zirconium alloys are used because they absorb relatively few neutrons and have good heat transfer properties.

1.2.3.1.4 Rod Cluster Control Assemblies

Rod cluster control (RCC) assemblies are used for reactor startup or shutdown, to follow load changes, and to control small transient changes in reactivity. The control elements of the RCC assembly consists of cylindrical neutron absorber rods (control rods, having approximately the same dimensions as a fuel rod and connected at the top by a spider-like bracket to form rod clusters. The control rods, which are stainless steel tubes encapsulating a neutron absorber material, extend the fuel length of the fuel assembly when fully inserted.

1.2.3.1.5 Burnable Absorber

Aluminum oxide-boron carbide burnable absorber material in placed the fuel assembly to provide additional reactivity control during reactor cycles. This material depletes during the reactor cycle in the same fashion as uranium-235.

1.2.3.1.6 Reactor Startup Neutron Sources

Reactor startup neutron sources must be used because of fuel configuration and the initially low core activity.

Neutron sources are of two types: 1) a primary source, which is active for initial reactor startup and startup early in the life of the first core; and 2) a secondary source, used for later startup of the reactor and which is activated during the operation of the reactor. The primary source normally are a californium isotope. The secondary sources contain a mixture of antimony and beryllium (Sb-Be).

The primary and secondary sources are similar to a control rod in mechanical construction. Both types of source rods are clad in stainless steel. The secondary source rods contain Sb-Be pellets which are not initially active. The primary source rods contain sealed capsules of source material at a specified axial position. Cladding encapsulation is completed by seal-welding the end plugs.

1.2.3.2 Maximum Quantity of Material per Package

The maximum quantity of radioisotopes in the contents of the package is limited to such quantity that is contained in a single fuel assemblies or the maximum number of fuel rods that may be transported in a fuel rod pipe. The fissile material is low enriched uranium less than 5 wt% uranium-235. The maximum quantity of fissile material is contained in approximately 32 kg of uranium-235. The fuel pellets are fabricated from Enriched Commercial Grade uranium as defined in ASTM C 996 (Ref. 1) and summarized in Table 1-1. Individual fuel rods are wrapped in a protective plastic sleeve. When the rod pipe is filled with the correct number of rods, a plastic disc is inserted to protect the ends of the fuel rods. The space between the plastic disc and the rod pipe is filled with “bubble wrap” so that the rods are secured axially. Fuel assemblies are wrapped in a polyethylene sleeve.

Table 1-1. Contents Specification

	Enriched Commercial Grade
U-232	0.0001 µg/gU
U-234	11.0 X 10^3 µg/g^{235}U
U-236	250 µg/gU
Tc-99	0.01 µg/gU
Alpha Activity Np / Pu	< 0.4 Bq/gU
Total Gamma Activity	< 5000 MeV Bq/kg

Enriched commercial grade uranium contents is unirradiated uranium with an A2 value that is unlimited on the basis of the isotopic mixtures given in ASTM C996. Enriched commercial grade uranium is a Type A quantity of radioactive material irrespective of the quantity of radioactive material.

Packaging materials such as a sleeve used to protect the fuel assembly or fuel rods during transport are limited to a maximum total of 2 kg.

1.2.4 Operational Features

Fork lift pockets and tubular legs are attached to the bottom Outerpack. Stacking brackets, which double as lift points, are attached to the top Outerpack and are located in eight (8) locations. The package must be uprighted onto one end for loading and unloading. Two lifting points are attached to the top nozzle end of the top Outerpack.

1.3 GENERAL REQUIREMENTS FOR ALL PACKAGES

1.3.1 Minimum Package Size

The smallest overall dimension of the Traveller packages is outer shell diameter, approximately 25 inches (64 cm). This dimension is greater than the minimum dimension of 4-inches specified in 10 CFR §71.43(a), TS-R-1 (634). Therefore, the requirements of 10 CFR §71.43(a), TS-R-1 (634) are satisfied by the Traveller packages.

1.3.2 Tamper-Indicating Feature

Two (2) tamper indicating seals (wire/lead security seal) are attached between the upper and lower Outerpack halves to provide visual evidence that the closure was not tampered. Thus, the requirements of 10 CFR §71.43(b), TS-R-1 (635) are satisfied.

The Traveller series of packages cannot be opened inadvertently. Positive closure of the Traveller packages is provided by high strength 3/4-inch hex head screws. Thus, the requirements of 10 CFR §71.43(c), TS-R-1(639) are satisfied.

1.4 APPENDICES

1.4.1 References

1. ASTM C 996-04, "Standard Specification for Uranium Hexaflouride Enriched to Less than 5% ^{235}U."

1.4.2 Engineering Drawings for Packaging

10004E58, Rev. 8 (Sheets 1-9)
10006E58, Rev. 5

Security-Related Information
Figure Withheld Under 10 CFR 2.390

SEE PRODUCT SPECIFICATION PDINF000 FOR SUPPLEMENTAL PRODUCT INFORMATION

DIMENSIONS ARE IN INCHES

THIRD ANGLE PROJECTION

Westinghouse

SAFETY RELATED ITEMS TRAVELLER XL & STD

SIZE	DRAWING NO	REV
E	10004E58	8

SCALE 1:1 SHEET 1 OF 9

Security-Related Information
Figure Withheld Under 10 CFR 2.390

SEE PRODUCT SPECIFICATION PDINFO00 FOR SUPPLEMENTAL PRODUCT INFORMATION

DIMENSIONS ARE IN INCHES

THIRD ANGLE PROJECTION

Westinghouse

SAFETY RELATED ITEMS TRAVELLER XL & STD

E | 10004E58 | 8

SHEET 2 OF 9

Security-Related Information
Figure Withheld Under 10 CFR 2.390

SEE PRODUCT SPECIFICATION PDINF000 FOR SUPPLEMENTAL PRODUCT INFORMATION

DIMENSIONS ARE IN INCHES

THIRD ANGLE PROJECTION

Westinghouse

SAFETY RELATED ITEMS TRAVELLER XL & STD

E | 10004E58 | 8

SHEET 3 OF 9

Security-Related Information
Figure Withheld Under 10 CFR 2.390

SEE PRODUCT SPECIFICATION PDINF000 FOR SUPPLEMENTAL PRODUCT INFORMATION

DIMENSIONS ARE IN INCHES

THIRD ANGLE PROJECTION

Westinghouse

SAFETY RELATED ITEMS TRAVELLER XL & STD

SIZE E | 10004E58 | REV 8

SHEET 4 OF 9

Security-Related Information
Figure Withheld Under 10 CFR 2.390

SEE PRODUCT SPECIFICATION PDINF000 FOR SUPPLEMENTAL PRODUCT INFORMATION

DIMENSIONS ARE IN INCHES

THIRD ANGLE PROJECTION

Westinghouse

SAFETY RELATED ITEMS TRAVELLER XL & STD

E | 10004E58 | 8

SHEET 5 OF 9

Security-Related Information
Figure Withheld Under 10 CFR 2.390

SEE PRODUCT SPECIFICATION
PDINF000 FOR SUPPLEMENTAL
PRODUCT INFORMATION

DIMENSIONS ARE IN INCHES

THIRD ANGLE PROJECTION

Westinghouse

SAFETY RELATED
ITEMS TRAVELLER
XL & STD

E | 10004E58 | 8

SHEET 6 OF 9

Security-Related Information
Figure Withheld Under 10 CFR 2.390

SEE PRODUCT SPECIFICATION PDINF000 FOR SUPPLEMENTAL PRODUCT INFORMATION

DIMENSIONS ARE IN INCHES

THIRD ANGLE PROJECTION

Westinghouse

SAFETY RELATED ITEMS TRAVELLER XL & STD

E | 10004E58 | 8

SHEET 7 OF 9

Security-Related Information
Figure Withheld Under 10 CFR 2.390

SEE PRODUCT SPECIFICATION PDINF000 FOR SUPPLEMENTAL PRODUCT INFORMATION

DIMENSIONS ARE IN INCHES

THIRD ANGLE PROJECTION

Westinghouse

SAFETY RELATED ITEMS TRAVELLER XL & STD

E | 10004E58 | 8

SHEET 8 OF 9

Security-Related Information
Figure Withheld Under 10 CFR 2.390

SEE PRODUCT SPECIFICATION PDINF000 FOR SUPPLEMENTAL PRODUCT INFORMATION

DIMENSIONS ARE IN INCHES

THIRD ANGLE PROJECTION

Westinghouse

SAFETY RELATED ITEMS TRAVELLER XL & STD

E | 10004E58 | 8

SHEET 9 OF 9

Security-Related Information
Figure Withheld Under 10 CFR 2.390

SEE PRODUCT SPECIFICATION PDINF000 FOR SUPPLEMENTAL PRODUCT INFORMATION

PRIMARY DIMENSIONS ARE IN INCHES

THIRD ANGLE PROJECTION

ALL TOLERANCES +/- 1/8" UNLESS OTHERWISE NOTED

M. ALES	03/29/04	
B. HEMPY	03/12/04	
S. PALMER	03/22/04	
J. COLE	03/22/04	
W. HERWIG	03/23/04	
G. SUMMER	03/22/04	

Westinghouse ELECTRIC COMPANY LLC - NUCLEAR FUEL COLUMBIA, SC USA

SHIPPING PACKAGE
LOOSE ROD PIPE

SIZE	DRAWING NO.	REV
E	10006E58	5

SCALE: 11 | WEIGHT: SEE DWG | SHEET 1 OF 1

SOLIDWORKS DRAWING DO NOT REVISE MANUALLY

TABLE OF CONTENTS

TABLE OF CONTENTS (cont)

TABLE OF CONTENTS (cont)

LIST OF TABLES

LIST OF TABLES (cont.)

LIST OF FIGURES

LIST OF FIGURES (cont.)

LIST OF FIGURES (cont.)

LIST OF FIGURES (cont.)

LIST OF FIGURES (cont.)

LIST OF FIGURES (cont.)

LIST OF FIGURES (cont.)

2.0 STRUCTURAL EVALUATION

This section presents the structural design criteria, weights, mechanical properties of material, and structural evaluations which demonstrate that the Traveller series of packages meet all applicable structural criteria for transportation as defined in 10 CFR 71[1] and TS-R-1[2].

2.1 DESCRIPTION OF STRUCTURAL DESIGN

The structural evaluation of the standard length Traveller (Traveller STD) and the longer length Traveller (Traveller XL) packages was performed with various tests and computer simulation using finite element analysis. The results of the computer simulations and testing are provided in the following sections. Supporting analyses and analyses of not-tested structural aspects are also provided.

The Traveller shipping package consists of two major fabricated components: 1) an Outerpack assembly, and 2) a Clamshell assembly. The Outerpack consists of a stainless steel outer shell for structural strength, a layer of rigid polyurethane foam for thermal and impact protection, and a stainless steel inner shell for structural strength. Polyethylene blocks are affixed to the inner shell of the Outerpack for criticality safety. See Section 6, Criticality Evaluation, for full criticality safety description. The Clamshell consists of an aluminum container to structurally enclose the contents. Neutron absorber panels are affixed to the inner faces of the Clamshell. Rubber shock mounts separate and isolate the Clamshell from the Outerpack assembly. See Figure 2-1 for an exploded view of the Traveller STD package.

2.1.1 Discussion

The designs of the Traveller STD and Traveller XL unirradiated fuel shipping packages are the same except for length (and therefore weight). Details of the packages, including dimensions, and materials can be found in Section 1, General Information. Both packages consist of an Outerpack, and a Clamshell. Positive closure of the Outerpack is accomplished by means of high strength stainless steel bolts. The number of bolts is the same for the XL and STD designs, thus the loading per bolt is lower for the STD design. There are 48 bolts ¾-inch bolts in the Outerpack, 24 attaching the hinge sections to the lower Outerpack and 24 attaching the upper Outerpack to the hinge sections. To remove the upper Outerpack, the 24 bolts must be removed. In the preferred approach, the Outerpack is opened when it is in a vertical orientation by removing the 12 bolts attaching the upper Outerpack to the hinges on one side. This allows the upper Outerpack to be opened on the other hinge sections, like a door. The design loadings for both packages are below the ultimate design loads for the Outerpack bolts. The worst case forces for the package are presented in Section 2.12.3.2.2, Horizontal Side Drops, and a discussion regarding the design allowable is presented in Section 2.12.3.7, Evaluation, Analysis and Detailed Calculations, and Section 2.12.3.9, Bolt Factor of Safety Calculation. Further evidence of the adequacy of the Outerpack bolts is demonstrated through 9m drop testing whereby only one (1) Outerpack bolt failed in a total of nine (9) 9m drop tests. The single bolt that failed did so as a

1. Title 10, Code of Federal Regulations, Part 71 (10 CFR 71), Packaging and Transportation of Radioactive Material, January 1, 2004 Edition

2. TS-R-1 1996 Edition (Revised), Regulations for the Safe Transport of Radioactive Material.

result of direct impact with the drop pad. The Clamshell is closed using ¼-turn nuts which lock latches on the doors of the assembly.

The Outerpack bolts and the Clamshell closure mechanisms have been subjected to the drop conditions of 10 CFR 71 and TS-R-1 without failure. Therefore, these designs are more than adequate to withstand the loads experienced during normal conditions of transport.

This page intentionally left blank.

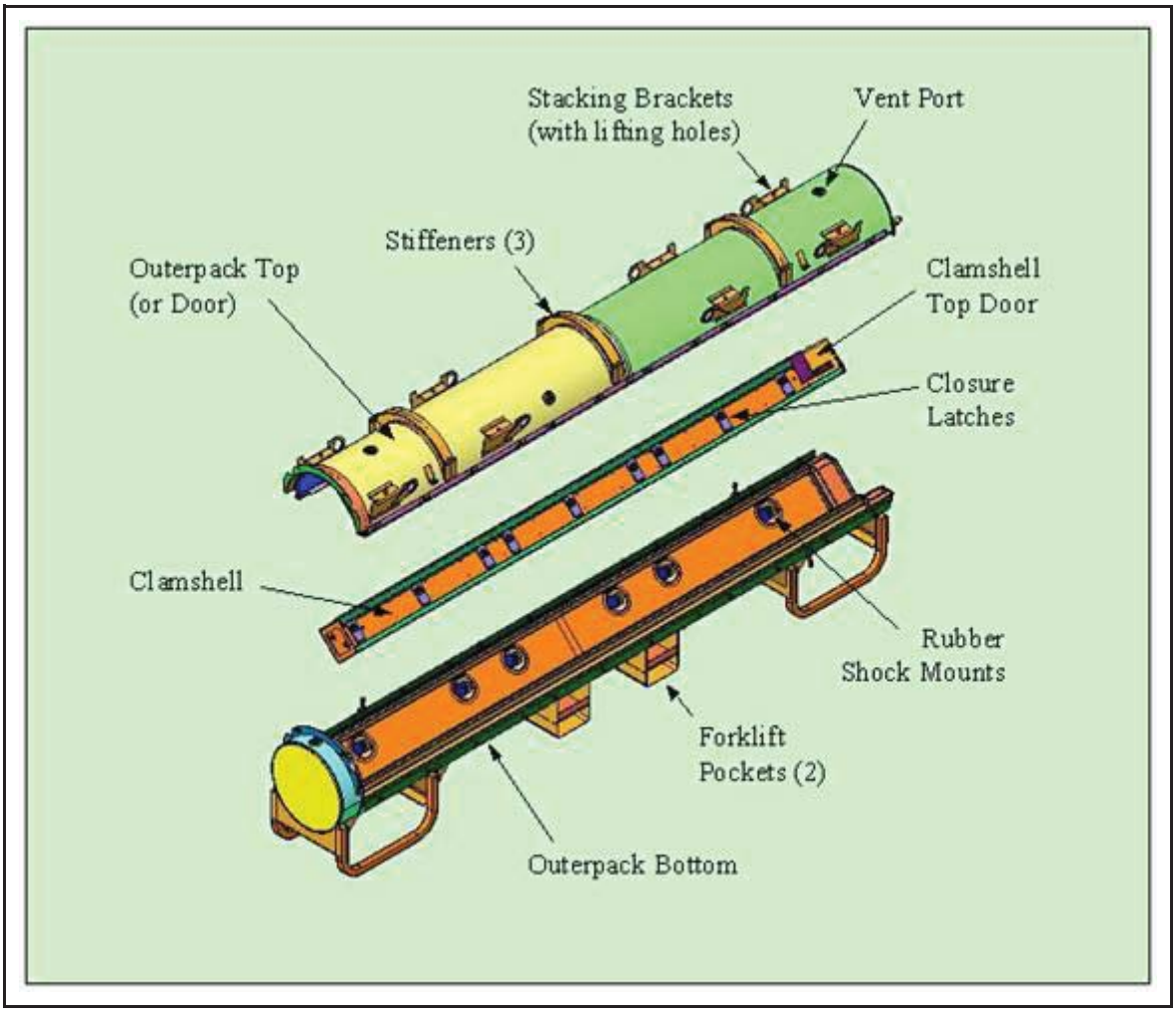

Figure 2-1 Traveller STD Exploded View

Closure of the Outerpack is provided by (12) ¾-10UNC hex head bolts, which allows the top half of the Outerpack assembly to swing open on a series of hinges. The Outerpack top half or "door" may be opened in either direction, depending on which bolts are removed. Optionally, the top Outerpack assembly may also be completely removed by removal of (24) ¾-10UNC hex head bolts. Closure of the Traveller STD and Traveller XL Clamshells are provided by latch assemblies that are secured with nine (9) ¼-turn nuts, and eleven (11) ¼- turn nuts, respectively.

The Traveller packages are not pressure sealed from the ambient environment, therefore, no differential pressures can occur within the package.

Handling of the packages is performed using the forklift pockets on the lower Outerpack. Handling may also utilize the lifting holes in the stacking brackets on the upper Outerpack.

Standard fabrication methods are utilized to fabricate the Traveller series of packages. Visual weld examinations are performed on all welds of the Traveller packages in accordance with AWS D1.6. and ASME Section III, Subsection NF-5360, for stainless steel and aluminum respectively.

2.1.2 Design Criteria

2.1.2.1 Basic Design Criteria

Evidence of performance for the Traveller XL package is achieved by (1) empirical evaluations using full-scale packages and (2) large-strain capable Finite Element Analysis (FEA). The Traveller XL is bounding due to its increased weight and length when compared to Traveller STD. The criteria that was used for impact evaluation is a demonstration that the containment and confinement systems maintain integrity throughout Normal Conditions of Transport (NCT) and Hypothetical Accident Condition (HAC) certification testing. That is, it is necessary to demonstrate that there is no release of material, no loss of moderator or neutron absorber, no decrease in Outerpack geometry, and no increase in Clamshell geometry. The as-found condition of the package (packaging and contents) is the baseline configuration for the criticality safety evaluation that can be found in Chapter 6, Criticality Evaluation.

A detailed discussion related to Traveller XL design criteria, can be found in Appendix 2.12.3, Mechanical Design Calculations for the Traveller XL Shipping Package.

2.1.2.2 Miscellaneous Structural Failure Modes

2.1.2.2.1 Brittle Fracture

The primary structural materials of the Traveller packages are austenitic stainless steel (ASTM A240 Type 304 SS) and 6000 Series aluminum (extruded components 6005-T5, all else 6061-T6). These materials do not undergo a ductile-to-brittle transition in the temperature range of interest [i.e., down to -40°F (-40°C)], and thus do not require evaluation for brittle fracture.

2.1.2.2.2 Fatigue

Because the shells of the Outerpack are constructed of ductile stainless steel and they are formed into a very stiff body with low resulting stresses, no structural failures of the Outerpack due to fatigue will occur. Because the Clamshell is structurally isolated from the Outerpack through the rubber shock mounts, no Clamshell fatigue will occur. The Clamshell is, for practical purposes, decoupled from the Outerpack through the rubber shock mounts. These rubber shock mounts also provide excellent damping to the Clamshell.

2.1.2.2.3 Buckling

For normal condition and hypothetical accident conditions, the Clamshell which structurally encloses the fuel, will not buckle due to free or puncture drops. This behavior has been demonstrated via full-scale testing of the bounding Traveller XL package.

2.1.3 Weights and Centers of Gravity

The Traveller XL weight bounds the Traveller STD weight as shown in Table 2-1. The calculated weight breakdown for the major individual subassemblies, including the shipping components for both packages, is listed below. For licensing purposes, the maximum bounding Traveller XL design weight is assumed to be 5,230 lb (2,372 kg).

Table 2-1 Summary of Traveller STD and Traveller XL Design Weights

	Traveller STD	Traveller XL
Max. Fuel Assembly Weight, lb (kg)	1650 (748)	1971 (894)
Max. Tare Weight, lb (kg)	2850 (1293)	3255 (1476)
Design and Licensing Basis Gross Weight, lb (kg)	4500 (2041)	5230 (2372)

The center of gravity of both Traveller packages is approximately at the geometric center of the Outerpack, i.e., approximately 23 inches above ground level, at the axial mid-station for both packages. Appendix 2.12.2, Container Weights and Centers of Gravity, shows the overall dimensions, locations of the centers of gravity for both packages, and detailed major component weights.

2.1.4 Identification of Codes and Standards for Package Design

The Traveller packages are evaluated with respect to the general standards for all packaging specified in 10 CFR §71.43, and TS-R-1 (paragraphs 606 – 649, as applicable). The fabrication, assembly, testing, maintenance, and operation will be accomplished with the use of generally accepted codes and standards such as ASME, ASTM, AWS. Special processes will be documented with procedures that will be evaluated and approved.

2.2 MATERIALS

2.2.1 Material Properties and Specifications

Mechanical properties for the materials used for the structural components of the Traveller packages are provided in this section. Temperature-dependent material properties for structural components are primarily obtained from Section II, Part D, of the ASME Boiler and Pressure Vessel (B&PV) Code. The analytic evaluation of the Traveller packages is via computer simulation (ANSYS/LS-DYNA®), only the material properties specific to the analysis portion and computer simulation portion of the evaluation are given. Table 2-2 lists the materials used in the Traveller packages and summarized key properties and specifications. More detailed material properties can be found in Appendix 2.12.3, Mechanical Design Calculations for the Traveller XL Shipping Package, and Appendix 2.12.4, Drop Analysis for the Traveller XL Shipping Package.

All materials used in the fabrication of the Certification Test Unit (CTU) meet 10 CFR 71 and TS-R-1 requirements. However, simulated neutron absorber plates were affixed to the inner faces of the Clamshell. These were fabricated from 1100-T0 aluminum ("dead soft" aluminum). These component plates did not contain boron, and were used to simulate the mechanical and thermal properties of the neutron absorber plates. The 1100-T0 aluminum was used due to its low mechanical properties. In production units, the actual neutron absorber plates will have insignificant differences in the material properties compared to the material used in the prototypes and CTU package.

2.2.2 Chemical, Galvanic, or Other Reactions

The Traveller series of packages are fabricated from ASTM A240 Type 304 stainless steel, 6000-series aluminum, borated 1100-series aluminum, polyurethane foam, and polyethylene sheeting. The stainless steel Outerpack does not have significant chemical or galvanic reactions with the interfacing components, air, or water.

The aluminum Clamshell is physically isolated, and environmentally protected, by the Outerpack and therefore will have negligible chemical or galvanic reactions with the interfacing components, air, or water. In addition, the Type 304 stainless steel fasteners which attach various Clamshell components represent a very small area ratio (cathode-to-anode ratio), which will render the reaction insignificant. Therefore, the requirements of 10 CFR §71.43(d), TS-R-1 (613) are met.

The Outerpack hinge bolts are zinc plated for the purpose of improving galling resistance which can be a significant problem when stainless steel fasteners are inserted in stainless steel threaded holes. The plating is not required for chemical or galvanic protection.

2.2.3 Effects of Radiation on Materials

There are no materials used in the Traveller packages which will be adversely affected by radiation under normal handling and transport conditions.

Table 2-2 Safety-Related Materials Used in the Traveller Packages

Material	Critical Properties	Reference Specifications/Codes	Comments
304 Stainless Steel	UTS: 75 ksi (517 MPa) YLD: 30 ksi (206 MPa) τ_{allow}: 18 ksi (124 MPa) E: 29.4 E6 psi (203 GPa)	ASTM A240 ASTM A276	Fully annealed material and not subject to brittle fracture.
6005-T5 Aluminum	UTS: 38 ksi (262 MPa) YLD: 35 ksi (241 MPa) τ_{allow}: 21 ksi (145 MPa) E: 10 E6 psi (69 GPa)	ASTM B221 ASTM B209	Reference standard UNS A96005
6061-T6 Aluminum	UTS: 38 ksi (262 MPa) YLD: 35 ksi (241 MPa) tallow: 21 ksi (145 MPa) E: 10 E6 psi (69 GPa)	ASTM B221 ASTM B209	Reference standard UNS A96061
Polyurethane Closed Cell Foam	Densities: 6 ± 1 pcf (0.096 ± 0.016 gm/cm^3), 10 ± 1 pcf (0.16 ± 0.016 gm/cm^3), 20 ± 2 pcf (0.32 ± 0.016 gm/cm^3) Crush Strengths: See Appendix 2.12.3	Westinghouse Specification PDSHIP02 ASTM D1621-94 ASTM D1622-93 ASTM D2842	Burn Characteristics verified by ASTM F-501, with exceptions noted in PDSHIP02.
UHMW Polyethylene	Specific Gravity: > 0.93 Molecular Wt: >3 million	ASTM D4020	N/A
Borated Aluminum Laminate Composite	Minimum areal densities: Borated Al Composite: 0.024 g/cm^2	Westinghouse Specification PDSHIP04 ASTM E748	The minimum areal densities are defined for the finished plate or laminate final thickness of 0.125" ± 0.006" (3.175 mm ± 0.153 mm). No structural credit is taken for the neutron poison plates.
Ceramic Insulation (Paper and Felt)	Max. use temp: >1800°F (982°C) Conductivity: ≤ 1.2 Btu-in/hr-ft^2 @ 500°F, (0.173 W/m-K @ 260°C)	N/A	The paper thickness is 0.0625" (1.59 mm), and the blanket thickness is 0.25" (6.35 mm)

2.3 FABRICATION AND EXAMINATION

2.3.1 Fabrication

The Traveller packages (XL and STD) are manufactured using standard fabrication techniques. No exotic materials or processes are required. Safety related items which are needed for criticality safety purposes have specific manufacturing specifications which clearly delineate all necessary codes, standards, and specifications required to meet design intent. All fabrication specifications are listed on the engineering drawings.

The fabrication processes of the Traveller include basic processes such as cutting, rolling, bending, machining, welding, and bolting. All welding is performed in accordance with ASME Section IX.

The manufacturing flow of the Traveller units includes fixturing of the inner and outer shells of the upper and lower Outerpack assemblies. Individual closure components are then aligned and welded in place. Sub-assemblies such as the forklift pockets, leg structures and stacking brackets are assembled in a parallel manner and appended to the main assemblies at appropriate times. Upon welding closure of the assemblies, the upper and lower Outerpack assemblies are secured together and poured with polyurethane foam material. Pouring of this material is tightly controlled through the foam manufacturing specification.

When the Traveller is filled with foam, it is ready for final assembly and installation of the Clamshell which has followed a parallel fabrication process. One difference for the Clamshell is that the faces are manufactured extrusions as opposed to “off-the-shelf” material. The extrusions are fabricated to industry standard specifications. Upon integration of the Clamshell to the Outerpack, final assembly and light grit blasting conclude the manufacturing process.

2.3.2 Examination

Manufacture of the Traveller XL and Traveller STD packages shall be performed in accordance with strict Quality Assurance (QA) requirements. Included in the manufacture of the packages are examinations to verify that each package is being built to the required specifications. These examinations include the following:

1. Receipt inspections whereby the received components are visually inspected for workmanship, overall part quality, dimensional compliance, and material certification compliance.

2. All welds (which shall be performed by qualified welders/processes) shall be visually examined by a qualified inspector in accordance with AWS D1.6 and ASME Section III, Subsection NF-5360, for stainless steel and aluminum respectively.

3. Examinations which evaluate form, fit, and function shall be performed on each package to verify its operability and assess its overall quality.

2.4 LIFTING AND TIE-DOWN STANDARDS FOR ALL PACKAGES

2.4.1 Lifting Devices

The lifting criteria is governed by 10 CFR §71.45(a) and TS-R-1 (607). 10 CFR §71.45(a) states that any lifting attachment that is a structural part of the package must be designed with a minimum safety factor of three against yielding when used to lift the package in its intended manner. In addition, it must be designed so that failure of any lifting device under excessive load would not impair the ability of the package to meet other requirements of 10 CFR 71. The following calculations are based on the features of the Traveller XL package which bounds the Traveller STD for these requirements. Lifting and tie-down are described in detail in Appendix 2.12.3, Mechanical Design Calculations for the Traveller XL Shipping Package.

2.5 GENERAL CONSIDERATIONS

The Traveller package structural evaluation consists of a combination of mechanical design calculations, finite element analysis, and testing. Table 2-3 shows the regulatory requirements and the means by which satisfactory compliance was demonstrated.

Table 2-3 Summary of Regulatory Requirements

Requirement Description	US NRC	TS-R-1	Applicable Condition	Means Demonstrated
Lifting attachments	10 CFR 71.45(a)	TS-R-1, § 607	General Package Standard	Mech. Design Calc.
Tie-Down devices	10 CFR 71.45(b)(1,2)	TS-R-1, § 636	General Package Standard	Mech. Design Calc.
Design temperatures between –40°F (-40°C) and 158°F (70°C)	10 CFR 71.71(c)(1,2)	TS-R-1, § 637 and 676	General Package Standard	Mech. Design Calc.
Internal/External Pressure	10 CFR 71.71(c)(3,4)	TS-R-1, § 615	Normal transport condition	Mech. Design Calc.
Vibration	10 CFR 71.71(c)(5)	TS-R-1, § 612	Normal transport condition	Mech. Design Calc.
Water spray	10 CFR 71.71(c)(6)	TS-R-1, § 721	Normal transport condition	Mech. Design Calc.
Compression/Stacking test	10 CFR 71.71(c)(9)	TS-R-1, § 723	Normal transport condition	Mech. Design Calc.
Penetration	10 CFR 71.71(c)(10)	TS-R-1, § 724	Normal transport condition	Mech. Design Calc.
Immersion	10 CFR 71.73(c)(6)	TS-R-1, § 729	Accident transport condition	Mech. Design Calc.

2.5.1 Evaluation by Test

The development of the Traveller packages included mechanical scoping tests to quantify the critical characteristics of the components or subsystems of the design. These scoping tests included:

1. Outerpack Hinge Strength-to-Failure Testing
2. Hinge Alignments Tests
3. Foam Pouring Tests
4. Foam Burn Tests (pail type)
5. Clamshell Hinge Strength-to-Failure Testing
6. Clamshell Weld Tests

7. Clamshell impact tests
8. Impact limiter testing including "pillow" impact testing

The scoping tests provided designers with performance data. However, proof of performance in the Traveller package was obtained through full-scale testing. As such, these tests were not required to be performed in accordance with full QA standard. However, all full-scale Traveller XL packages were fabricated and tested under all QA requirements.

The development of the Traveller consisted of essentially three (3) full-scale test campaigns. These campaigns consisted of what are called the Prototype units (2), the Qualification Test Units (QTU) (2), and finally the Certification Test Units (CTU) (1). In general, these packages are very similar. The overall configuration of the Outerpack and Clamshell remain essentially identical throughout the design evolution. With each test campaign, the design was modified to increase structural or thermal margin, or to reduce excess design margin when appropriate. The significant design changes from Prototype to CTU were:

1. The reduction in Outerpack shell thicknesses from 11 gage (0.120", 0.30 cm) to 12 gage (0.105", 0.27 cm),

2. The adjusting of polyurethane foam densities (first a lowering of density for structural reasons, then an increase for improve thermal performance),

3. The addition of a thin stainless steel covering of the moderator blocks,

4. The replacement of short individual Outerpack hinges with a continuous Outerpack hinge,

5. A redesign of the Clamshell head attachment configuration, and finally,

6. A reduction in the number and size of the Outerpack hinge bolts.

The purpose of the computer simulation was to assist in evaluating these minor changes and predict performance of the modified packages. The computer simulation was also used to show the impact of initial test conditions (temperature of package) and manufacturing variability (foam density tolerances, skin thickness variations, etc.). These factors showed negligible effects on the overall performance of the packages. Details can be found in Appendix 2.12.4, Drop Analysis for the Traveller XL Shipping Package.

A summary of the development and testing of the Traveller XL full-scale test packages is described in Table 2-5, and the detailed results of each test are described in Appendix 2.12.5, Traveller Drop Test Results.

2.5.2 Evaluation by Analysis

Analysis consisted of mechanical design calculations and finite element analysis. Mechanical design calculations are described in detail in Appendix 2.12.3. Finite element analysis, utilizing LS-DYNA software, is described in detail in Appendix 2.12.4.

Table 2-4 gives a summary of the regulatory requirements that are demonstrated through mechanical design calculations.

Table 2-4 Summary of Traveller Mechanical Analysis

Requirement Description	Allowable Design Value(s) or Acceptance Criteria	Calculated Value
Lifting attachments	Tensile Yield Stress, σ_y < 30 ksi Shear Yield Stress, τ_y < 18 ksi Weld shear Yield Stress, τ_y < 12 ksi Hoist Screw Shear Stress, τ < 72 ksi Coupling Nut Shear Stress, τ < 18 ksi Hoist Ring Tensile Stress, τ < 130 ksi	**Hole tear-out (4-pt. lifting)** XL: τ = 5,230 psi < 18 ksi STD: τ = 6,364 psi < 18 ksi **Weld shear (4-pt. lifting)** XL: τ = 7,565 psi < 12 ksi STD: τ = 9,205 psi < 12 ksi **Forklift** XL Bending: σ = 17,528 psi < 30 ksi STD Bending: σ = 26,260 psi < 30 ksi XL Weld shear: τ = 3,533 psi < 12 ksi STD Weld shear: τ = 6,080 psi < 12 ksi **Hoist Ring Assembly** Bolt shear: τ = 50,619 psi < 72 ksi Coupling Nut Shear Stress: τ = 17,671 psi< 18 ksi Hoist ring tensile: σ = 35,659 psi < 130 ksi
Tie-Down	Tensile Yield Stress, σ_y < 30 ksi	No tie down systems on package
Temperatures Effects	No brittle fracture No impact from Differential Thermal Expansion (DTE)	No brittle fracture No DTE Impact
Internal/External Pressure	Compressive Yield Stress, σ_y < 30 ksi	No stress developed
Vibration	No impact on structural performance $f_{natOP} > f_{nat\ TRANS}$	No impact, 23 Hz > 3.7-8 Hz
Water spray	No impact on structural performance	No impact
Compression/Stacking	Weld shear Yield Stress, τ_y < 12 ksi Compressive Yield Stress, σ_y < 30 ksi Elastic Stability (Critical Buckling), F < Pcr	**Stacking Bracket:** Weld shear: τ = 4,729 psi < 12 ksi Bending: σ = 1,827 psi < < 30 ksi **Outerpack Buckling:** Buckling: 26,150 lb < 78,583 lb **Leg Support Buckling:** Buckling: 3,269 lb < 71,978 lb
Penetration	No perforation of outer skin	Bounded by 1.0m HAC pin-puncture; No perforation of outer skin.
Immersion	Compressive Yield Stress, σ_y < 30 ksi	No stress developed

2.6 NORMAL CONDITIONS OF TRANSPORT

2.6.1 Heat

The thermal evaluation for the heat test is described and reported in Section 3, Thermal Evaluation.

2.6.1.1 Summary of Pressures and Temperatures

There is no pressure seal in the Traveller series of packages. Therefore, there is no pressure build up within the package. Maximum temperature for the following sections were evaluated to 158°F (70°C) and minimum temperatures to -40°F (-40°C).

2.6.1.2 Differential Thermal Expansion

The effects differential thermal expansion for the Traveller series of packages is negligible due to the design of the package. The most significant differential is between the aluminum Clamshell and the fuel assembly, and is less than 0.25 inches. The differential thermal expansion is accommodated by rubber-cork spacers between the Clamshell and fuel assembly.

Ultra-high Molecular Weight (UHMW) polyethylene does have a significantly higher coefficient of thermal expansion (CTE) when compared to Type 304 stainless steel. For this reason, the moderator panels are segmented along their lengths to accommodate the differential thermal expansion between the polyethylene and the inner stainless steel shells of the Outerpack. Additionally, oversized holes in the polyethylene panel are used to accommodate the effects of both temperature extremes.

See Appendix 2.12.3, Mechanical Design Calculations for the Traveller XL Shipping Package, for detailed differential thermal expansion calculations.

2.6.1.3 Stress Calculations

The Traveller packages are fabricated from relatively thin sheet metal parts which are not subject to thermal gradients generated from the interior of the package. The packages are also not sealed to the environment, therefore pressure stress is negated. The most significant stress potential occurs from the differential expansion rates of the bolted polyethylene moderator panels to the inner steel shells of the Outerpack. This potential stress is also negated by design, whereby the panels are made in sections and the bolt clearances and gaps between panels are adequately sized to allow unrestrained growth and contraction.

Successful testing of full scale Traveller XL packages indicates that the stresses associated with differential thermal expansion of the various packaging components are negligible.

2.6.1.4 Comparison with Allowable Stresses

As discussed in Section 2.6.1.3, Stress Calculations, further evaluation of stresses associated with differential thermal expansion for the various Traveller package components is not required.

2.6.2 Cold

The materials used in construction of the Traveller packages are not degraded by cold at -40°C (-40°F). Stainless steel and aluminum exhibit no brittle fracture at these temperatures. Therefore, the requirements of 10 CFR §71.71(c)(2) and TS-R-1 (618) are satisfied.

2.6.3 Reduced External Pressure

Since the Traveller series of packages are not sealed against pressure, there can not be any significant differential pressure. *See Appendix 2.12.3.2.4.1 for additional explanation.*

2.6.4 Increased External Pressure

Since the Traveller series of packages are not sealed against pressure, there can not be any significant differential pressure. *See Appendix 2.12.3.2.4.1 for additional explanation.*

2.6.5 Vibration

The package must be evaluated to consider the effects of normal vibration on the design performance. The isolation system is designed to dampen normally induced vibrations from transport, and is not fundamental to the safe operation of the package. However, the Outerpack must maintain its structural integrity during transport to maintain a safe transport condition as specified in 10 CFR §71.71(5), TS-R-1 (612). Typical attachment to a transport conveyance for the Traveller packages includes nylon straps or chain mounted both over the package and on the gusset tray connected to the support legs pointed inboard. The loading configuration can be modeled as a simply supported beam. Furthermore, the Outerpack is conservatively modeled considering only the outer shell at the first mode of vibration. The typical natural frequency range for transportation vehicles, $f_{nat\ TRANS}$, is 3.7-8 Hz. The natural frequency of the Outerpack can be determined from: l

$$f_{natOP} = a\sqrt{(EIg/l^3)/m}$$

where a=1.57 (primary mode coefficient assuming hinge-hinge end conditions for additional conservatism), E = 29.4E6 psi, I = 634 in^4, m = 2834 pounds, g = 386.4 in/s^2 and l = 226.2 in. Substituting values:

$$f_{natOP} = 1.57\sqrt{[(29.4E6)(634)(386.4)/(226.2)^3]/2834} \text{ 1/s (Hz)}$$

$$f_{natOP} = 1.57\sqrt{220} \text{ Hz}$$

$$f_{natOP} = 23 \text{ Hz}$$

Since the natural frequency of the Outerpack is greater than the natural frequency typical of a transportation vehicle, resonance of the Outerpack is not expected and normally induced vibrations will not preclude the package from performing its design function.

The rubber shock mounts effectively isolate and dampen loads and vibrations to the Clamshell and its contents. No resonant vibration conditions which could fatigue the Clamshell shall occur during normal conditions of transport.

There are several natural frequencies of the shock mount system depending on direction of movement. The dominant frequency is for vertical movement. This frequency is between 5.9 and 6.7 Hz (for Traveller XL) depending on the weight of the fuel assembly being transported. The fore and aft pitch frequency is slightly higher (6.9-7.9 Hz) but has a lower amplitude. Road tests have been performed with the suspension system to measure amplitudes during shipping. Figure 2-1A is characteristic of the results seen. When the truck travels over a bump, the clamshell initially sees relatively large accelerations (2-3 g's) but this oscillation quickly damps out to accelerations less than 1 g. This 300 mi trip involved approximately five and a half hours on the road with 1.4×10^5 total cycles.

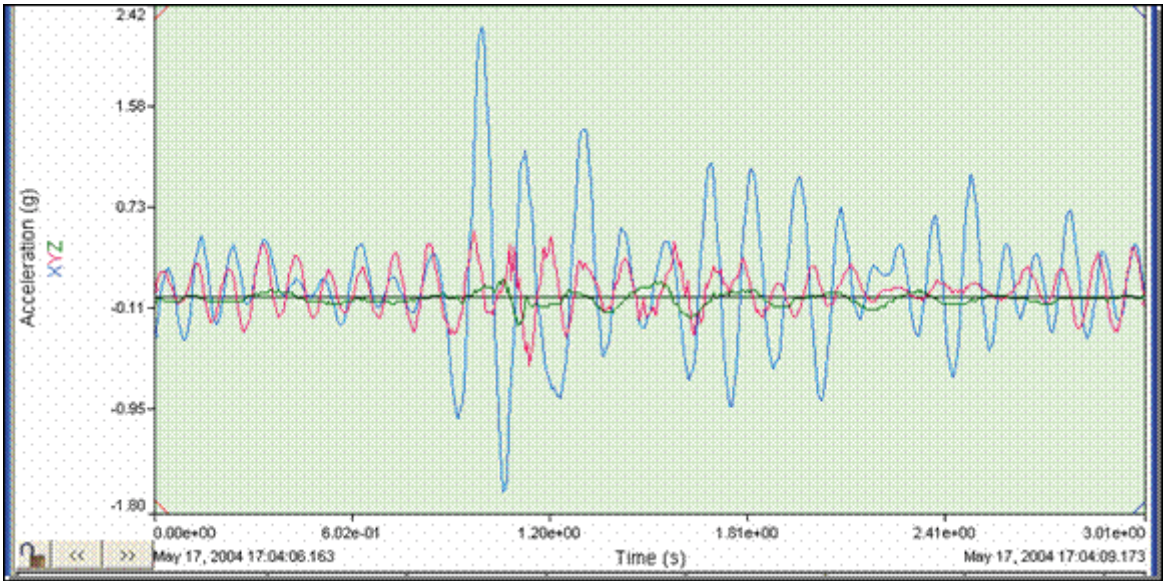

Figure 2-1A Sample of Clamshell Accelerations Measured During Road Test (May 11, 2004)

2.6.6 Water Spray

The materials of construction utilized for the Traveller packages are such that the water spray test identified in 10 CFR §71.71(c)(6), TS-R-1 (721), will have negligible effect on the package. Further, the Traveller Outerpack is cylindrical, and is specifically shaped to negate water collection. Since the Outerpack shell is fabricated from ASTM A240 Type 304 SS, the water spray will not impact the structural integrity of the package.

2.6.7 Free Drop

Since the gross weight of the bounding Traveller XL package is approximately 5,000 kg (11,000 lb), a 1.2 m (4 feet) free drop is conservatively required per 10 CFR §71.71(c)(7), TS-R-1 (722). As discussed in Appendix 2.12.5, Traveller Drop Test Results, 1.2 m drops were performed on the Traveller CTU as an initial condition for subsequent Hypothetical Accident Condition (HAC) tests.

The Traveller packages are well protected during drop testing. In particular, the leg structure including fork lift structure, stacking structure, and upper Outerpack stiffener I-beam structure, all protect the Traveller during impact. Traveller CTU free drop testing and engineering evaluations indicated that this testing have negligible impact on the integrity of the package. However, the orientation selected for the free drop testing was a low angle slap-down, approximately 10 degrees, with the package inverted. The basis for selection of this orientation was that this orientation offered the greatest opportunity to stress the welded joints at the ends of the package. Detailed descriptions of the test results are given in Appendix 2.12.5, Traveller Drop Test Results. Examinations following the prototypic and CTU testing proved the ability of the Traveller packaging to maintain its structural and criticality control integrity. Therefore, the requirements of 10 CFR §71.71(c)(7) are satisfied.

This page intentionally left blank.

2.6.8 Corner Drop

The corner drop test does not apply, since the gross weight of the package exceeds 100 pounds (50 kg), as specified in 10 CFR §71.71(c)(8) or 100 kg (221 lb) as specified in TS-R-1 (722).

2.6.9 Compression – Stacking Test

The compressive load requirement of 10 CFR §71.71(c)(9), TS-R-1 (723) is satisfied by the Traveller packages. Details of the analysis can be found in Appendix 2.12.3, Mechanical Design Calculations for the Traveller XL Shipping Package.

2.6.10 Penetration

The 1 m (40 inch) drop of a 1 ¼-inch (3.2 cm) diameter, 6 kg (13 pound), hemispherical end steel rod, as specified in 10 CFR §71.71(c)(10), TS-R-1 (724), is of negligible consequence to the Traveller series of packages. This conclusion is due to the fact that the Traveller packages are designed to minimize the consequences associated with the much more limiting case of a 1 m (40 inch) drop of the entire package onto a puncture rod, as discussed I Section 2.7.3, Puncture. The 12-gauge (2.7 mm) minimum thickness of the outer shell of the Outerpack is not damaged by the penetration event. Therefore, the requirements of 10 CFR §71.71(c)(10), TS-R-1 (724), are satisfied.

2.7 HYPOTHETICAL ACCIDENT CONDITIONS

When subjected to the hypothetical accident conditions as specified in 10 CFR §71.73, the Traveller package meets the performance requirements specified in Subpart E of 10 CFR 71, and TS-R-1 (726-737 as applicable). This conclusion is demonstrated in the following subsections, where the most severe accident condition is addressed and the package is shown to meet the applicable design criteria. The method of demonstration is through both computer analysis and by testing. The loads specified in 10 CFR §71.73 are applied sequentially, per Regulatory Guides 7.8 and 7.9 (draft).

The Traveller XL Certification Test Unit (CTU) test results are summarized in Section 2.7.7, Summary of Damage, with details provided in Appendix 2.12.5, Traveller Drop Test Results. Additional full-scale test results conducted prior to the certification tests are also included in Appendix 2.12.5. These tests describe the improvements to the Traveller XL design, substantiate the basis for the most severe hypothetical accident condition, and were used to validate the computer simulations.

The following table summarizes the development of the Traveller XL shipping package from the first prototype through the Certification Test Unit, or CTU. As can be seen, satisfying the thermal test requirements proved more difficult than expected. However, the culmination of the development effort has yielded a shipping package that has been thoroughly tested and meets the requirements of both 10 CFR 71 and TS-R-1.

Table 2-5 Summary of the Development of the Traveller

Traveller XL	Test Sequence(s)	Structural Performance	Fire/Thermal Performance
Prototype-1 Drop testing: Jan 27-28, 2003 Burn Testing: Feb 28, 2003	Objective: FEA validation - 9 m low angle slap down (14.5 degrees) - 9 m high angle (71 degrees) - 1 m pin puncture (through CG, low angle) - 35 minute pool fire burn test.	- Outerpack – Satisfied requirements. Minor, local damage only. - Clamshell – Satisfied requirements for 9 m low angle test. Failed requirements for 9 m high angle test. Satisfied 1 m pin puncture test.	Outerpack failed to prevent ignition of polyethylene sheets in one location. Clamshell temperature away from interior combustion satisfied fire requirements.
Comments: The Traveller XL Prototype-1 demonstrated robust structural performance, except for the Clamshell head(s) attachment which was not adequate. The most probable root cause of ignition of polyethylene sheeting was polyurethane foam combustion products entering the inside of the Outerpack as a result of holes drilled into inner Outerpack shell for thermocouples. No seals were used in the Outerpack for conservatism. Fire testing failed to prevent ignition of the combustible materials in the Outerpack. However, the components not adjacent to the internal fire remained well within thermal limitations, thus, demonstrating that the Outerpack had sufficient thermal resistance to external heat flow into package. **Design Changes as a Result of Testing:** Additional bolts were added to secure the top Clamshell head for Prototype-2 testing (see below). The package was subjected to the applicable tests for Normal and Hypothetical Accident conditions as described below. Following this series, the package was modified again to assess the robustness of the design. The center Outerpack hinge bolts were removed (1 of 3 bolts) from each hinge section. The number of locking pins on the Clamshell latches was also reduced, from 18 to 12.			
Prototype-2 Drop Testing: Jan 30, 2003 Burn Testing: N/A	- 1.2 m low angle slapdown (20 degrees) - 1 m pin puncture (through CG, low angle) - 9 m high angle (72 degrees) **Bolts and locking pins removed (described above)** - 9 m end drop (bottom end down) - 9 m horizontal (feet down) - 9 m horizontal (side down)	- Outerpack – Satisfied requirements for all 9 m drops and pin puncture tests. Minor, local damage only. - Clamshell – Satisfied requirements for first 9 m drop. Bottom head separated in second 9 m drop (bottom end drop) because the fuel assembly was not properly seated against bottom Clamshell head as a result of prior drop. No other significant damage.	- Prototype 2 was not subjected to HAC fire testing.

Table 2-5 (cont.) Summary of the Development of the Traveller

Traveller XL	Test Sequence(s)	Structural Performance	Fire/Thermal Performance

Comments:

The performance of the Prototypes (1 & 2) associated with the first testing campaign clearly demonstrated the robustness of the Overpack and Clamshell (except for the Clamshell head attachments). In all, six (6) drops were performed on 2 full-scale prototypes from 9 m. The Outerpack retained its overall integrity and functionality. Most importantly, all design features important to criticality safety performed as intended. Moderator blocks and simulated neutron absorber plates remained intact and attached to their respective structural components.

Design Changes as a Result of Testing:

Based on the robust structural performance of the Prototype units, several design changes were made to the Traveller XL for subsequent testing in the second test campaign. The Traveller units fabricated for the second campaign were called the Qualification Test Units, or QTUs. A total of two units were fabricated and tested. The significant changes to the QTUs were as follows:

1. The Outerpack stainless steel shells were reduced from 11 gauge (0.1196 in., 3.04 mm) to 12 gauge (0.1046 in., 2.66 mm). This change was made primarily to lower weight and reduce excessive structural margin.
2. The hinge bolts were reduced in both number and size, from ten 7/8" (2.22 cm) diameter bolts to ten ¾" (1.91 cm) bolts. This change was made to reduce excessive design margin.
3. A total of 2 seal materials were added to the design to act as: 1) an environmental seal, and 2) to minimize hot gases from entering the Outerpack seams.
4. The Outerpack leg structure, circumferential stiffeners, stacking brackets, and forklift pocket structures were changed. These changes were made for simplified manufacturing purposes and to reduce excessive design margin.
5. The polyurethane foam density of the center section of the package was reduced from 11 pcf to 10 pcf. The axial limiter foam sections of the package were also reduced from 16 pcf to 14 pcf. This change was made to lower the impact deceleration, and therefore loads experienced by the Clamshell.
6. The Clamshell extrusions were made thicker, from a nominal 0.375" (0.95 cm) to 0.438" (1.11 cm). This change was made primarily to eliminate welding of the heads to the extrusions. Bolted connections were utilized to attach the heads.
7. The welded simulated poison plates were redesigned for a bolted connection. This change was made to reduce the distortion of the aluminum Clamshell extrusions due to welding.
8. The Clamshell door locking latches were redesigned for quarter-turn nuts. This change was made for manufacturing and aesthetic purposes.
9. The Clamshell axial restraint system for restraint of the fuel assembly was redesigned. This change was made to simplify the fuel handling.

Table 2-5 Summary of the Development of the Traveller (cont.)

Traveller XL	Test Sequence(s)	Structural Performance	Fire/Thermal Performance
QTU-1 Drop Testing: Sep 11, 2003 Burn Testing: Sep 15, 2003	- 1.2 m low angle slapdown (10 degree) - 9 m high angle (72 degrees) - 1 m pin-puncture (83 degrees at bottom end) - 37 minute pool-fire burn test.	- Outerpack – Satisfied requirements for both drops and pin puncture tests. Minor, local damage only. - Clamshell – Satisfied requirements for both drops and pin puncture tests.	Failed to prevent ignition of the polyethylene sheeting inside the Outerpack. Temperatures inside the Outerpack exceeded design limits. The package was extinguished approximately 1 hour after the conclusion of the pool fire testing.
Comments: The Traveller XL QTU-1 demonstrated robust structural performance. No Outerpack bolts failed. The Outerpack did not separate, and the pin puncture did not perforate the inner or outer shells nor did it effect the Clamshell in any detrimental way. One hour after the pool fire, the package burning was extinguished. Upon inspection of the QTU-1 unit, it was determined that excessive distortion of the Outerpack shells between the hinges, allowed sufficient hot gases to ignite the polyethylene sheeting on the top half of the Outerpack. The burnt polyethylene sheeting was directly in line with the gaps in between the hinges. The burnt zones (4) were located only on the upper half of the Outerpack. This is most likely due to the flanges on the mating Outerpack halves which preferentially directs incoming gases to the upper portion of the Outerpack. **Design Changes as a Result of Testing:** Based on unsuccessful fire testing of the QTU-1 unit, the QTU-2 unit was modified for improved thermal performance. Since the QTU-2 had already been drop tested in accordance with 10 CFR 71, and TS-R-1 requirements, only minor modifications were deemed acceptable. Only changes considered for the QTU-2 were ones that would not have affected the drop characteristics and performance. The changes made to the QTU-2 unit subsequent to drop testing are listed as follows: 1. The 10 short Outerpack hinge sections were removed and replaced with 8 (four per side) long hinge sections that butted together forming a continuous hinge covering essentially all of the Outerpack mating seams. 2. The polyethylene moderator sheeting (both top and bottom sections) was covered with 26 gage stainless steel sheet metal. This sheet material was welded to the inner shells of the Outerpack along the sides of the covers, the ends (both top and bottom) were sealed with adhesive. The coverings therefore, were not completely welded closed.			
QTU-2 Drop Testing: Sep 11, 2003 Burn Testing: Oct 20, 2003	- 1.2 m low angle slapdown (10 degrees) - 9 m end drop (bottom end down) - 1 m pin puncture (22 degrees through CG) - 32 minute pool-fire burn test.	- Outerpack – Satisfied requirements for both drops and pin puncture tests. Minor, local damage only. - Clamshell – Satisfied requirements for both drop tests and thermal tests. No failures were noted in any structure, or fasteners. The maximum temperature of the Clamshell and its contents never exceeded design limits	- Failed to prevent ignition of the polyethylene sheeting inside the Outerpack. However, the maximum temperature of the Clamshell and contents remained below 200°C. The package was extinguished approximately 7 hours after the conclusion of the pool fire testing.

Table 2-5 Summary of the Development of the Traveller (cont.)

Traveller XL	Test Sequence(s)	Structural Performance	Fire/Thermal Performance

Comments:

The Traveller XL QTU-2 demonstrated robust structural performance. No Outerpack bolts failed. The Outerpack did not separate, and the pin puncture did not perforate the inner or outer shells nor did it effect the Clamshell in any detrimental way.

Seven hours after the pool fire, the package burning was extinguished. During this seven hour period there was continuous low level smoldering. Upon inspection of the QTU-2 unit, it was determined that ignition occurred at the bottom end of the package. This was most likely caused by distortion of the Outerpack halves in the area of the bottom end where the impact limiter warped away from the top Outerpack half during the fire. The continuous hinge sections also did not cover the last 3 inches of the Outerpack seams on both sides of the package, which may have allowed additional hot gases to enter the package. The hot gas ingress occurred at a location were there was exposed polyurethane foam (the inner axial limiter foam) due to the thin stainless steel limiter cover being punched out by the Clamshell. This was an expected consequence of the bottom end drop.

The long sheet metal covers which were welded along their sides but applied adhesive at the ends did not perform as anticipated. The covers distorted during the testing and opened the adhesive joint. This allowed the polyethylene moderator to ignite. The areas around the shock mounts also were not covered with sheet metal thus exposing the moderator to the conditions inside the Outerpack. These exposed areas showed signs of burning in post-test examinations.

The QTU-2 test demonstrated that the polyethylene sheeting must be completely welded, or “canned”, by sheet metal to prevent ignition. However, this test was further evidence that the “bulk” heating of the inside of the Outerpack was acceptable, even with burning occurring within the Outerpack. This is a result of the fact that there is insufficient oxygen to support large amounts of burning. It was estimated that over the 7.5 hours of total burning, only about 10-15% of the moderator material was consumed.

Design Changes as a Result of Testing:

Based on the structural success of the QTU units and the thermal failures of the units, several changes were made to the design. These changes are listed below:

1. The 26 gage moderator sheet metal covers were redesigned so that the polyethylene was completely encapsulated by sheet metal. This mandated the use of sheet metal “cones” around each shock mount. Additionally, thin ceramic insulating material was incorporated between the moderator sheet and the metal covers, around the cones, and over a length of 30 inches at both the top and bottom ends. The ceramic “paper” is nominally 0.06 inches (0.15 cm) in thickness. Ceramic felt was also incorporated to fill the voids under the shock mount cones and at the ends of the moderator sheets.
2. The thin sheet metal impact limiter cover which were design to be punched out by high angle Clamshell impacts were redesigned to have thicker (0.25", 0.64 cm) puncture-resistant plates. These “pillows” were separate structures that were tested in a separate series of mechanical and thermal tests prior to CTU testing. The purpose of the pillows was to prevent polyurethane foam from becoming exposed to the inside of the outerpack, even in end drops. The pillow also incorporated a thick (0.25", 0.64 cm) plate at its base to act as a heat capacitor for incoming heat during the fire testing. Finally, the void space between the pillow and the outer sections of the impact limiters was filled with ceramic felt and paper to further reduce the heat load to the pillows and the internal contents of the Outerpack.
3. The foam density within the inner section of the impact limiters, or pillows, was reduced from 7 pcf to 6 pcf to allow more crushing of the foam. This change was made to lower the impact forces on the Clamshell and its contents.

Table 2-5 Summary of the Development of the Traveller (cont.)

Traveller XL	Test Sequence(s)	Structural Performance	Fire/Thermal Performance
4. The four (4) long Outerpack hinge sections were lengthened to cover all of the Outerpack seams. There existed a nominal 3 inch (7.6 cm) uncovered section at the bottom end. 5. The bottom limiter cover which curves around the bottom impact limiter was extended an additional 1.5 inches axially. Ribs (or lips) were added to this cover, and to the bottom limiter, to further reduce the ingress of hot gases. 6. The foam density in the outer sections of impact limiters was increased from 14 pcf to 20 pcf to reduce the heat flow through these sections. 7. The polyethylene moderator sheets were redesigned for manufacturing purposes. 8. The silicone rubber Omega seal, was replaced with acrylic impregnated fiberglass braided tubing. This change was made to eliminate a potential source of combustion inside the Outerpack. The design changes listed above were retrofitted onto the QTU-1 unit (which had already been burned). The QTU-1 unit was then instrumented and taken through a series of fire tests in an effort to quantify the thermal design margins associated with these design changes. This testing was considered necessary to quantify the thermal design margins before the final Certification Test Unit (CTU) test article was tested. The modified unit was tested twice. It was first burned for 40 minutes, then it was re-burned for another 30 minutes the following day. The results of the tests were excellent. The impact limiter pillow temperature never exceeded 120°C, and the data confirms the primary heating to the inside of the Outerpack is by conduction. Based on the successful testing of the modified QTU-1 article, the design changes were incorporated in the manufacturing of the Traveller XL CTU package.			
CTU Drop Testing: Feb 5, 2004 Burn Testing: Feb 10, 2004	- 1.2 m low angle slapdown (9 degrees) - 9 m end drop (bottom end down) - 1 m pin puncture (21 degrees through CG, directly onto Outerpack hinge) - 32 minute pool-fire burn test.	- Outerpack – Satisfied requirements for both drops and pin puncture tests. Minor, local damage only. - Clamshell – Satisfied requirements for both drop tests and thermal tests. The Clamshell retained its shape and remained closed and latched after drop testing.	Clamshell – Satisfied requirements for fuel containment and criticality safety. The Clamshell and its contents remained below a maximum of 150°C.
The Traveller XL CTU demonstrated robust structural performance. No Outerpack bolts failed and the Outerpack retained its circular pre-test shape. The Outerpack did not separate, and the pin puncture did not perforate the inner or outer shells nor did it affect the Clamshell in any detrimental way. Minor weld failures on the Outerpack, in the region near the impact, were observed in post-test examinations. These failures had negligible effect on the performance of the CTU. The two (2) quick release pins on the cover lips detached during the drop test, therefore, they could not be used where they were intended, in the burn test (as such, they were not re-installed for the burn testing).			

Table 2-5 Summary of the Development of the Traveller (cont.)

Traveller XL	Test Sequence(s)	Structural Performance	Fire/Thermal Performance

The impact limiter pillows performed as intended, however, they did not crush as much as intended due to the inherent axial flexibility of the 17x17 XL fuel assembly. The moderator sheeting remained completely contained within the sheet metal covering. A small brown spot was observed on the back side of one moderator sheet attached to the Outerpack top half. A very small amount of flow occurred away from the hot spot. This melt spot was small, affecting only a few cubic centimeters of material.

The Clamshell was found intact and closed, and the simulated poison plates maintained their attached position with very little distortion. Minor damage was observed at the location of the impact with the pillow, however, the damage had negligible effect on the performance of the Clamshell. All closure nuts remained intact with no signs of distortion or stress.

The most significant observation from the post-test examinations were 20 cracked fuel rod bottom end plug welds. These cracks occurred in the regions corresponding to the corners of the bottom nozzle. At these corners, the buckled bottom nozzle has steep faces (in excess of 45 degrees), which was exacerbated by the characteristically long legs of the 17XL assembly. The angled faces apply a side force to the local fuel rods as they are decelerated in the impact. The largest crack occurred in a fuel rod located in the outermost row within the assembly. The crack in the rod had a maximum width of approximately 0.075" (1.91 mm). This width is not sufficiently large enough for loss of fuel from the rod. Further, in all cases of cracked rods, the bottom end plugs did not separate. Therefore, fuel pellets are prevented from exiting any of the cracked rods.

Design Changes as a Result of Testing:

The CTU satisfied the HAC drop-test and burn-test requirements in all aspects. However, as with any development program, improvements can be envisioned after every series of tests. Based on the results of the CTU tests, several minor changes shall be incorporated into production units to enhance the performance of the package. There changes do not change the performance or characteristics of the package, but merely improve the safety margin of the package by incorporating rather obvious improvements as listed below. The basis for the change is also listed below:

1. The studs which hold the moderator blocks to the upper Outerpack half failed during the drop testing. The moderator remained contained within the sheet metal covering. However, the number of 3/8" (0.95 cm) diameter studs shall be increased by 50% on the top Outerpack assembly only.
2. The bottom impact limiter pillow is welded at the top plate to the Outerpack inner plate. This weld is design to break in a high angle impact. It performed well in the drop test, however, it did not completely break. This joint shall be redesigned with a small groove cut into the inner plate to form a weakened break point. The break shall therefore not necessarily occur at the weld location.
3. The quick release pins used to secure the bottom end seam flange cover failed during drop testing but had negligible effect on the performance (intended for thermal performance only). Therefore, they were not used in the thermal test and will not be used in production units.

The figure below (Figure 2-1B) shows the impact limiter, or Pillow, assembly (shown without insulation). This assembly is shown installed in the Traveller package bottom (the configurations are the same for STD and XL packages) in Figure 2-1C. The weld between the bottom plate (yellow) and the puncture plate (red) is also shown. During testing this weld failed as expected, however, it did not completely allow the components to separate. This design change weakens the bottom plate by reducing its thickness to a nominal 0.025" thickness, as shown in Figures 2-1D and 2-1E. A .25 inch wide channel was added to weaken the part.

Table 2-5 (cont.) Summary of the Development of the Traveller			
Traveller XL	**Test Sequence(s)**	**Structural Performance**	**Fire/Thermal Performance**

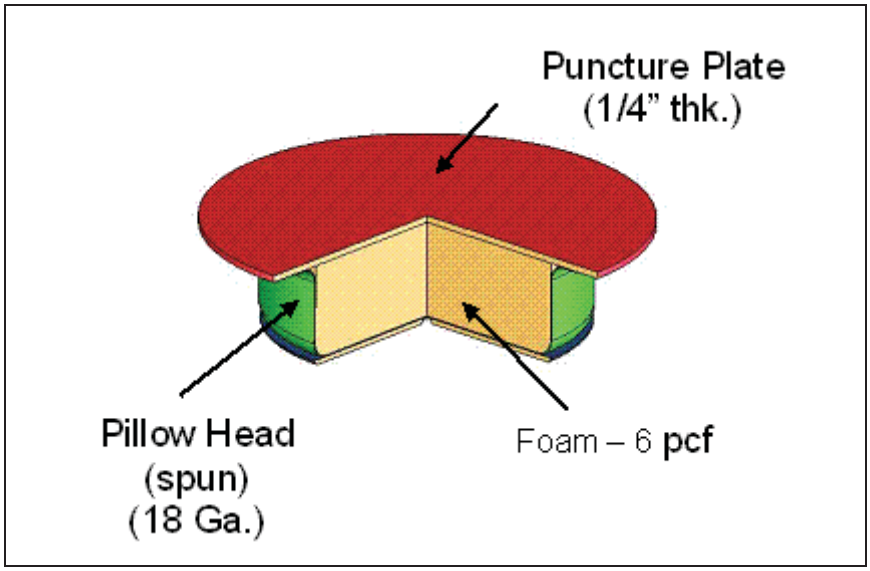

Figure 2-1B Impact Limiter "Pillow" Assembly

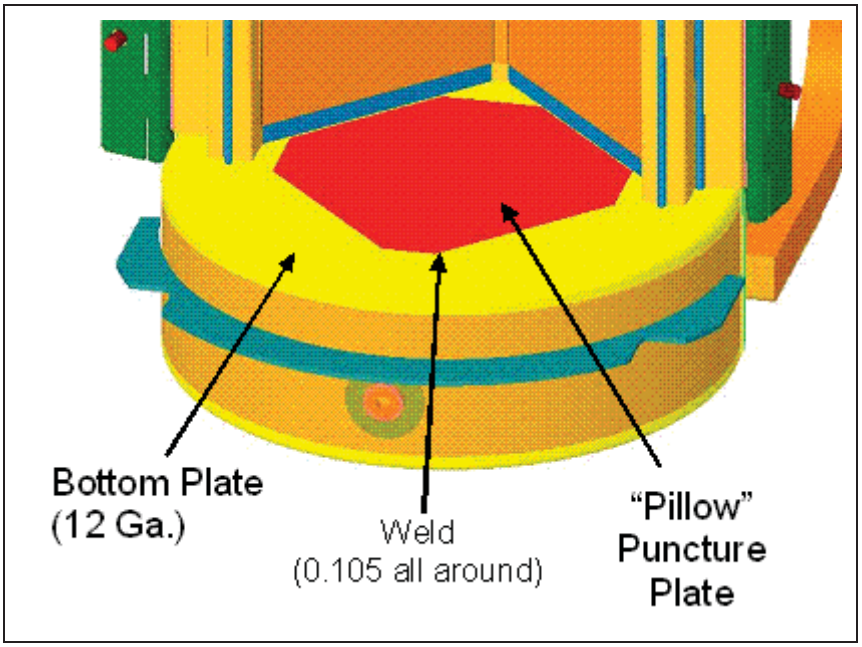

Figure 2-1C Container Bottom End

Table 2-5 (cont.) Summary of the Development of the Traveller			
Traveller XL	**Test Sequence(s)**	**Structural Performance**	**Fire/Thermal Performance**

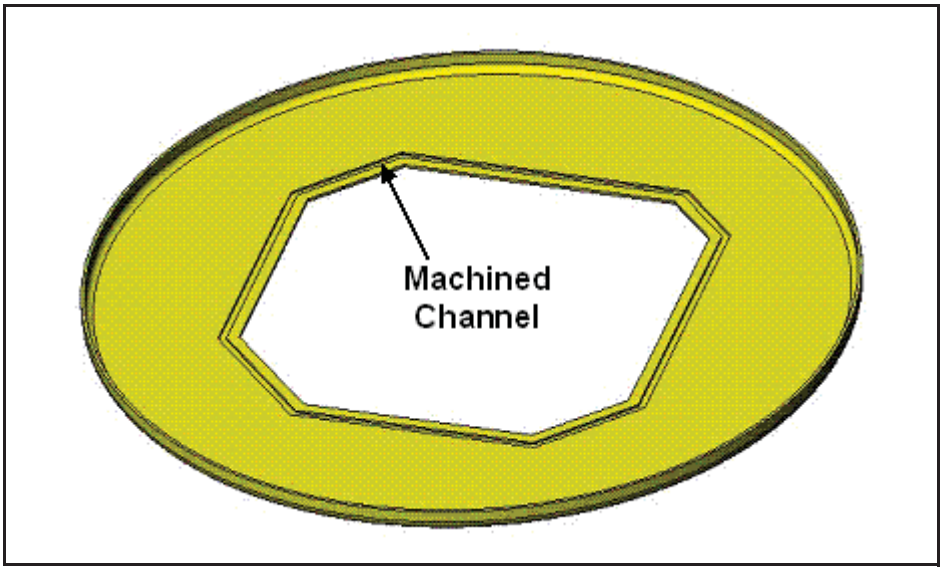

Figure 2-1D Impact Limiter "Pillow" Assembly

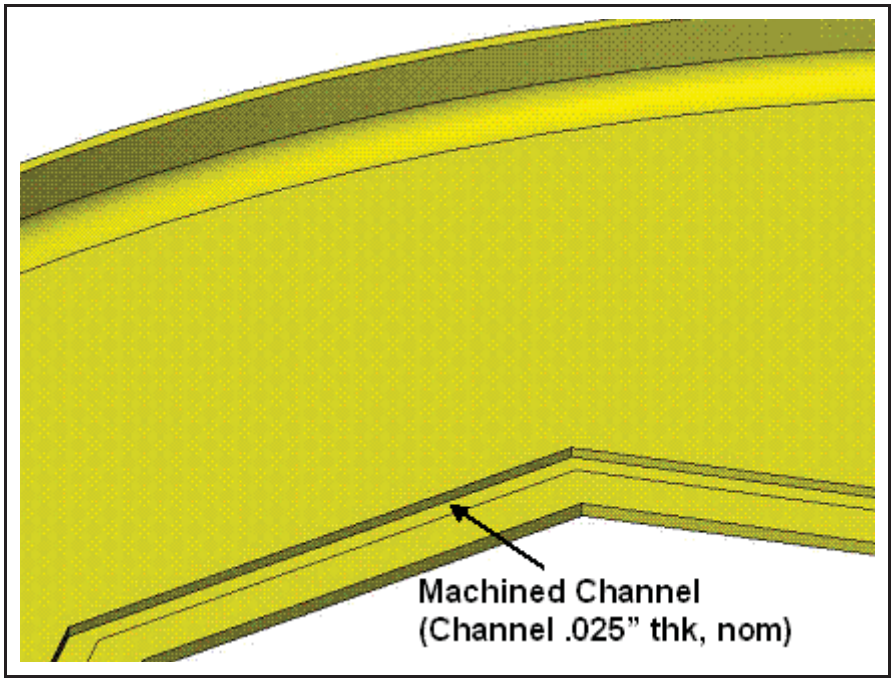

Figure 2-1E Bottom Plate – Viewed from Inside

Table 2-5 (cont.) Summary of the Development of the Traveller

Traveller XL	Test Sequence(s)	Structural Performance	Fire/Thermal Performance

The CTU design included a pinned connection (2 quick release pins – 0.5" diameter) between Outerpack halves at the bottom end of the package. Quick release pins were designed to help prevent the halves from warping and opening a gap locally during fire testing. Figure 2-1F shows the location of the quick release pins. During drop testing, the pins failed, therefore, they could not be used in the fire testing

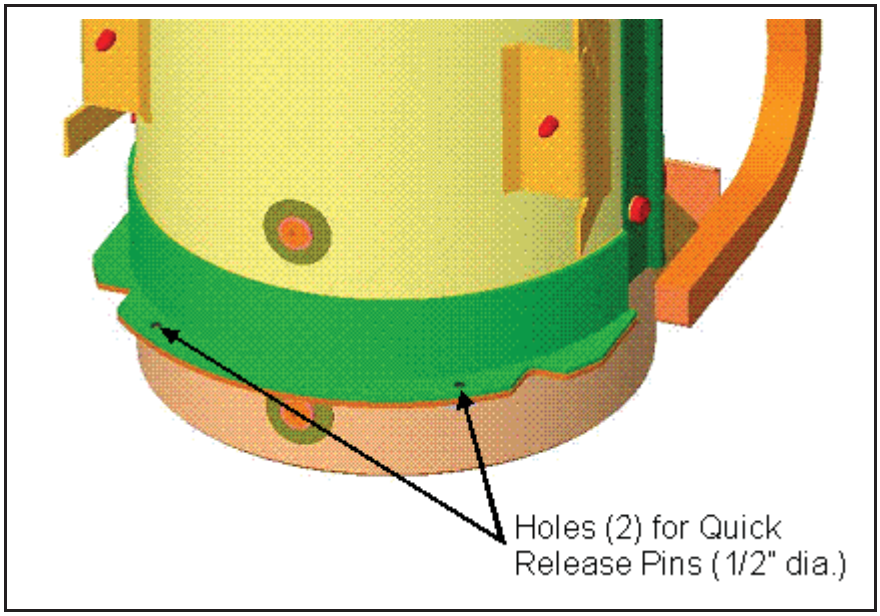

Figure 2-1F CTU Package Bottom End

This page intentionally left blank.

2.7.1 Free Drop

Subpart F of 10 CFR 71, TS-R-1 (727) requires that a 9-meter (30 foot) free drop be considered for the Traveller series of packages. The free drop is to occur onto a flat, essentially unyielding, horizontal surface, and the package is to strike the surface in an orientation for which the maximum damage is expected. The free drop is addressed by test, in which the most severe orientation is used. The free drop precedes both the puncture and fire tests. The ability of the Traveller packages to adequately withstand this specified drop condition is demonstrated via drop testing of the full-scale Traveller XL Certification Test Unit (CTU). The Traveller XL variant bounds the shorter and lighter Traveller STD design. Simulations using finite element analysis are performed to demonstrate the response of the package to free drop tests with the Clamshell axial spacer and removable top end plate.

2.7.1.1 Technical Basis for the Free Drop Tests

To properly select a worst case package orientation for the 9 m (30 feet) free drop event, the foremost item that could potentially compromise the criticality control integrity of the Traveller series of packages must be clearly identified.

The criticality control integrity may be compromised by four methods: 1) excessive movement of the fuel rods such that they form a critical geometry, 2) damage/destruction of the neutron absorber and polyethylene sheeting, 3) degradation of the neutron absorber/polyethylene sheeting and/or 4) other structural damage that could affect the nuclear reactivity of an array of packages.

For the above considerations, testing and FEA predictive methodology must include orientations that affect the Clamshell geometry and integrity. Throughout the development of the Traveller XL, minor design changes were made to optimize the structural and thermal performance of the package.

A total of nine (9) 30 foot (9 m) free drops were performed using full-scale prototypes at a variety of orientations to determine the most severe orientation and to assist in benchmarking the computer simulation model. Based on these tests, and the predictions of the analytic analyses, it was determined that the most severe 9 m free drop orientation was a bottom-end down drop due to; 1) the relatively high deceleration, 2) the greatest opportunity for lattice expansion of the fuel, and 3) the greatest opportunity for fire damage as a result of the subsequent pool-fire thermal testing.

The bottom-down end drop causes the greatest damage to the axial impact limiters, or “pillows.” These pillows were incorporated as a re-design from QTU-2 testing whereby the Clamshell punched through the plate covering the inner section of the axial impact limiter. This exposed foam later burned within the interior of the Outerpack and ignited the moderator panels. The concept of a puncture plate was redesigned to incorporate a “puncture resistant” plate. The inner foam limiter was therefore protected by the puncture resistant plate (1/4" thk, 0.64 cm), and was enclosed by a spun metal “can” welded to the plate to completely seal the pillow assembly. CTU test results confirmed that no polyurethane foam was exposed as a result of the bottom-down end impact.

The long bottom nozzle “legs” associated with the Westinghouse 17x17 XL fuel assembly are considered the most severe because they allow considerable strain of the bottom nozzle (particularly the flow plate, or

adapter plate) during a bottom-down end drop. The bowed adapter plate offers the greatest opportunity to damage fuel rods during the impact.

The top-down end drop produces significantly lower deceleration due to buckling of the axial clamp bolts. As these buckle, considerable energy is absorbed, thus lower the buckling of the top nozzle. By comparison, the bottom-down end drop is more severe.

2.7.1.2 Test Sequence for the Selected Tests

Analyses indicated and testing demonstrated that the puncture tests did not cause any damage to the package that would lead to further damage in the fire test, and neither did they compromise package containment or confinement. Therefore either order in which the 9m drop test and the puncture test are performed is equally valid.

TS-R-1, para 727, states that the drop test sequence shall be such that, upon completion, the specimen will have suffered such damage as to lead to maximum damage in the thermal test that follows. The TS-R-1 advisory document, TS-G-1.1, expands on this, saying that the assessment of maximum damage should consider what affect the drops have on package containment, shielding, and confinement. TS-G-1.1 further cautions that the most damaging package orientation may not be a flat impact onto the bar top surface, but an angle in the range 20° –30° range, because such an angle causes tearing of the outer skin as well as puncturing.

Section 2.7.3.1 discusses the technical basis for the puncture test, indicating that the greatest possibility of cumulative damage to this package occurs when the pin puncture is located within the area of impact of the 9m drop. Thus, maximum damage would occur when the puncture test follows the 9m drop test. During the Traveller development period, several test specimens were subjected to puncture drops onto different parts of the package in an effort to determine which location was most damaging. In one instance the drop test sequence was altered to assess whether or not a different order would cause more damage. As mentioned above, it was found that the puncture tests did not cause any damage to the package that would jeopardize either package containment or confinement. Therefore either order in which the 9m drop test and the puncture test are performed is equally valid.

Section 2.7.3.2 summarizes the results from the puncture drop tests. The several puncture tests are described in detail in the SAR and are summarized below.

Test Specimen	SAR	Test Sequence	Inspection Results
FEA Analysis	2.12.3.2.7	Two cases modeled: – Horizontal drop onto belly – Horizontal drop onto hinge	• Predicted unlikely that the outer shell would be penetrated in either case • (Good agreement between FEA results and prototype test results
Prototype I	2.12.4.1	**(1) 9m Drop** – Bottom nozzle drop – 71° angle CG over corner on hinge **(2) Puncture** – Package at 20° angle upside down over center of gravity	• Outerpack outer skin was locally indented 1.63" • Impact punch zone width was 10.5" • Pin did not perforate the outer skin • Internal inspection findings – small dent about 7/16" to 1/2" and 15" wide resulted from the pin puncture test • Moderator blocks were not impacted by the pin test.

Test Specimen	SAR	Test Sequence	Inspection Results
Prototype II	2.12.4.1	**(1) Puncture** – Drop onto package side – Package at 20° angle, CG **(2) 9m Drop** – Top nozzle drop – 72° angle CG over corner	• Outerpack outer skin was locally indented about 2" • Impact punch zone was 10" tall and 14" wide • Pin did not perforate the inner and outer shell • Moderator blocks and neutron poison plates maintained position
Qualification Test Unit I	2.12.4.2.1	**(1) 9m Drop** – Top nozzle drop – 72° angle CG over corner **(2) Puncture** – Drop onto top nozzle end – Package at 83° angle – Dropped on hinge to add to damage from 9m drop	• Indention was approximately 1-1/2" deep • Additional tearing of the joint was noted which resulted in measured tear of approximately 1-1/8" • Moderator blocks and neutron poison plates maintained position
Qualification Test Unit II	2.12.4.2.2	**(1) 9m Drop** – Bottom nozzle drop – 90° angle **(2) Puncture** – Drop onto underbelly of package – Package at 22° angle	• Damage zone was 9" long x 6" wide x 2-7/8" deep • Moderator blocks and neutron poison plates maintained position
Certification Test Unit	2.12.4.3	**(1) 9m Drop** – Bottom nozzle drop – 90° angle **(2) Puncture** – Drop onto side of package, onto hinge – Package at 21° angle	• 6" length of hinge dented length to a maximum depth of 1.375" • Hinge separation of 1/2" from package about 7-1/2" from the impact point towards the top nozzle end • Hinge knuckles were not compromised • Moderator blocks and neutron poison plates maintained position

2.7.1.3 Summary of Results from the Free Drop Tests

Successful HAC free drop testing of the Traveller XL CTU certification unit indicates that the various structural features are adequately designed to withstand the 9 m (30 foot) free drop event. The most important result of the testing program was the demonstrated ability of the bounding Traveller XL package to maintain its criticality safety integrity.

Significant results of the free drop tests, including the thermal test, are as follows:

1. There was no breach or distortion of the Clamshell aluminum container.
2. There was no evidence of melting or material degradation on the polyethylene sheeting.
3. The Outerpack remained closed and structurally intact.
4. A small number of rods (20) were cracked during drop testing (only seen in bottom-end drops).
5. Rod damage has been at the end of the rods only. No damage anywhere else.
6. None of the end plugs have separated from the rods.
7. No pellet material is lost from the cracked rods.

Further details of the free drop test results are provided in Appendix 2.12.5, Traveller Drop Test Results.

2.7.2 Crush

The crush test specified in 10 CFR §71.73(c)(2), TS-R-1 (727) is required only when the specimen has mass not greater than 500 kg (1,100 pounds), an overall density not greater than 1,000 kg/m^3 (62.4 lb/ft^3), and radioactive contents greater than 1,000 A2, not as special form. The gross weights of the Traveller packages are greater than 500 kg (1,100 pounds). Therefore, the dynamic crush test of 10 CFR §71.73(c)(2), TS-R-1 (727) is not applicable to the Traveller series of packages.

2.7.3 Puncture

Subpart F of 10 CFR 71 requires performing a puncture test in accordance with the requirements of 10 CFR §71.71(c)(3), TS-R-1 (727). The puncture test involves a 1 m (40 inch) drop onto the upper end of a solid, vertical, cylindrical, mild steel bar mounting on an essentially unyielding, horizontal surface. The bar must be 15 cm (6 inches) in diameter, with the top surface horizontal and its edge rounded to a radius of not more than 6 mm (1/4 inch). The minimum length of the bar is to be 20 cm (8 inches). The ability of the bounding Traveller XL packages to adequately withstand this specified drop condition is demonstrated via testing of numerous full-scale Traveller XL prototypes and the Certification Test Unit (CTU).

2.7.3.1 Technical Basis for the Puncture Drop Tests

To properly select a worst case package orientation for the puncture drop test, items that could potentially compromise criticality integrity of the Traveller package must be clearly identified. For the Traveller XL package design, the foremost item to be addressed is the integrity of the Clamshell and the neutron moderation and absorption materials (i.e., neutron absorber plate and polyethylene sheeting).

The integrity of the Clamshell and the criticality control features may be compromised by two methods: 1) breach of the Clamshell boundary, and 2) degradation of the neutron moderation/control materials due to fire.

For the above reasons, testing must consider orientations that attack the Outerpack closure assembly, which may result in an excessive opening into the interior for subsequent fire event, and/or the Clamshell which contains the fuel assembly. Based on prototype testing and computer simulations of the pin puncture event, the pin puncture has insufficient energy to cause significant damage to the Outerpack hinge closure system nor to the Clamshell (including components within the Clamshell).

The greatest possibility of cumulative damage to the package occurs when the pin puncture is located within the area of impact of the 9m drop. These locations further attack the welded joints adjacent to the crushed area between the Outerpack outer shell and the end cap. Many pin puncture locations were tested in prototype testing, and all had insignificant impact on the structural and thermal performance of the package. See Table 2-2 above, and Appendix 2.12.5, Traveller Drop Test Results, for more information regarding pin puncture testing.

Based on the above discussion, the Traveller XL CTU was specifically evaluated at a “new” location. The pin puncture was located such that the pin impacted directly on an Outerpack hinge at a low impact angle. This test had not previously been performed, and it was desired to test the hinge’s ability to take a pin impact and still perform its important function of thermally protecting the seam between Outerpack bottom and top assemblies. The thermal protection offered by the hinge is described in more detail in Section 3.

2.7.3.2 Summary of Results from the Puncture Drop Test

Successful HAC puncture drop testing of the CTU indicates that the various Traveller XL packaging features are adequately designed to withstand the HAC puncture drop event. The most important result of the testing program was the demonstrated ability of the bounding Traveller XL to maintain its structural integrity. Significant results of the puncture drop testing are as follows:

1. Minor damage to the Outerpack and Outerpack hinge

2. No affect on the structural or thermal performance of the package.

3. There was no evidence of separation of the Outerpack seam which would allow hot gases to enter the Outerpack.

4. No evidence of movement occurred that would have significantly affected the geometry or structural integrity of the Clamshell.

5. There was no evidence of loss of contents from the Clamshell due to the puncture events.

6. There was no evidence of deterioration of the polyethylene sheeting in the subsequent fire event.

7. There was no evidence of deterioration of the borated-aluminum sheeting (simulated) in the subsequent fire event.

Further details of the puncture drop test results are provided in Appendix 2.12.5, Traveller Drop Test Results.

2.7.4 Thermal

Subpart F of 10 CFR 71, TS-R-1 requires performing a thermal test in accordance with the requirements of 10 CFR §71.71(c)(4), TS-R-1 (728). To demonstrate the performance capabilities of the Traveller packaging when subjected to the HAC thermal test specified in 10 CFR §71.71(c)(4), TS-R-1 (727), a full-scale CTU was burned in a fully engulfing pool fire. The test unit was subjected to a 9 m (30 foot) free drop, and a 1.2 m (4 foot) puncture drop, prior to being burned, as discussed above. Further details of the thermal performance of the Traveller XL CTU are provided in Section 3, Thermal Evaluation.

Type K thermocouples were installed on the exterior surface of the packaging (each side, top, and bottom) to monitor the package's temperature during the test. In addition, passive, non-reversible temperature indicating labels were installed on the Clamshell, fuel assembly, and inner surfaces of the Outerpack.

The CTU was exposed to a minimum 800ºC (1,475ºF), 30-minute pool fire. As discussed in Appendix 2.12.5, Traveller Drop Test Results, the package was orientated such that the Outerpack was on its side. This orientation offered the greatest opportunity for formation of a chimney and thus result in maximum combustion of the Outerpack foam and degradation of the polyethylene sheeting.

Following the minimum 30-minute fire, the CTU was allowed to cool naturally in air, without any active cooling systems.

2.7.4.1 Summary of Pressures and Temperatures

The accident case pressure is assumed to be 0 psig since the Outerpack and Clamshell are not sealed.

The peak temperatures for the Clamshell, as recorded by five (5) temperature indicating strips, was 104ºC (217ºF). No loss of material was observed in the polyethylene material.

2.7.4.2 Differential Thermal Expansion

Fire testing of a full-scale Traveller XL package indicates that the stresses associated with differential thermal expansion of the various components are negligible.

2.7.4.3 Stress Calculations

Successful fire testing of a full-scale Traveller XL CTU package, as well as prior tested prototypes, indicates that the stresses associated with differential thermal expansion of the various packaging components are negligible.

2.7.4.4 Comparison with Allowable Stresses

As discussed in Section 2.7.4.3, Stress Calculations, further evaluation of stresses associated with differential thermal expansion for the various Traveller package components is not required.

Successful HAC thermal testing of the CTU indicates that the various Traveller packaging design features are adequately designed to withstand the HAC thermal test event. The most significant result of the testing program was the demonstrated ability of the Traveller XL CTU to maintain its criticality control integrity, as demonstrated by post-test inspection of; the moderator and poison materials, the remaining polyurethane foam, and the integrity of the Clamshell.

Further details of the thermal test results are provided in Appendix 2.12.5, Traveller Drop Tests Results and Section 3, Thermal Evaluation.

2.7.5 Immersion – Fissile Material

Subpart F of 10 CFR 71 requires performing an immersion test for fissile material packages in accordance with the requirements of 10 CFR §71.73(c)(6), TS-R-1 (733). Because of the seal configuration (see Section 1, General Information), the Traveller STD and Traveller XL packages are not leak-tight under external overpressure. Under the immersion test, water will fill all internal void space. Because of the pressure equalization, the packaging structure is therefore not subjected to loading during these tests.

2.7.6 Immersion – All Packages

Subpart F of 10 CFR 71 requires performing an immersion test for fissile material packages in accordance with the requirements of 10 CFR §71.73(c)(6), TS-R-1 (729). Because of the seal configuration (see Section 1, General Information), the Traveller STD and Traveller XL series of packages are not leak-tight under external overpressure. Under the immersion test, water will fill all voids. Because of the pressure equalization, the packaging structure is therefore not subjected to loading during these tests.

As the package model criticality study assumes the worst-case flooding scenario, the Traveller XL CTU is exempted from this water immersion test.

2.7.7 Summary of Damage

As discussed in the previous sections, the cumulative damaging effects of the free drops, puncture drop, and thermal tests were satisfactorily withstood by the Traveller XL CTU. Subsequent examinations of the CTU confirmed that integrity of the criticality control components was maintained throughout the test series. The geometry of the Clamshell remained essentially unchanged from the pretest condition. In addition, the Fuel Assembly was well protected and experienced damage that was within acceptance criteria. Therefore, the requirements of 10 CFR §71.73, TS-R-1 (726-729) have been adequately satisfied.

2.8 ACCIDENT CONDITIONS FOR AIR TRANSPORT OF PLUTONIUM

Not applicable.

2.9 ACCIDENT CONDITIONS FOR FISSILE MATERIAL FOR AIR TRANSPORT

Application to be made at a later date.

2.10 SPECIAL FORM

The contents of the Traveller series of packages do not classify as special form material.

2.11 FUEL RODS

In the Traveller XL and STD packages, the fuel rods within the package provide containment for the nuclear fuel. This containment was successfully demonstrated in 3 full-scale test campaigns comprising a total of nine (9) 30 foot free drops, and the corresponding 1.3 meter free-drops and pin puncture tests. These tests resulted in 100% containment of the fuel pellets within rod of every fuel assembly.

For all 9-meter drop test orientations except for the bottom-down end drop (long axis of package aligned with the gravity vector), every fuel rod survived with no damage except slight to moderate buckling of the cladding. Rod pressure test sampling was routinely performed on these fuel assemblies. Except for the bottom-down end drop, all of the rods sampled remained intact and pressurized. All rods visually appeared in excellent condition.

A total of two (2) full-scale Traveller XL packages (QTU-2 and CTU) were tested in a bottom-down end drop orientation. Both of these fuel assemblies (dummy Westinghouse 17x17 XLs) experienced a small percentage of rods with cracked welds in the location of the bottom end plug. In the worst case assembly (CTU), post-test inspection of the fuel assembly indicated that approximately 7.5% of the fuel rods were visibly cracked at the end plug weld zone. The average magnitude of the crack widths measured approximately 0.030 inches (0.76 mm) encompassing about one-half of a rod diameter. This minor cracking is considered insignificant since fuel pellets of diameter 0.374 inches (9.50 mm) are approximately 12.5 times larger than the average visible crack widths. A crack width of 0.075 inches (1.91 mm) was the largest observed. This width is not sufficient for fuel pellets to escape. Therefore, the containment system satisfies its requirement of containing loss of fuel.

Due to the nature of the bottom-down end impact, the fuel rod array is tightly packed and forced into the bottom nozzle. As the bottom nozzle buckles, the rods located nearest the corners of the adapter plate experience a side loading due to the deformed shape of the plate. This moment is sufficient to crack the weld, however, it is clearly not sufficient to completely break off the bottom end plug since the array of rods is so tightly packed. No complete separation of the bottom end plug was observed in any fuel rods for both fuel assemblies. Therefore, the fuel pellets are safely contained within each fuel rod. Further details can be found in Appendix 2.12.5, Traveller Drop Tests Results.

2.11.1 Rod Pipe

The Traveller Clamshell is primarily designed to transport PWR fuel assemblies. To accommodate loose fuel rods, a rod pipe has been designed. It is a 304 stainless steel rod pipe with a maximum diameter of 6.625 inches (6" Schedule 40 pipe), maximum length 200 inches, and a maximum loaded weight of 1650 lbs.

The loose rod pipe is a relatively rigid structure as compared to a fuel assembly. The rod pipe is a single structural member closed by rigid mechanisms. Because the fuel assembly is less stiff than the rod pipe, the fuel assembly is more likely to deform plastically from localized buckling.

The rod pipe is fit to conform into the clamshell axially with a rubber spacer, and is restrained laterally by the bent flanges with foam rubber "clamps" similar to retraining a fuel assembly at the spacer grid locations.

The TRAVELLER response to the 9-meter HAC drop test resulted in the kinetic energy due to the combined mass of the fuel assembly and clamshell being absorbed by the outerpack impact limiter and minor fuel assembly buckling. As a result, the strain damage to the fuel assembly was minimal, and the clamshell retained its pre-test geometry and its structural integrity even though the full stroke of the impact limiter was not utilized. When subjected to the 9-meter impact test described in 10CRF71.73, the rod pipe is expected to utilize the full stroke of the impact limiter due to their rigidity. The resulting applied impact force to the rod pipe is expected to be less then that imparted to the fuel assembly. Furthermore, the rod pipe is expected to act in a coupled manner similar to the fuel assembly and result in similar load paths. With the maximum mass of 1650 pounds, the rod pipe will have less impact energy imparted on their rigid structure as well. The maximum rod pipe mass is less than the maximum fuel assembly mass used in the 9-meter impact test. Therefore, the performance of the TRAVELLER packaging with rod pipe contents would be similar to and bounded by the performance of the TRAVELLER packaging that was demonstrated by the 9-meter HAC drop with the fuel assembly contents.

This page intentionally left blank.

2.12 APPENDICES

2.12.1 References

None.

2.12.2 Container Weights and Centers of Gravity

2.12.3 Mechanical Design Calculations for the Traveller XL Shipping Package

2.12.4 Drop Analysis for the Traveller XL Shipping Package

2.12.5 Traveller Drop Test Results

2.12.6 Supplement to Drop Analysis for the Traveller XL Shipping Package – Clamshell Axial Spacer Structural Evaluation

2.12.7 Supplement to Drop Analysis for the Traveller XL Shipping Package – Clamshell Removable Top Plate Structural Evaluation

2.12.2 Container Weights and Centers of Gravity

2.12.2.1 Container Weights

This section provides the Traveller XL and Traveller STD weight breakdown to determine design and licensing weights, and centers of gravity for each package. The Design and Licensing Basis Gross Weight is calculated from the Nominal Total Weight plus the 2.3% manufacturing variability. The maximum tare weight is the Design and Licensing Basis Gross Weight less the maximum fuel assembly weight. Maximum tare and Design and Licensing weights are rounded up to the nearest tenth after the maximum tare weight is determined.

Table 2-6 Summary of Traveller STD and Traveller XL Weights

	Traveller STD	Traveller XL
Nominal Outerpack Weight, lb (kg)	2368 (1074)	2670 (1211)
Max. Fuel Assembly Weight, lb (kg)	1650 (748)	1971 (894)
Nominal Clamshell Weight, lb (kg)	378 (171)	467 (212)
Nominal Total Weight, lb (kg)	4396 (1994)	5108 (2317)
Desgin and Licensing Basis Gross Weight, lb (kg)	4500 (2041)	5230 (2372)
Max. Tare Weight, lb (kg)	2850 (1293)	3255 (1476)

2.12.2.2 Centers of Gravity

This section provides the location of the center of gravity for empty Traveller XL and Traveller STD packages.

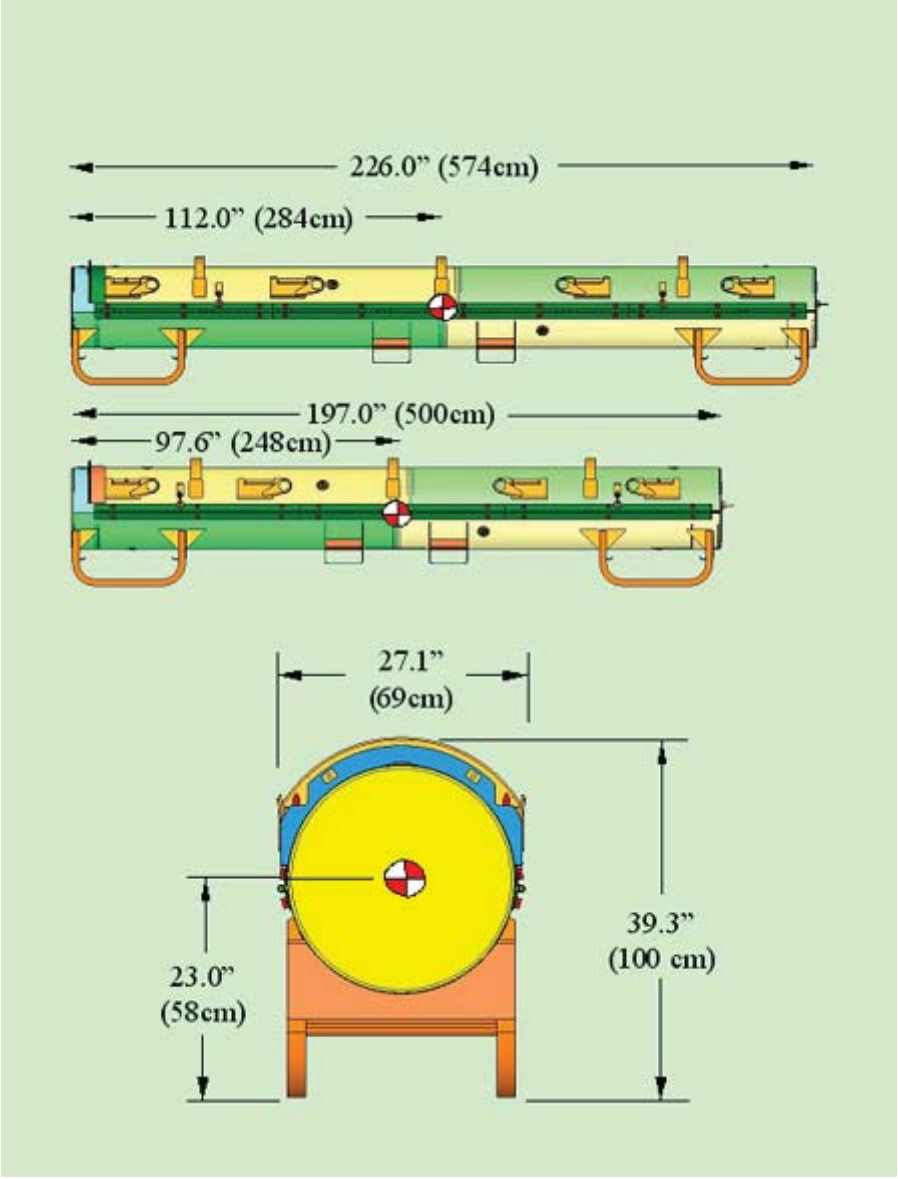

Figure 2-2 Traveller XL and Traveller STD Dimensions and Center of Gravity (Note: End View is Common to both Models)

2.12.3 Mechanical Design Calculations for the Traveller XL Shipping Package

During Traveller package development, normal transport and hypothetical accident condition testing were performed to demonstrate package compliance to test conditions described in 10 CFR 71 and TS-R-1. For those requirements not demonstrated by testing, a mechanical analysis was performed to demonstrate package compliance. This section outlines the non-tested requirements to be satisfied and provides an analysis for each requirement.

The Traveller XL package is depicted in Figure 2-3. The exterior view of the Outerpack is shown. The internal packaging including the Clamshell is shown in Figure 2-4. The Traveller XL package structurally and mechanically bounds the Traveller STD package because it is more massive and longer than the Traveller STD except for cases of stacking where the Traveller STD bounds the Traveller XL. Additionally, the computer simulations and full-scale testing of the Traveller XL units demonstrate a robust design with considerable safety margins with respect to all structural and mechanical requirements.

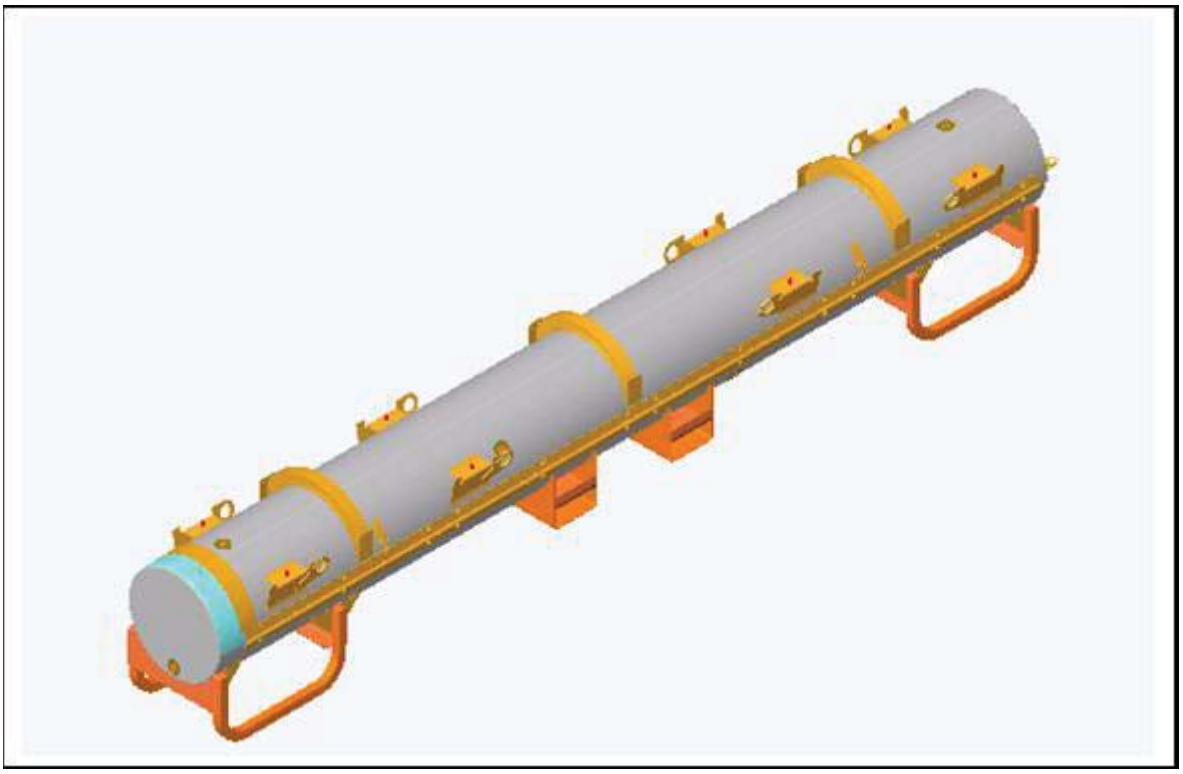

Figure 2-3 Westinghouse Fresh Fuel Shipping Package, the Traveller XL

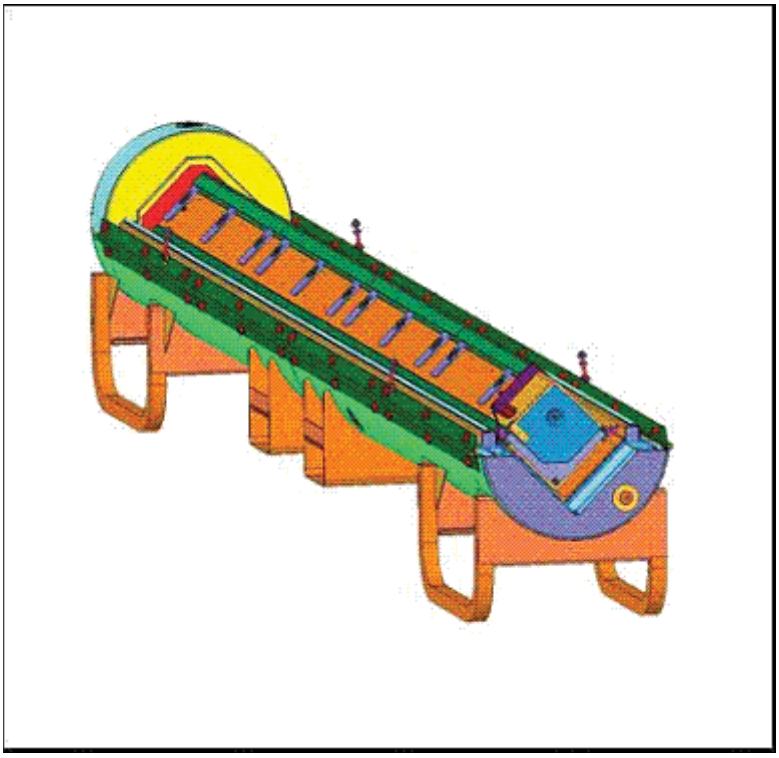

Figure 2-4 Internal View of the Traveller Shipping Package

2.12.3.1 Analysis Results and Conclusions

These analyses were performed to demonstrate Traveller XL package compliance to the mechanical requirements described in 10 CFR 71 and TS-R-1 for which no formal testing was conducted. These calculations bound the lighter, shorter Traveller STD unit. The applicable requirements were summarized in Table 2-3. The results of the design calculations (where applicable), acceptance criteria, and conditional acceptance shown in Table 2-4. Based on the results in Table 2-4, the Traveller package is shown to be compliant to mechanical requirements described in 10 CFR 71 and TS-R-1

Table 2-7 has been deleted.

Table 2-8 has been deleted.

Assumptions

The calculations to determine the maximum Outerpack allowable stresses for yield, shear, and weld shear are based on the properties of ASTM A240 Type 304 Stainless Steel. It is further assumed that the weld consumable possess greater mechanical properties than that of the base metal. Hence, the mechanical properties of the base metal will be employed for weld stress analysis. The reference drawings included in this analysis represent the Certification Test Unit (CTU) Traveller XL, which was fabricated for the drop and fire tests.

Acceptance Criteria

The Traveller package was structurally evaluated to demonstrate compliance to the conditions described in Table 2-3. The package's Outerpack structure is composed of ASTM A240 Type 304 Stainless steel. The mechanical properties are of listed below:

- Tensile strength, Minimum: 75 ksi
- Yield strength, Minimum: 30 ksi

For mechanical analysis where tensile, shear, or weld shear stresses were determined, the acceptance criteria was as follows:

- Maximum allowable tensile yield stress, $\sigma_y = 30$ ksi
- Maximum allowable shear stress, $\tau_{max} = .6\sigma_y = 18$ ksi
- Maximum allowable weld shear stress, $\tau_{weld} = .4\sigma_y = 12$ ksi

The material constant Young's Modulus for 304 Stainless steel is:

$$E = 29.4E6 \text{ psi}$$

2.12.3.2 Calculations

Nine mechanical conditions were evaluated for Traveller package. These conditions are outlined in Table 2-3. Standard engineering methods were used for these calculations.

2.12.3.2.1 Input

The design loads were determined according to the criteria described in 10 CFR 71 and TS-R-1, 1996 where appropriate. The Traveller XL package weight bounds the Traveller STD design as shown in Table 2-6. The total weights for each Traveller design include shipping components where applicable.

Table 2-9 has been deleted.

Lifting – The lifting criteria is governed by 10 CFR 71.45(a) and TS-R-1, Paragraph 607. 10 CFR 71.45(a) states that any lifting attachment that is a structural part of the package must be designed with a minimum safety factor of three against yielding when used to lift the package in its intended manner. In addition, it must be designed so that failure of any lifting device under excessive load would not impair the ability of the package to meet other requirements of 10 CFR 71. The applied loads to the package lifting attachments are then:

For the case of Traveller XL:

$$F_l = 3W_{XL}$$
$$F_l = 3(5{,}230) \text{ lb}$$
$$F_l = 15{,}690 \text{ lb for the Traveller XL}$$

For the case of stacked Traveller STD:

$$F_l = 3W_{2STD}$$
$$F_l = 3(2*4{,}500) \text{ lb}$$
$$F_l = 27{,}000 \text{ lb}$$

Tie-Downs – The tie-down requirements are described in 10 CFR 71.45(b)(1,2) and TS-R-1, Paragraph 636. 10 CFR 71.45 states that a system of tie-downs that is a structural part of the package must be capable of withstanding, without generating stress in excess of its yield strength, a static force applied to the center of gravity having the following components:

- Vertical: 2 g
- Axial: 10 g
- Transverse: 5 g

Thus, the applied tie-down loads for the Traveller are:

- Vertical: 10,460 lb
- Axial: 52,300 lb
- Transverse: 26,150 lb

Design Temperatures between -40°F (-40°C) and 158°F (70°C) – The package must account for temperatures ranging from -40°F (-40°C) to 158°F (70°C) per TS-R-1 (637), and from -40°F (-40°C) to 100°F (38°C) per 10 CFR 71.71(c)(1,2). Thus, the bounding temperature range to consider for package design is -40°F (-40°C) to 158°F (70°C). The analysis of the Traveller package will consider the effects of temperature on thermally induced stress.

Internal/External Pressure – The package must account for the effects of external pressure conditions. The effects of reduced and increased external pressure are described in 10 CFR 71.71(c)(3,4) and TS-R-1 (615). The reduced external pressure is 25 kPa (3.5 psi) absolute, and the increased external pressure is 140 kPa (20 psi) as stated in 10 CFR 71.71.

Water Spray – A water spray test is required for the Traveller package to consider the effects of excessive rainfall on the structural integrity of the package. The water spray test is described by 10 CFR 71.71(c)(6) and TS-R-1 (721). The water spray test is to simulate a rainfall rate of approximately 5 cm/hr (2 in/hr) for at least one hour.

Compression/Stacking Test – The Traveller package must be subjected to a static compression test per by 10 CFR 71.71(c)(9) and TS-R-1 (723). Both regulations require that the applied load by the greater of the following:

An equivalent load of five times the mass of the package or the equivalent of 13 kPa (2 psi) multiplied by the vertically projected area of the package. Evaluating each case:

Case 1

The applied stacking force for case 1 is:

$$Fs = 5W_{XL}$$

$$Fs = 5(5230) \quad \text{lb}$$

$$Fs = 26{,}150 \quad \text{lb}$$

Case 2

The applied stacking force for case 2 is:

$$Fs = (Length)(OD)(P)$$

$$Fs = (226.2)(27.1)in^2(2)\,psi$$

$$Fs = 12{,}260 \text{ lb}$$

Thus, the applied stacking load is Fs = 26,150 lb.

Penetration – The penetration test is an impact test described by 10 CFR 71.71(c)(10) and TS-R-1 (724). The package must be subject to the impact of the hemispherical end of a vertical steel cylinder of 3.2 cm (1.25 in) diameter and a mass of 6 kg (13 lb) dropped from 1 m (40 in) onto the surface of the package that is expected to be the most vulnerable to puncture.

Immersion – The immersion test is a hypothetical accident condition test that evaluates the effects of static water pressure head on the structural integrity of the package. The test condition is described by 10 CFR 71.73(c)(6) and TS-R-1 (729). The regulations state that the package must be immersed under a head of water of at least 15 m (50 ft) for at least 8 hours in the most damaging orientation. For demonstration purposes, an external gauge pressure of 150 kPa (21.7 psi) is considered to meet the test conditions.

2.12.3.2.2 Lifting

Traveller XL Four Point Lift – The Traveller package is crane lifted using a 4-point lift with attachment points located on the stacking bracket. Figure 2-5 shows a sample package with the lifting configurations. The assumed sling angle is 30°. The applied load, Fl = 15,690 lb.

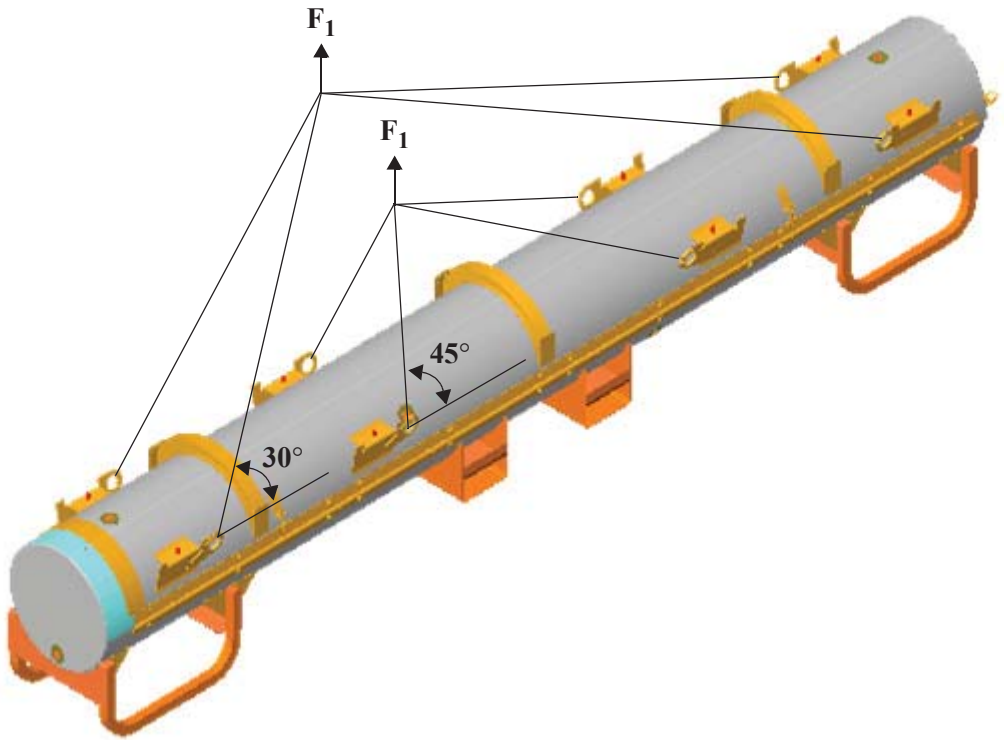

Figure 2-5 Traveller XL Lifting Configurations

Based on the lifting configuration, the applied load transferred to each lifting hole, F, is:

$$F = \frac{\frac{F_l}{4}}{\sin 30}$$

$$F = \frac{15{,}690}{4} / .5 \text{ lb}$$

$$F = 7{,}845 \text{ lb/hole}$$

The applied forces and resultant components for a single lifting hole are shown in Figure 2-6.

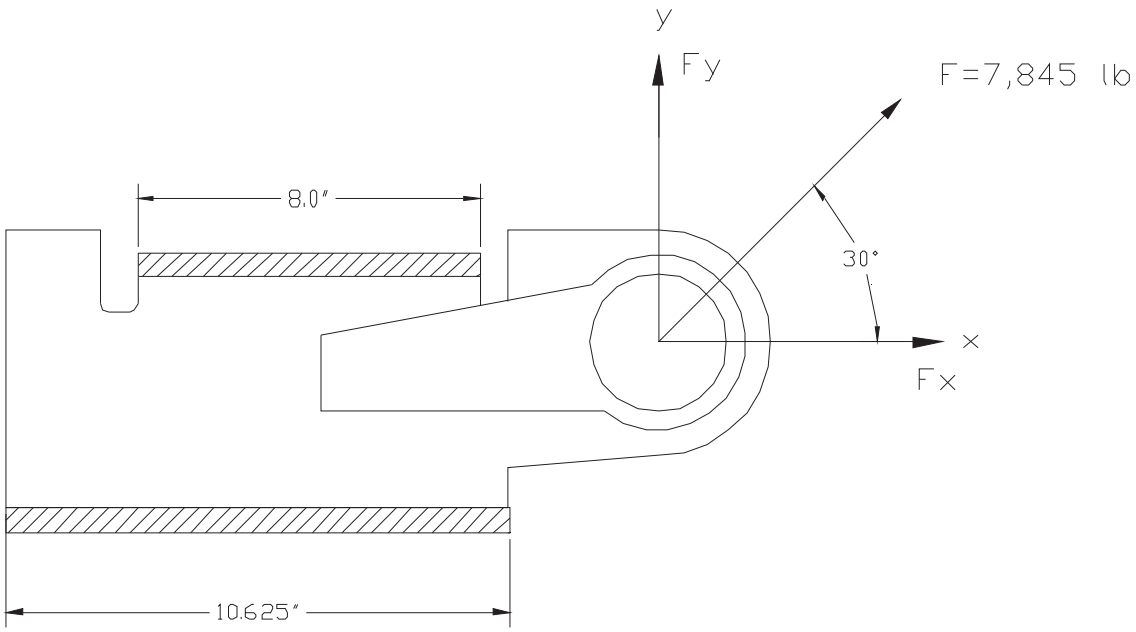

Figure 2-6 Lifting Hole Force Detail

The resulting force components are then:

$$F_x = F(\cos 30)$$

$$F_x = 7{,}845(0.866) \text{ lb}$$

$$F_x = 6{,}794 \text{ lb, and}$$

$$Fy = F(\sin 30)$$

$$Fy = 7{,}845(0.50) \text{ lb}$$

$$Fy = 3{,}923 \text{ lb}$$

The lifting bracket consists of ASTM A276 SS plate with an attached lifting eye. The lifting eye is 0.25" thick ASTM A276 SS plate and is reinforced with a 0.25" plate doubler. A lifting bracket detail is shown in Figure 2-7.

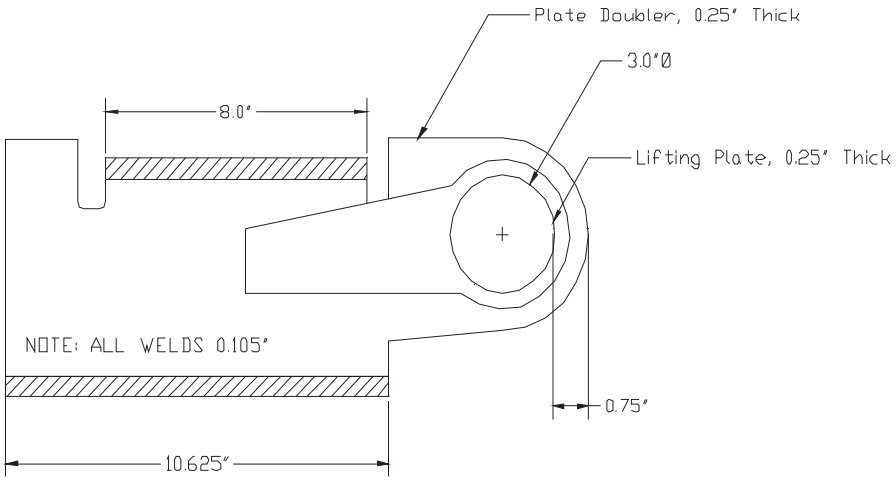

Figure 2-7 Lifting Bracket Fabrication Detail

The lifting analysis consists of two calculations: 1) hole tear-out and, 2) weld strength.

The hole tear-out is assumed to occur at the minimum 0.75" section of material in the lifting eye plate. From Table 2-4, the maximum allowable Shear Yield Stress, τ_y is 18 ksi. The stressed area is the minimum thickness of 0.5" times the section width of the tear out, 0.75" and double shear is assumed. Thus,

$$A = 2(.75)(.5) \text{ in}$$

$$A = 0.75 \text{ in}$$

The elemental volume stress state is described by the Mohr's Circle as shown in Figure 2-8. The resulting stress on the element due to applied load of 7,500 lbs is:

$$\sigma_{x'} = F / A$$

$$\sigma_x = 7{,}845 / .75 \text{psi}$$

$$\sigma_x = 10{,}460 \text{ psi}$$

The maximum shear stress on the element is then:

$$\tau_{\max} = \sqrt{\left[\frac{(\sigma_{x'} - \sigma_{y'})}{2}\right]^2 + \tau_{x'y'}^{\ 2}}$$

$$\tau_{\max} = \sqrt{\left[\frac{(10{,}460 - 0)}{2}\right]^2 + 0^2}$$

$$\tau_{\max} = 5{,}230 \text{ psi}$$

Shear tear-out of the hole is not expected since $\tau_{\max} = 5{,}230$ psi $< \tau_{allowx} = 18{,}000$ psi.

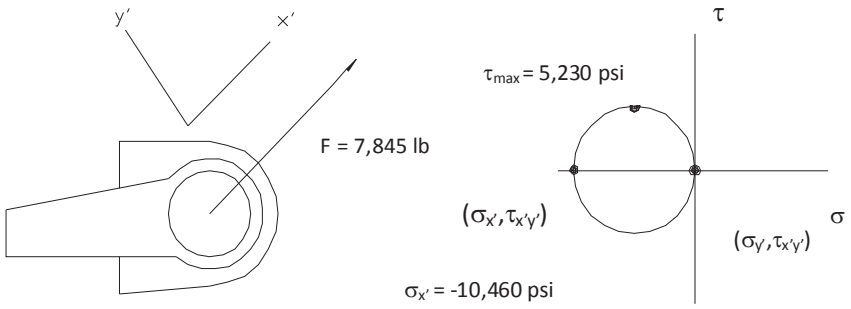

Figure 2-8 Hole Tear-out Model and Mohr's Circle Stress State

The weld attaching the lift plates to the Outerpack shell are required to demonstrate that they are adequate to preclude local weld yielding. The analysis assumes that one of the wire ropes is non–functional and three of the four welds bear the lifting load. The weld shear stress is found by $\tau_{weld} = F/A$, where F is the applied vertical or horizontal load and A is the weld area. The assumed weld area is:

$A = hl \sin 45$, where l is (.75)(10.625+8") = 13.97" from Figure 2-6, and h is the weld thickness, 0.105".

The applied loads are F_x = 6,794 lbs in the vertical direction and Fy = 3,923 in the horizontal direction. The weld stresses are then:

$$\tau_x = F_x/A \quad \text{and} \quad \tau_y = F_y/A$$

Substituting values,

$\tau_x = 6{,}794/(.105)(13.97)(.707)$ psi

$\tau_x = 6{,}551$ psi, and

$$\tau_y = F_y \big/ A$$

$\tau_y = 3{,}923/(.105)(13.97)(.707)$ psi

$\tau_y = 3{,}783$ psi

The stresses τ_x and τ_y are perpendicular to each other, and the resulting weld shear stress is:

$$\tau = \sqrt{\left(\tau_x^{\,2} + \tau_y^{\,2}\right)}$$

$$\tau = \sqrt{(6{,}551^2 + 3{,}783^2)}$$

$\tau = 7{,}565$ psi

The welds are sufficient to prevent local yielding since $\tau_{\max} = 7{,}565$ psi $< \tau_{allowx} = 12{,}000$ psi.

Traveller STD Four Point Lift – The Traveller STD package may be crane lifted using a 4-point lift with attachment points located on the inner stacking bracket. Figure 2-9 shows sample STD packages with the lifting configuration. The assumed sling angle is 45° since the inner lifting brackets are utilized. The applied load is $F_l = 27{,}000$ lb from Section 2.12.3.2.1. The methodology is the same as for the Traveller XL since the load path and structure is assumed nearly identical. However, the force components are greater:

$$F = \frac{F_l}{4} \Big/ \sin 45$$

$$F = \frac{27{,}000}{4} \Big/ .707 \text{ lb/hole}$$

$F = 9{,}546$ lb/hole

.

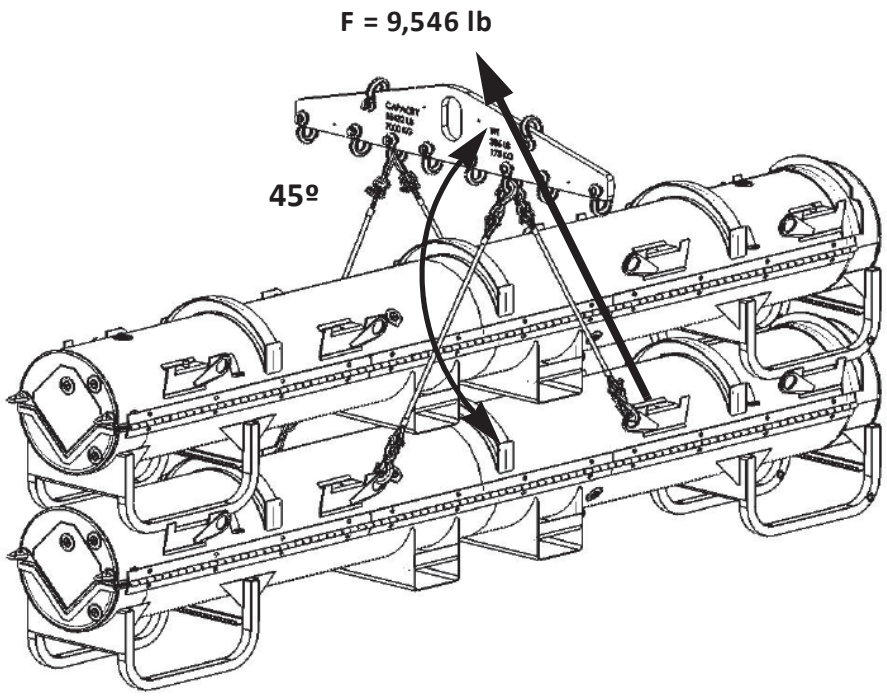

Figure 2-9 Traveller STD Stacked Lifting Configuration

Substituting into the force component geometric relationships:

$$F_x = Fy = 6{,}750 \text{ lb}$$

These resultant forces result in the following hole tear-out and weld shear loads using the same equations shown for the Traveller XL and substituting Traveller STD values:

Hole tear-out

$$\tau_{\max} = 6{,}364 \text{ psi}$$

Shear tear-out of the hole is not expected since $\tau_{\max} = 6{,}364$ psi < $\tau_{allowx} = 18{,}000$ psi.

Weld Shear

$$\tau = 9{,}205 \text{ psi}$$

The welds are sufficient to prevent local yielding since $\tau_{\max} = 9{,}205$ psi < $\tau_{allowx} = 12{,}000$ psi.

Forklift Analysis – During package lift by a forklift, only the center portion of the package is supported by the forklift extension arms. Consequently, the package is subject to a bending load due to the unsupported weight of the package. The loading conditions include a single Traveller XL and two stacked Traveller STDs.

For the bending evaluation, the Traveller package is conservatively modeled as a cantilever beam with the length equal to half of the overall Traveller length. For XL, L_f = 113.1 inches and the design lifting load is distributed over the length of the package as shown in Figure 2-10a. The outer shell is the only assumed structure of the package carrying the bending load. This calculation is repeated for Traveller STD with L_f = 98.6 inches. The design weights are calculated in Section 2.12.3.2.1. as 15,690 and 27,000 pounds for Traveller XL and two Traveller STD stacked, respectively.

The forklift pockets weldments are also subjected to a shear load during lifting as the forks will apply a normal force along the top plate as shown in Figure 2-10b. Both the Traveller XL and Traveller STD doubled stacked conditions are evaluated.

Bending

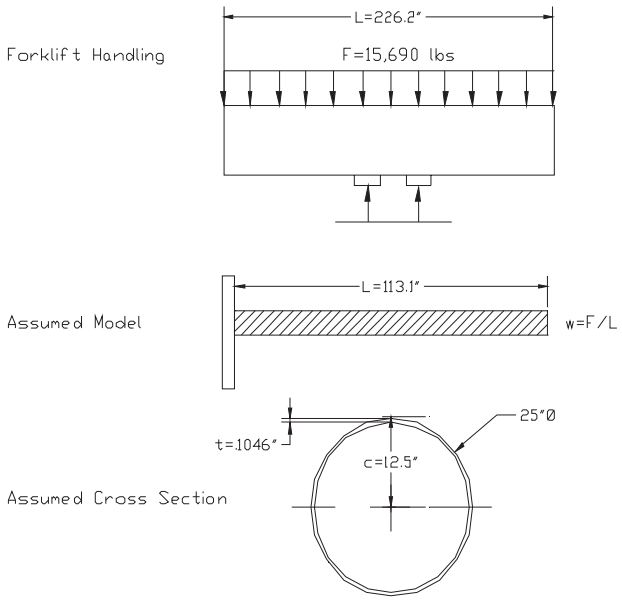

Figure 2-10a Forklift Handling XL Model and Assumed Cross Section

The bending stress can be determined from the classic flexure equation:

$$\sigma = \frac{Mc}{I}$$, where

c is the distance from the neutral axis to the outer fibers, M is the applied bending moment, and I is the moment of inertia of the section.

The applied moment is given by:

$$M = \frac{wL^2}{2}$$

where w equals F/L from Figure 2-10a. The value for w is:

$$w = \frac{F}{L}$$

$$w = \frac{15{,}690}{113.1} \text{ lb/in} = 139 \text{ lb/in}$$

Thus,

$$M = \frac{(139)(113.1)^2}{2} \text{ in-lb}$$

$$M = 889{,}017 \text{ in-lb}$$

The moment of inertia for the shell, I, is calculated as follows:

$$I = \frac{\pi}{4}(R_o^4 - R_i^4)$$

where R_o = 12.5" and R_i = (12.5 – .1046)", R_i = 12.395".

Thus,

$$I = \frac{\pi}{4}(12.5^4 - 12.395^4) \text{ in}^4$$

$$I = 634 \text{ in}^4$$

The bending stress is then:

$$\sigma = \frac{(889{,}017)(12.5)}{634} \text{ psi}$$

$$\sigma = 17{,}528 \text{ psi}$$

Forklift loading is not expected to impact the XL package by bending since $\sigma = 17{,}528$ psi < $\sigma_{yield} = 30{,}000$ psi.

In the case of the Traveller STD stacked:

$$w = \frac{27{,}000}{98.6} \text{ lb/in} = 274 \text{ lb/in}$$

$$M = \frac{(274)(98.6)^2}{2} \text{ in-lb}$$

$$M = 1{,}331{,}909 \text{ in-lb}$$

The bending stress is then:

$$\sigma = \frac{(1{,}331{,}909)(12.5)}{634} \text{ psi}$$

$$\sigma = 26{,}260 \text{ psi}$$

Forklift loading is not expected to impact the STD package by bending since $\sigma = 26{,}260$ psi < $\sigma_{yield} = 30{,}000$ psi.

As previously noted, the model conservatively assumes the outer shell is loaded, and the actual Outerpack structure with foam would provide even greater margin against bending.

Weld Shear

The forklift pocket (Item 01 in Figure 2-10b) weldments are also subjected to a shear load during lifting as the forks will apply a normal force along the top plate (Item 02) bottom surface as shown in Figure 2-10b. There are two cases to be evaluated: Traveller XL and Traveller STD doubled stacked. The applied forces are:

$F_l = 15{,}690$ lb for the Traveller XL

$F_l = 27{,}000$ lb for two Traveller STDs stacked

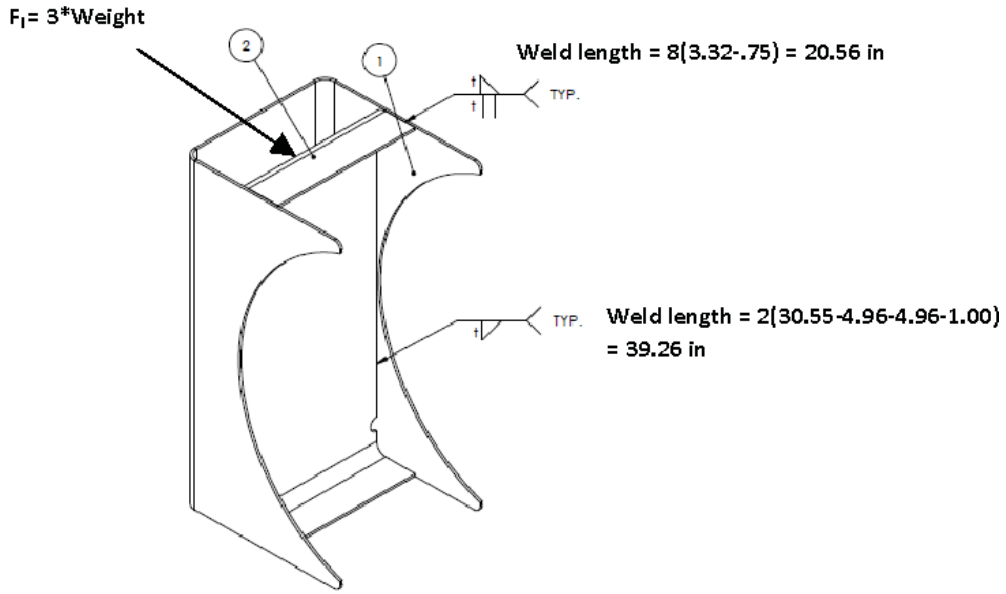

Figure 2-10b Forklift Pocket Weld Detail

The assumed weld area is:

$A = hl \sin 45$, where l is (20.56"+39.26") = 59.82" and h is the weld thickness, 0.105".

The weld stresses are then:

$$\tau_{xL} = {F_{xL}}/{A} \text{ and } \tau_{STD} = {F_{STD}}/{A}$$

Substituting values for Traveller XL,

$$\tau_{xL} = {15{,}690}/{(.105)(59.82)(.707)} \text{ psi}$$

$$\tau_{xL} = 3{,}533 \text{ psi}$$

The welds are sufficient to prevent local yielding since $\tau_{XL} = 3{,}533$ psi < $\tau_{allowx} = 12{,}000$ psi.

Substituting values for Traveller STD,

$$\tau_{STD} = {27{,}000}/{(.105)(59.82)(.707)}$$

$$\tau_{STD} = 6{,}080 \text{ psi}$$

The welds are sufficient to prevent local yielding since $\tau_{STD} = 6{,}080$ psi < $\tau_{allowx} = 12{,}000$ psi.

Bolts

During package lift for fuel loading and unloading, the package is hoisted using the two rings attached to the top nozzle end of the Outerpack top. The hoist rings attach to the Outerpack using two 3/8-16 UNC Grade 8 Medium-Carbon socket head cap screws per hoist ring into a welded nut. The four screws and are subject to shear loading in the most limiting case. The screws are fabricated to a minimum proof load of 120,000 psi. The load per bolt is the design lifting load of 15,690 pounds distributed by the four bolts. Thus, the load per bolt is 3,923 pounds. The allowable axial stress is the yield stress of 120,000 psi and the allowable shear stress is .6Sy, 72,000 psi. The stressed area is 0.0775 in^2. The applied stress is then:

$$\tau = {F}/{A}$$

$\tau = {}^{3,923}\!/_{.0775}$ psi

$\tau = 50{,}619$ psi, which is less than the allowable shear stress of 72,000 psi as well as the axial allowable stress of 120,000 psi and is acceptable.

Coupling Nut

When the package is vertical, the coupling nut will be subject to a shear load. The nut is 3/8-16 and the material is 304 stainless steel. The allowable shear stress is 18,000 psi.

The stressed area of the internal thread is found by:

$A = .7845(D - \frac{.9743}{n})^2$ where D is the nominal diameter 0.375 inches, and n is the number of threads per inch; 16.

$A = .0775$ in^2

The shear area An is found by:

$$An = (3.1416)(n)(Le)(Ds\min)\left[\frac{1}{2n} + .57735(Ds\min - En\max)\right] \text{in}^2$$

where:

n =	16
Le =	0.269
Ds_min =	0.364
En_max =	0.340

Thus, $An = 0.222$ in^2. The shear stress is then:

$\tau = {}^{F}\!/_{A}$

$\tau = {}^{3,923}\!/_{.222}$ psi

$\tau = 17{,}671$ psi, which is less than the allowable material shear stress of 18,000 and is acceptable.

Hoist Ring

After the package is in the vertical position, the hoists will be loaded in tension. The applied tensile stress for normal up-ending is found from $\sigma = P/A$. The load per 3/8 inch diameter hoist ring is:

$P = 15{,}690/2$ lbs

$P = 7{,}845$ lbs

The tensile stress per hoist ring is:

$\sigma = 7{,}845/[2][(\pi)(0.375^2)/4]$

$\sigma = 7{,}845/0.22$ psi

$\sigma = 35{,}659$ ksi.

Since the allowable tensile yield strength is 130 ksi minimum, the hoist ring satisfies the lifting requirements.

2.12.3.2.3 Tie-Down Analysis

The Traveller packages are secured to the transport conveyance by means of strapping across the top of the package(s) and placing a chain inboard from the welded plate at the package legs. Since there are no structural devices designed for tie-down, a tie-down analysis is not required.

2.12.3.2.4 Design Temperature Analysis –40°F (-40°C) and 158°F (70°C)

The materials of construction of the Traveller Outerpack include ASTM A240 Type 304 Stainless Steel for the shells and low density, closed cell polyurethane impact limiter/thermal insulator (10 pcf along the axis, 6 pcf inside the top and lower pillows, and 20 pcf between the top and lower pillows). The Clamshell is comprised of ASTM B209/B221 Type 6005-T5 Aluminum. As demonstrated in the below sections, the package is suitable for transport operations over the required design temperature range.

Brittle Fracture – Aluminum alloys, including 6005-T5 Aluminum, do not exhibit a ductile-to-brittle temperature transition; consequently, neither ASTM nor ASME specifications require low temperature Charpy or Izod tests of aluminum alloys. Thus, brittle fracture of the aluminum components is not expected. Austenitic steels such as 304 Stainless Steel have a Face Centered Cubic (FCC) structure and consequently exhibit a ductile-to-brittle transition at cryogenic temperatures near -297°F (-183°C). Thus, brittle fracture of the stainless steel components is not expected.

Mechanical Properties For Design Temperature Range – The range of tensile and yield strength of 6005 series Aluminum over the design temperature range will not preclude the package from performing its intended design function. Figure 2-11 provides the temperature dependent yield and tensile strengths typical for a 6000-series aluminum up to approximately 212°F (100°C). Furthermore, the recommended operating temperature of aluminum alloys for structural applications is up to a temperature of 400°F (204°C), which is well below the maximum design temperature of 158°F (70°C).

The range of tensile and yield strength of 304 stainless steel over the design temperature range will not preclude the package from performing it intended design function. Figure 2-12 provides the temperature dependent yield and tensile strengths for 304 SS up to approximately 194°F (90°C).

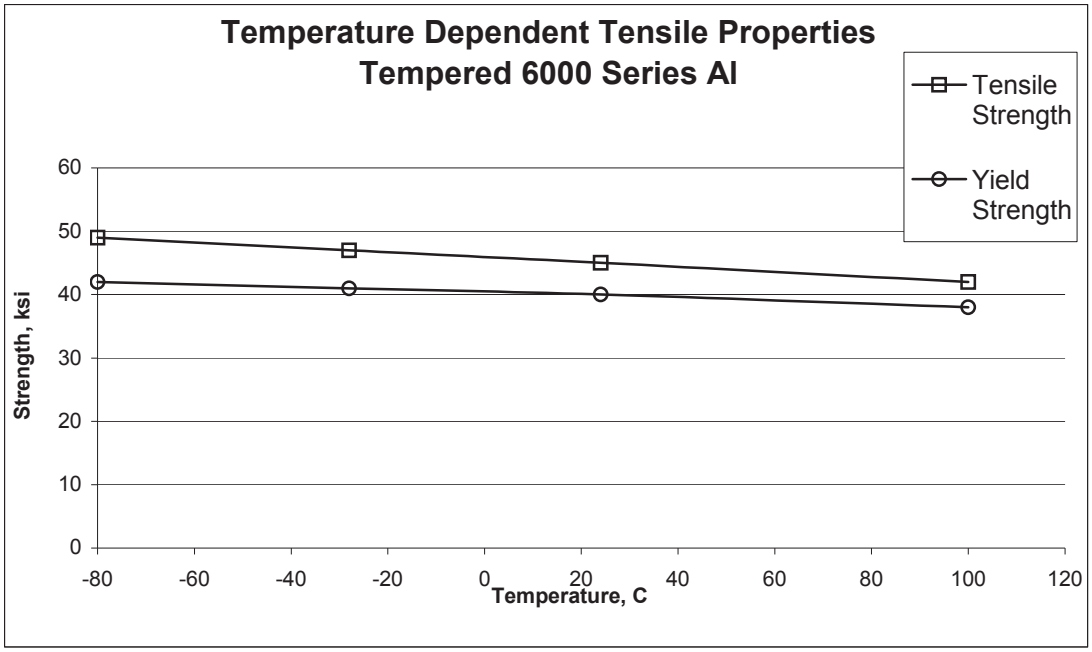

Figure 2-11 Typical Temperature Dependent Tensile Properties for Tempered 6000 Series Al

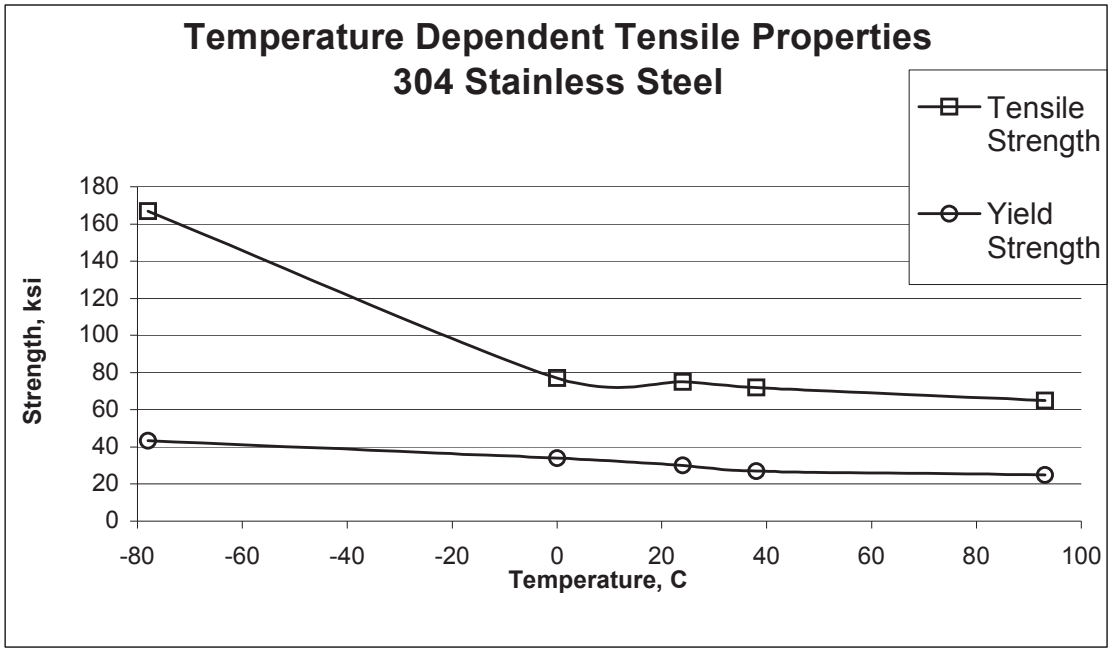

Figure 2-12 Temperature Dependent Tensile Properties for 304 SS

Temperature Evaluation of Foam – The foam is used as a crushable impact limiter and a special thermal insulator. This section only considers the mechanical properties since the thermal functions are evaluated in Section 3, Thermal Evaluation. The foam exhibits a general increase in compressive strength as temperature decreases. Figures 2-13, 14 and 15 show the compressive strength for the 10 pcf (pound per cubic foot), 20 pcf, and 6 pcf foam as a function of temperature, respectively. Of interest is the area under each temperature curve from 0-60% strain (the recommended energy absorption operation range of the foam). For each foam density, the temperature range considered does not significantly impact the energy absorption characteristics. Also, Figures 2-15 show that the compressive strength difference between –29°C and 24°C are relatively similar indicating at -40°C the behavior of the foam will not significantly change. Figure 2-16 provides the temperature dependent strength of each foam density at 10% strain from -54°C to 82°C. The curves show essentially a linear increase in crush strength as temperature decreases. Therefore, the impact properties of the foam are acceptable for use in the temperature range from -40°F (-40°C) to 158°F (70°C).

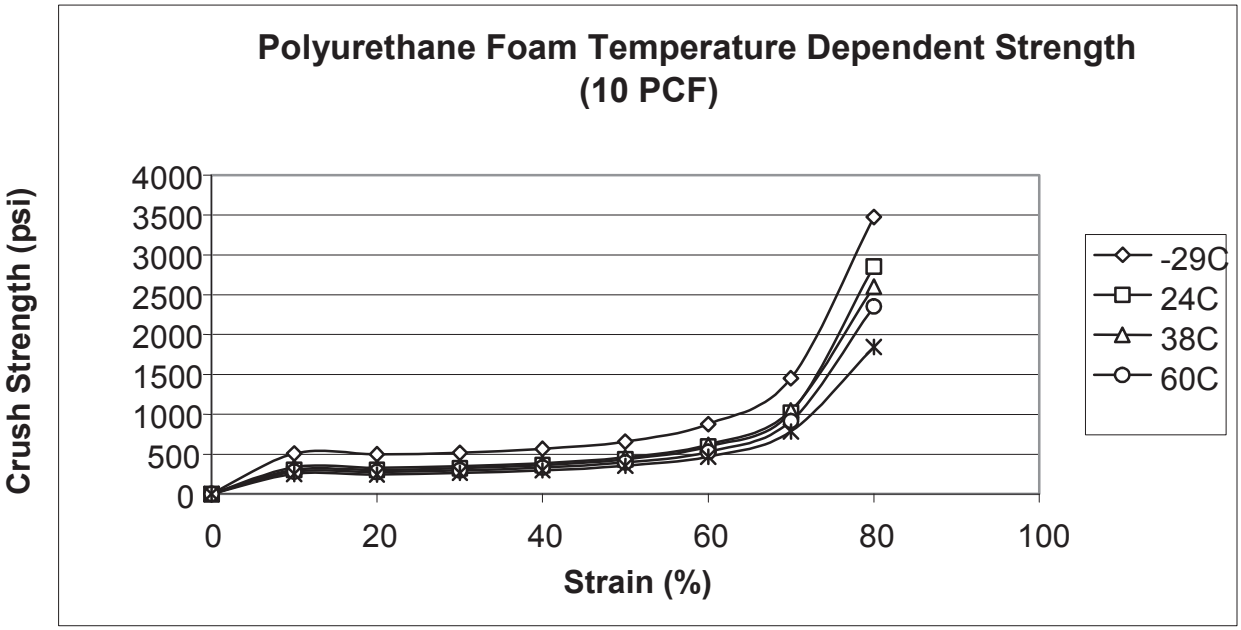

Figure 2-13 Temperature Dependent Crush Strength for 10 PCF Polyurethane Foam

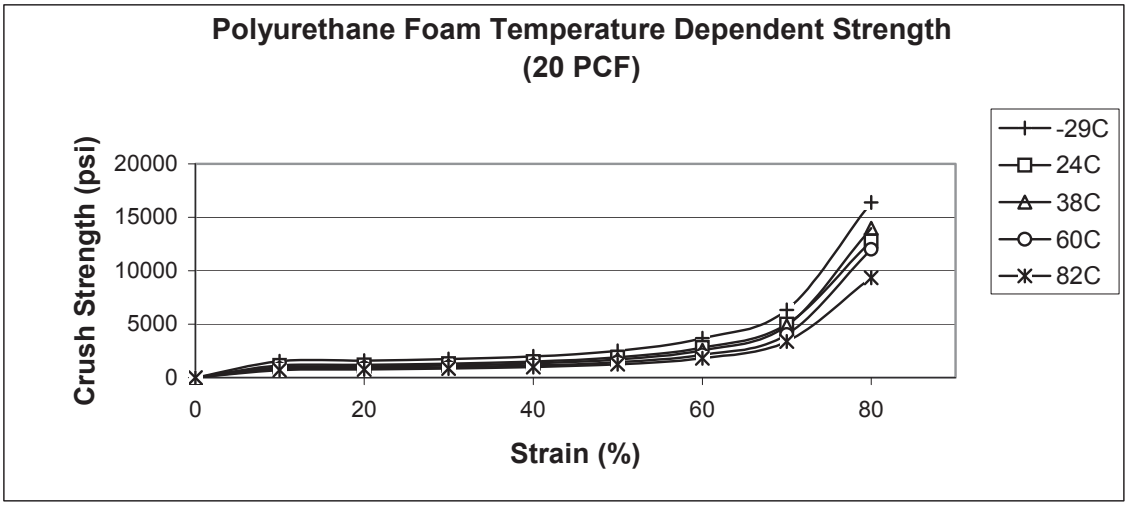

Figure 2-14 Temperature Dependent Crush Strength for 20 PCF Polyurethane Foam

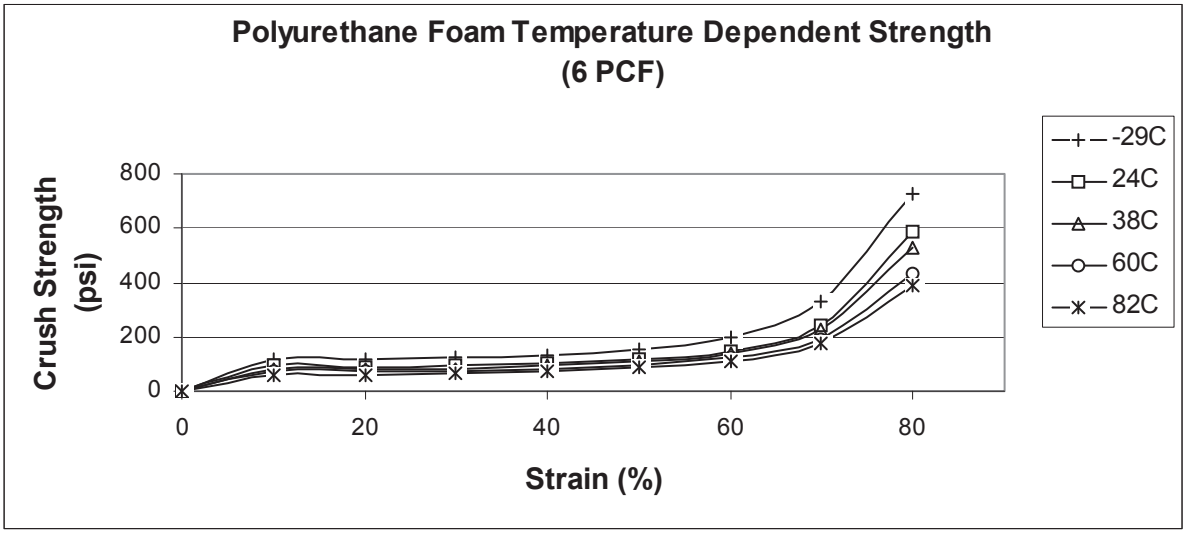

Figure 2-15 Temperature Dependent Crush Strength for 6 PCF Polyurethane Foam

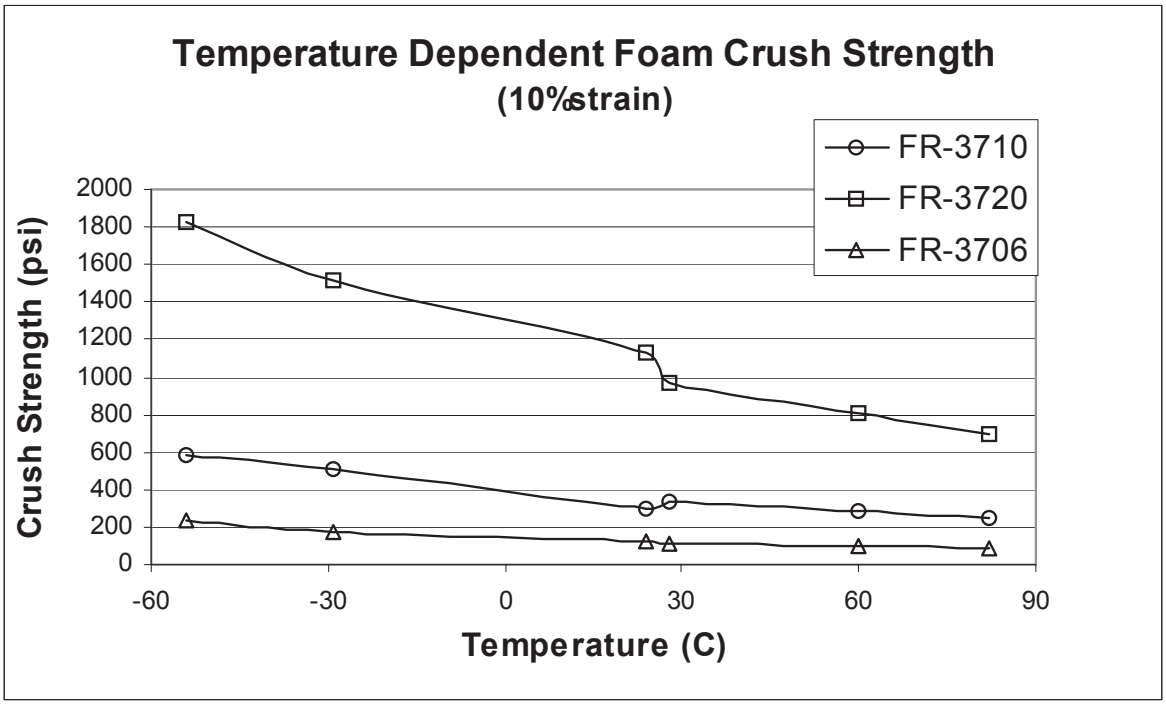

Figure 2-16 Temperature Dependent Crush Strength for Traveller Foam at 10% Strain

Differential Thermal Expansion – Differential thermal expansion (DTE) is expected to only impact the fuel assembly and Clamshell interface. The Outerpack is not under physical constraints and can accommodate thermal growth. Differential thermal expansion between the foam and the stainless steel shells of the Outerpack is easily accommodated by the elastic properties (low modulus value) of the foam.

However, the Ultra-high Molecular Weight (UHMW) polyethylene does have a significantly higher coefficient of thermal expansion (CTE) when compared to 304 stainless steel. For this reason, the moderator panels are segmented along their lengths to accommodate the differential thermal expansion between the polyethylene and the inner stainless steel shells of the Outerpack. Holes in the polyethylene segments are used to attached the panels to the inner Outerpack shells using threaded studs. These studs must not be loaded by the individual panel differential thermal expansion, or contraction. For this reason, each hole drilled into the polyethylene panel is significantly large to preclude thermally induced stresses in the bolt studs. The following calculation addresses this case.

The polyethylene moderator blocks are attached by 0.375 inch diameter weld studs on the inner skin of the on the Outerpack. The weld studs penetrate the moderator blocks through 0.563 inch diameter holes). The blocks are mounted with a nominal gap, block to block, of 0.260 inches. The coefficients of thermal expansions are:

- 304 stainless steel 9.6 ì in/in-F
- UHMW polyethylene 72 – 111 ì in/in-F

Using the worst difference in expansion coefficients, 100 ì in/in-F, the gaps between the blocks will accommodate heat up from 70° to 167°F. In addition, there is an additional 0.094 inch of clearance between the weld studs and each side of the holes in the polyethylene that will allow blocks with less than nominal clearance to slide in a direction to provide uniform clearance along the length of the Traveller.

Because the polyethylene's coefficient of expansion is much greater than stainless steel, interference between moderator blocks is not an issue when temperature drops. Instead, it is the interference between the blocks and the weld studs. Based on nominal clearances and a maximum distance of 17.0 inches from outboard hole-to-outboard hole, the package temperature can drop from 70°F to -41°F before the polyethylene is stressed. Most of the moderator blocks have significantly smaller distances between the outboard holes (6.5 to 12.5 inches) allowing them to accommodate larger temperature changes.

See Licensing drawings for additional details.

Analyzing the DTE between the fuel assembly and the Clamshell is evaluated assuming fuel loading is performed at 70°F (21°C) and shipped to a cold environment of -40°F (-40°C) since the aluminum will tend to contract more than the fuel assembly. The thermal growth is found by the familiar equation:

> $\Delta L = \alpha(\Delta T)L_o$, where ΔL is the total growth, L_o CS is the original length of the Clamshell (202 inches), $L_{o\ FA}$ is the original length of the fuel assembly (188.86 inches, per drawing 1453E86), ΔT is the temperature change (110°F), and α is the coefficient of thermal expansion.
>
> For Aluminum, α = 13 μin/in-°F. For Zircalloy, α = 2.79 μin/in-°F.

The differential thermal growth between the Clamshell and the fuel assembly is then:

DTE = $\{\Delta L = \alpha(\Delta T)L_{oCS}$ Al $\}$- $\{\Delta L = \alpha(\Delta T)L_{oFA}$ Zirlo$\}$

= {13e-6x110x202} inches- {2.79e-6x110x188.86} inches

= 0.29-0.058 inches

Thus,

DTE =0.23 inches (the fuel assembly grows 0.23 inches relative to the Clamshell).

The combined thickness of the base cork rubber and axial clamp cork rubber is 0.50 inches and can accommodate the growth due to differential thermal expansion. Thus, DTE is not a concern. Since the total differential growth associated with the XL Clamshell is greater than the STD Clamshell, it is the bounding calculation.

2.12.3.2.4.1 Internal/External Pressure

The Traveller package utilizes silicone foam rubber seals to preclude dust and other contaminants from entering the package. These seals are not continuous, and do not form an airtight pressure boundary. The package does not maintain a boundary between pressure gradients and is not designed to be pressurized during transport. Thus, internal/external reduced pressure will not impact the structural integrity of the package.

2.12.3.2.4.2 Vibration

The package must be evaluated to consider the effects of normal vibration on the design performance. The isolation system is designed to dampen normally induced vibrations from transport, and is not fundamental to the safe operation of the package. However, the Outerpack must maintain its structural integrity during transport to maintain a safe transport condition. Typical package attachment to a transport conveyance for the Traveller includes nylon straps or chain mounted both over the package and on the gusset tray connected to the support legs pointed inboard. The loading configuration can be modeled as a simply supported beam. Furthermore, the Outerpack is conservatively modeled considering only the outer shell at the first mode of vibration. The typical natural frequency range for transportation vehicles, $f_{nat\ TRANS}$, is 3.7-8 Hz . The natural frequency of the Outerpack can be determined from.

$$f_{natOP} = a\sqrt{(EIg/l^3)/m}$$

where a=1.57 (primary mode coefficient assuming hinge-hinge end conditions for additional conservatism), E=29.4E6 psi, I=634 in^4, m = 2,834 pounds, g = 386.4 in/s^2 and l = 226.2 in (distance from gusset tray to gusset tray). Substituting values:

$$f_{natOP} = 1.57\sqrt{[(29.4E6)(634)(386.4)/(226.2)^3]/(2{,}834)}\ 1/s\ (Hz)$$

$$f_{natOP} = 1.57\sqrt{220} \text{ Hz}$$

$$f_{natOP} = 23 \text{ Hz}$$

Since the natural frequency of the Outerpack is greater than the natural frequency typical of a transportation vehicle, resonance of the Outerpack is not expected and normally induced vibrations will not preclude the package from performing its design function.

2.12.3.2.5 Water Spray

The Traveller Outerpack is cylindrical, and shaped so that water will not be collected. Since the shell is fabricated of 304 SS, the water spray will not impact the structural integrity of the package.

2.12.3.2.6 Compression/Stacking test

The Traveller package must demonstrate elastic stability for a 5 g static load. No credit is taken for the circumferential stiffeners or the forklift support tubes. The analysis assumes the stacking load is uniformly distributed over the four outermost stacking brackets on the Outerpack. Figure 2-17 depicts the shell compression/stacking model.

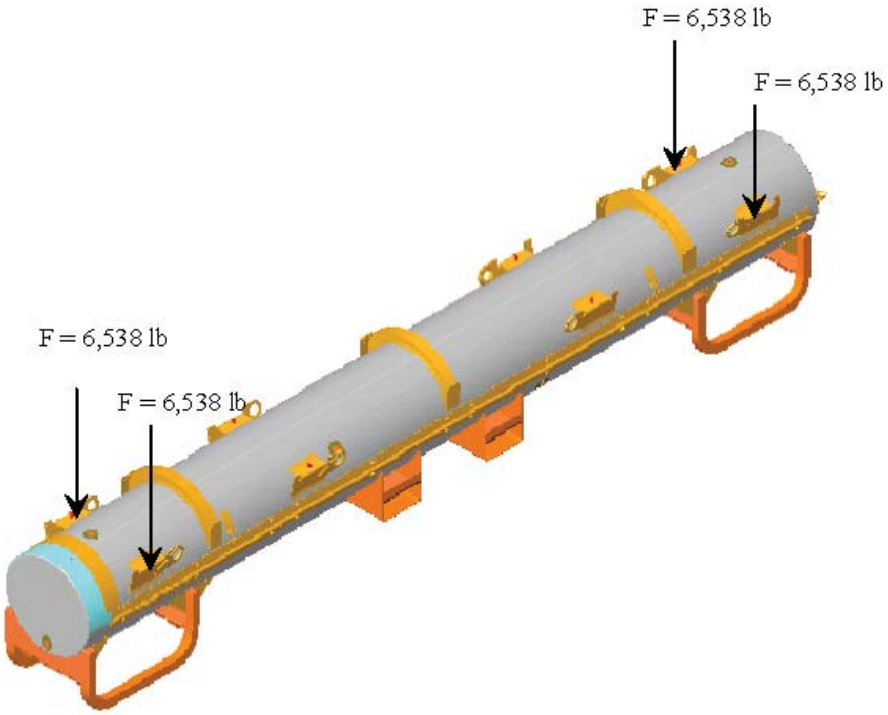

Figure 2-17 Compression/Stacking Requirement Analysis Model

The applied stacking force for the stacking test was determined to be:

Fs = 26,150 lb from Section 2.12.3.2.1.

The load path is assumed to follow through the welds of the stacking brackets, through the Outerpack side, and then to the leg supports. This assumption is based on the package stacking configuration or the placement of weight on the package top. Each loaded section will be analyzed for its structural integrity.

Stacking Bracket – The stacking bracket is expected to experience a shear load on the weld during stacking. The loading configuration for a single bracket is shown in Figure 2-18.

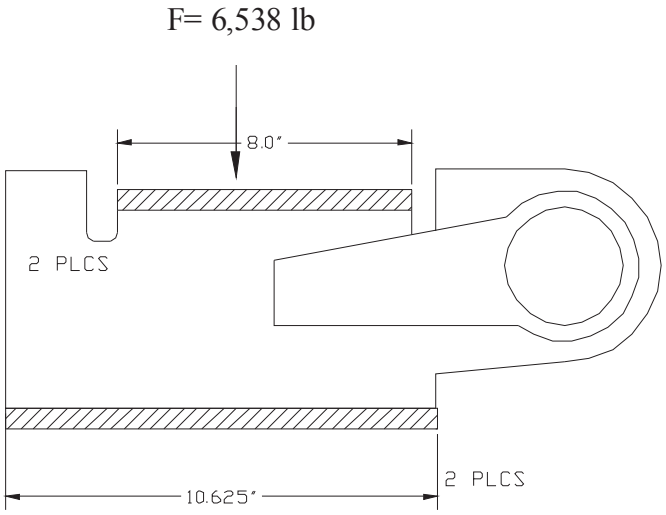

Figure 2-18 Stacking Force Model on Stacking Bracket

The load on each stacking bracket is found by dividing the applied load of 26,150 pounds by the four brackets that support the load:

F = 26,150 lb

F = 6,538 lb

The weld shear stress is found by $\tau_{weld} = F/A$, where F is the applied vertical or horizontal load and A is the weld area. The assumed weld area is the total weld area of each bracket and is found by:

$A = hl \sin 45$, where l is (10.625" + 8") = 18.625" from Figure 2-18 and h is the weld thickness, 0.105".

The weld stress is then:

$$\tau = F/A$$

Substituting values,

τ = 6,538/(.105)(18.625)(.707) psi

τ = 4,729 psi, which is less the allowable weld shear stress of 12 ksi.

2.12.3.2.6.1 Outerpack Section

The stacking bracket is expected to experience a compressive load through the package side cross section during stacking as the force follows the projected load path The loading configuration and model for the Outerpack section is shown in Figure 2-19.

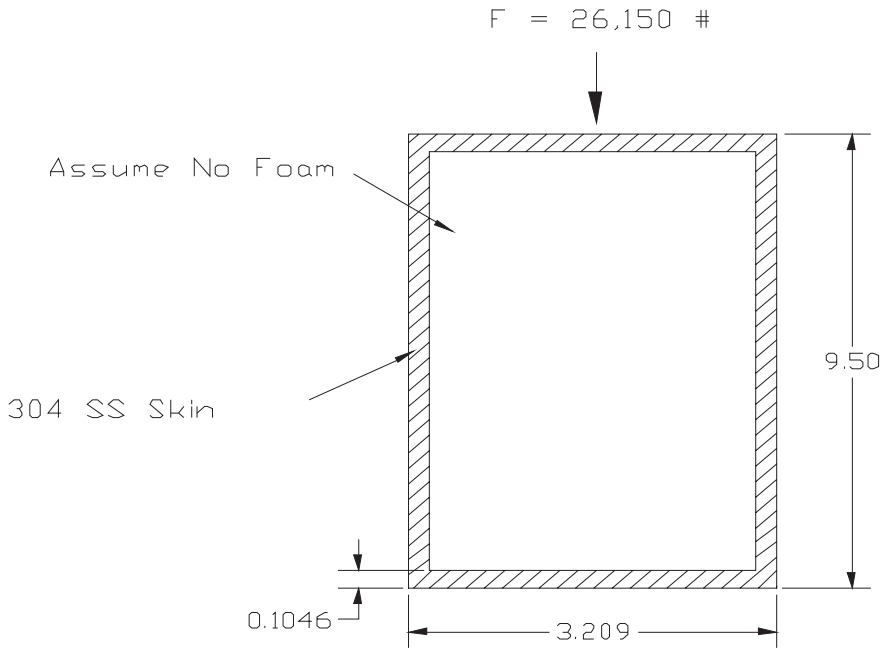

Figure 2-19 Outerpack Section Compression Model

The evaluation first examined the slenderness ratio of this section to determine if buckling is applicable. The model conservatively assumed no structural credit for the foam. In addition, the model assumed the force path section is from the base of the stacking bracket to the top of the support leg. The cross section consisted of a rectangular section of dimensions 9.50" x 3.209" with a wall thickness of 0.1046". The critical buckling load will be calculated and compared to the actual load to determine elastic stability of the Outerpack section.

The slenderness ratio, SR, can be expressed as:

$$SR = l / k$$

where l is the effective length, 9.50 inches, and the radius of gyration, k, is:

$$k = \sqrt{I / A}$$

For the Outerpack section, the moment of inertia, I, and the cross section area, A are:

$$I = \left(wl^3 - w_i l^3{}_i\right)/12 \text{ in}^4$$

$$I = \left(3.209\{9.50\}^3 - 3.0\{9.29\}^3\right)/12 \text{ in}^4$$

$$I = 28.8 \text{ in}^4$$

$$A = wl - w_i l_i \text{ in}^2$$

$$A = \left(3.209\{9.50\} - 3.0\{9.29\}\right) \text{ in}^2$$

$$A = 2.62 \text{ in}^2$$

Thus, the value for k is:

$$k = \sqrt{28.8 / 2.62} \text{ in}$$

$$k = 3.32 \text{ in}$$

The corresponding slenderness ratio is then:

$$SR = 9.50 / 3.32 \text{ in/in}$$

$$SR = 2.86$$

The limiting slenderness ratios for columns are as follows:

Long Columns

$\left(l/k\right)_1 = \sqrt{\frac{2\pi^2 CE}{\sigma_y}}$ where the end condition C is conservatively assumed to be unity, E is Young's Modulus, and σ_y is the tensile yield stress.

Substituting values:

$$\left(l/k\right)_1 = \sqrt{\frac{2\pi^2 (29.4E6)}{30000}}$$

$$\left(l/k\right)_1 = 139$$

Short Columns

$$\left(l/k\right)_2 = .282\sqrt{\frac{Al^2}{\pi^2 I}}$$

Substituting values:

$$\left(l/k\right)_2 = .282\sqrt{\frac{2.62(9.50)^2}{\pi^2 28.8}}$$

$$\left(l/k\right)_2 = .257$$

Thus, .257< 2.86 (SR) < 139 and the Outerpack section is considered an intermediate column. The critical load for this column is given by:

$$P_{cr} = A(\sigma_y - \left\{\frac{\sigma_y}{2\pi}\frac{l}{k}\right\}^2 \frac{1}{CE})$$

$$P_{cr} = 2.62(30000 - \left\{\frac{30000}{2\pi}\frac{9.50}{3.32}\right\}^2 \frac{1}{29.4E6})$$

$$P_{cr} = 78{,}583 \text{ lb}$$

Since the actual load of 26,150 pounds is less than the critical buckling load of 78,583 pounds, the Outerpack section is considered stable during compression from stacking.

2.12.3.2.6.2 Leg Support

The leg support is expected to experience a compressive load through the straight top cross section during stacking as the force follows the projected load path The loading configuration and model for the leg support section is shown in Figure 2-20. There are eight (8) leg sections of 2"x2"x.120" 304 SS tubing of approximately 10" length, The expected load for each leg section is 26,150/8 pounds, or 3,269 pounds.

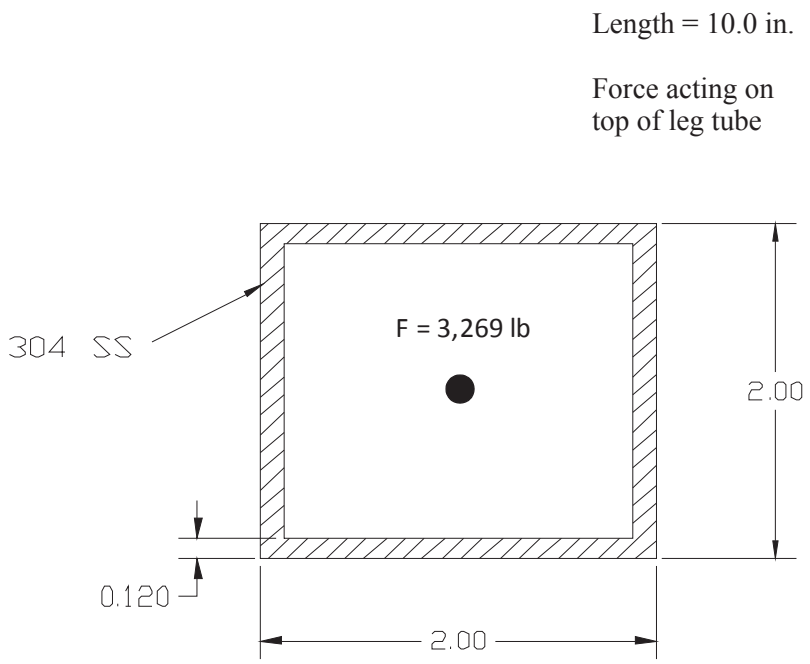

Figure 2-20 Leg Support Section Compression Model

The evaluation will first consider the slenderness ratio of this section to determine if buckling is applicable. The critical buckling load will be calculated and compared to the actual load to determine elastic stability of the leg support section.

The slenderness ratio, SR, is:

$$SR = l / k$$

where l is the effective length, 10.0 inches, and the radius of gyration, k, is:

$$k = \sqrt{I/A}$$

For the Outerpack section, the moment of inertia, I, and the cross section area, A are:

$$I = \left(wl^3 - w_i l^3{}_i\right)/12 \text{ in}^4$$

$$I = \left(2.0\{10.0\}^3 - 1.76\{10.0\}^3\right)/12 \text{ in}^4$$

$$I = 20 \text{ in}^4$$

$$A = wl - w_i l_i \text{ in}^2$$

$$A = \left(2.0\{10.0\} - 1.76\{10.0\}\right) \text{ in}^2$$

$$A = 2.4 \text{ in}^2$$

Thus, the value for k is:

$$k = \sqrt{20/2.4} \text{ in}$$

$$k = 2.9 \text{ in}$$

The corresponding slenderness ratio is then:

$$SR = 10.0/2.9 \text{ in/in}$$

$$SR = 3.4$$

The limiting slenderness ratios for columns is:

Long Columns

$\left(l/k\right)_1 = \sqrt{\dfrac{2\pi^2 CE}{\sigma_y}}$ where the end condition C is conservatively assumed to be unity, E is Young's Modulus, and σ_y is the tensile yield stress.

Substituting values:

$$\left(l/k\right)_1 = \sqrt{\frac{2\pi^2 (29.4E6)}{30000}}$$

$$\left(l/k\right)_1 = 139$$

Short Columns

$$\left(l/k\right)_2 = .282\sqrt{\frac{Al^2}{\pi^2 I}}$$

Substituting values:

$$(l/k)_2 = 0.282\sqrt{\frac{2.4(10.0)^2}{\pi^2 20}}$$

$$(l/k)_2 = .31$$

Thus, .31< 3.4 (SR) < 139 and the leg support section is considered an intermediate column. The critical load for this column is:

$$P_{cr} = A(\sigma_y - \left\{\frac{\sigma_y}{2\pi}\frac{1}{k}\right\}^2 \frac{1}{CE})$$

$$P_{cr} = 2.4\left(30{,}000 - \left\{\frac{30{,}000}{2\pi}\frac{10.0}{2.9}\right\}^2 \frac{1}{29.4E6}\right)$$

$P_{cr} = 71{,}978$ lb

Since the actual load of 3,269 pounds is less than the critical buckling load of 71,978 pounds, the leg support section is considered stable during compression from stacking.

2.12.3.2.7 Penetration

The penetration test can be characterized as a localized impact event on the outer skin of the Outerpack. The energy imparted onto the outer skin is equal to the potential energy of the falling pin:

$PE = mgh$, where the mass of the pin is 13 lb and the drop height is 40 inches. To obtain correct units of energy, the gravitational constant g_c must be used in the energy equation. Thus,

$$PE_{penetration} = \frac{(13)(40)(32.2)}{32.2} \text{ in-lb (ft*s2)/ft*s2}$$

$$PE_{penetration} = 520 \text{ in-lb.}$$

By comparison, the energy locally imparted to the outer skin from the pin-puncture drop test is determined from the dropped package mass and the drop height. The mass of the package is 5,230 lb, and the drop height is 40 inches. Thus,

$$PE_{pin} = {mgh}/{g_c} = mh$$

PE_{pin} = (5,230)(40) in-lb.

PE_{pin} = 209,200 in-lb.

Pin puncture drop tests have demonstrated that the outer skin was not perforated as a result of impact onto the pin. Since the impact energy of the pin puncture drop test is approximately 400 times greater than that of the pin penetration, the pin puncture drop test bounds the pin penetration. Thus, the pin penetration impact is not expected to result in any significant structural damage to the Outerpack.

2.12.3.2.8 Immersion Analysis

The Traveller package uses acrylic fiberglass seals for thermal protection and to preclude dust and other contaminants from entering the package. The seals are not continuous around the perimeter of the package and do not form a pressure boundary. In the event of water submersion, the inner portion of the package will fill with water creating equal hydrostatic pressure on the Outerpack and Clamshell surfaces. This condition would not result in a stress gradient through the Outerpack or Clamshell. Thus, immersion will not impact the structural integrity of the package.

2.12.4 DROP ANALYSIS FOR THE TRAVELLER XL SHIPPING PACKAGE

The primary method for evaluating the performance of the Traveller under hypothetical accident condition scenarios was actual testing of full-scale prototype packages. During the development program eighteen drop tests were conducted using a variety of orientations. Most of the drops were from greater than 9m. The drop tests are summarized in Table 2-5 and reported in detail in Section 2.12.4.

To supplement the actual test data, a finite element analysis (FEA) study was conducted using two models that were developed for the Traveller XL package. The first FEA model was based on the design of the two prototypes that were tested in January 2003. The second FEA model was based on the design of the two Qualification Test Units that were tested in September 2003. The QTU (actual package and FEA model) incorporated the modifications that were made to the design as a result of the prototype test results.

The objectives of the drop analysis effort were:

- Demonstrate that the first model acceptably predicted actual test results. This was accomplished by comparing the permanent mechanical deformations that resulted from the actual prototype drops with those predicted by the FEA model.

- Assist in the evaluation of test results. Because the FEA prototype model acceptably predicted actual test results, it could be used with confidence as a tool to evaluate possible changes to the packaging design in order to finalize a design that would pass the hypothetical drop tests.

- Assist in planning final tests. The FEA results, combined with the data obtained by prototype drop testing, were used to establish drop orientations for the qualification test unit (QTU) and certification test unit (CTU) tests.

Limitations were observed in the FEA process. For example, mesh density limitations meant that actual stress and strain predicted values could not be considered highly accurate. The models could identify regions of high stress and strain but could not accurately predict component failure unless predicted values were significantly above or below failure points. Instead, the models were developed to evaluate relative deformations, decelerations and energy absorption between drop orientations. The analyses provided a qualitative means for comparing predicted stresses and strains for different drop orientations to allow intelligent selection of drop orientations for testing. The Traveller program utilized extensive full-scale tests to prove the acceptability of the Traveller design. These tests results are described in sections 2.12.4 below and the results are compared with the FEA in this section.

2.12.4.1 Conclusion and Summary of Results

2.12.4.1.1 Conclusion

Analysis indicates that the Traveller XL shipping package complies with 10 CFR 71 and TS-R-1 requirements, respectively for all drop orientations. Test orientations which are most challenging are a 9 meter vertical drop with the bottom end of the package hitting first as shown in Figure 2-52A and a 9 meter

CG-forward-of-corner drop onto the TN end of package with an 18° forward rotation, Figures 2-44 and Figure 2-45. The former has the greatest potential to damage the fuel assembly and the latter is most damaging to the shipping package itself. Based on this analysis, successful drop tests in these two orientations are adequate to demonstrate that the Traveller XL design meets/exceeds the HAC drop test requirements.

2.12.4.1.2 Summary of Results

Analyses were conducted for horizontal side drops, center-of-gravity-over-corner onto the top nozzle drops, and vertical drops onto the top nozzle and bottom nozzle. A significant amount of analytical data is presented in the following sections. Below is an summary of the major points in the order presented:

Determination of Most Damaging Orientations

- The most damaging orientation for the outerpack may not be most damaging for the fuel assembly. Because of the robust design of the packaging, drop orientations that were most damaging to the fuel assembly took precedence.

- Analysis of drop orientations most damaging to the outerpack focused on three orientations: horizontal drop onto the side, vertical end drop (top and bottom nozzle end), and near-vertical drop (center-of-gravity over corner).

- Analysis of drop orientations most damaging to the fuel assembly focused on the vertical end drop (top and bottom nozzle end).

Most Damaging Orientations to Outerpack

- Horizontal drop onto the side gave highest predicted outerpack loads.

- CG forward of corner onto top predicted to be most damaging to outerpack because of potential damage that might compromise package ability to survive the thermal test.

- Damage to the Traveller XL shipping package from the HAC drop tests is predicted to be minor and primarily involves localized deformations in the region of impact. Both the Outerpack and Clamshell structures remain intact and closed.

Most Damaging Orientations to Fuel Assembly

- Bottom nozzle end drop predicted to be more damaging than top nozzle end drop.

- Fuel assembly damage is predicted to be confined to the top or bottom region depending on drop orientation. This damage primarily involves localized buckling and deformation of the nozzles.

Temperature and Foam Density Effects

- Temperature and foam density have a minor effect on drop performance of the Traveller XL package.

- For the orientation predicted most damaging to the Outerpack, a package with nominal foam density and dropped at "normal temperature" (75°F) experiences 8.5 and 13.7% higher loads than, respectively, one containing low density foam and dropped at 160°F or one containing high density foam and dropped at -40°F, Figure 2-62.

- Fuel assemblies in packages containing the highest allowable density foam and dropped at the lowest temperature extreme will experience accelerations that are very similar to those in packages with lowest allowable density foam and dropped at the highest temperature extreme, Figure 2-63. However, the accelerations at these extremes are only 5% greater than for a package dropped at 75°F containing nominal density foam.

- Bottom nozzle end drop predicted to be more damaging than top nozzle end drop.

Pin Puncture

- Analysis indicates that the Traveller XL is capable of withstanding the 1 m pin puncture test. The steel outer skin should not be ruptured.

- A maximum indentation of 67 mm is predicted for the 1 m pin puncture test when the package is impacted from underneath and dropped horizontally with its CG directly above the pin. during this test.

Comparison of Prototype Test Results to Analysis Predicted Results.

- There was good overall agreement between predicted and actual drop performance. This is evident by comparisons of predicted and actual permanent deformations, failed parts, and measured and predicted accelerations at specific positions on the Outerpack and Clamshell.

Bolt Factor-of-Safety Calculations.

- The Traveller XL shipping package will survive the HAC drop tests in any orientation with few or no closure bolt failures. Horizontal side drops onto the hinges or latches, Figures 26A and B, result in the highest hinge/latch bolt loads. The analyses indicate ten ¾-10 stainless steel bolts/side are sufficient to ensure the Outerpack remains closed during such drops. The miminum predicted factor of safety for the Outerpack latch and hinge bolts is 1.12.

[Rev 2 redistributed this information in Section 2.12.3.1 above.]

2.12.4.2 Predicted Performance of the Traveller Qualification Test Unit

2.12.4.2.1 Most Damaging Drop Orientations

A primary objective of this study was to determine the worst case drop orientation(s) for the HAC drop tests. This requirement is to drop test the shipping package in orientations that most damage: a) the shipping package, and b) the fuel assembly. It was quickly realized that the most damaging orientation for the shipping package, would not necessarily be the same for the fuel assembly. Based on the robust performance of the Traveller XL drop units during testing, orientations that were most severe to the fuel assembly became more significant.

Determination of the worst case orientation for the shipping package was facilitated by the Traveller XL computer analysis and results of the prototype tests. Many orientations can be eliminated from consideration due to inherent design features of the Traveller. For example, the circumferential stiffeners on the upper Outerpack, and the legs/forklift pocket structure, Figure 2-21, greatly reduce the crushing of the Outerpack since they crush prior to impact of the main body of the Outerpack. Drop orientations where one or the other

of these structures directly contacts the drop pad, Outerpack damage is reduced in comparison to orientations where these features are not impacted. This is because the energy absorbed in crushing these features cannot be absorbed by the Outerpack.

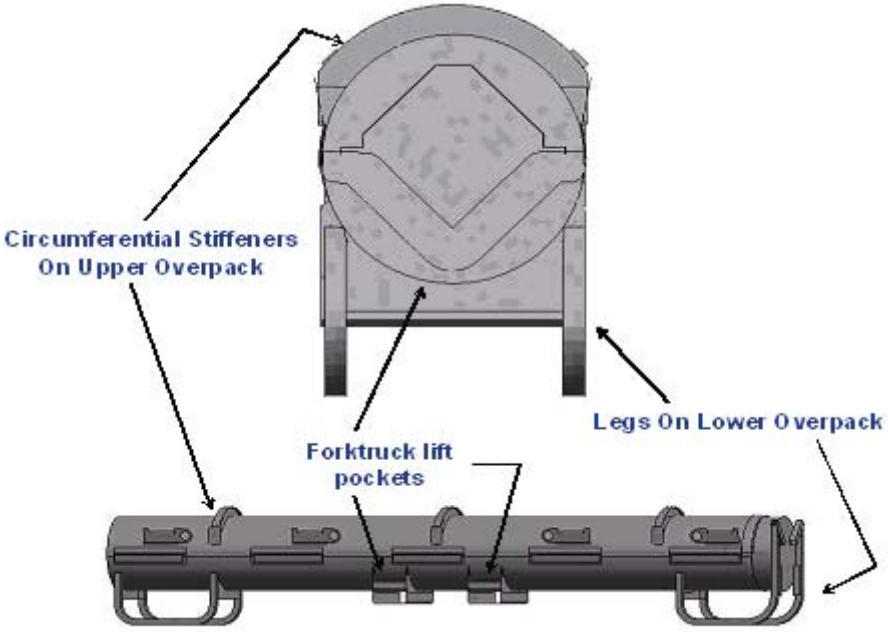

Figure 2-21 Traveller Stiffeners, Legs, and Forklift Pockets

Test results supported this hypothesis. Indeed, in the two available tests of relevance, these features absorbed almost all the energy and very little damage was incurred by the Outerpack. For example, Prototype-1, Test 1.1 was a low angle slap down test resulting in extensive crushing of the upper Outerpack stiffeners, Figure 2-22. Aside from this crushing, very little Outerpack damage was incurred. Prototype-2, Test 3.2 was the second example. In this test, the Outerpack was dropped horizontally onto its legs from 9 m. This resulted in significant crushing of the Outerpack legs and feet, Figure 2-22B, and the forklift supports, not shown. However, the Outerpack was otherwise not significantly damaged.

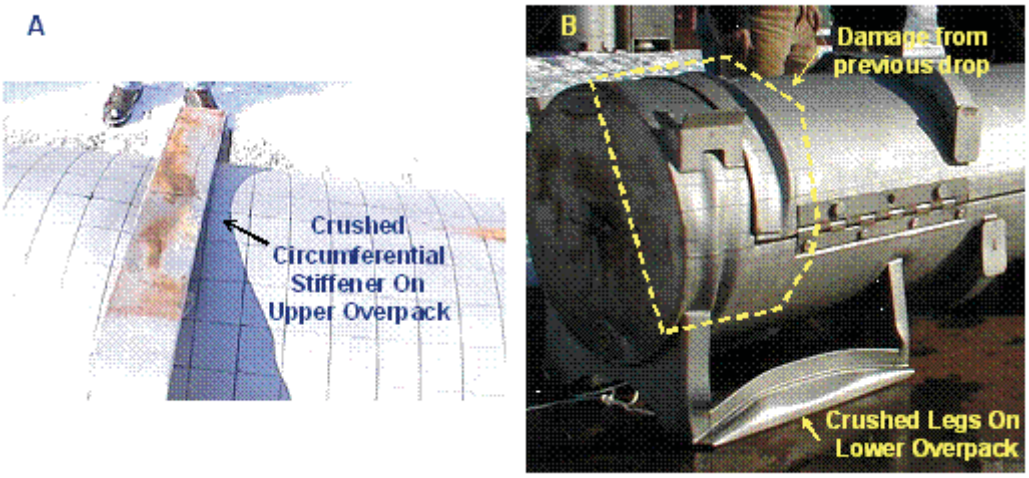

Figure 2-22 Results of Prototype Drop Test

Alternately, neither the stiffeners, nor legs hit first for orientations in which the Outerpack ZX plane defined in is perpendicular to the impact surface, Figure 2-23. Such orientations include side drops or slap downs onto the hinged sides of the Outerpack and vertical drops onto the either end of the package. Thus, our analysis of the most damaging Outerpack orientations focused on these orientations.

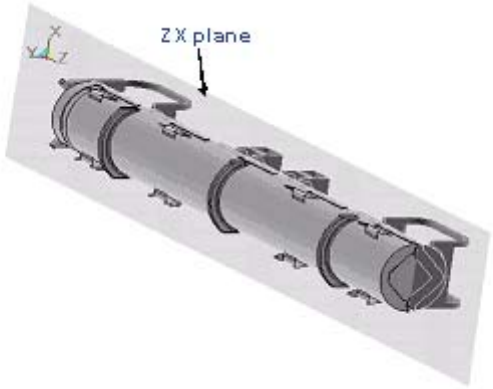

Figure 2-23 Side Drop Orientation

Determining which drop orientations in the ZX plane most damage the shipping package was also facilitated by the Traveller XL design itself. In particular, “slap down” drops, low- to medium-angle impacts where one end of the package hits before the other, as shown in Figure 2-24, divide the impact energy primarily between the top and bottom impact limiters. Generally, this energy is absorbed in a manner that induces relatively little damage for this design. An example of the damage associated with a 15° slap down is shown in Figure 2-25. This figure reflects the damage obtained in Test 1.1 of the Prototype test campaign.

Figure 2-24 Low Angle Drop Orientation

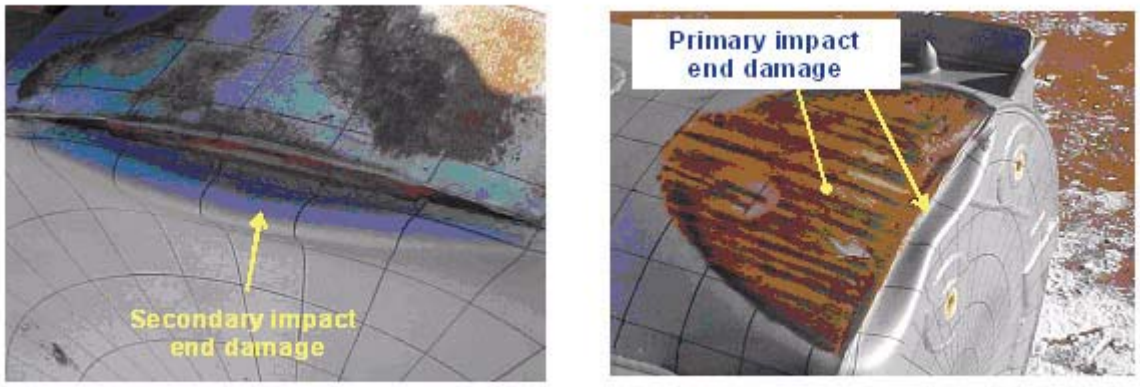

Figure 2-25 Damage from Prototype Low Angle Drop (Test 1.1)

The shipping package may be dropped in some orientations outside the ZX plane and still not be protected by its stiffeners and legs/forklift pocket structure, Figure 2-21. In vertical and nearly vertical orientations, the impact limiter will hit the drop pad first. In these cases, the primary impact energy may be entirely absorbed by the impact limiters and Outerpack walls with little, if any, being channeled into the stiffeners or legs. Indeed, the stiffeners and legs provide no benefit unless the shipping package actually falls over for a secondary impact.

Thus, analysis of orientations most damaging to the Outerpack was focused on horizontal drops onto the Outerpack side (i.e., onto the hinges/latches), vertical drops (onto either end of the package) and nearly vertical drops.

2.12.4.2.2 Horizontal Side Drops

The two possible orientations for a horizontal side drop test involve either a drop onto the opening or latched side of the Outerpack, Figure 2-26A, or a drop onto the permanently (or semi-permanently) hinged side, Figure 2-26B.

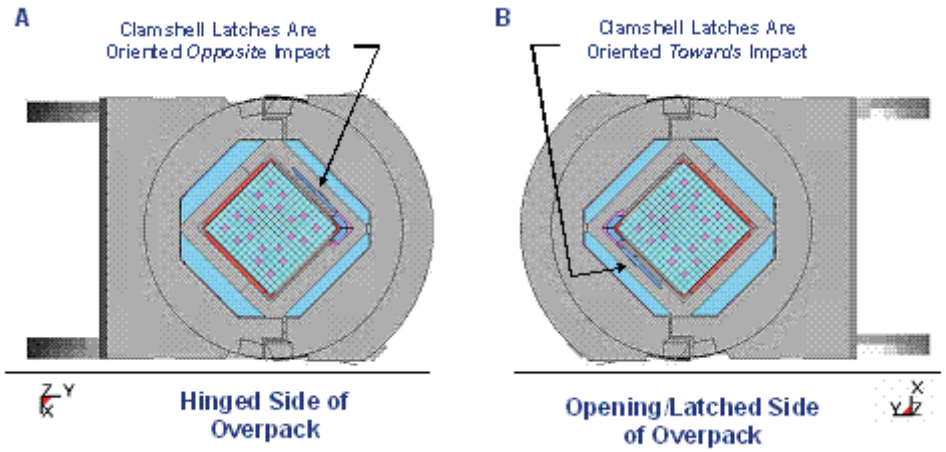

Figure 2-26 Horizontal Drop Orientation

Energy and Work Histories – Global energy and work for the Outerpack horizontal side drops are shown in Figures 2-27 and 2-28. The similarity of these two drops is reflected in these plots. Both plots (as do all the 9.14m (30ft) drops reported herein for the qualification unit) have an initial total energy (TE) of 204 kJ. This value correctly reflects the initial velocity (v) of 13.4 m/s applied to the 2,270 kg (5,005 lb) package mass (m) since our simulation is initiated at the end of Outerpack free fall from 9.14 m (30 ft.); the total energy is comprised only of kinetic energy (KE), and $KE = \frac{1}{2}mv^2$. Total energy remains nearly constant throughout both drop simulations. This reflects the relatively small overall deformations predicted for this drop, i.e., the almost negligible external work done by the package under gravity loading. In both simulations, the event was essentially completed within 10 milliseconds as seen by the flattening of the kinetic energy and internal energies after that time. Moreover, acceptable levels of hourglass, sliding, and stonewall energies were obtained although the sliding energy ultimately reached 10% of the internal energy. This latter issue is not critical since it occurs after the maximum Outerpack/drop pad force has been reached.

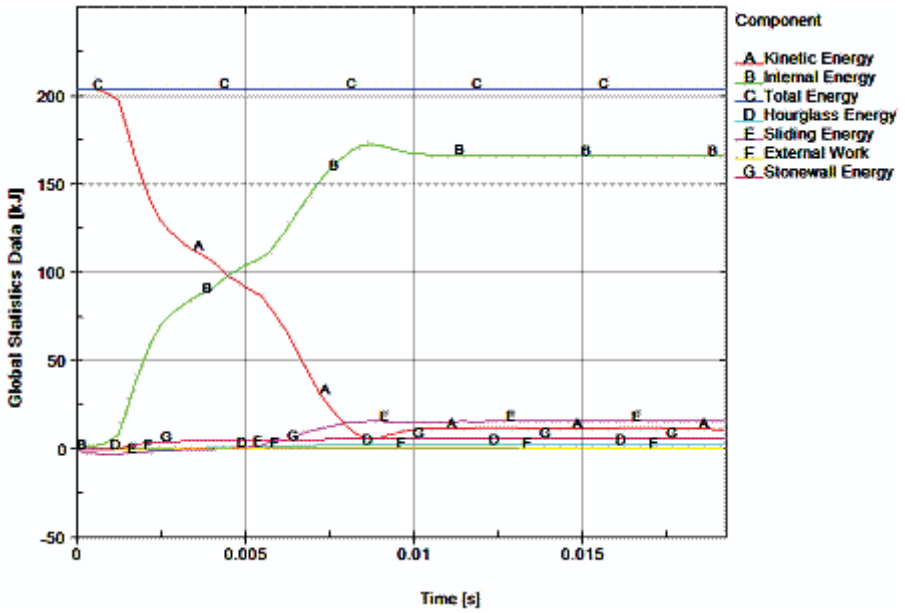

Figure 2-27 Predicted Energy and Work for 9m Horizontal Drop Onto Outerpack Hinges

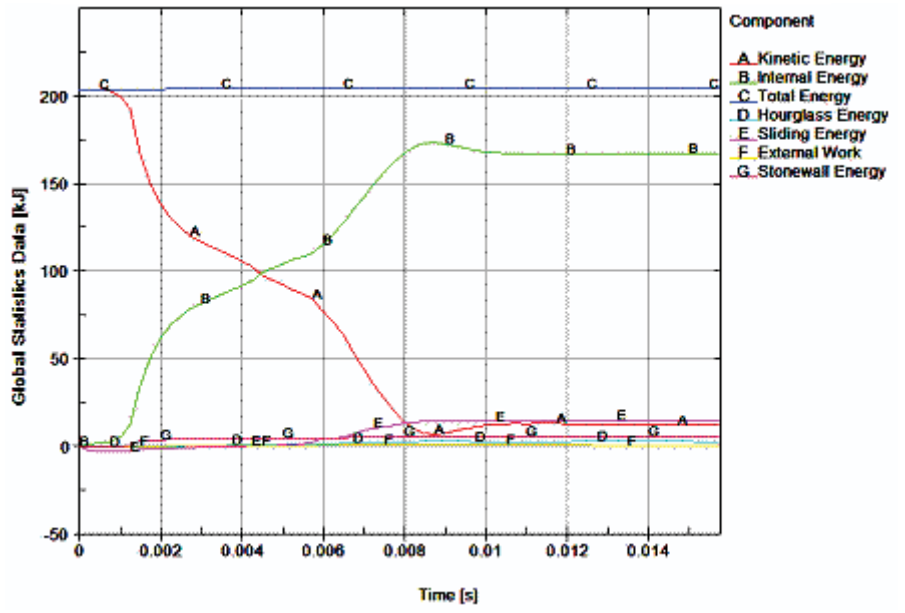

Figure 2-28 Predicted Energy and Work Histories for a 9m Horizontal Drop Onto the Outerpack Hinges

Rigid Wall Forces – Neglecting the very soft shock mounts that tie them together, the Traveller XL shipping package consists of an essentially de-coupled Outerpack and Clamshell/fuel pair. Indeed, the predicted drop scenario consists of the Outerpack crushing onto the pad while the Clamshell/fuel assembly continues falling until it hits the inner surfaces of the Outerpack. Then the Outerpack, Clamshell, and fuel assembly crush further onto the pad. This scenario is reflected in the rigid wall force history shown in Figure 2-29.

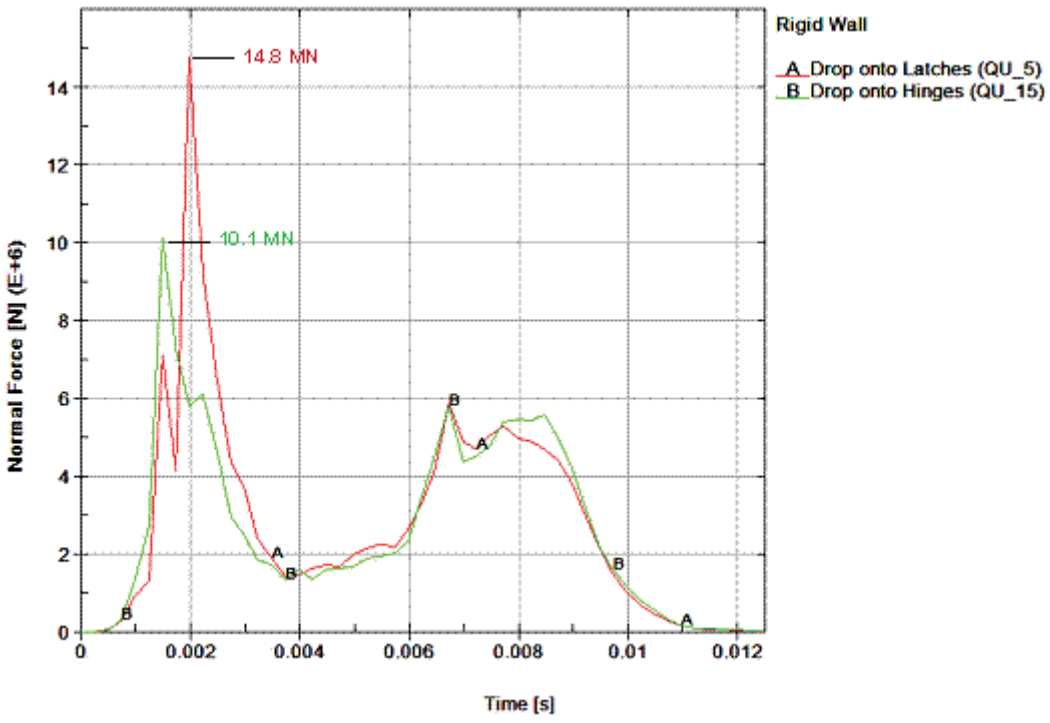

Figure 2-29 Predicted Rigid Wall Force Histories for 9m Horizontal Drops Onto the Outerpack Latches and Hinges

In Figure 2-30A, the initial impact between the Outerpack and pad is seen in the first 4 milliseconds, peaking at approximately 1.5 milliseconds for the drop onto hinge (run QU_15) and 2.0 milliseconds for the drop onto latches (run QU_5). This disparity is attributed to slight errors in the model geometrical definition (rather than to any actual non-symmetry within the design itself). Further, we postulate resolution of this disparity would lower the predicted forces for the drop onto Outerpack latch simulation (run QU_5) and increase those for the simulated drop onto the Outerpack hinges (run QU_15). However, we choose not to resolve this difference but simply used the QU_5 predictions as a bounding and conservative case. At approximately 4.0 milliseconds, the force between the Outerpack and drop pad has decreased and it appears the Outerpack might soon rebound. However, the Clamshell/fuel assembly then contacts the inner surface of the Outerpack and drives it into back into the drop pad, Figure 2-30B.

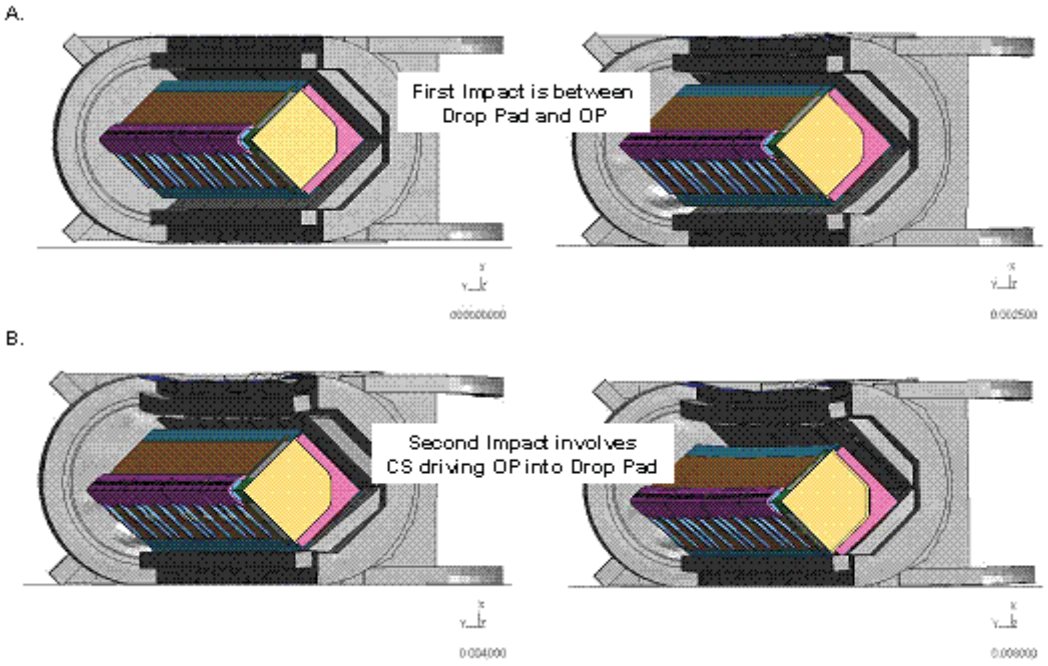

Figure 2-30 De-coupled Impacts for 9 m Horizontal Side Drop

The forces between the Outerpack and drop pad during the first portion of a horizontal side drop are the highest predicted forces for any orientations analyzed. However, these forces are so high because the deformations (i.e., cushioning) are small. Thus, despite the high forces, the package (Outerpack and Clamshell) should be relatively undamaged provided its components remain closed. For the Outerpack, this requires that the majority of the Outerpack latch/hinge bolts do not fail. In the case of the Clamshell, the latch bolts, the top and bottom end plate bolts, and, as will be described, the lipped/groove interfaces between the Clamshell end plates themselves (top end) and between the Clamshell doors and plate (bottom end) must not be comprised. During Prototype testing the robustness of these features was confirmed, as no Outerpack bolts failed, and the Clamshell latches remained closed.

Note that the Clamshell cross-sectional shape is predicted to stay essentially unchanged during the horizontal side drops, Figure 2-30. This is due in large part to the moderator blocks which form a "cradle" for the Clamshell. These moderator blocks prevent the Clamshell from radically changing shape as might otherwise happen since three of the Clamshell edges are either hinged or latched. This is an important structural benefit of the conformal shape of the interior of the Outerpack.

Outerpack Hinge Bolts – The Outerpack hinges are secured to the Outerpack with Type 304 stainless steel bolts, Figure 2-31. The bolts securing the bottom flange of the hinge (or latch) to the lower Outerpack are not removed during normal operation. Thus, the number of bolts used in this area is not critical from a user/operation standpoint. However, the bolts securing the top half of the latch to the upper Outerpack must be removed whenever the package is opened. Thus, the desire is to minimize the number of these bolts while

still insuring the package is not compromised during HAC drop tests. As such, the development of the Traveller XL design started with three 7/8" diameter (2.2 cm) for each hinge segment. A total of five (5) hinge segments per Outerpack side were utilized. The second Prototype unit therefore was tested with only 2 of 3 bolts in each hinge section (10 per side) to verify that design margins were present in the design.

Based on the successful testing of 10 bolts per side, evaluations were initiated to determine if smaller ¾" diameter (1.91 cm) bolts had sufficient strength to sustain impact loads. These were shown to be acceptable. The QTU-1 and QTU-2 units were dropped with ten ¾" (1.91 cm) bolts on each side.

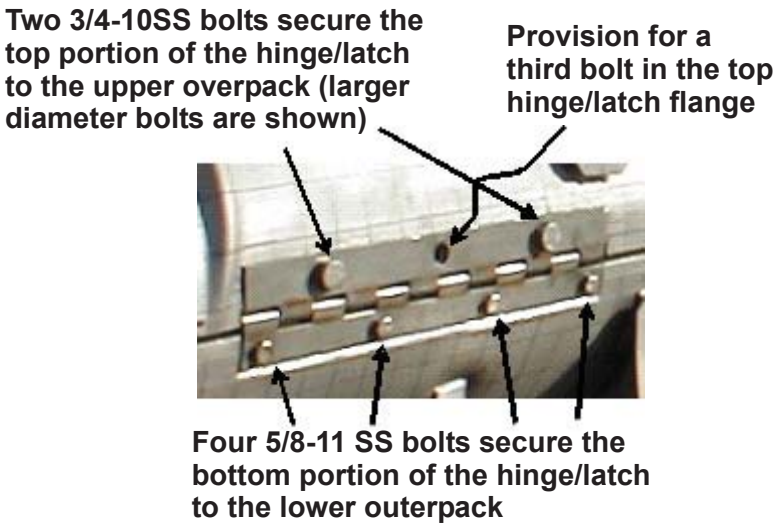

Figure 2-31 Bolts on Prototype Outerpack

Prototype-2, Test 3.3 was a side drop in which two 7/8-9 stainless steel bolts were used to secure the top portion of the hinge to the upper Outerpack and four 5/8-11 stainless steel bolts were used to secure the bottom hinge flange to the lower Outerpack. In this test, no bolts were broken. Our analyses indicate two ¾-10 stainless steel bolts/latch and hinge are sufficient to insure the Outerpack remains closed during the 9m side drop. This is seen by reviewing the predicted safety factors of the top latch bolts when the package is dropped on its latching side, Figure 2-26B. As shown in Table 2-10, the minimum factor-of-safety (FS) for the top Outerpack latch bolts was 2.15 based on the bolt minimum tensile (125 ksi). This minimum was calculated for a latch bolt when the Outerpack was dropped onto its latched side, Figure 2-26B.

Table 2-10 Top Outerpack Latch Bolt Minimum Factors of Safety (FS) for 9m Side Dropped		
ID (Figure 2-32)	FS/Time	
	Dropped On OP Latches (Figure 2-30B)	Dropped On OP Hinges (Figure 2-30A)
B917	2.22/0.0082 s	2.20/0.0077 s
B921	**2.15/0.0065 s**	2.21/0.0065 s
B923	2.16/0.0065 s	2.17/0.0065 s
B927	2.20/0.0062 s	2.18/0.0065 s
B929	2.19/0.0057 s	2.19/0.0062 s
B933	2.19/0.0067 s	2.20/0.0077 s
B935	2.20/0.0067 s	**2.16/0.0065 s**
B939	2.18/0.0065 s	2.18/0.0065 s
B941	2.21/0.0085 s	2.23/0.008 s
B945	2.32/0.0045 s	2.43/0.0045 s

Figure 2-32 Bolt Labels for Right Outerpack

Hinge bolt FS for horizontal 9m side drops on the latched and hinged side of the Outerpack are shown in Table 2-10. If the shipping package were exactly symmetrical, FS for the hinge bolts calculated for a drop on the Outerpack hinges would correspond with those for the latch bolts when the package was dropped onto the latches, etc. However, this was not the case as can be seen by comparing the results shown in Table 2-10 with those in Table 2-11. This small irregularity is primarily attributed to slight errors in the model geometrical definition and to a lesser extent on actual non-symmetry within the design itself. The analysis indicates little likelihood of compromising the Outerpack closure during a 9m side drop.

Table 2-11 Top Outerpack Hinge Bolt Minimum Factors of Safety (FS) for 9m Side Drop		
ID (Figure 2-33)	FS/Time	
	Dropped On OP Latches (Figure 2-30B)	Dropped On OP Hinges (Figure 2-30A)
B947	2.34/0.0025 s	2.20/0.0077 s
B951	3.05/0.0027 s	2.21/0.0065 s
B953	2.58/0.0022 s	2.17/0.0065 s
B957	2.93/0.0022 s	2.18/0.0065 s
B959	2.82/0.0017 s	2.19/0.0062 s
B963	3.19/0.0017 s	2.20/0.0077 s
B965	2.52/0.0022 s	**2.16/0.0065 s**
B969	2.22/0.0117 s	2.18/0.0065 s
B971	2.52/0.0055 s	2.23/0.008 s
B975	2.54/0.0032 s	2.43/0.0045 s

For the CTU and production designs, minor changes to the design were made to improve burn test performance, as well as simplify manufacturing. To ensure a conservative design, two additional bolts were added on each side of the Outerpack full-length hinge sections. Therefore, the CTU and production packages utilize 12 bolts per side per hinge leaf. This change allowed the reduction of the planned high strength (125 ksi ultimate strength) bolt to be replaced with a lower strength bolt, since there are more bolts, and since the 70 ksi bolts were marginal in performance. It should also be noted that the Prototype-2 package was dropped on its side from 9 m and showed no visible signs of strain on any of the bolts. One explanation for this may be that friction is ignored in the calculation of bolt factors of safety.

The increase in number of bolts, 20%, (= 12/10) and the increase in strength of the allowable bolt material, ASTM A193 Class 1 B8, of 7% (= 75 ksi/70ksi – 1) causes the factors of safety of the worst bolt in a side drop to be reduced from 2.15 to 1.12. Since this is the greatest loading for any orientation, all bolts have an adequate safety margin.

Figure 2-33 Bolt Labels for Left Outerpack

Clamshell Keeper Bolts – The inner Clamshell is restrained during shipment by eleven (11) quarter-turn latches as shown in Figure 2-34. This design was incorporated after Prototype testing, primarily for improved handling characteristics. One half of the latch, the latch handle, is welded to the one Clamshell door hinge. The portion of the latches which is physically turned to allow opening and closing is attached to the opposite door is called the "keeper." Each keeper is attached to the Clamshell door with ½-13 stainless steel bolts.

Factors-of-safety for the Clamshell keeper bolts are shown in Table 2-12. The analyses indicate that these bolts are unlikely to fail during side drops onto either the Outerpack latches or Outerpack hinges. Further, the modeling of the fuel assembly as a rigid structure likely makes little difference to these predictions since the fuel rods would not be expected to buckle in this drop orientation.

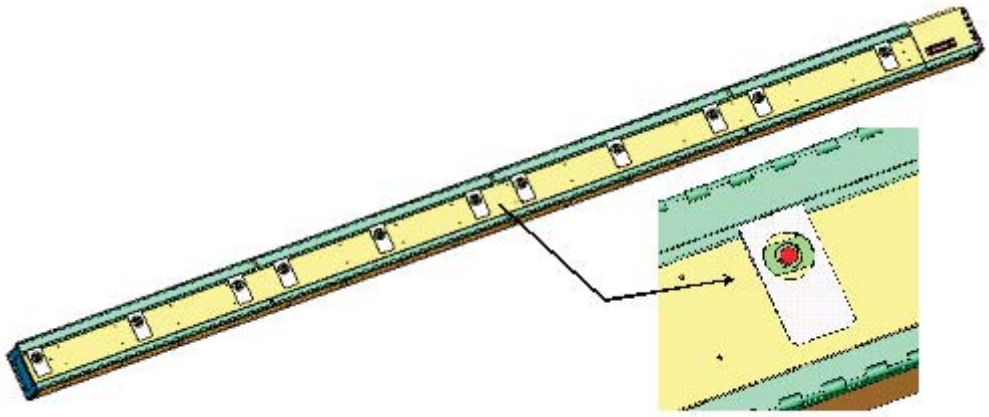

Figure 2-34 Clamshell Closure Latches and Keeper Bolts

Table 2-12 Clamshell Keeper Bolt Minimum Factors of Safety for 9m Side Drop		
ID (Figure 2-35)	FS/Time	
	Dropped On OP Latches (Figure 2-30B)	Dropped On OP Hinges (Figure 2-30A)
B6271277	2.10/0.0067 s	**1.72/0.006 s**
B6271278	2.15/0.007 s	**1.72/0.0085 s**
B6271279	3.17/0.0062 s	3.36/0.0075 s
B6271280	2.12/0.0072 s	4.40/0.01 s
B6271281	2.90/0.008 s	4.03/0.0092 s
B6271282	2.50/0.0082 s	2.48/0.0067 s
B6271283	3.70/0.0055 s	2.16/0.0067 s
B6271284	2.56/0.007 s	1.84/0.0062 s
B6271285	**1.93/0.0072 s**	2.64/0.008 s
B6271286	2.62/0.0072 s	3.00/0.0082 s
B6271287	1.94/0.0075 s	2.29/0.0082 s

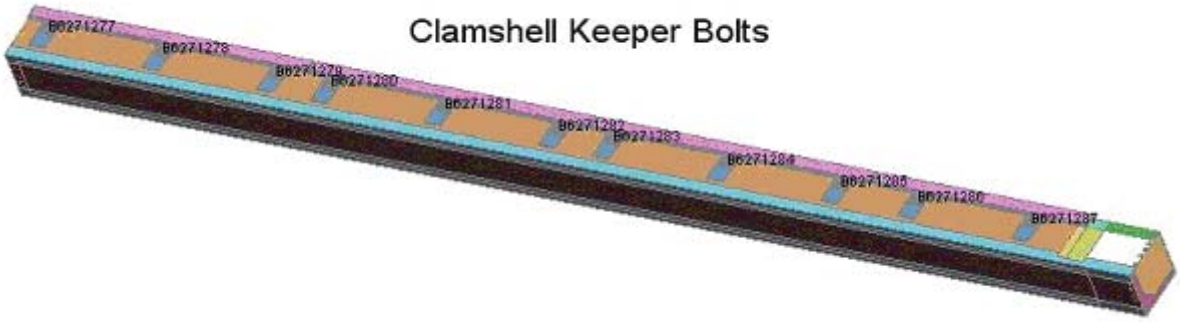

Figure 2-35 Clamshell Keeper Bolt Labels

Clamshell Top and Bottom Plate Bolts – In addition to the Clamshell latch bolts, there are thirty ½-13 stainless steel bolts securing the Clamshell top and bottom end plates. The twenty bolts securing the top end plate are distributed five per side as shown in Figure 2-36A. These bolts are not removed during normal operation and are permanently adhered to the plates. The ten bolts securing the bottom end plate are distributed equally to the two walls of the Clamshell V-shaped bottom extrusion as shown in Figure 2-36B. These bolts are also permanently adhered.

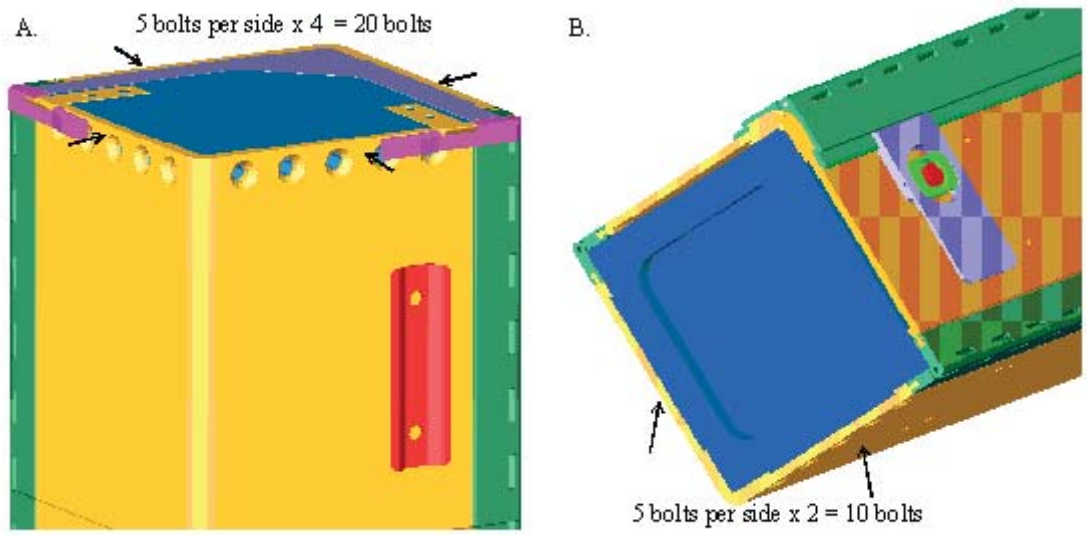

Figure 2-36 Clamshell Top and Bottom End Plates

The analyses indicates that none of the Clamshell bolts at the top and bottom ends will fail during a side drop on either the Outerpack latches or Outerpack hinges. This is evident from the minimum factors of safety shown in Tables 2-14, 2-15 and 2-16. (Our modeling of the fuel assembly as a rigid structure likely makes little difference to these predictions since the fuel rods would not be expected to buckle in this drop orientation.)

Table 2-13 Clamshell Bottom Plate Bolt Minimum Factor of Safety for 9m Side Drops

ID (Figure 2-37)	FS/Time	
	Dropped on OP Latches (Figure 2-30B)	Dropped on OP Hinges (Figure 2-30A)
B6168785	**2.39/0.0047 s**	**2.33/0.0107 s**
B6168786	2.84/0.0070 s	4.29/0.0065 s
B6168787	6.40/0.0092 s	6.96/0.0062 s
B6168788	9.56/0.0092 s	6.26/0.0062 s
B6168789	6.62/0.0190 s	3.96/0.0060 s
B6168794	3.84/0.0062 s	5.43/0.0102 s
B6168793	19.4/0.0050 s	7.61/0.0102 s
B6168792	13.5/0.0087 s	7.88/0.0102 s
B6168791	4.37/0.0065 s	3.57/0.0055 s
B6168790	2.41/0.0060 s	2.48/0.0050 s

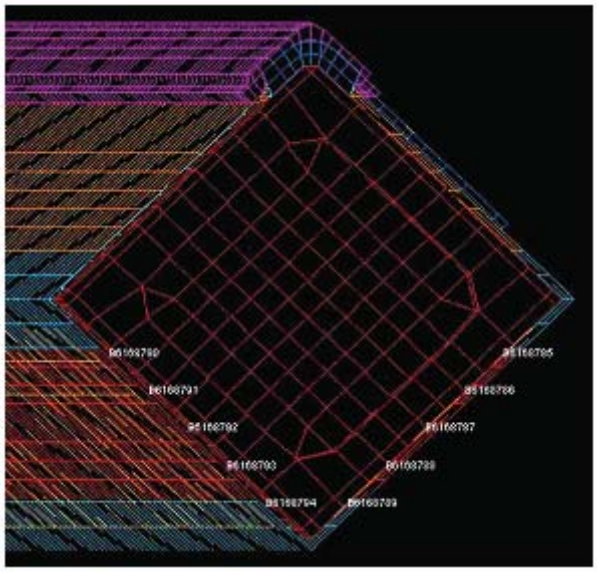

Figure 2-37 Clamshell Bottom Plate Bolt Labels

Table 2-14 Clamshell Grooved Top Plate Bolt Minimum Factors of Safety for 9m Side Drops

ID (Figure 2-38)	FS/Time	
	Dropped on OP Latches (Figure 2-30B)	Dropped on OP Hinges (Figure 2-30A)
B6168781	4.19/0.006 s	5.21/0.0052 s
B6168780	21.1/0.0065 s	12.67/0.0057 s
B6168779	32.1/0.0077 s	21.22/0.0057 s
B6168778	17.5/0.0095 s	33.37/0.007 s
B6168773	2.29/0.0065 s	**2.73/0.005 s**
B6168774	**2.25/0.0062 s**	4.97/0.0087 s
B6168775	3.88/0.0075 s	33.54/0.0092 s
B6168776	24.5/0.0057 s	52.4/0.0077 s
B6168777	13.2/0.0057 s	54.49/0.009 s
B6168769	2.99/0.0052 s	4.77/0.006 s

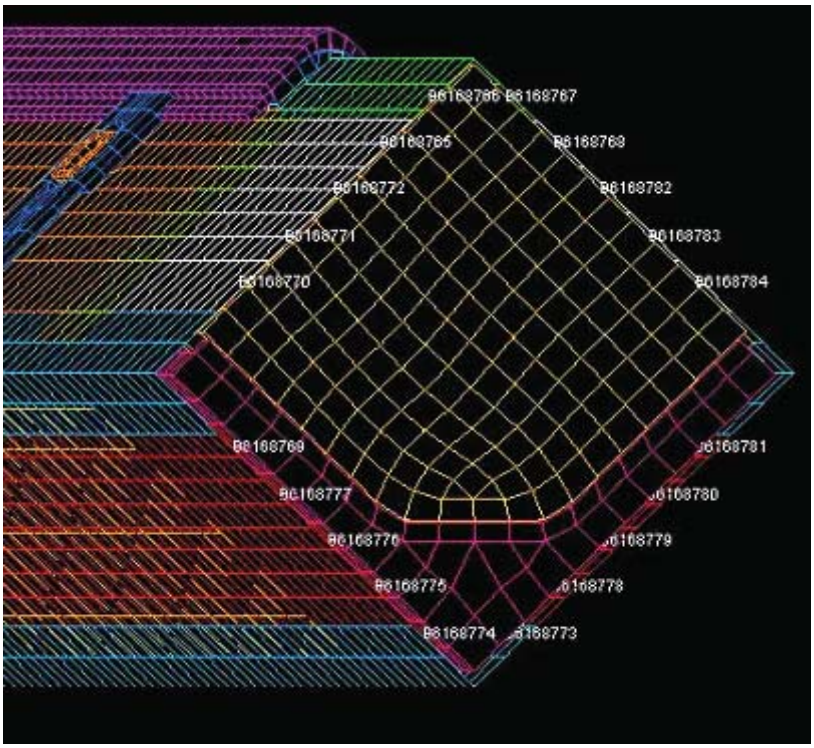

Figure 2-38 Clamshell Bottom Plate Bolt Labels

Table 2-15 Clamshell Lipped Top Plate Bolt Minimum Factors of Safety for 9m Side Drops

ID (Figure 2-38)	FS/Time	
	Dropped on OP Latches (Figure 2-30B)	Dropped on OP Hinges (Figure 2-30A)
B6168770	2.32/0.005 s	3.38/0.0077 s
B6168771	5.65/0.005 s	10.4/0.006 s
B6168772	5.95/0.005 s	11.6/0.007 s
B6168765	9.29/0.0085 s	18.8/0.0065 s
B6168766	7.27/0.0057 s	7.99/0.007 s
B6168767	6.54/0.007 s	6.58/0.006 s
B6168768	9.68/0.007 s	11.7/0.006 s
B6168762	9.14/0.007 s	9.16/0.006 s
B6168783	6.18/0.0085 s	5.65/0.0122 s
B6168784	4.22/0.008 s	2.25/0.0047 s

Clamshell Top End Plate Joint – One goal of the Traveller package design was to minimize the time and effort associated with loading and unloading the fuel. This necessitated the number of bolts that had to be removed during these operations be as kept as low as possible. To accomplish this, the top end of the Clamshell consists of two interlocking plates as shown in Figure 2-39. One of these plates is grooved and is permanently attached to the V-shaped lower portion of the Clamshell, Figure 2-36A. The other has a lip and is permanently attached to an upper housing above the Clamshell doors, Figure 2-39. This groove-and-lip design should indeed facilitate rapid loading and unloading, however, the joint must not separate to any significant extent during the HAC drop tests that the fuel rods might slip out of the Clamshell.

Fortunately, our analysis indicates that the separation during impact is small, Figure 2-40. Furthermore, the separation is transient/temporary as can be seen by the reduction in the separation distance in the later stages of the analysis, Figure 2-40B compared with Figure 2-40A. These predicted results were obtained from the analysis of the Outerpack drop onto its latches. In this case, the Clamshell latches are positioned underneath the fuel, towards the ground, Figure 2-26B. Analysis of the Outerpack drop onto its hinges yielded similar results although the predicted separation of this joint was slightly less.

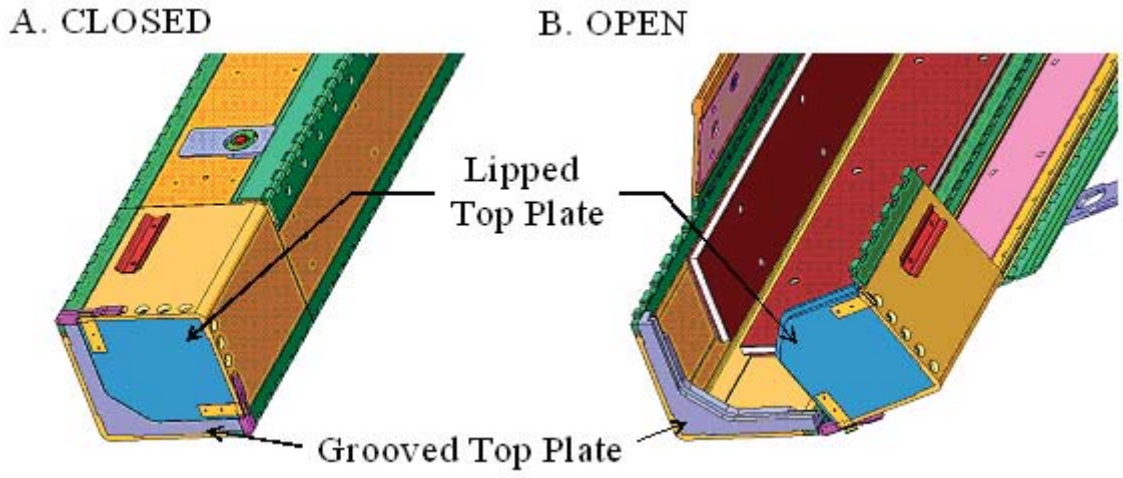

Figure 2-39 Clamshell Doors

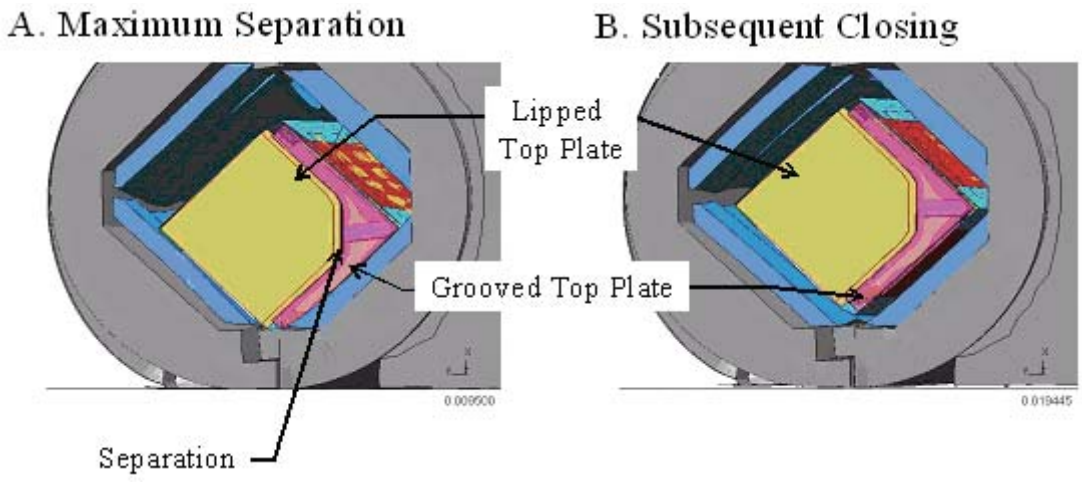

Figure 2-40 Clamshell Response during Side Drop

Clamshell Bottom End Plate/Door Joints – In keeping with the goal of minimizing the time and of loading and unloading the fuel, no bolts must be removed at the bottom end of the Clamshell during these operations. To accomplish this, the bottom Clamshell plate and doors have an interlocking feature consisting of a lip on the bottom end plate and corresponding grooves in both Clamshell doors, Figure 2-41. As described previously for the top end, these joints also do not separate to the extent that a fuel rod could slip through the opening

.

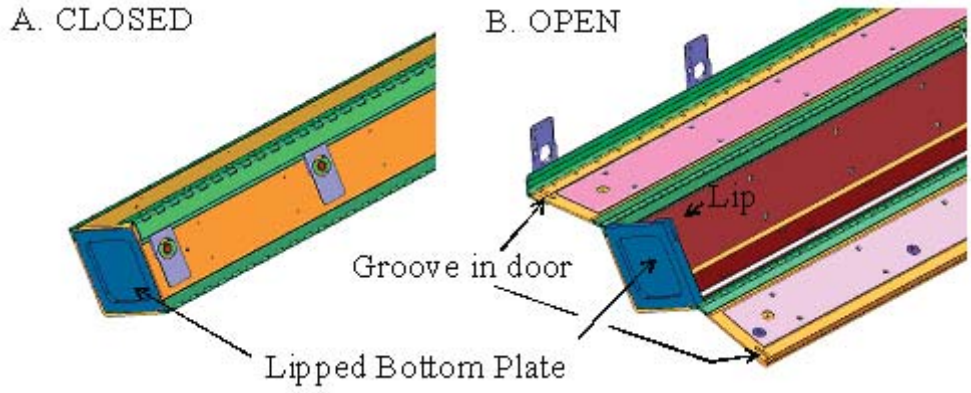

Figure 2-41 Clamshell Doors at Bottom Plate

A small separation of one of these joint during impact is predicted, Figure 2-42. Because the separation is at the upper joint is small, it is not possible that a fuel rod could slip through this joint. Furthermore, the other joint is predicted to remain closed and the bottom end plate should remain intact. These predicted results were obtained from the analysis of the Outerpack drop onto its latches. In this case, the Clamshell latches are positioned underneath the fuel, towards the ground, Figure 2-26B. As with the joint at the top Clamshell plate, the predicted separation of this joint was slightly less for a drop onto the Outerpack hinges.

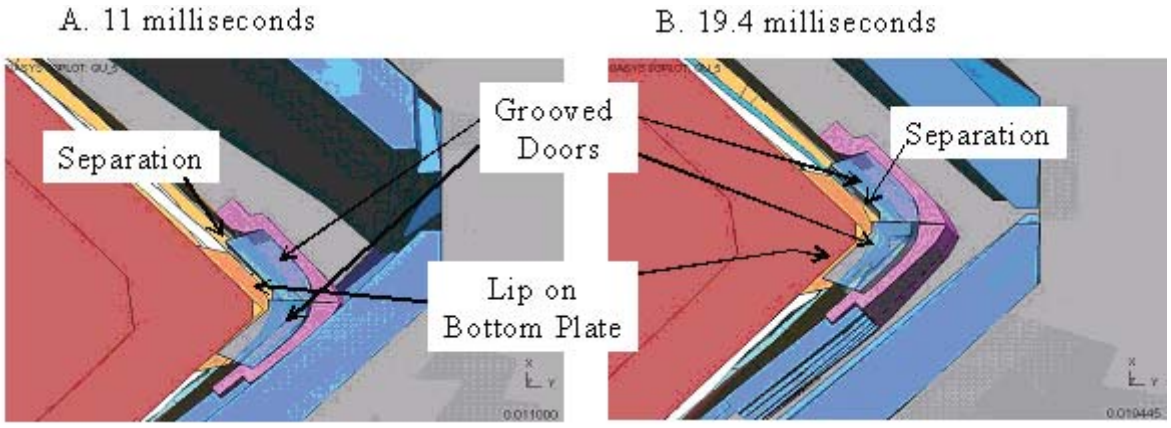

Figure 2-42 Predicted Response of Clamshell Bottom Plate and Doors During 9m Horizontal Drop onto Outerpack Latches

2.12.4.2.3 "CG-over-Corner" and "CG-forward-of-Corner" Drops onto Top Nozzle End of Package

As indicated in Figure 2-43, almost vertical orientations may result in the package center of gravity (CG) being positioned directly above the impacting corner of the package. When this occurs, the drop is designated as a "CG-over-corner" impact. In a CG-over-corner impact, the shipping package will initially continue translating in the direction of impact without rotating. However, deformation of the impacted corner may eventually result in the package tilting and falling over.

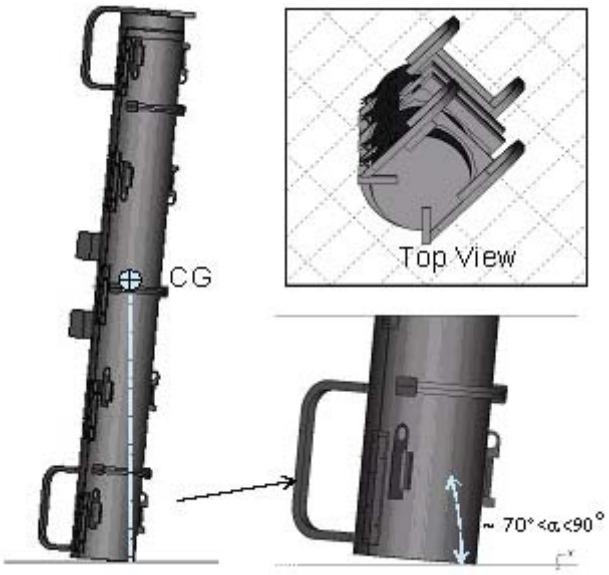

Figure 2-43 Top Nozzle Analysis Drop Orientation

CG-over-corner impacts direct all the drop energy to only a portion of the impact limiter Thus, except for a specific feature of the Traveller XL package, a CG-over-corner impact (either onto the top or bottom end of the package) would probably be the most damaging "nearly vertical" drop. However, as subsequently shown, some drops onto the top nozzle at angles that put the CG forward of the impact corner, i.e., in the "fall" direction of Figure 2-44, are predicted to be more damaging. This is because the resulting deformation involves the Outerpack top corner bending about an (imaginary) axis between the knuckles of the first hinge and latch Figure 2-45.

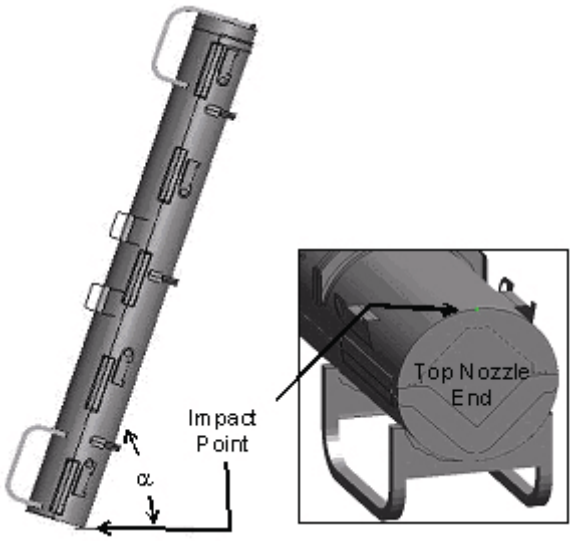

Figure 2-44 Location of Impact

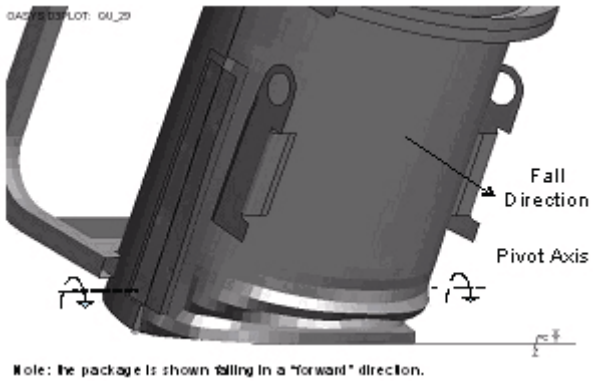

Figure 2-45 Damage to Outerpack During Angled Drop onto Top Nozzle End of Package

The most damaging drop orientation for the Outerpack is a top nozzle down, CG-forward-of-corner configuration having an 18° rotation (α=72°), see Figure 2-44. With smaller rotations, the detrimental opening of the Outerpack seam is predicted to be less despite a greater amount of energy being absorbed by the impact limiter. This is because portions of both the upper and lower Outerpack assemblies contact the drop pad and this significantly reduces their relative motion. With larger rotations, Outerpack seam opening is also predicted to be less. This is because the pivot axis moves well in front of the hinge knuckles in Figures 2-45 and 2-46.

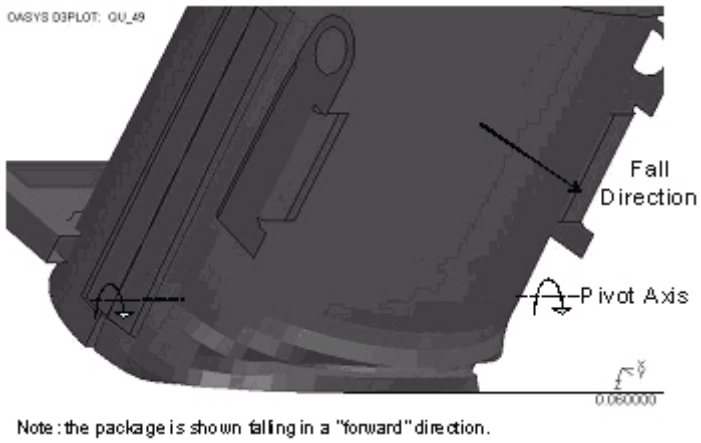

Figure 2-46 Predicted Deformation of Outerpack Top Nozzle Impact Limiter

For the subsequent 1 meter pin puncture drop, the premise is that this is the worst possible additional damage for the Outerpack seam to be further opened. Thus, the most damaging pin puncture orientation following a CG-forward-of-corner test is clearly one where the damaged face of the Outerpack is perpendicular to the pin as depicted in Figure 2-47. The combination of these scenarios; a high angle drop followed by a pin puncture in the location of the initial impact was the basis for the QTU-1 unit testing.

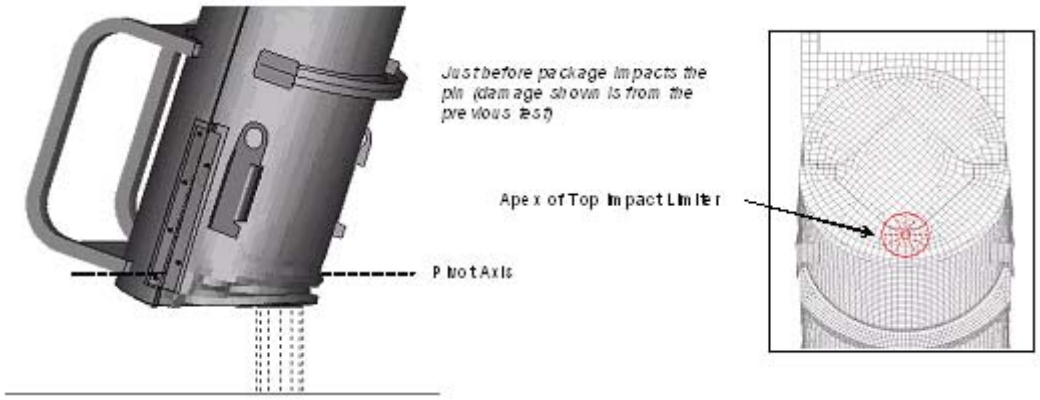

Figure 2-47 Predicted Pin Puncture Orientation after a CG-Forward-of-Corner Test

The FEA of the pin drop incorporated package deformations and stresses calculated to result from the 9m drop. The methodology for including the deformation and stresses involved defining the nodal coordinates in the pin puncture model as the deformed nodal positions of the previous analysis plus a rigid-body-rotation to locate the "model with previous damage" to the proper position/orientation for the pin puncture test. The element stresses were extracted from the first analysis and included as initial stresses in the second analysis.

Finally, from a computation standpoint, it was not practical to compute the secondary impact. This is because the secondary impact is preceded by a lengthy free-fall. Long (multi-day) computations would have been required to run an analysis through the free-fall and secondary impact. Fortunately, secondary impacts for such nearly vertical drops as this are known not to cause much additional damage. This is especially so for the Traveller XL design which will be protected by the circumferential stiffeners on the upper Outerpack. Thus, not having predictions of the secondary impact should be no limitation.

"**Worst Case Drop Angle" Determination** – As previously discussed, our damage criterion for the CG-forward-of-corner drops onto the top nozzle end of the package was the degree of separation between the upper and lower Outerpack assemblies. Three orientations: 11, 18, and 25° were investigated and it was determined that an angle of 18° resulted in the most separation, Figure 2-48.

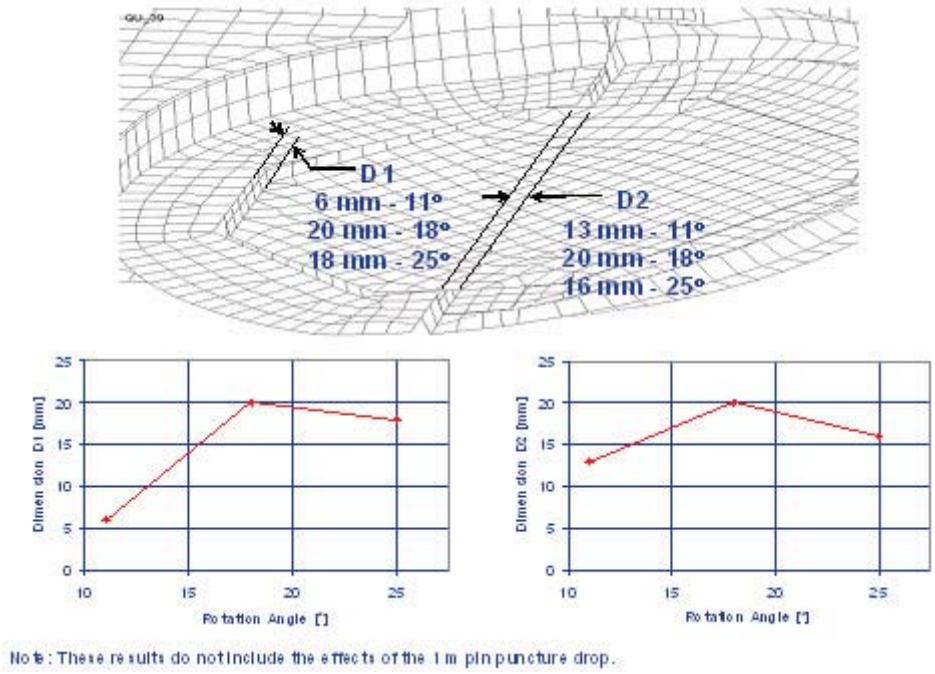

Figure 2-48 Outerpack Top Separation vs. Drop Angle

Energy and Work Histories – Predicted global energy and work histories for the primary impact of three CG-forward-of-corner drops onto the top nozzle end of the package are shown in Figure 2-49. These plots were obtained for forward rotations of 11, 18, and 25°, respectively. As before, the initial total energy (TE) of 204 kJ and increases slightly during the run in concert with the external work due to gravity. In each of these plots, the internal energy (IE) and kinetic energy (KE) traces become flat between 50-60 milliseconds into the impact event. This indicates completion of the primary impact and initiation of rollover. (Rollover and secondary impact were not numerically investigated as previously justified.) Note as drop rotation angle decreases, the internal energy absorbed by the Outerpack is predicted to increase. However, as explained earlier, this should not result in the largest Outerpack seam opening. Finally, hourglass, sliding and stonewall energies are low in each plot. This indicates overall numerically sound analyses. However, late in the analysis, hourglass energy does reach 4.1% of the total energy. While this is a low percentage, the hourglass error is concentrated in the XL pins (PID 10764) and the Clamshell cushioning pads (PIDS 2003 and 2013) in the vicinity of impact. An investigation of this error which involved using fully integrated elements found the energy previously dissipated as hourglass deformation was now (correctly) forced into the bottom impact limiter. This had only a marginal effect on the predicted force in the primary impact of Figure 2-50 and Figure 2-62. However, it did reduce predicted FA accelerations by about 17% (from the 47.3 g's shown in Figure 2-63 to 39.3 g's.). This latter effect was not significant enough to change any conclusions within the report.

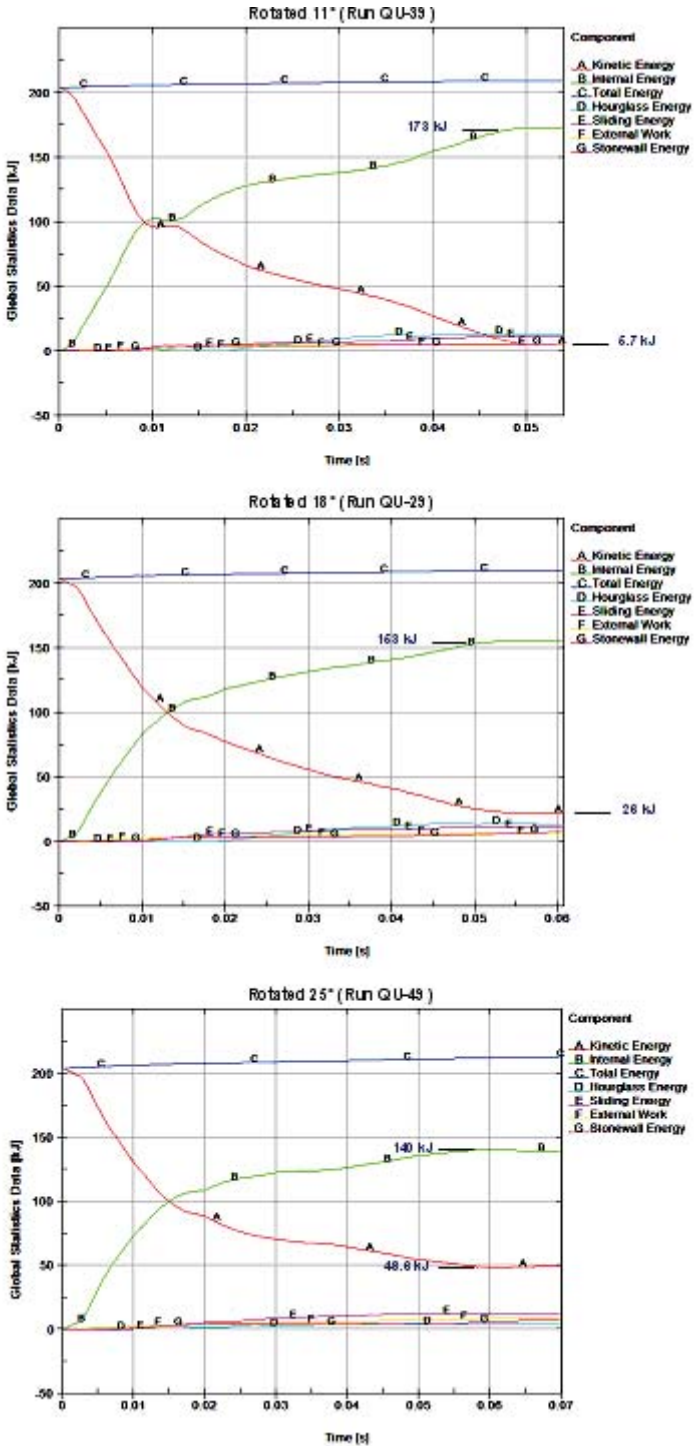

Figure 2-49 Predicted Energy and Work Histories for 9 m CG-over-Corner Drop onto the Top Nozzle End at Various Angles

Rigid Wall Forces – The predicted rigid wall force histories are shown in Figure 2-50 for CG-forward-of-corner drops on to the top end of the package rotated 11, 18, and 25°. These plots show only the primary impact (since the secondary impact due to fall-over was not calculated). The primary impact is divided into two separate events. From impact onset to approximately 25 milliseconds, the Outerpack impacts the drop pad while the Clamshell is still in free-fall. (This is due to the de-coupling between Outerpack and Clamshell previously discussed in section 2.1.1.1.1.) Secondly, the Clamshell hits the inner surfaces of the Outerpack and drives it back into the drop pad from approximately 25 milliseconds into the impact until about 70 milliseconds. Figure 2-50 shows the highest predicted loads for the Outerpack in these three orientations will be encountered at an 11° rotation. This agrees with the previous prediction that as drop rotation angle decreases, the internal energy absorbed by the Outerpack increases.

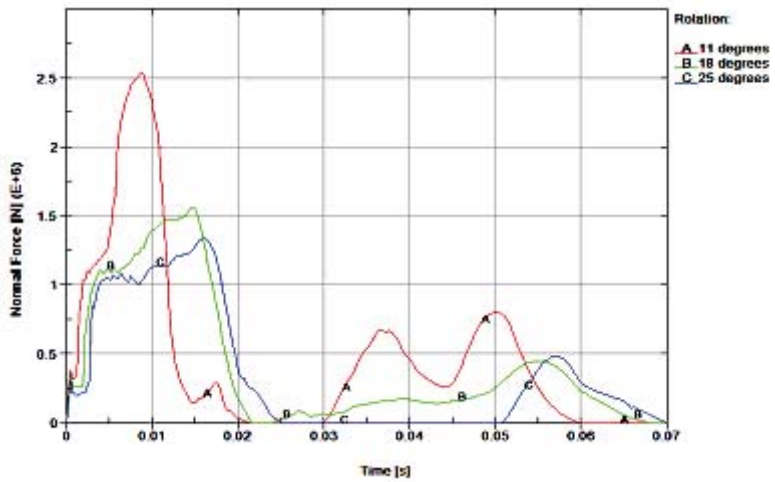

Figure 2-50 Predicted Rigid Wall Forces

As previously stated, the primary concern with CG-forward-of-corner drops onto the top nozzle end of the package is whether or not the thermal integrity needed to protect against the 30 min burn test will be compromised. It was shown that the deformation most likely to induce such damage is greatest when the Traveller XL package is rotated approx. 18° forward from a vertical orientation Figure 2-48. The main concern with the higher loads sustained and additional energy absorbed by the Outerpack at smaller rotation angles is if this jeopardized the Outerpack bolts. This issue is addressed in the following section.

Outerpack Hinge/Latch Bolts – The analysis indicates there is little likelihood of the Outerpack latch and hinge top bolts failing during a 9m CG-forward-of-corner drop onto the top end of the package. This is evident from the relatively high predicted factors of safety for these bolts, Tables 2-16 and 2-17.

Table 2-16 Top Outerpack Latch Bolt Minimum Factors of Safety for 9m CB-Forward of Corner Drops			
ID (Figure 32)	**FS/Time**		
	11° Forward Rotation	**18° Forward Rotation**	**25° Forward Rotation**
B917	3.80/0.0143 s	7.57/0.0102 s	5.08/0.0105 s
B921	3.94/0.014 s	6.89/0.0247 s	6.19/0.0102 s
B923	3.10/0.0225 s	2.63/0.0245 s	3.87/0.0245 s
B927	3.28/0.0227 s	2.70/0.0247 s	4.04/0.0262 s
B929	2.61/0.012 s	2.29/0.0112 s	2.36/0.0147 s
B933	2.45/0.0065 s	2.25/0.0112 s	2.38/0.0147 s
B935	**2.22/0.0117 s**	**2.22/0.0072 s**	**2.22/0.008 s**
B939	**2.22/0.0117 s**	**2.22/0.0072 s**	**2.22/0.0075 s**
B941	2.23/0.0032 s	2.23/0.0052 s	2.23/0.0057 s
B945	**2.22/0.0057 s**	2.23/0.0077 s	2.23/0.0097 s

Table 2-17 Top Outerpack Hinge Bolt Minimum Factors of Safety for 9m CB Forward of Corner Drops			
ID (Figure 33)	**FS/Time**		
	11° Forward Rotation	**18° Forward Rotation**	**25° Forward Rotation**
B947	3.59/0.014 s	6.37/0.0337 s	5.13/0.0105 s
B951	3.73/0.014 s	7.49/0.0232 s	6.17/0.0135 s
B953	2.95/0.0225 s	3.04/0.0245 s	4.19/0.0322 s
B957	3.19/0.0225 s	3.26/0.0245 s	4.30/0.0322 s
B959	2.65/0.0065 s	2.32/0.0115 s	2.34/0.0147 s
B963	2.51/0.0065 s	2.27/0.011 s	2.40/0.0122 s
B965	2.21/0.0062 s	2.21/0.0243 s	2.21/0.0077 s
B969	2.22/0.006 s	2.21/0.0235 s	2.23/0.0072 s
B971	**2.20/0.006 s**	**2.20/0.0095 s**	**2.20/0.0110 s**
B975	2.22/0.0055 s	2.23/0.0072 s	2.23/0.0077 s

It should also be noted that the latch and hinge bolts nearest impact were predicted to have the smallest (although still very adequate) safety factors. This is logical.

Clamshell Keeper Bolts – Our analysis indicates there is little likelihood of the Clamshell keeper bolts failing during a 9m CG-forward-of-corner drop onto the top nozzle end of the package. This is evident from the relatively high predicted factors of safety for these bolts, Table 2-18.

Table 2-18 Clamshell Keeper Bolt Minimum Factors of Safety for 9m CG-Forward-of-Corner Drops

ID (Figure 35)	FS/Time		
	11° Forward Rotation	18° Forward Rotation	25° Forward Rotation
B6271277	5.86/0.0255 s	8.71/0.038 s	10.86/0.0237 s
B6271278	5.75/0.027 s	4.79/0.0285 s	4.43/0.0277 s
B6271279	22.6/0.029 s	8.46/0.0287 s	6.63/0.0237 s
B6271280	17.4/0.0258 s	10.89/0.026 s	3.29/0.0225 s
B6271281	13.38/0.023 s	12.31/0.0522 s	7.96/0.024 s
B6271282	19.48/0.0455 s	8.13/0.0375 s	8.85/0.0282 s
B6271283	16.85/0.0207 s	5.41/0.0332 s	5.78/0.0258 s
B6271284	33.54/0.0285 s	8.89/0.0392 s	7.3/0.0252 s
B6271285	17.56/0.0405 s	11.32/0.0132 s	11.69/0.0197 s
B6271286	14.73/0.016 s	9.67/0.0415 s	8.09/0.024 s

It should be noted that the keeper bolt nearest impact was predicted to have the smallest (although still very adequate) safety factor.

Clamshell Top and Bottom Plate Bolts – The analyses indicate that none of the Clamshell bolts at the top and bottom ends will fail during a 9m CG-forward-of-corner drop onto the top nozzle end of the package. This is evident from the minimum factors of safety shown in Tables 2-19, 2-20 and 2-21. (The modeling of the fuel assembly as a rigid structure likely makes little difference to these predictions since the fuel rods would not be expected to buckle in this drop orientation.)

Table 2-19 Clamshell Bottom Plate bolt Minimum Factors of Safety for 9m CG-Forward-of-Corner Drops

ID (Figure 37)	FS/Time		
	11° Forward Rotation	18° Forward Rotation	25° Forward Rotation
B6168785	**2.36/0.0495 s**	**2.38/0.0245 s**	2.50/0.0197 s
B6168786	8.27/0.0497 s	5.85/0.0243 s	4.48/0.0235 s
B6168787	100.3/0.0262 s	94.5/0.0225 s	60.8/0.0235 s
B6168788	97.8/0.0262 s	112/0.0515 s	89.5/0.0235 s
B6168789	51.1/0.0227 s	27.0/0.0230 s	43.3/0.0437 s
B6168794	40.2/0.0222 s	31.0/0.0317 s	27.7/0.0317 s
B6168793	99.9/0.0262 s	83.3/0.0305 s	59.3/0.0385 s
B6168792	100.7/0.0618 s	86.7/0.0202 s	44.2/0.0402 s
B6168791	11.2/0.0412 s	6.55/0.0202 s	7.69/0.0200 s
B6168790	2.84/0.0412 s	2.43/0.0205 s	**2.33/0.0280 s**

Table 2-20 Clamshell Grooved Top Plate Bolt Minimum Factors of Safety for 9m CG-Forward-of-Corner Drops

ID (Figure 38)	FS/Time		
	11° Forward Rotation	18° Forward Rotation	25° Forward Rotation
B6168781	2.33/0.0182 s	2.29/0.0187 s	2.31/0.0197 s
B6168780	3.86/0.0397 s	5.32/0.0200 s	4.32/0.0200 s
B6168779	2.84/0.049 s	6.08/0.0510 s	12.06/0.0217 s
B6168778	2.31/0.039 s	2.34/0.0447 s	2.37/0.0470 s
B6168773	2.25/0.0367 s	2.26/0.0430 s	2.26/0.0410 s
B6168774	**2.23/0.0367 s**	**2.22/0.0427 s**	**2.22/0.0410 s**
B6168775	2.31/0.0387 s	2.30/0.0435 s	2.32/0.0467 s
B6168776	2.91/0.0485 s	5.39/0.0555 s	9.58/0.0465 s
B6168777	7.04/0.0495 s	6.20/0.0467 s	4.84/0.0205 s

Table 2-21 Clamshell Lipped Top Plate Bolt Minimum Factors of Safety for 9m CG-Forward-of-Corner Drops			
ID (Figure 38)	**FS/Time**		
	11° Forward Rotation	**18° Forward Rotation**	**25° Forward Rotation**
B6168770	1.76/0.0165 s	1.81/0.0180 s	1.77/0.0195 s
B6168771	1.79/0.0207 s	1.77/0.0177 s	1.75/0.0197 s
B6168772	1.78/0.0360 s	1.76/0.0477 s	1.80/0.0117 s
B6168765	1.76/0.0350 s	1.76/0.0170 s	1.73/0.0135 s
B6168766	1.77/0.0125 s	1.77/0.0150 s	**1.72/0.0125 s**
B6168767	1.78/0.0200 s	**1.75/0.0150 s**	**1.72/0.0127 s**
B6168768	1.77/0.0362 s	1.76/0.0152 s	1.76/0.0277 s
B6168762	1.76/0.0362 s	1.77/0.0510 s	1.76/0.0187 s
B6168783	1.77/0.0192 s	1.77/0.0155 s	1.77/0.0202 s

Clamshell Top End Plate Joint – The analyses indicate the Clamshell top end plate joint (Figure 2-39) will separate slightly, but not come completely apart during CG-forward-of-corner impacts. In particular, the lip on the top plate is predicted to remain within the groove in the V-shaped top plate along both edges but slip completely out in the middle. This is shown in Figure 2-51 for the CG-forward-of-corner drop rotated 11°. It should be noted that this separation is predicted to be permanent, not transient. It should also be noted that predicted deformations were similar but lesser for CG-forward-of-corner drops rotated 18° and 25°. However, in these latter two orientations, the lip on the top plate is predicted to remain within the groove in the V-shaped top plate along its entire length. **This extent of deformation was not observed in full-scale testing of Traveller XL prototypes and is therefore conservative**.

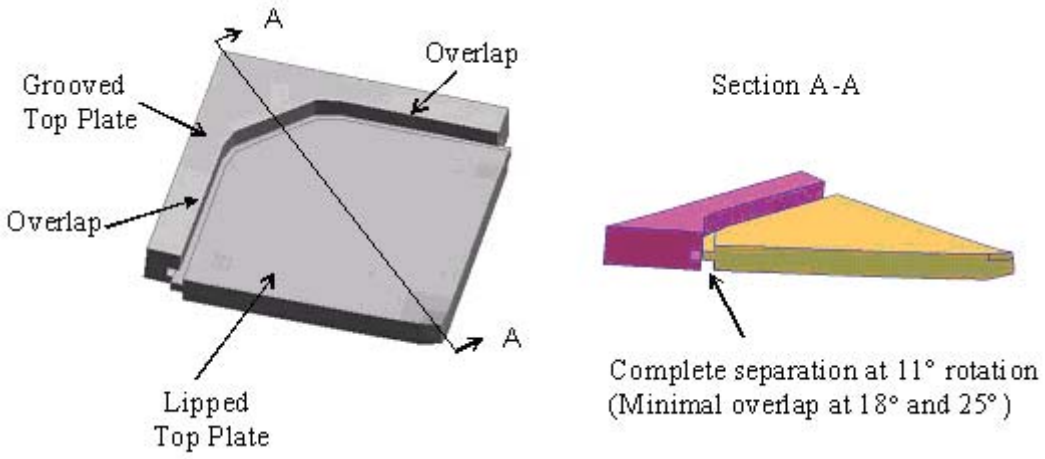

Figure 2-51 Clamshell Top Plate Geometry

Clamshell Bottom End Plate/Door Joints – The analyses indicated the Clamshell bottom end plate is minimally loaded during CG-forward-of-corner drops onto the top end of the shipping package. These trivial loads are not reported herein.

In summary, horizontal side drops onto the Outerpack hinges/latches result in the highest predicted Outerpack loads. Even so, a CG-forward-of-corner drop onto the top nozzle end of the package with 18° forward rotation, Figure 2-48 is predicted most damaging to the Outerpack. This is because the predicted opening of the seam between the upper and lower Outerpack assemblies may compromise the ability of the Traveller XL shipping package to withstand the 30 minute HAC burn test. Drop tests are described in Appendix 2.12.5 and the fire tests are described in Section 3, all of which demonstrate that this is not a serious concern.

2.12.4.2.4 Orientation Predicted Most Damaging to the Fuel Assembly

Determining the drop orientation most damaging to a fuel assembly is greatly facilitated by the geometry of the assembly itself. In particular, the fuel rods within a fuel assembly are very long (4.4 m or more), slender (approx. 9 mm), and relatively flexible. Thus, they are quite susceptible to buckling. For this reason, our hypothesis is that drop orientations which impart the highest axial loads to the assembly are most damaging. Buckling of the fuel rods is also of paramount importance with respect to criticality safety. For criticality safety, fuel rods must not be allowed to buckle in a configuration which results in an unsafe nuclear condition. See Section 6 for a complete description of the criticality safety of the Traveller packages.

Obviously, highest axial loads are generated by vertical or nearly vertical loadings. Near-vertical orientations may impart higher loads to a portion of the fuel rods than the average load applied to a fuel rod in truly vertical drops. However, in these orientations, the adjacent rods or Clamshell structure will provide lateral support. Thus, our focus was entirely on (truly) vertical drops for fuel assembly damage, Figure 2-52. Vertical orientations result in higher impact loads because the larger footprint impacts the ground and therefore the system is stiffer than a high angle orientation where the initial contact is a point which "grows" a footprint.

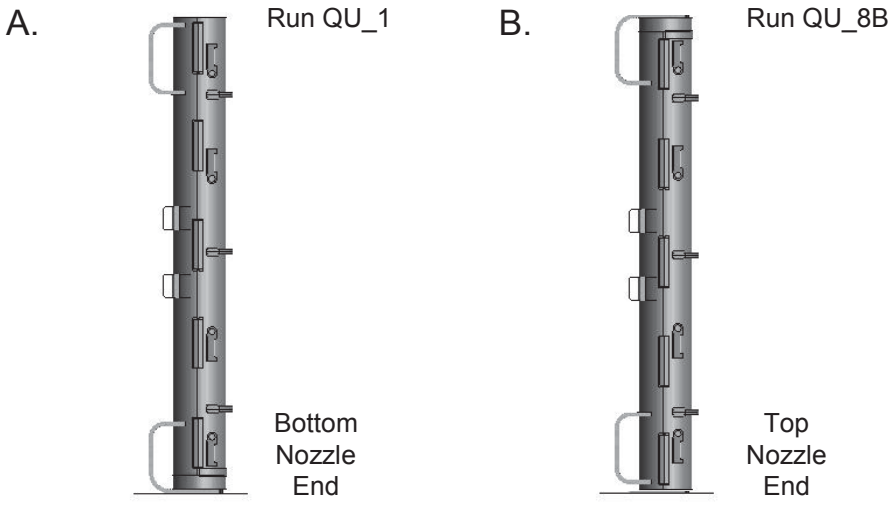

Figure 2-52 Traveller Drop Orientations Analyzed For Maximum Fuel Assembly Damage

The tendency of the fuel rods to buckle proved a severe modeling limitation because post-buckling behavior was simply beyond our current modeling capability. Post-buckling involves one or more buckled fuel rods impacting a nearby rod or Clamshell wall. These collisions involved a large momentum transfer because the fuel rods are so heavy. In our model, the mesh of the walls and nearby rods and was simply not capable of properly absorbing this energy. The result was the analysis aborted almost immediately once any fuel rods buckled. This was due to "negative volumes" (highly distorted solid elements) which resulted from the inability of the Clamshell walls, as meshed, to properly absorb the momentum transferred from the fuel rods. This occurred in all analyses we attempted and often with as much as 30 percent of the drop energy not yet absorbed. The mesh of the surrounding structure was simply not capable of properly absorbing this energy. Successful resolution of this problem would have required significantly finer meshes of both the fuel rods and surrounding structure and perhaps many other changes. From a practical standpoint, this level of analysis is beyond the capabilities of current computer systems. Rather, the fuel rods and associated fuel assembly structure (i.e., the grids), except for the top and bottom nozzles, were converted into a rigid part using the LS-DYNA® deformable-to-rigid option. This prevented the fuel rods from buckling and eliminated the associated problems with negative volumes allowing an analysis that absorbed all the available energy.

This approach prevented any associated loading of the structure surrounding the sides of the fuel assembly (the Clamshell walls), forfeiting the ability to predict the maximum loads and stresses on the Clamshell walls and latches in regions adjacent to the fuel rods. Since the fuel nozzles and other structures near the Clamshell top and bottom ends were kept deformable, Clamshell loads and stresses at the ends of the Clamshell were still fairly accurate. Further, the energy not transferred to the Clamshell walls was now forced into other structures – primarily the fuel assembly nozzles (which were kept deformable) and the end impact limiters in the case of axial drops. Thus, our analyses should be non-conservative for Clamshell regions adjacent to the fuel rods, accurate for the Clamshell top and bottom ends, and probably overly conservative for the displacements in the Outerpack impact limiters.

2.12.4.2.5 Vertical Drops

Our analysis determined that a vertical drop onto the bottom end of the package would be more damaging to the fuel assembly than a drop onto the top end. This is because the Clamshell is subjected to larger impact forces and the fuel assembly must withstand larger accelerations.

Energy and Work Histories – Global energy and work for vertical drops onto the top and bottom end of the package are shown in Figures 2-53 and 2-54, respectively. As before, both plots have an initial total energy (TE) of 204 kJ. The total energy rises slightly, reflecting the external work done by the package under gravity loading. Hourglass, sliding, and stonewall energies were small relative to the total energy. This indicates a good overall numerical analysis was obtained in both simulations.

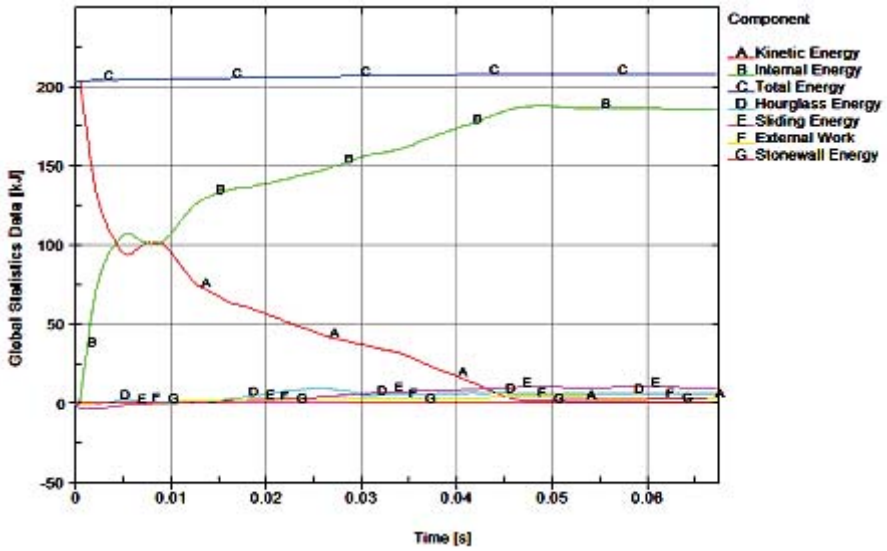

Figure 2-53 Predicted Energy and Work Histories for a 9m Vertical Drop Onto the Top Nozzle End of the Package

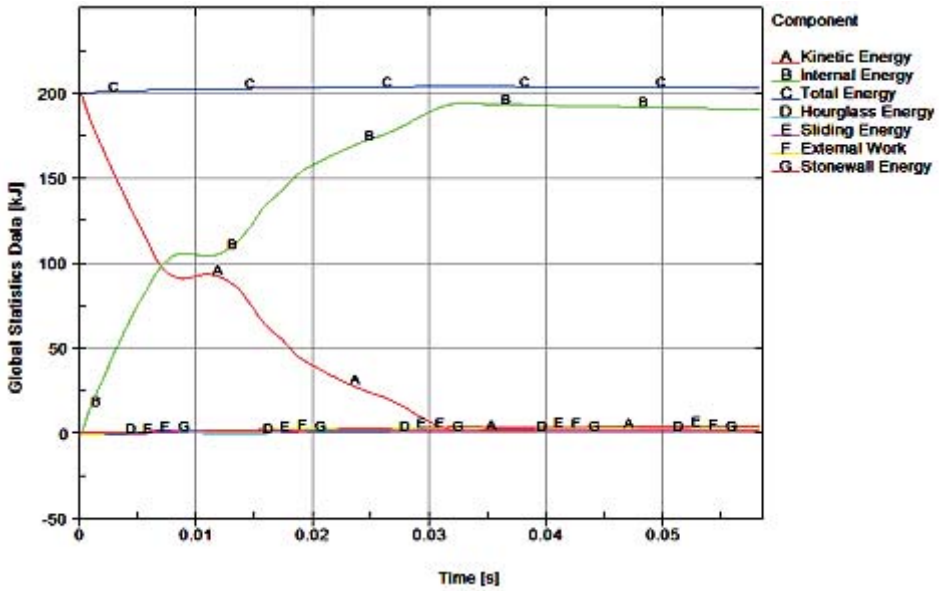

Figure 2-54 Predicted Energy and Work Histories for a 9m Vertical Drop Onto the Bottom Nozzle End of the Package

Rigid Wall Forces – Predicted force histories between the Outerpack and drop pad are shown in Figure 2–55 for top and bottom end vertical drops. The near de-coupling of the Clamshell and Outerpack is clearly evident in both simulations. In the drop onto the bottom end of the package, the initial impact between

Outerpack and drop pad has a 12 milliseconds (approx.) duration. The Clamshell is not involved in this impact as it is still in free-fall (neglecting the small forces of the shock mounts.) At approximately 15 milliseconds into the simulation, the Clamshell contacts the inner surface of the bottom impact limiter and pushes it back into the drop pad. The Clamshell and Outerpack impact further into the drop pad while the fuel assembly is now essentially decoupled from the Clamshell and still in free-fall. As the Outerpack and Clamshell begin to re-bound (at ~25 milliseconds into the simulation) the fuel assembly impacts the Clamshell and all three components (Outerpack, Clamshell and fuel assembly) crash back into the drop pad. The shipping package begins to rebound at approximately 31 milliseconds into the simulation and has left the drop pad after 45 milliseconds. A similar scenario is evident for the vertical drop onto the top nozzle end of the package.

Referring to Figure 2-55, it is noted that the predicted maximum Outerpack load for the top end drop is more than 2X that for the bottom end drop (5.1 versus 2.5 MN, respectively). This shows the higher cushioning capability of the bottom impact limiter design. Further, this indicates that bolts in the Outerpack hinges and latches in the vicinity of impact will be loaded more significantly in a vertical drop onto the top end of the package. Finally, the predicted 5.1 MN load on the Outerpack for a vertical top end drop is still 2-3X less than that predicted for horizontal side drops, Figure 2-29.

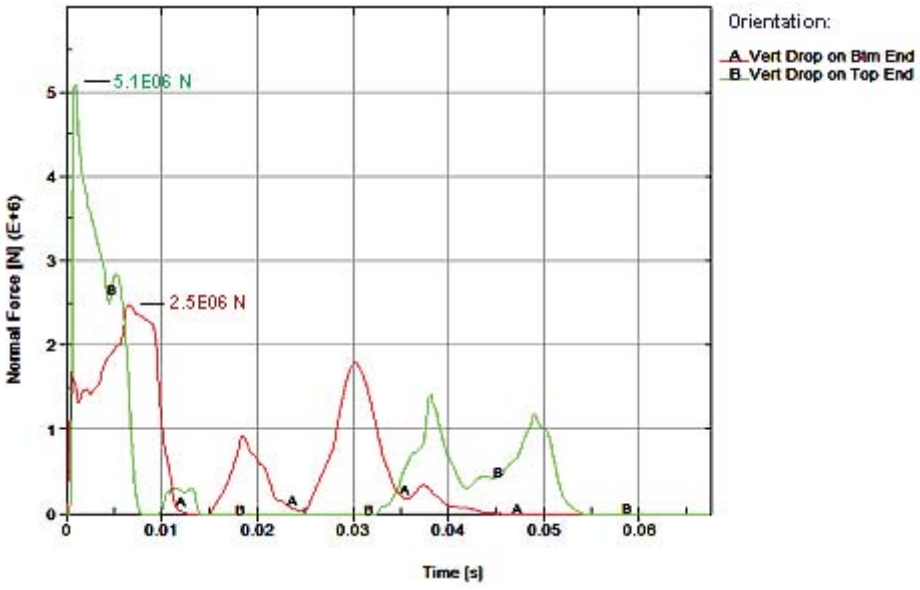

Figure 2-55 Predicted Rigid Wall Histories for 9m Vertical Drops onto the Bottom (QU-1) and Top (QU-8B) Ends of the Package

Clamshell Loads and Accelerations – The force between Clamshell and impact limiter was determined for vertical drops by specifying contacts between the CS top and bottom plates and the innermost impact limiter covers. For drops onto the top end of the package, this required defining contacts between the two CS top plates (the grooved and the lipped plate) and the innermost plate of the top impact limiter and summing

the predicted forces. This technique was only used for vertical drops because these are the only drop orientations in which the Clamshell impacts into only one surface.

Results are shown in Figure 2-56 (for the primary impact only as previously explained.) Note that the force is zero until almost 9 milliseconds into the drop simulation (which starts right before the Outerpack hits the drop pad. This is the time it takes the Clamshell to fall through the approximate 120 mm sway space separating the Clamshell and inner and the top and bottom impact limiters.

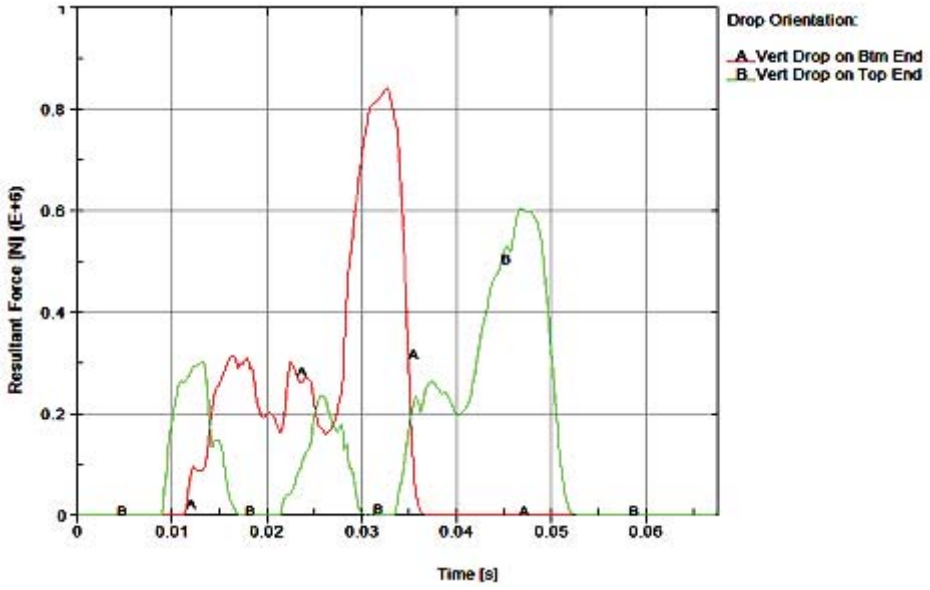

Figure 2-56 Predicted Force Between Clamshell and Impact Limiter for 9m Vertical Drops

Note also in Figure 2-56 that drops onto the bottom end of the package are more severe for the Clamshell than those onto the top end. Indeed, predicted CS loads for vertical drops onto the top and bottom end of the package are, respectively, 605 and 843 kN. These loads resulted in higher accelerations for the fuel assembly (FA) as well. As shown in Figure 2-57, predicted FA accelerations are 102 and 126 g's, respectively, for drops onto the bottom and top ends of the package.

The predicted sequence for a drop onto the bottom nozzle end of the package is shown in Figure 2-58. Impact between the Clamshell and inside covering of the bottom impact limiter occurs at approximately 13 milliseconds into the simulation; the maximum load between CS and bottom impact limiter is predicted to occur at approx. 33 milliseconds; and, the Clamshell is in full rebound by 40 milliseconds. Note the predicted crushing of the bottom nozzle legs shown in Figure 2-58.

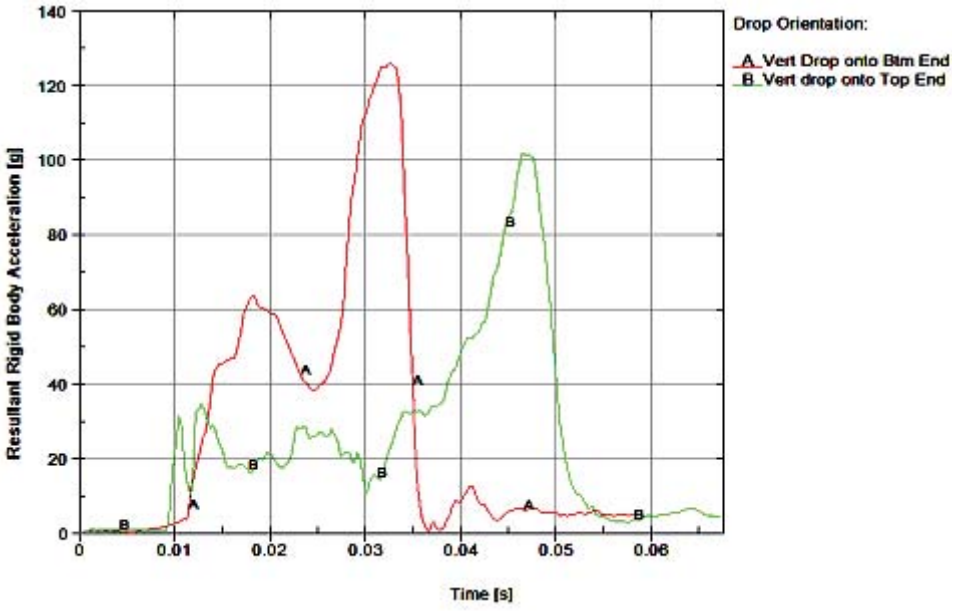

Figure 2-57 Predicted Fuel Assembly Accelerations for 9m Vertical Drops

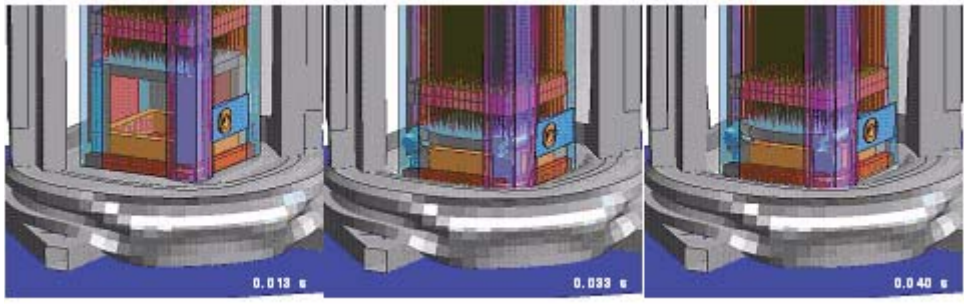

Figure 2-58 Impact Between Clamshell and Bottom Impact Limiter for Vertical Drop onto Bottom End of Package

It is interesting to note the Clamshell and top impact limiter are predicted to collide three times during the primary impact of top end drops. These impacts are depicted in Figures 2-59, 2-60 and 2-61. As shown in Figure 2-59, the first impact involves the Clamshell hitting the top impact limiter from free-fall (at ~9 milliseconds) and the XL pins and top nozzle hold-down posts buckling under the load of the fuel assembly until the top nozzle slides off the hold-down posts (at ~17 milliseconds.) The Clamshell now begins to rebound and leaves the top impact limiter. However, as shown in Figure 2-60, the fuel assembly

continues its downward motion and the top nozzle contacts the midsection of the hold-down posts at about 21.5 milliseconds. At approximately 30.5 milliseconds, Figure 2-60, the hold-down posts are predicted to break near their connection to the cross member connecting them. Then, the fuel assembly pushes the Clamshell back into the top impact limiter. This momentarily removes the fuel assembly loading from the Clamshell and it no longer is pushed into the Outerpack. However, the FA continues falling and the top nozzle begins pushing into the cross member at approximately 33.5 milliseconds. The FA continues its downward fall until motion is arrested at approximately 53 milliseconds, Figure 2-61.

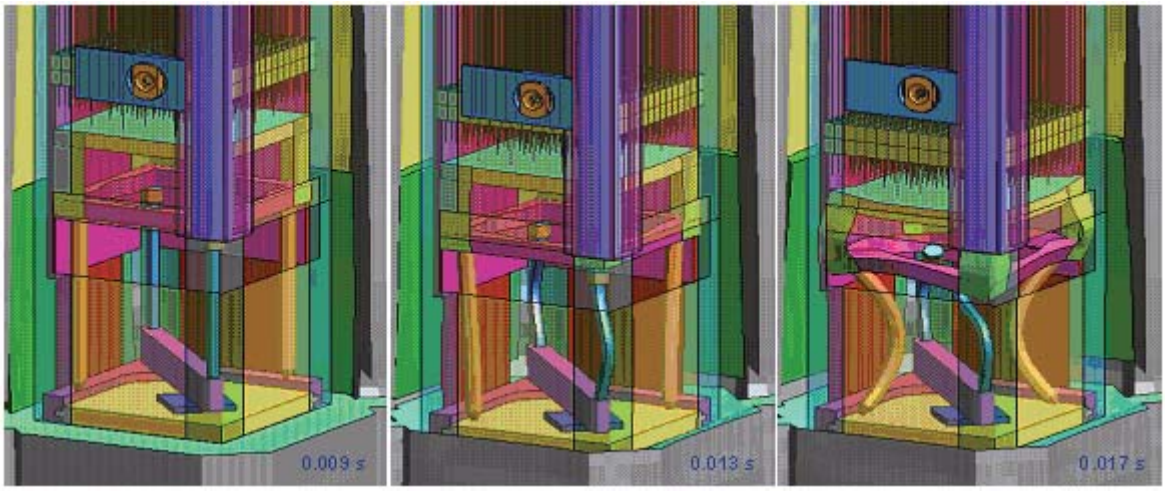

Figure 2-59 First Impact Between Clamshell and Top Impact Limiter for Vertical Drop onto Top End of Package

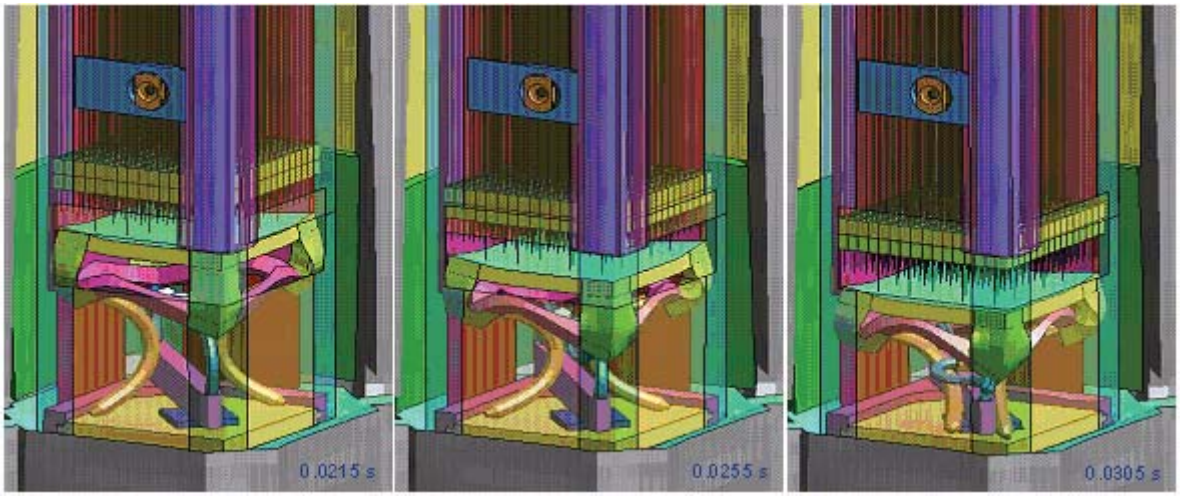

Figure 2-60 Second Impact Between Clamshell and Top Impact Limiter for Vertical Drop onto Top End of Package

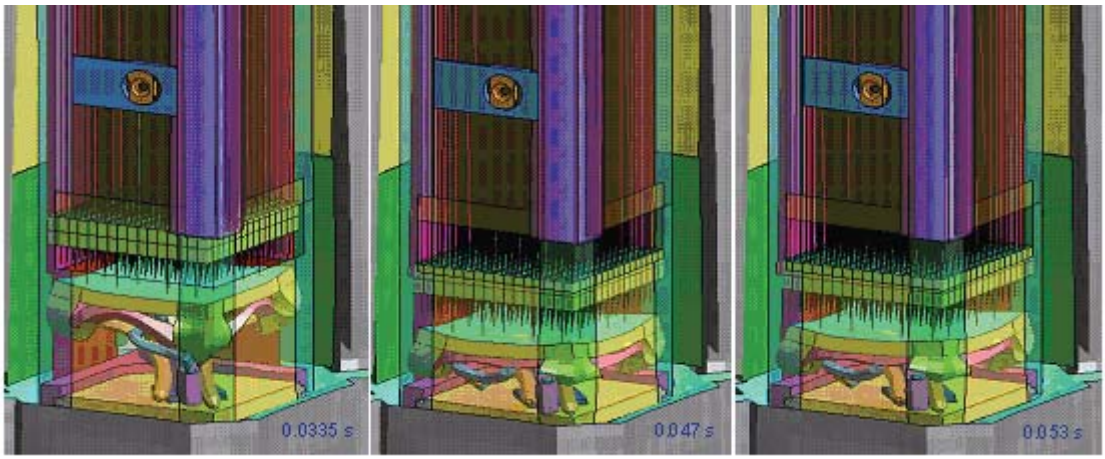

Figure 2-61 Third Impact Between Clamshell and Top Impact Limiter for Vertical Drop onto Top End of Package

From the results shown in this section, we conclude that a CG-forward-of-corner drop onto the top nozzle end of the package with an 18° forward rotation, Figures 2-44 and 2-45 is most damaging to the Outerpack. Further, as also shown, we conclude that the drop most damaging to a fuel assembly is a vertical one onto the bottom nozzle end of the package, Figure 2-52A. Thus, successful drop tests in these two orientations are an adequate demonstration that the Traveller XL design meets/exceeds the HAC drop test requirements.

2.12.4.2.6 Temperature and Foam Density Effects

The Traveller XL package must be capable of passing the HAC drop tests at any temperature within the range -40 to 160°F. Furthermore, foam crush strength is also directly related to foam density. The drop orientation previously determined most damaging to the Outerpack was selected to study the effect of temperature and density (the 9 meter CG-forward-of-corner drops onto the TN end of package with an 18° forward rotation, Figure 2-44). Our finding is that a Traveller XL package with nominal foam density and at "normal temperature" (75°F) experiences slightly higher Outerpack loads when dropped in this orientation compared with packages containing low density foam and dropped at 160°F or containing high density foam and dropped at -40°F, see Figure 2-62. In particular, the predicted maximum Outerpack load for the 75°F temperature/nominal density scenario is 1.69 MN. This is 8.5% more than the maximum load predicted for the -40°F/high density scenario and 13.7% more than that for the 160°F/low density scenario. Our analyses also indicates fuel assemblies in packages containing the highest allowable density foam and dropped at the lowest temperature extreme will experience accelerations that are very similar to those in packages with lowest allowable density foam and dropped at the highest temperature extreme, see Figure 2-63. However, the accelerations at these extremes are only 5% greater than for a package dropped at 75°F containing nominal density foam. Thus, temperature and foam density have a minor effect on drop performance of the Traveller XL package.

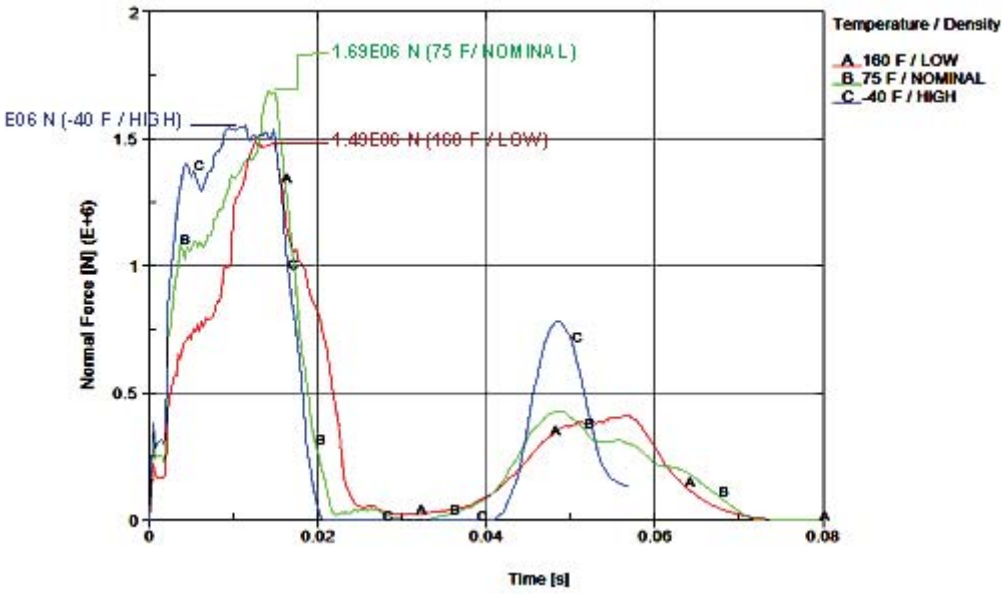

Figure 2-62 Predicted Temperature and Foam Density Effect on Outerpack/Drop Pad Interface Forces (9m CG-Forward-of-Corner with 18° Rotation Drop onto the Top End of the Package)

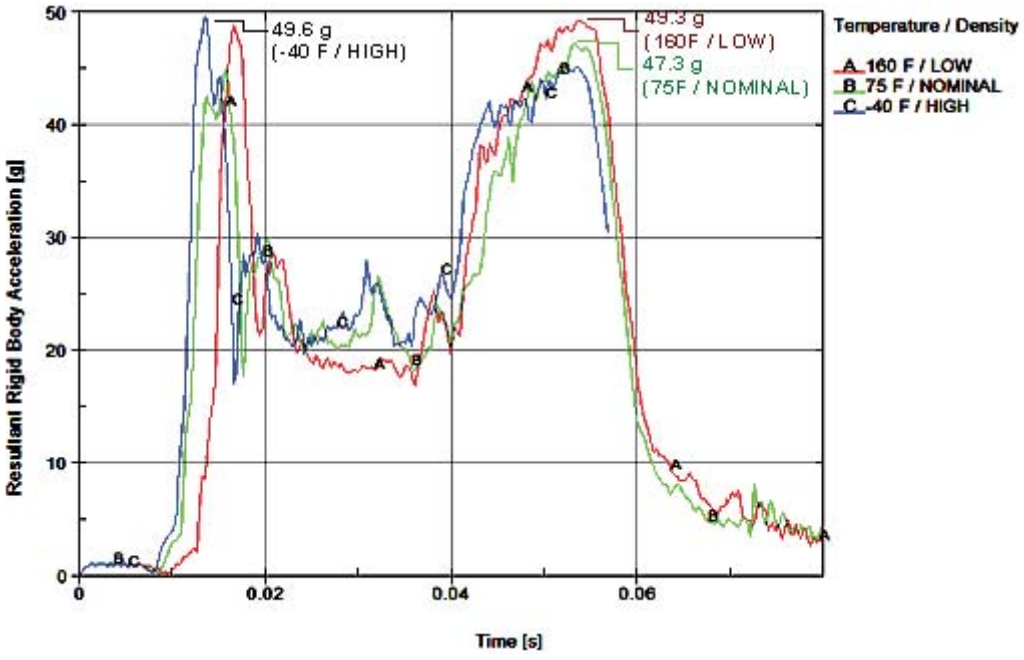

Figure 2-63 Predicted Temperature and Foam Density Effect on Outerpack/Drop Pad Accelerations (9m CG-Forward-of-Corner with 18° Rotation Drop onto the Top End of the Package)

In addition, the 9 meter vertical bottom-end down drop was analyzed using material properties for -40°C (-40°F) with foam density at the upper end of the tolerance band and 71°C (160°F) with foam density at the lower end of the tolerance band. The predicted results were compared with each other and with those at 24°C (75°F) and nominal foam density previously reported in Section 2.12.3.2.5. The results support the conclusions obtained from analysis of the 9 meter CG-forward-of-corner drops: temperature and variation in foam density due to manufacturing tolerances have only a minor effect on the drop performance of the Traveller package.

Temperature/foam tolerance effects for the 9 meter vertical drop onto the bottom nozzle end of the package were evaluated for the three previously noted conditions. Both predicted outerpack/drop pad force histories and fuel assembly accelerations were compared as shown in Figures 2-63A and 2-63B.

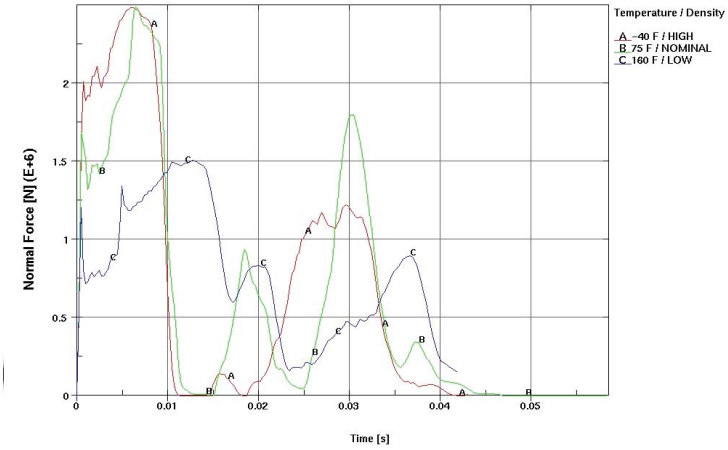

Figure 2-63A Predicted Temperature and Foam Density Effect on Outerpack/Drop Pad Interface Forces (9m Vertical Drop onto the Bottom End of the Package)

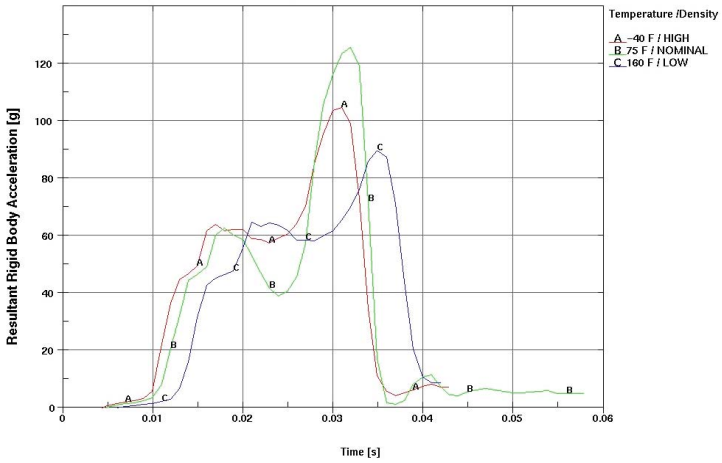

Figure 2-63B Predicted Temperature and Foam Density Effect on Fuel Assembly Acceleration (9m Vertical Drop onto the Bottom End of the Package)

Both of these figures predict that the highest forces occur when the package is 24°C (75°F) with the package having nominal foam density. (This does not necessarily mean that a package dropped at 24°C/75°F having foam densities at either the high or low end of the tolerance band would have had lower outerpack/drop pad forces and lower FA accelerations since that was not investigated.) In particular, the predicted maximum outerpack load for the 75°F (24°C)/nominal foam density scenario was 2.5E6 N. This was equal to that predicted for -40°C (-40°F) with foam density at the upper end of the tolerance band and about 67% greater than the 1.5E6 N load predicted for 71°C (160°F) with foam density at the lower end of the tolerance band. Moreover, a maximum FA acceleration of 126 g's was predicted for drops at 24°C (75°F) with the package having nominal foam density. This was approximately 20% higher than the 105 g's predicted for the -40°C (-40°F) with foam density at the upper end of the tolerance band scenario and approximately 40% higher than the 90.1 g's predicted for 71°C (160°F) with foam density at the lower end of the tolerance band case.

Energy and Work Histories – The predicted global energy and work histories for the package at 75°F containing nominal density foam was previously shown in Figure 2-29 (18° rotation.) This information is repeated in Figure 2-64 along with the corresponding results for a package dropped at 160°F with low density foam and at -40°F and high density foam. Although not discernable from these graphs, the initial total energies were slightly different for the three runs. In particular, the initial energy for the 160°F/low foam density run was 202 kJ, 204 kJ for the 75°F/nominal foam density run, and 205 kJ for the -40°F/high foam density run. These slight differences were obviously a result of the slight differences in predicted weight. Hourglass, sliding, and stonewall energies were small relative to the total energy. This indicates good overall numerical analyses.

2.12.4.2.7 Pin Puncture

In addition to the 9m drops, the package must survive a "pin puncture" test. The pin puncture test involves dropping the shipping package onto a flat-headed (15 cm diameter with 6 mm chamfer all around) steel pin from a 1 m height. The orientation of the package and location of pin impact must be chosen to achieve the greatest damage to the package.

The pin damage investigation consisted of two approaches. First, the pin drop was analyzed, based on maximum impact forces imparted to the Outerpack. Then, the cumulative damage that a pin drop could cause following a 9 m drop was studied. The latter study was naturally based on the 9 m drop predicted to cause the most Outerpack damage.

Maximum Loads – Our analysis indicates the shipping package will be subjected to the higher loads when dropped in a horizontal orientation, Figure 2-65A, compared to an inclined one Figure 2-65B. For example, when the package is tilted 20° (with the top nozzle end of the package towards the ground), our analysis predicts the maximum impact load is 561 kN. This is 10% less than the 624 kN load predicted for a fully horizontal drop Figure 2-66.

This page intentionally left blank.

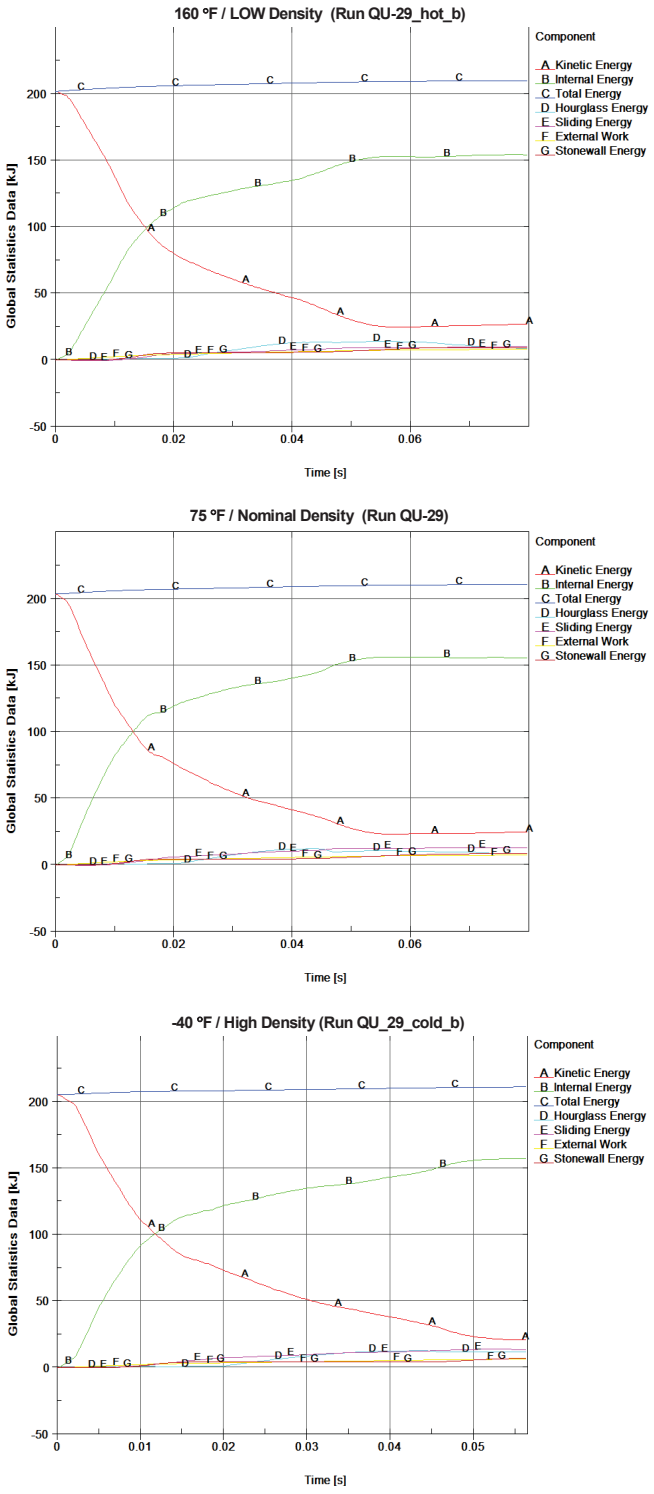

Figure 2-64 Predicted Energy and Work Histories at Various Temperatures

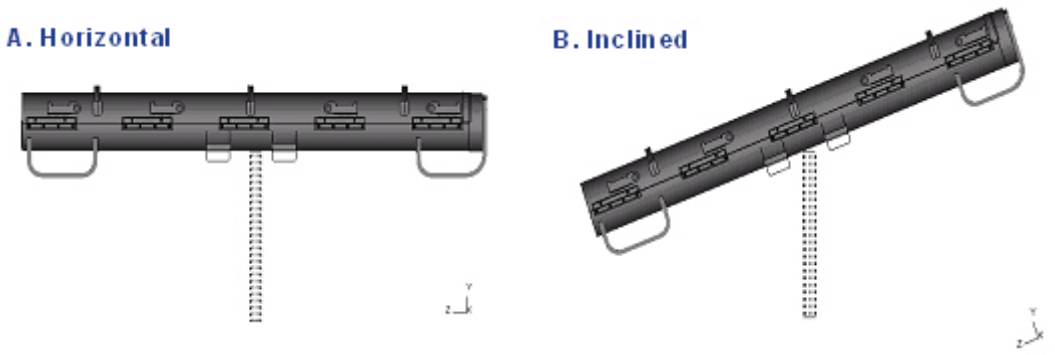

Figure 2-65 Pin Drop Orientation

A comparison of predicted fuel assembly accelerations is shown in Figure 2-67. Note the fuel assembly is predicted to experience approximately 9% higher accelerations in a fully horizontal pin drop than one inclined at 20 degrees.

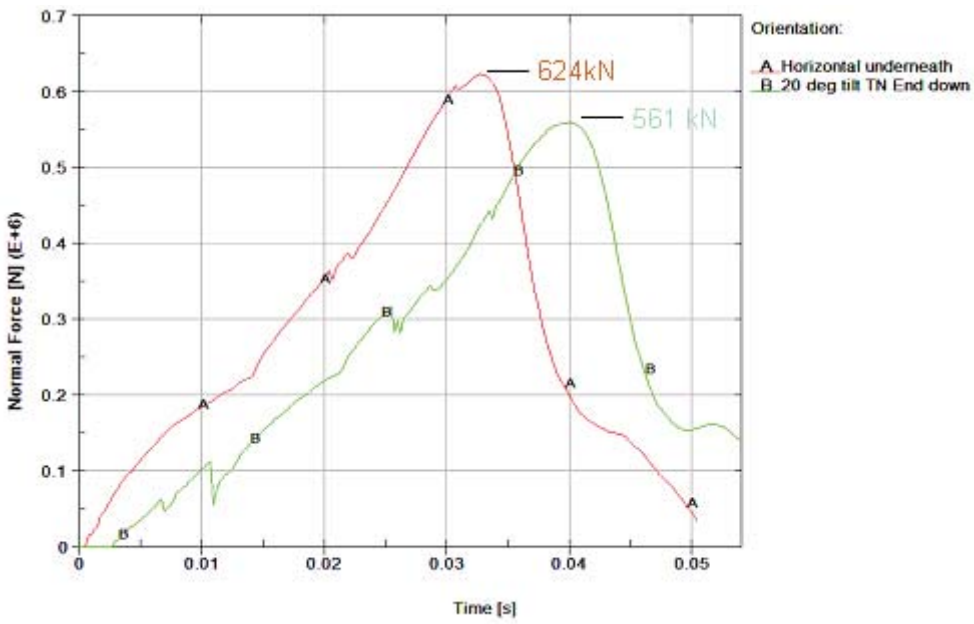

Figure 2-66 Predicted Outerpack/Pin Interference Forces (1m Drop onto 15mm Diameter Steel Pin)

Thus, a fully horizontal pin puncture drop produces higher Outerpack loads and fuel assembly accelerations than inclined pin puncture drops.

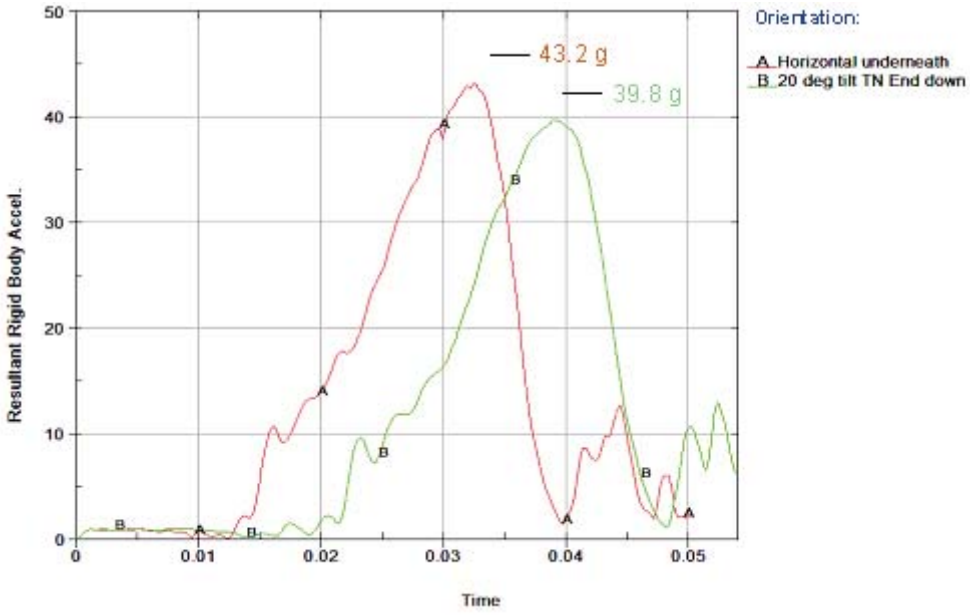

Figure 2-67 Predicted Fuel Assembly Accelerations (1m Drop onto 15mm Diameter Steel Pin)

Worst Horizontal Pin Drop – Two axial rotations were compared when studying the horizontal pin puncture drops. These were the previously described orientation in which the pin impacts the shipping package from underneath, Figure 2-65A, and one where the pin impacts the Outerpack hinges, Figure 2-68. In both cases, the pin was positioned directly under the package CG.

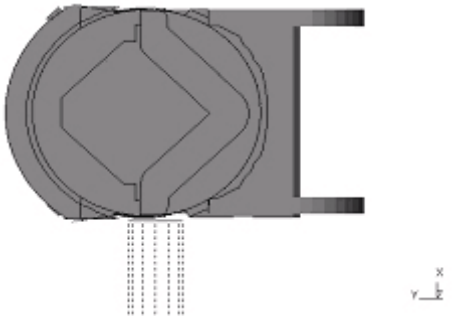

Figure 2-68 Pin Drop onto Outerpack Hinges

Interestingly, predicted Outerpack loads were practically the same for a horizontal pin puncture to the underneath side of the Outerpack and a pin impact directly to a hinge, Figure 2-69. However, there was less cushioning for the fuel assembly in the latter drop. This is evident from the predicted fuel assembly accelerations of 43.2 g's for the impact to the underneath region of the Outerpack and 82.1 g's for the hinge impact, Figure 2-70.

In fact, all of these pin puncture orientations were tested using full-scale Traveller XL units. In all cases, the pin puncture tests were passed without any puncturing of the outer skins of the units, nor any detrimental effects to the Clamshell/fuel assembly, or criticality safety aspects of the package.

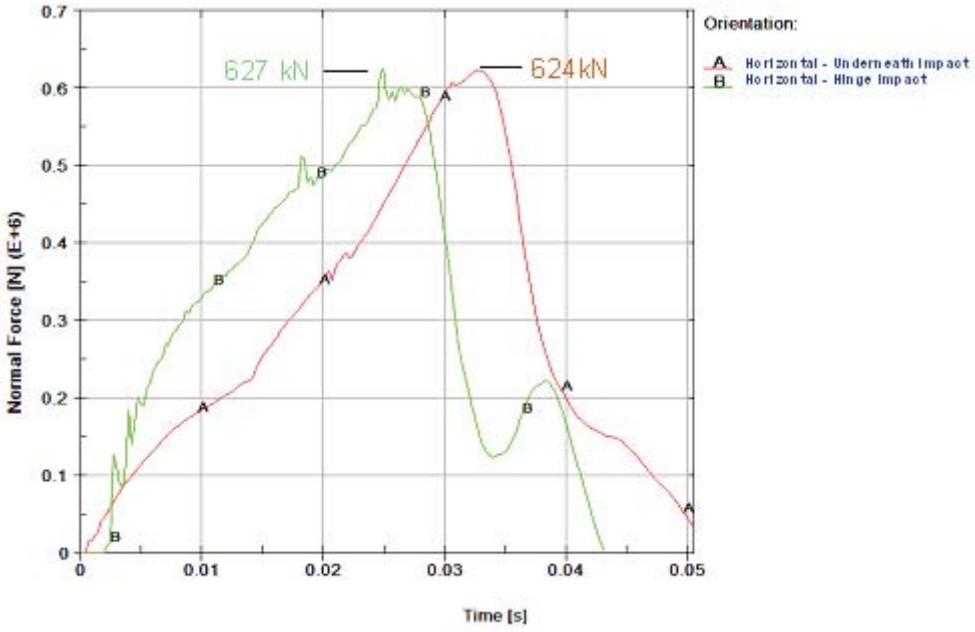

Figure 2-69 Predicted Outerpack/Pin Interface Forces (1m Drop onto 15mm Diameter Steel Pin)

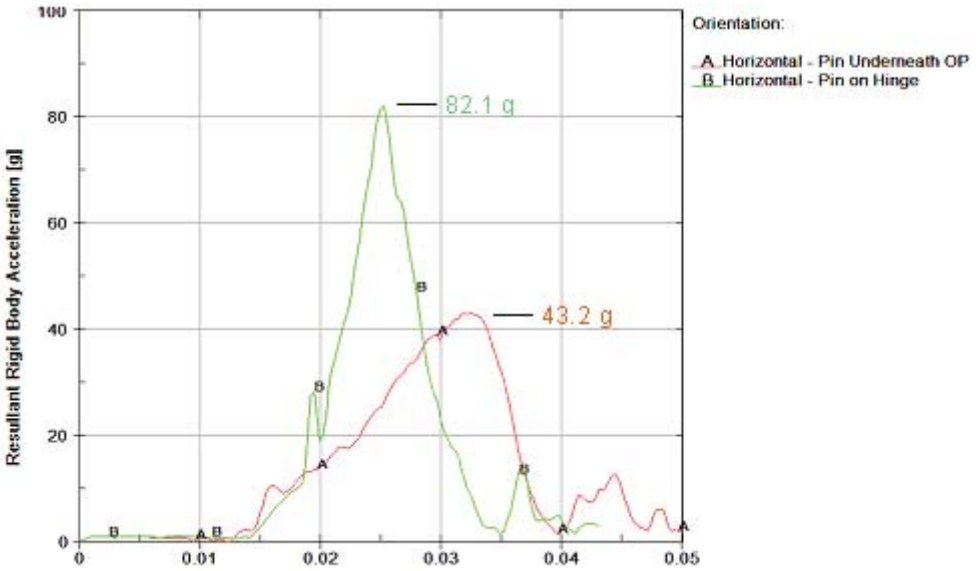

Figure 2-70 Predicted Fuel Assembly Accelerations (1m Drop onto 15mm Diameter Steel Pin)

Energy and Work Histories – Global energy and work for the 1 m pin puncture drops discussed above are shown in Figures 2-71, 2-72 and 2-73. These plots have an initial total energy (TE) of 22.3 kJ. This value correctly reflects the initial velocity (v) of 4.43 m/s applied to the 2,270 kg package mass (m) since our pin puncture simulations are initiated at the end of Outerpack free fall from 1 m; the total energy is comprised only of kinetic energy (KE), and $KE = \frac{1}{2} mv^2$. Total energy rises about 8% in these drop simulations. This reflects the work done by the package under gravity loading, i.e., the bending of the shipping package around the pin. Depending on drop orientation, the event was completed within 4 to 5 milliseconds as seen by the flattening of the kinetic energy and internal energies after that time. Moreover, acceptable levels of hourglass, sliding, and stonewall energies were obtained. This indicates a good overall numerical analysis was obtained in each simulation.

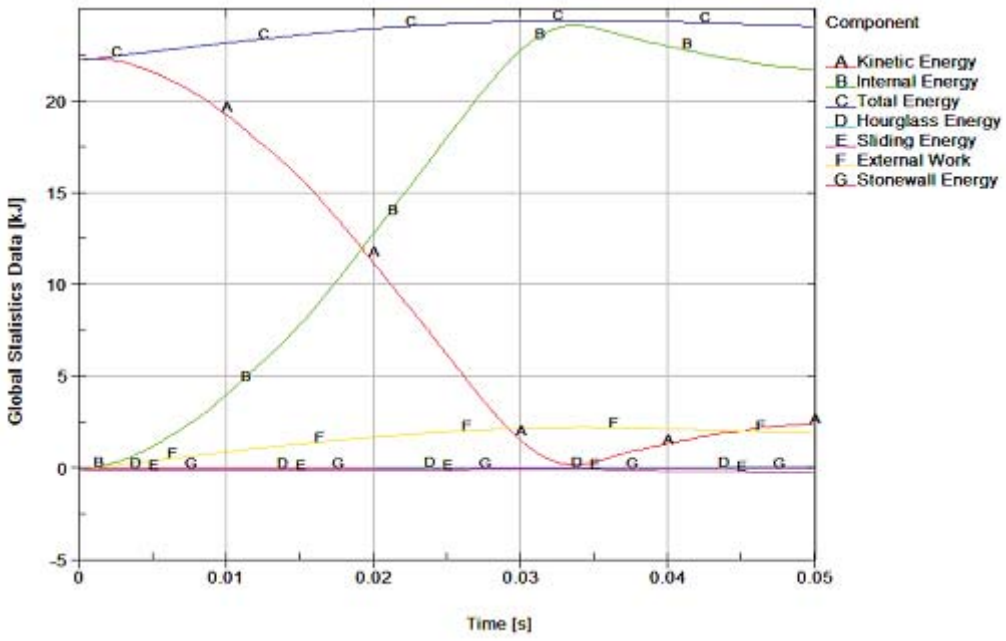

Figure 2-71 Predicted Energy and Work Histories for a 1 m Horizontal Pin Drop (Pin Underneath the Package CG)

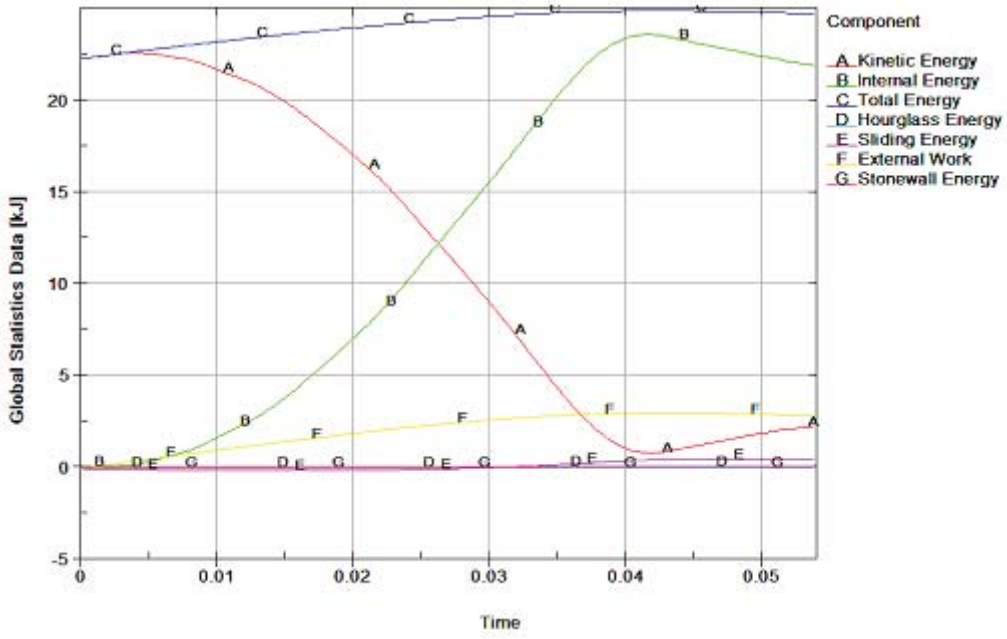

Figure 2-72 Predicted Energy and Work Histories for a 1 m Tilted Pin Drop (20° Tilt With TN End Down

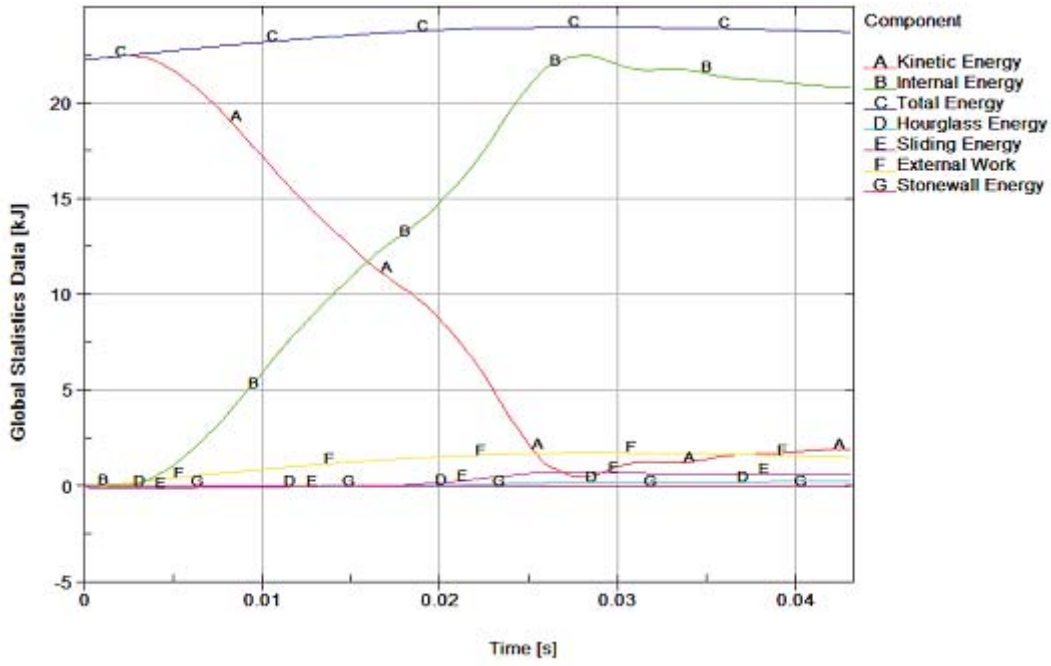

Figure 2-73 Predicted Energy and Work Histories for a 1 m Horizontal Pin Drop (Pin Hitting Hinge at Package CG)

Maximum Pin Indention – Predicted maximum pin indention for the horizontal underneath, inclined, Figure 2-65 and hinge pin puncture drops Figures 2-68 were, 67, 54 and 50 mm, respectively. This is shown in Figure 2-74.

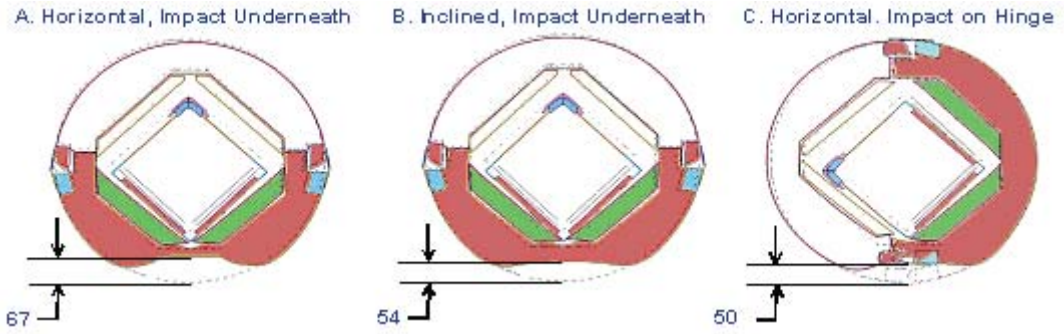

Figure 2-74 Comparison of Predicted Maximum Pin Indentions

Outer Steel Skin Damage – Predicted maximum plastic strains in the steel skin were only 12.6 and 15.7% for the horizontal and 20° tilted pin puncture simulations Figures 2-65A and 2-65B, respectively. These values are much less than the allowable 46.7% failure strain. Thus, it is unlikely the steel skin will be ruptured by the pin puncture test. Initial testing of the Traveller XL Prototype units were demonstrated that 11 gage (0.120" nominal thickness, 3.0 mm) 304 stainless steel had little difficulty passing the pin puncture tests. Those full-scale tests, in addition to the analytic work discussed previously, allowed designers the confidence to reduce the thickness of the Outerpack shells to 12 gage material (0.105" nominal thickness, 2.7 mm). Therefore, the QTU and CTU packages were all fabricated using 12 gage sheet material of the outer shells. Pin drop tests of QTU-1, QTU-2 and CTU packages confirmed that 12 gage material survived the pin puncture tests without failure.

Cumulative Damage – As previously stated, analysis of cumulative pin damage was based on the 9 m drop predicted to cause the most Outerpack damage. Indeed, this analysis placed the pin 1 m under, and normal to, the region of the top impact limiter which was (previously) predicted to flatten during the 9 meter CG-forward-of-corner drop onto the TN end of package with an 18° forward rotation Figures 2-64 and 2-25. The position of the pin was at the apex of the top impact limiter Figure 2-67. This location was chosen since it would most exacerbate the opening of the Outerpack seam predicted from the 9 m drop analysis.

Deformations, strains, and stresses from the previous 9 m analysis were used as the initial starting point for the cumulative pin puncture drop analysis. Inclusion of deformations was accomplished by use of the LSTC/LSPOST[1] capability to output deformations at the appropriate time (state) in LS-DYNA keyword format. The corresponding strains and stresses from the 9m analysis were written to a file (in LS-DYNA keyword format) via the LS-DYNA *INTERFACE_SPRINGBACK_DYNA3D command. A new master 1 m pin puncture analysis keyword file was created that defined all parts, materials, nodes (with deformed

1. LSPOST is the pre- and postprocessor by LSTC provided with LS-DYNA.

positions), element connectivity, loading, etc. Stresses and strains were then brought into the analysis by use of the LS-DYNA *INCLUDE and *STRESS_INITIALIZATION commands.

Maximum Loads – The Westinghouse analysis indicates the shipping package is subjected to higher loads when dropped on a previously damaged end than in any other orientation analyzed, including a drop onto a hinge. Indeed the maximum predicted Outerpack load was 734 kN for the 2nd hit Figure 2-75. This is 17% higher than the 627 kN predicted for a drop onto the Outerpack hinge Figure 2-69. The greater load is attributed to the lower cushioning available due to the foam in being highly compressed during the 9m drop. Even so, the maximum predicted fuel assembly acceleration was just 38.2 g's Figure 2-76.

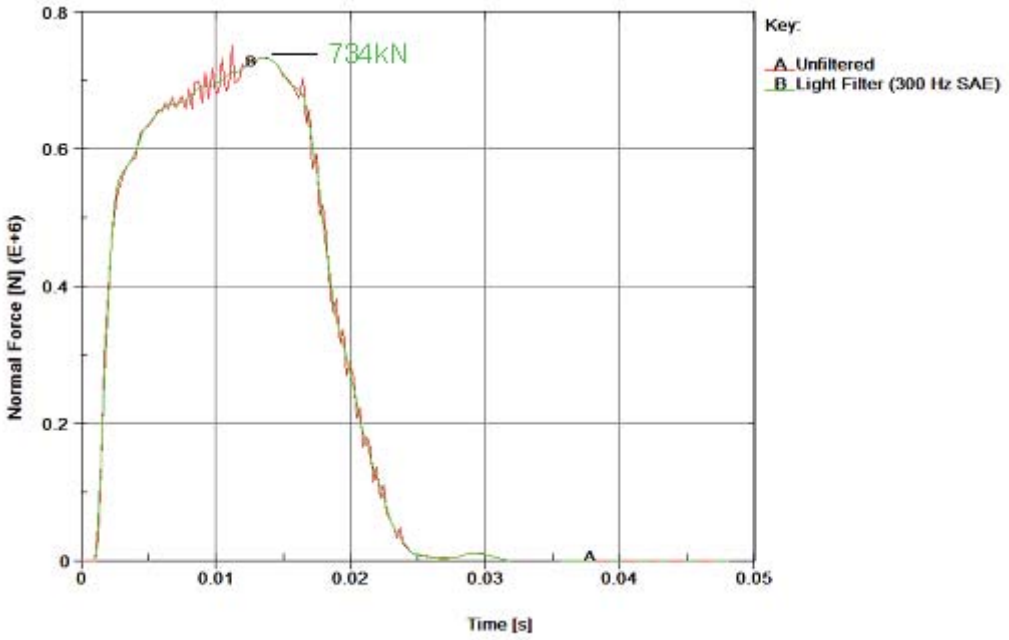

Figure 2-75 Predicted Outerpack/Pin Interface Forces (1 m Drop onto 15 mm Diameter Steel Pin After 9m Drop)

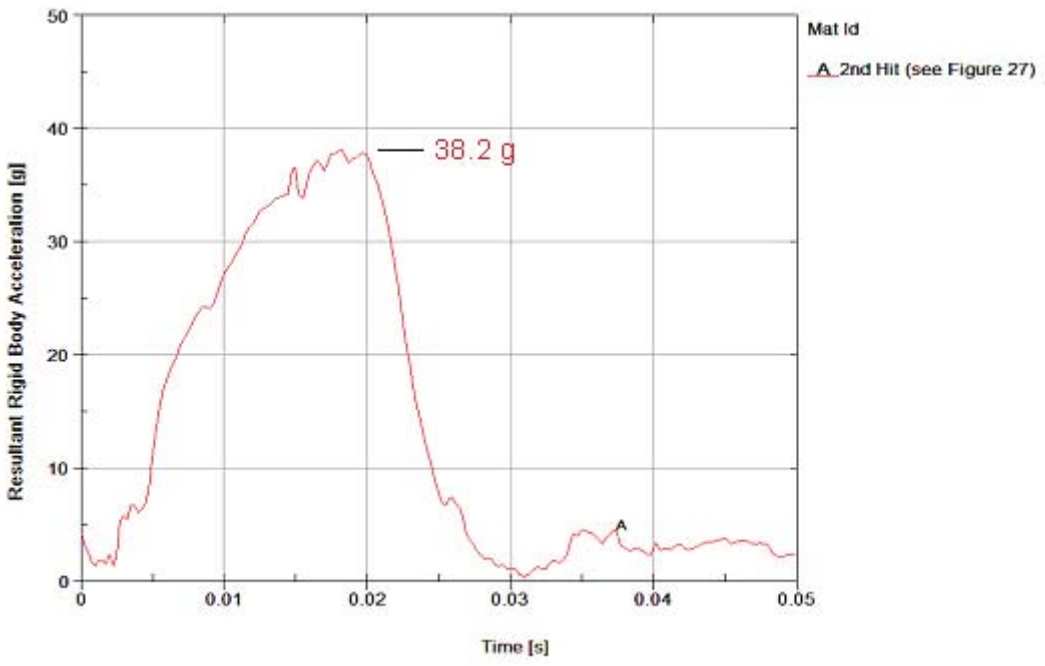

Figure 2-76 Predicted Fuel Assembly Accelerations (1 m Drop onto 15mm Diameter Steel Pin after 9 m Drop)

Additional Damage – As previously discussed, our primary concern for this sequence of drops (a 9 m CG-forward-of-corner drop onto the top nozzle end of the package followed by the 1 m pin puncture) was the extent of Outerpack seam opening Figure 2-28. Our measures of Outerpack seam opening, D1 and D2 (see Figure 2-48), would increase from 20 to 22.9 mm and from 20 to 22.2 mm, respectively.

Energy and Work Histories – Predicted global energy and work for the 1 m pin puncture drop following a 9 m CG-forward-of-corner drop onto the top nozzle end of the package is shown in Figure 2-77. The sliding energy in this plot is related to the initial penetration between the crushed impact limiter foam and outer steel skins. It is not necessarily an error. Moreover, the predicted increase in damage due to the pin puncture test simply does not warrant further investigation of this issue.

Pin Puncture Summary – Our analyses indicate the Traveller XL package is very capable of withstanding the 1 m pin puncture test. Indeed, it was determined that the likelihood of rupturing the outer steel skin is very low. Thus, the 1 m pin puncture test is a relatively benign test for the Traveller XL package. These conclusions were confirmed by the prototype test results as subsequently discussed.

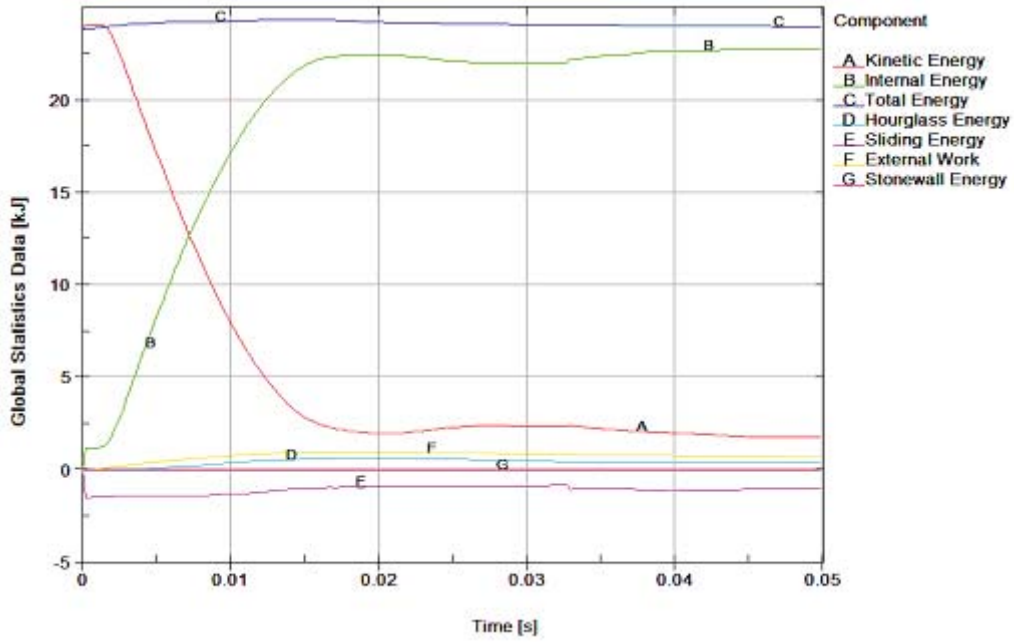

Figure 2-77 Predicted Energy and Work Histories (1 m Drop onto 15 mm Diameter Steel Pin after 9 m Drop)

2.12.4.3 Comparison of Test Results and Predictions

Two prototype Traveller XL packages were drop tested on January 28 and 29, 2003. Details of these tests are provided in Appendix 2.12.5, Traveller Drop Test Results.

Results from the extensive prototype tests in January, 2003 were reviewed to find the best ones for comparison with FEA predictions. Comparison cases were chosen to include tests with prototype units which did not have extensive previous test damage, those which represented a unique test configuration (i.e., the pin puncture) and those in which accelerometer data was obtained. The four selected cases are identified in Table 2-22 and Figure 2-78.

There was good overall agreement between predicted and actual drop performance of the prototype Traveller XL package. This is evident by comparisons of predicted and actual permanent deformations, failed parts and measured and predicted accelerations at specific positions on the Outerpack and Clamshell.

Table 2-22 Prototype Tests Used to Compare with Analysis					
Test ID (corresponds to [6])	**Analysis ID**	**Drop Height [m]**	**$\grave{E}_x$**	**$\grave{E}_z$**	**Comment**
1.1, 9 m Low Angle	C1-25	9.1	14.5°	180°	T/N primary impact on OP top
1.2, 9 m CG-over-corner	C1-31	9.1	-71°	90°	B/N primary impact on OP hinge
2.2, 1 m Pin-puncture	Punc2-2nh	1.04	20°	135°	CG (Axial) on OP topside, T/N end down
2.3, 9 m CG-over-corner	C1-29	9.1	108°	0°	T/N primary impact on OP top

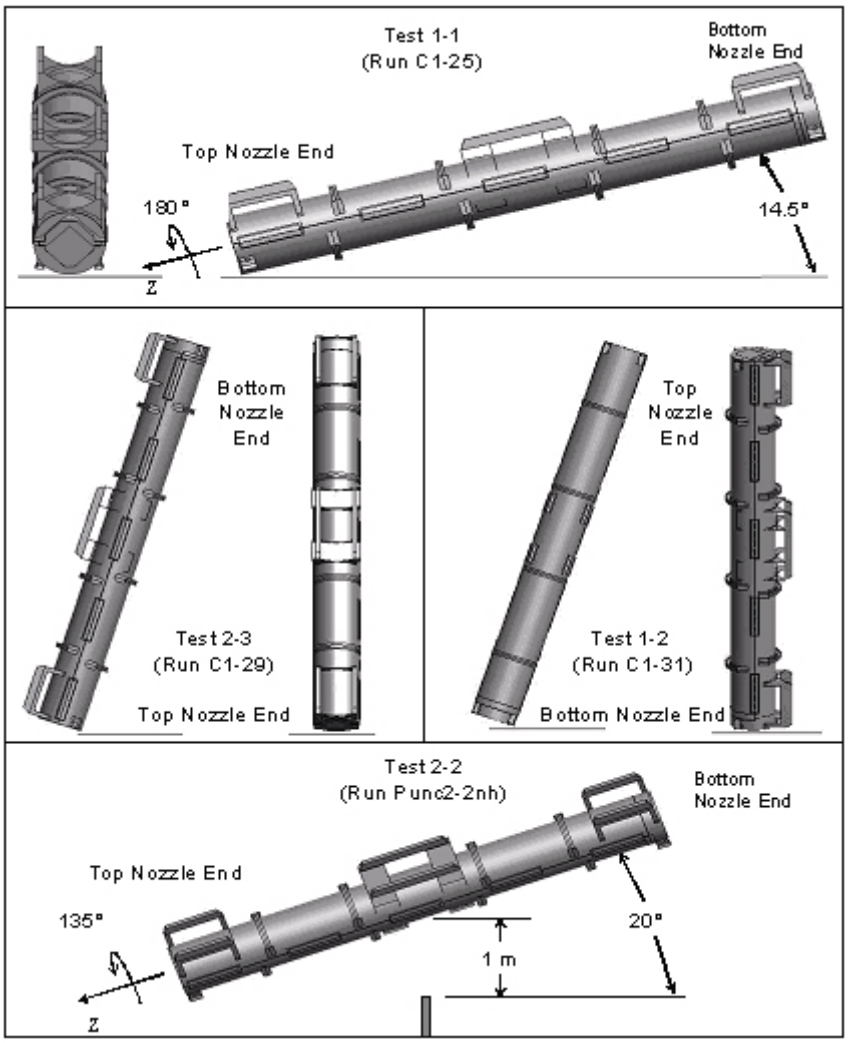

Figure 2-78 Prototype Drop Tests Used To Benchmark Analysis

2.12.4.3.1 Prototype Unit-1 Test 1.1

Prototype Unit-1, Test 1.1 was chosen for the first comparison. As indicated in Table 2-22 and Figure 2-78, this was an inclined drop from 9.1 meters onto the upper Outerpack (the unit was rotated 175° about its long axis and inclined 14.5° with the end of the package nearest the top of the fuel assembly hitting first.[1] Four frames taken from a video recording of test 1.1 are shown in Figure 2-79. These frames show the test sequence was comprised of the initial impact on the top nozzle end of the package (frame 1), rollover (frames 2 and 3), and a secondary impact to the bottom nozzle end of the package (frame 4).

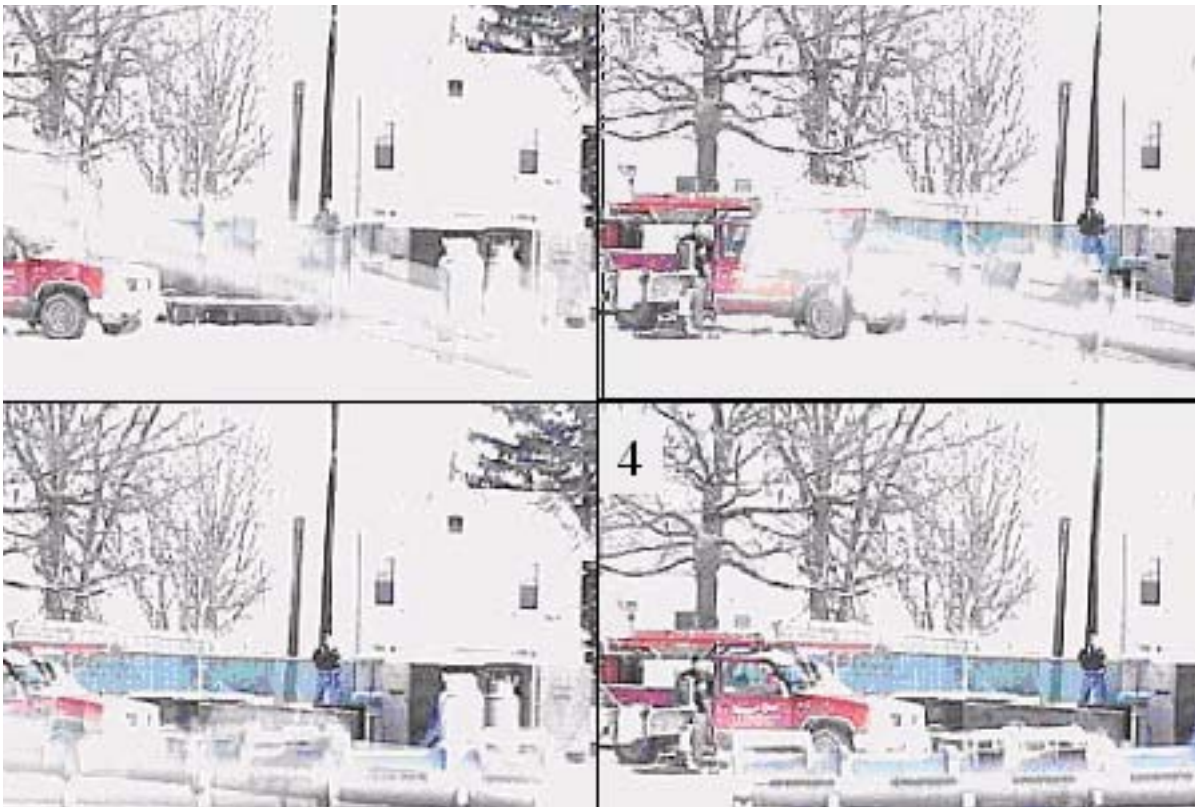

Figure 2-79 Prototype Unit 1 Drop Test

Deformations – As reported in, test 1.1 produced noticeable permanent deformations in several locations of the Outerpack and no significant permanent deformations in the Clamshell. Outerpack permanent deformations were primarily at the ends of the package.

1. This will be referred to as the "top nozzle end" of the package. Likewise, the end of the package nearest the bottom of the fuel assembly will be called the "bottom nozzle end."

An overall sense of the correspondence between predicted and actual Outerpack permanent deformations may be obtained by reviewing Figures 2-80 through 2-87. Quantitative comparison between predicted and documented measurements is given in Table 2-23.

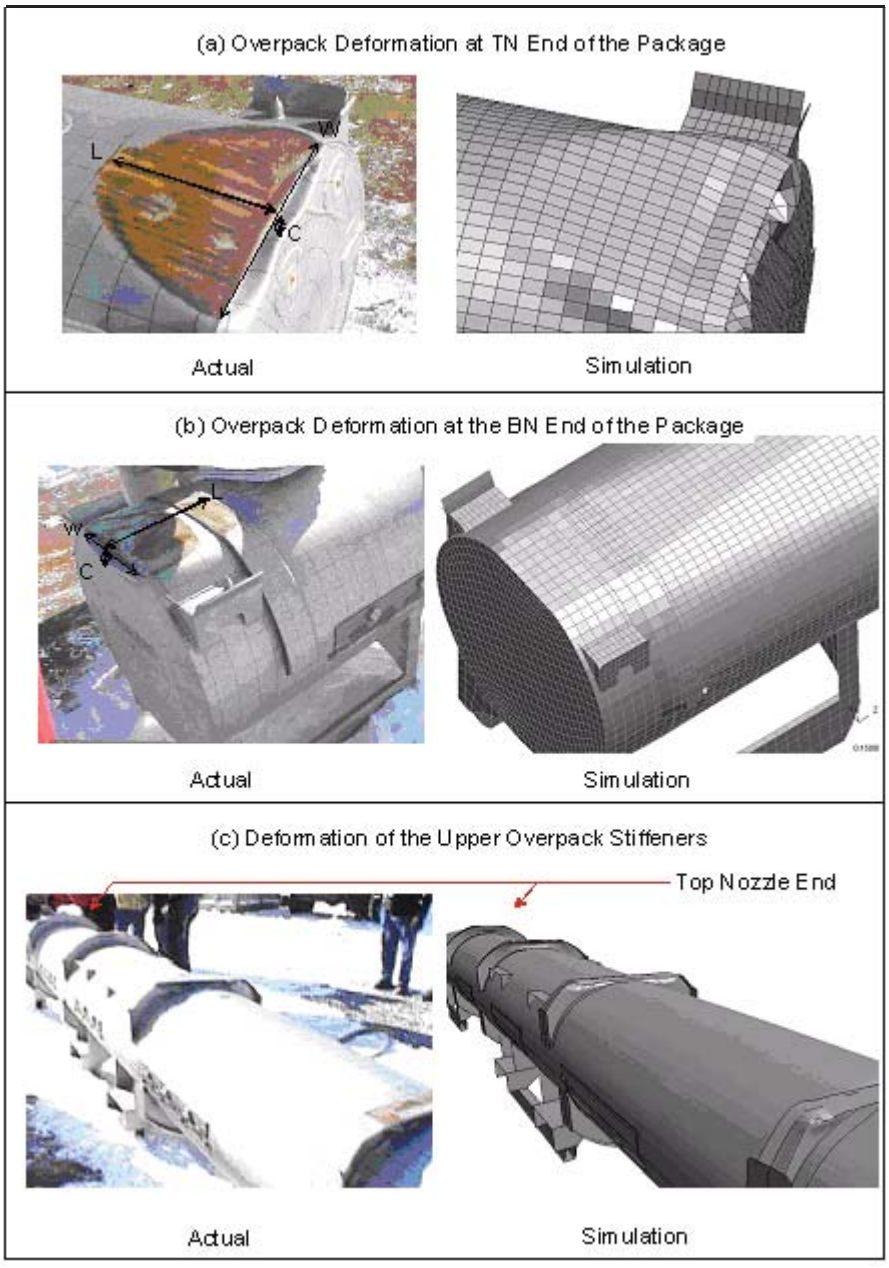

Figure 2-80 Comparison of Test 1.1 with Analytical Results

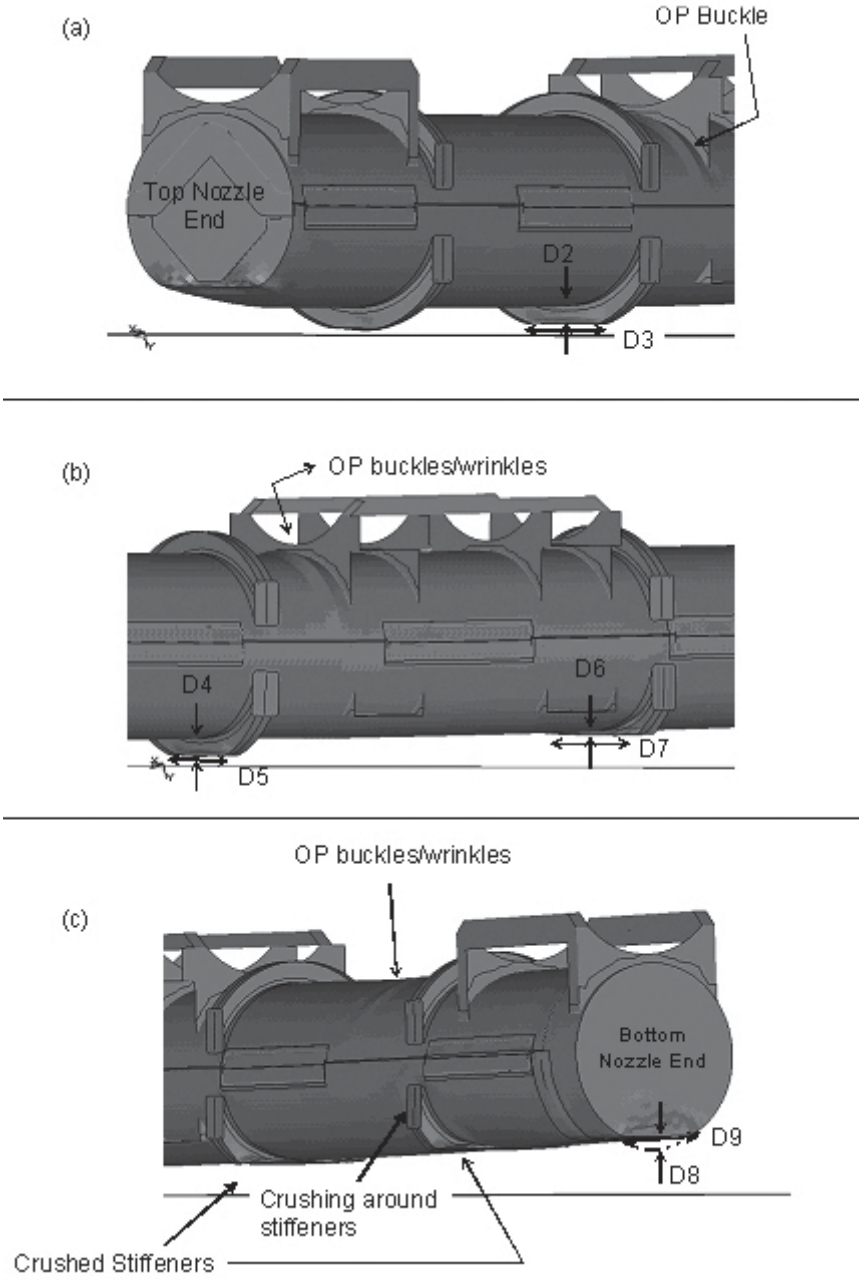

Figure 2-81 Comparison of Test 1.1 with Analytical Results

Table 2-23 Comparison of Predicted and Actual Deformations for Test 1-1

Item	Location	Measured (Reference 6)		Predicted		Nodes used to make Prediction		Difference	Conservative
		(in)	(mm)	(in)	(mm)				
1	Top nozzle end								
	Dim L in Figure 2-80	9.0	229	11.9	302	192658	134223	32.2%	Yes
	Dim W in Figure 2-80	12.0	305	14.6	371	134052	134170	21.7%	Yes
	Dim C in Figure 2-80	1.5	38	1.65	42	134062	223918	10.0%	Yes
2	Bottom nozzle end								
	Dim W in Figure 2-80	11.5	292	11.9	302	214342	190946	3.5%	Yes
	Dim L in Figure 2-80	10.57	268	13.0	330	94120	213639	23.0%	Yes
	Dim C in Figure 2-80	0.75	19	1.5	38	93833	214433	100.0%	No
3	Upper Overpack Stiffeners								
	Dim D2 in Figure 2-81	0.8	19	0.7	17	115715	115853	-10.7%	Yes
	Dim D3 in Figure 2-81	N/A		11.9	303	115702	116484	-	
	Dim D4 in Figure 2-81	2.4	60	2.2	56	112621	112759	-6.4%	No
	Dim D5 in Figure 2-81	N/A			-			-	
	Dim D6 in Figure 2-81	N/A		1.0	26	109526	110131	-	
	Dim D7 in Figure 2-81	16.0	406	18.4	468			15.1%	Yes
	Dim D8 in Figure 2-81	N/A			-			-	
	Dim D9 in Figure 2-81	23	584	22.6	574			-1.7%	No
							Average Difference:	22.4%	

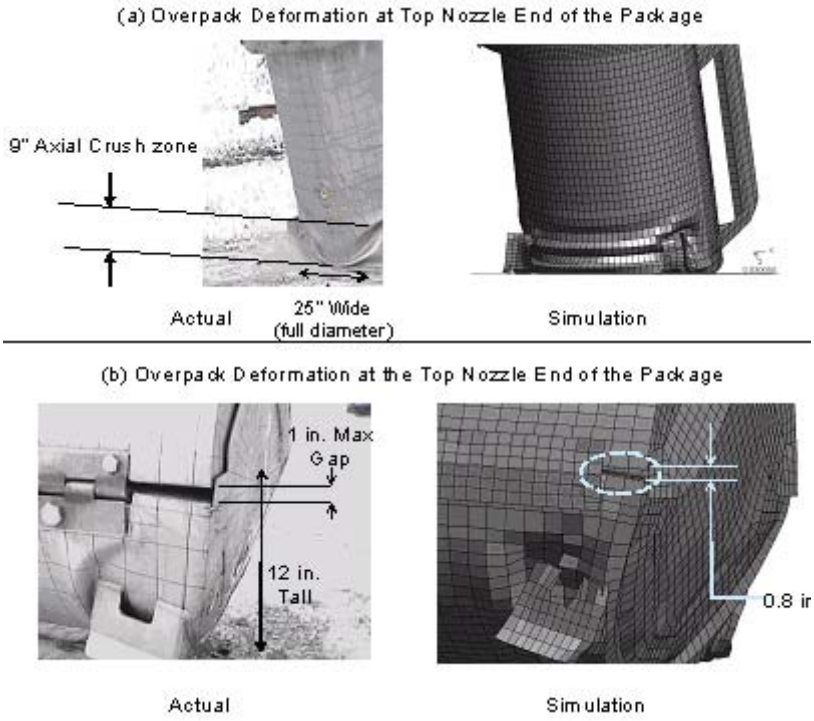

Figure 2-82 Deformations at End of Package

Figure 2-83 Internal Deformations at Inside Outerpack

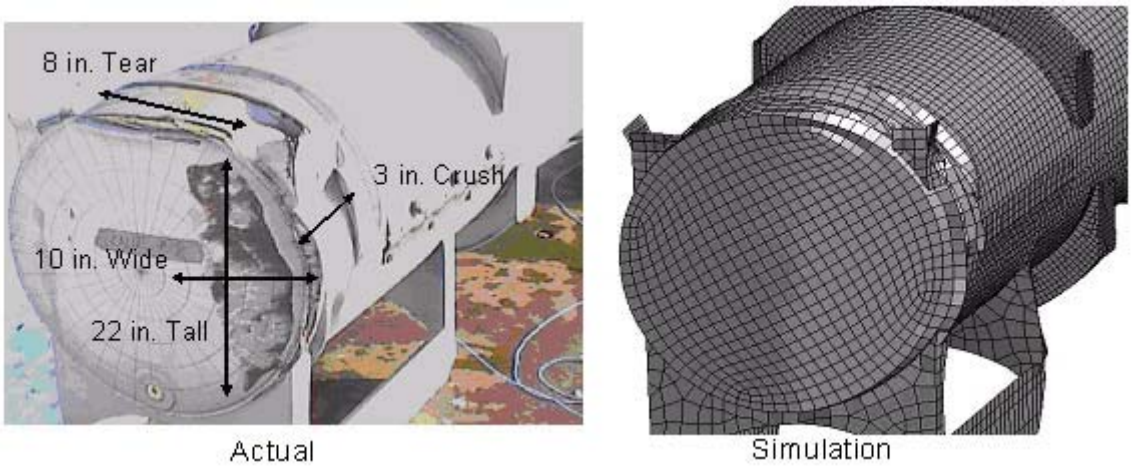

Figure 2-84 Outerpack Deformations at Bottom Nozzle End of Package

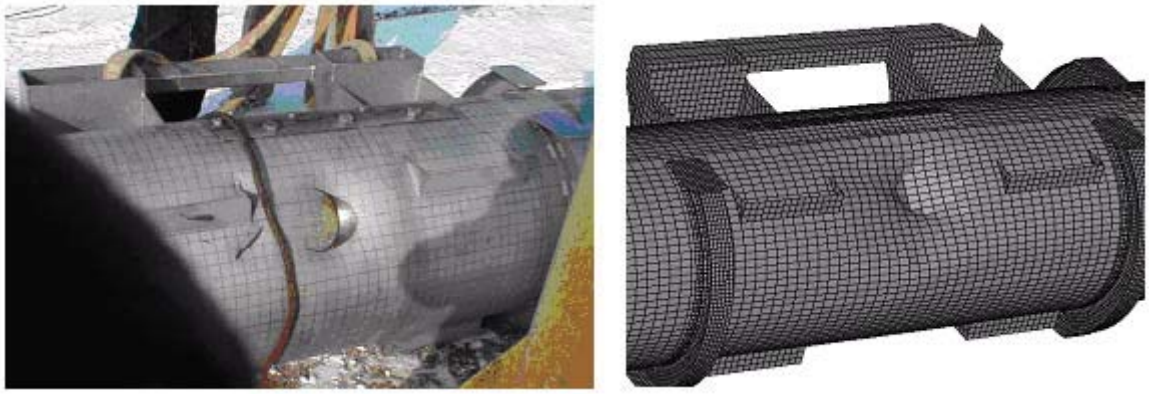

Figure 2-85 Pin Puncture Deformations

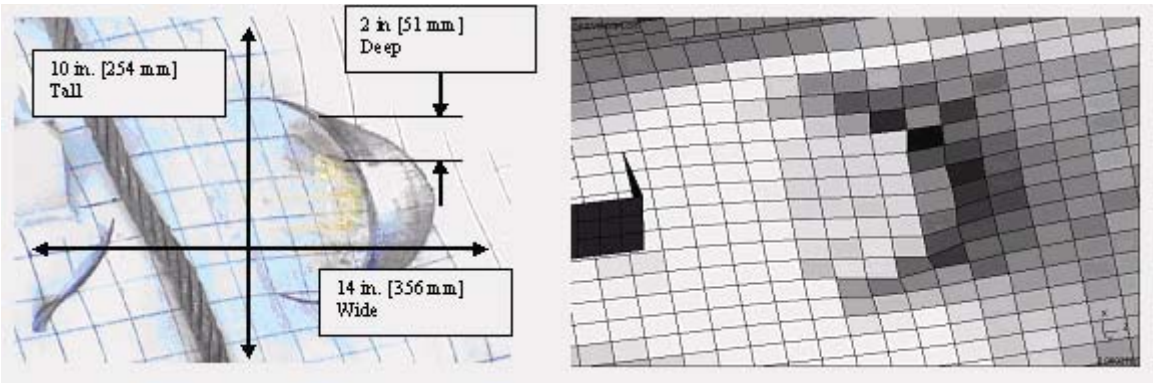

Figure 2-86 Dimensions of Pin Puncture Deformations

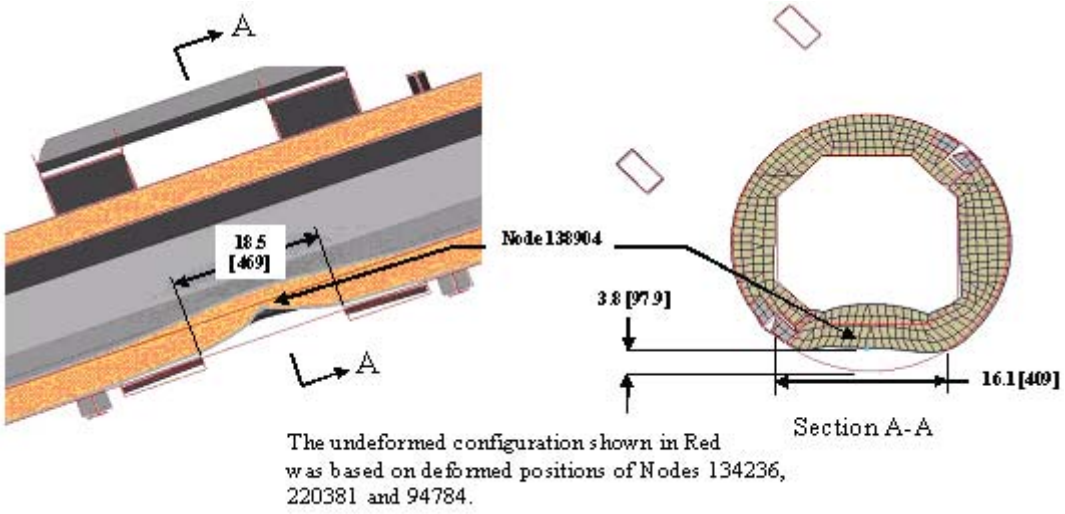

Figure 2-87 Outerpack Predicted Deformations of Pin Drop

2.12.4.3.2 Accelerations

Vertical accelerations (Y-direction) measured during test 1.1 are compared with the FE-based predictions in Figures 2-88 through 2-92. Agreement was good. Indeed, discrepancies between the two could easily be attributed to the inherent error associated with obtaining such data.

For the Outerpack, both measured and predicted traces contained two peaks, Figure 2-88. These corresponded to the two impacts associated with this test as illustrated in Figure 2-78. (Note: the larger acceleration with the secondary impact should not be interpreted as meaning larger forces were associated with the second impact. Rather, the larger magnitude simply reflects that the accelerometer was much nearer the secondary impact end.) While there were two visible peaks, the measured response was very small for the primary impact. For the secondary impact, the predicted acceleration was 1270 g's. This was in accordance with the measured peak acceleration which indicated accelerations were greater than 950 g's.

For unknown reasons, the accelerometers on both the Clamshell top and bottom plates gave erroneous readings late into the drop. This is clearly evident from accelerometer data in Appendix 2.12.5 that the accelerometers "saturate" for over 0.025 seconds and provide no meaningful response afterwards. Thus, only the first 0.05 seconds of the Clamshell data was compared in this report. For the accelerometer on the Clamshell top plate, measured and predicted accelerations corresponding to the first impact (at time 0.01 seconds in Figure 2-90) were 555 g's. This was also in accordance with measurements which indicated a peak acceleration greater than 525 g's was experienced. As shown in Figure 2-91, peak accelerations of 205 g's were measured on the Clamshell bottom plate. The corresponding predicted acceleration is also shown. Note the peak predicted acceleration was 155 g's.

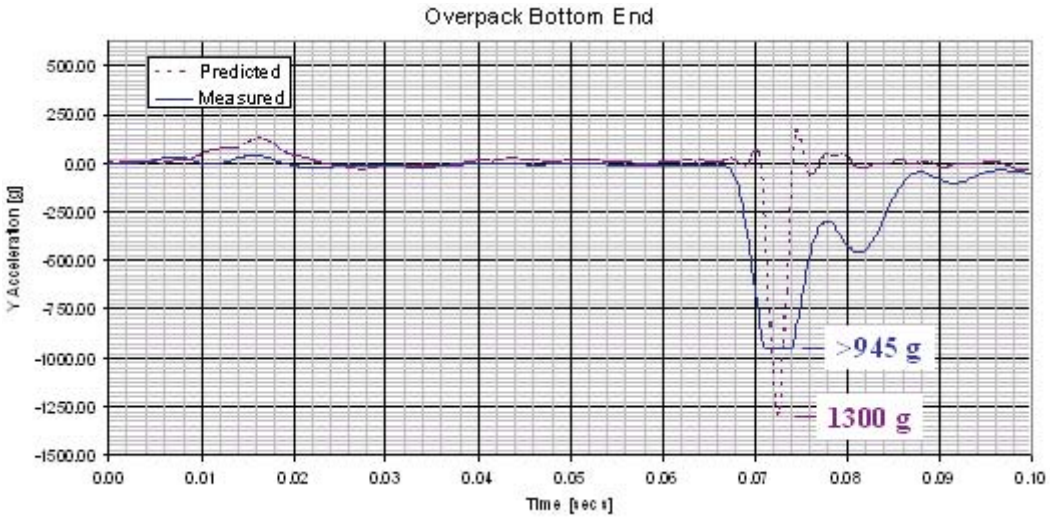

Figure 2-88 Predicted and Measured Y Accelerations

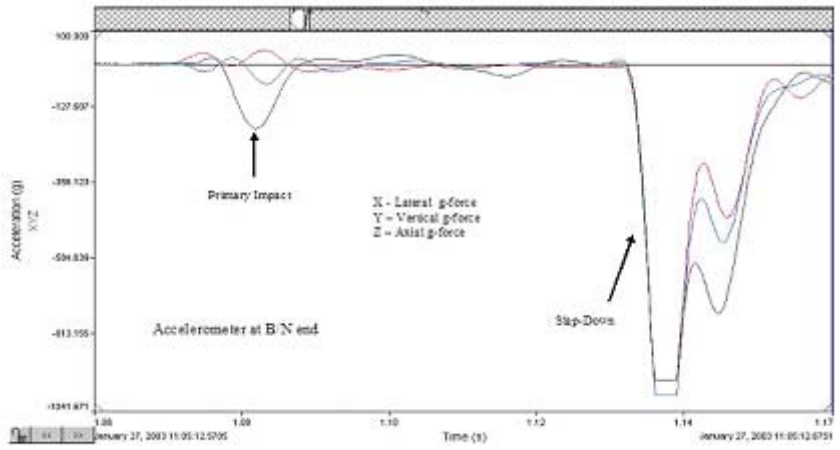

Figure 2-89 Three Axis Measured Accelerations

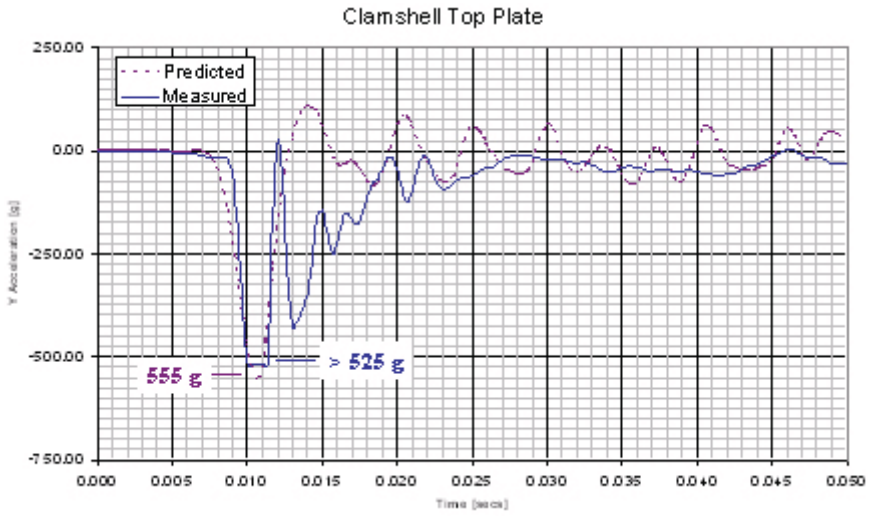

Figure 2-90 Predicted and Measured Y Accelerations

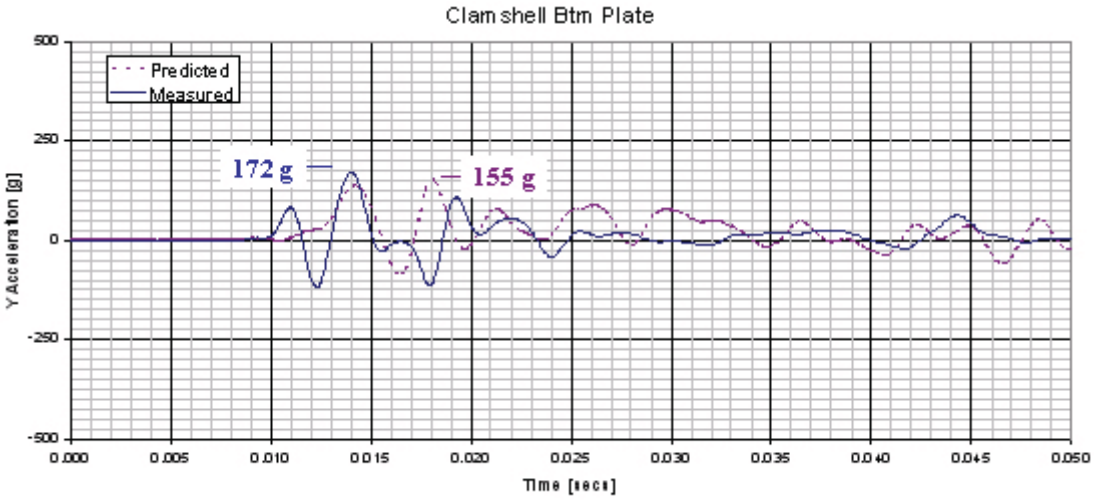

Figure 2-91 Predicted and Measured Y Accelerations

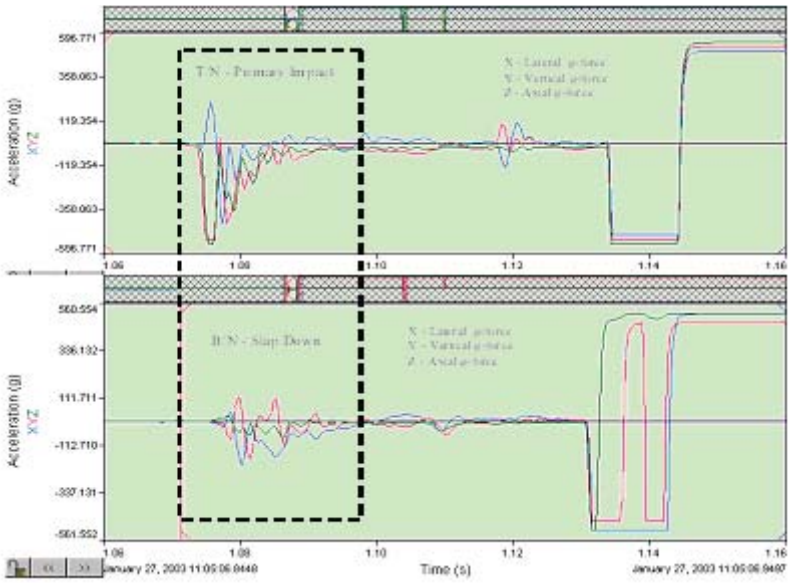

Figure 2-92 Measured Primary and Secondary Accelerations

2.12.4.4 Discussion of Major Assumptions

The many assumptions used to develop the LS-DYNA non-linear finite element stress code, including those needed to model the materials and impact, were found valid for simulating drop tests of the Traveller XL package. It is clearly evident from comparisons between prototype test results and predictions that the key physical phenomena governing shipping container impacts is captured within the LS-DYNA code.

The only major additional assumption was that bowing of the fuel assembly did not result in excessive additional loading of the Clamshell side walls, hinges and latches. Test results showed this was a valid assumption.

LS-DYNA 960 build no. 1647 (single precision, MPP) was used in these calculations because it has the very needed “no put-back” contact capability. However, the official quality tested and assured version is currently DYNA 960 build no. 1106 (single precision, MPP) which does not have the no put-back contact capability. ARUP is expecting to officially release LS-DYNA 970 (probably build no. 3858) in late October, 2004. This version, which does have the no put-back capability, must be installed and tested on the claxgen computers. Then a Traveller XL drop test case must be run to verify results in this calculation note correspond with results from the quality-assured version of LS-DYNA.

2.12.4.5 Calculations

2.12.4.5.1 Method Discussion

The finite element method was used to determine the loads, displacements, accelerations, strains, etc. of a Traveller XL shipping package containing an XL fuel assembly when dropped on a flat surface from 9 m and onto a 15 mm diameter pin from 1 m. The LS-DYNA explicit finite element code was used. This software was selected because it allowed the analysis to include the effects of large deformation, large strain, material non-linearity, contact, and failure of connections between parts and assemblies.

The goal of the analysis was to predict the deformation and damage that the Traveller XL shipping package and contained fuel will experience when subjected to the HAC impact tests. Although it would have been more conservative, it was not feasible to build a model which allowed failure of all joints and any deformation pattern. Such a model would have been unduly complex and calculation intensive and have required extraordinary development time. Rather, the Traveller XL prototype and qualification unit finite element models were constructed with consideration of all probable relative displacements, contact and failures. The premise in choosing this deliberately restrictive approach was that it would not affect accuracy because it would include provisions for the actual deformation and damage. Test results substantiated the accuracy of the prototype unit model, see Appendix 2.12.5.

The models described herein were primarily developed to aid in determining the drop orientations and number of drops needed to meet the HAC requirements. Thus, any point on the Outerpack outer periphery was a potential impact point and there was no one point in which a finer mesh could be afforded. Thus, the actual strains and stresses determined in the model can not be considered refined. Rather, the relative deformations, decelerations and energy absorption between drop orientations should be considered. This limitation applies to both models of the prototype unit and the qualification unit.

Model Descriptions – A basic description of the Traveller XL prototype and qualification units is discussed in section 1 above. All design details are available in and. Details of the finite element models are described in the following two sections.

In both models, units were tonnes (mass), millimeters (length), seconds (times) and Newtons (force).

2.12.4.5.2 Prototype Models

The Prototype models, Units 1 and 2, were constructed from many input files, Figure 2-94. These files defined various details of the model and were included with, or without, transformations of coordinates and renumbering of identities as the model was assembled.

The main file, Apr6.key, contains the control cards, specifies outputs, contact definitions, and many attributes common to more than one subassembly. The major subassemblies were the Outerpack, Clamshell, and fuel assembly. These were defined in the OP.key, CS.key, and XL_FAr.key files, respectively. These subassemblies are detailed in Figures 2-95 through 2-97. A total of 363,646 elements were used in the model (199128 shells, 150717 solids and 13801 beams).

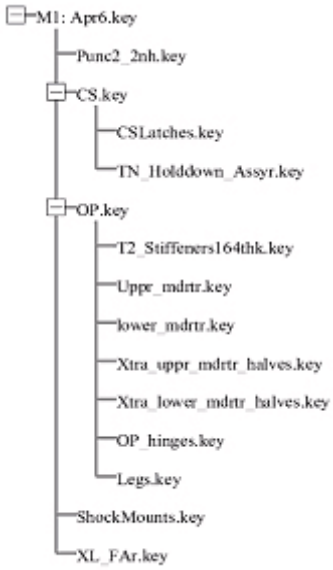

Figure 2-93 FEA Model Input Files

The orientation for each run was defined in individual load case files. Obviously, only one load case file and one material file was invoked per run.

The Clamshell Figure 2-96 is mounted to the Outerpack, Figure 2-94 with 22 rubber shock mounts. These shock mounts were modeled as discrete elements (springs). The stiffness of these elements was 92.7 N/mm in the global X direction, 135.4 N/mm in the global Y direction and 42.3 N/mm in the global Z direction. These values were obtained through tests. These details are included in the 'ShockMounts.key' file.

Predicted model weight for the Prototype units was 2.39 tonnes (5258 lbs). This matched the Prototype unit's 5065 lb. average weight within 3.8%.

Predicted model weight for the Qualification units was 2.27 tonnes (4994 lbs). This matched the Qualification unit's 4786 lb. average weight within 4.4%.

The Traveller program performed drop tests as input into the design process. As a result, there were changes in the design of the Traveller between the prototypes discussed on page 2-130 and the qualification test units described on page 2-133. The changes resulted in slightly different weights as noted in the descriptions.

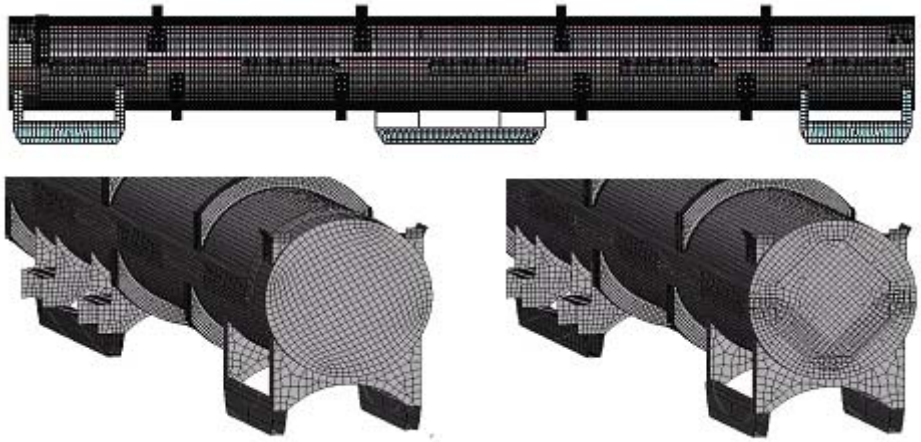

Figure 2-94 Outerpack Mesh in Prototype Model

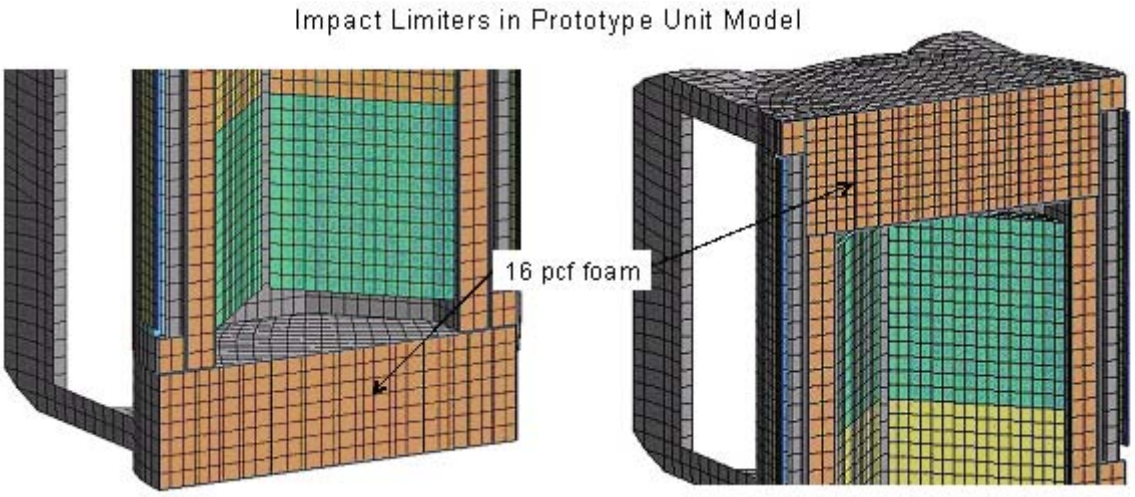

Figure 2-95 Impact Limiter in Prototype Unit Model

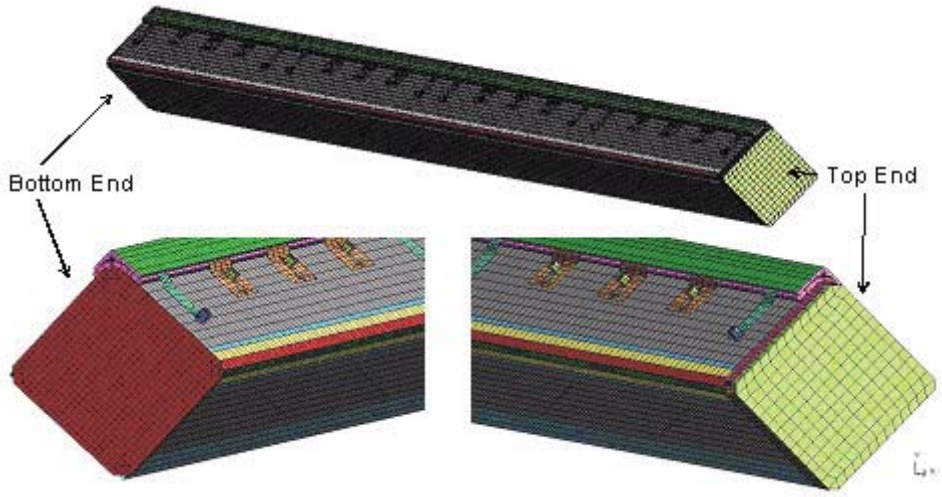

Figure 2-96 Clamshell Mesh in Qualification Unit Model

Figure 2-97 Fuel Assembly in Both Prototype and Qualification Unit Models

The Outerpack hinge details are shown in Figure 2-98. There were three bolts in the upper hinge plate in the Prototype models and only two for the Qualification unit models (shown). The bolts were modeled as spotweld beams. The spotweld beams and hinge plate shared nodes. The spotweld beam node at the hinge block was tied with LS-DYNA's NODAL_RIGID_BODIES. It should be noted that the manner of modeling the bolts allows for compression loading of the bolt, whereas in reality compression loads are not typically carried in bolted joints. However, in the horizontal side impact drops, the bolt heads themselves may impact the drop pad and compressive bolt loads are expected. Thus, our bolt model should be accurate in instances where compressive loads are developed and conservative elsewhere. The hinge pin was simulated using the LS-DYNA REVOLUTE_JOINT feature.

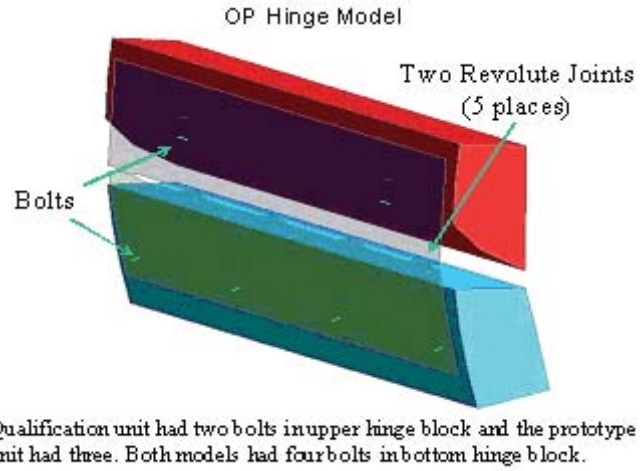

Figure 2-98 Outerpack Hinge Model

2.12.4.5.3 Qualification Unit Models (QTUs)

As with the Prototype units, the QTUs were constructed from many input files, see Figure 2-99. These files defined various details of the model and were included with, or without, transformations of coordinates and renumbering of identities as the model was assembled.

The main file, Aug19.key, contains the control cards, specifies outputs, contact definitions, and many attributes common to more than one subassembly. The major subassemblies were the Outerpack, Clamshell, and fuel assembly. These were defined in the OPs.key, CS_06_26sl6.key, and FA_remesh_FRslip.key files, respectively. The Outerpack and Clamshell subassemblies are detailed in Figures 2-101, 2-102 and 2-103 (The fuel assembly model was very similar to the one depicted previously in Figure 2-97. A total of 361,333 elements were used in the model (185985 shells, 157031 solids and 18317 beams).

The orientation for each run was defined in individual load case files. Likewise, the material property date was defined in three files which represented three different temperatures and foam densities. Obviously, only one load case file and one material file was invoked per run.

The Clamshell, Figure 2-102 is mounted to the Outerpack, Figure 2-100, with 14 rubber shock mounts. These shock mounts were modeled as discrete elements (springs). Outerpack hinge details were described in the previous section, see Figure 2-98.

Predicted model weight was 2.27 tonnes (4994 lbs). This matched the qualification unit's 4786 lb. average weight within 4.4%.

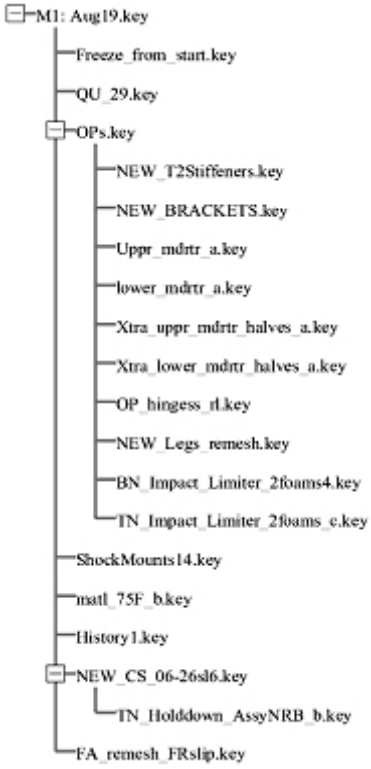

Figure 2-99 FEA Input Files

2.12.4.5.4 Qualification Unit – Outerpack Model Details

The FE model of the outerpack is shown in Figures 2-100 through 2-101A. Key features of the outerpack include the combination circumferential stiffeners/legs, the forklift pockets, the upper and lower outerpack halves, the hinges/latches on the sides, the stacking brackets, and the circumferential stiffeners on the upper outerpack. These features were included in the FE model as described below.

The circumferential stiffeners/legs and forklift pockets (Figure 2-100A) were modeled using 4-node Belytschko-Tsay shell elements (LS-DYNA elform = 2). These elements were integrated at three locations through the thickness using Gaussian quadrature. 1,008 of these elements were used to model the forklift pockets and 4,436 were used modeling the legs.

Both the circumferential stiffeners/legs and forklift pockets are welded to the lower outerpack outer casing. In the model, these parts were attached to one another using a penalty based tied contact algorithm (LS-DYNA's TIED_NODES_TO_SURFACE_OFFSET contact algorithm).

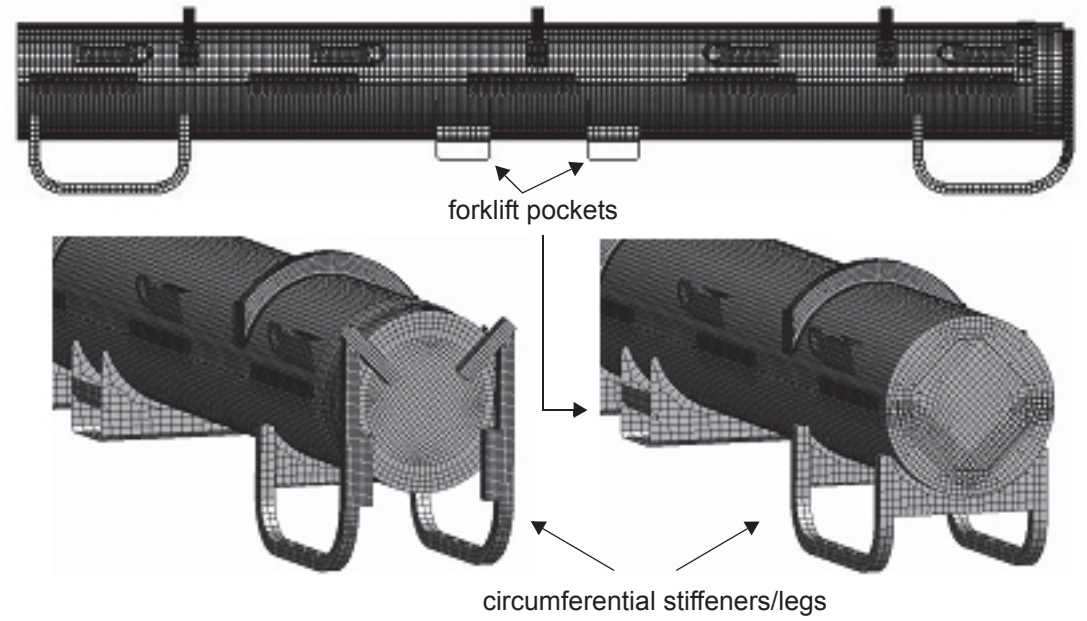

Figure 2-100 Outerpack Mesh in Qualification Unit Model

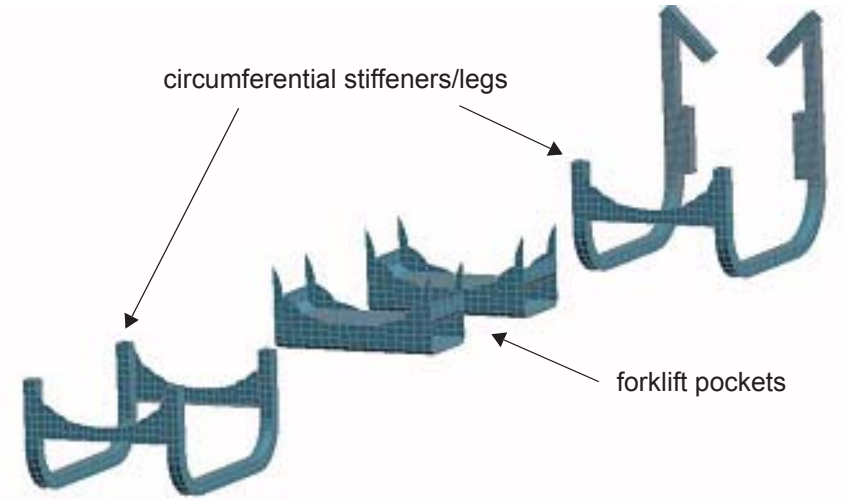

Figure 2-100A FE Meshes of Outerpack Legs and Forklift Pockets

The FE model of the QTU lower outerpack is depicted in Figures 2-100B and 2-100C. In addition to the previously mentioned circumferential stiffeners/legs, the lower outerpack is comprised of a long thick-walled "half-barrel" body and an impact limiter attached to one end (Figure 2-100A). The "half barrel" body is a sandwich construct of 10 pcf foam encased in 0.105 inch thick 304 stainless steel (Figure 2-100C). The outer steel casing was modeled using the same element formulation and integration scheme used for the

circumferential stiffeners/legs. 19,516 elements were required. The 10 pcf foam was modeled using 8 node selectively reduced fully integrated solid elements (LS-DYNA elform = 2) in conjunction with a material formulation developed especially for crushable foam (LS-DYNA material type = 63). Modeling the 10 pcf foam in the lower outerpack required 36,617 elements. Since this foam was poured-in-place, it is adhered to the stainless steel casing. This was modeled by enforcing tied contact between the outer nodes of the foam and the casing. The moderator blocks in the lower outerpack were modeled using 26,368 constant stress solid elements (LS-DYNA elform =1). Linear elastic material properties were used. The moderator blocks were attached to the lower outerpack using four bolts each for the full length moderator sections and two bolts each for the half-length moderator sections at the ends. These bolts were modeled using beam elements (LS-DYNA elform = 9) with a "spot weld" material formulation (LS-DYNA material type = 100.) Contacts between the moderator blocks, the lower outerpack, and the clamshell were defined using a penalty-based contact algorithm that accounts for shell thicknesses and for self contact as well as contact between different parts (LS-DYNA's AUTOMATIC_SINGLE_SURFACE contact algorithm). Contact stiffness was found by dividing the nodal mass by the square of the time step size with a scale factor to ensure stability (LS-DYNA's SOFT=1 contact option.) This approach was used because the foam has stiffness that is one or more orders of magnitude less than the metal parts. (Contact would possibly have broken down with other approaches that basically use the minimum stiffness of the two contact surfaces.)

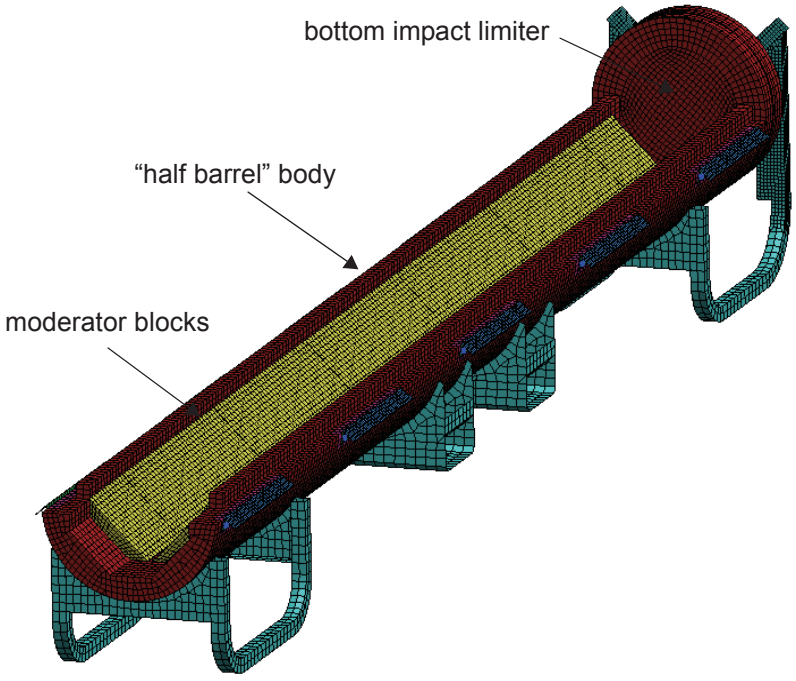

Figure 2-100B Lower Outerpack Mesh for Qualification Unit Model

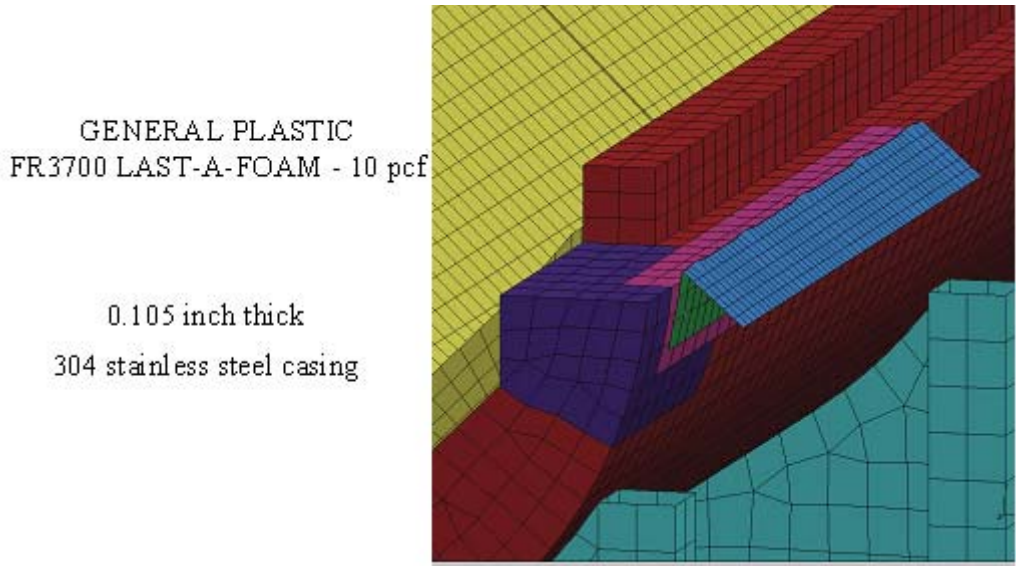

Figure 2-100C Qualification Unit Model Mesh Detail

The FE model of the QTU upper outerpack is depicted in Figure 2-100D. It primarily consists of a long thick-walled "half-barrel" body and an impact limiter attached to one end (Figure 2-100D). The "half barrel" body is a sandwich construct of 10 pcf foam encased in 0.105 inch thick 304 stainless steel. The outer steel casing was modeled using the same element formulation and integration scheme used for the circumferential stiffeners/legs and lower outerpack casing. 18,634 elements were required. The 10 pcf foam was modeled using 8 node selectively reduced fully integrated solid elements (LS-DYNA elform = 2) in conjunction with a material formulation developed especially for crushable foam (LS-DYNA material type = 63). Modeling the 10 pcf foam in the lower outerpack required 36,094 elements. Since this foam was poured-in-place, it is adhered to the stainless steel casing. This was modeled by enforcing tied contact between the outer nodes of the foam and the casing. The moderator blocks in the upper outerpack were modeled using 26,368 constant stress solid elements (LS-DYNA elform = 1). Linear elastic material properties were used. The moderator blocks were attached to the upper outerpack using four bolts each for the full length moderator sections and two bolts each for the half-length moderator sections at the ends. These bolts were modeled using beam elements (LS-DYNA elform = 9) with a "spot weld" material formulation (LS-DYNA material type = 100). Contacts between the moderator blocks, the upper outerpack, and the clamshell were defined using a penalty-based contact algorithm as described for the lower outerpack.

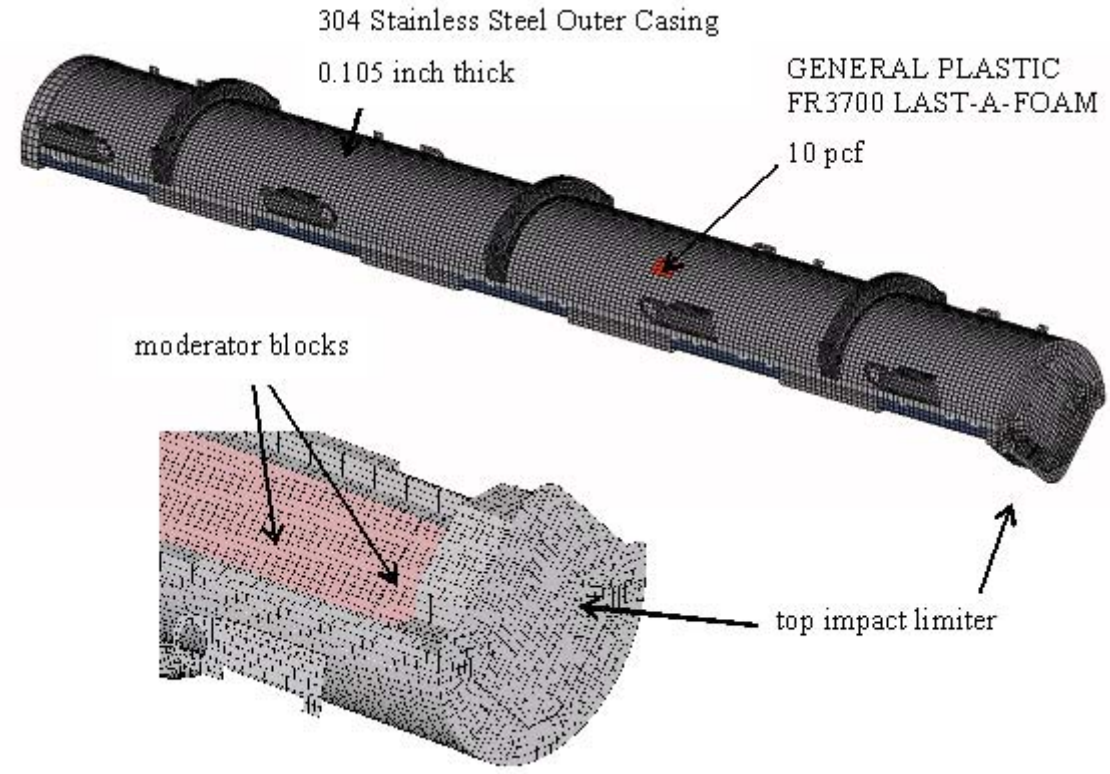

Figure 2-100D Upper Outerpack Mesh for Qualification Unit Model

Model details of the impact limiters are shown in Figure 2-101. Both consisted of two separate foam pieces: a 7 pcf foam block was placed inboard nearest the clamshell and 14 pcf foam covered both ends of the overpacks. These foam pieces were separated and covered by stainless steel. The foams were modeled using the same element formulation and material model as described for the 10 pcf foam in the overpack "barrels" except that each foam density had its own stress-strain curve. The 7 pcf foam in the bottom impact limiter was modeled with 2112 solid elements; the 14 pcf foam was modeled with 4480. The 7 pcf foam in the top impact limiter was modeled with 5248 elements; the 14 pcf foam was modeled with 1755 elements. Because these foams were "cut-to-fit," they were not bonded to the steel cases. Thus, contact between the steel casings and the foam was defined using LS-DYNA's AUTOMATIC_SINGLE_SURFACE contact algorithm as previously described (for contact between the lower outerpack, moderator blocks and clamshell).

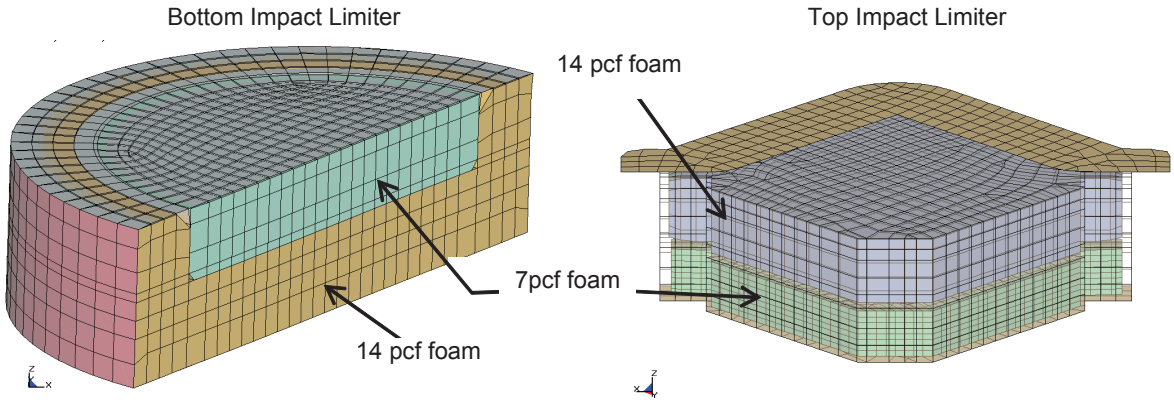

Figure 2-101 Impact Limiter Meshes in Qualification Unit Model

The stacking brackets and circumferential stiffeners on the upper overpack (Figure 2-100D) were modeled using the same element formulation and integration scheme used for the circumferential stiffeners/legs and outerpack casings. 4,404 of these elements were used to model the stiffeners and 1,376 were used modeling the stacking brackets. Both the stiffeners and brackets were secured to the upper outerpack casing using a tied contact algorithm as described for the circumferential stiffeners/forklift pockets and lower overpack casing.

The bolts which secure the outerpack hinges/latches are all that prevent the upper and lower outerpacks from separating upon impact. This was simulated in the model by replication of each physical part of the hinge/latch assemblies. In particular, hinge/latch assemblies including mounting blocks, hinge leaves, and the bolts were modeled (see Figure 2-98 and associated description in Section 2.12.3.5). These assemblies were attached to the upper and lower overpacks via tied (penalty-based) constraints. This methodology permitted relative rotations between the upper and lower outerpacks along the axes of the hinges/latches while resisting any relative translations. Thus, the model forced the overpack latch bolts to prevent the displacement shown in Figure 2-101A. This allowed predicted deformations at the outerpack seam to be realistic (e.g., Figures 2-30B and 2-74.)

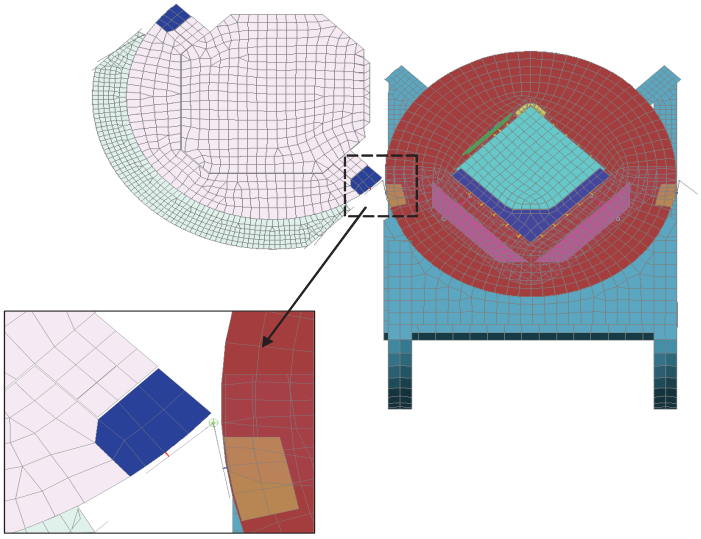

Figure 2-101A Hinge/Latch Feature in Qualification Unit Model

2.12.4.5.5 Qualification Unit – Clamshell Model Details

The FE model of the clamshell is shown in Figures 2-102 through 2-102C. Key features of the clamshell include: the clamshell top assembly, the V-shaped extrusion, the two doors including the hinges, middle latch and locks, and the bottom plate. These features were included in the FE model as described below.

The clamshell top assembly has two major features. First it can swivel from either side to allow access to the top portion of the fuel assembly. This is shown in Figure 2-102A where the CS head is swiveling about its right side. This feature was built into the FE model using the LS-DYNA revolute joint elements. (This is very similar to what was done for the overpack hinges/latches.)

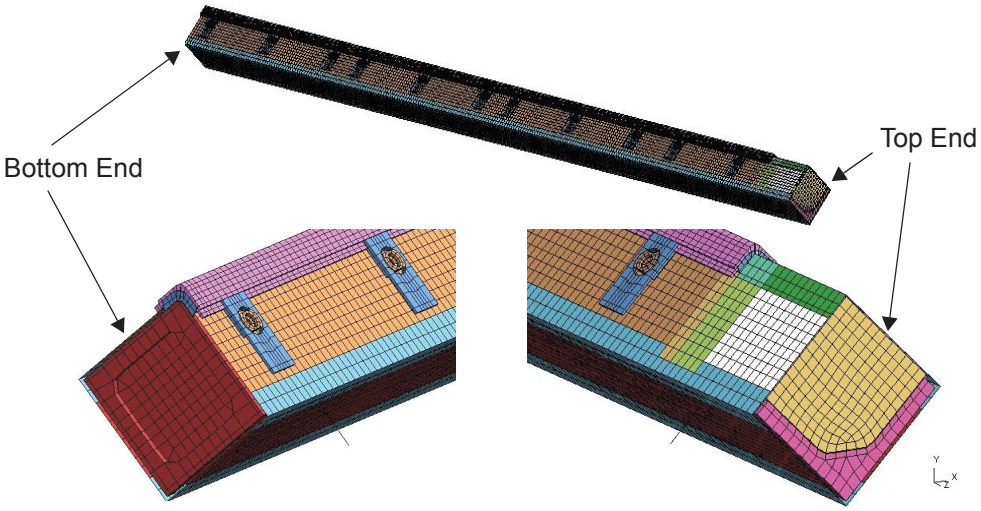

Figure 2-102 Clamshell Mesh in Qualification Unit Model

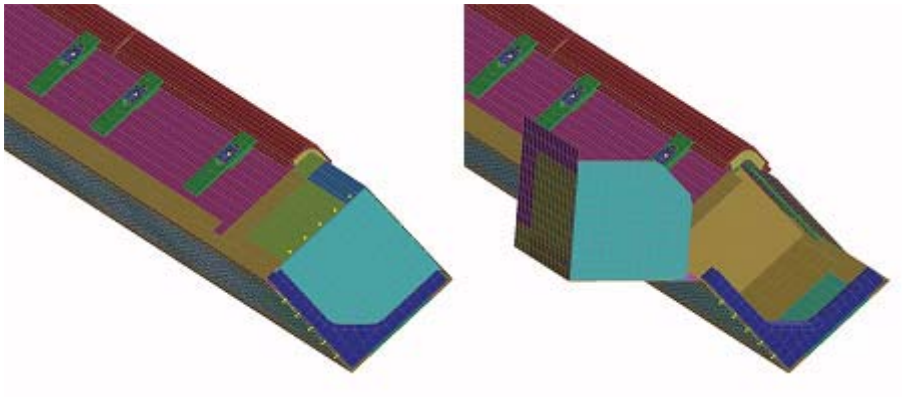

Figure 2-102A Clamshell Top Head in Qualification Unit Model

The second major feature was the top nozzle hold-down bars as shown in Figure 2-102B. Although this hardware has length adjustments to accommodate different fuel assembly heights, the hold-down bar was modeled for the height of an XL fuel assembly. If other fuels were to be modeled, the hold-down bars would need to be scaled in the z-direction. The hold-down bars were modeled with 8 node solid elements and contact between the top nozzle and other fuel and clamshell parts in the near vicinity was defined using LS-DYNA's AUTOMATIC_SINGLE_SURFACE contact algorithm.

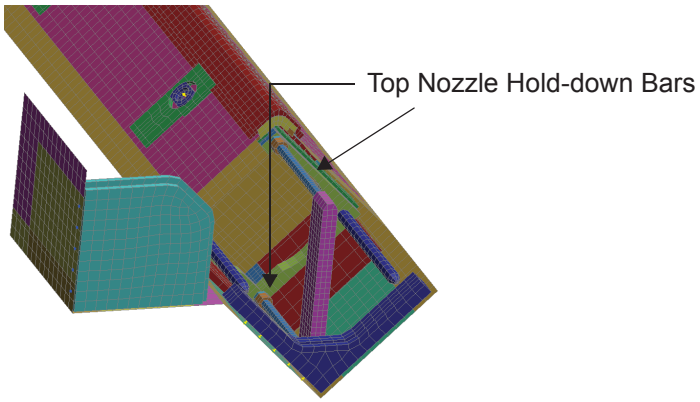

Figure 2-102B Clamshell Top Nozzle Hold-down Bars in Qualification Unit Model

The model of the clamshell latch and hinges allow the doors to rotate about the hinge centerlines as depicted in Figure 2-102C. These features were added using the LS-DYNA revolute joint element as already described.

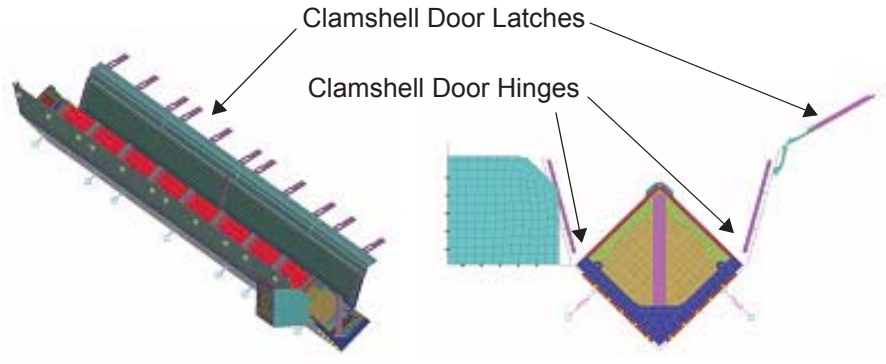

Figure 2-102C Clamshell Hinges and Latches in Qualification Unit Model

2.12.4.6 Model Input

Information needed to construct finite element models of the prototype and qualification units included load and boundary condition details, the stiffness and density of the comprising materials, the shipping package geometry, and the interconnections between the various shipping container subassemblies.

Drop Orientation and Initial Conditions – For modeling convenience, different drop orientations were modeled by changing the velocity and gravitational fields instead of rotating the model relative to the

This page intentionally left blank.

model global axes. Loadings were therefore specific to each drop orientation. Further, each analysis was initiated just prior to impact with the shipping package positioned just above the impact surface, having an initial velocity based on drop height (9.14 m for the free drops and 1 m for the pin puncture), and undergoing earth's gravitational pull. This analysis approach minimized computation effort since only minimal calculations of the shipping package during free-fall were needed. The required calculations were as follows.

2.12.4.6.1 Initial Velocity Magnitude (Speed)

The velocity, V, of any object having fallen for a drop height, h, in a constant gravitational field, g, is:

$$V = \sqrt{2gh}$$

Thus, using 9810 mm/s as the value of g, the calculated magnitude of the initial velocities (speed) for the 9 meter free drop and 1 meter pin puncture tests were as shown in Table 2-24.

Table 2-24 Initial Velocities 9 Meter Drop and 1 Meter Pin Puncture Analyses

Test	Drop Height [m]	Initial Velocity (Speed) [mm/s]
9 m drop		
Prototype model	9.0	13288
Qualification model	9.14 (30 ft)	13389
Pin Puncture		
Prototype & Qualification models	1.0	4429

Velocity and Gravitational Fields – In general, a complete description of the position and orientation of an object in 3-dimensional space requires three coordinates and three direction cosines. However, for these drop tests, specification of only two direction cosines is sufficient. This is because both the drop pad and impact pin may be modeled as two-dimensional rigid walls or surfaces. In other words, these items have no distinct feature with respect to the shipping package that requires specification of the angle θ_y in Figure 2-103. Thus, only the angles θ_x and θ_Z are needed to define the velocity and gravitational fields.

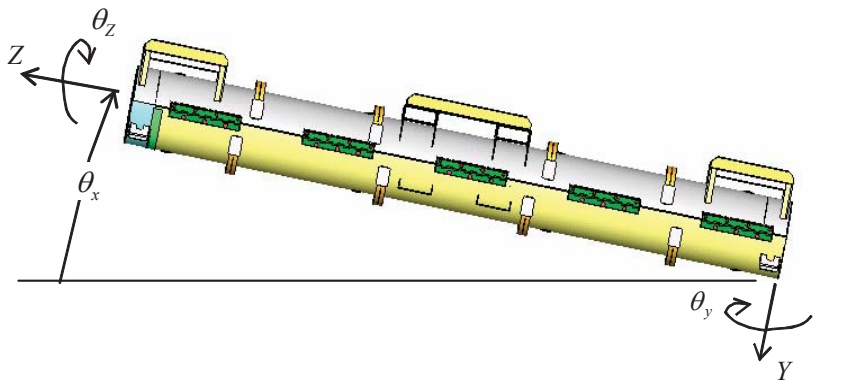

Figure 2-103 Package Drop Angle

Using the angles θ_X and θ_Z shown in Figure 2-69, the velocity and gravitational fields are, respectively,

$$v = A^T \begin{Bmatrix} 0 \\ -V \\ 0 \end{Bmatrix}$$

and

$$a = A^T \begin{Bmatrix} 0 \\ g \\ 0 \end{Bmatrix}$$

where

$$A = \begin{bmatrix} \cos\theta_z & \sin\theta_z & 0 \\ \cos\theta_x \cdot \sin\theta_z & \cos\theta_z \cdot \cos\theta_x & -\sin\theta_x \\ \sin\theta_x \cdot \sin\theta_z & \sin\theta_x \cdot \cos\theta_z & \cos\theta_x \end{bmatrix}$$

The normal to the plane of impact (drop pad surface or pin face) is given by

$$n = A^T \begin{Bmatrix} 0 \\ -1 \\ 0 \end{Bmatrix}$$

The initial velocity field was implemented into the finite element model with the *INITIAL_VELOCITY command in LS-DYNA. The gravity field was applied using the *LOAD_BODY_GENERALIZED command. Finally, the impact plane was defined using the *RIGIDWALL_PLANAR or *RIGIDWALL_GEOMETRIC_CYLINDER commands. This approach allowed the drop orientation to be changed without altering the model coordinates. It should be noted that the gravity load was applied as a ramped load as shown in Figure 2-70. This was done as a precaution to minimize any numerical oscillations. However, this was probably unnecessary – applying the full gravity load at time zero would most likely produced equivalent results.

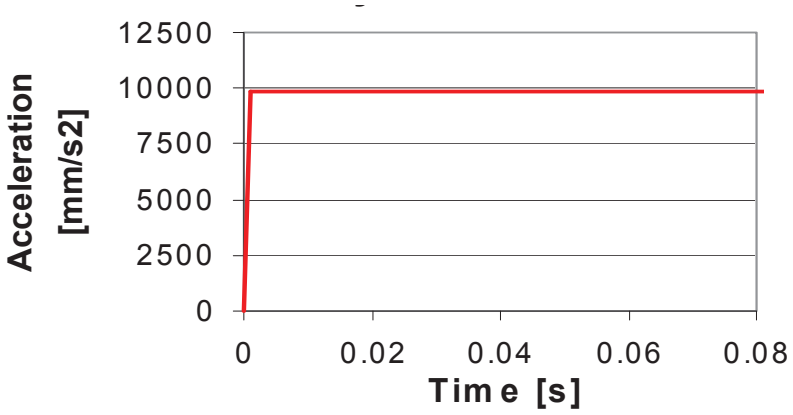

Figure 2-104 Gravity Load Profile

2.12.4.6.2 Material Properties

The crush strength of the polyurethane foam used in the Traveller XL package (LAST-A-FOAM® from General Plastics Manufacturing Company) is strongly influenced by temperature. For example, the perpendicular-to-rise dynamic crush strength of 10 pcf foam at 40% strain is approximately 940 psi at -40°F, 550 psi at 75°F, and just 338 psi at 160°F. Furthermore, foam crush strength is also directly related to foam density. Per the foam procurement specification, density is held within ±1 pcf for the 7 and 10 pcf foam and ±10% for the 14 pcf foam. Both effects were included in our analyses. This was accomplished by specifying the foam crush strength at highest temperature (160°F) and lowest density (nominal density minus 1 pcf or 10%) and at lowest temperature (-40°F) and highest density (nominal density plus 1 pcf or 10%). Foam stress-strain curves used in the qualification unit analysis are shown in Figure 2-105. These were obtained from General Plastics data except that; 1) the curves were extended past General Plastics' recommend maximum strain limit to fully compressed (100% strain) using linear regressions of the last three known points, and 2) the two most crushable foams (6 pcf @160°F and 7 pcf @75°F) were made to follow the 8 pcf @ -40°F curves at strains above 50%, Figure 2-105). The latter adjustment was needed to prevent the foam elements from inverting under the high strains (i.e., this prevented "negative volumes").

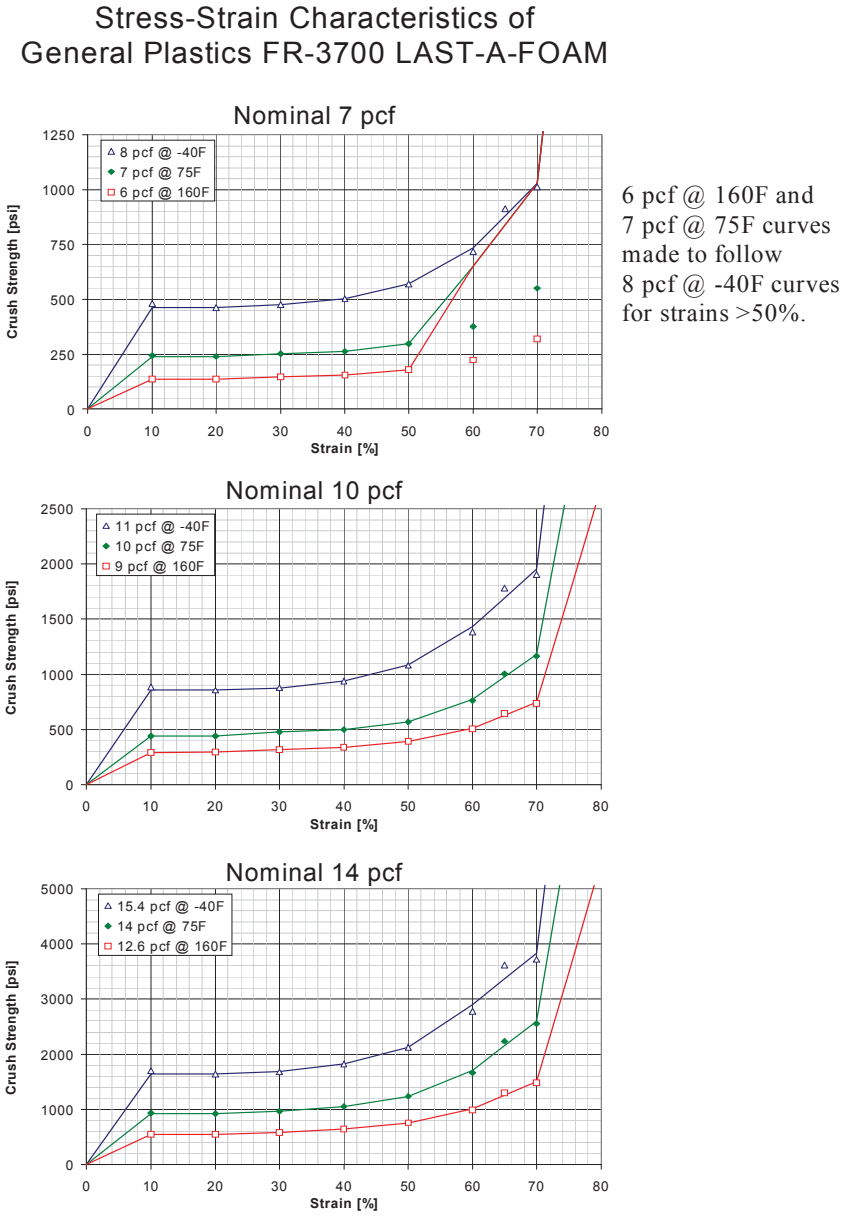

Figure 2-105 Stress Strain Data for LAST-A_FOAM

The use of a linear elastic material model from 0-10% strain was selected to evaluate the effects of temperature and foam density on drop test reaction forces. From Section 2.12.3.2.6, foam linear data demonstrated that temperature and foam density have a minor effect on the drop test response of the Traveller. The use of true stress-strain data ranging from 0-10% would not impact the conclusions of the comparative analysis.

A typical comparison of foam stress-strain behavior demonstrates that the available strain energy of a linear model is less than that observed with true stress-strain data. The use of true stress-strain data is expected to result in greater foam deflection when compared to linear modeling. Since greater crushing would absorb more kinetic energy, the predicted reaction force of the outerpack using true stress-strain data is expected to be less compared to linear data. It is concluded that the use of linear stress-strain data in the 0-10% range adds additional conservatism to the model.

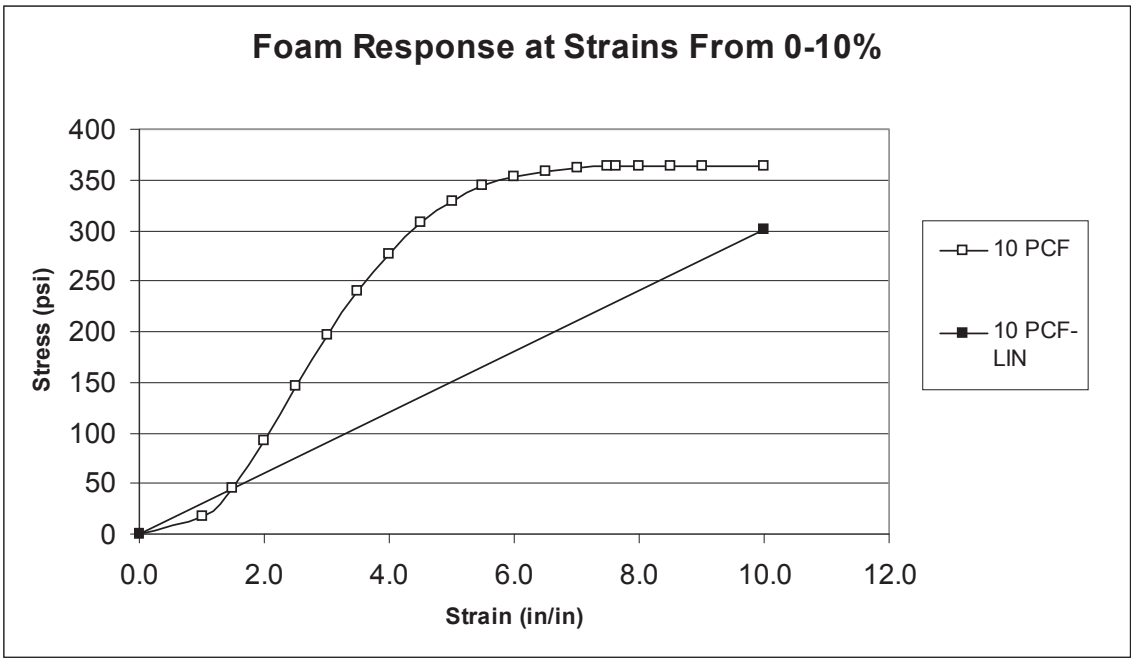

Figure 2-105A Foam Response at Strains from 0-10%

Stress strain characteristics for the 304 stainless steel used in these analyses are shown in Figure 2-106. The 75°F characteristics were obtained from pull tests of samples used in the prototype unit. Based on MIL_HDBK-5H "Metallic Materials and Elements for Aerospace Vehicle Structures," see Figure 2-107, performance at 160°F was estimated by lowering both yield and ultimate strengths to 90% of their values at 75°F. Similarly, the performance at minus 40°F was estimated by raising yield and ultimate strengths to, respectively, 112 and 132% of their values at 75°F, Figure 2-107.

This page intentionally left blank.

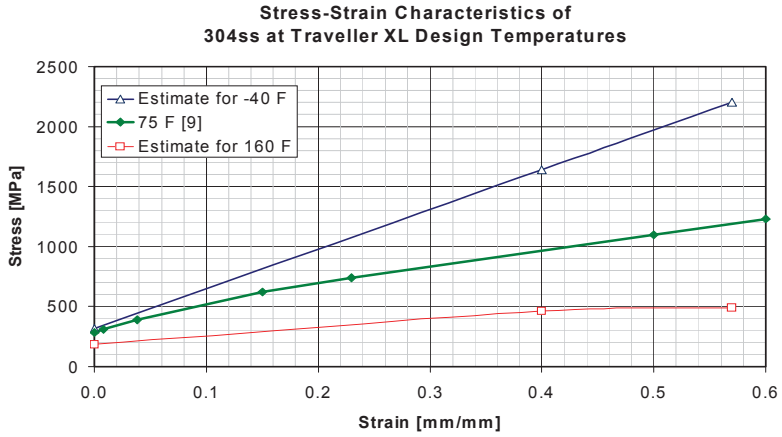

Figure 2-106 Stress-Strain Curves for 304 Stainless Steel

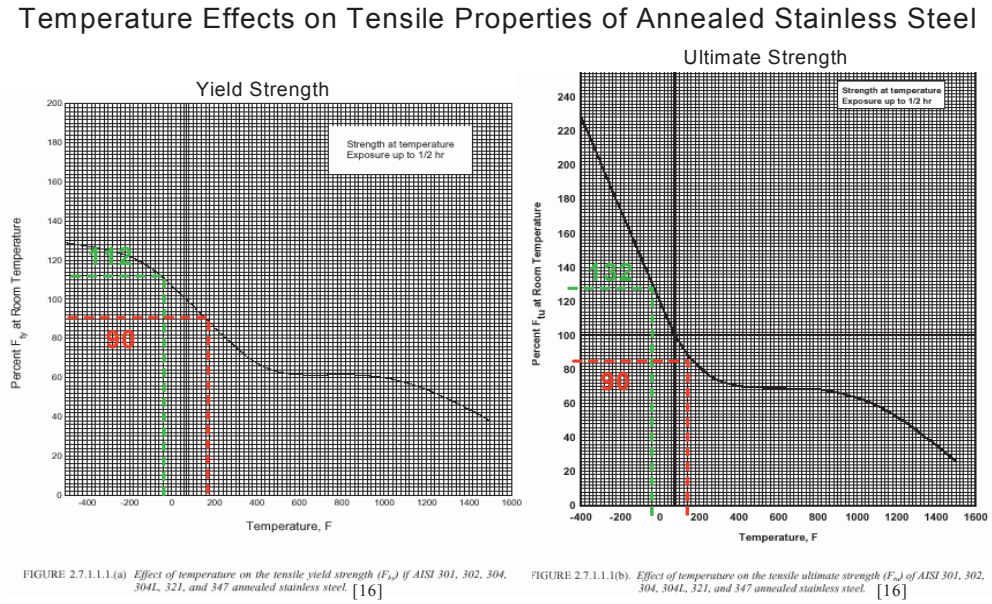

Figure 2-107 Temperature Effects on Tensile Properties of Annealed Stainless Steel

Estimated stress strain characteristics for the 6005-T5 aluminum used in these analyses are shown in Figure 2-108. The 75°F characteristics are typical of those for 6061-T6 used in the aerospace and automotive industries.[1] The 6005-T5 properties are similar based on their similar yield and ultimate strength and elongation. Because there was no available temperature dependent data, the curves for -40°F and 160°F were estimated based on the temperature dependence of aluminum alloy 6061T6. This was judged acceptable because alloy 6061-T6 is very similar to 6005-T5. However, for conservatism, we doubled

1. This data is not published. However, a similar curve is available from ALCAN

the impact that temperature had on 6061-T6 when estimating the temperature dependence of 6005-T5. For example, yield and ultimate strengths of 6061-T6 at 160°F is expected to be 6 and 4% less than at 75°F, Figure 2-109. However, we estimated these quantities for 6005-T5 by lowering the 75°F values by 12 and 8%. Likewise, when estimating the performance of 6006-T5 at -40°F, we increased the yield and ultimate strengths at 75°F by 8 and 12%, respectively. This is twice the reported impact this temperature reduction has on 6061-T6, Figures 2-109.

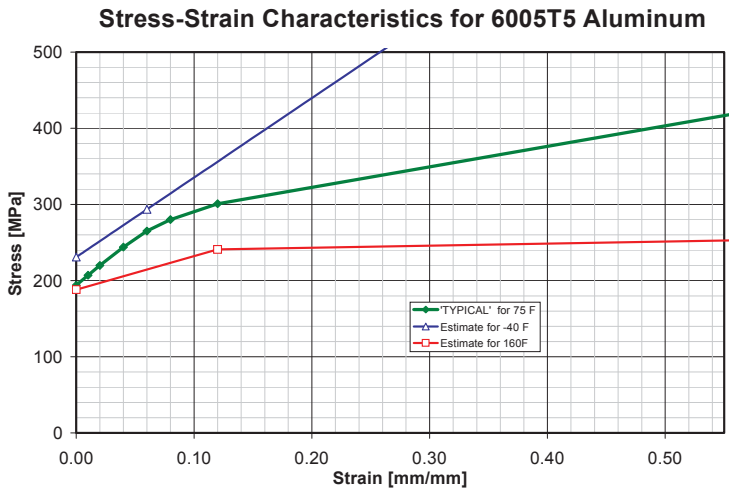

Figure 2-108 Stress-Strain Characteristics of Aluminum in Clamshell

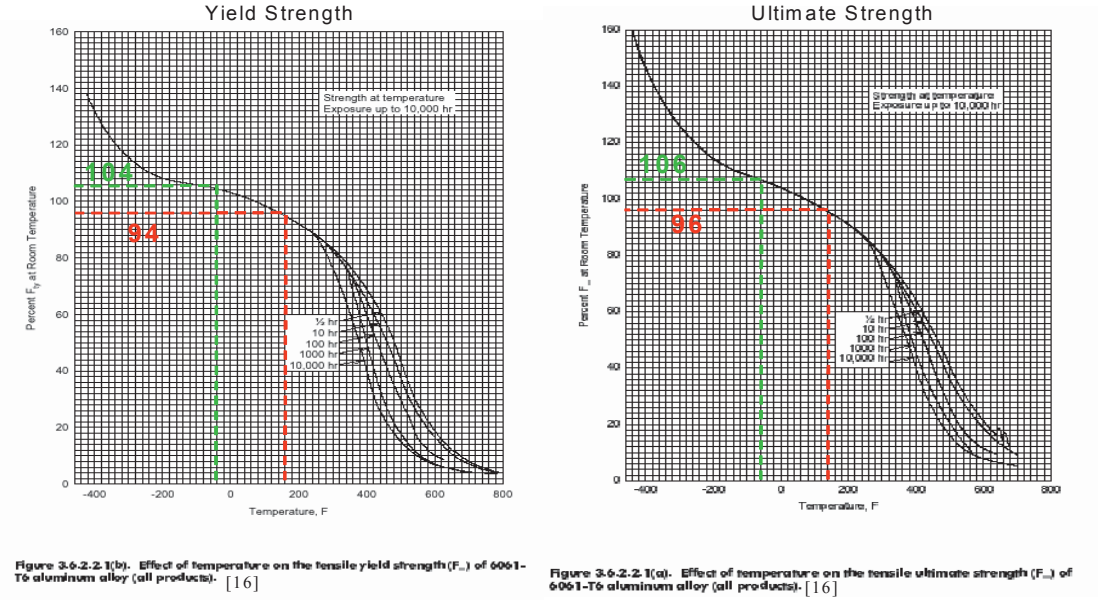

Figure 2-109 Temperature Effects on Tensile Properties of Aluminum in Clamshell

Finally, modulus of elasticity and Poisson's ratio are also influenced by temperature. However, this effect is minimal and was neglected in this highly inelastic analysis. Thus, elastic properties determined at 75°F were used in the model. These are shown in Table 2-25.

Table 2-25 Summary of Elastic Properties

Material	Modulus of Elasticity [GPa]	Poisson's Ratio
304 stainless steel	206.7[a]	0.32[a]
6005T5 aluminum	70 [10]	0.3 [10]
Foam	0.37[b]	N/A

Notes:
a. This value of modulus is approximately 8% higher than the 192.0 GPa recommended at Westinghouse. This Poisson's ratio is approximately 23% higher than the 0.26 recommendation. However, these elastic values were consistently used and these differences likely had little effect in this highly non-elastic analysis.
b. Determined by using stress value at 10% strain instead of offset yield point.

2.12.4.7 Evaluations, Analysis and Detailed Calculations

Many billions of calculations required in these analyses were performed on the HPJ6000 workstation cluster (claxgen1, 2, 3 and 4). However, three additional sets of calculations were required. These were; 1) the calculations of the gravity and velocity fields and the orientation for the rigid wall surface or pin, 2) calculations of bolt factors of safety, and 3) calculations of accelerations from differentiated velocities. Example Calculations of Impact Plane Normal, Gravity Field, and Velocity Field

Horizontal Drop onto Outerpack Latches – A horizontal drop onto the Outerpack latches is shown in Figure 2-26. Using the coordinate system shown in Figure 2-103, this orientation is obtained when $\theta_X = 0$ and $\theta_Z = 90°$. Further, V=13,389 mm/s for a 9.14 m drop, Table 2-24, and g=9810 mm/s^2. Thus,

$$A = \begin{bmatrix} 0.0 & 1.0 & 0.0 \\ 1.0 & 0.0 & 0.0 \\ 0.0 & 0.0 & 1.0 \end{bmatrix},$$

$$n = \begin{bmatrix} 0.0 & 1.0 & 0.0 \\ 1.0 & 0.0 & 0.0 \\ 0.0 & 0.0 & 1.0 \end{bmatrix}^T \cdot \begin{Bmatrix} 0 \\ -1 \\ 0 \end{Bmatrix} = \begin{Bmatrix} 1 \\ 0 \\ 0 \end{Bmatrix},$$

$$v = \begin{bmatrix} 0.0 & 1.0 & 0.0 \\ 1.0 & 0.0 & 0.0 \\ 0.0 & 0.0 & 1.0 \end{bmatrix}^T \cdot \begin{Bmatrix} 0 \\ -13{,}389 \\ 0 \end{Bmatrix} = \begin{Bmatrix} -13{,}389 \\ 0 \\ 0 \end{Bmatrix},$$

and

$$g = \begin{bmatrix} 0.0 & 1.0 & 0.0 \\ 1.0 & 0.0 & 0.0 \\ 0.0 & 0.0 & 1.0 \end{bmatrix}^T \cdot \begin{Bmatrix} 0 \\ 9{,}810 \\ 0 \end{Bmatrix} = \begin{Bmatrix} 9{,}810 \\ 0 \\ 0 \end{Bmatrix}.$$

Example Calculation of Bolt Factor of Safety – The equation below is utilized to calculate bolt factor of safety. For example, suppose a Clamshell bolt is subjected to an axial force of 5,134 lb_f and shear forces of 925 and 3380 lb_f. A factor of safety is calculated by first calculating the "Actual" (load) using these values of load, Table 2-26.

$$\begin{aligned} Actual &= \left(\frac{F_{axial}}{FN\_ult}\right)^2 + \left(\frac{F_{yshear}}{FS\_ult}\right)^2 + \left(\frac{F_{zshear}}{FS\_ult}\right)^2 \\ &= \left(\frac{5{,}134}{12{,}070}\right)^2 + \left(\frac{925}{6{,}040}\right)^2 + \left(\frac{3{,}380}{6{,}040}\right)^2 \\ &= 0.5175 \end{aligned}$$

This value must be divided into the "Allowable" which is 1.0. Thus, the factor of safety for the bolt in this example is 1.93. (These loads correspond to those predicted for the Clamshell keeper bolt which is third down from the top end of the Clamshell during a horizontal side drop onto the latches at time 0.0072s. The calculated value for factor of safety corresponds to that shown in Table 2-11.

Description of Acceleration Calculations – Predicted accelerations, as shown in Figures 2-88 through 2-92, were obtained by differentiating predicted nodal velocities sampled at a frequency of 4 KHz and applying a "light" (SAE 180 Hz) filter. This technique was used because the finite-difference technique used in LS-DYNA yields very noisy accelerations. These nodal accelerations are indeed accurate in an average sense, but not in an absolute value. The differentiated velocity technique allowed the true trend in accelerations to be discerned. The calculations were accomplished with the LS-POST program.

2.12.4.8 Accelerometer Test Setup

Prior to testing, piezoelectric accelerometers were mounted on the Outerpack and Clamshells of both test prototypes. The intent was to measure the accelerations at a few critical points so that the forces involved in the drops would be better known and so that the FEA results could be validated.

Three accelerometers were positioned on the Prototype Unit-1 Test series 1, Figure 2-110. One accelerometer was on the Clamshell top plate and thus was near the initial impact end. The other two were positioned on the secondary impact end at the Clamshell bottom plate and bottom impact limiter. Further details of this instrumentation are available in Appendix 2.12.5.

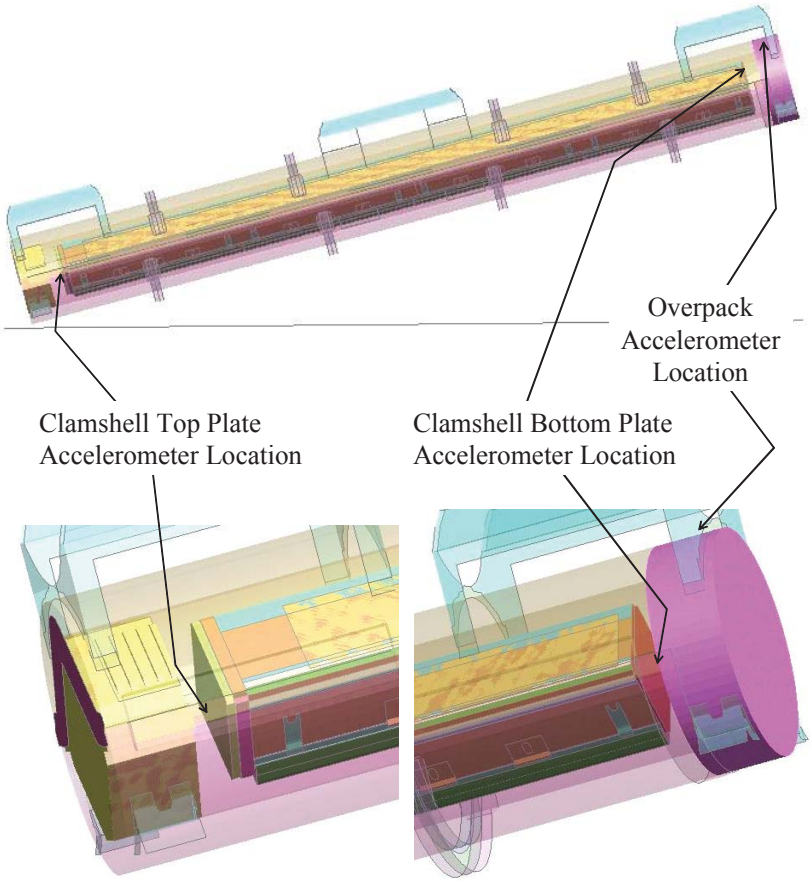

Figure 2-110 Accelerometer Locations on Prototype Unit 1

2.12.4.9 Bolt Factor of Safety Calculation

Bolt factors of safety (FS)

$$F.S. = \frac{\text{Allowable}}{\text{Actual}} \tag{H-1}$$

were based on the failure criteria

$$\left(\frac{F_{axial}}{FN\_ult}\right)^2 + \left(\frac{F_{yshear}}{FS\_ult}\right)^2 + \left(\frac{F_{zshear}}{FS\_ult}\right)^2 \geq 1. \tag{H-2}$$

This commonly-used criterion was chosen because it accounts for the effects of both axial and shear forces. (Note: the left side of equation H-2 is the "Actual" in equation H-1 and the "Allowable" is unity.)

The loads in equation H-2 were determined from the finite element analysis; the tensile and shear strengths are shown in Table 2-26. Initially, the tensile strengths were estimated from the tensile to proof strength ratios for Grade 2 bolts, Tables 2-27 and 2-28, obtained from. Use of the ratios obtained for Grade 2 bolts was justified because the proof strengths of these bolts should be just above Grade 2 levels based on their minimum strength of 70 ksi. However, bolt strengths estimated in this manner did not result in adequate factors of safety for each Outerpack bolt when the Traveller XL package was dropped horizontally, Figure 2-26. However, the specification for the Outerpack bolts was changed in the design of the CTU unit. The new bolt specification for CTU and production packages is ASTM A193 Class 1 B8 which has an ultimate tensile strength minimum of 75 ksi. Additionally, the number of Outerpack hinge bolts has increased to 12 bolts per side on the top leaf and bottom hinge leaf for both the XL and STD packages. This increase in the number of bolts, and the increase in strength results in a factor of safety of 1.12 for the bounding Traveller XL's worst bolt, in the worst case bolt failure orientation (the side drop).

Table 2-26 Bolt Strength Summary

Location	Size	Thread Area [in^2] [13]	Minimum Yield Strength [ksi]	Estimated Minimum Proof Strength [lbf](1)	Ratio of Tensile to Proof Strength(2)	FN_ult [lbf]	NS_ult [lbs](5)
CS bolts	1/2"-13	0.142	70 [14]	8,940	1.35	12,070(3)	6,040
Bottom OP hinge bolts	5/8"-11	0.226	70 [14]	14,240	1.35	19,200(3)	9,600
Top OP hinge bolts	3/4"-10	0.334	70 [14]	21,040	1.34	28,200(3)	14,100
			100 [18]	30,060	N/A	41,750(4)	20,900

Notes:
(1) 0.9 * thread area * min yield strength
(2) Based on estimated proof strength and Table 2-28
(3) Estimated min proof strength * ratio of Tensile to proof strength
(4) Minimum Ultimate Tensile Strength of 125 ksi * thread area
(5) 0.5 *FN_ult

Table 2-27 Strengths of Various Classifications of Bolts [14]

Nominal Dia of Product and Threads per in	Stress Area, in^2	Grade 1		Grade 2		Grade 4		Grades 5 and 5.2		Grade 5.1		Grade 7		Grades 8, 8.1, and 8.2	
		Proof Load, lb	Tensile Strength min, lb	Proof Load, lb	Tensile Strength min, lb	Proof Load, lb	Tensile Strength min, lb	Proof Load, lb	Tensile Strength min, lb	Proof Load, lb	Tensile Strength min, lb	Proof Load, lb	Tensile Strength min, lb	Proof Load, lb	Tensile Strength min, lb
Coarse-Thread Series – UNC															
No. 6-32	0.00909	–	–	–	–	–	–	–	–	750	1,100	–	–	–	–
8-32	0.0140	–	–	–	–	–	–	–	–	1,200	1,700	–	–	–	–
10-24	0.0175	–	–	–	–	–	–	–	–	1,500	2,100	–	–	–	–
12-24	0.0242	–	–	–	–	–	–	–	–	2,050	2,900	–	–	–	–
1/4-20	0.0318	1,050	1,900	1.750	2,350	2,050	3,650	2,700	3,800	2,700	3,800	3,350	4,250	3,800	4,750
5/16-18	0.0524	1,750	3,150	2,900	3,900	3,400	6,000	4,450	6,300	4,450	6,300	5,500	6,950	6,300	7,850
3/8-16	0.0775	2,550	4,650	4,250	5,750	5,050	8,400	6,600	9,300	6,600	9,300	8,150	10,300	9,300	11,600
7/16-14	0.1063	3,500	6,400	5,850	7,850	6,900	12,200	9,050	12,800	9,050	12,800	11,200	14,100	12,800	15,900
1/2-13	0.1419	4,700	8,500	7,800	10,500	9,200	16,300	12,100	17,000	12,100	17,000	14,900	18,900	17,000	21,300
9/16-12	0.182	6,000	10,900	10,000	13,500	11,800	20,900	15,500	21,800	15,500	21,800	19,100	24,200	21,800	27,300
5/8-11	0.226	7,450	13,600	12,400	16,700	14,700	25,400	19,200	27,100	19,200	27,100	23,700	30,100	27,100	33,900
3/4-10	0.334	11,000	20,000	18,400	24,700	21,700	38,400	28,400	40,100	–	–	35,100	44,400	40,100	50,100
7/8-9	0.462	15,200	27,700	15,200	27,700	30,000	53,100	39,300	55,400	–	–	48,500	61,400	55,400	69,300
1-8	0.606	20,000	36,400	20,000	36,400	39,400	69,700	51,500	72,700	–	–	63,600	80,600	72,700	90,900
1-1/8 - 7	0.763	25,200	45,800	25,200	45,800	49,600	87,700	56,500	80,100	–	–	80,100	101,500	91,600	114,400
1-1/4 - 7	0.969	32,000	58,100	32,000	58,100	63,000	111,400	71,700	101,700	–	–	101,700	127,700	116,300	145,400
1-3/8 - 6	1.155	38,100	69,300	38,100	69,300	75,100	132,800	85,500	121,300	–	–	121,300	153,600	138,600	173,200
1-1/2 - 6	1.405	46,400	84,300	46,400	84,300	91,300	161,600	104,000	147,500	–	–	147,500	186,900	168,600	210,800

Table 2-28 Bolt Strength Ratio

Size	Tensile to Proof Strength Ratio					
	Grade 1	Grade 2	Grade 4	Grades 5, 5.1 and 5.2	Grade 7	Grades 8, 8.1 and 8.2
½-13	1.81	1.35	1.77	1.40	1.27	1.25
5/8-11	1.83	1.35	1.73	1.41	1.27	1.25
¾-10	1.82	1.34	1.77	1.41	1.26	1.25

2.12.5 TRAVELLER DROP TESTS RESULTS

Three series of full scale drop tests have been performed on the Traveller package to evaluate the performance of the design. This appendix will summarize structural performance of the Traveller during these tests. The objectives, test articles, results and lessons learned will be described. The three series were:

- Prototype Tests
- Qualification Tests
- Certification Tests

2.12.5.1 Prototype Test Unit Drop Tests

Testing was conducted at Columbiana High Tech Company (CHT) in Columbiana, Ohio during the week of January 27-30, 2003 (Ref. 3).

An as-built Traveller package prototype is shown in Figures 2-111 and 2-112. Figure 2-111 shows the internal packaging including the 17x71 XL fuel assembly, Clamshell, and moderator blocks. Figure 2-112 shows the closed Outerpack. The prototype packages employed 11 pcf foam along the axial section of the package and 16 pcf foam in the endcaps. Furthermore, the Outerpack consisted of 11 gage inner and outer skin. Each package also contained 22 shock mounts to connect the Clamshell to the Outerpack.

Test Series 1 – Test series 1 was conducted on January 27th through 28th and included two 9 meter drop tests plus a pin-puncture test. The package's test weight was 5072 pounds. Drop orientations are shown in Figure 2-113 and Table 2-29.

The Outerpack retained its basic circular pre-test shape except for localized plastic deformation from the 9 meter drop tests and the pin-puncture test. One bolt on the lower Outerpack hinge failed after completion of the last 9 meter drop test. The Outerpack did not separate after any impacts, and the pin did not perforate the inner or outer shell. The internal damage was minimal. The fuel assembly's envelope decreased from 8.418" nominal to 8.25" maximum after the first 9 meter drop test, and reduced further to 8.13" maximum after second 9 meter drop test. Fuel rod gaps globally decreased (the fuel envelope decreased), but local expansion was noted between a few rods with a maximum measured gap of .188" for the first 9 meter drop test and .625" maximum measured gap for second 9 meter drop test (compared to the nominal gap of .122"). The polyethylene moderator blocks and aluminum neutron "poison plates" maintained position. The Clamshell doors remained closed, but the top and bottom heads were separated from the Clamshell. The separation was caused by the fuel assembly deceleration forces reacting against the clamshell end plate. The bearing force of the bolts (a shear effect on the top head plate) from impact was sufficient to fail the material in the bolt slots for both head pieces. The fuel inspection indicated that no fuel rods had ruptured, and that the axial position of fuel rods maintained location between bottom and top nozzle. The failure the clamshell endplates was due to the bolt slots being modified as a result of warping of the clamshell during fabrication.

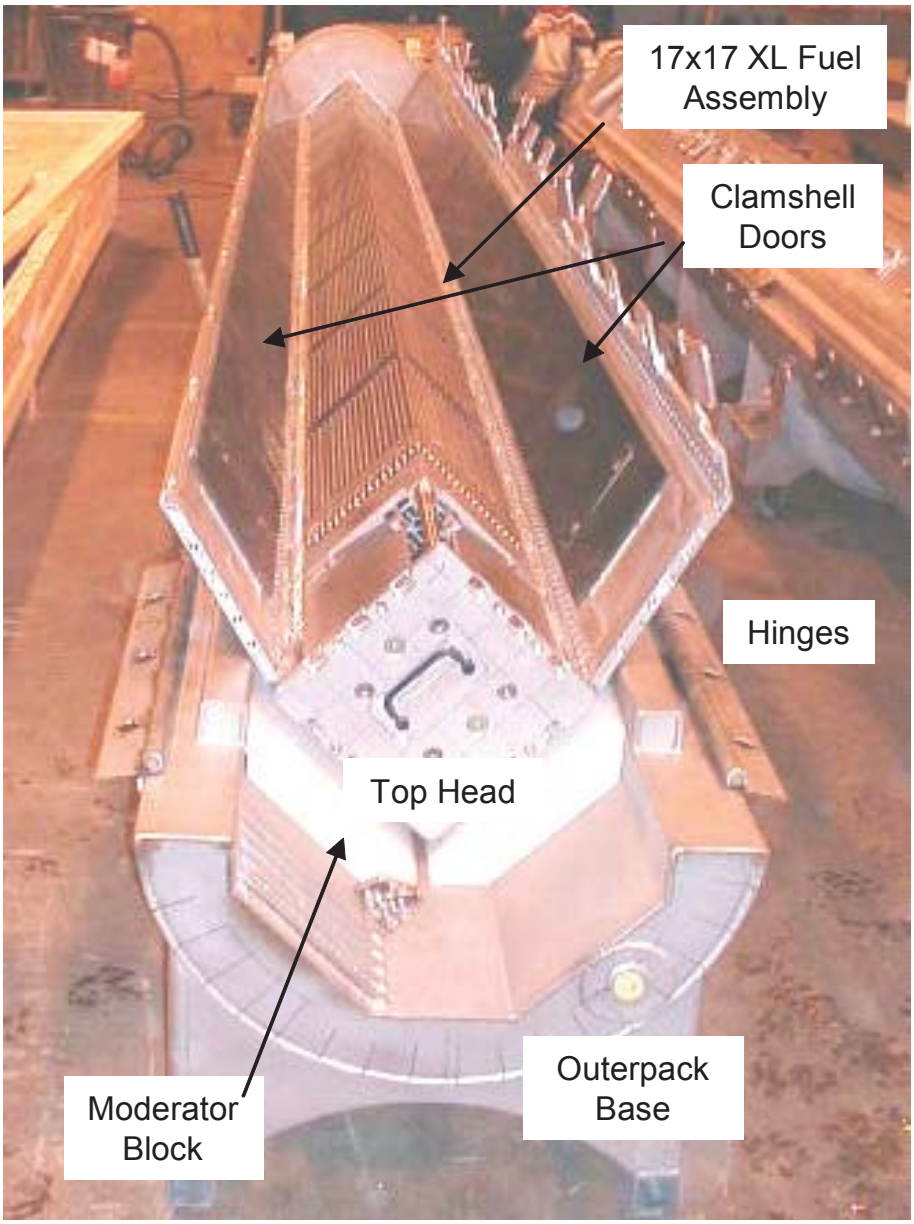

Figure 2-111 Traveller Prototype Internal View

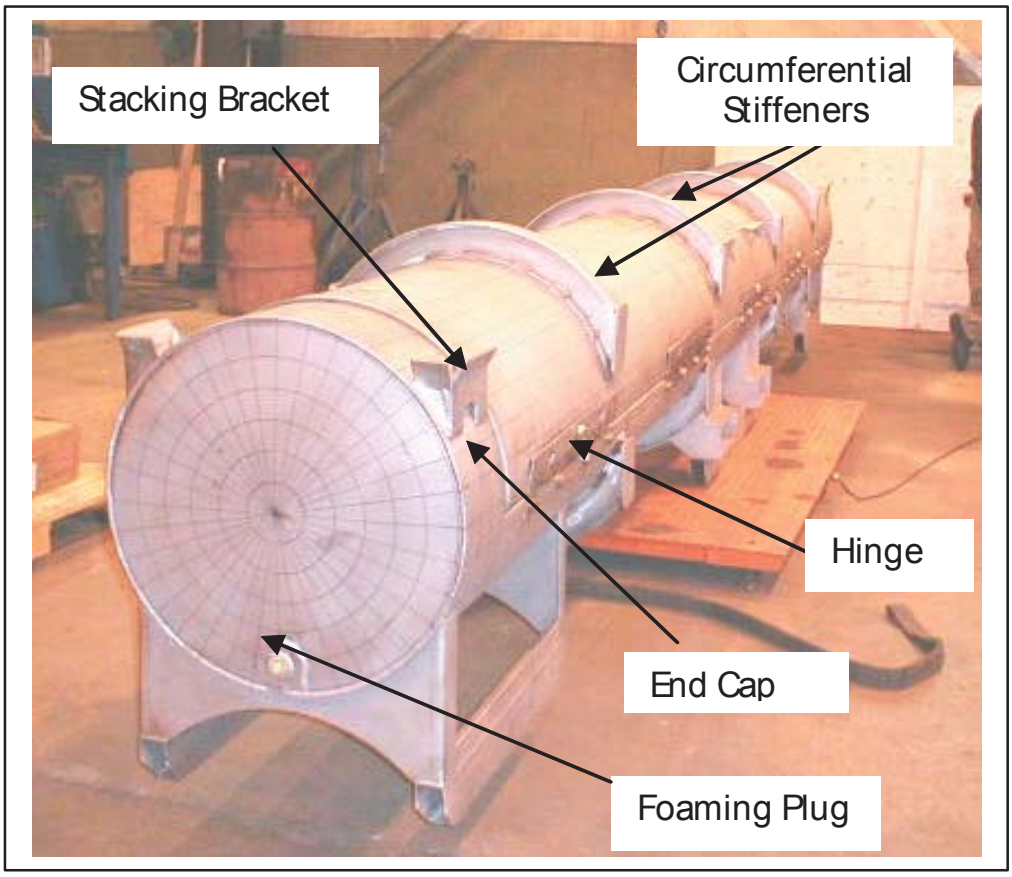

Figure 2-112 Traveller Prototype External View

Table 2-29 Series 1 As-Tested Drop Conditions

Test Sequence	Test Pitch Attitude	Test Roll Attitude	Impact Location
1.1) 9 m Low Angle	14.5°	180°	T/N primary impact on OP top
1.2) 9 m CG-over-corner	71°	90°	B/N primary impact on OP hinge
1.3) 1 m Pin-puncture	20°	180°	Center of Gravity (Axial) on OP top, T/N end down

Test 1.1 – The Outerpack retained its basic circular pre-test shape except for localized plastic deformation from the 9 meter drop test. Impact zones from the drop test were localized at the nozzle impact locations on the package ends. The Outerpack did not separate after the impact, and no bolt failures on the Outerpack hinge were noted. The top nozzle damage zone consisted of local crush approximately 12" wide, 9" axially and a maximum crush of approximately 1.5". The circumferential stiffeners were crushed (Figure 2-114) and inhibited global crushing on the Outerpack. The bottom nozzle damage zone consisted of local crush approximately 11.5" wide, a maximum crush of approximately 3/4", and axially from the package end to

the edge of the stiffening ring. The internal damage was minimal as shown in Figures 2-113 and 2-114. The polyethylene moderator blocks and aluminum neutron "poison plates" maintained position. The Clamshell doors remained closed, but the Clamshell bulged outwardly approximately 0.25" locally at the grid locations in a section 54" long at the bottom nozzle end. The fuel inspection indicated that no fuel rods had ruptured, and that the axial position of fuel rods maintained location between bottom and top nozzle. The average measured fuel envelope decreased from 8.418" nominally to 8.25" maximum, and the maximum measured fuel rod gap was found to be 0.188" locally (observed at one or two rods along the envelope) compared to the nominal gap of 0.122". Figures 2-114 and 2-115 summarize the results of this drop test.

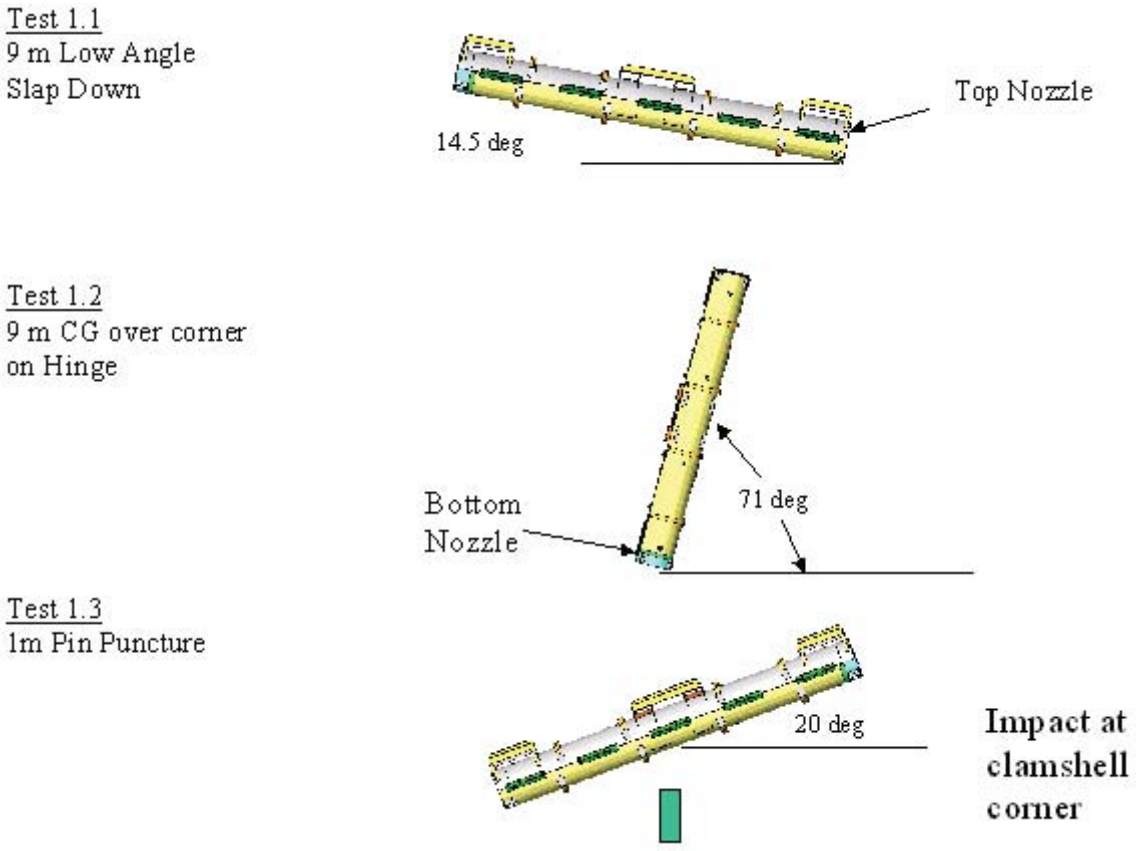

Figure 2-113 Drop Orientations for Prototype Test Series 1

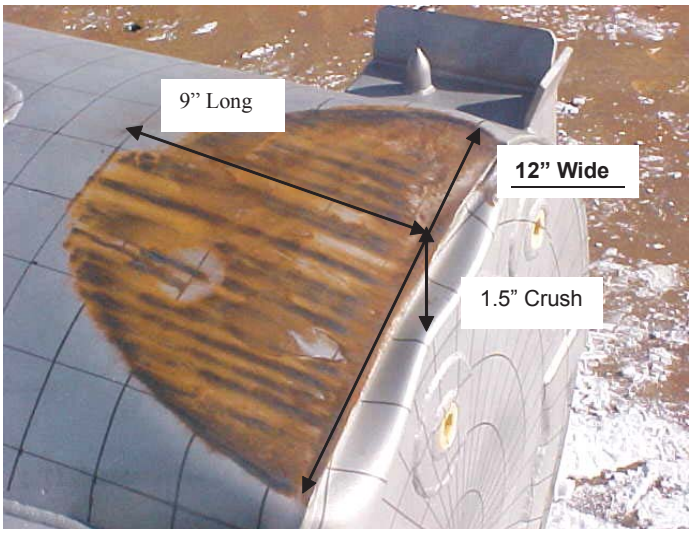

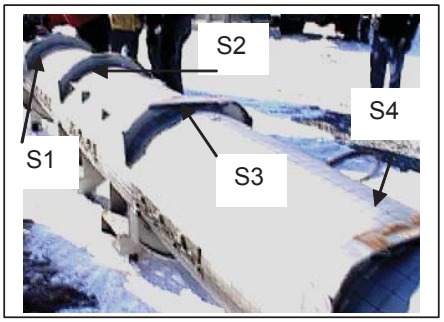

Stiffening rings show progressive damage from T/N

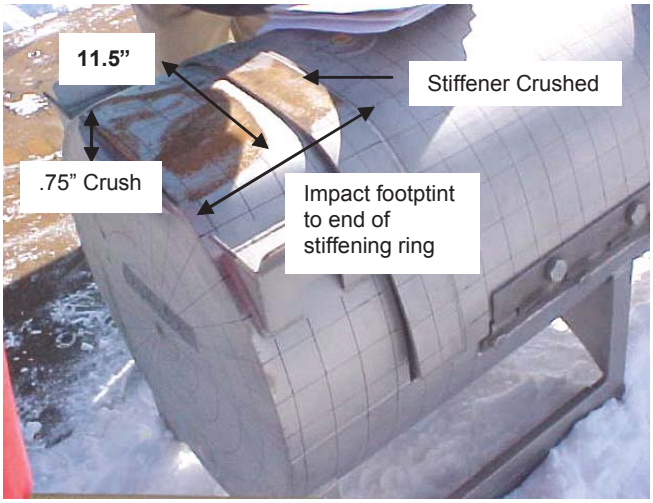

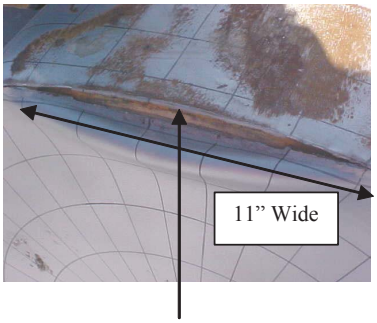

Small tear at Bottom End cap/Plate Seam

Figure 2-114 Traveller Prototype Exterior After Test 1.1

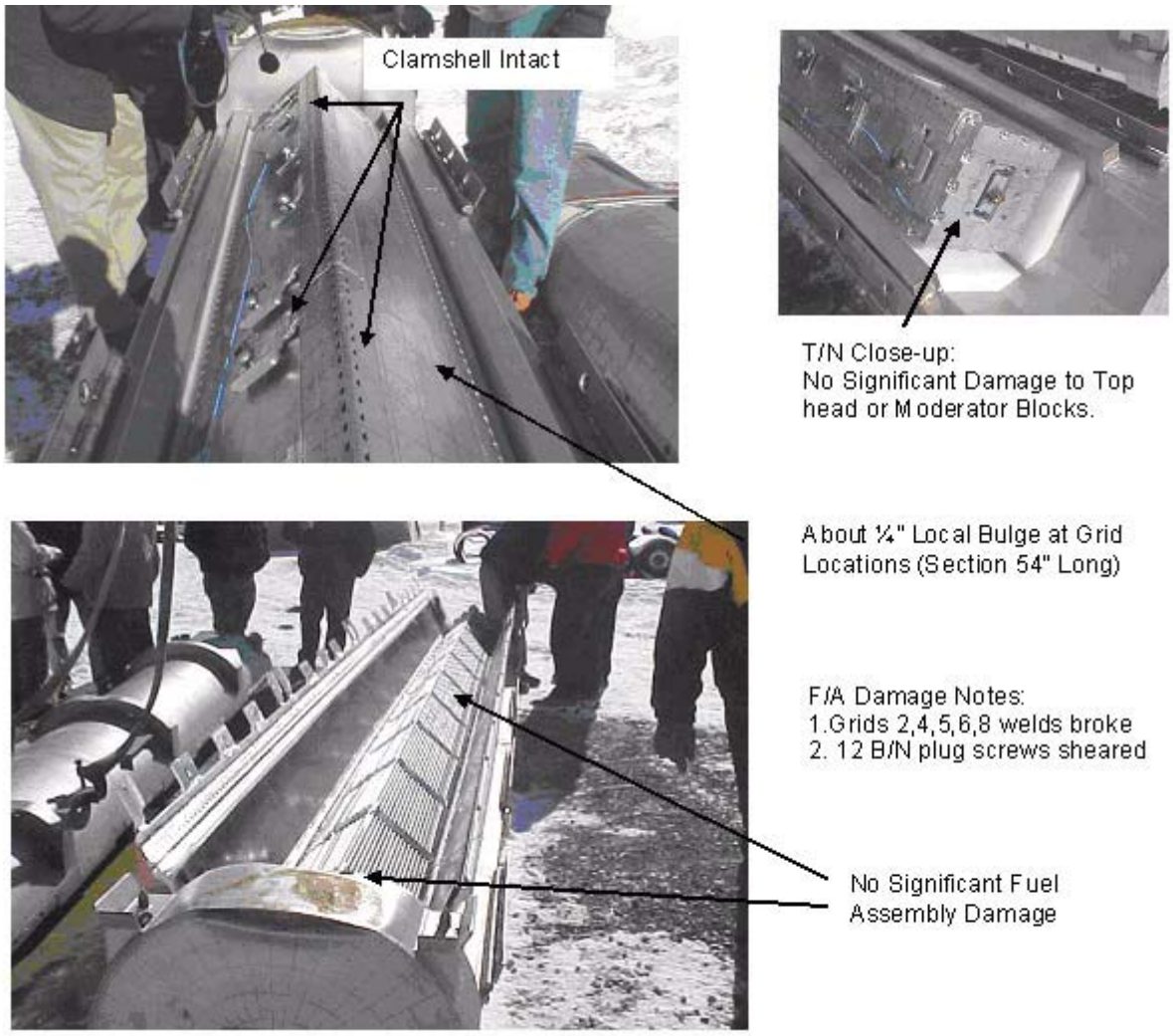

Figure 2-115 Traveller Prototype Interior After Test 1.1

Test 1.2 – The Outerpack retained its basic circular pre-test shape except for localized plastic deformation from the 9 meter drop test. Impact zones from the drop test were localized at the nozzle impact locations on the package ends. The Outerpack did not separate after the impact. One bolt failure on the Outerpack lower hinge, top nozzle end was noted. The bottom nozzle damage zone consisted of local crush approximately 10" wide, 22" tall and a maximum crush of approximately 3". The impact encompassed the stacking bracket which caused local buckling at the top/bottom Outerpack joint. A small ripple occurred in the Outerpack at this location. In addition, a tear in the Outerpack end cap measuring 8" wide resulted from the impact The top nozzle damage zone consisted of local crush approximately 6" wide, 13" long and a maximum crush of approximately 1/4". The relatively small amount of crushing is attributed the stacking bracket impacting the Outerpack in a normal direction and spreading the load more uniformly along the Outerpack length. The internal damage was more substantial than the previous drop test. The polyethylene moderator blocks and aluminum neutron“poison plates” maintained position. The Clamshell doors remained closed, but the top

and bottom head pieces separated from the Clamshell. The separation was caused by material shear-out as the top head connector bolts beared against the bolt slots. The bearing force of the bolts (a shear effect on the top head plate) from impact was of sufficient load to fail the material in the bolt slots for both head pieces. The fuel inspection indicated that no fuel rods had ruptured, and that the position of fuel rods maintained axial location between bottom and top nozzle. The maximum measured fuel envelope compressed from 8.25" after test 1.1 to 8.13", and the maximum measured fuel rod gap increased from 0.188" to 0.625" locally (observed at one or two rods along the envelope). The fuel rod gap expansion was also localized to Grids P, 1, 2, 3, and 4. In addition, Grid 2 failed by means of the weld joint tearing on the grid corner. External and internal results are summarized in Figures 2-116 and 2-117.

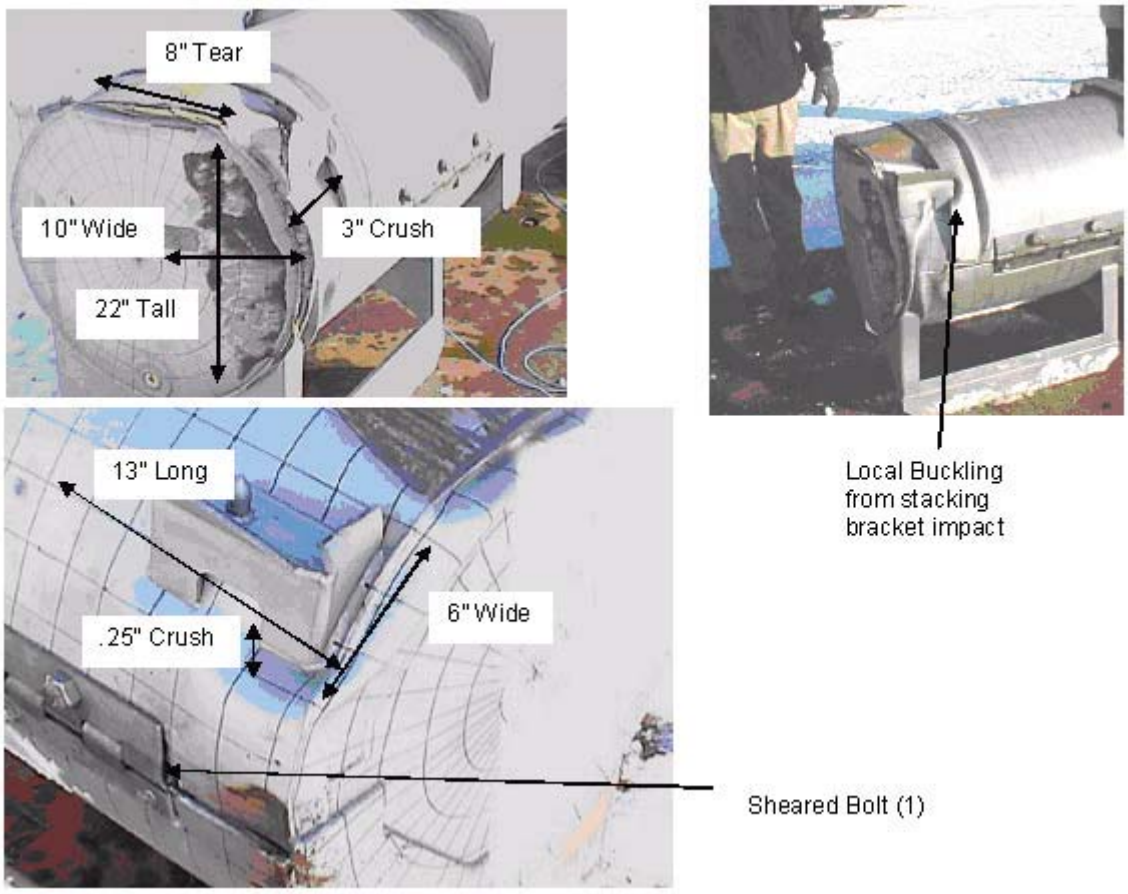

Figure 2-116 Traveller Prototype Exterior After Test 1.2

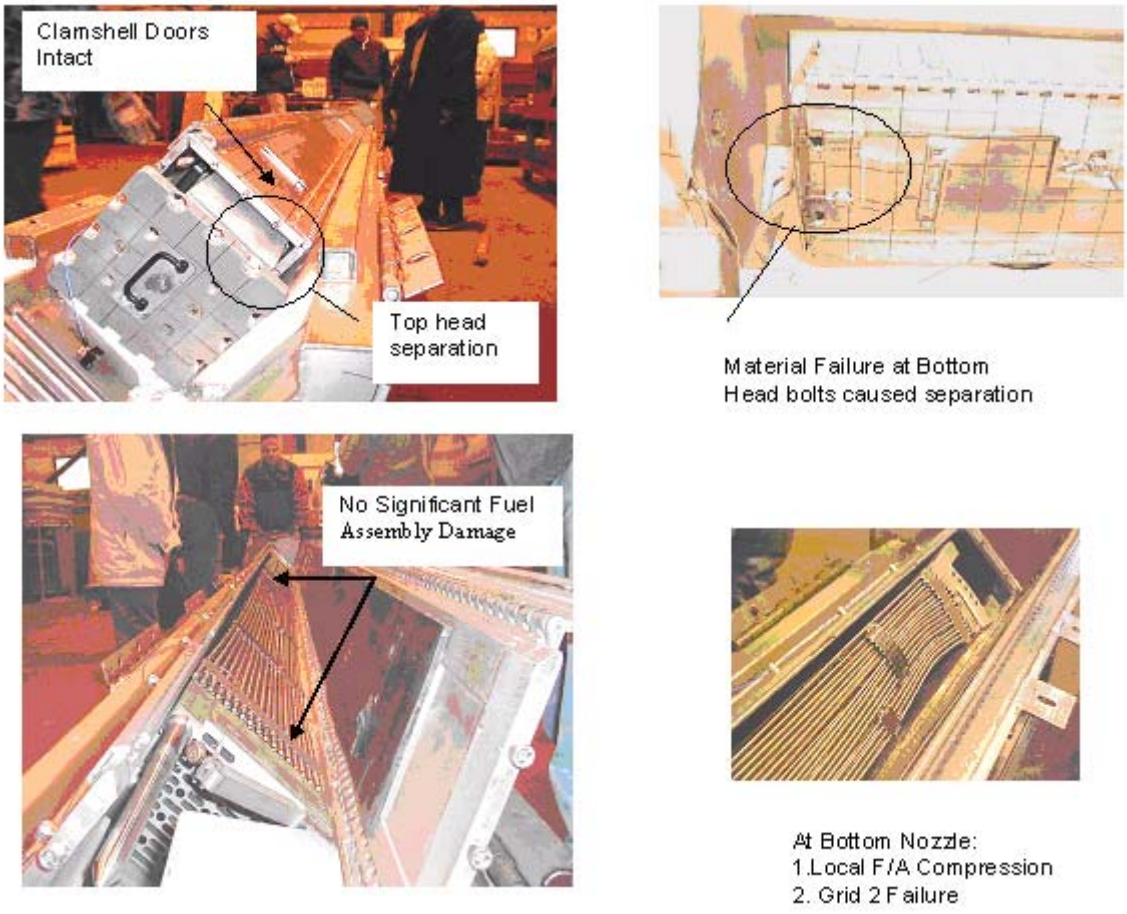

Figure 2-117 Traveller Prototype Interior After Test 1.2

Piezoelectric accelerometers were mounted on the Clamshell and Outerpack for drop tests 1.1 and 1.2. On the Clamshell, one 0-500 g accelerometer was mounted on the top head, and the other 0-500 g accelerometer on the bottom head. On the Outerpack, one 0-1000 g accelerometer was mounted on the underside of the bottom nozzle end (secondary impact location for test 1.1). After test 1.1, the accelerometer on the top head was replaced. The locations of these accelerometers are shown in Figure 2-117A. Figure 2-118 shows the accelerometer traces for the Clamshell from test 1.1. On the primary impact end (top nozzle), the accelerometer saturated in the vertical and axial directions, and the peak lateral deceleration was 453 g. The peak deceleration was 203 g and the resultant vector deceleration sum was 247 g at the secondary impact end (bottom nozzle).

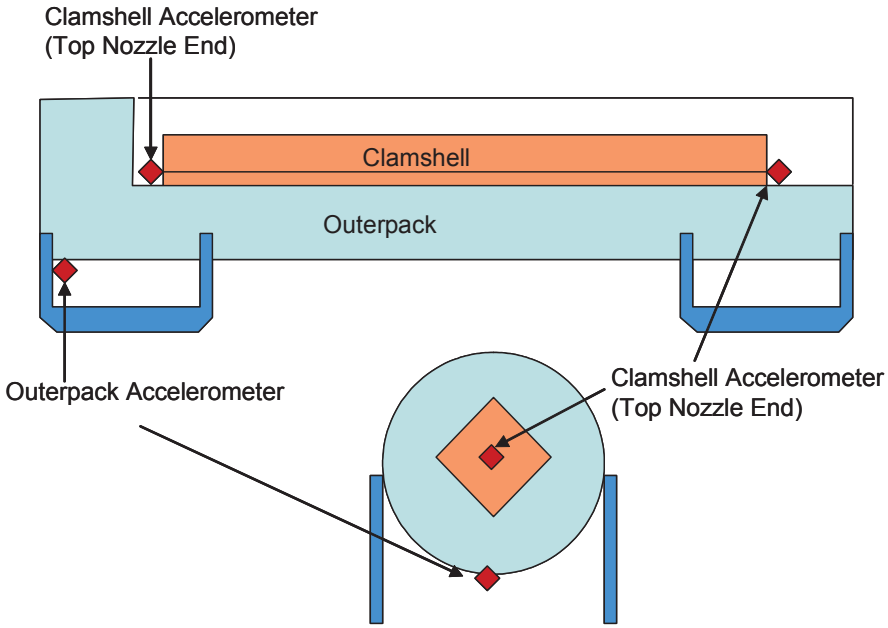

Figure 2-117A Accelerometer Locations on Prototype Drop Test

The 0-1000 g accelerometer trace is for the Outerpack is shown in Figure 2-119. The Outerpack vector deceleration sum for the primary impact measured 204 g, and the peak deceleration force measured 191 g in the vertical direction. The slap-down (secondary impact) resulted in decelerations which saturated each directional accelerometer.

The deceleration data for test 1.1 is summarized in Table 2-30.

This page intentionally left blank.

Table 2-30 Measured Decelerations in Prototype Test 1.1				
Accelerometer Position	Measured Deceleration Force, g			
	Vertical	Lateral	Axial	Vector Sum
Clamshell T/N end	>500	435	>500	N/A
Clamshell B/N end	205	118	78	247
Outerpack – Primary Impact	191	59	42	204
Outerpack – Slap Down	>1000	>1000	>1000	N/A

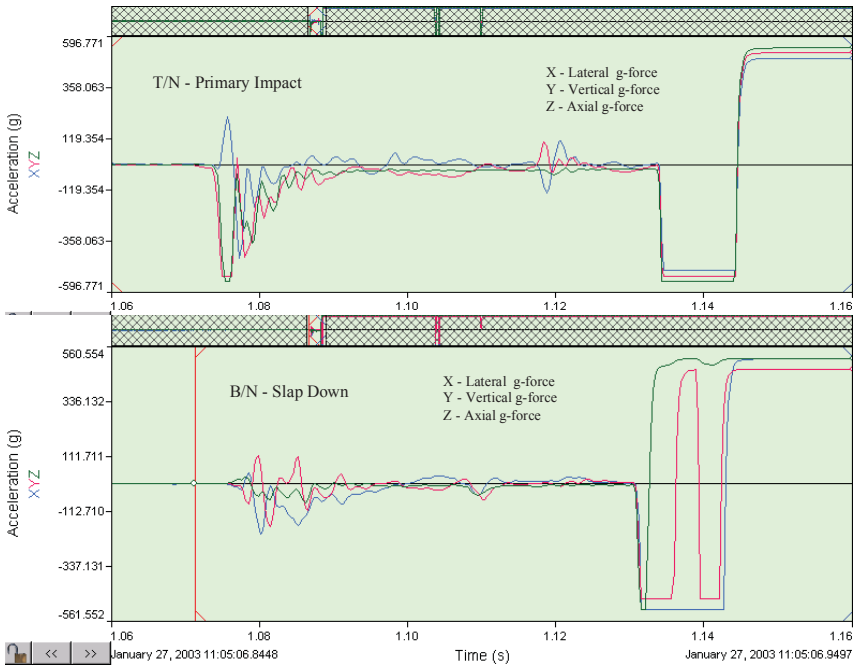

Figure 2-118 Clamshell Accelerometer Trace for Prototype Test 1.1

The top head accelerometer was replaced prior to test 1.2. Due to damaged instrumentation, no data was recorded for the bottom head or the Outerpack. The primary impact occurred on the bottom nozzle end. The top head accelerometer measured the deceleration trace of the primary impact as shown in Figure 2-119. The vector deceleration sum of the primary impact measured 417 g, and the peak deceleration force measured 260 g in the axial direction. The deceleration data for test 1.2 is summarized in Table 2-31.

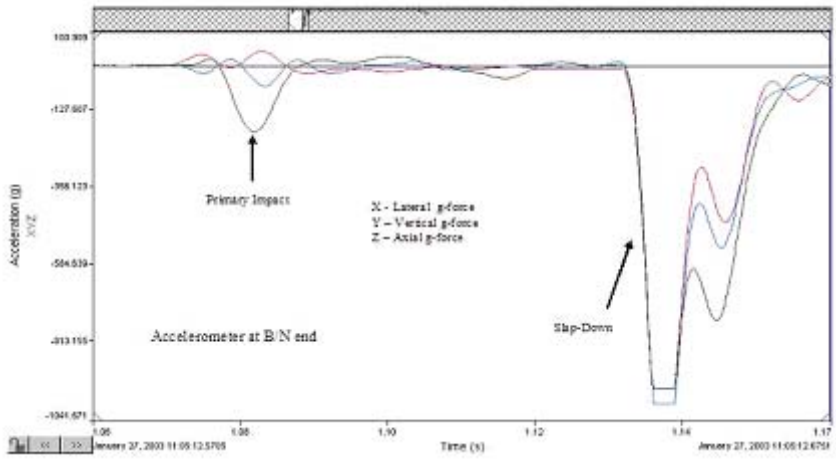

Figure 2-119 Outerpack Accelerometer Trace for Prototype Test 1.1

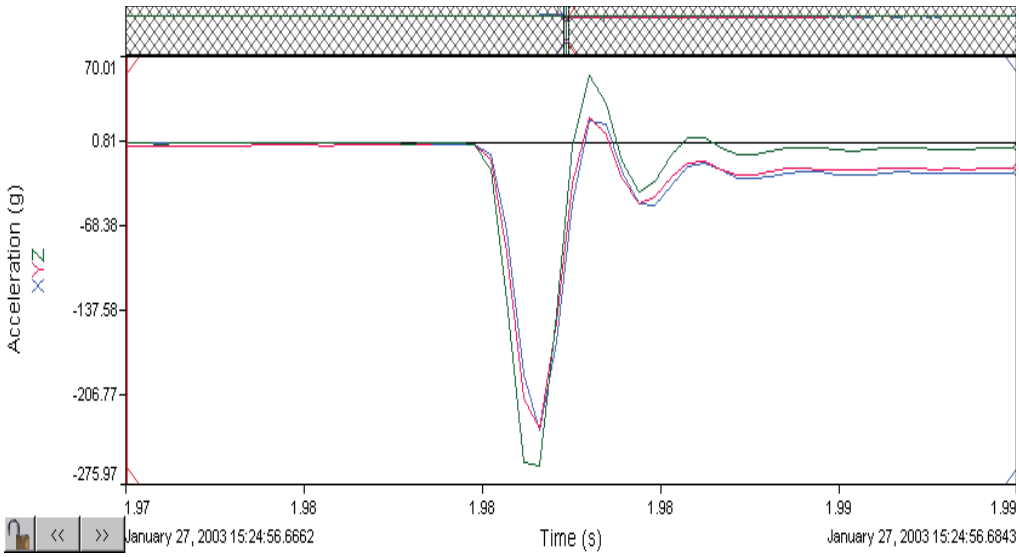

Figure 2-120 Clamshell Accelerometer Trace for Prototype Test 1.2

Table 2-31 Measured Accelerations in Test 1.2

Accelerometer Position	Measured Deceleration Force, g			
	Vertical	Lateral	Axial	Vector Sum
Clamshell T/N end	230	232	260	417
Clamshell B/N end	No data	No data	No data	N/A
Outerpack – Primary Impact	No data	No data	No data	N/A
Outerpack – Slap Down	No data	No data	No data	N/A

Test 1.3 – The 1-meter pin puncture test resulted in little damage to the package. The outer skin of the Outerpack was locally punched approximately 1.63" and the width of the impact was approximately 10.5" as shown in Figure 2-121. The impact did not perforate the outer skin. The subsequent inspection of the inner side of the Outerpack top indicated that a small dent approximately 7/16" to 1/2" and 15" wide resulted from the pin puncture test. The moderator blocks were not impacted by the pin test.

Test Series 2 – Test series 2 was conducted on January 30th (Table 2-32) and included a 1.2-meter Normal accident condition free drop, a 1-meter pin-puncture test, and a 9-meter free drop test. The package's test weight was 5057 pounds.

The cumulative external damage from the regulatory drop test sequence was localized to plastic deformation at the impact zones. There was no significant changes in the Outerpack geometry, and no bolt failures were noted. Upon an internal inspection, the pin did not perforate the inner or outer shell. The internal damage was minimal. The fuel assembly's envelope decreased from 8.418" nominal to 8.25" maximum. Fuel rod gaps globally decreased (the fuel envelope decreased), but local expansion was noted between a few rods with a maximum measured gap of .188" compared to the nominal gap of .122". The polyethylene moderator blocks and aluminum neutron "poison plates" maintained position. The Clamshell doors remained closed, and the modified top head and bottom heads maintained position. A subsequent fuel inspection indicated that no fuel rods had ruptured, and that the axial position of fuel rods maintained location between bottom and top nozzle.

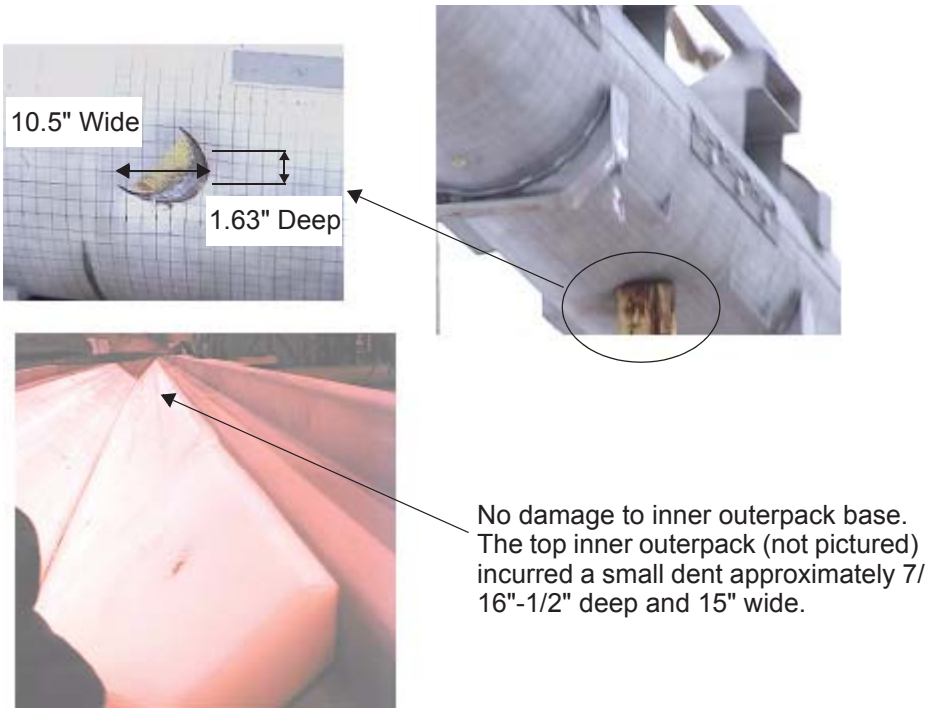

Figure 2-121 Traveller Prototype After Test 1.3

Table 2-32 Prototype Test Series 2

Test Sequence	Test Pitch Attitude	Test Roll Attitude	Impact Location
2.1) 1.2-m NAC drop	20°	180°	B/N primary impact on OP top
2.2) 1-m Pin-puncture	20°	135°	CG (Axial) on OP topside, T/N end down
2.3) 9-m CG-over-corner	72°	180°	T/N primary impact on OP top

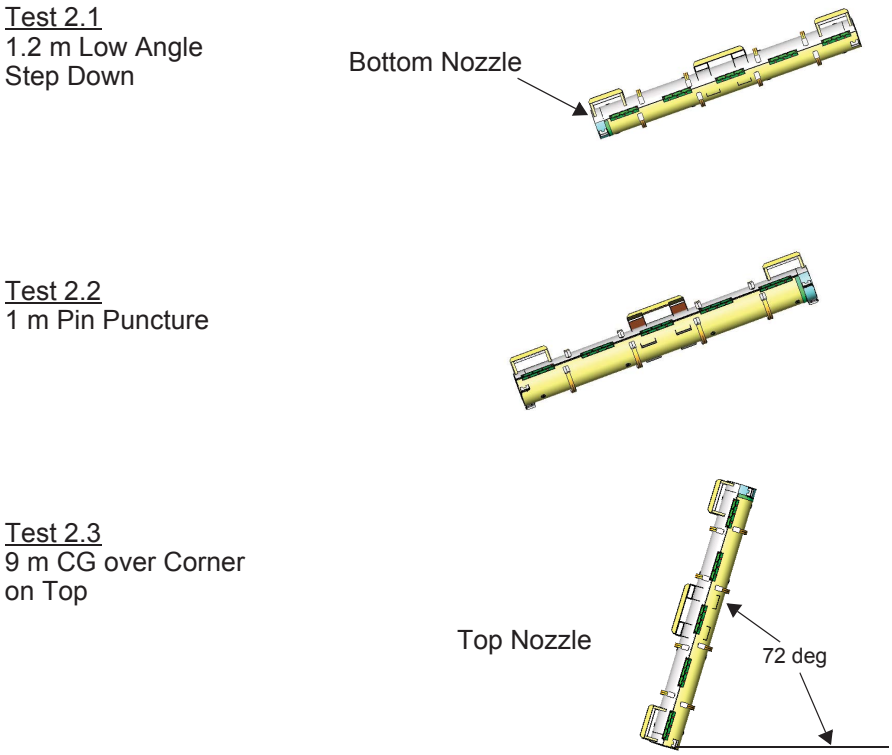

Figure 2-122 Drop Orientations for Traveller Prototype Test Series 2

Test 2.1 – The 1.2 meter normal condition drop test resulted in minimal damage to the Outerpack. The impact created an impact zone at the bottom end 9" wide, 2.5" in axial length, and crushed the Outerpack .75" as shown in Figure 2-123. Two stiffeners near the Outerpack center crushed approximately .75" over a width of 6". The energy absorption of the circumferential stiffeners precluded damage to the secondary impact end (top nozzle).

Test 2.2 – The second test of this drop sequence was a 1-meter pin drop on the package side, Figure 2-122. The 1-meter pin puncture test resulted in little damage to the package. The outer skin of the Outerpack was locally punched in approximately 2"as shown in Figure 2-124. The impact punch zone was 10" tall and the width of the impact was approximately 14". The impact did not perforate the outer skin.

Test 2.3 – The 9-meter drop test resulted in local damage to the primary impact region (top nozzle end). The secondary impact region was in the vicinity of the impact region of the 1.2-meter free drop and did not result in additional damage. From Figure 2-125, the damage zone was approximately 25" wide, 12" tall, and produced a crush zone approximately 9" axially. Due to the impact attitude, the Outerpack top tended to shear relative to the Outerpack bottom. A gap approximately 1" resulted from the impact, but did not comprise the Outerpack closure. No bolt failures were noted.

In general, the test sequence resulted in minimal Clamshell and fuel damage. The top nozzle end of the Clamshell was slightly bowed in a localized region at the top nozzle end (Figure 2-126), but did not result in fuel expansion. The modified top and bottom head pieces remained intact, and no shock mount failures were noted. The fuel inspection indicated that the assembly had moved axially toward the top nozzle 3-3/8" as a result of the spacer movement. There was no significant fuel damage at the bottom nozzle. Also the top nozzle region of the fuel assembly incurred some local damage. The guide pins buckled. Four (4) fuel rods moved axially (maximum of 1"), but did not extend beyond the neutron poison plates. The fuel inspection also indicated that no fuel rods had ruptured. The fuel rod gap measurements indicated the maximum measured fuel rod gap increased from 0.122" nominally to 0.188" locally (observed at one or two rods along the envelope). The measured fuel envelope compressed from 8.418" nominally to 8.25" maximum. The moderator blocks did not move from their original position even though two studs were sheared off. The pin-puncture test produced a 24" long by 5/8" deep dent on the inner Outerpack surface.

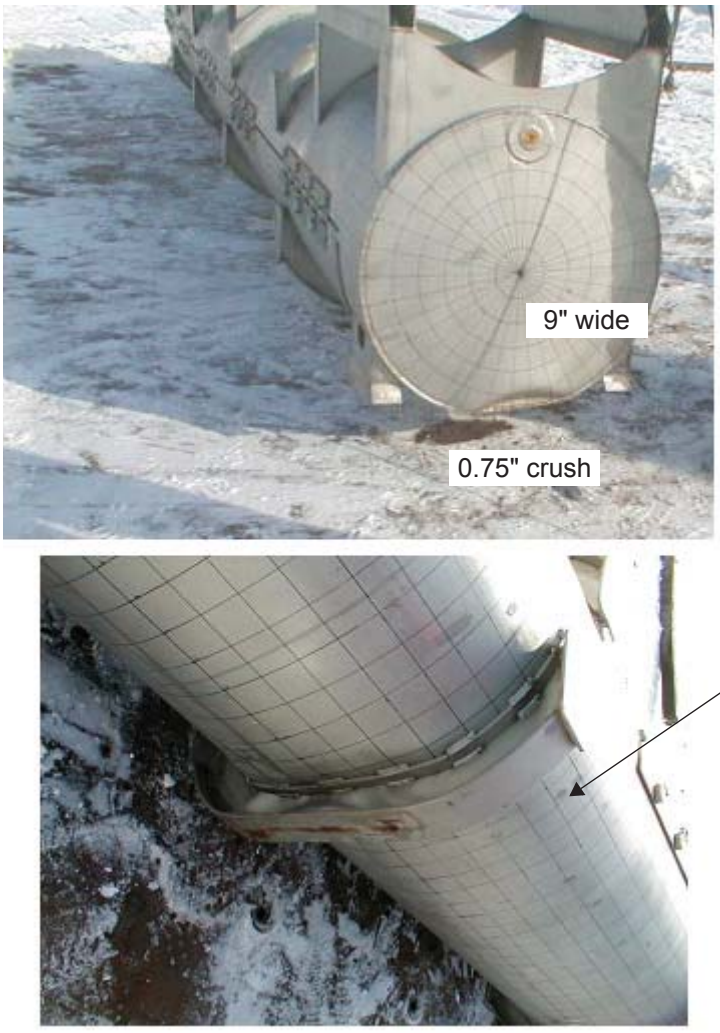

Figure 2-123 Traveller Prototype After Test 2.1

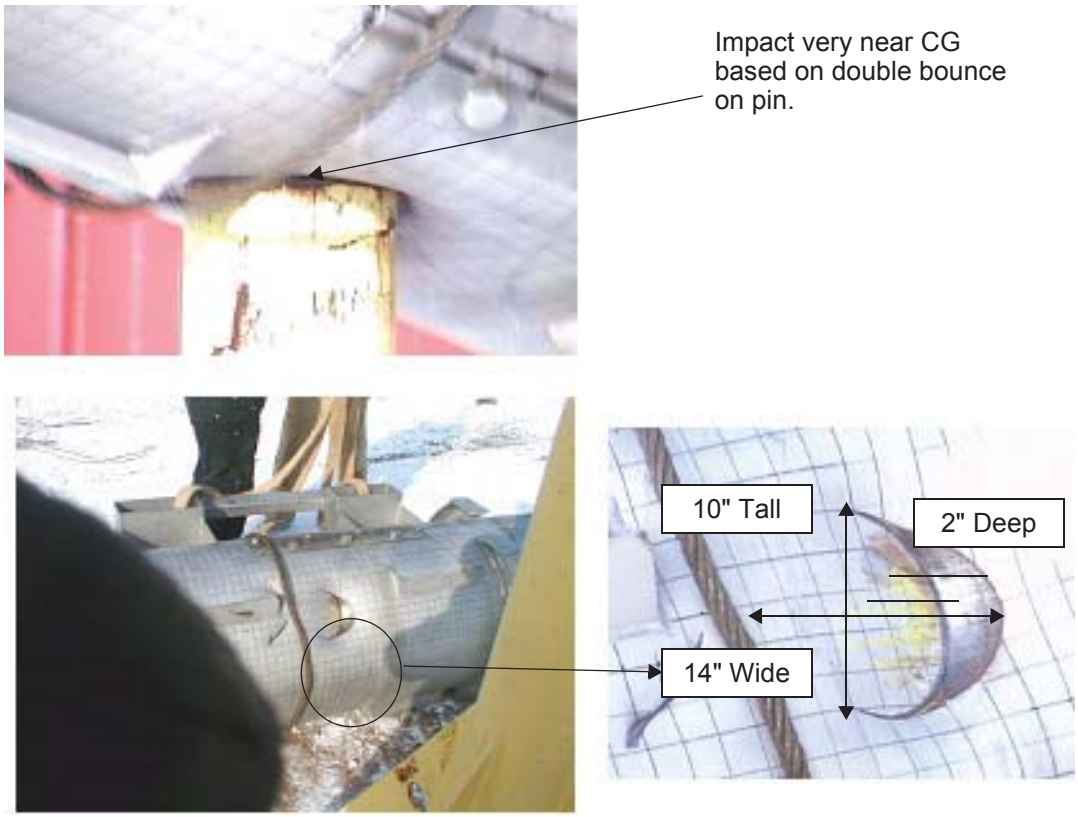

Figure 2-124 Traveller Prototype After Test 2.2

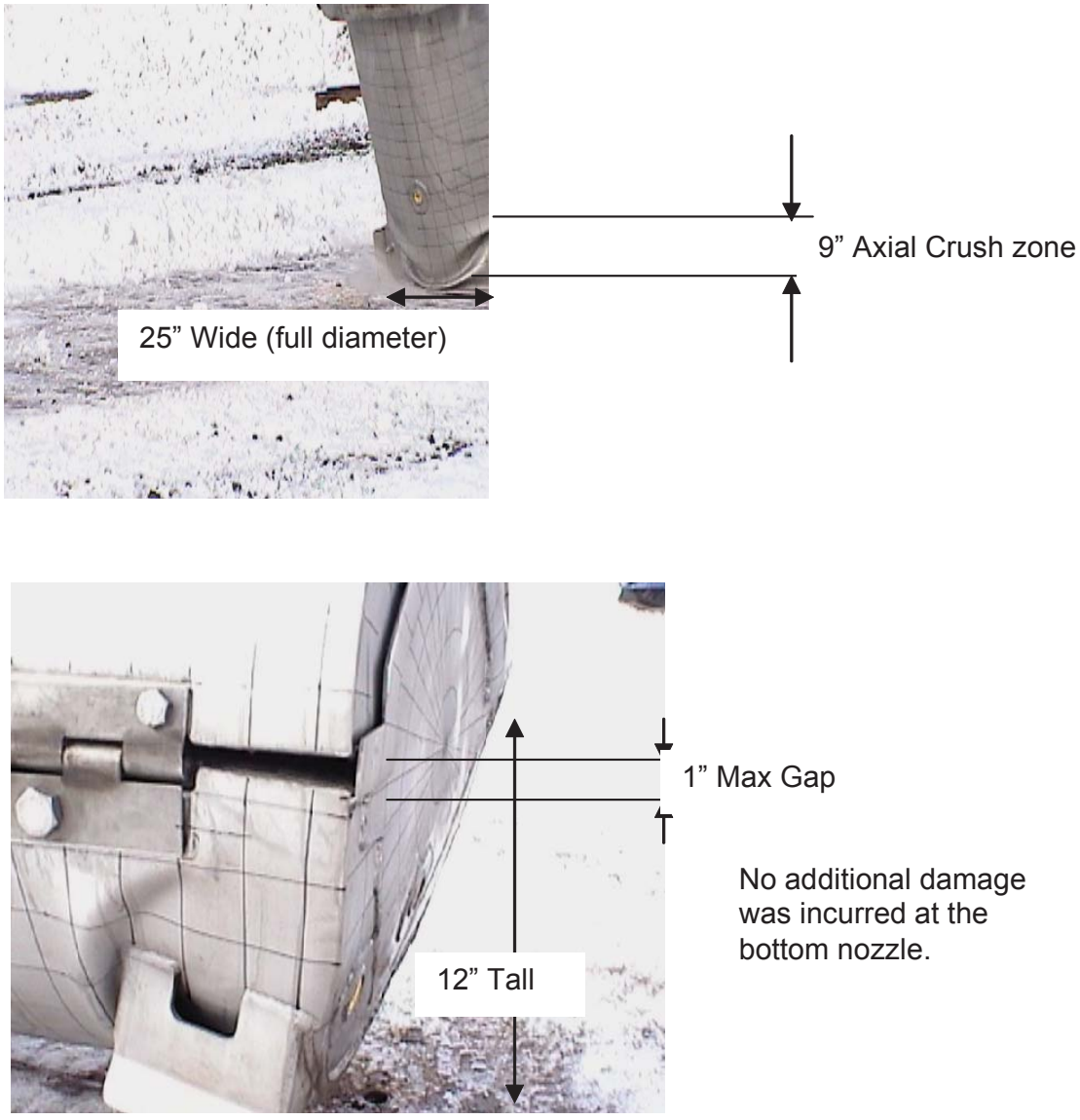

Figure 2-125 Traveller Prototype After Test 2.3

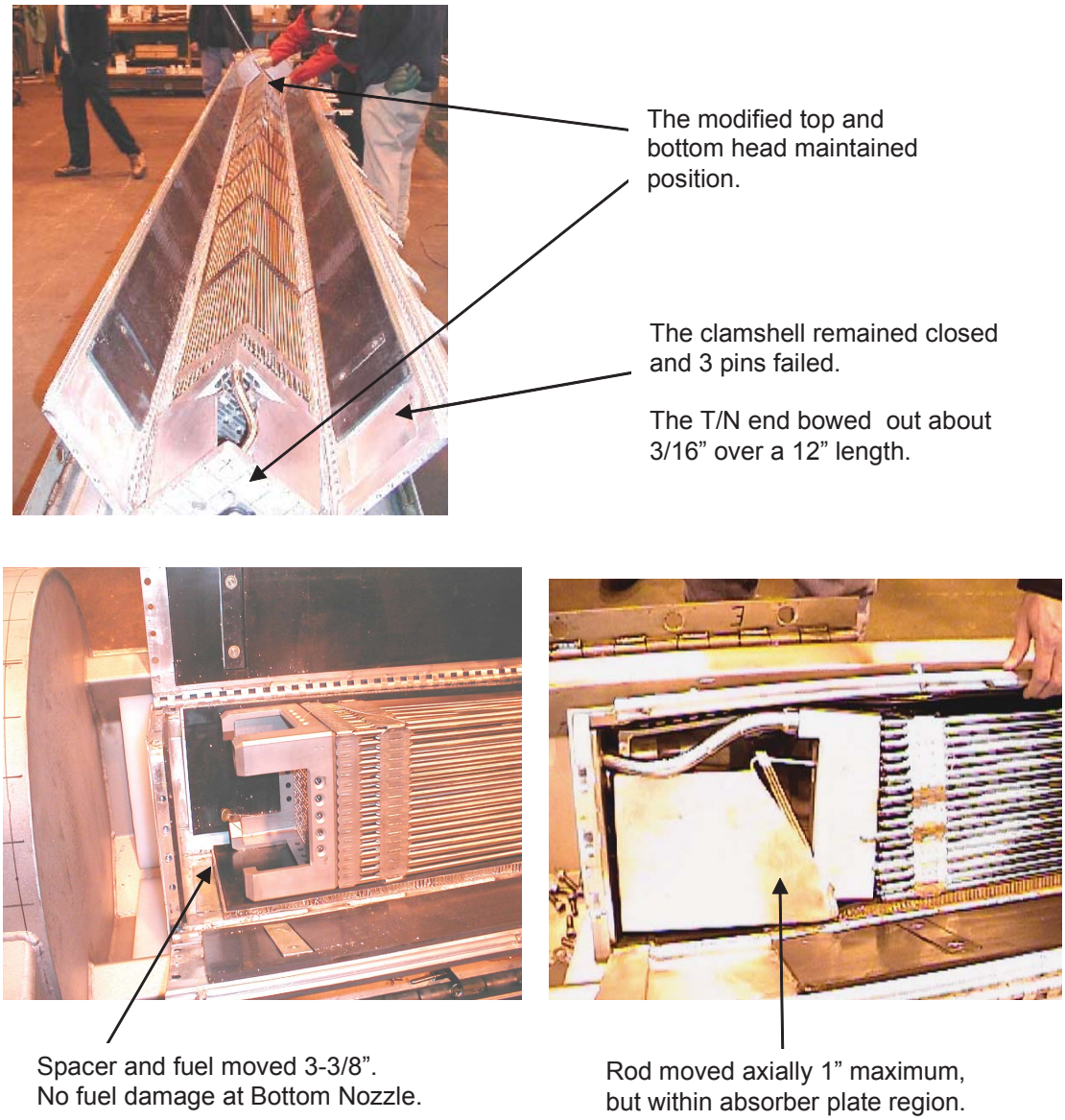

Figure 2-126 Traveller Prototype Interior After Test Series 2

Test Series 3 – Test Series 3 consisted of three 9-meter drop tests conducted to evaluate design features of the Outerpack after modifications to the Clamshell and Outerpack. The test sequence and measured drop attitudes are summarized in Table 2-33. The test series employed was Prototype 2 that had been used for test Series 2. The purpose of this test series was to evaluate design features and evaluate design margin. External damage assessments were performed following each supplementary drop test, and a general internal assessment was conducted after the completion of test 3.3. However, the inspections for this test series were

not intended for use in nuclear criticality safety analysis. Prior to test 3.1, the following modifications were made to the package:

- Removed 1 bolt from each of the 5 top Outerpack hinges (reduced bolt count by 33%).
- Removed sheet metal from endcap inner surface
- Removed 2 of the 5 pins that secure each Clamshell clip

Table 2-33 Traveller Prototype Drop Tests Performed in Test Series 3

Test Sequence	Test Pitch Attitude	Test Roll Attitude	Impact Location
3.1) 9-m Axial End drop	90°	0°	B/N impact
3.2) 9-m Flat drop	0.5°	0°	Impact on OP feet
3.3) 9-m Side drop	0°	270°(90°CCW)	Impact on OP hinges

Figure 2-127 shows that the Outerpack sustained minimal damage. The Outerpack remained closed and no bolts failed after the completion of drop test series 3. The first drop test of this series resulted in slight crushing (approximately 1-5/8" deep) at the bottom nozzle end. The crushed circumferential stiffeners precluded excessive Outerpack damage as the package slapped down after the axial drop. Drop test 3.2 crushed the feet and forklift supports completely, but otherwise did not comprise the Outerpack structural integrity. The direct hinge impact (test 3.3) did not fail any hinges or result in any substantial damage to the Outerpack.

The cumulative overall damage to the Clamshell was also minimal as shown in Figure 2-127. The Clamshell retained its geometry, no Clamshell clip pins failed, and no shock mount failures were noted. The notable Clamshell damage was located at the bottom head, which was separated from the Clamshell by the impacting fuel, Figure 2-128. It is presumed that the 3-3/8" gap from the Clamshell bottom plate to the base of the fuel assembly bottom nozzle provided sufficient distance for the fuel assembly to attain enough kinetic energy to separate the Clamshell bottom head upon impact.

The fuel was in good condition. No measurements were taken since this test series was qualitative in nature.

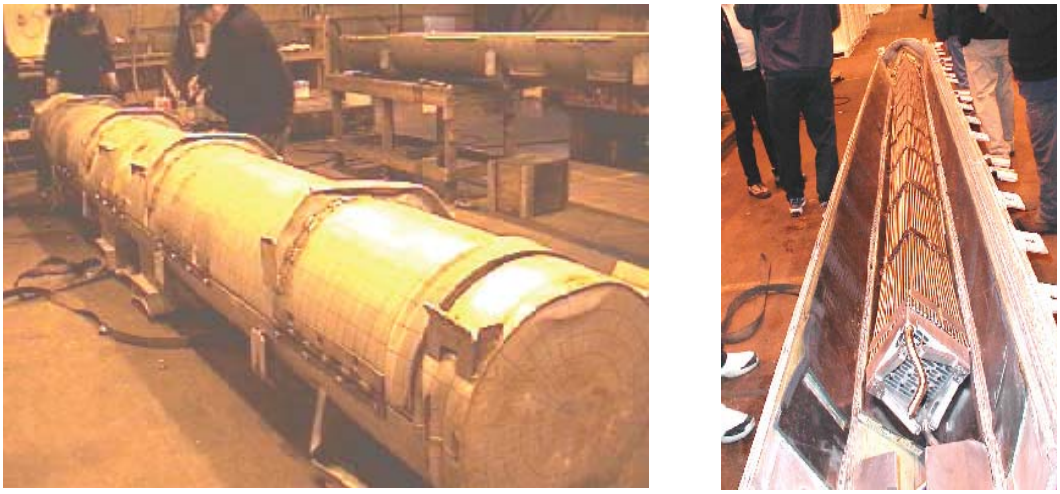

Figure 2-127 Traveller Prototype Clamshell and Bottom Impact Limiter After Test Series 3

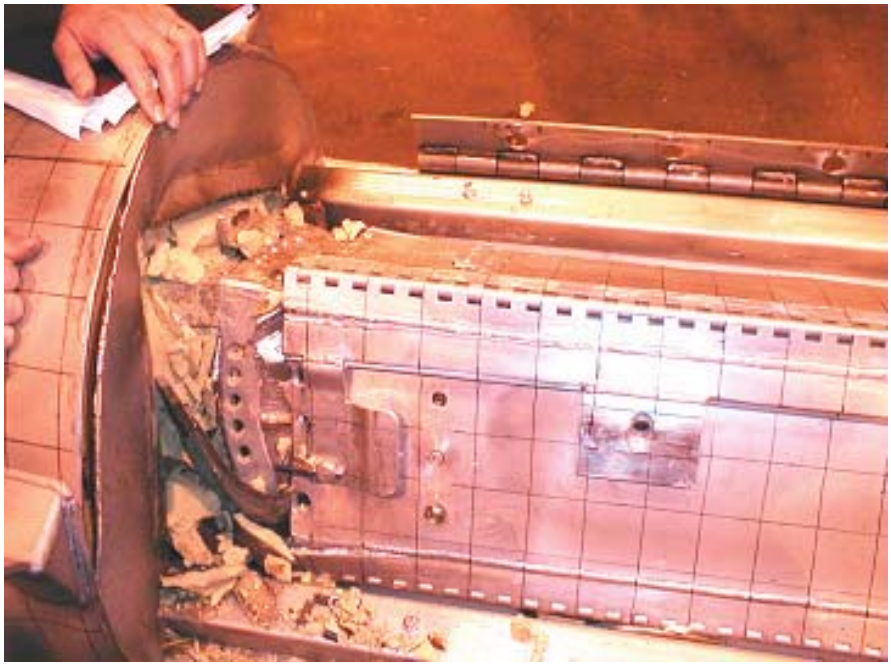

Figure 2-128 Traveller Prototype Clamshell and Bottom Impact Limiter After Test Series 3

Minor design modifications were recommended for the Traveller package based on this testing. The top and bottom heads required additional bolting to preclude Clamshell separation. The number of Clamshell clip retaining pins (and clips) could be reduced. It was found that sufficient design margin against material failure existed allowing the Outerpack gage metal can be reduced slightly in thickness. In addition, the number of Outerpack bolts can be reduced on the top hinge by at least 1/3.

2.12.5.2 Qualification Test Unit Drop Tests

The following section delineates the second of three (3) full-scale testing campaigns of the Traveller development program. This campaign utilized two units called Quality Test Units, or QTU-1 and 2. A total of two (2) QTUs were built and tested, with minor changes to improve burn performance incorporated into the second QTU article.

2.12.5.2.1 QTU Test Series 1

Test series 1 was conducted on the afternoon of September 11 and included a 50 inch (1.27 m) slap down, a 33.3 feet (10.15 m) center of gravity-over-corner free drop test, and a 42 inch (1.07 m) pin-puncture test. The package's test weight was 4793 pounds (Table 2-34). The internal inspection of the fuel assembly was conducted after completion of the fire test on September 16, 2003.

Table 2-34 QTU-1 Measured Weight

Test Weights	Nominal	Actual
Weight of Outerpack (Empty):	3033 lb	**3032** lb
Weight of Clamshell (Empty):	425 lb	**400** lb
Weight of package (Empty):	3477 lb	**3432** lb
Total package test weight:	5422 lb	**4793** lb

Test series 1 was conducted on the afternoon of September 11 and included a 50.75 inch (1.29 m) slap down, a 33.3 feet (10.15 m) free drop test, and a 42 inch (1.07 m) pin-puncture test. QTU1 pre-test data and observations are shown in Form 1A. The test sequence and measured drop attitudes are summarized in Table 2-35 and shown in Figure 2-129. A pitch angle of 72 degrees was measured along the outerpack surface for Test 1.2. The angle of 108 degrees should be located as shown in Figure 2-129. The reference to "hinge side" in Test 1.3 indicates the package side that pivots, rather than the actual hinge. The impact point of Test 1.3 (Figure 2-132) was on the top nozzle end and on the pivot (left) side of the package. A fuel damage assessment was conducted after the completion of the hypothetical fire condition test conducted on September 16, 2003 at the South Carolina Fire Academy near Columbia, SC.

The Outerpack retained its basic circular pre-test shape except for localized plastic deformation at the top nozzle end accumulated from the drop test series. No bolts failed on the Outerpack after completion of the drop test series. The Outerpack did not separate after any impacts, and the pin did not perforate the inner or outer shell. The most notable Outerpack damage was the resulting joint tear of approximately 1-1/8" at the Outerpack corner located at the top, left hinge side. The fuel assembly damage was minimal. At the top nozzle portion, the fuel assembly locally expanded from 8.375" nominal to 8.625" maximum over a length of approximately 2-3". The fuel rod gaps were globally unchanged but local expansion was noted between one rod near Grid 10 with a maximum measured gap of 0.250". The resulting measured maximum local pitch was 0.625 inches. Three rods were found to be in contact with each other while the remaining rods

were nominally positioned. Intermediate grids 2-7 were buckled locally, but the fuel rod envelope was unchanged. The bottom nozzle portion of the fuel assembly was slightly compressed from 8.375" nominally to 8.250" measured. Based on the condition of the fuel assembly, the Clamshell was concluded to have performed successfully. The fuel inspection also indicated that no fuel rods had visibly ruptured, and that the axial position of fuel rods maintained location between bottom and top nozzle.

Table 2-35 QTU-1 Drop Test Orientations

Test Article ID	F/A Type	Test Sequence	Test Pitch Attitude	Test Roll Attitude	Design Feature Tested
QTU1	17x17 XL	P1.1)1.2 m, NAC, Low angle[1]	10°	180°	Operations of hinges/doors
		P1.2)9 m CG-over-Corner[1]	108°	90°	OP hinge shear, CS latches
		P1.3)1 m Pin-puncture[1]	83°	90°	Joint Integrity – Fire test

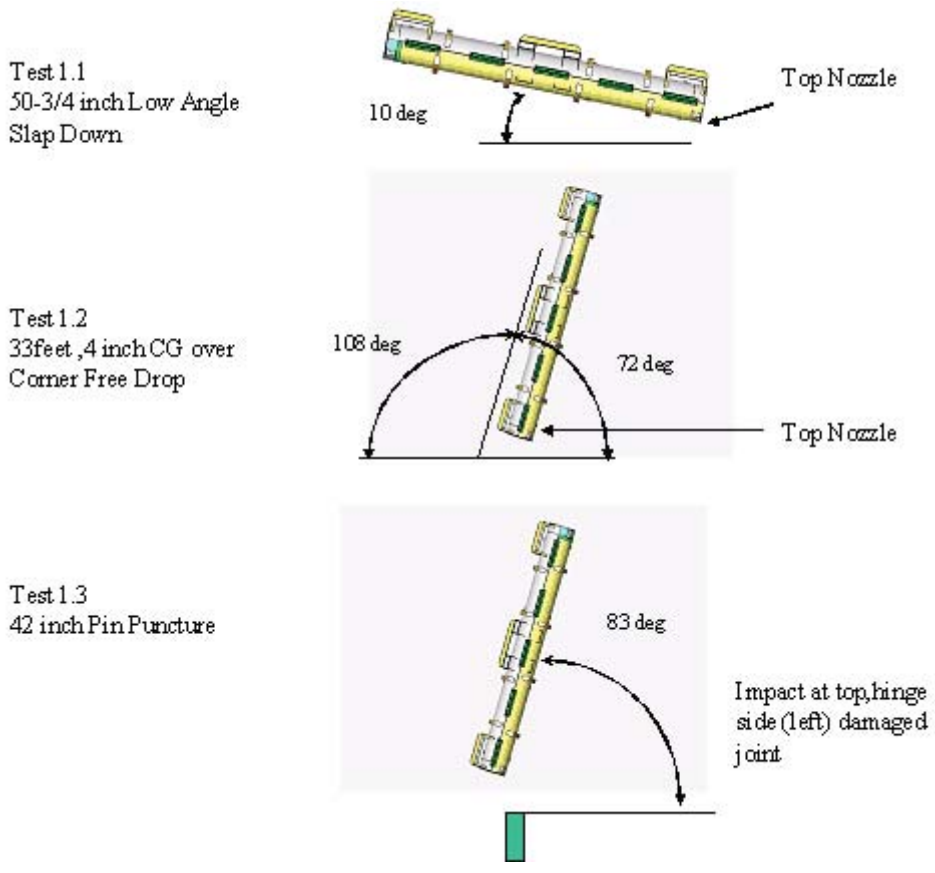

Figure 2-129 Drop Orientation for QTU Test Series 1

Test 1.1 – The 50.75 inches (1.29 m) drop onto the Outerpack lid was performed first. As shown in Figure 2-130, this drop resulted in a small indention in the outer skin of the Outerpack.

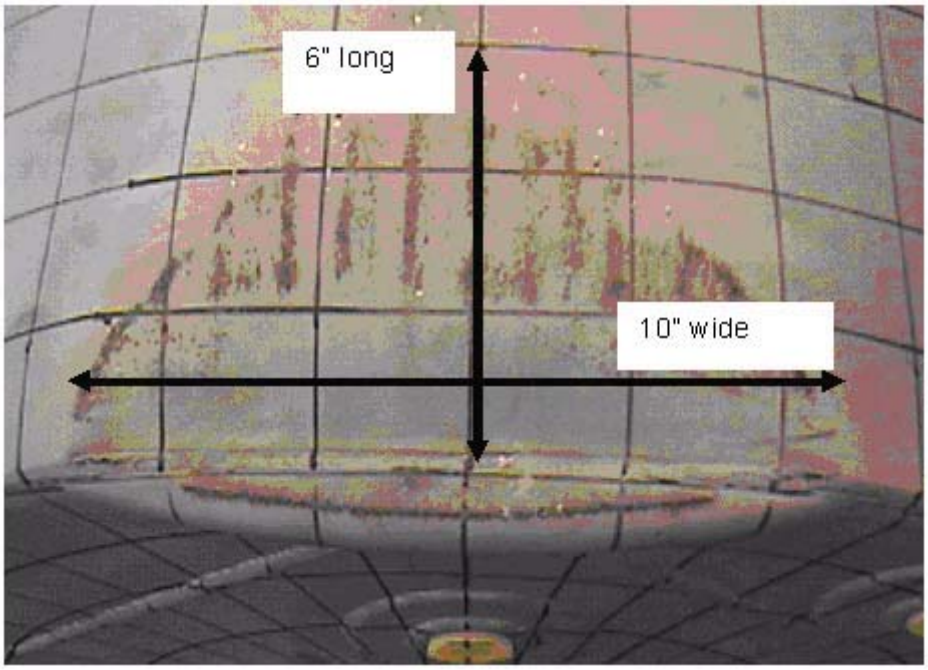

Figure 2-130 QUTU-1 Outerpack After Test 1.1

Test 1.2 – The 33.3-foot free drop resulted in localized damage to the top nozzle end region. One of the hoist rings was sheared off as a result of the impact, Figure 2-131. The impact opened a small tear at the top and bottom Outerpack seam (also in circled region). The entire 25" diameter face of the top nozzle end was dented approximately 3-1/2". The stiffeners were also dented across their tops, but were intact. Two welds located at the bottom nozzle end stiffener were broken, but this did not compromise the stiffener position.

Test 1.3 – The pin puncture test was located in the top left (hinge) side of the Outerpack top nozzle end. The objective of the test was attempt to increase the Outerpack separation incurred by the previous 33.3-ft drop. Additional tearing of the joint was noted which resulted in measured tear of approximately 1-1/8". The indention resulting from the pin puncture was approximately 1-1/2" deep (Figure 2-132).

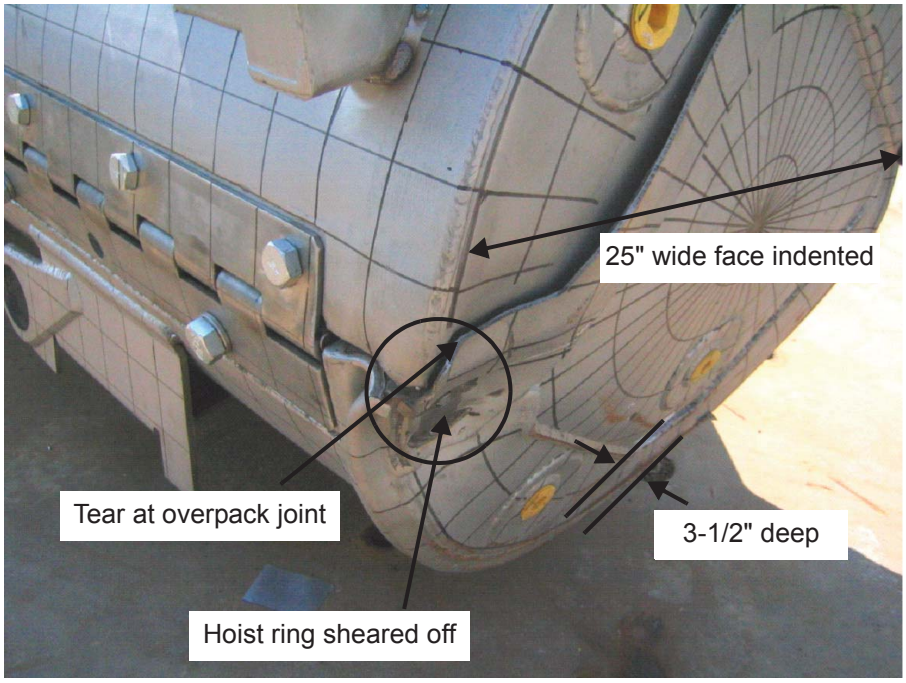

Figure 2-131 QTU-1 Outerpack After Test 1.2

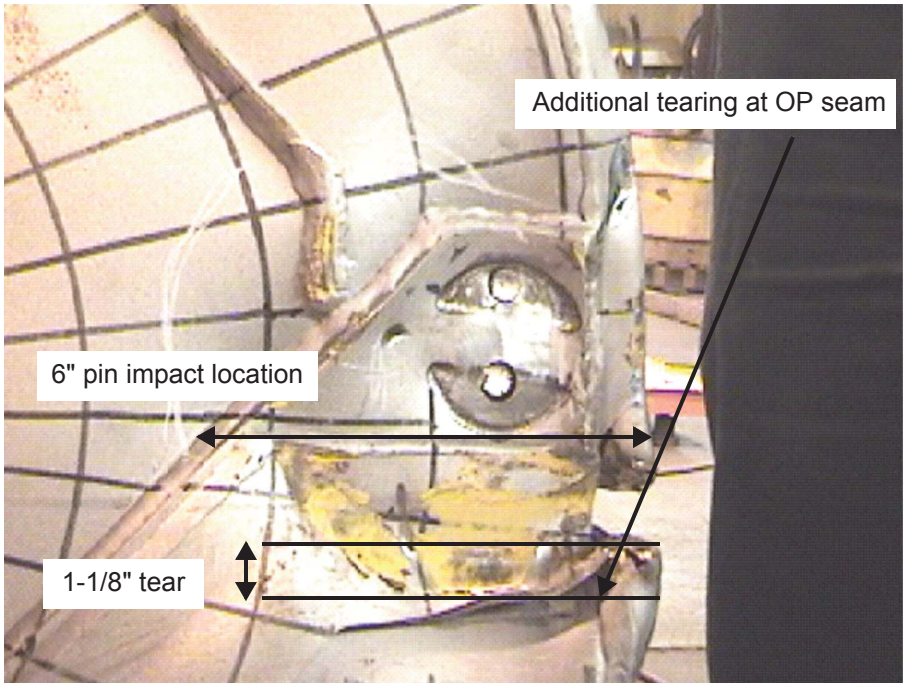

Figure 2-132 QTU-1 Outerpack After Test 1.3

QTU-1 was not opened until after the fire test. The Clamshell and fuel assembly were examined for damage at that time. The fuel assembly of QTU-1 was essentially undamaged, Figure 2-133. The most damage occurred at the top nozzle section where an area of approximately 2-3" in length increased from 8.375" nominal to 8.625". Grid 10 was torn, and all other grids were buckled but intact. The nozzles were essentially undamaged. The impact resulted in buckling of the core line-up pins attached to the top nozzle. The fuel rods appeared visibly undamaged.

The fuel assembly in QTU-1 was measured before the test and after the burn test at locations shown in Figure 2-134. Table 2-36 provides the pretest dimensions. Tables 2-37 and 2-38 provide the post test dimensions.

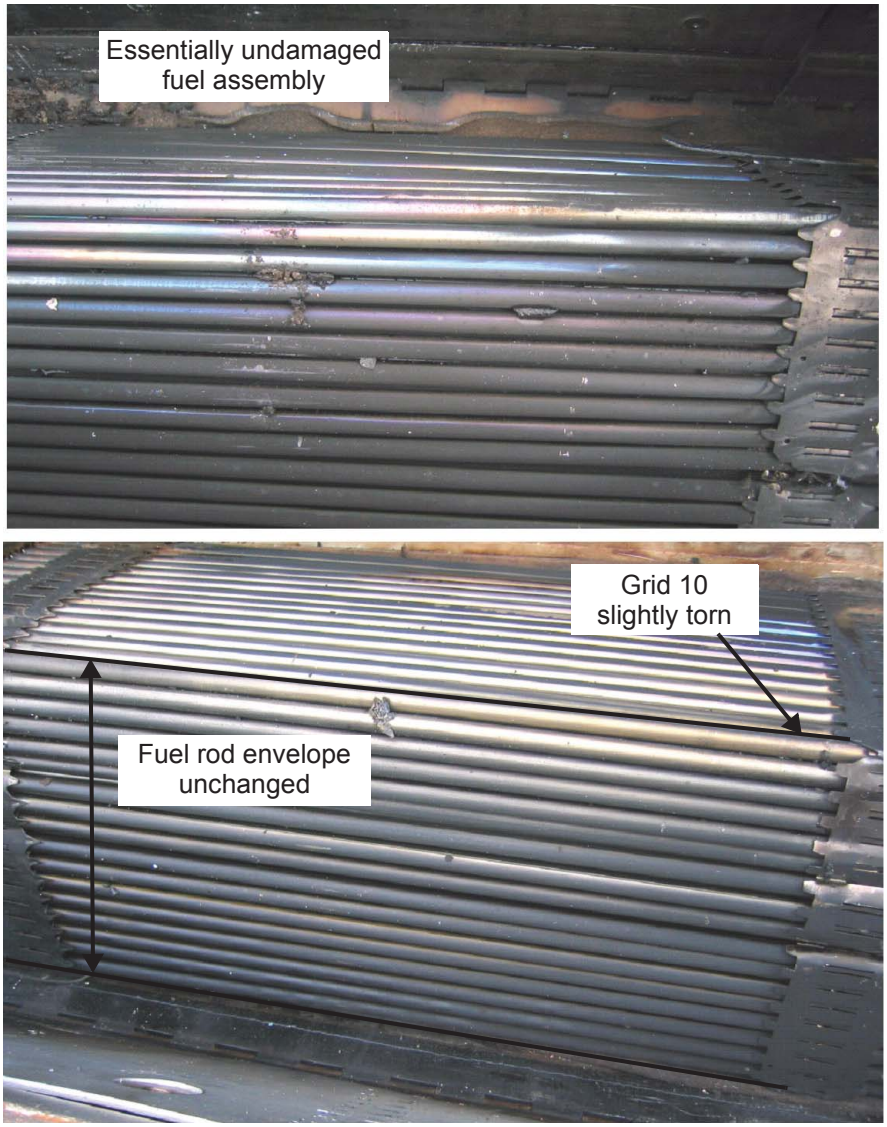

Figure 2-133 QTU-1 Fuel Assembly After Drop and Burn Tests

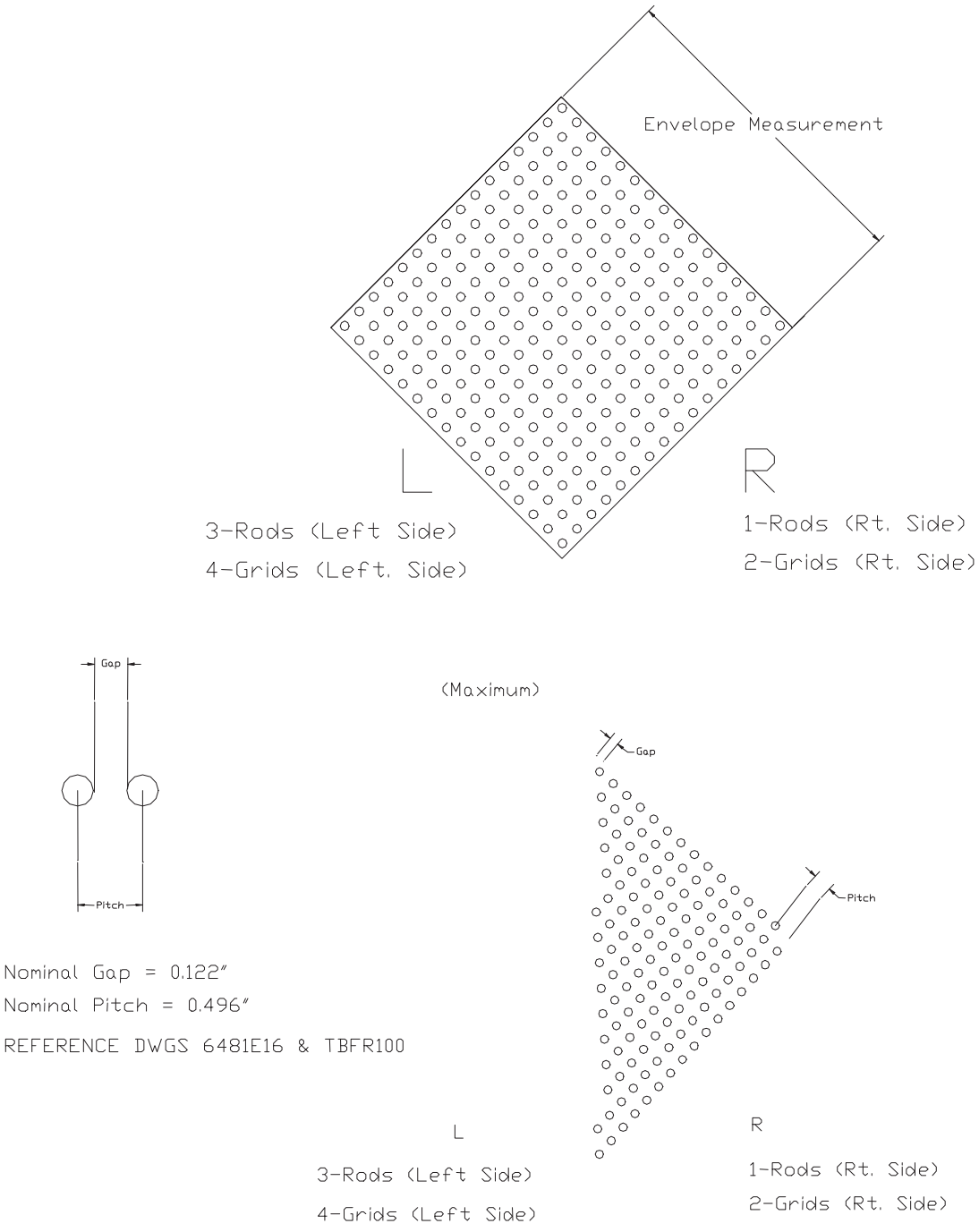

Figure 2-134 Measurements Made on QTU-1 Fuel Assemblies Before and After Drop Tests

Table 2-36 Key Dimensions of QTU-1 Fuel Assembly Before Testing

Fuel Assembly ID: 503007, B/N # 02-6703

F/A Location	Fuel Envelope (inches)	Gap (inches)	Pitch (inches)
B/N – Grid 1	1 – 8.330 2 – 8.455 3 – 8.250 4 – 8.446 8.375 Meas. Nominal*	L – 0.122 R – 0.123 0.125 Meas. Nominal*	L – 0.497 R – 0.498 0.500 Meas. Nominal*
Grid 1 – Grid 2	1 – 8.338 2 – 8.418 3 – 8.326 4 – 8.415 8.375 Meas. Nominal*	L – 0.124 R – 0.124 0.125 Meas. Nominal*	L – 0.499 R – 0.499 0.500 Meas. Nominal*
Grid 2 – Grid 3	8.375 Meas. Nominal*	L – 0.123 R – 0.120 0.125 Meas. Nominal*	L – 0.498 R – 0.495 0.500 Meas. Nominal*
Grid 3 – Grid 4	8.375 Meas. Nominal*	0.125 Meas. Nominal*	0.500 Meas. Nominal*
Grid 4 – Grid 5	8.375 Meas. Nominal*	0.125 Meas. Nominal*	0.500 Meas. Nominal*
Grid 5 – Grid 6	8.375 Meas. Nominal*	0.125 Meas. Nominal*	0.500 Meas. Nominal*
Grid 6 – Grid 7	8.375 Meas. Nominal*	0.125 Meas. Nominal*	0.500 Meas. Nominal*
Grid 8 –- Grid 9	8.375 Meas. Nominal*	0.125 Meas. Nominal*	0.500 Meas. Nominal*
Grid 9 – Grid 10	8.375 Meas. Nominal*	0.125 Meas. Nominal*	0.500 Meas. Nominal*
Grid 10 – T/N	8.375 Meas.Nominal*	0.125 Meas. Nominal*	0.500 Meas. Nominal*

Note:

* Measured nominal values were measured to nearest 1/8".

Table 2-37 QTU-1 Fuel Assembly Grid Envelope After Testing

Fuel Assembly Envelope Inspection Table

Location	Envelope Dimension, Inches		Maximum Fuel Rod Gap from Form 1F (Nominal Gap = 0.122")
	Left Side, LS	Right Side, RS	
Between B/N and Grid 1	8.125	8.250	0.250
Between Grids 1 and 2	8.125	8.000	0.250
Between Grids 2 and 3	8.000	8.250	0.188
Between Grids 3 and 4	8.375	8.375	0.125
Between Grids 4 and 5	8.375	8.375	0.125
Between Grids 5 and 6	8.375	8.375	0.188
Between Grids 6 and 7	8.375	8.375	0.188
Between Grids 7 and 8	8.375	8.375	0.188
Between Grids 8 and 9	8.375	8.375	0.188
Between Grids 9 and 10	8.375	8.500	0.250
Between Grid 10 and T/N	8.500	8.625	0.250
MAXIMUM VALUE	8.500	8.625	0.250

Table 2-38 QTU-1 Fuel Rod Pitch Data After Testing

Fuel Rod Pitch Inspection Table

Location	Maximum Gap, inches		Maximum Pitch
	Left Side, LS	Right Side, RS	
Between B/N Grid 1	0.250	0.188	0.625
Between Grids 1 and 2	0.250	0.250	0.625
Between Grids 2 and 3	0.188	0.188	0.563
Between Grids 3 and 4	0.125	0.125	0.500
Between Grids 4 and 5	0.125	0.125	0.500
Between Grids 5 and 6	0.125	0.188	0.563
Between Grids 6 and 7	0.125	0.188	0.563
Between Grids 7 and 8	0.188	0.188	0.563
Between Grids 8 and 9	0.188	0.188	0.563
Between Grids 9 and 10	0.125	0.250	0.625
Between Grid 10 and T/N	0.125	0.250	0.625
MAXIMUM VALUE	0.250	0.250	0.625

2.12.5.2.2 QTU Test Series 2

Test series 2 was conducted on the afternoon of September 11 and included a 50 inch (1.27 m) slap down, a 33.4 feet (10.18 m) free drop test, and a 42 inch (1.07 m) pin-puncture test. The test sequence and measured drop attitudes are summarized in Table 2-39 and shown in Figure 2-135. Weights for QTU-2 are recorded on Table 2-40.

Table 2-39 QTU Series 2 As-Tested Drop Conditions

Test Article ID	F/A Type	Test Sequence	Test Pitch Attitude	Test Roll Attitude	Design Feature Tested
QTU2	17x17 XL	P2.1) 1.2-m, NAC, Low angle(1)	10°	180°	Operations of hinges/doors
		P2.2) 9-m End (B/N)(1)	90°	0°	Lattice exp., FR axial position
		P2.3) 1-m Pin-puncture(1)	22°	0°	OP stiffness

Note:
(1) Actual test heights are reported in Figure 163 and post-test forms.

Table 2-40 QTU-2 Weights

Test Weights	Nominal	Actual
Weight of Outerpack (Empty):	3033 lb	**2611** lb
Weight of Clamshell (Empty):	425 lb	**400** lb
Weight of package (Empty) :	3477 lb	**3011** lb
Total package test weight:	5422 lb	**4778** lb

The Outerpack retained its basic circular pre-test shape except for localized plastic deformation accumulated from the 1.2 meter and 33.4 foot (10.18m) drop test. Damage zones from the drop test were localized to impact locations on the package end. The Outerpack did not separate after the impact, and no bolt failures on the Outerpack hinges were noted. From Figure 2-136, the 1.2 meter free drop resulted in a local crush zone at the top nozzle end measuring approximately 9-1/2" wide, 6" long axially and 7/8" deep. The Outerpack damage from the 33.4 foot drop, Figure 2-136 consisted of local crumple zone approximately 7" long maximum as demonstrated by the buckled Outerpack at the bottom nozzle end. A small weld tear was noted on each side of the Outerpack where the leg stand is connected to the end cap. The pin puncture damage was isolated to the impact point located at the package center-of-gravity. From As shown in Figure 2-138, pin puncture damage zone was an indented oval of measured dimensions 9" long by 6" wide and 2-7/8" deep.

The Clamshell was essentially undamaged from the drop test series, Figure 2-138. No change in the Clamshell grid markings were noted indicating that the Clamshell had not bulged outward (nor compressed). The polyethylene moderator blocks and aluminum neutron “poison plates” maintained position. The fuel assembly was found to be within the confines of the Clamshell and intact. The impact resulted in a slight ovalizing of the fuel assembly at the bottom nozzle region. Figure 2-139 shows the approximate angle of ovality is 118° at Grid 1 location. Localized expansion from 8.375" nominal to 8.625" was measured over a length of approximately 12" (30.48cm). The maximum fuel rod gap measured was 0.722 inches resulting in a maximum measured fuel rod pitch of 1.097 inches. The top nozzle portion of the tested fuel assembly was essentially undamaged. The axial position of fuel rods maintained location between bottom and top nozzles.

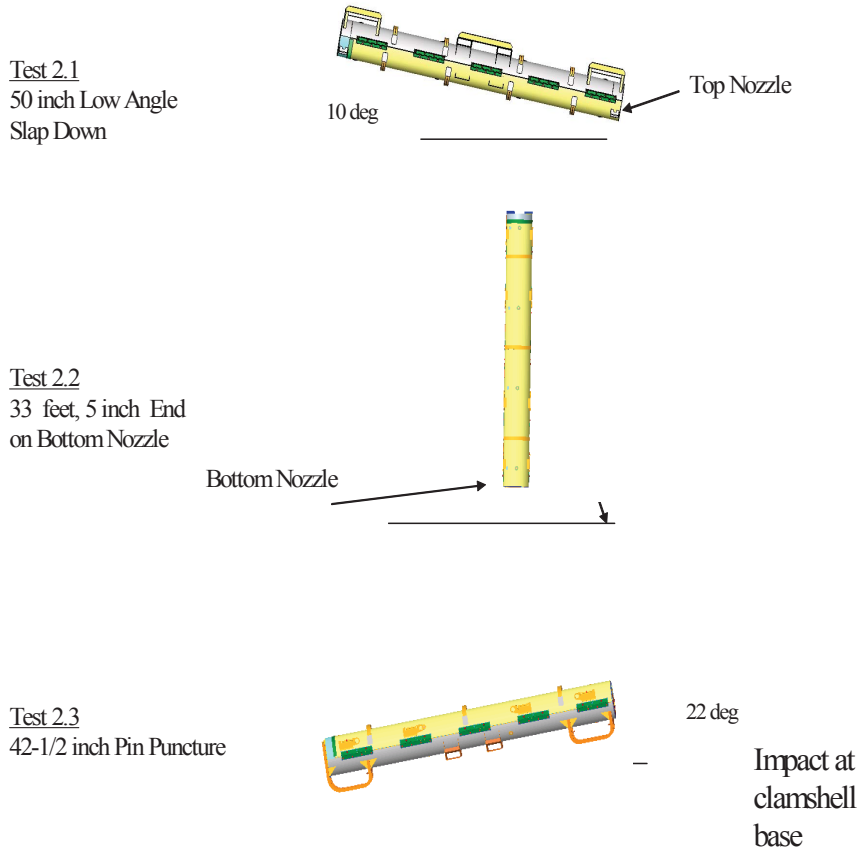

Figure 2-135 QTU Test Series 2 Drop Orientations

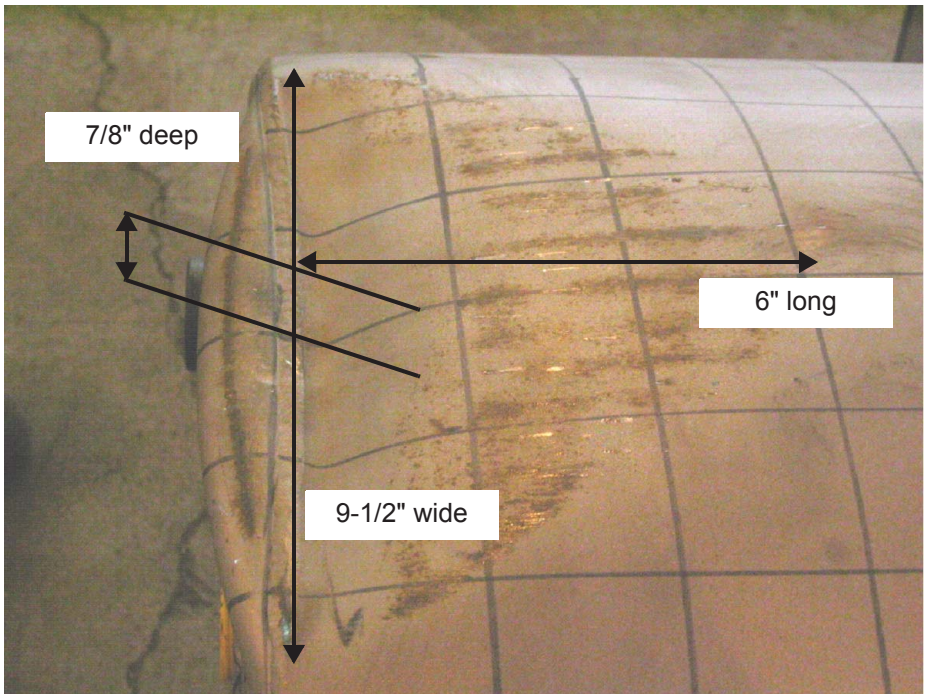

Figure 2-136 QTU Outerpack After Test 2.1

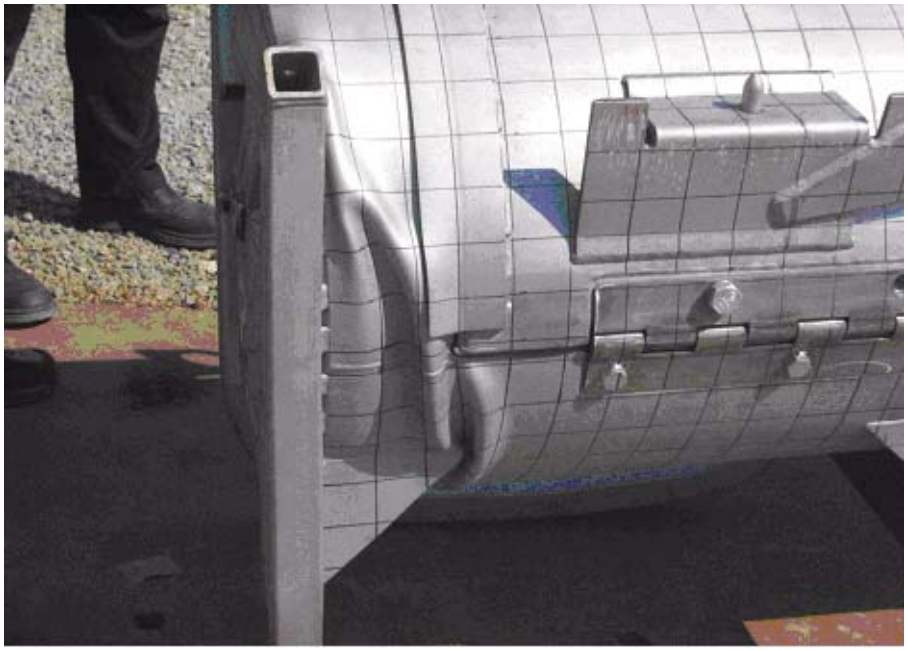

Figure 2-137 QTU Outerpack After Test 2.2

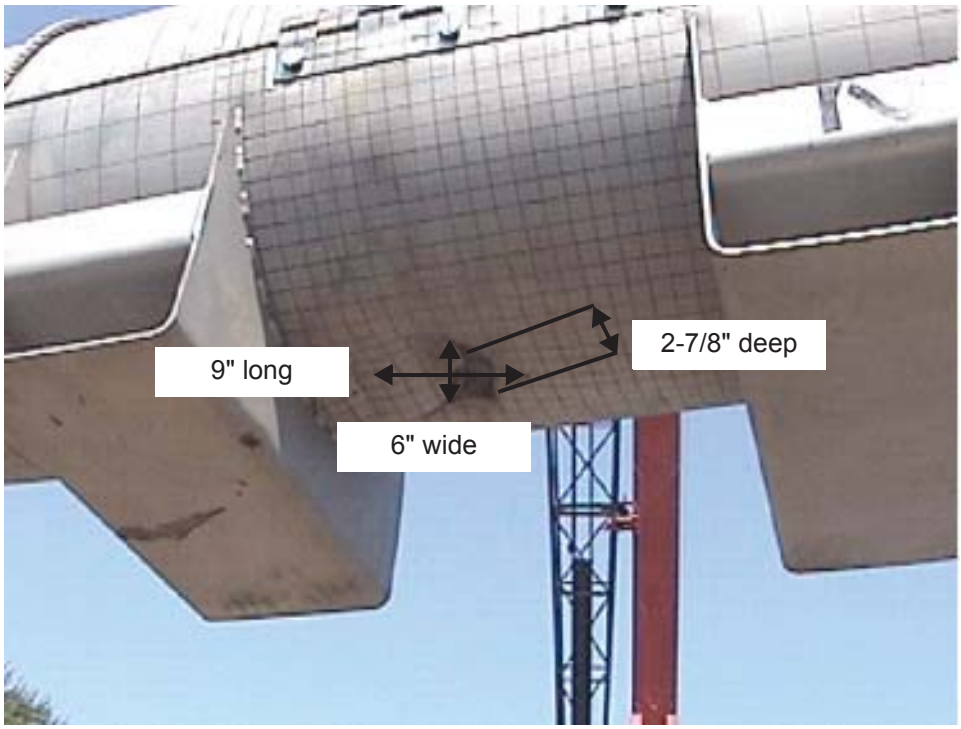

Figure 2-138 QTU Outerpack After Test 2.3

The fuel assembly in QTU-1 was measured before the test and after the burn test at locations shown in Figure 2-134 above. Table 2-41 provides the pretest dimensions. Tables 2-42 and 2-43 provide the post test dimensions.

The post-test inspections concluded that the tested configuration of the Traveller Outerpacks and Clamshells were acceptable. Furthermore, the tests concluded that Test Series 1 imparted the most damage to the Outerpack, and Test Series 2 imparted the most damage to the fuel assembly. Also, testing demonstrated that the Traveller Outerpack is suitable for transport with two top Outerpack bolts per hinge. The post-test geometry of the fuel assemblies for both test series was also acceptable.

In summary, testing demonstrated the Traveller package is suitable for compliance to normal and hypothetical mechanical drop test conditions described in 10 CFR 71 and TS-R-1.

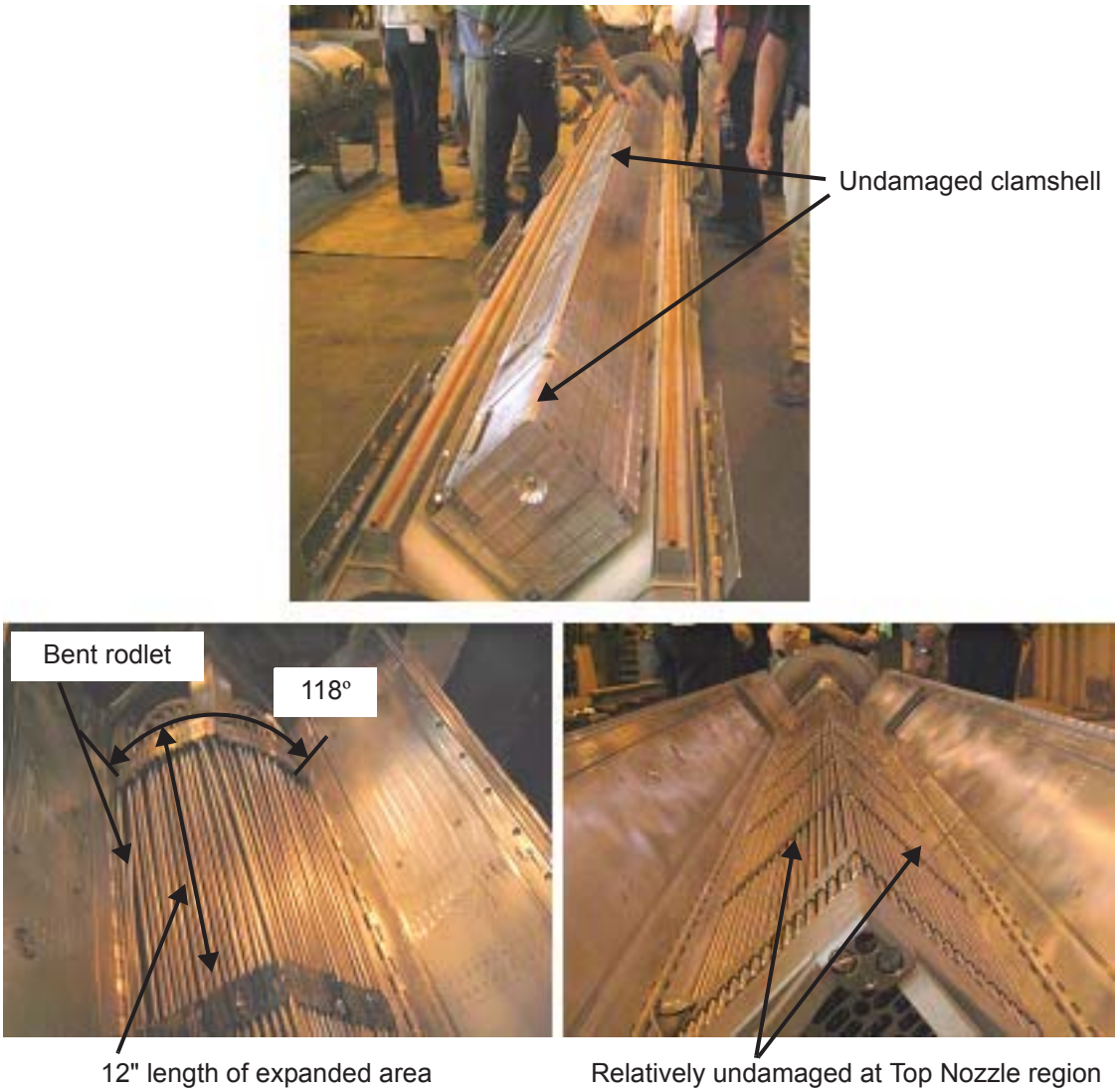

Figure 2-139 QTU-2 Clamshell and Fuel Assembly After Drop Tests

Table 2-41 Key Dimensions of QTU-2 Fuel Assembly Before Testing

Fuel Assembly ID: 503005, B/N # 97-2480Y

F/A Location	Fuel Envelope (inches)	Gap (inches)	Pitch (inches)
B/N – Grid 1	1 – 8.356 2 – 8.463 3 – 8.329 4 – 8.430 8.375 Meas. Nominal*	L – 0.124 R – 0.123 0.125 Meas. Nominal*	L – 0.499 R – 0.498 0.500 Meas. Nominal*
Grid 1 – Grid 2	1 – 8.325 2 – 8.415 3 – 8.319 4 – 8.420 8.375 Meas. Nominal*	L – 0.121 R – 0.123 0.125 Meas. Nominal*	L – 0.496 R – 0.498 0.500 Meas. Nominal*
Grid 2 – Grid 3	1 – 8.333 2 – 8.410 3 – 8.329 4 – 8.411 8.375 Meas. Nominal*	L – 0.121 R – 0.123 0.125 Meas. Nominal*	L – 0.496 R – 0.498 0.500 Meas. Nominal*
Grid 3 – Grid 4	1 – 8.311 2 – 8.435 3 – 8.310 4 – 8.24 8.375 Meas. Nominal*	L – 0.124 R – 0.123 0.125 Meas. Nominal*	L – 0.499 R – 0.498 0.500 Meas. Nominal*
Grid 4 – Grid 5	8.375 Meas. Nominal*	0.125 Meas. Nominal*	0.500 Meas. Nominal*
Grid 5 – Grid 6	8.375 Meas. Nominal*	0.125 Meas. Nominal*	0.500 Meas. Nominal*
Grid 6 – Grid 7	8.375 Meas. Nominal*	0.125 Meas. Nominal*	0.500 Meas. Nominal*
Grid 8 – Grid 9	8.375 Meas. Nominal*	0.125 Meas. Nominal*	0.500 Meas. Nominal*
Grid 9 – Grid 10	8.375 Meas. Nominal*	0.125 Meas. Nominal*	0.500 Meas. Nominal*
Grid 10 – T/N	8.375 Meas. Nominal*	0.125 Meas. Nominal*	0.500 Meas. Nominal*

Note:
* Measured nominal values were measured to nearest 1/8".

Table 2-42 QTU-2 Fuel Assembly Grid Envelope After Testing

Fuel Assembly Envelope Inspection Table

Location	Envelope Dimension, Inches		Maximum Fuel Rod Gap from Form 2F (Nominal Gap = 0.122")
	Left Side, LS	Right Side, RS	
Between B/N and Grid 1	8.625	8.500	0.722
Between Grids 1 and 2	8.000	7.938	0.539
Between Grids 2 and 3	7.938	7.688	0.316
Between Grids 3 and 4	7.813	7.625	0.137
Between Grids 4 and 5	8.063	7.875	0.153
Between Grids 5 and 6	8.250	8.250	0.143
Between Grids 6 and 7	8.375	8.375	0.146
Between Grids 7 and 8	8.375	8.375	0.141
Between Grids 8 and 9	8.375	8.375	0.162
Between Grids 9 and 10	8.375	8.375	0.141
Between Grid 10 and T/N	8.438	8.438	0.127
MAXIMUM VALUE	8.625	8.500	0.722

Table 2-43 QTU-2 Fuel Rod Pitch Data After Testing

Fuel Rod Pitch Inspection Table

Location	Maximum Gap, inches		Maximum Pitch, inches
	Left Side, LS	Right Side, RS	
Between B/N and Grid 1	0.722	0.501	1.097
Between Grids 1 and 2	0.539	0.501	0.914
Between Grids 2 and 3	0.250	0.316	0.691
Between Grids 3 and 4	0.137	0.125	0.512
Between Grids 4 and 5	0.153	0.132	0.528
Between Grids 5 and 6	0.142	0.143	0.518
Between Grids 6 and 7	0.145	0.146	0.521
Between Grids 7 and 8	0.141	0.138	0.516
Between Grids 8 and 9	0.162	0.122	0.537
Between Grids 9 and 10	0.139	0.141	0.516
Between Grid 10 and T/N	0.127	0.123	0.502
MAXIMUM VALUE	0.722	0.501	1.097

2.12.5.3 Certification Test Unit Drop Tests

A Traveller XL package was fabricated by Columbiana High Tech to serve as the certification test unit (CTU), Figures 2-140 and 2-141 and Table 2-44. This unit was subjected to a regulatory drop test performed February 5, 2004 in Columbiana, Ohio. The test included a 50 inch (1.27 m) slap down, a 32.8 feet (10.0 m) free drop test impacting the bottom nozzle, and a 42 inch (1.07 m) pin-puncture test, Figure 2-142 and Table 2-45. The CTU package was thermally saturated for approximately 15 hours prior to testing at a temperature of about 17ºF (-8.3ºC). At the time of testing the temperature was approximately 24ºF (-4.4ºC). The package's test weight was 4863 pounds.

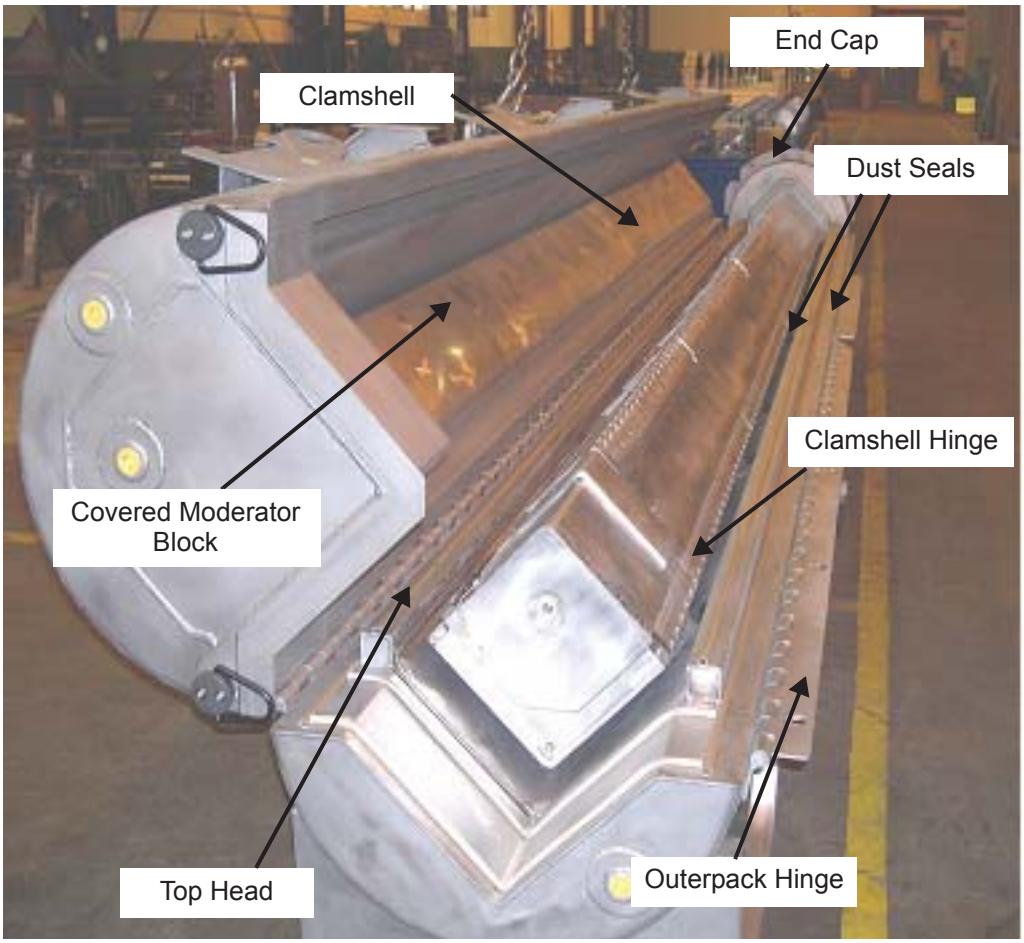

Figure 2-140 Traveller CTU Test Article Internal View

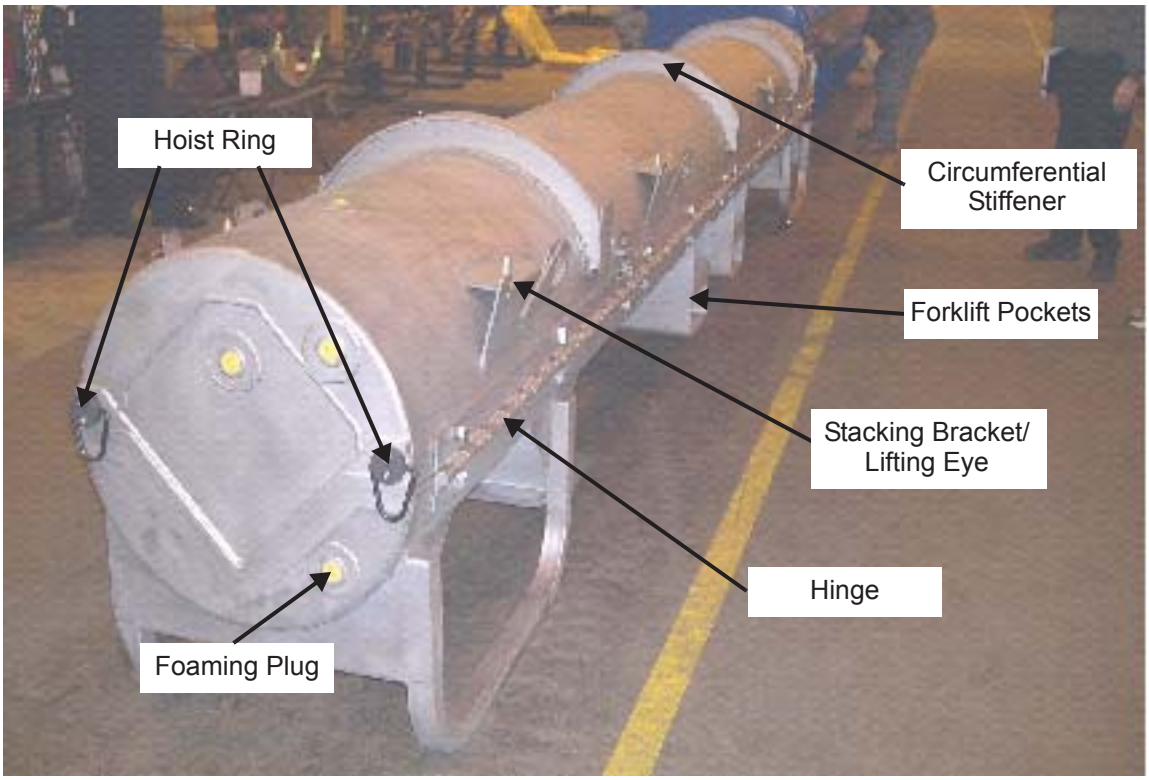

Figure 2-141 Traveller CTU External View

Table 2-44 Test Weights

	Nominal* Wt	Actual Wt
Weight of Outerpack (Empty):	2633 lb	2671 lb
Weight of Clamshell (Empty):	425 lb	440 lb
Weight of package (Empty) :	3058 lb	3111 lb
Total package test weight:	4810 lb	4863 lb

Note:
* Nominal total weight includes only Fuel Assembly since drop test was conducted without RCCA. Maximum expected design weight is estimated to be 5071 pounds (Ref. 3). The top Outerpack section weight is 1063 pounds empty and the bottom Outerpack section weight is 1608 pounds empty.

Exterior Inspections After Drop Tests – The exterior of the package was examined after each drop. The inspections found that the Outerpack retained its circular pre-test shape except for localized plastic deformation at the ends. No hinge bolts failed on the Outerpack, the Outerpack did not separate, and neither the inner nor outer shell were perforated in the pin drop test.

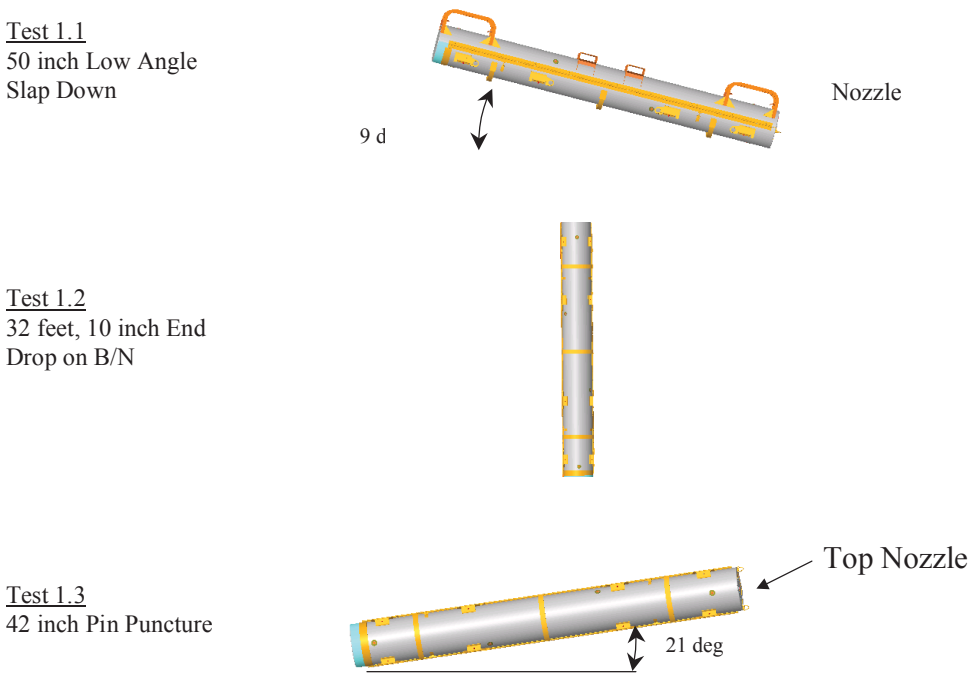

Figure 2-142 CTU Drop Test Orientations

Table 2-45 CTU Drop Test Orientations

Test Article ID	F/A Type	Test Sequence	Test Pitch Attitude	Test Roll Attitude	Design Feature Tested
CTU	17x17 XL	P1.1) 1.2-m, NCT, Low angle[1]	9°	180°	Operations of hinges/doors
		P1.2) 9-m End Drop[1]	90°	0°	Lattice exp., FR axial position
		P1.3) 1-m Pin-puncture[1]	21°	90°	Hinge structural integrity

Test 1 – The 1.2 meter drop test resulted in a localized dent at the top nozzle end, and near the bottom nozzle end, the stiffener was dented over a length of about 8". Figures 2-143 and 2-144 shows the damage observed. The normal condition drop produced only local damage to the impact area. The depth of the crush was minimal.

Test 2 – The 9m (32.8-foot) free drop resulted in localized damage to the bottom nozzle end region. The two bottom nozzle stiffener keeper pins were detached as a result of the impact. The impact created a circumferential ripple located at 9" (bottom Outerpack) and 12" (top Outerpack) from the package bottom

end. The ripple resulted in a 1/2" crumple impact, which effectively shortened that section of the package slightly. Two stitch welds located inside the bottom nozzle end stiffener were broken, but this did not compromise the stiffener position. The bottom nozzle end cap stiffener separated to form a 1-3/16" gap, and the gap between the hinge and the cover lip was measured to be approximately 7/16". The hinge at the bottom nozzle end was separated about 1/16" from the Outerpack skin surface after the drop test. Figures 2-145 – 2-147 shows the damage observed.

Test 3 – The pin puncture test was located on the hinge of the Outerpack at approximately the axial center of gravity. The impact zone locally dented 6" of hinge length to a maximum measured depth of approximately 1-3/8", Figure 2-148. The hinge knuckles were not compromised as a result of the test. Hinge separation of 1/2" was noted about 7-1/2" from the impact point towards the top nozzle end.

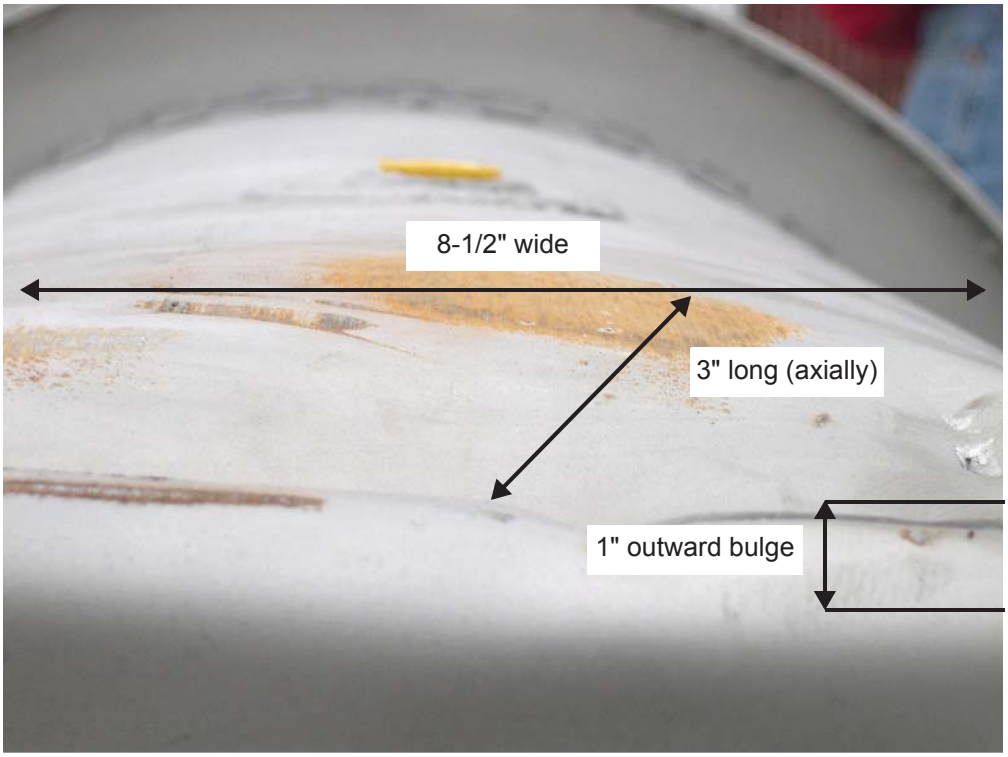

Figure 2-143 Top Nozzle End Outerpack Impact Damage

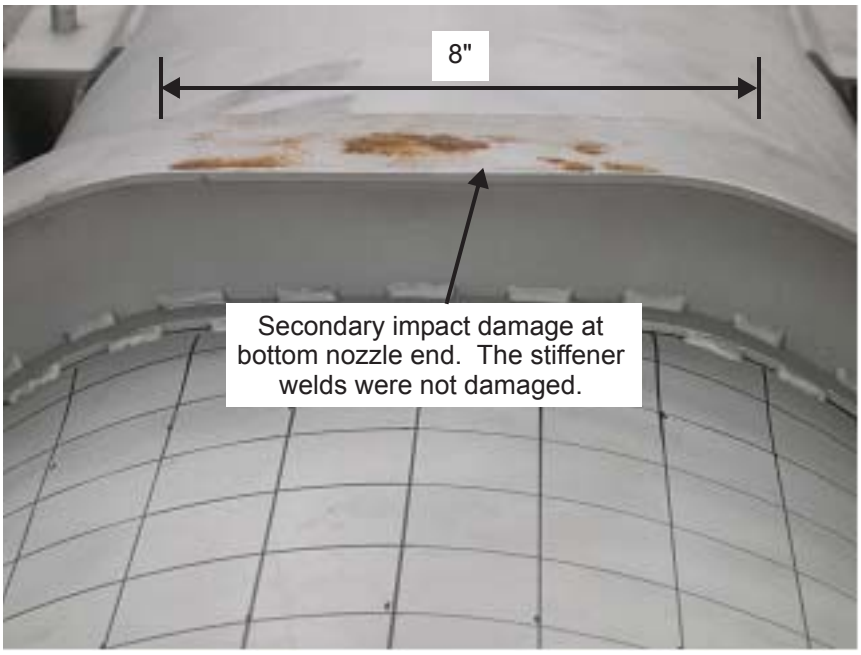

Figure 2-144 CTU Outerpack Stiffener After Test 1

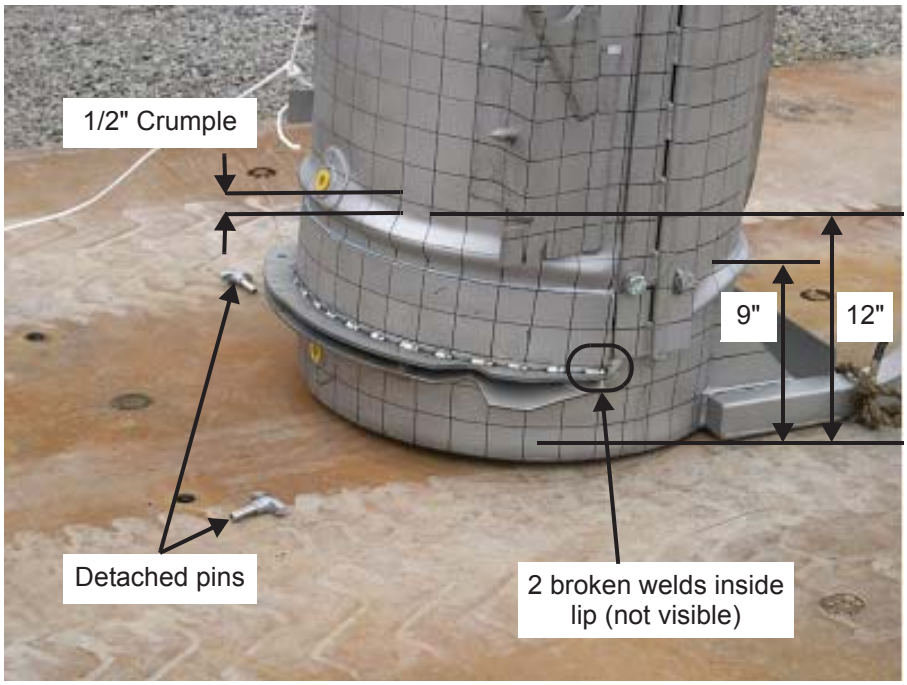

Figure 2-145 CTU Outerpack After Test 2

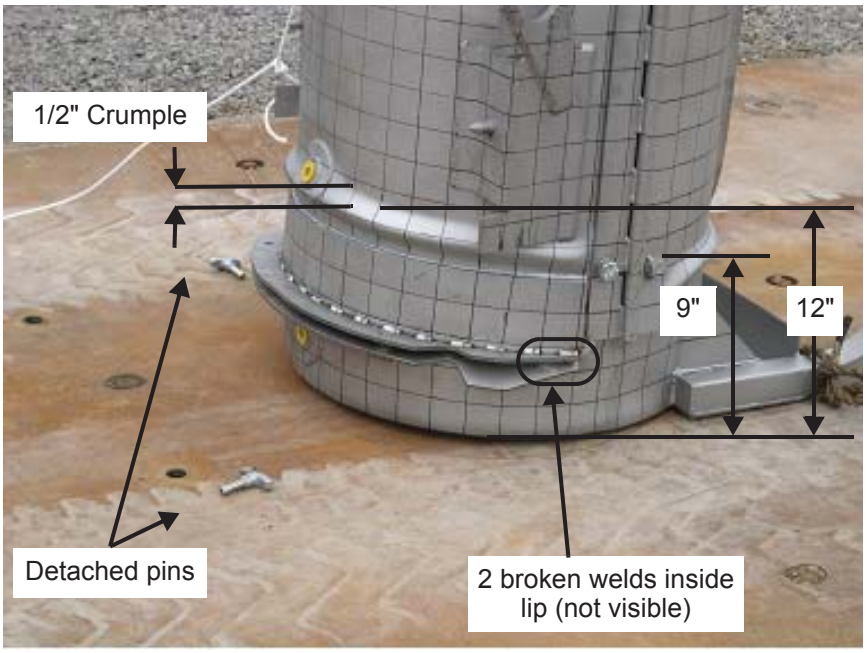

Figure 2-146 CTU Outerpack After Test 2

Figure 2-147 Hinge Separation at Bottom Nozzle End From Test 2

Figure 2-148 CTU Outerpack After Test 3

Interior Inspection Results – The CTU was sent to the South Carolina Fire Academy for the burn test immediately after the drop tests were completed. The package was not opened until the following week, approximately five hours after the fire test was completed. In general, the drop test and fire test resulted in minor damage to the Traveller internal structural components. The Clamshell was found intact and closed, Figure 2-149, and the simulated poison plates maintained position. All shock mounts were found to be visibly intact. At the bottom Clamshell plate, a 2-1/2" and a 2-3/4" piece of end lip sheared off. The measured gap was less than 1/16" and in the axial direction. The axial location of the fuel rods maintained position between the bottom and top nozzle. Finally, the moderator blocks were found to be intact and essentially undamaged after the completion of the drop and fire test. The moderator stud bolts on the top Outerpack were found sheared off, but the moderator cover maintained the moderator position. The stainless steel moderator cover was removed and the polyethylene moderator was examined. As shown in Figure 2-150, the moderator was intact and essentially undamaged.

Figure 2-151 provides the damage sketch overlaying the pre-tested fuel assembly for comparative purposes. For the 20" span from the bottom nozzle to Grid 2 of the fuel assembly, the fuel rod envelope expanded from 8-3/8" average nominal to 9-3/16". The grid envelope expanded from 8-7/16" nominal to 8-5/8" over the same 20" axial distance. The maximum measured fuel rod pitch in this region increased from 0.496" nominal to 0.990". This was caused by a single bent rod which was bent outward approximately 1/2". Otherwise, the typical pitch pattern consisted of 2 rod rows touching and the remaining 14 rows at nominal pitch, Figure 2-152.

Figure 2-149 CTU Clamshell After Drop and Fire Tests

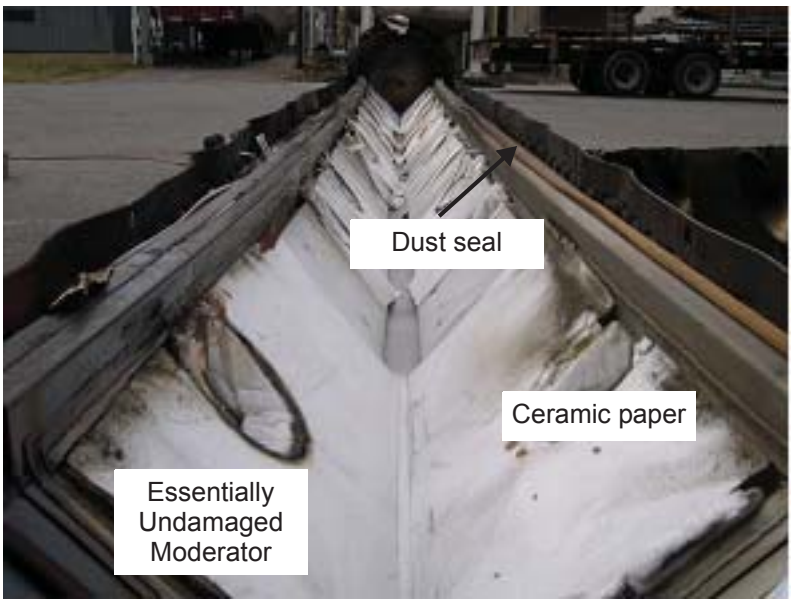

Figure 2-150 Outerpack Lid Moderator After Testing

For a length of 10" above Grid 2, the fuel rod envelope compressed from 8-3/8" nominal to 8-1/4". This slight compression is due to the single top rod slightly compressed inward. Above this 10" region, the single rod bent outward about 1/2" for a length of approximately 25".

For the 25" length from between Grids 2 and 3 and up to Grid 4, the single rod resulted in a measured envelope of 8-7/8", but the remaining envelope of 16 rows was slightly compressed (about 1/16"). The maximum pitch caused by the single rod was 0.740" compared to 0.496" nominal. Otherwise, the average pitch was nominal.

For the remainder of the fuel assembly from Grid 4 to the top nozzle, the fuel rod envelope compressed about 0.15" and the grid envelope compressed about 1/4". The average pitch decreased from 0.496" to 0.459" in this region.

Grid 1 was severely buckled, and the ovality was measured to be 120º for a length of about 20", Figure 2-153. Grids 2 and 3 were broken at the top corner, but otherwise intact. Grids 4-10 were relatively undamaged. The fuel inspection also indicated that 7.5% (20 of 265 rods) were cracked at the end plug locations (Figure 2-154). The average crack width measured was approximately 0.030" (30 mils) and the average length was 50% of the rod diameter. The cracked rods were located at the four corners, indicating the vertical impact created symmetrical impact forces to be transmitted through the bottom nozzle and fuel rods (Figure 2-155).

The fuel assembly in QTU-1 was measured before the test and after the burn test at locations shown in Figure 2-134 above. Table 2-46 provides the pretest dimensions. Tables 2-47 through 2-50 provide the post test dimensions.

2.12.5.4 Application to Higher Contents Weights

As discussed in section 2.12.3.2, the vertical drops on the bottom nozzle end of the package were determined to be the most damaging to the fuel assembly. Therefore, vertical drops were performed in the last two drop tests series, QTU-2 and CTU. This provided the maximum challenge to the fuel assembly and the clamshell heads. The tests were performed with lead filled fuel assemblies that did not incorporate rod cluster control assemblies (RCCA) or other internals. This was done because the RCCA, although adding weight, would increase the rigidity of the fuel assembly. This increased rigidity would decrease the forces on the clamshell walls. Additionally, when the fuel assembly is shipped with an RCCA, an additional axial restraint is provided to secure the total payload.

The two vertical drop tests are summarized below:

QTU-2 – 9 m drop test

Outerpack wt.	2611 lbs
Clamshell wt.	400 lbs
FA wt.	1767 lbs

Total wt.	4778 lbs
Drop ht	33.4 ft (10.2 m)

CTU – 9 m drop test

Outerpack wt.	2671 lbs
Clamshell wt.	440 lbs
FA wt.	1752 lbs
Total wt.	4863 lb
Drop ht	32.8 ft (10.0 m)

Drop heights greater than 9 m were used to bound maximum possible weights and other uncertainties. Because potential energy is directly proportional to drop height the bounding weights for each test result as:

QTU-2 at 9 meters

FA wt.	2000 lb
FA & Clamshell wt.	2453 lb
Total package wt.	5409 lb

CTU at 9 m

FA wt.	1947 lb
FA & Clamshell wt.	2433 lb
Total package wt.	5398 lb

During the vertical drop, the fuel assembly remains stationary with respect to the clamshell until the clamshell hits the outerpack impact limiter and begins to decelerate. When the outerpack hits the ground, it quickly decelerates as the foam and outerpack metal skin absorb the outerpack kinetic energy. As shown Figures 2-136 and 2-137, the amount of deformation to the outerpack was very small with a total crush of the outside of the bottom impact limiter < 0.5 inches (averaged).

The dynamic characteristics of the actual test performed with QTU-2 from 10.2 m are slightly different than a 9.0 m drop of a heavier package (and heavier fuel assembly), as described below. The terminal velocity of the test was approximately 14.2 m/s instead of the 13.3 m/s from a 9.0 meter drop. This will result in slightly different impact times between the clamshell and outerpack. The magnitude of this difference can be estimated with the following assumptions:

- Although the outerpack impact limiter has a total crush of approximately 0.5 inches (0.013 m) before the clamshell impact, the interior dimensions of the outerpack remain essentially the same as before impact.

- Initial separation distance between the clamshell and outerpack interior of 4.0 inches (0.102 m)

- There are no interaction between the clamshell/fuel assembly and the outerpack occurs until the clamshell hits the inside of the outerpack.

The actual QTU-2 drop was performed with a gross weight of 4778 lbs (2167 kg) from a 10.2 meter height. This is compared with a second theoretical Traveller drop test with a gross weight of 5409 lbs (2452 kg) from a 9.0 meter height. The outerpack cavity on QTU-2 was approximately eight inches longer than clamshell inside that cavity.

In the actual QTU-2 drop, the Traveller was falling at 14.2 m/s when the outerpack hits the ground. Assuming the clamshell was in its nominal position, it would continue to fall over a distance of four inches (0.102 m) before it hits the inside of the outerpack impact limiter. It takes the clamshell approximately 7.2 milliseconds for the clamshell to hit the inside of the outerpack after the outerpack comes to rest. This is calculated by:

$$0.102 = 14.15\ t + 0.5\ 9.81\ t^2$$

In the theoretical Traveller drop, the clamshell package velocity at the time of outerpack impact is 13.2 m/s. If the clamshell is in the nominal position within the outerpack cavity, it will take approximately 7.7 milliseconds for the clamshell to hit the inside of the outerpack after the outerpack comes to rest. This is calculated by:

$$0.102 = 13.29\ t + 0.5 \times 9.81\ t^2$$

This results in a time difference between the two scenarios of 0.5 milliseconds. If the clamshell is located the maximum distance from the bottom impact limiter (8 inches or 0.204 m) the time to hit the impact limiter increases to 14.5 milliseconds and 15.3 milliseconds for the actual and theoretical drops respectively. In this case, there is a time difference of 0.8 milliseconds.

This simplified analysis does not include the deformation of the outerpack and the resulting deceleration profile which is not instantaneous. The FEA model provides a reasonable estimation of these deformations and predicts that the clamshell will hit the interior of the outerpack 15 milliseconds after the outerpack touches the ground (section 2.12.3.2.5). Because a small portion of the outerpack deformation is elastic, the outerpack probably rebounds slightly. The rebound was not observed in the tests but the FEA model does predict it to occur approximately 25 milliseconds after the outerpack impact.

The analysis above does show, however, the relative magnitude of the two different situations. The time difference between the actual drop and theoretical drop described above is only 0.5 to 0.8 milliseconds. This difference will not cause the clamshell to hit during the outerpack rebound (approximately 10 milliseconds

after clamshell contact) and the actual positions and velocities of the Traveller components will not be significantly different between the two drop scenarios.

The comparison above was made for the QTU-2 test. The general observations are applicable to the CTU tests however As a result, the QTU-2 and CTU test drops justify payload weights significantly higher than the 1767 and 1752 lb fuel assemblies actually used in the testing.

2.12.5.5 Conclusions

Three series of drop tests were performed during the development and certification of the Traveller shipping package. This included two prototype units, two qualification test units and one certification test unit. Design improvements were made at each step based on the results of the drop tests and subsequent fire tests. The drop test series included a regulatory normal free drop of 1.2 meters, a 9-meter end drop onto the bottom nozzle, and a 1-meter pin-puncture test on the hinge. Minor structural Outerpack damage indicated that the Traveller Outerpack design satisfied the hypothetical accident condition defined in 10 CFR 71 and TS-R-1. Furthermore, the Clamshell was found to meet the acceptance criteria of the test by maintaining closure and its pre-test shape. The post-test geometry of the fuel assembly was determined to meet the acceptance criteria since only local expansion was noted in the lower 20" of the bottom nozzle region and the cracked rod gaps were all measured less than a pellet diameter.

In summary, testing demonstrated the Traveller package is suitable for compliance to normal and hypothetical mechanical drop test conditions described in 10 CFR 71 and TS-R-1.

This page intentionally blank.

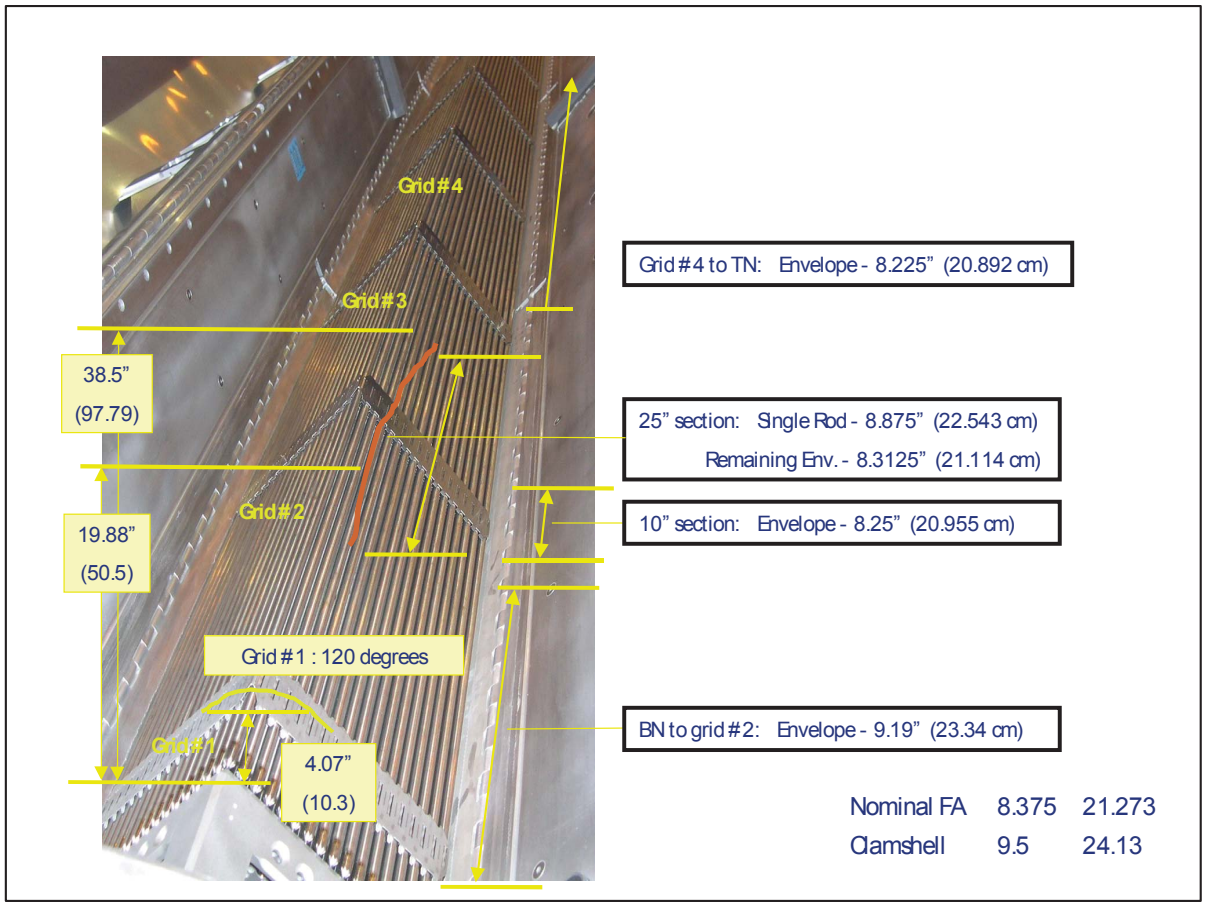

Figure 2-151 Fuel Assembly Damage Sketch and Pre-test Assembly

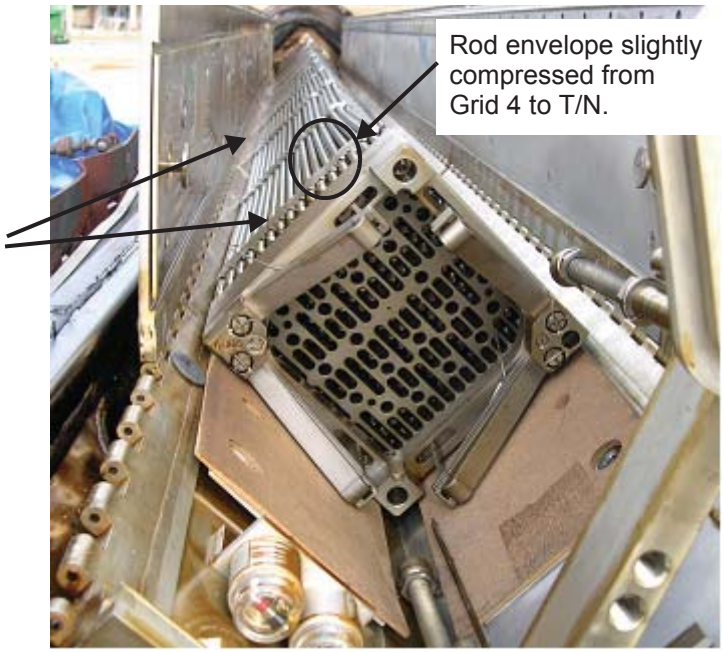

Figure 2-152 CTU Fuel Assembly After Testing

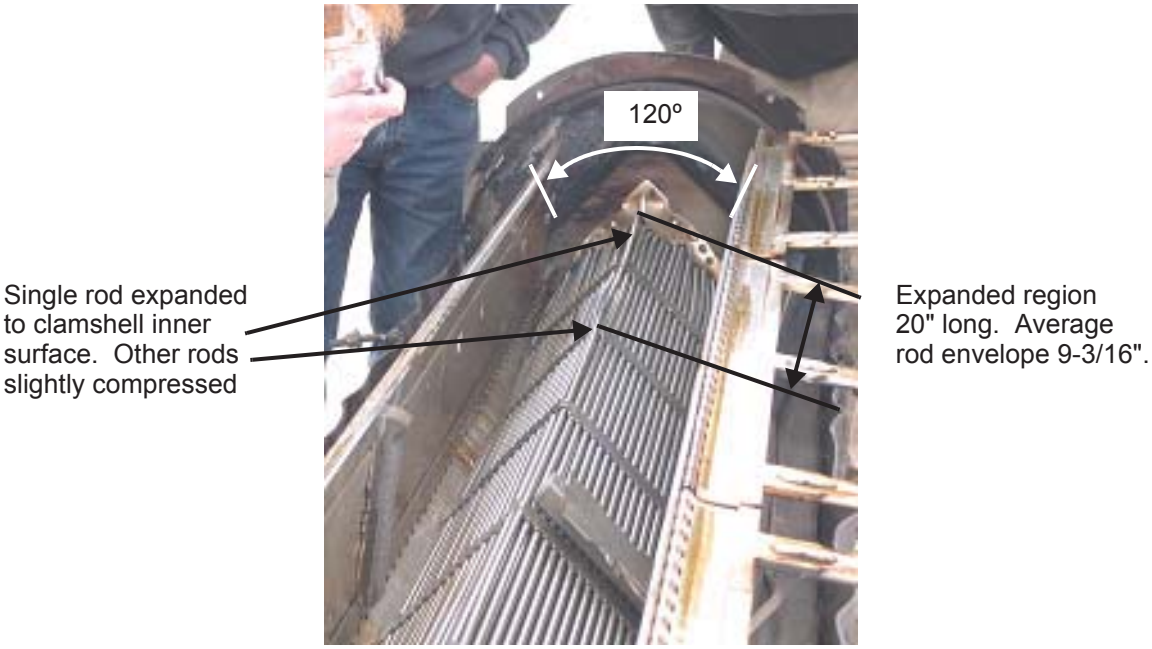

Figure 2-153 CTU Fuel Assembly Top End After Testing

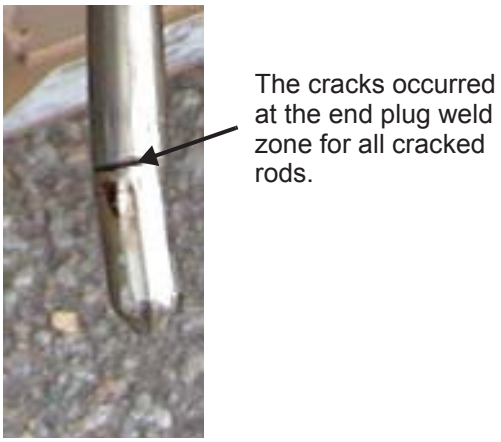

Figure 2-154 Cracked Rod From CTU Fuel Assembly

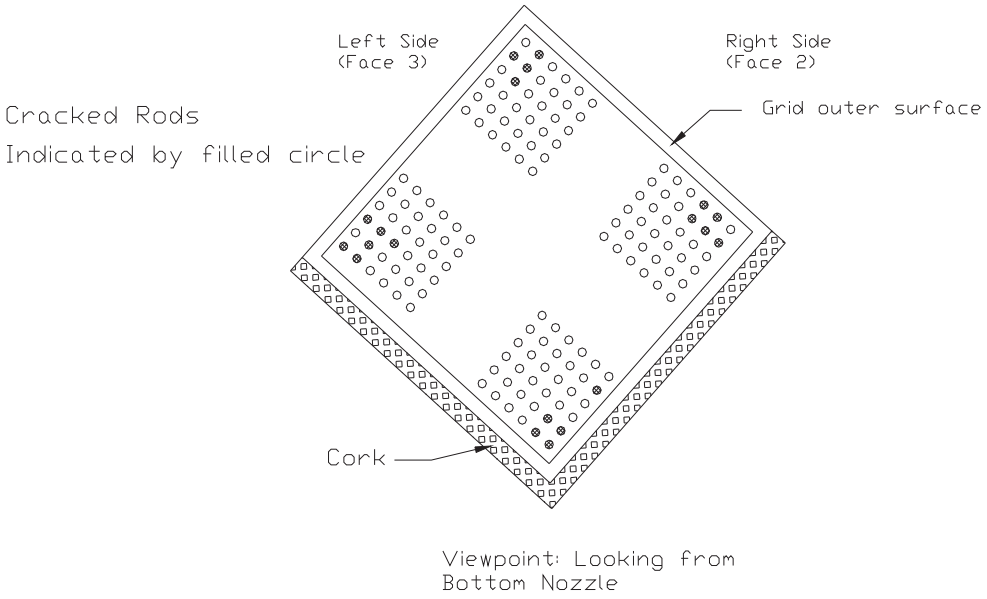

Figure 2-155 Cracked Rod Locations on CTU Fuel Assembly

Table 2-46 Fuel Assembly Key Dimension Before Drop Test

Fuel Assembly ID: T/N # LM1F2N

F/A Location	Fuel Envelope (inches)	Gap (inches)	Pitch (inches)
B/N – Grid 1	1: 8-3/8 2: 8-7/16 3: 8-3/8 4: 8-7/16	L – 0.123 R – 0.121	L – 0.498 R – 0.495
Grid 1- Grid 2	1: 8-3/8 2: 8-7/16 3: 8-3/8 4: 8-7/16	L – 0.123 R – 0.124	L – 0.497 R – 0.499
Grid 2- Grid 3	1: 8-3/8 2: 8-7/16 3: 8-3/8 4: 8-7/16	L – 0.121 R – 0.121	L – 0.495 R – 0.495
Grid 3- Grid 4	1: 8-3/8 2: 8-7/16 3: 8-3/8 4: 8-7/16	L – 0.123 R – 0.123	L – 0.497 R – 0.498
Grid 4- Grid 5	Rods: 8-3/8 Grids: 8-7/16	0.121	0.495
Grid 5- Grid 6	Rods: 8-3/8 Grids: 8-7/16	0.123	0.498
Grid 6- Grid 7	Rods: 8-3/8 Grids: 8-7/16	0.122	0.497
Grid 7- Grid 8	Rods: 8-3/8 Grids: 8-7/16	0.123	0.497
Grid 8- Grid 9	Rods: 8-3/8 Grids: 8-7/16	0.123	0.498
Grid 9- Grid 10	Rods: 8-3/8 Grids: 8-7/16	0.121	0.495
Grid 10 – T/N	Rods: 8-3/8 Grids: 8-7/16	0.122	0.497
AVERAGE	Rods: 8-3/8 Grids: 8-7/16:	0.122	0.497

Note:
* Measured fractional values were measured to nearest 1/16". Measured decimal values were measured to the nearest 0.001".

Table 2-47 CTU Fuel Assembly Grid Envelop Dimensions After Testing

Location	Measured Grid Envelope Dimension, Inches	
	Left Side, LS	Right Side, RS
Grid 1	9-0	8-3/4
Grid 2	8-7/16	8-3/8
Grid 3	9-1/2	9-1/2
Grid 4	8-1/8	8-1/4
Grid 5	8-1/8	8-1/4
Grid 6	8-1/4	8-1/4
Grid 7	8-1/8	8-3/16
Grid 8	8-5/16	8-3/16
Grid 9	8-5/16	7-7/8
Grid 10	8-3/8	8-1/2
MAXIMUM VALUE	9-1/2	9-1/2

Table 2-48 CTU Fuel Assembly Rod Envelope Data After Testing

Fuel Assembly Rod Envelope Inspection Table

Location	Measured Envelope Dimension, In.		Calculated Maximum Fuel Rod Pitch from Form 1G (Nominal Pitch = 0.496")
	Left Side, LS	Right Side, RS	
Between B/N and Grid 1	9-0	8-3/4	0.566
Between Grids 1 and 2	8-5/16 (1)	8-5/16 (1)	0.990
Between Grids 2 and 3	8-1/2	8.-0	0.740
Between Grids 3 and 4	8-7/16	8-1/2	0.715
Between Grids 4 and 5	8-3/16	8-3/16	0.472
Between Grids 5 and 6	8-3/16	8-3/8	0.578
Between Grids 6 and 7	8-1/16	8-1/16	0.550
Between Grids 7 and 8	8-3/8	8-3/16	0.541
Between Grids 8 and 9	8-0	7-13/16	0.483
Between Grids 9 and 10	8-3/8	8-1/2	0.498
Between Grid 10 and T/N	8-3/8	8-0	0.497
MAXIMUM VALUE	9-0	8-3/4	0.990

Note:
(1) A single rod was measured to the inner Clamshell surface (9-1/2"). See Figure 2-153.

Table 2-49 CTU Fuel Assembly Rod Envelope After Testing

Fuel Assembly Rod Envelope Inspection Table

Location	Measured Envelope Dimension, In.		Calculated Maximum Fuel Rod Pitch from Form 1G (Nominal Pitch = 0.496")
	Left Side, LS	Right Side, RS	
Between B/N and Grid 1	9-0	8-3/4	0.566
Between Grids 1 and 2	8-5/16 (1)	8-5/16 (1)	0.990
Between Grids 2 and 3	8-1/2	8.-0	0.740
Between Grids 3 and 4	8-7/16	8-1/2	0.715
Between Grids 4 and 5	8-3/16	8-3/16	0.472
Between Grids 5 and 6	8-3/16	8-3/8	0.578
Between Grids 6 and 7	8-1/16	8-1/16	0.550
Between Grids 7 and 8	8-3/8	8-3/16	0.541
Between Grids 8 and 9	8-0	7-13/16	0.483
Between Grids 9 and 10	8-3/8	8-1/2	0.498
Between Grid 10 and T/N	8-3/8	8-0	0.497
MAXIMUM VALUE	9-0	8-3/4	0.990

Note:
(1) A single rod was measured to the inner Clamshell surface (9-1/2"). See Figure 2-153.

Table 2-50 CTU Fuel Rod Gap and Pitch Inspection After Testing

Fuel Rod Gap and Pitch Inspection Table

Location	Measured Maximum Gap, Inches		Calculated Maximum Pitch, Inches
	Left Side, LS	Right Side, RS	
Between B/N Grid 1	0.093 (between rows 9 & 10)	0.193 (between rows 6 & 7)	0.566
Between Grids 1 and 2	0.616 (out-lying rod only)	0.563 (out-lying rod only)	0.990
Between Grids 2 and 3	0.207 (one rod) Others touching	0.366 (one rod) Others touching	0.740
Between Grids 3 and 4	0.336	0.340	0.715
Between Grids 4 and 5	0.099	0.050	0.472
Between Grids 5 and 6	0.204	0.084	0.578
Between Grids 6 and 7	0.173 (between rows 2 & 3) Others Nominal	0.176 (between rows 6 & 7) Others Nominal	0.550
Between Grids 7 and 8	0.166	0.064	0.541
Between Grids 8 and 9	0.109	0.060	0.483
Between Grids 9 and 10	0.124	0.090	0.498
Between Grid 10 and T/N	0.123	0.074	0.497
MAXIMUM VALUE	0.616	0.563	0.990

Note:
The pitch is calculated by adding the measured gap to the fuel rod diameter.

2.12.6 SUPPLEMENT TO DROP ANALYSIS FOR THE TRAVELLER XL SHIPPING PACKAGE –CLAMSHELL AXIAL SPACER STRUCTURAL EVALUATION

2.12.6.1 Background

The XL Clamshell may be configured to include an aluminum spacer assembly to ship fuel types that normally would ship inside a Traveller STD package as shown in Figure 2-158. The structural performance of the spacer assembly in a bottom-down 9m hypothetical drop is evaluated to determine if there is any buckling of the spacer, a 6-inch Schedule 40 aluminum pipe, that could then damage or deform the Clamshell.

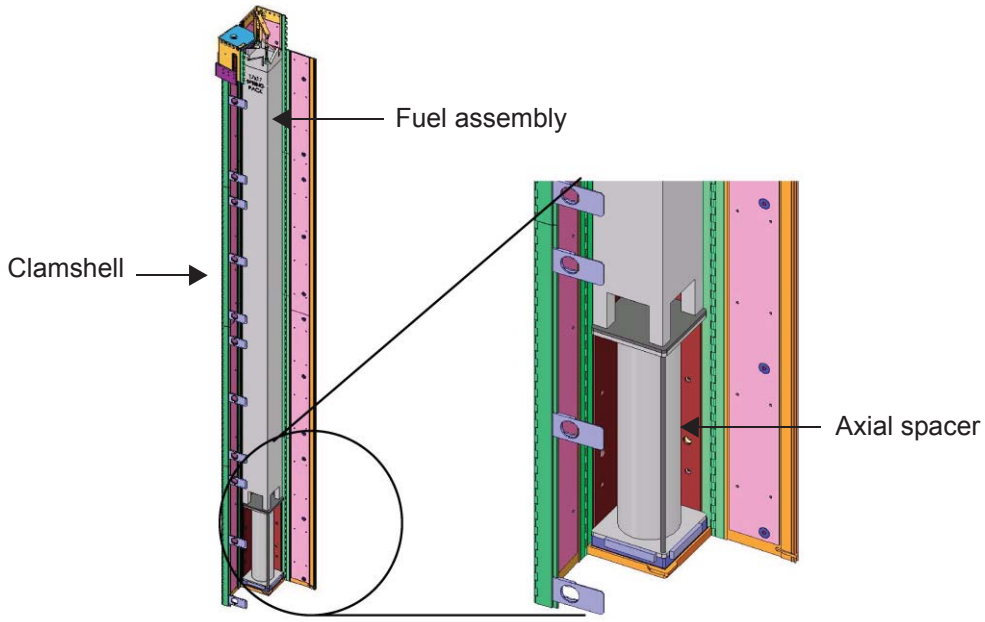

Figure 2-156 Axial Spacer below Fuel Assembly in Traveller XL Clamshell

The fuel assembly is assumed to be restrained in the clamshell to prevent any secondary impact within the clamshell. The spacer below the fuel assembly, when needed, and a top axial restraint restrain the contents to the clamshell, and as such the clamshell and contents decelerate as a coupled mass. The top axial restraint, fuel assembly structure, or spacer may absorb kinetic energy during the deceleration that results from an end drop impact.

Any structural deformation of the spacer assembly shall not change the shape of the clamshell or compromise the ability of the clamshell to confine the fuel assembly. The clamshell panel doors shall remain securely closed, end plates shall remain securely in place, hinges attaching the panel doors and multi-point cammed latch shall remain intact, and dimensions of the clamshell shall not be altered.

The primary impact with the unyielding surface occurs on the Outerpack end impact limiter. The Outerpack decelerates quickly within a few milliseconds of the primary impact because the contact area of the end surface is large and stiff, and there is no significant rebound. The Outerpack is completely decelerated by the time a secondary impact occurs inside the package as the Clamshell, suspended in the lower Outerpack on rubber mounts, continues to fall and contact the inside surface of the end impact limiter.

A crushable foam "pillow" is integrated into the end impact limiter to absorb kinetic energy from the secondary impact between the Clamshell and inside surface of the lower Outerpack end impact limiter. This pillow is a solid disk made from 6 pcf polyurethane foam. It has a nominal diameter of 12.00 inches (305 mm) and a nominal height of 3.60 inches (91 mm). The stiffer foam in the Overpack end impact limiter, 20 lb/cu. ft. (0.32 g/cc) density, is located below and around the soft pillow. This stiffer component end impact limiter functions to decelerate the Outerpack at all high drop angle orientations.

2.12.6.2 Conclusions

Results of the simulated bottom-down 10m impact predict that there is no significant risk of damage to the Clamshell due to buckling of the spacer assembly. The 28.94 inch (735.1mm) long spacer assembly is too short to fail in a classic Euler buckling manner. Instead, the spacer pipe locally may crumple near its bottom and top ends during the impact. This local crumpling does not result in large column bowing displacements that could impart forces on the Clamshell panel doors or base.

2.12.6.3 Detailed Calculations and Evaluations

A Traveller TX finite element (FE) model of the entire package was originally used to simulate the impact testing. A new LS-DYNA Traveller model was created to simulate features of the TX package affected by the end impact orientation. The new model is more efficient and was used to evaluate the structural performance of the axial spacer in the vertical end impact.

Assumptions

Specific assumptions used in the FEA simulation are as follows:

1. The assumed mass of the 17STD FA (1,496 lbs, 678 kg) includes the heaviest core component, a Rod Control Cluster Assembly (RCCA) (180 lbs, 82 kg), Reference 5. The total FA mass was therefore, 1,676 lbs (760 kg) (RCCA dwg: 1554E27).

2. The FA is modeled with distributed point-element masses and is therefore not elastic. This is very conservative since actual drop testing revealed the weak axial stiffness of a FA (it vibrates and bows during end impacts).

3. The drop height was conservatively increased from 9m to 10m.

4. The FA bottom nozzle and spacer assembly were modeled without any restraints and they are therefore free to rotate/tilt. In actuality, the FA itself would keep the bottom nozzle relatively horizontal and the Clamshell walls will further restrain both items.

5. The majority of the mass of the Outerpack has not been included in this analysis because it does not significantly affect the Clamshell impact. More specifically, the Outerpack impact event is finished within only a few milliseconds, therefore the bottom limiter is simply waiting for the Clamshell impact into it. This assumption has been validated in a separate run which did include the remaining Outerpack mass.

6. The foam crush characteristics include extrapolation from 80% crush to 100% crush for model stability purposes. As mentioned earlier, actual pillow crushing was measured to be only about 50%. This is because the FA is not a rigid "hammer" that has no axial elasticity. This effect has been proven to be quite significant. However, in these simulations, the severe impact of the rigid-mass modeling of the fuel assembly was used. In some cases, this forces the crush curves to be extrapolated to 100%.

7. The longest spacer assembly is considered the bounding FA/Spacer combination.

8. LS-DYNA incorporates strain capability into the plastic regions of metallic material properties, therefore the "strain hardening" effects for aluminum were included in the model. These values are difficult to obtain, and therefore engineering judgement was used to assume the modulus after the yield. This was assumed to be a very low, linear value, of 268 MPa. This is almost no strain hardening from yield to failure.

Method

The Lawrence Livermore, LS-DYNA® finite element code was used to determine the loads, displacements, accelerations, strains, etc. of a Traveller XL shipping package containing a 17x17STD fuel assembly with RCCA when dropped onto a flat unyielding surface from a height of 10m. LS-DYNA 970, Revision 5434a, is a general purpose finite element code for analyzing the large deformation dynamic response of structures. This software was selected because it allows the analysis to include the effects of large deformation, large strain, material non-linearity, contact, and failure of materials.

Only the bottom end of the FA is modeled, the remainder of the assembly mass is simulated through point-mass elements. The weight of the remainder of the Clamshell is also modeled with point-mass elements. The Clamshell is an aluminum box with a solid 1 inch thick bottom plate. The spacer assembly is modeled with the 1.25 inch (31.8 mm) thick bottom rubber pad included, however, the 3/8 inch (9.5 mm) thick rubber pad on the top surface was not modeled.

Figure 2-157 shows components, materials, and meshing for the FEA simulation. The material properties assumed for the aluminum, stainless steel, and the crushable foams, and rubber pad are summarized in Tables 1 through 5. The compressive strength difference between the crushable foams is shown in Figure 2-158. Figure 2-159 shows the stress-strain curve of the 304 Stainless Steel properties used in the LS-Dyna simulation.

The appropriate properties of neoprene rubber for this simulation are difficult to determine exactly. Further, neoprene rubber does not obey Hook's law because it exhibits non-linear behavior. For this simulation, a value of 6.21 MPa was used for the shear modulus (G) of the 30 mm thick lower rubber pad.

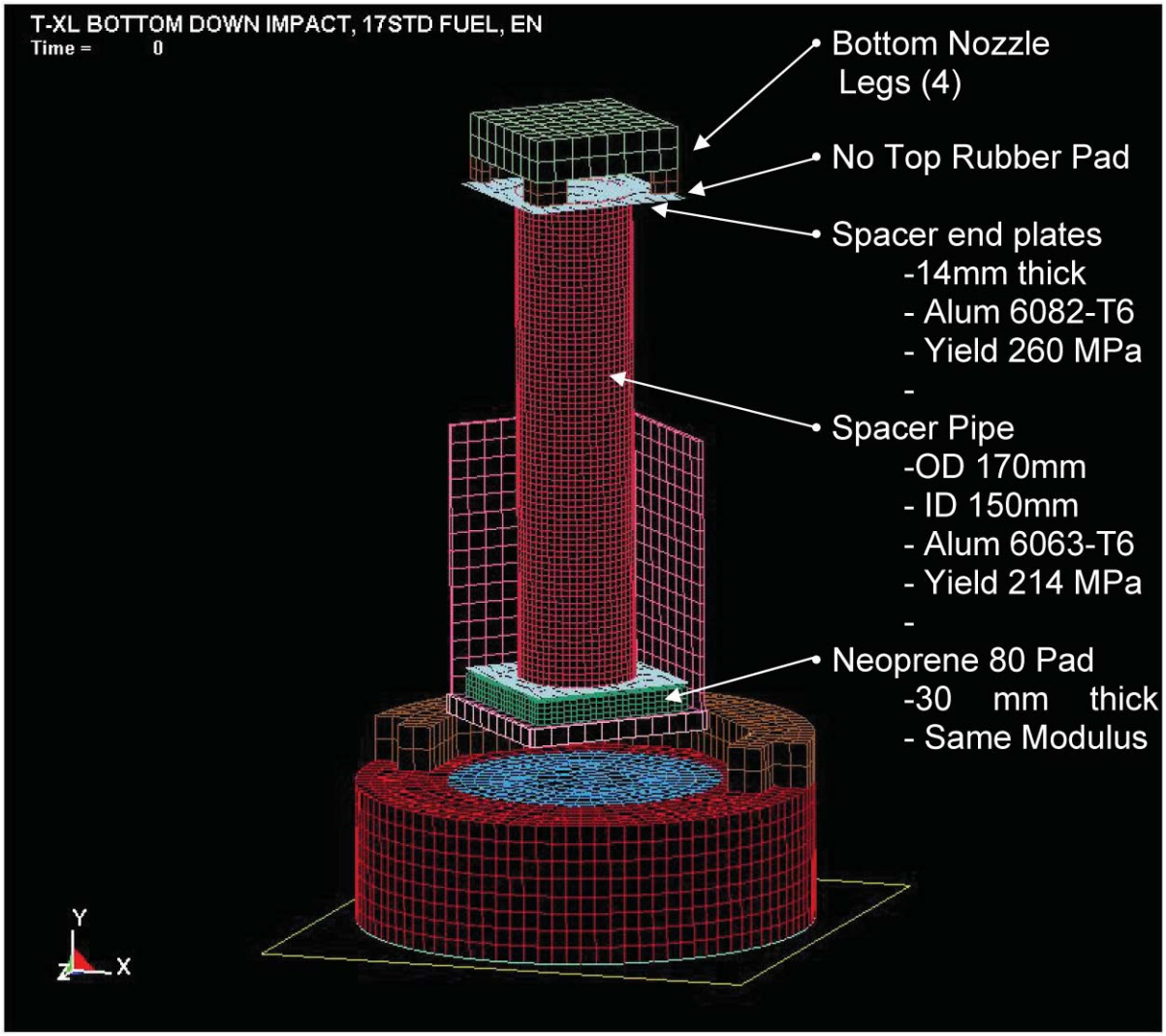

Figure 2-157 FEA Model – Axial Spacer

Table 2-51 Dimension and Material Properties of Axial Spacer	
Support Pipe:	
Exterior Diameter - mm (in):	170 (6.69)
Interior Diameter - mm (in):	150 (5.91)
Length - mm (in):	671.1 (26.42)
Wall Thickness - mm (in):	10 (0.39)
Material	6063-T6
Yield Strength - MPa (Ksi)	214 (31.0)*
Base Plates:	
Thickness - mm (in)	14 (.55)
Length - mm (in):	228.6 (9.00)
Material	6082-T6
Yield Strength - MPa (Ksi)	262 (38.0)*
Top Rubber Pad:	
Length - mm (in):	228.6 (9.00)
Thickness - mm (in)	10 (0.39)
Material	Neoprene 80
Bottom Rubber Pad:	
Length - mm (in):	228.6 (9.00)
Thickness - mm (in)	30 (1.18)
Material	Neoprene 80
Rod Handle:	No
Side Rubber Pad:	No
Total Assembly Length - mm (in):	735.1 (28.94)

Table 2-52 Aluminum Properties

Aluminum Properties			
6005-T5 and 6061-T6 Aluminum at 75 degrees F			
Property	**Symbol**	**Value**	**Units**
Density	RO	2.71E-09	Mg/mm^3
Modulus	E	70	kN/mm^2 (GPa)
Poisson's Ratio	PR	0.30	dimensionless
Yield Strength	SIGY	0.241	kN/mm^2 (GPa)
Hardening Modulus	ETAN	0.25	kN/mm^2
Failure Strain	FAIL	0.35	In compression

Table 2-53 Annealed 304 Stainless Steel Properties

Annealed 304 SS Properties			
Property	**Symbol**	**Value**	**Units**
Density	RO	8.00E-09	Mg/mm^3
Modulus	E	203	kN/mm^2 (GPa)
Poisson's Ratio	PR	0.30	dimensionless

Table 2-54 Crushable Foam Properties

Crushable Foam Properties			
	Density	**Modulus**	**Poisson's Ratio**
	Mg/mm^3	(MPa)	(dimensionless)
6 pcf Last-A-Foam	9.61E-11	30.14	0
10 pcf Last-A-Foam	1.60E-10	66.23	0
20 pcf Last-A-Foam	2.24E-10	192.76	0

Table 2-55 Neoprene (60 durometer) Properties

Neoprene (Rubber) at 75 degrees F			
Property	**Symbol**	**Value**	**Units**
Density	RO	9.13E-10	Mg/mm^3
Shear Modulus	G	6.21E+00	MPa

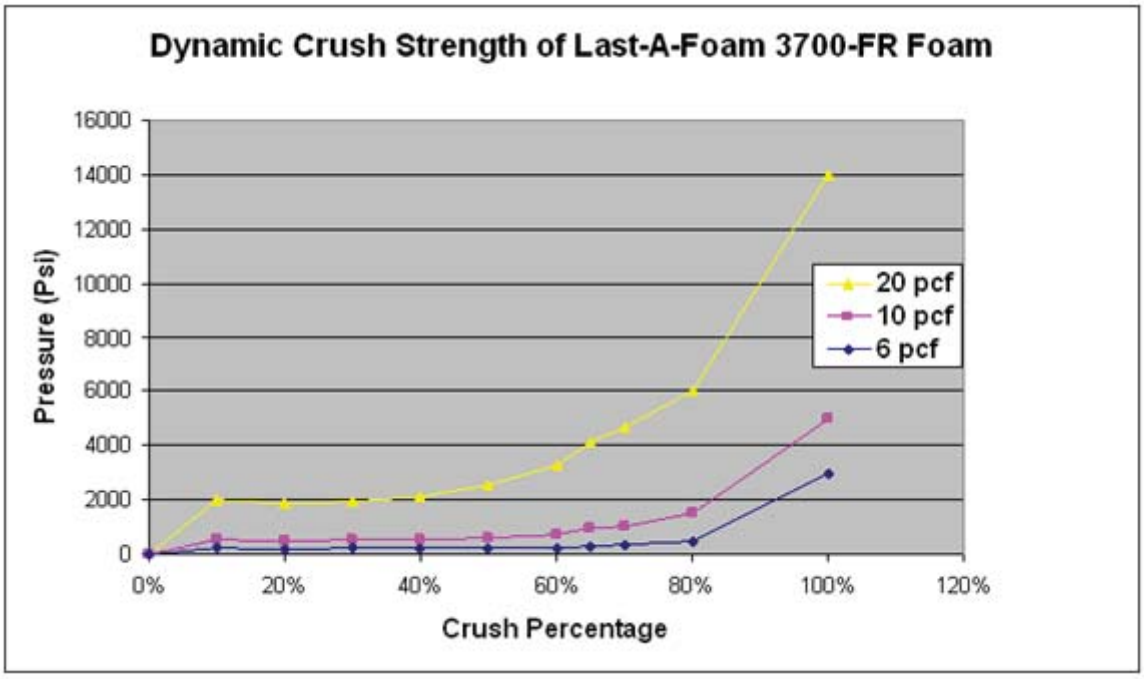

Figure 2-158 Dynamic Crush Strengths for Foam Materials Utilized in the Traveller

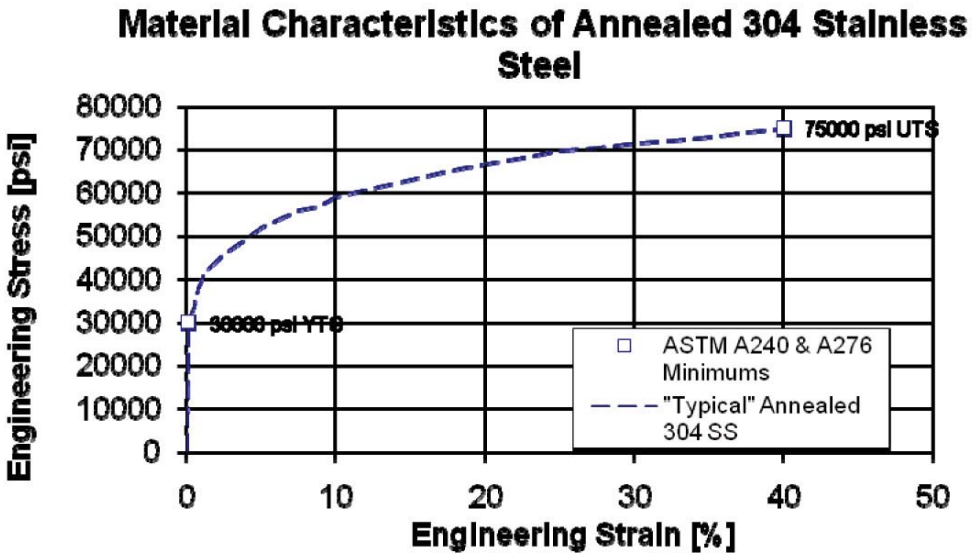

Figure 2-159 Annealed 304 Stainless Steel Stress-Strain Characteristics

Calculation Results

The 10m initial drop height of the Traveller simulation yields an impact velocity of 45.93 ft/sec (14 m/s). The FEA simulation shown in Figure 2-160 predicts deformation of the top spacer end plate, but no buckling or plastic deformation of the spacer pipe. From the displacement history of the top surface of the pillow shown in Figure 2-161, the total crush distance into the end impact limiter is approximately 94 mm (3.70 in). Figure 2-162 shows the kinetic energy history (mJ) of the axial spacer model.

Figure 2-160 Deformed Model with Axial Spacer at 23 ms (the end of the impact)

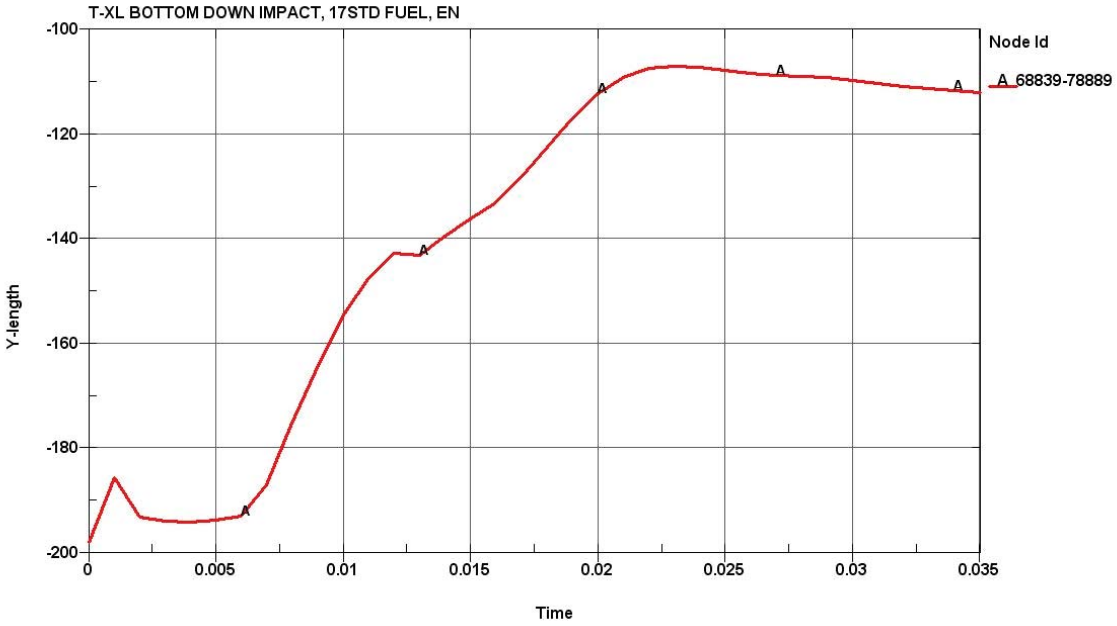

Figure 2-161 Predicted Total End Crushing (mm) with Axial Spacer

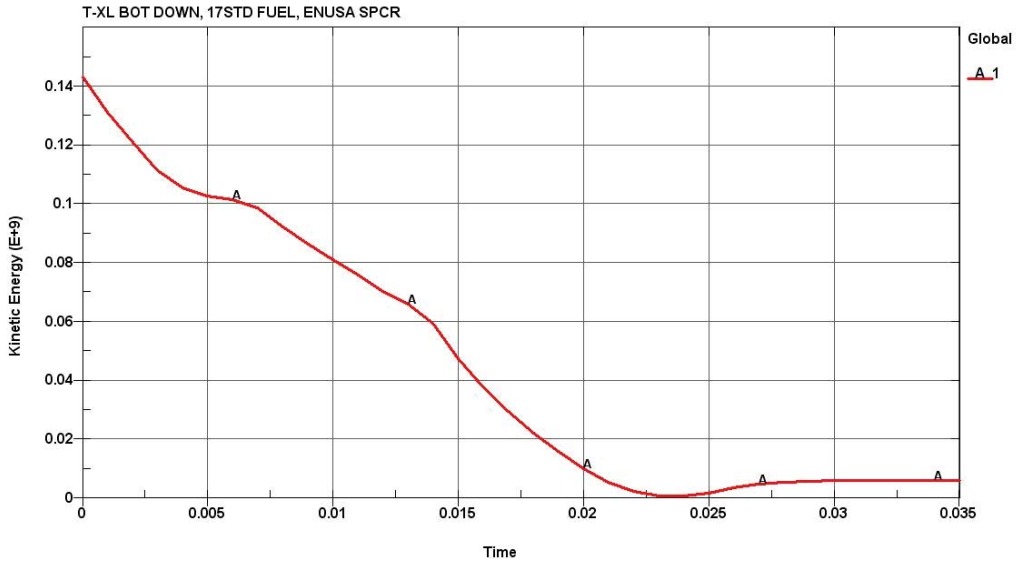

Figure 2-162 Kinetic Energy History (mJ) of the Axial Spacer Model

Validation

The many assumptions used to develop the LS-DYNA non-linear finite element stress code, including those needed to model the materials and impact, are validated by comparing the simulation results to the actual drop tests for the Traveller XL. Comparisons between certification test unit results and FEA simulation demonstrates that physical phenomenon governing shipping package impacts are simulated with adequate fidelity using the LS-DYNA model.

The pillow from a 10.0 m free drop impacting the bottom end of the package, CTU Test 1.2, was observed to crush approximately 1.8 inches. The simulation with axial spacer predicted the end limiter assembly (pillow and high density end limiter) is crushed 92 mm (3.62 inches). The simulation predicts more absorption of the kinetic energy in the end impact limiter than observed in the actual drop test. This is due primarily to the assumption in the simulation that the fuel assembly is a rigid mass while for the actual drop test there was a significant energy absorbed in the deformation of the fuel assembly bottom nozzle and fuel rods during the deceleration.

In addition to the comparison energy absorbed by the end impact limiter, the axial force required to cause buckling of the spacer pipe, P_{cr}, can be estimated using the Euler buckling equation assuming that neither end is fixed (Reference: Shigley, "Mechanical Engineering Design", 3rd Edition, page 115):

$P_{cr} = \pi^2 \times E \times I / L^2$, where

E = Modulus of elasticity, 1.00E+07 psi

I = Moment of inertia, $\pi/64 \times (D^4 - d^4)$, D=Outer diameter, d=Inner diameter

L = Length of the column

Using the dimensions from Table 1 the critical axial force is calculated as follows:

$I = \pi/64 \times (6.69^4 - 5.91^4) = 38.44$

$P_{cr} = \pi^2 \times$ 1.00E+07 psi $\times 38.44 / 26.42^2 =$ 5.44E+06= lbf

Assuming a conservative fuel assembly gross weight of 2,000 lbs and a deceleration of 200 g, the maximum load on the spacer would be approximately 400,000 lbs. This is significantly lower critical Euler values calculated for the axial spacer pipe. This result is consistent FEA simulation that predicted no buckling of the axial spacer.

Computer Code Input Files

CTUWSPCR.K Bottom-down end drop from 10m, with 17STD fuel and ENUSA Spacer Assy (dwg: CECT100, rev 1). This is Traveller XL pkg, production type, with 6pcf pillow. Temp = 75 F, Nominal foam densities

References

1. SFAD-10-72, Revision 2 (July 6, 2010), "Analysis of a Traveller XL Package in a Hypothetical Bottom-Down Impact With 17x17 STD Fuel and Spacer Assembly."

2.12.7 SUPPLEMENT TO DROP ANALYSIS FOR THE TRAVELLER XL SHIPPING PACKAGE – CLAMSHELL REMOVABLE TOP PLATE STRUCTURAL EVALUATION

2.12.7.1 Background

The fuel assembly is assumed to be restrained in the clamshell to prevent any secondary impact within the clamshell. The spacer below the fuel assembly, when needed, and an axial restraint restrain the contents to the clamshell, and as such the clamshell and contents decelerate as a coupled mass. The top end axial restraint, fuel assembly structure, or spacer may absorb kinetic energy during the deceleration that results from an end drop impact.

Operational experience with Traveller package revealed that some fuel types could not be loaded or unloaded vertically with existing customer handling tools. In particular, the 17x17 XL fuel with guide pins could not be vertically loaded/unloaded into the Traveller due to an interference between the handling tool and the Clamshell Shear Lip. Figure 2-163 shows the 17x17 XL top nozzle with the handling tool attached and fully seated. Figure 2-164 shows the potential interference. The tool cannot be installed or removed without tilting the fuel handling tool and potentially damaging the fuel assembly.

Additional evaluation revealed similar interference issues when handling fuel assemblies which include Core Component Assemblies (CCA). A new Clamshell top head configuration was designed to eliminate the interference from the Shear Lip. Both the original Fixed Top Plate (FTP) configuration and an alternate configuration called the Removable Top Plate (RTP) are described in Section 1 of the Safety Analysis Report (SAR).

The primary impact with the unyielding surface occurs on the Outerpack end impact limiter. The Outerpack decelerates quickly within a few milliseconds of the primary impact because contact area of the end surface is large and stiff, and there is no significant rebound. The Outerpack is completely decelerated by the time a secondary impact occurs inside the package as the Clamshell, suspended on rubber mounts, continues to fall and contact the inside surface of the end impact limiter.

A crushable foam “pillow” is integrated into the end impact limiter to absorb kinetic energy from the secondary impact between the Clamshell and inside surface of the Outerpack end impact limiter. This pillow is a solid disk made from 6 pcf polyurethane foam. It has a diameter of 12.00 inches (305 mm) and a height of 3.60 inches (91 mm). The stiffer foam in the Overpack end impact limiter, 20 lb/cu. ft. (0.32 g/cc) density, is located below and around the soft pillow. This stiffer component end impact limiter functions to decelerate the Outerpack at all high drop angle orientations.

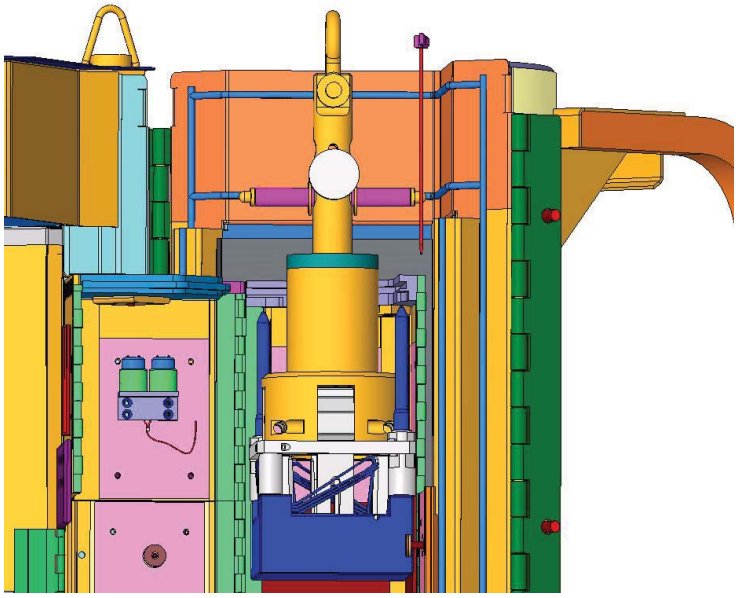

Figure 2-163 Fuel Handling Tool Grappled to a 17x17 Top Nozzle (in blue) within the Opened Outerpack and Clamshell

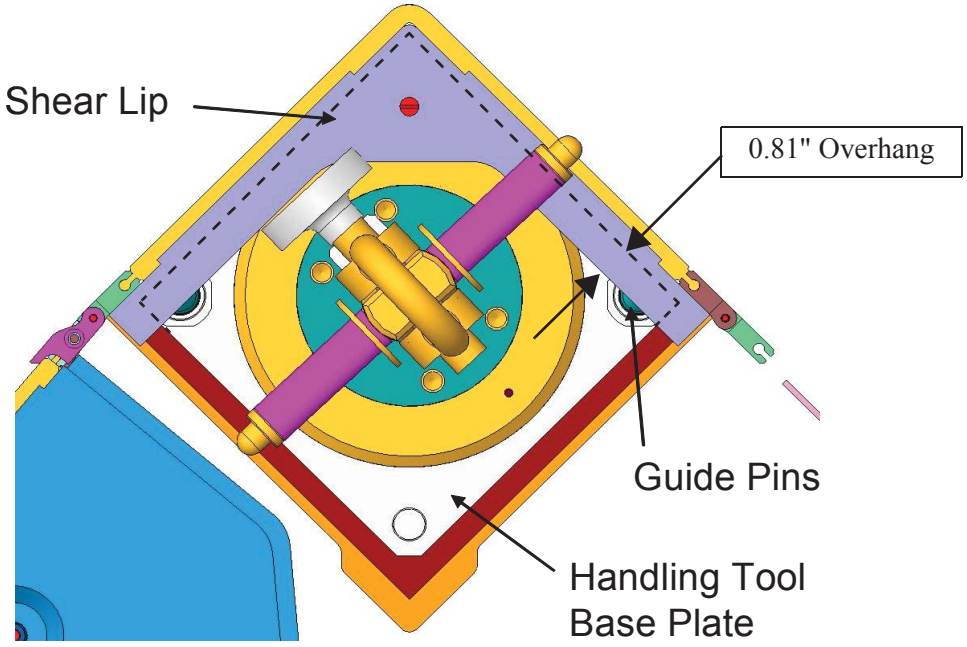

Figure 2-164 Fuel Handling Tool Shown Attached to a 17x17 XL Fuel Assembly and Behind the Overhanging Shear Lip

2.12.7.2 Conclusions

One of the most damaging orientations for the Clamshell and contents during impact is the end over center of gravity. The top-down impact challenges the integrity of the Clamshell's top end plate. End over center of gravity drop testing was performed using a certification test unit (CTU) and simulated using a finite element (FE) model. Both the actual drop tests and the FE model showed that the FTP design was acceptable. Simulation of the drop test with the RTP shows that this alternate end top plate design is also acceptable.

The screw fasteners that secure the top end plate components to the top access door and clamshell base are the weakest structure in either the FTP or RTP. These screws resist shear forces resulting from the secondary impact of the fuel assembly or fuel rod box on the top end plate during an end drop. Each screw is a stainless steel flat head cap screw, ½ inch diameter -13 threads per inch (1/2-13). These screw fasteners are not subject to large shear forces because the fuel assembly or rod container is restrained in the Clamshell to prevent secondary impact on the end plate.

2.12.7.3 Detailed Calculations and Evaluations

A Traveller XL finite element (FE) model of the entire package was originally used to simulate the impact testing. A new LS-DYNA Traveller model was created to simulate features of the XL package affected by the end impact orientation. The new model is more efficient and was used to evaluate the structural performance of the axial space in the vertical end impact.

Method

The Lawrence Livermore, LS-DYNA® finite element code was used to determine the loads, displacements, accelerations, strains, etc. of a Traveller XL shipping package containing a 17x17 XL fuel assembly with RCCA when dropped onto a flat unyielding surface from a height of 10m. LS-DYNA 970, Revision 5434a, is a general purpose finite element code for analyzing the large deformation dynamic response of structures. This software was selected because it allows the analysis to include the effects of large deformation, large strain, material non-linearity, contact, and failure of materials.

Only the top end of the FA is modeled, the remainder of the assembly mass is simulated through point-mass elements. The weight of the remainder of the Clamshell is also modeled with point-mass elements. The Clamshell is an aluminum box with a solid 1 inch thick top plate. Figure 2-165 shows components and meshing for the FEA simulation.

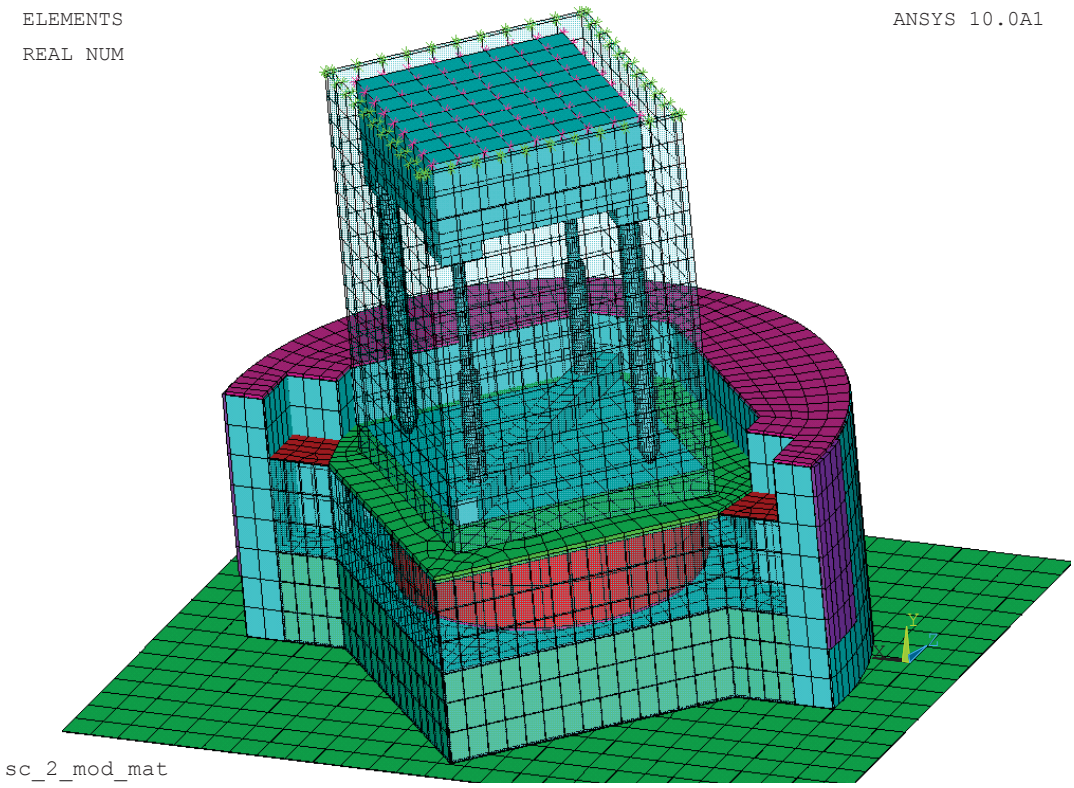

Figure 2-165 Traveller Top End Plate FEA Model

Calculation Results

The LS-Dyna model was also used to evaluate the maximum shear forces in the shear bar screws (simulated as the shear forces at the interfaces between the top plate and the extrusion walls). The peak shear force of the worst wall (i.e. across 5 screws) still showed a factor of safety of approximately 2.02 using conservative assumptions (i.e. ignoring friction between the wall and the plate for example).

The complete impact event for the RTP design without guide pins is shown in Figure 2-166 at various times. Figure 2-167 shows the rigid wall impact force history of RTP model and Figure 2-168 shows the kinetic energy history (mJ) of the axial spacer model.

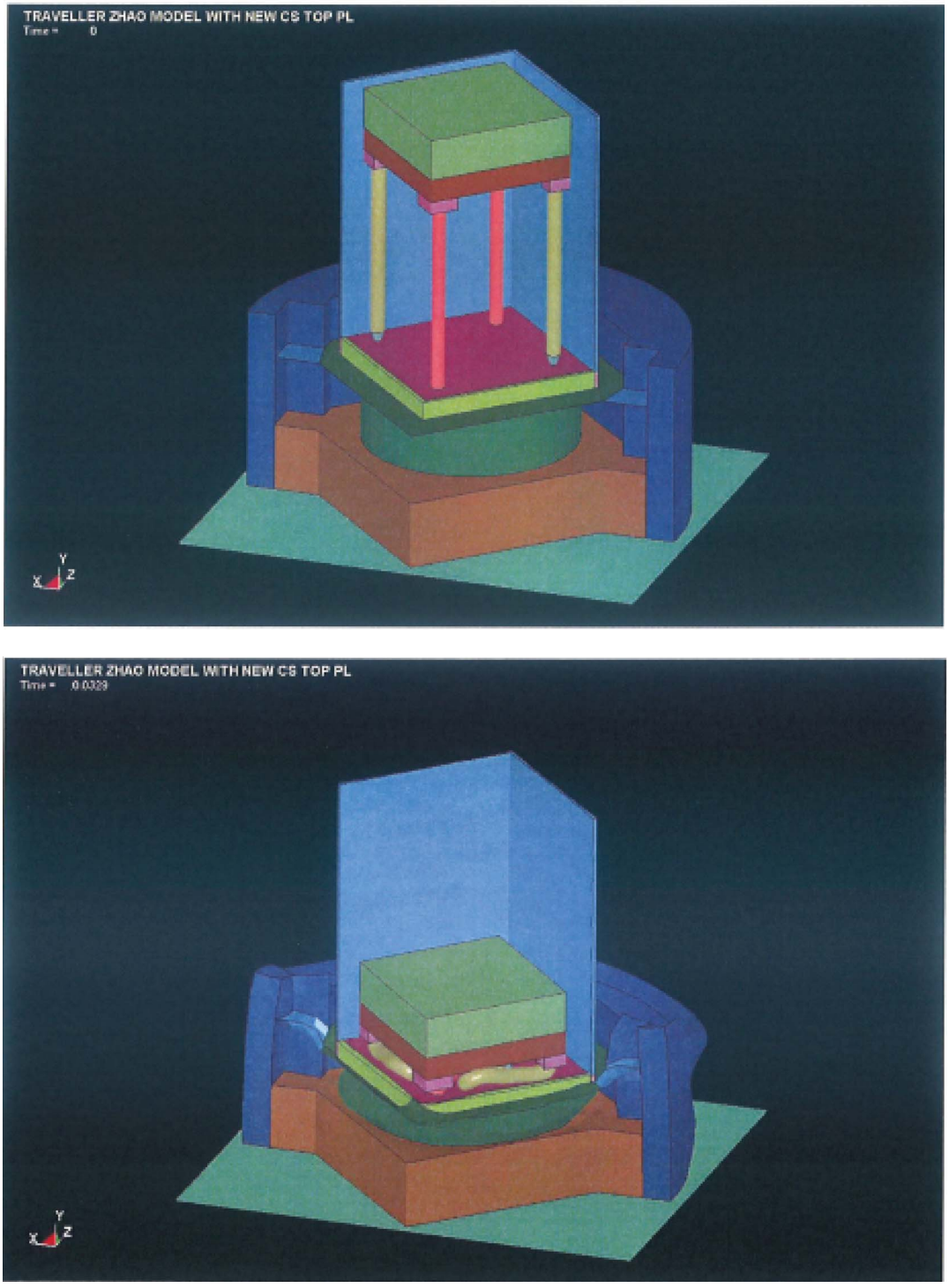

Figure 2-166 RTP Model at Beginning of Impact (0 ms) and End of Impact (33 ms)

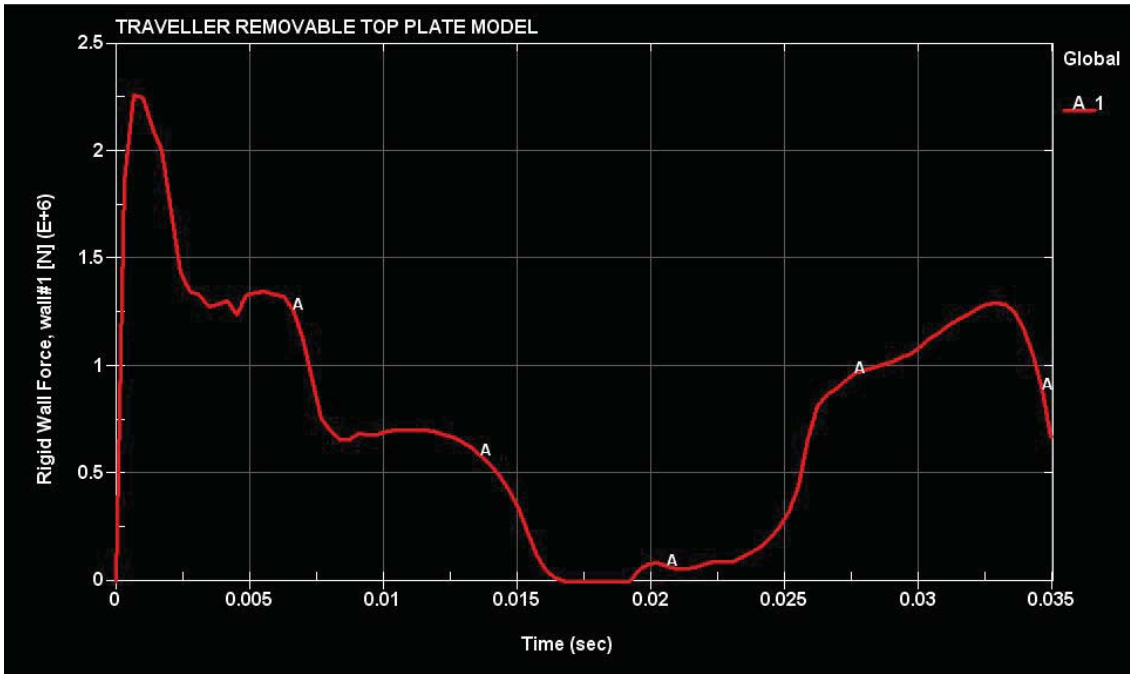

Figure 2-167 Rigid Wall Impact Force History of RTP Model

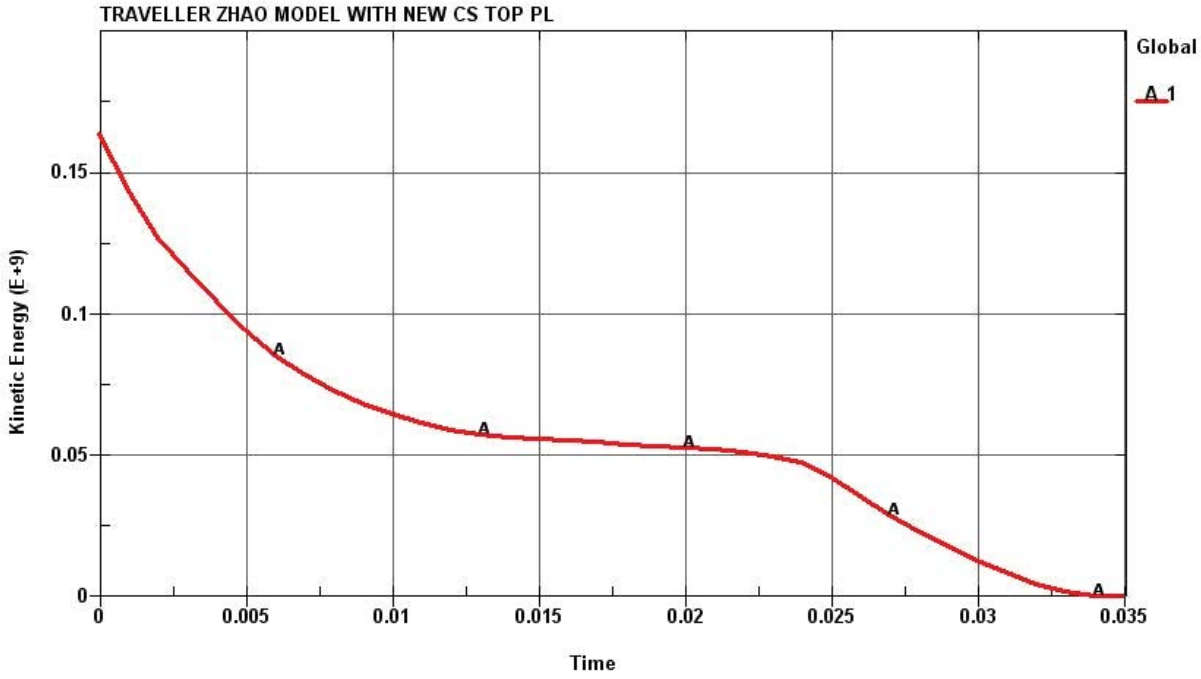

Figure 2-168 Kinetic Energy History of RTP Model (mJ vs s)

Validation

The many assumptions used to develop the LS-DYNA non-linear finite element stress code, including those needed to model the materials and impact, are validate by comparing the simulation results to the actual drop tests for the Traveller XL. Comparisons between certification test unit results and FEA simulation demonstrates that physical phenomenon governing shipping package impacts is simulated with adequate fidelity using the LS-DYNA model.

The buckling of the axial clamp studs and the Pillow are very similar to the previous the drop tests done with the qualification test unit (QTU). Figure 2-169 shows prediction of the post drop deformed shape of the top nozzle compared to the actual dropped nozzle.

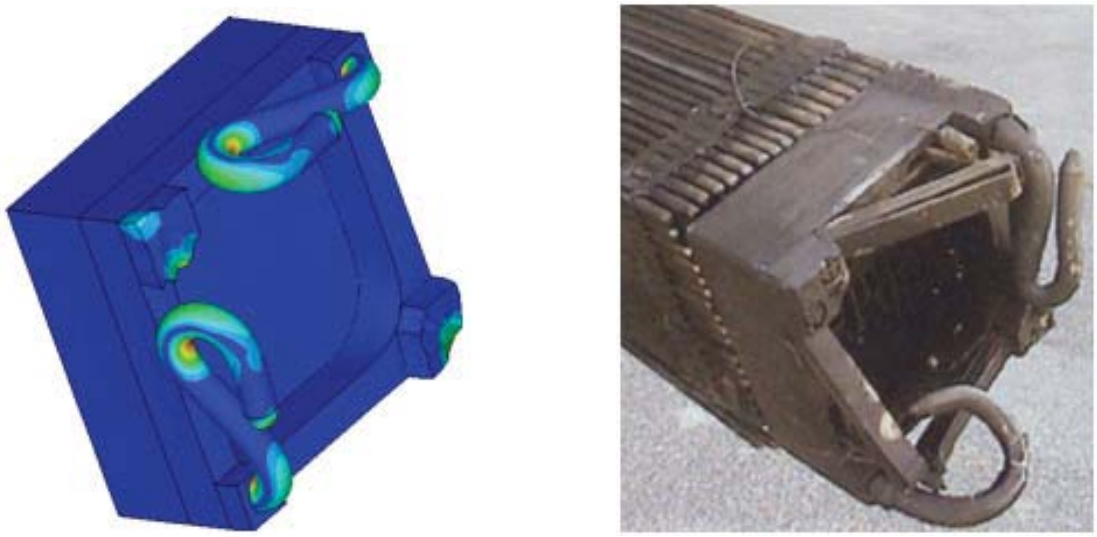

Figure 2-169 Comparison of Simulated Top Nozzle Damage (left) to Drop Test (right)

Computer Code Input Files

QTU1_9 w big axial studs 3.k	Traveller Top Nozzle Impact Study, New Top Plate Model

References

1. SFAD-09-184, Revision 1 (May 24, 2010) "ER 09-6 – Engineering Review Data Package for Revised Traveller Shear Lip"

TABLE OF CONTENTS

LIST OF TABLES

LIST OF FIGURES

LIST OF FIGURES (cont.)

3.0 THERMAL EVALUATION

The Traveller series packages are limited to use for transporting unirradiated, low enriched uranium, nuclear reactor core assemblies. There is no packaging design feature for heat removal because the contents does not contain heat generating radioactive material. The use of polyethylene as a moderator requires controlled heat-up during accident conditions, to prevent loss of hydrogen within the moderator.

3.1 DESCRIPTION OF THERMAL DESIGN

3.1.1 Design Features

The Traveller series packages, as described in section 2, utilize an aluminum Clamshell to contain a single unirradiated nuclear fuel assembly. The Clamshell is mounted within a cylindrical Outerpack fabricated from 304 stainless steel and flame retardant polyurethane foam. The stainless steel/foam sandwich provides thermal insulation during hypothetical fire conditions. Most of the heat capacity is within the Outerpack, provided by the polyethylene moderator, the aluminum Clamshell and the fuel assembly itself reducing the peak temperatures within the package.

The fuel rods, that contain the radioactive material, are designed to withstand temperatures of 1204°C (2200°F) without substantial damage. The primary temperature limitation is the polyethylene moderator located on the inside surface of the Outerpack. Polyethylene was selected because it retains its chemical composition and therefore its hydrogen content past melt temperature (between 120° and 137°C). Because of its very high viscosity, it will not flow significantly and will not change chemical composition unless significant amounts of high temperature oxygen are present (320-360°C).

The design and test strategy employed for the Traveller was to utilize design approaches that had previously passed the thermal test requirements. A review of previous designs and associated test results led to the selection of a stainless steel/polyurethane sandwich for the Outerpack. Based on this design approach, scoping tests and thermal analysis were performed to size the Outerpack structure. These analyses showed that sufficient polyurethane was incorporated to effectively insulate the interior of the Outerpack. As described in section 3.3.1 below, anticipated heat transfer due to conduction and radiation was so low that peak temperatures within the Outerpack would be below the melt temperature of the polyethylene and well below its ignition temperature. The primary concern was hot gas flow into the interior of the Outerpack. If both inner and outer skins of the Outerpack are ripped or if the seam between the Outerpack door and base are opened during the drop tests, hot gas from the fire could flow through the Outerpack significantly increasing its temperature. The Outerpack was made sufficiently robust that the defined drops did not create air infiltration paths within the Outerpack.

During the development process, three Traveller test articles were built. All were subjected to drop testing. Afterwards, these units were subjected to multiple burn tests. The information obtained during tests was incorporated into the final design of the Traveller Certification Test Unit (CTU). The CTU was subjected to drop testing as described above (Section 2.12.4). The CTU was then transported to Columbia, SC where it was burned in accordance with 10CFR71.73(c)(4) and TS-R-1, paragraph 728(a).

The package survived the test with maximum internal temperatures less than 180°C. The results of this test are described in section 3.5 and appendix 3.6.4.

3.1.2 Contents Decay Heat

Decay heat and radioactivity of the contents are not applicable for this package type.

3.1.3 Summary Tables of Temperatures

The maximum temperatures that affect structural integrity, containment, and criticality for both normal conditions of transport and hypothetical accident conditions are provided in Table 3-1. The table also includes the maximum measured temperature of the package components. All measured temperatures are within the limits specified. These results show that hypothetical accident thermal conditions will not materially affect the fuel assembly, the neutron poison plates, clamshell or the polyethylene moderator

During hypothetical accident conditions, the polyurethane insulation in the Outerpack protects the interior from excessive heat up. The Clamshell and its contents will not experience temperature increases significantly greater than 100°C. Therefore, room temperature material properties adequately describe the Clamshell and fuel assembly. The polyurethane foam will experience significant temperatures during the hypothetical accident. Because the lack of data at higher temperatures, the thermal analysis assumed foam properties above 340°C were equivalent to dry air. As shown by tests described in section 3.5 below, this approximation reasonably bounded actual properties.

Table 3-1 Summary Table of Temperatures for Traveller Materials

Material	Temperature Limit and Rational (C)	Measured Temperature in CTU Fire Test (C)(1)
Uranium oxide	2750 (melt) 1300 (compatibility with zirconium)	104
Zircalloy	1850 (melt)	104
Aluminum	660 (melt)	104
Stainless steel	1480-1530 (melt)	177(2)
UHMW Polyethylene	349 (boiling/ignition)	177(2)
Fiberglass seals (Thermojecket S)	1000°F (long term)	Temperature not measured/ Seals present after fire test
Silicone Rubber Gasket	500°F (long term)	Seals not present after fire test
Shock Mounts (fully cross-linked natural rubber)	greater than 300 (combustion)	177(2)
Refractory fiber felt insulation	2300°F (melt)	177(2)

Notes:
(1) Temperature measurements made by non-reversible temperature strips. Exact time of peak temperature can be inferred from analysis. See section 3.3-1.
(2) One location was unreadable on inside Outerpack shell. See section 3.6-4.

3.1.4 Summary Tables of Maximum Pressures

The Traveller Outerpack surrounds the Clamshell and fuel assembly. It has two silicone foam rubber seals to prevent rain, dirt, dust and spray from entering the package. The seals are not continuous, however, to avoid producing an air-tight seal. The Traveller Clamshell is not air tight and cannot maintain a different pressure than the air surrounding it. The double wall Traveller Outerpack also incorporates acetate seal plugs that melt in the event of a fire allowing decomposition products from the polyurethane insulate to vent to the outside air. Therefore, the Traveller interior pressure will always maintain itself in approximate equilibrium with external air pressure.

3.2 MATERIALS PROPERTIES AND COMPONENT SPECIFICATIONS

3.2.1 Materials Properties

The Traveller package series is fabricated primarily from four materials: 304 stainless steel, 6005 aluminum, Ultra-High Molecular Weight (UHMW) polyethylene, and flame retardant polyurethane foam. The Outerpack is fabricated from stainless steel and the polyurethane foam. The interior Clamshell holding the fuel assembly is fabricated from aluminum. The polyethylene is used as a neutron moderator and is located on the inside walls of the Outerpack, between the Outerpack and Clamshell. The important room temperature material properties are provided in Table 3-2.

The melt temperature of the polyurethane foam is not provided because it is a thermoset material that decomposes before melting. The urethane foam selected for use will be a fire retardant foam that, when heated above 204.4°C, produces an intumenscent char that seals voids and continues to provide insulation. This process is endothermic and produces gasses that must be vented. Vent plugs are placed along the length of the package to provide this venting. All Outerpack components containing polyurethane foam will have at least one vent plug.

The fuel assembly significantly affects the response of the overall package during a hypothetical fire. Because the fuel assembly may account for as much as 40% of the total package weight, the thermal capacity of the fuel assembly has a significant effect interior temperature. Key materials for the 17x17 XL fuel assembly to be shipped in the Traveller XL package is shown in Table 3-3.

Table 3-2 Room Temperature Properties of Key Traveller Materials

Material	Density	Melt Temp	Conductivity	Specific Heat
304 Stainless Steel	8.3 g/cc .29 lb/in^3	1400-1455°C 2550-2650°F	14.2 W/m-K 8.2 BTU/hr-ft-F	0.5 J/g-°C 0.12 BTU/lb-°F
6005 Aluminum	2.8 g/cc .098 lb/in^3	582-652°C 1080-1210°F	167 W/m-K 96.1 BTU/hr-ft-F	0.88 J/g-°C 0.21 BTU/lb-°F
UHMW polyethylene	.932-.945 g/cc .0337 - .0341 lb/in^3	125-138°C 257-280°F	0.42 W/m-K .24 BTU/hr-ft-F	2.2 J/g-°C 0.526 BTU/lb-°F
Polyurethane Foam	0.166 g/cc .0058 lb/in^3	NA	0.041 W/m-K .023 BTU/hr-ft-F	1.15 J/g-°C 0.275 BTU/lb-°F
Fiberglass seals (Thermojecket S)	NA(2)	538°C(1) 1000°F	NA(2)	NA(2)
Silicone rubber gasket	NA(2)	-73 to 250°C(1) -100 to 500°F	NA(2)	NA(2)
Refractory fiber felt insulation	0.097 g/cc .0035 lb/in^3	1260°C 2300°F	.06 W/m-K .034 BTU/hr-ft-F	1.0 J/g-°C 0.239 BTU/lb-°F

Notes:
(1) Temperature range that the gasket material and adhesive will withstand.
(2) Packaging weather gasket is to keep dust, dirt and spray from getting inside the Outerpack.

Table 3-3 Room Temperature Properties of Key Fuel Assembly Materials

Material	Mass in FA	Melt Temp	Conductivity	Specific Heat
304 Stainless Steel	22 kg 49 lb	1400-1455°C 2550-2650°F	14.2 W/m-K 8.2 BTU/hr-ft-F	0.5 J/g-°C 0.12 BTU/lb-°F
Inconel	2.7 kg 6 lb	1354-1413°C 2470-2580°F	14.9 W/m-K 8.6 BTU/hr-ft-F	0.44 J/g-°C 0.106 BTU/lb-°F
Zircalloy 4	150 kg 330 lb	1850°C 3360°F	21.5 W/m-K 12.4 BTU/hr-ft-F	0.285 J/g-°C 0.0681 BTU/lb-°F
Uranium dioxide	608.3 kg 1341 lb	2750°C 4982°F	5.86 W/m-K 3.39 BTU/hr-ft-F	0.237 J/g-°C 0.0565 BTU/lb-°F

3.2.2 Component Specifications

Stainless steel and aluminum materials are procured to ASTM A24 304 SS and ASTM B209/B221 respectively. Welding is performed in accordance with ASME Section IX and inspected per AWS D1.6. The polyurethane foam is poured in accordance with approved procedures and specifications.

3.3 GENERAL CONSIDERATIONS

Thermal evaluations of the Traveller were performed by analysis and actual test. The Traveller package utilizes a double wall, insulated, Outerpack to protect an interior box (Clamshell) containing a fuel assembly and blocks of polyethylene moderator. Because of the large length to diameter ratio (8.8), heat transport in most of the package is primarily radial. The thermal analysis performed examined this heat transport path. The seam burn tests, examined radial heat flow with prototypical gas infiltration through the Outerpack seams. The impact limiter burn tests, examined and measured the heat transport through the ends of the package. The final QTU burn test combined all of the possible heat transport mechanism and demonstrated the suitability of the design.

3.3.1 Evaluation by Analysis

The thermal model of the Traveller package was created to examine the response to the hypothetical fire accident conditions described in 10 CFR 71 and IAEA Regulations for the Safe Transport of Radioactive Material, Section VII-728. This analysis was performed to bound the anticipated response and was done by analyzing the response of the package at 800°C external conditions with a fire emissivity of 0.9 and a package emissivity of 0.8 as defined by 10CFR71.73. The analysis was also performed assuming an average fire temperature of 1000°C anticipated during an actual burn test. The analytical burn model did not include potential damage to the Outerpack because:

- Minimum damage was anticipated after drop test
- The anticipated minor damage would not have a significant impact of global performance
- The combined uncertainty of the package damage combined with uncertainty in modeling gas flow patterns around the package made a detailed thermal analysis undesirable.

The analysis results show that the outer skin of the package quickly rises to thermal equilibrium with the fire. The internal components heat up more slowly due to the insulation capability of the polyurethane foam between the inner and outer shell of the Outerpack. Fuel and Clamshell temperatures increase by approximately 50°C and are well within acceptable levels, see Figure 3-1 and Figure 3-2. This analysis is described in greater detail in appendix 3.6.1.

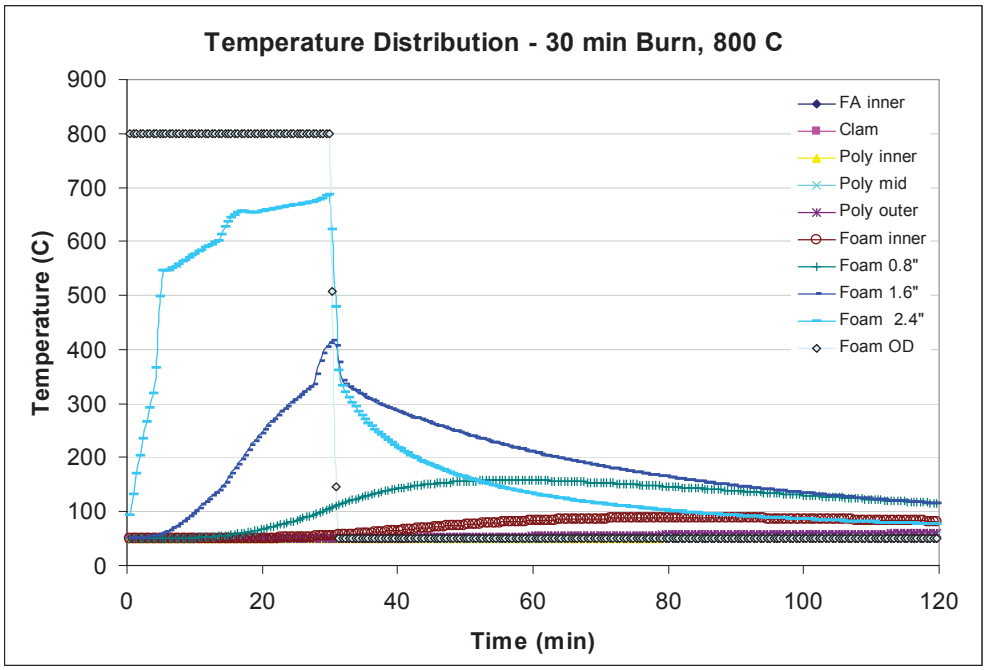

Figure 3-1 Calculated Radial Temperature Distribution for 30 Minute Fire (800°C)

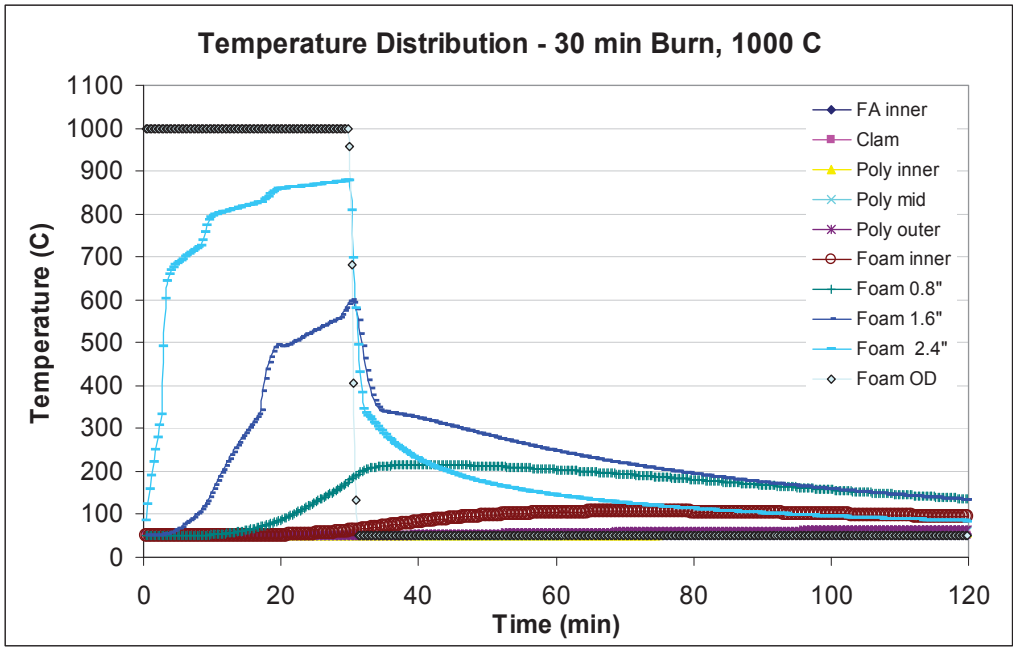

Figure 3-2 Calculated Radial Temperature Distribution for 30 Minute Fire (1000°C)

3.3.2 Evaluation by Test

Traveller performance under hypothetical accident conditions specified in 10CFR71.73 (c) and IAEA Regulations for the Safe Transport of Radioactive Material, Section VII-728 was initially calculated using the SCALE 4.4 thermal analysis code. The performance was subsequently demonstrated in a series of partial burn tests exposing selective portions of a full-scale package to pool fire conditions exceeding the hypothetical accident conditions. Finally, a full scale package was subjected to a full scale, fully engulfing, pool fire exceeding hypothetical accident conditions.

Two separate partial burn tests were performed to verify the final Traveller design. The first was the seam burn test. This test was designed to simulate the flow of hot gas through the Outerpack seams at the hinged joint between the Outerpack base and the Outerpack door and to measure the resulting heat transfer. The second, was the impact limiter burn test. This test subjected the end of a Traveller package to pool fire conditions to measure heat transfer at the package ends. These partial burn tests were then followed by a burn test of the qualification test article. This test, which followed the regulatory drop tests, completely immersed the full scale test unit in a pool fire for more than 30 minutes in flames significantly hotter than 800°C.

3.3.2.1 Seam Burn Test

The seam burn tests were designed to measure performance of different design approaches of protecting polyethylene moderator from excessive heat during the hypothetical fire conditions. Previous burn tests had revealed a tendency for package structures to deform in pool fires potentially allowing hot gasses to enter the package. The tests, performed in a previously burned package with large gaps left between the upper and lower Outerpack to allow hot gases to enter the package. One section, used as a control, had no protection for interior structures. The second section covered the Outerpack seam with stainless steel hinges to model a design with essentially continuous hinges. The third section used 26 gage stainless steel to cover the moderator blocks. The steel cover sheet was stitch welded in place, leaving gaps for combustion air to enter. The test approach is described in appendix 3.6.2

The first burn was of the control section. During the 30 minute burn, internal temperatures rose within the test section throughout the test due to the gap deliberately left in the seam between Outerpack base and lid Peak internal temperatures over 500°C were observed, Figure 3-3.

The second test burn was of the section protected with essentially continuous hinge material. This section had a similar gap between the Outerpack base and lid, but gas flow through the package was minimized by the hinge sections. This burn lasted for 35 minutes with internal temperatures rising to 75°C (from an initial temperature of 35°C). After the burn was completed, interior temperatures continued to rise, peaking after 30 minutes at approximately 100°C.

The third test section was burned for 35 minutes as well. The internal temperatures measured show temperatures rose at a much higher rate than in the second test. This was expected because of the large gapes in the Outerpack seam (varying between 0.5 and 1.5 inches at the bottom seam). One thermocouple showed temperature at the bottom moderator blocks rose above 350°C within 25 minutes after the start of the burn.

After the pool fire was extinguished, some smoke was observed at the top Outerpack seam. This corresponded with a high temperature measurement on the moderator surface. Later examination showed that a small section of moderator burned for a limited period of time.

The seam burn tests showed that, where the Outerpack seam was covered by a hinge, that hot gas ingestion was virtually eliminated. Peak internal temperatures were approximately 100°C. With gaps in the Outerpack seams, peak internal temperatures exceeded the 350°C, the ignition temperature of polyethylene. Covering the moderator with stainless reduced the heat up rate, even with larger seam gaps, but moderator combustion took place near gaps in the stainless steel cover sheet. The tests showed that the best approach to prevent moderator combustion is to incorporate continuous hinge sections to prevent hot gas ingestion. The tests also showed that, to prevent combustion of moderator, assuming higher temperatures are experienced within the package, the stainless steel cover must be welded closed to prevent significant amounts of oxygen from reaching the polyethylene.

Figure 3-3 Seam Burn Test

3.3.2.2 Impact Limiter Burn Test

The seam burn tests described above examined the performance of the center portion of the package. The impact limiter burn test examined the thermal performance of the bottom end of the Traveller package. Both burns engulfed the bottom impact limiter and approximately 1.2 meters (four feet) of the package beyond the bottom impact limiter. Thermocouples were mounted at 16 locations inside and outside the package. The

test unit was mounted over the small weir built for the seam burn tests and burned for 40 minutes, Figure 3-4. Because the ambient temperature dropped below freezing during the night, initial temperatures inside the package started the test at approximately 0°C. Temperatures within the impact limiter pillow climbed to between 70 and 95°C depending on location during and after the burn test. Temperatures within the Outerpack interior cavity varied from 50 to 320°C. The only temperature measurements above 200°C were at locations near the outside skin of the Outerpack and well away from the moderator or impact limiter pillow.

The relatively high temperature observed at the Outerpack top seam led to questions of heat transfer. Was hot gas entering past the lip on the Outerpack door, or was the temperatures the result of heat conduction through the metal of the impact limiter bulkhead? The impact limiter burn test was therefore repeated but with Kaowool insulation stuffed into the Outerpack upper seam to prevent hot gasses from entering the package from that location. A 30 minute burn was performed in the late afternoon, so the initial temperatures inside the package were higher than the previous day. Temperatures within the Outerpack interior cavity varied from 80 to 340°C with the high temperatures being the closest to the Outerpack outer skin. Temperatures within the impact limiter pillow climbed to between 70 and 95°C depending on location during and after the burn test. The Outerpack top seam temperature rose to the same levels with insulation stuffed into the seam, demonstrating that the primary heat transport mechanism in this region is conduction. The slightly faster heat up rate can be attributed to several factors including the fact that the polyurethane insulating foam in the Outerpack had already been burned in earlier tests. These tests are described in greater detail in appendix 3.6.3 below.

Figure 3-4 December 15, Impact Limiter Burn Test

3.3.3 Margins of Safety

The Traveller protects its contents with a polyurethane insulated, double walled, stainless steel Outerpack. This Outerpack provides sufficient insulation to prevent significant heat conduction and maintain low interior temperatures during a hypothetical fire accident. The Outerpack also incorporates design features that prevent convective heat transfer. The tests described in 3.3.2 above, identified features (continuous hinge lengths and a large lip over the bottom seam) that prevent hot gases from entering the Outerpack seams. The results of these tests, as described in sections 3.5.2 and appendices 3.6.3 and 3.6.4 show that internal temperatures remain low when the Outerpack seams are adequately protected. These features were incorporated into the CTU test article and the production design. When the CTU was tested, significant margins of safety were observed as illustrated by Table 3-1 above. The most temperature sensitive component, the polyethylene moderator blocks, have an additional level of protection. The blocks are sealed by stainless steel cover sheets and are insulated at the ends. In the event that local conditions exceed the combustion temperature of the polyethylene, the moderator is protected by an insulating air gap (and refractory fiber felt insulation at the ends). Additionally, the moderator is isolated from oxygen preventing significant combustion.

3.4 THERMAL EVALUATION UNDER NORMAL CONDITIONS OF TRANSPORT+

The package will only be used to ship non-irradiated nuclear fuel. The contents contains no heat generating radioactive material. Therefore, the surface temperature of the package will not rise above ambient temperatures. As such, there is no need to evaluate by analysis or perform tests to demonstrate the maximum package surface temperature. All materials used within the Traveller package retain their desired properties over the entire range of possible ambient temperatures. The package is not hermetically sealed allowing interior pressure to adjust with changes in elevation and allowing expansion/contraction of internal air during temperature changes.

3.5 THERMAL EVALUATION UNDER HYPOTHETICAL ACCIDENT CONDITIONS

The primary verification of the Traveller's performance in a hypothetical accident was demonstrated in the burn test of a full-scale package loaded with a simulated fuel assembly. This unit was identified as the certification test unit (CTU). According to 10 CFR71.73 "Thermal. Exposure of the specimen fully engulfed, except for a simple support system, in a hydrocarbon fuel/air fire of sufficient extent, and in sufficiently quiescent ambient conditions, to provide an average emissivity coefficient of at least 0.9, with an average flame temperature of at least 800ºC (1475ºF) for a period of 30 minutes, or any other thermal test that provides the equivalent total heat input to the package and which provides a time averaged environmental temperature of 800ºC. The fuel source must extend horizontally at least 1 m (40 in), but may not extend more than 3 m (10 ft), beyond any external surface of the specimen, and the specimen must be positioned 1 m (40 in) above the surface of the fuel source. For purposes of calculation, the surface absorptivity coefficient must be either that value which the package may be expected to possess if exposed to the fire specified or 0.8, whichever is greater; and the convective coefficient must be that value which may be demonstrated to exist if the package were exposed to the fire specified. Artificial cooling may not be applied after cessation of external heat input, and any combustion of materials of construction, must be allowed to proceed until it terminates naturally." (The IAEA Regulations for the Safe Transport of Radioactive Material, Section VII-728 have similar specifications.)

A Traveller XL package was fabricated by Columbiana High Tech to serve as the certification test article. This unit was subjected to a regulatory drop test performed February 5, 2004 in Columbiana, Ohio. This package was transported to the South Carolina Fire Academy in Columbia, South Carolina on February 6. The package was installed in the burn pool and subjected to a 32 minute burn test on February 10, 2004. Although the Outerpack had suffered minor damage that allowed some urethane decomposition products to escape into the package interior, the fuel assembly, Clamshell, and polyethylene moderator were essentially undamaged.

The testing was conducted on a calm day. To further minimize the impact of winds, the burn pool was surrounded with an insulated steel diffuser that extended to the top of the package and expanded the effective fire area. The maximum distance between the package and the diffuser was less than the 3 meters maximum proscribed distance, Figures 3-5 and 3-6.

Twenty-two, inconel sheathed type-K thermocouples were used to measure flame temperature immediately around the Traveller and the Outerpack outer skin as shown in Figure 3-7. Before and during the pool fire, temperature measurements were made at 16 locations using type K thermocouples located. During the test temperatures were measured at six locations on the package skin, at twelve locations inside the pool fire, at four locations using directional flame thermometers (DFTs) facing away from the package, and from outside the fire using two optical thermometers.

Figure 3-5 Pool Fire Test Facility

Figure 3-6 Traveller CTU During Pool Fire Test

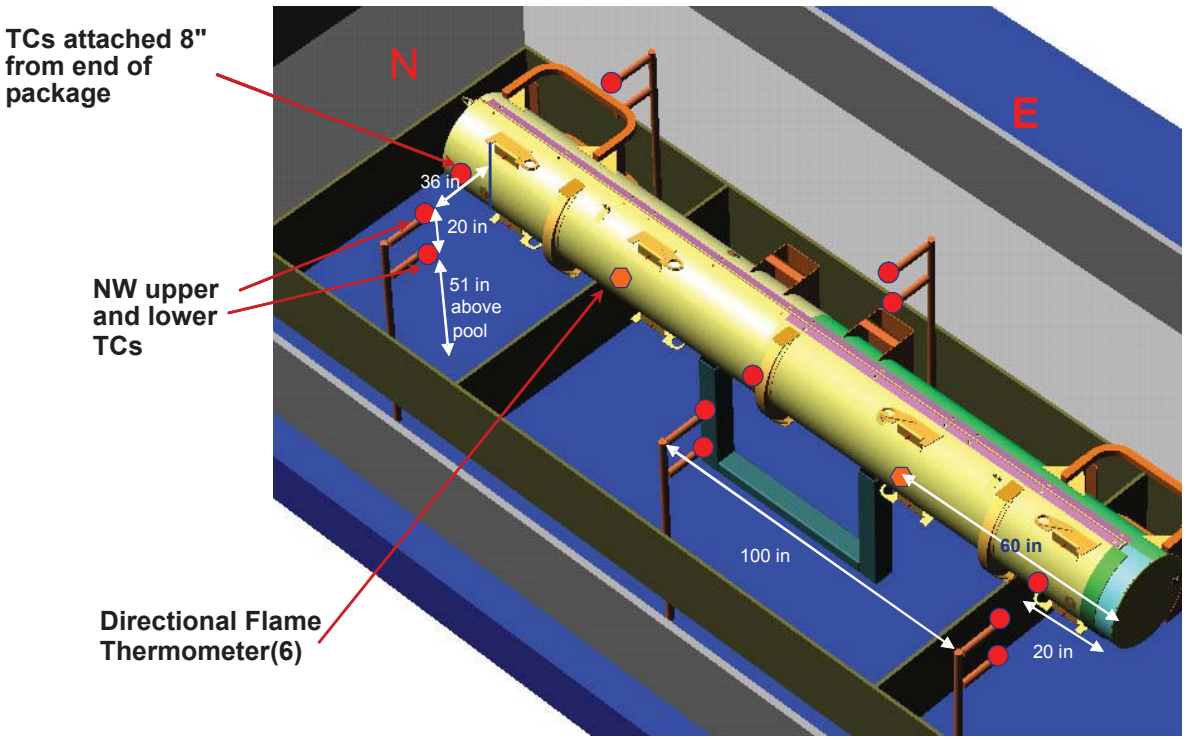

Figure 3-7 Thermocouple Locations Measuring Fire Temperature During CTU Burn Test

3.5.1 Initial Conditions

The package was covered with a canvas tent approximately 16 hours before the burn test. Two 44 kWth (150,000 BTU/hr) kerosene heaters were used, alternately, to maintain air temperature within the tent to above 37°C. The heaters were secured and the tent removed approximately 75 minutes before the beginning of the fire test. Air temperature around the package at this time averaged at 50°C (122°F). The air temperature and outside surface temperature dropped to approximately 5°C (41°F). Additional information can be found in appendix 3.6-4.

3.5.2 Fire Test Conditions

The CTU burn test was performed on a cool, calm, lightly overcast morning. The test article was located on a stand in a water pool. Fuel was pumped into manifolds under the surface of the pool to provide an even distribution of fuel for the pool fire. Approximately one minute after the fuel on the surface of the pool was ignited, the test article was completely engulfed. The fuel system continued to pump fuel into the fire until 32 minutes after the pool was lit. The pool fire was extinguished approximately one minute later. Fire temperatures were measured using four directional flame thermometers (DFTs) and 12 thermocouples suspended in the fire 0.9 m (3 feet) from the surface of the package. The 30 minute average temperatures measured by the DFTs were 833°C (1531°F). The 39 minute average temperature measured by the thermocouples suspended in the fire was 859°C (1578°F). Two, hand-held, optical thermometers that measured flame temperature from outside the pool supplemented these measurements. The average readings made with these thermometers was 958°C (1757°F).

3.5.3 Maximum Temperatures and Pressures

Temperatures were measured on the CTU Outerpack outer skin using six type K thermocouples, attached by screws. These thermocouples were located as shown in Figure 3-7 above. The 30 minute average temperature measured by these thermocouples was 904°C (1659°F). Temperatures inside the CTU Outerpack were measured using 13 sets of non-reversible temperature strips. One set on the inner stainless steel skin covering the Outerpack lid moderator was unreadable. All of the remaining temperature strips on the Outerpack lid recorded temperatures of 177°C (351°F) or below. Temperatures on the inside surface of the top and bottom impact limiters were 116 (241°F) and 149°C (300°F) respectively. Temperatures inside the Clamshell were below 104°C (219°F). An example of the temperature strip sets attached to the Outerpack lid moderator cover sheets is shown in Figure 3-8.

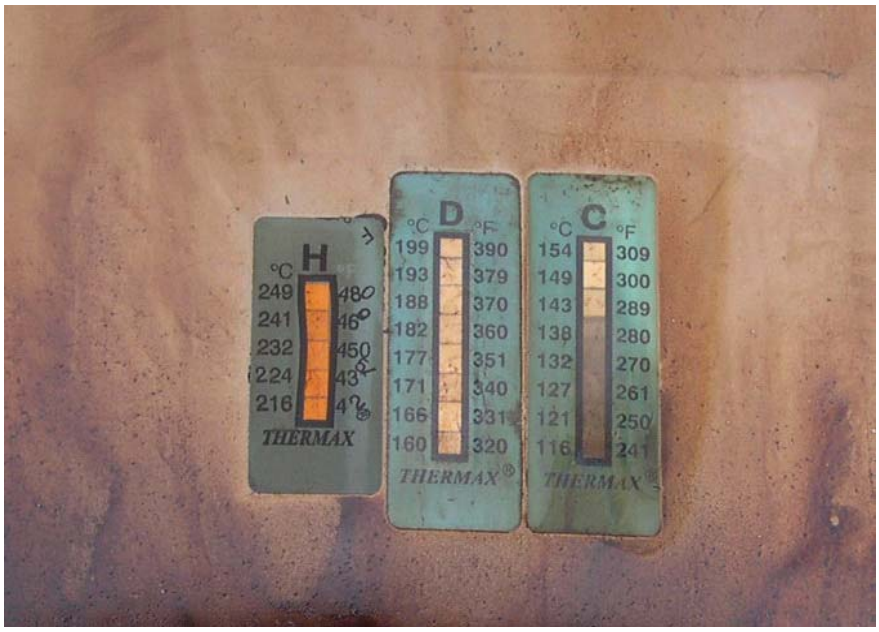

Figure 3-8 Temperature Strip Condition After CTU Burn Test

Although the thermal testing was done with the fiberglass seal, the detailed evaluation of the package after test revealed that the Outerpack hinge was the effective heat shield [1]. The temperature of the moderator blocks during this testing never reached even 100ºC, well below the ignition temperature of the polyethylene moderator blocks or melting temperature of the aluminum clamshell material. The braided fiberglass gasket material alone was not an effective heat shield and did not provide any significant barrier to limiting the heat-up of the interior of the package during the thermal testing. The fiberglass seal was retained to provide packaging weather gasket to keep dust, dirt and spray from getting inside the Outerpack. The seal material may be either braided fiberglass or soft conformable silicone rubber as shown in Figure 3-8A.

The Traveller package design is non-pressurized and cannot retain internal pressure. Weather gasketing seals are discontinuous to prevent internal pressurization during the hypothetical fire and during normal variations in temperature and atmospheric pressure. The polyurethane foam space between the inner and outer shells of the Outerpack is protected from pressurization through the use of vent plugs. Every internal foam compartment within the Outerpack is protected by at least one acetate vent plug that will melt in the event of a fire and allow the internal spaces to vent. As a result, no significant increase in pressure was observed during the testing, nor is anticipated in any hypothetical accident condition.

The Traveller design surrounds the fuel assembly and polyethylene moderator with an insulated outer package. As a result, the outer surface of the package quickly reaches equilibrium with the fire while the interior remains cool. This is indicated by analysis and by the burn tests described above. The peak temperature measured on the Clamshell and the moderator covers were consistent between the seam burn test, the impact limiter burn test and the CTU burn test. All temperatures remained below 177°C and most locations remained below 100°C. No significant thermal damage was observed in the fuel assembly,

Clamshell or moderator blocks after the fire test. Moderator blocks were weighed before and after the fire test. No measurable reduction in mass was found.

.

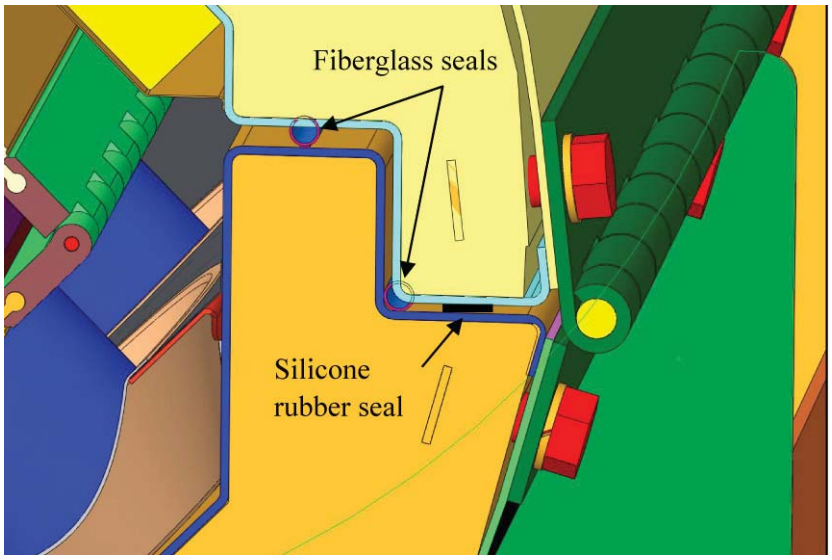

Figure 3-8A Outerpack Flange Joint Showing Location of Packaging Weather Seal Gasket Options (1) Fiberglass Seal or (2) Silicone Rubber Seal

3.5.4 Accident Conditions for Fissile Material Packages for Air Transport

Application will be made for air transport at a later date.

This page intentionally left blank.

3.6 APPENDICES

The following appendices are included to provide amplifying information on material contained elsewhere in section 3.

- 3.6.1: References
- 3.6.2: Traveller Thermal Analysis
- 3.6.3: Traveller Seam Burn Tests
- 3.6.4: Traveller Impact Limiter Burn Tests
- 3.6.5: Traveller Certification Test Unit (CTU) Burn Test

3.6.1 References

1. CN-NFPE-09-86, (7/14/2009), "Justification for Removal of Traveller Heat Seal," Westinghouse Proprietary Class 2.

This page intentionally left blank.

3.6.2 Traveller Thermal Analysis

A simplified computer model was developed using the HEATING7.2 code distributed by Oak Ridge National Laboratory as a part of SCALE 4.4. The model was built in cylindrical coordinates using the simplified geometry shown in Figure 3-9. This simplification was possible because:

- Primary temperature variations occur in the Outerpack foam that is cylindrical on the outside
- Simplifying interior foam surface by making it cylindrical is conservative
- The large length to diameter ratio (8.9:1) minimize end effects
- The ends have twice the thickness of polyurethane foam as the sides further reducing end effects

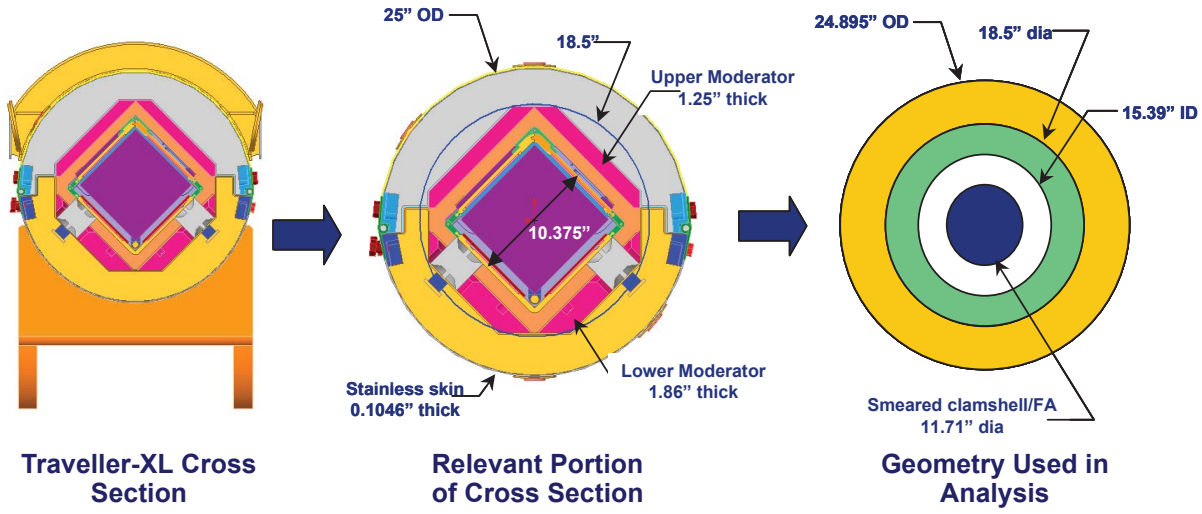

Figure 3-9 Approach Used to Generate Analytical Model Geometry

Three material regions were used in the analysis: Polyurethane foam with an average density of 10 lb/ft^3, Polyethylene, and a smeared mixture representing the mid-section of the Clamshell and fuel assembly.

The Clamshell and fuel assembly region was modeled as a heat sink representing a 17x17 XL fuel assembly within the 9.50 inch (24.13 cm) inside dimension aluminum Clamshell. Because the end effects were to be ignored in this model, the fuel assembly nozzles and the Clamshell end plates were not included in this calculation. This resulted in the following material ratios:

- Aluminum Clamshell – 359.7 lb (163.2 kg) with a specific heat of 0.23 BTU/lb-°F (0.96 J/g-°C),
- Uranium Dioxide – 1341 lb (608.3 kg) with a specific heat of 0.0565 BTU/lb-°F (0.237 J/g-°C)
- Zircalloy 4 – 330 lb (149.7 kg) with a specific heat of 0.0681 BTU/lb-°F (0.285 J/g-°C)

The Traveller XL Clamshell is 202.0 inches (513.1 cm) long. The heat sink region weighs 2031 lb (921.1 kg), has an average specific heat of 0.891 BTU/lb-°F (0.373 J/g-°C) and a smeared density of 0.0934 lb/in^3 (2.58 gm/cc).

A volumetric average conductivity was generated for the Clamshell and fuel assembly region by calculating a volume smeared conductivity by using the ratio of conductivity to volume for each material.

- Aluminum Clamshell – 3560 in^3 (58,300 cc) with a conductivity of 104 BTU/hr-ft-F (182 W/m-K)
- Uranium Dioxide – 3380 in^3 (54,500 cc) with a conductivity of 3.39 BTU/hr-ft-F (5.86 W/m-K)
- Zircalloy 4 – 1400 in^3 (23,000 cc) with a conductivity of 12.4 BTU/hr-ft-(21.5 W/m-K)

Total volume used in the Clamshell/fuel assembly region is 21,700 in^3 (356,000 cc). This results in a smeared conductivity of 18.3 BTU/hr-ft-F (32.1 W/m-K). This approximation is valid only because the heat input rate is very low allowing the region to be almost isothermal, even with low conductivities.

The Traveller XL Outerpack contains approximately 426 lb (193 kg) of UHMW polyethylene with specific heat of 0.526 BTU/lb-°F (2.2 J/g-°C) and a conductivity of 24 BTU/hr-ft-°F (0.42 W/m-°C). The total length of the moderator within the Outerpack is approximately 206 inches (523 cm). For the geometry defined for the model, this results in a smeared polyethylene density of 0.0249 lb/in^3 (0.689 g/cc) which is 74% of predicted minimum density. The polyethylene acts as a heat sink and an insulation of primary heat sink.

The polyurethane foam room-temperature properties are given in Table 3-5. The properties change significantly, however, as the foam temperature increases resulting in pyrolization which occurs between 600 and 650°F (316 and 343°C). After charring, the material has the general appearance of very low density carbon foam. For the analytical model, the room temperature specific heat and conductivity were used up to 600F. Above 650°F, the temperature dependent conductivity of air was used instead. Between 600 and 650°F, foam specific heat is assumed to drop to zero.

Table 3-4 Temperature Dependent Thermal Conductivity Used to Model Polyurethane Foam

Temperature (F)	Conductivity (BTU/hr-ft-F)	Conductivity (W/m-K)
100	.0230	.0398
600	.0230	.0398
650	.0249	.0431
700	.0268	.0464
800	.0286	.0495
1000	.0319	.0552
1500	.0400	.0692
2000	.0502	0.0869

The surface emissivity of the foam was set at 0.8. The first analysis performed modeled a 30 minute fire with flame temperature of 800°C. This analysis, Figure 3-1, showed significant temperature variation through the thickness of the polyurethane foam. Peak temperatures on the inside surface of the foam reached 100°C approximately 80 minutes after the beginning of the fire (50 minutes after the fire was put out).

Because the planned fire test facility burns at a higher temperature, the same analysis was performed assuming a 1000°C fire temperature. As shown in Figure 3-3, peak temperature within the polyethylene (at the interface between the polyurethane foam and the polyethylene) was calculated to reach 106°C. This is below the 125 – 138°C melt temperature of the polyethylene and well below the temperature that the melted polyethylene viscosity is low enough to flow easily.

The thermal analysis performed demonstrated several important features/characteristics of the design. Because of the urethane foam insulating the Outerpack, exterior skin temperatures quickly rise to near equilibrium with the fire outside the package. The clamshell and fuel assembly temperature, rise very slowly due to the insulation and the specific heat of the aluminum clamshell, polyethylene moderator, and the fuel assembly. The primary mechanisms that can result in significantly higher internal temperatures is hot gas infiltration during the fire and internal combustion during and after the fire test. We do not believe that these mechanisms can be accurately predicted by analysis. As a result, the Traveller team chose to demonstrate the package using pool fire tests, culminating with a full-scale fire test.

The seam burn tests with continuous hinge sections demonstrated approximately 60°C temperature rise during and after the test which was in close agreement with the 50°C temperature rise predicted by the analysis. The CTU burn test demonstrated internal temperatures between 116° and 177°C. This is 112° to 173°C higher than the air temperature that morning. These values are only 66° to 127°C higher than the equilibrium package temperatures maintained by heaters before the fire. As noted above, the external skin temperature at the middle of the package was significantly higher at the middle. Secondly, the amount of hot gas entering the package at different locations along the length clearly affects the local internal temperatures. Greater quantities of hot gas probably entered that package at that location.

Because of the fundamental limitations of the analysis (e.g., inability to predict precise geometry changes during the fire) the analysis model was never refined and exact agreement was never anticipated with test results. The analysis does illustrate the fundamental mechanisms involved and the general characteristics of the package response, assuming no significant gas infiltration or geometry changes.

3.6.3 Traveller Seam Burn Tests

This test examined two methods of protecting the polyethylene to prevent combustion and/or significant melting. One was the use of continuous hinges to seal the gap at the seam and the second was to cover the moderator with stainless steel sheet to prevent combustion. A third test section was also created to act as the test control. This section did not have any additional protection for the moderator.

The test was performed as series of three burns, heating the reference or control section, the section with additional hinge to model a package with continuous hinges, and the section with stainless covering over the moderator respectively. The first burn lasted 30 minutes. The two subsequent burns lasting for 35 minutes. A small pool fire (approximately 30 x 80 inches) was be created under the region of the package to be tested, Figure 3-10. Each region was approximately 57 cm (22.4 inches) across separated from the adjacent test region by 61 cm (24 inches) of refractory fiber felt insulation. This insulation was stuffed between the Clamshell and the moderator to prevent air flow from the section being tested to other test regions within the prototype package. The test regions were selected based having intact moderator left from previous tests. The test section with stainless steel cover over the moderator was selected based on the minimum distortion of the inner Outerpack shell and moderator blocks. The outside of the package was insulated on the bottom and sides using at least 2.5 cm (one inch) of refractory fiber felt insulation. This insulation will extend at least 1.2 m (48 inches) from each end of the test region, Figure 3-11.

Six thermocouples were attached in each test section. Two were screwed to the moderator bottom edge nearest the seam, one was screwed to the moderator/Outerpack where the two moderator blocks meet, one was screwed to the moderator block near the top seam, one was screwed to the Clamshell J-clip, and one was run through the bottom seam to hang approximately four inches below the package in the flames. Thermocouple connections and Teflon coated wires were routed out of the package at each end.

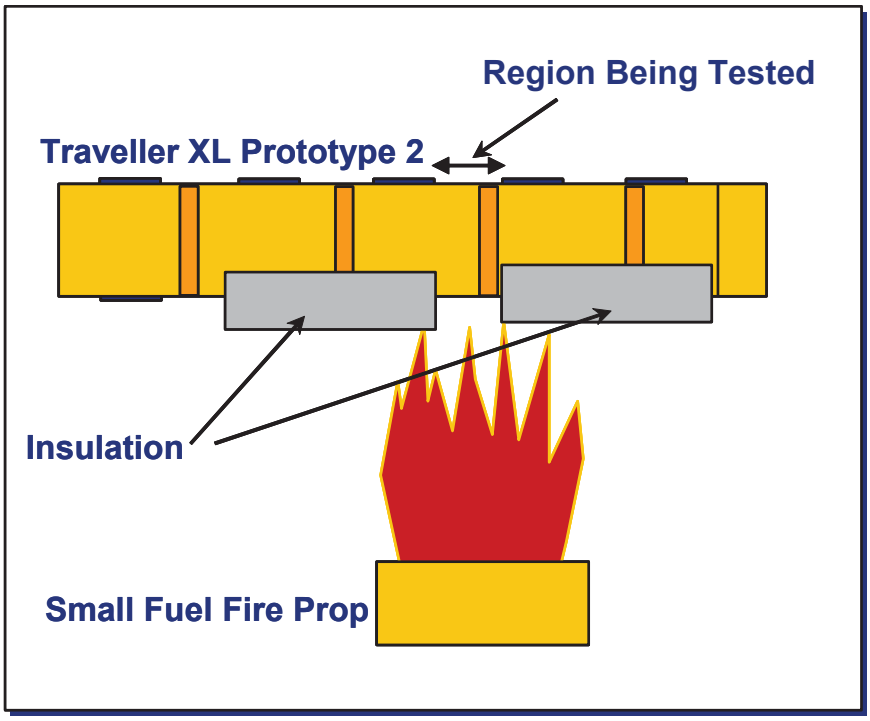

Figure 3-10 Seam Burn Test Orientation

Figure 3-11 Package Exterior Wrapped with Ceramic Fiber Insulation

3.6.3.1 Test Results

The first test burn was on the unprotected, control section of the package on October 3. Due to strong winds, flames did not stay on the test section. As a result, temperatures remained low and ultimately the thermocouple wires were burnt before the test was completed. Afterward, the weir was modified to extend the height up to the bottom of the package to confine the flames to the test region.

The burn of the control section was then repeated on October 6. The new weir confined the fire to the test section and temperatures rose within the test section throughout the test, Figure 3-12. After the pool fire was extinguished, burning polyurethane was observed along the top seam of the package and at the bottom seam of the test section. This was extinguished after approximately 10 minutes and the package was opened. Significant moderator was lost.

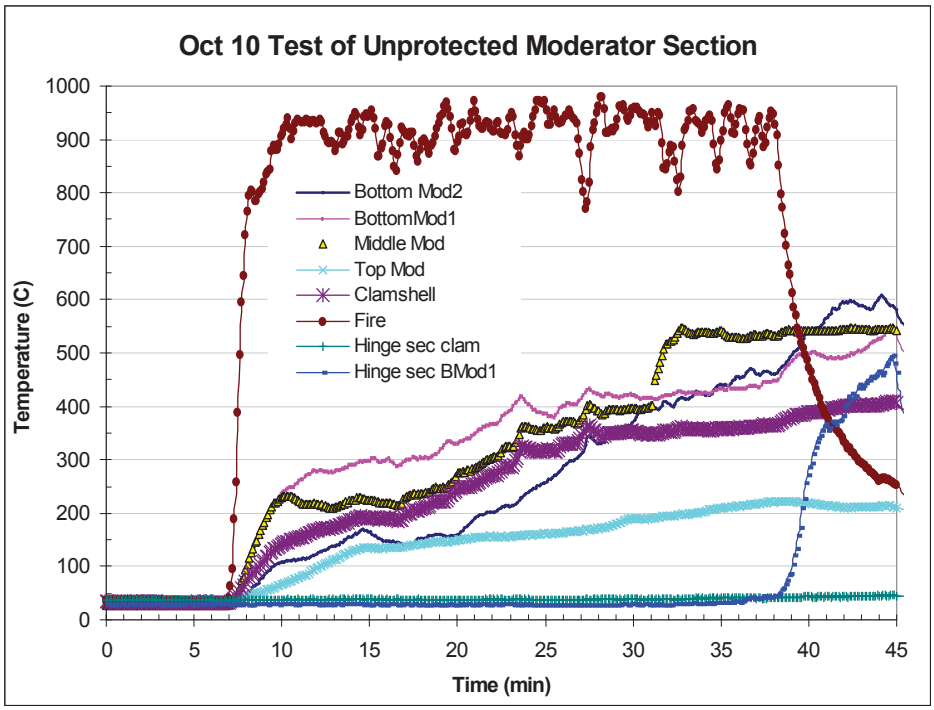

Figure 3-12 Measured Temperatures During Second Burn of the Control Section

The package was then closed, reinsulated, and the section modeling continuous hinges tested. This burn lasted for 35 minutes instead of the 30 minutes in the previous test. Thermocouple data, Figure 3-13, was incomplete because two of the channels (the external fire temperature and the middle moderator thermocouples) were bad. The latter produced very noisy data indicating that a connector was bad and the former did not change values throughout the test. Subsequent inspection revealed that the thermocouple itself was broken at the Outerpack seam. The data that was gathered from the internal thermocouples in the hinge test section and in the adjacent control section showed little change in internal temperatures. Temperatures rose very slowly during the burn test, with internal temperatures reaching a peak of 75°C at

the end of the test. After this data was collected and saved, additional temperature data was collected during the next 30 minutes after the burn, Figure 3-14. Temperatures slowly increased to approximately 100°C. This is consistent with thermal analysis that shows that heat transfer by conduction through the Outerpack polyurethane foam will continue to add heat to the interior for over an hour after the beginning of the burn, see section 3.1.

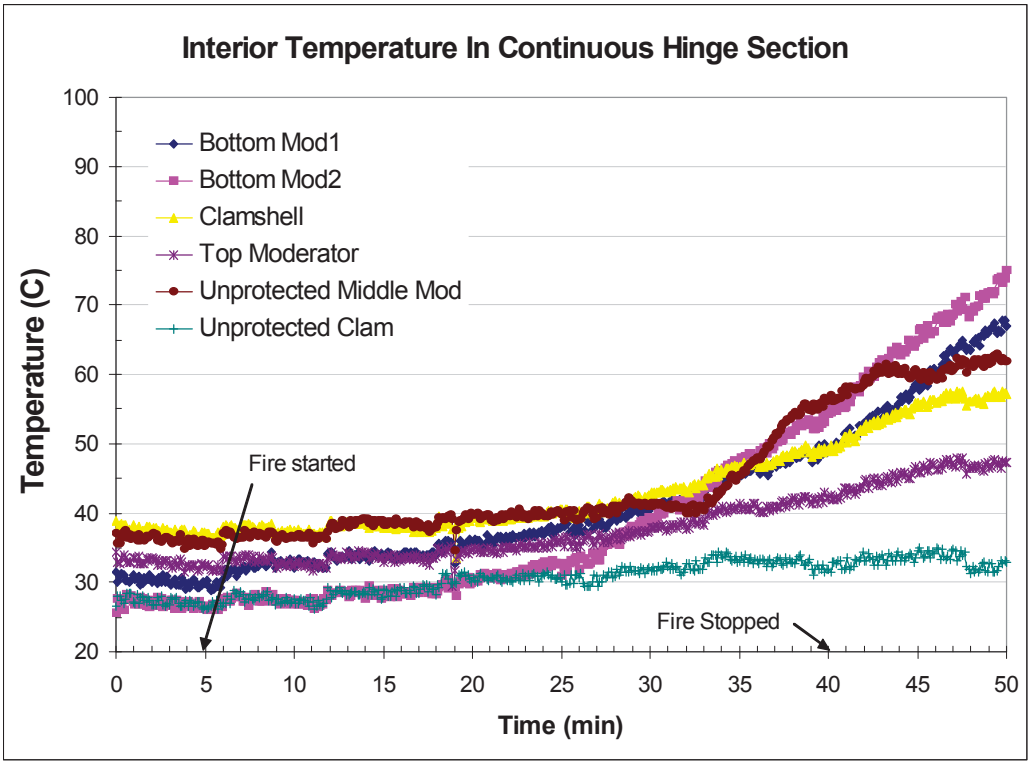

Figure 3-13 Interior Temperature Measurements During Test of Continuous Hinge Section

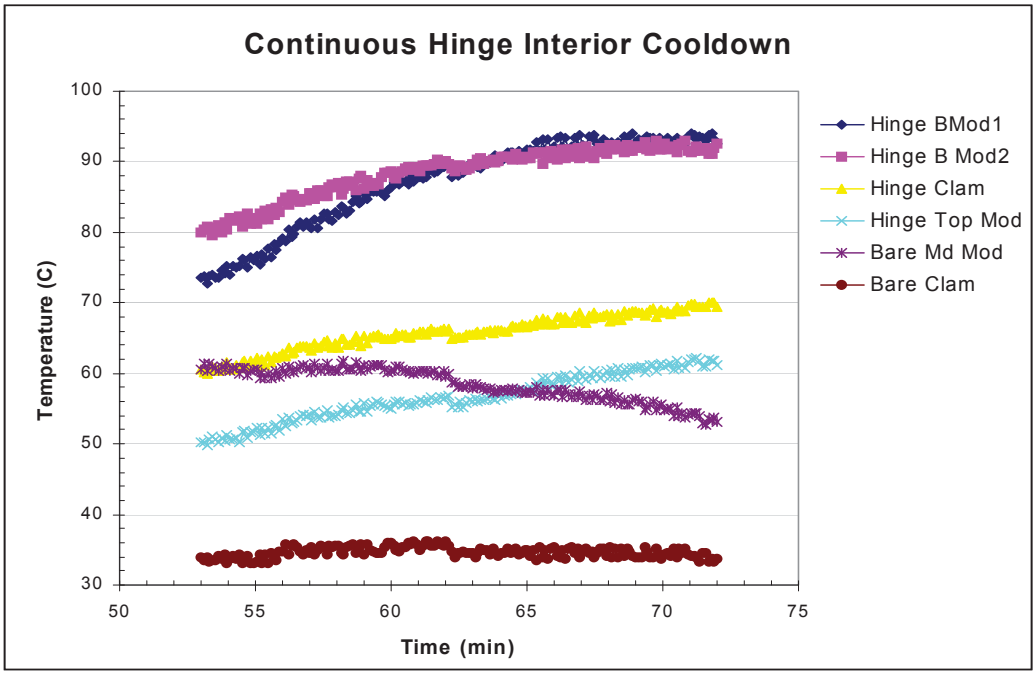

Figure 3-14 Interior Temperature Measures After Test of Continuous Hinge Section

The package was then moved on the test stand and positioned with the third test section, the covered moderator, over the burn weir. This section was burned for 35 minutes as well. The internal temperatures measured, Figure 3-15, show temperatures rose at a much higher rate than in the second test. This was expected because of the large gapes in the Outerpack seam (varying between 0.5 and 1.5 inches at the bottom seam), Figure 3-16. One thermocouple showed temperature at the bottom moderator blocks rose to above 350°C within 25 minutes after the start of the burn. After the pool fire was extinguished, some smoke was observed at the top Outerpack seam. This corresponded with an eventual rise in moderator temperature at one location after the external fire had been extinguished. After approximately 15 minutes, the package was cooled by water spray and removed from the burn pool. When opened, there was not initial sign of damage. After the stainless steel covering the moderator was removed, however, it was confirmed that small amounts of the moderator had burned.

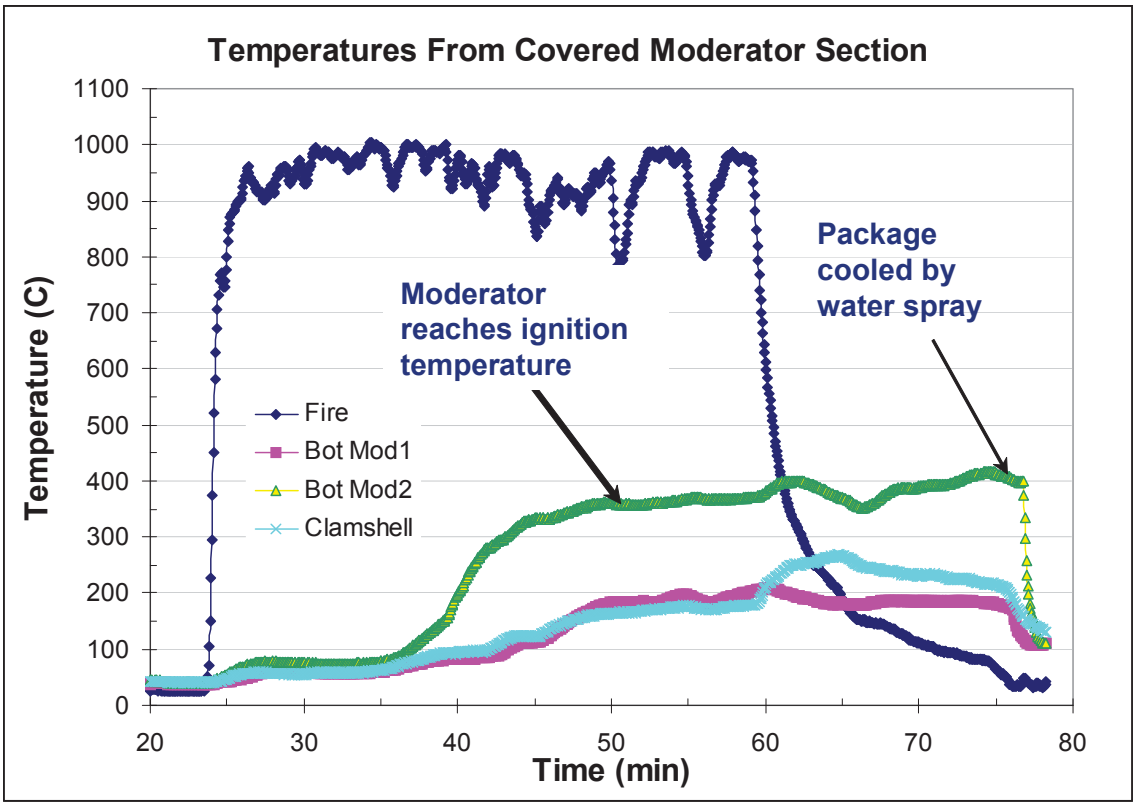

Figure 3-15 Interior Temperature Measurements During Test of Covered Moderator Section

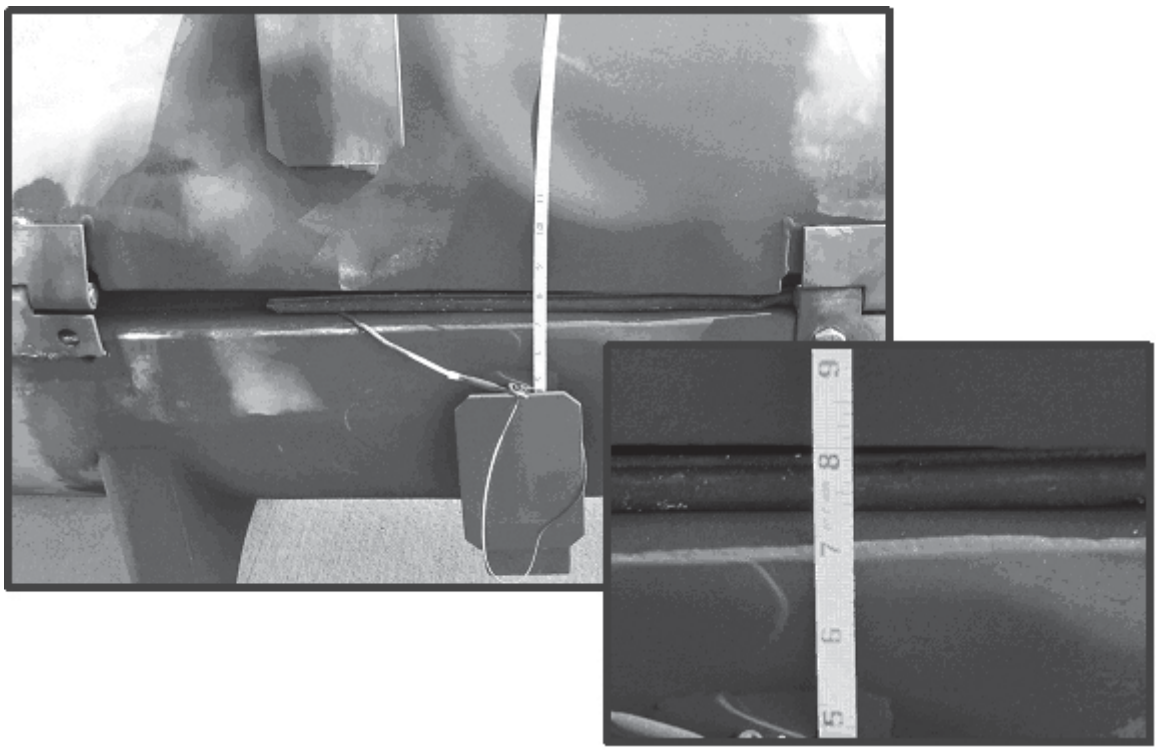

Figure 3-16 Gaps in Outerpack Bottom Seam at Covered Moderator Test Section

3.6.3.2 Conclusions

Tests showed that, where the Outerpack seam was covered by a hinge, that hot gas ingestion was virtually eliminated. Peak internal temperatures were approximately 100°C. With gaps in the Outerpack seams, peak internal temperatures exceeded the 350°C ignition temperature of polyethylene. Covering the moderator with stainless did appear to reduce heatup rate, even with larger seam gaps, but moderator combustion took place anyway. The tests showed that the best approach to prevent moderator combustion is to incorporate continuous hinge sections to prevent hot gas ingestion during the burn test.

3.6.4 Traveller Impact Limiter Burn Tests

A Traveller package was subjected to two burn tests after being tested in a full series of regulatory drops. This test series focused on the heat transfer characteristics of the bottom end of the package. This end is referred to as the bottom impact limiter. The top and bottom impact limiters are divided into two regions with high (20 lb/ft^3) density foam in the outer regions and low density foam (6 lb/ft^3) pillows inside. The foam pillow is separately encased in stainless steel with a 0.64 cm (0.25 inch) impact plate to minimize the chance of exposing the foam. Each pillow also has a 0.64 cm (0.25 inch) thick plate out the outer end as a heat sink to reduce peak temperatures in a fire. The foam pillow is also separated from the inside end of the outer impact limiter foam with approximately 0.32 cm (0.125 inches) of refractory fiber felt insulation.

During both tests, the package was instrumented with 16, inconel sheathed, type K thermocouples (Omega part numbers XCIB-K-4-2-10 and XCIB-K-2-3-10). Seven thermocouples were mounted on or around the impact limiter pillow, one midway through the outer impact limiter foam, and one on the outer impact limiter skin, Figure 3-17. The remaining seven thermocouples were mounted inside the Outerpack. The location of the thermocouples is shown in Figure 3-18.

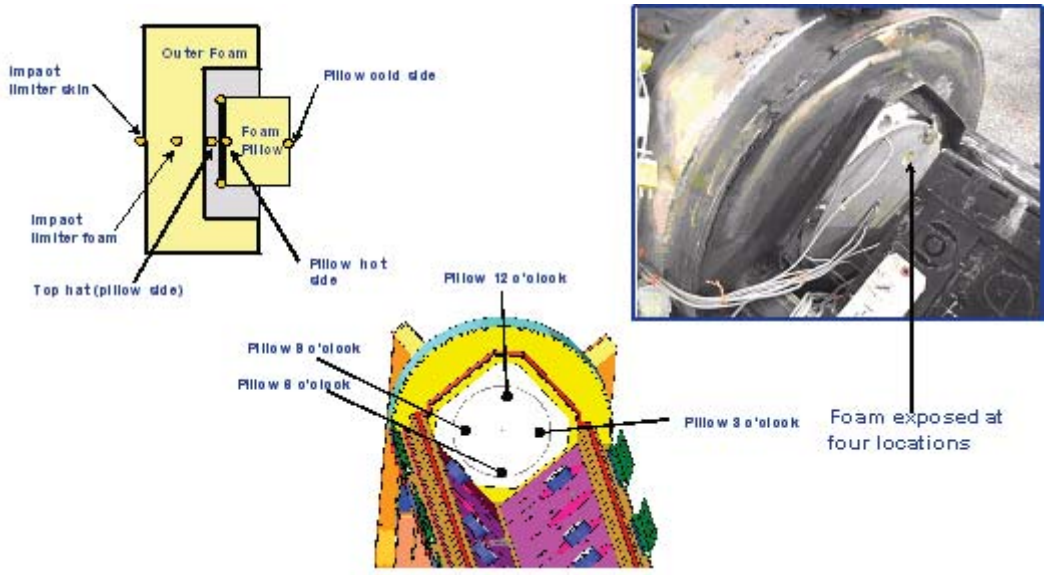

Figure 3-17 Thermocouple Locations in Impact Limiter

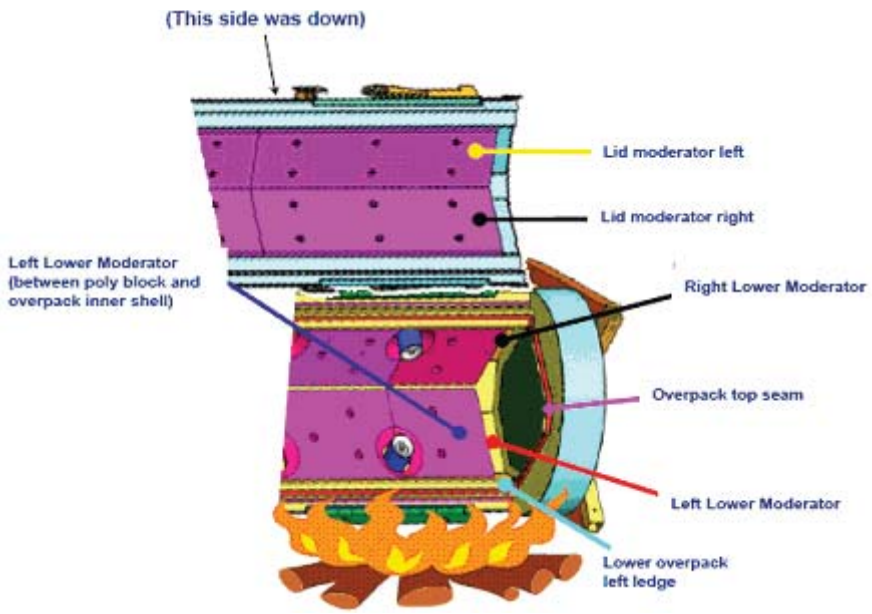

Figure 3-18 Thermocouple Locations in Outerpack Interior

The thermocouples were connected to thermocouple wire extensions using standard Type K plugs connecting the thermocouples to 20 gage type K extension wire. The 16 thermocouple cables were connected to two data acquisition systems. One system used an Omega OM-CP-OCTTEMP 8-channel data logger. This unit was set in operation before the test using a laptop computer and stored data from each channel at a rate of 12 samples per minute. After the test was completed, the data was download to the same laptop computer. The second system used an 8-channel Omega INET-100 external A/D box connected to an INET-230 PC-Card controller with a INET 311-2 power supply. This recorded data directly into the laptop computer allowing these channels to be monitored during the test.

Additional data was taken on external temperatures using two OMEGA OS523 handheld optical thermometers during the December 15 test. These units were used to measure flame temperatures and outside package skin temperature after the pool fire was extinguished.

A previously drop tested unit was modified to incorporate these changes in the bottom impact limiter and was subjected to two burns, one on December 15, and the second on December 16. Both burns engulfed the bottom impact limiter and approximately 3 feet of the package above the bottom impact limiter. Thermocouples were mounted at 16 locations inside and outside the package. Data from eight of the thermocouples were recorded by a laptop PC based Instrunet system that allowed data to be monitored in real time. The other eight channels were recorded using a battery powered Omega data logger.

3.6.4.1 First Impact Limiter Burn (December 15)

The test unit was mounted over the small weir built for the seam burn tests and burned for 40 minutes, Figure 3-19. Because the ambient temperature dropped below freezing during the night, initial temperatures inside the package started the test at approximately 0°C. Temperatures within the impact limiter pillow climbed to between 70 and 95°C depending on location during and after the burn test, Figure 3-20. Temperatures within the Outerpack interior cavity varied from 50 to 320°C, Figure 3-21.

Figure 3-19 December 15, Impact Limiter Burn Test

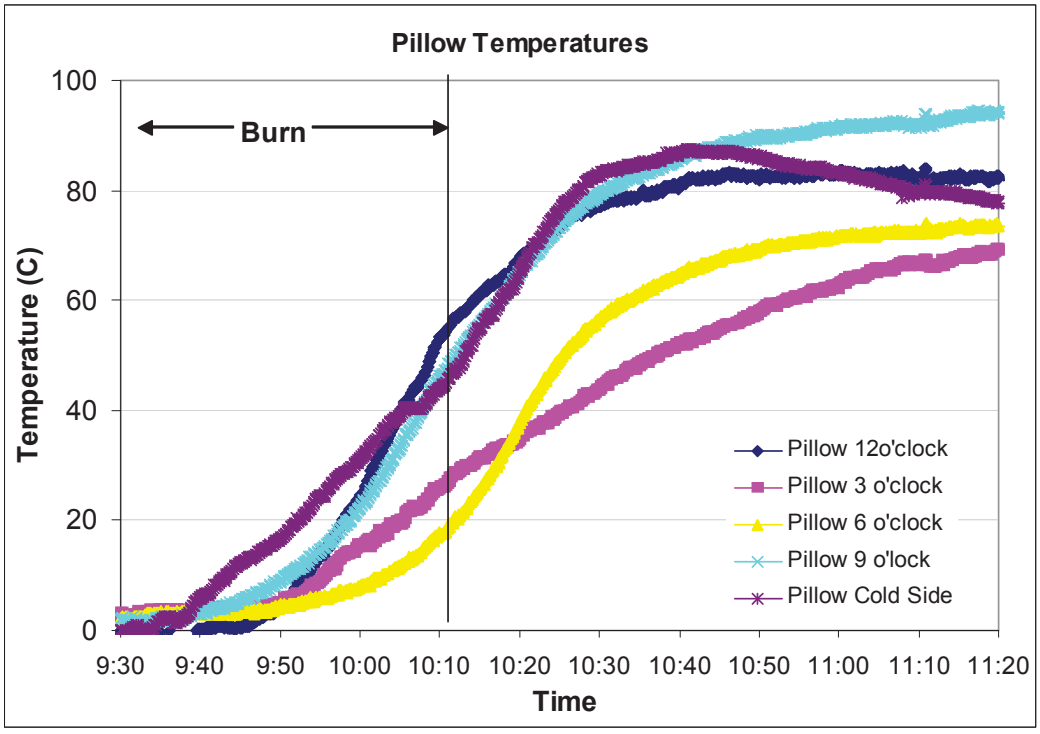

Figure 3-20 Impact Limiter Pillow Temperatures

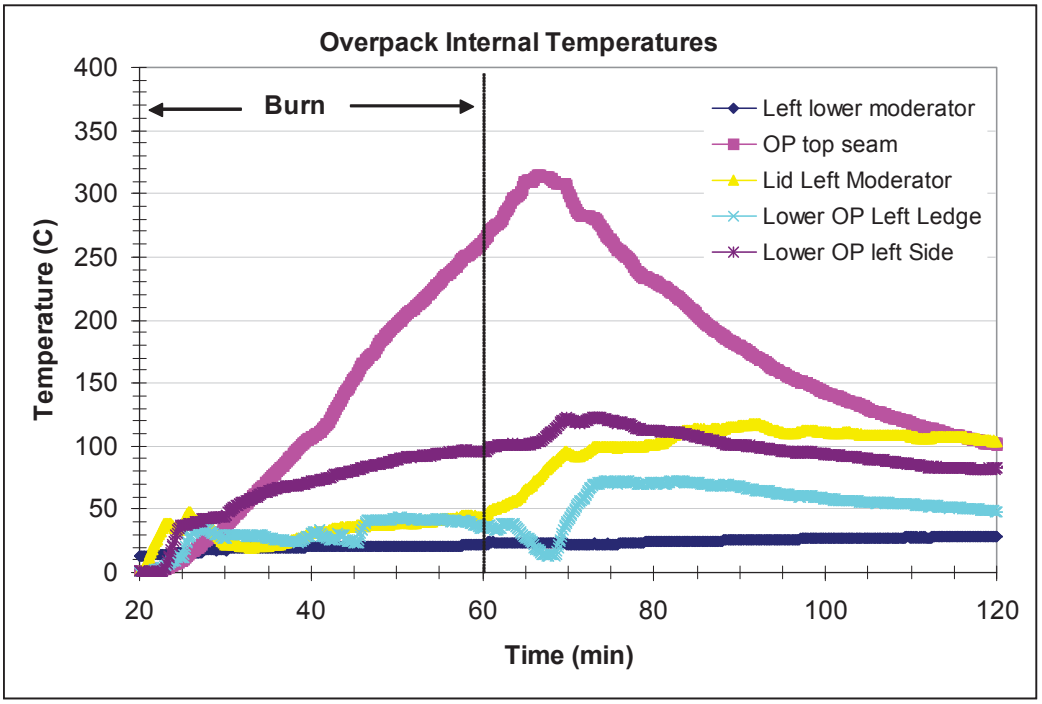

Figure 3-21 Internal Outerpack Skin Temperatures (December 15 Burn)

During this test, external temperatures were measured with two optical thermometers. Readings were taken every five minutes, Figure 3-22. After the test was completed, the Outerpack was opened. Other than a thin layer of soot lining the inside surfaces, there was no noticeable change in the Outerpack or Clamshell, Figure 3-23.

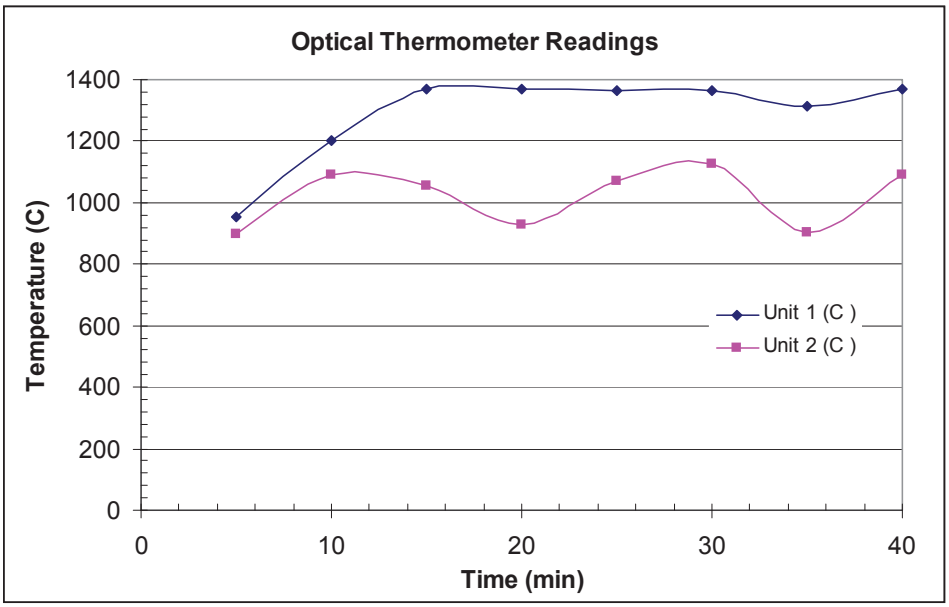

Figure 3-22 Flame Temperatures Measured by Optical Pyrometers

Figure 3-23 Outerpack Internals after December 15 Burn Test

3.6.4.2 Second Impact Limiter Burn (December 16)

The relatively high temperature observed at the Outerpack top seam led to questions of heat transfer. Was hot gas entering past the lip on the Outerpack door, or was the temperatures the result of heat conduction through the metal of the impact limiter bulkhead. The impact limiter burn test was therefore repeated but with Kaowool insulation stuffed into the Outerpack upper seam to prevent hot gasses from entering the package from that location, Figure 3-24. This burn lasted for 30 minutes, Figure 3-25. This test was performed in the late afternoon, so the initial temperatures inside the package were higher than the previous day. Temperatures within the Outerpack interior cavity varied from 80 to 340°C, Figure 3-26. Temperatures within the impact limiter pillow climbed to between 70 and 95°C depending on location during and after the burn test, Figure 3-27. The Outerpack top seam temperature rose to the same levels with insulation stuffed into the seam, demonstrating that the primary heat transport mechanism in this region is conduction.

Figure 3-24 Kaowool Layers on Outerpack Bottom Impact Limiter

Figure 3-25 December 16 Impact Limiter Burn

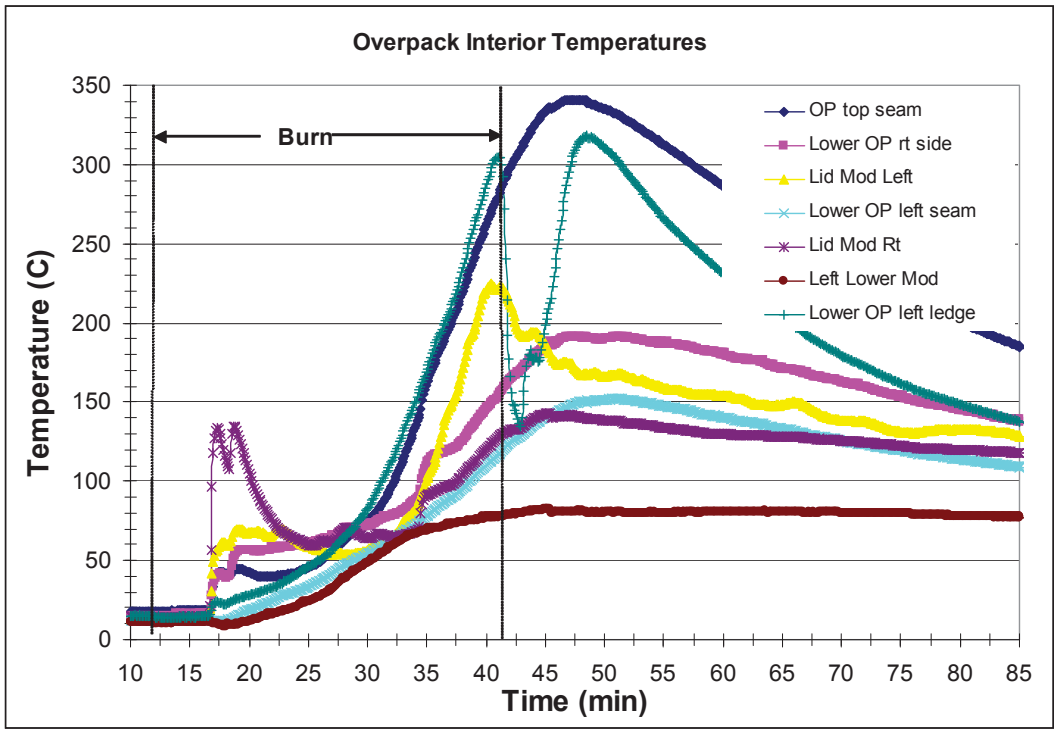

Figure 3-26 Internal Outerpack Skin Temperatures (December 16 Burn)

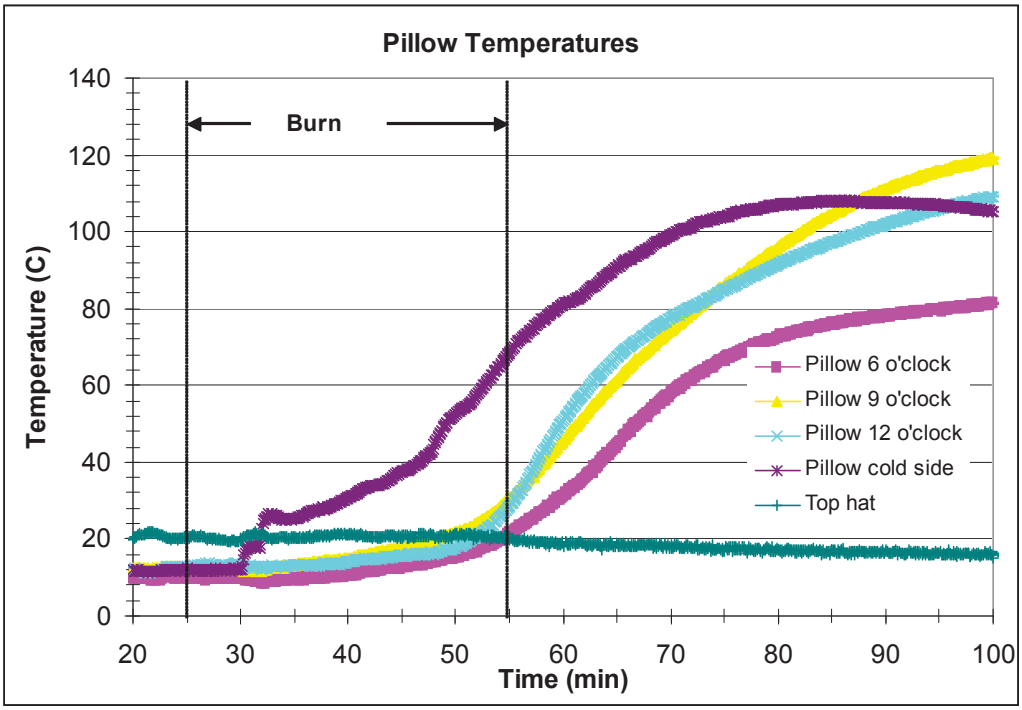

Figure 3-27 Impact Limiter Pillow Temperatures (December 16 Burn)

3.6.4.3 Test Conclusions

The purpose of the December 16 test was to repeat the previous day's test ensuring that hot gases did not flow around the Outerpack lid bottom lip. The heat up rate of the Outerpack top seam was slightly higher during the second burn than the first. Three factors may explain the higher temperatures during the second test.

- Foam in the impact limiter was charred during the first test resulting in higher heat transfer during the second test.

- The kaowool used to fill the bottom seam prevented the lid from closing as tightly as in the first test. This may have allow small amounts of combustion gas from the pool to enter the package

- During the first 5-6 minutes of the burn, fuel was sprayed directly on the outer skin of the package.

The test demonstrated that the revised impact limiter design will not overheat during a regulatory burn test. Even if the initial temperature is raised by 50°C, final temperature of the impact limiter pillow is anticipate to be less than 150°C. The test also demonstrated that very little gas is entering the Outerpack through the side or top seams. The interior skin is heating up however, due to conduction through metal parts of the Outerpack and through the polyurethane foam. The impact limiter tests results are conservative because the

foam in the cylindrical section of the package was not replaced and, therefore, did not provide the insulation that a unburnt package would have.

3.6.5 Traveller Certification Test Unit Burn Test

A Traveller XL package was fabricated by Columbiana High Tech to serve as the certification test article. This unit was subjected to a regulatory drop test performed February 5, 2004 in Columbiana, Ohio. This package was transported to the South Carolina Fire Academy in Columbia, South Carolina on February 6. The package was installed in the burn pool and burned February 10, 2004, Figure 3-28. Although the Outerpack had suffered minor damage that allowed some urethane decomposition products to escape into the package interior, the fuel assembly, Clamshell, and polyethylene moderator were essentially undamaged. (Please see section 2.12.4.2.3 in the Safety Analysis Report (pp 3-183 through 3-192) for description of the CTU drop tests and the resulting damage.)

The test was performed with the following objectives:

- Test Traveller package in manner that meets or exceeds regulatory requirements of TS-R-1 and 10CFR71.
- Demonstrate that the fuel assembly survives intact, without potential release of radioactivity.
- Demonstrate that the polyethylene moderator survives essentially intact retaining at least 90% of the hydrogen within the polyethylene.
- Demonstrate that the fuel assembly survives without cladding rupture caused by excessive temperatures inside the Clamshell

Figure 3-27A shows the orientation of the Certification Test Unit (CTU) for the thermal test. The bottom of the package was positioned approximately 1 meter from the top of the fire pool surface. The distance of the outer facility walls beyond the edge of the package were 67" at the ends and 71.5" at the sides

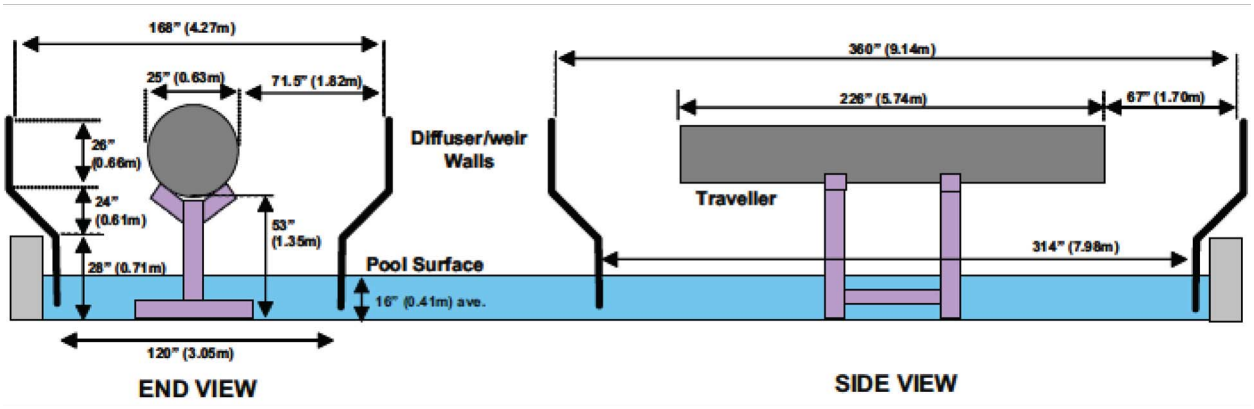

Figure 3-27A Orientation of CTU for Thermal Test

.During this test, the package was engulfed for approximately 32 minutes. Prior to the burn test, the package was heated overnight to ensure that the interior of the package remained above 38°C (100°F). During the test temperatures were measured at six locations on the package skin, at twelve locations inside the pool fire, at four locations using directional flame thermometers (DFTs) facing away from the package, and from outside the fire using two optical thermometers, Figure 3-29. The 30 minute average temperatures were 904°C (1659°F) on the package skin, 859°C (1578°F) within the flame, 833°C (1531°F) as measured by the DFTs, and 958°C (1757°F) as measured by the optical thermometers.

The fire test facility was originally designed to terminate the fire test by shutting off fuel flow and allowing the fuel at the surface of the pool to burn off. Testing revealed that, in some circumstances, excess fuel could buildup on the pool surface causing the fire to continue burning for five minutes or longer. As a result, a simple fire suppression system was added to the facility. A water hose was connected to a nearby fire hydrant, Figure 3-27B. This hose utilized a suction line to siphon standard fire suppressant foam into the line, Figure 3-27C. The hose discharged into a single pipe that fed into the pool a few inches above the water level. When activated, the system would inject foam horizontally onto the surface of the pool, well below the test article. When used in combination with the fuel shutoff valves, the pool fire was extinguished within 60 seconds. This system did not cool the test article when in use and the package was allowed to naturally extinguish itself after the test. This was demonstrated by the CTU burn test, where the polyurethane at the Outerpack vent ports continued to burn many minutes after the fire suppressant was used on the pool surface.

Figure 3-27B Fire Fighters Standing by Fire Suppression System

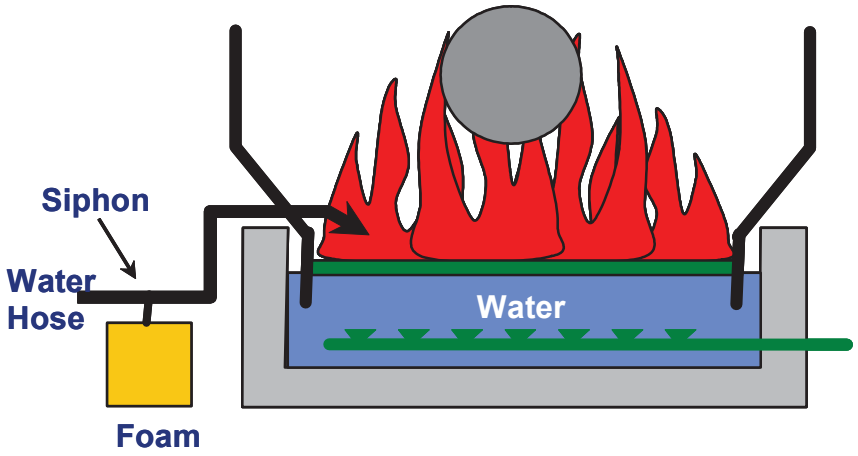

Figure 3-27C Approach to Suppress Pool Fire at End of Test

After the pool fire was extinguished, the package was removed from the pool and allowed to cool. Small amounts of smoke were observed to be coming from the package seams. The package was opened and the interior was examined. Significant amounts of polyurethane intumescence residue were observed along the Outerpack seam, Figure 3-30, and brown tar from the polyurethane was observed inside the package, Figure 3-31. Internal temperature strips recorded peak temperatures under 150°C throughout the package with one possible exception. Approximately 2 m (6 ft) from the bottom of the package, one set of temperature strips was unreadable due to heating and urethane deposits. An examination of the fuel assembly and the moderator blocks showed no significant heat damage.

Figure 3-28 Traveller CTU Burn Test

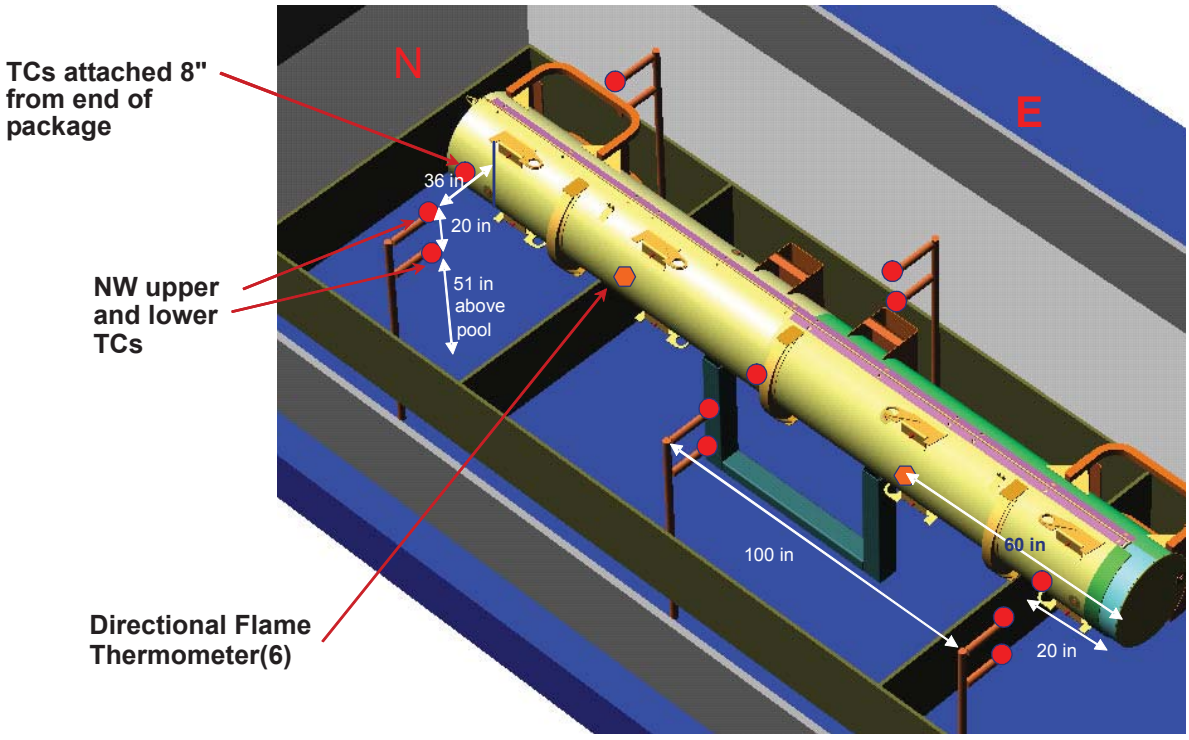

Figure 3-29 Thermocouple Locations on CTU Burn Test

Figure 3-30 Polyurethane Char in Outerpack Seam After Burn Test

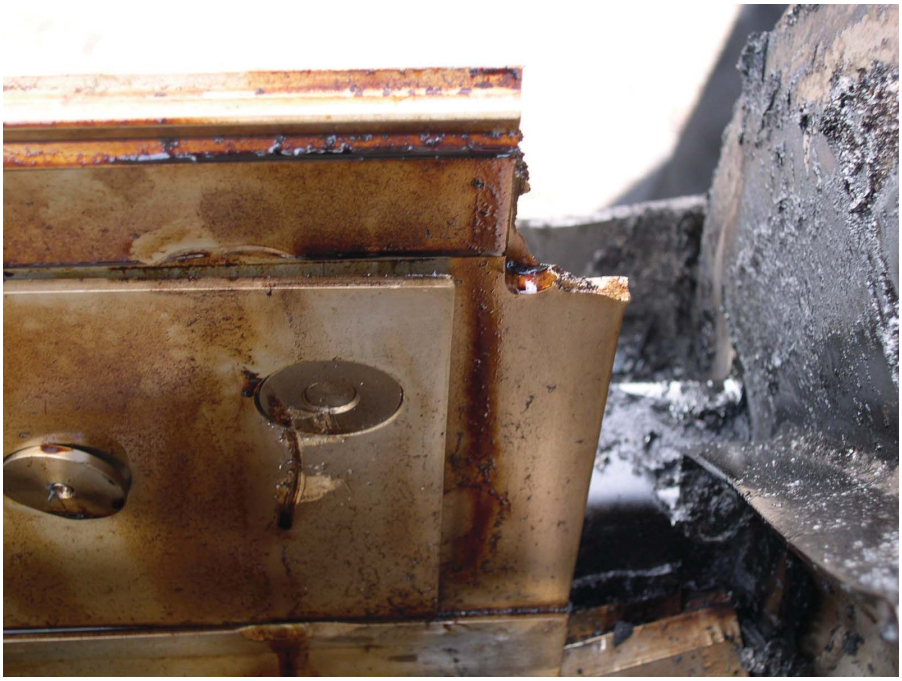

Figure 3-31 Brown Polyurethane Residue Inside Outerpack After Burn Test

The following test equipment was used to conduct the burn test:

- Video cameras (4)
- Digital camera
- Omega type K thermocouples with Inconel overbraided 10' leads to measure skin temperature and flame temperature depending on location (XCIB-K-4-2-10 with screw attachment ends and XCIB-K-3-2-10 with air hoods)
- Omega OM-CP-OCTTEMP data loggers (2)
- Omega USB recorder Data Acquisition Modules with weather tight electronics box
- Laptop computer
- Hand held optical pyrometer with adjustable emissivity setting (s)
- Adhesive temperature measurement strips (TL-E-170, TL-E-250, TL-E-330)
- Edmund Scientific Propeller Wind Anometer

The package rested on a steel support structure placed in a burn pool, Figure 3-32. The burn pool was limited by a water cooled weir and the fuel was evenly distributed throughout the pool. The pool was also surrounded by a steel diffuser, Figure 3-33. The top of the diffuser was approximately 1.6 m (5.4 ft) above the top of the pool surface, the height of the top of the test article.

The primary sensors used in the tests were Omega XCIB-K-4-12 thermocouples connected via approximately 50 ft of 20 gage type K, Teflon coated, extension wire. The type K thermocouples have standard limit of 4°F (2.2°C) or 0.75% between 32° and 2282°F (0° and 1250°C). The 20 gage chromega/ alomega wire has a resistance of 0.586 ohms per double foot of length. Two types of data recorders were used. Two Omega OM-CP-OCTTEMP 8 channel data recorders were used for 14 channels of data. These recorders have a -270° to 1370°C temperature measurement range for Type K thermocouples and 0.5°C accuracy for type K thermocouples. The recorders were purchased new from Omega and were used within the time limit of their original factory calibration. Eight channels of data were recorded using a Instrunet, data acquisition system with an INET-100 external A/D box connected to a Toshiba Satellite notebook computer running Windows XP Professional using a INET-230 PC card controller. This system, with Type K thermocouples has an accuracy of ±0.6°C between -50° and 1360°C. The lowest average temperatures from the CTU burn test were the DFT readings which had an 834°C, 30 minute average temperature. Adding the worst case thermocouple and data recorder errors results in a 6.8°C average error. This is not sufficient to lower average temperature below 800°C.

Figure 3-32 Test Stand for Fire Test

Figure 3-33 Test Setup with Steel Diffuser Plates

3.6.5.1 Test Procedures and Results

The Certification Test Unit 1 (CTU) was burn tested on February 10, 2004. Because the overnight temperatures dropped to near freezing, the package was covered with a tarp, Figure 3-34 and heated by two 150,000 BTU/hr (44 kWt) kerosene heaters used alternatively. The heaters maintained the air temperature under the tent between 40 and 80°C (104 and 176°F) with readings at one location climbing to 115°C (239°F). The heater was turned off shortly after 7:15 AM and the tarp was removed between 7:20 and 8:00 AM. Temperatures around the package were measured and recorded on the two data loggers. This data is shown on, Figures 3-35 and 3-36. The ambient temperature shown is air temperature outside of the heated tent.

This test was performed between 8:32 and 9:06 AM Tuesday morning. Fuel was added to the pool starting at 8:26 AM and continued until 150 gal had been added. The pool was lit at 8:32 and full engulfment was achieved one minute later. After full engulfment was achieved, fuel flow was adjusted to between 61 and 83 l/min (16 and 22 gal/min) depending on the flame coverage within the pool. The fuel flow was secured at 9:04 and the fire suppression system was activated one minute later. The pool fire was extinguished within approximately one minute, although burning polyurethane from the package reignited residual fuel at one end of the pool shortly afterwards. This was extinguished using the fire suppression system.

Figure 3-34 Test Article Under Tent to Maintain Temperature Overnight

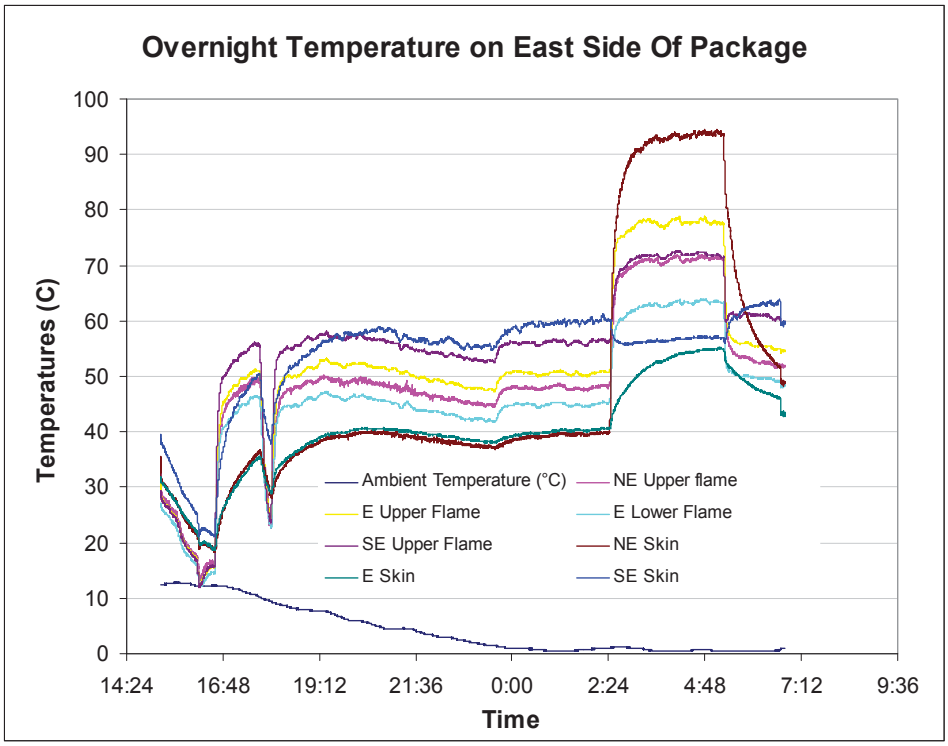

Figure 3-35 Overnight Temperatures on East Side of Test Article

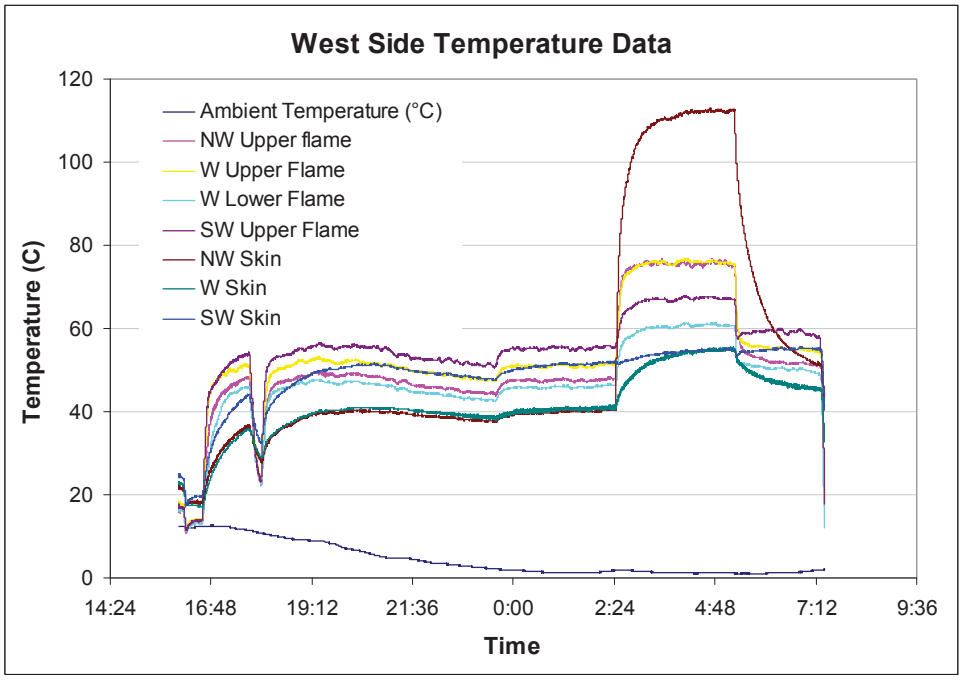

Figure 3-36 Overnight Temperatures on West Side of Test Article

During the fire test, data recorded by the instrument system was monitored in real time. This data included the following thermocouples:

- NE lower flame temperature (same height as center of test article)
- NE DFT
- SE DFT
- SE lower flame temperature
- NW lower flame temperature
- NW DFT
- SW DFT
- SW lower flame temperature

The data from the thermocouples within the fire is shown in, Figure 3-37. The data from the DFTs is shown in Figure 3-38.

Two data loggers were used to record a total of 14 channels of data. One data logger recorded temperatures on the east side of the CTU other, the west side of the CTU. Figures 3-39 and 3-40 show the skin temperature data collected on the east and west sides of the CTU. Figures 3-41 and 3-42 show data collected from the remaining thermocouples in the fire on the east and west sides respectively.

Twenty-two (22) thermocouples were used to measure external conditions on and around the Traveller package during the February 10, 2004 fire test. These sensors were located as shown in Figure 3-30 in the SAR. Due to the natural instability of open flames, combined with wind effects, these thermocouples were periodically uncovered. As shown in Figures 3-38 through 3-43, this resulted in large variations in measured temperature. These variations are largest at the corners of the pool fire where small disruptions in the flame would change air temperature at the thermocouple location. These disruptions were the smallest at the package skin because it was in the center of the pool fire.

Table 3-4A below, summarizes the thermocouple data for the test. Some of the thermocouples had average temperatures under 800°C but all experienced temperatures above 900°C during the test, demonstrating that the fire covered the complete pool area. Some of the minimum temperatures recorded are due to the time selected for the 30 minute average. A fire this size cannot start instantaneously, nor did it end instantaneously. As a result, the 30 minute period selected for averaging data includes data when some TC were beginning to heat up and when some were already cooling off after the fire. The data still shows that the average skin temperature, the average DFT temperature and the average temperature of TCs in the flame were all above 800°C for the 30 minute period selected.

Table 3-4A Summary of Recorded Temperatures During Burn Test

TC Location	30 Minute Ave (°C)	Max Temp (°C)	Min Temp (°C)
NE Lower Flame	727	959	275
NE Upper Flame	925	1245	493
E Lower Flame	926	1155	489
E Upper Flame	904	1163	532
SE Lower Flame	714	962	291
SE Upper Flame	924	1245	484
NW Lower Flame	630	906	329
NW Upper Flame	748	1059	458
W Lower Flame	997	1162	640
W Upper Flame	1027	1173	661
SW Lower Flame	827	1032	230
SW Upper Flame	1000	1213	598
NE DFT	804	907	454
SE DFT	801	964	338
NW DFT	854	1016	541
SW DFT	876	1003	594
NE Skin	878	1058	610
E Skin	917	1073	699
SE Skin	903	1088	542
NW Skin	725	990	492
W Skin	974	1080	682
SW Skin	1028	1143	719

Because the thermocouples in the corners of the pool were not engulfed as long as the package itself, the 30 minute average temperature for the corners is lower than in the center of the pool. The total average for all of the thermocouples in the flame was 862°C versus 812°C for the corner thermocouples in the flame. The DFT average readings are also lower for similar reasons. The DFTs insulated the thermocouple and attached face plate from convective heat transfer. Radiative heat transfer was dominate by design. Because these devices faced away from the package, they recorded equilibrium temperature based on radiation from the fire and reradiation to cold surfaces outside the fire, without contribution from convection. The skin temperature is an equilibrium temperature that includes convective heat transfer from hot combustion gasses. As a result, its temperatures should be higher.

As described in the discussion of thermal analysis results (section 3.6.1) the long length to diameter ratio of the Traveller package minimizes the role of axial heat transfer inside the package. Non-uniform external temperatures produce non-uniform internal temperatures during fire tests. This fundamental mechanism allowed useful data to be obtained in the seam burn and impact limiter burn tests described in sections 3.6.2 and 3.6.3. This mechanism was demonstrated by the very low clamshell temperatures measured adjacent to the heated sections in those tests. During the CTU burn test, the average skin temperature at the North end, middle and South end of the package was 801°, 946°, and 915°C respectively. Peak interior temperatures recorded by the non-reversible temperatures strips were 116°C at the North end of the package, 177°C at the middle of the package, and 143°C at the South end of the package. At the center of the package, where the average exterior skin temperature was 946°C, the corresponding interior temperatures were acceptable for all materials in the package.

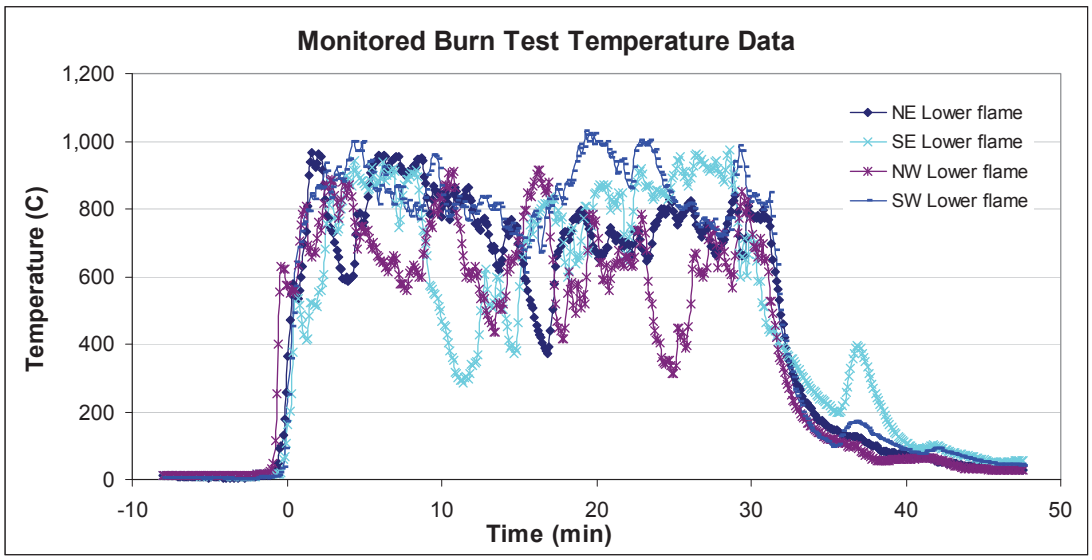

Figure 3-37 Fire Temperatures Measured at the Corners of the Pool

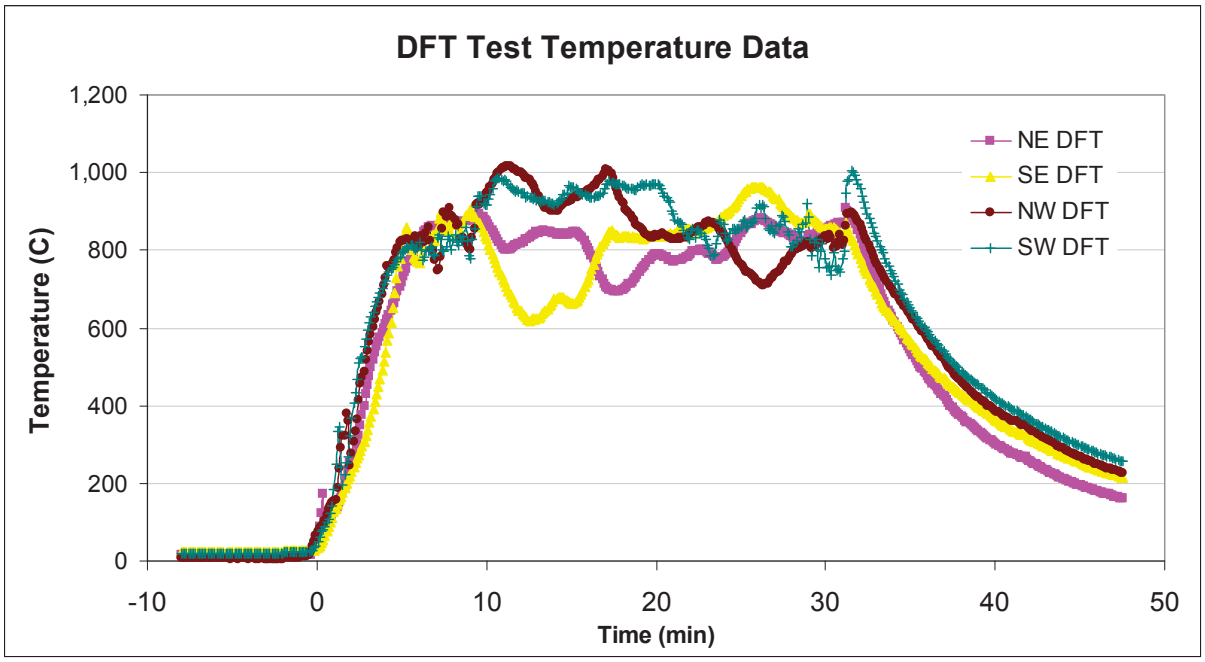

Figure 3-38 Data from Direction Flame Thermometers (DFTs)

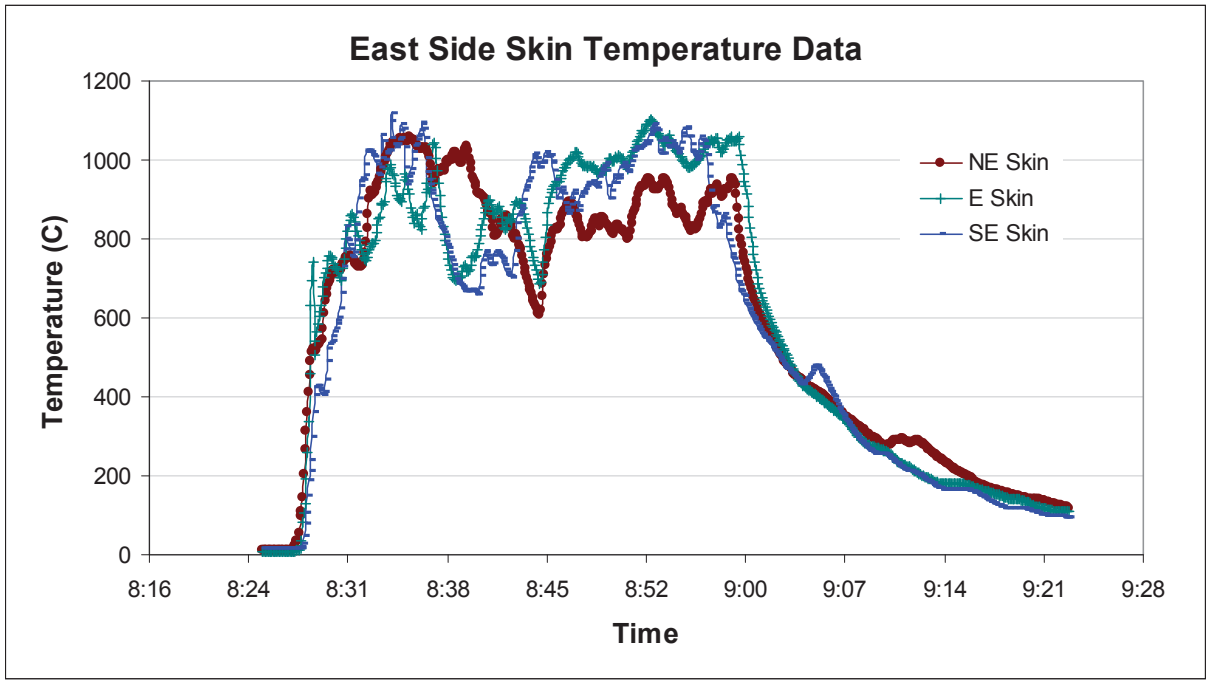

Figure 3-39 Skin Temperature Data from East Side of CTU

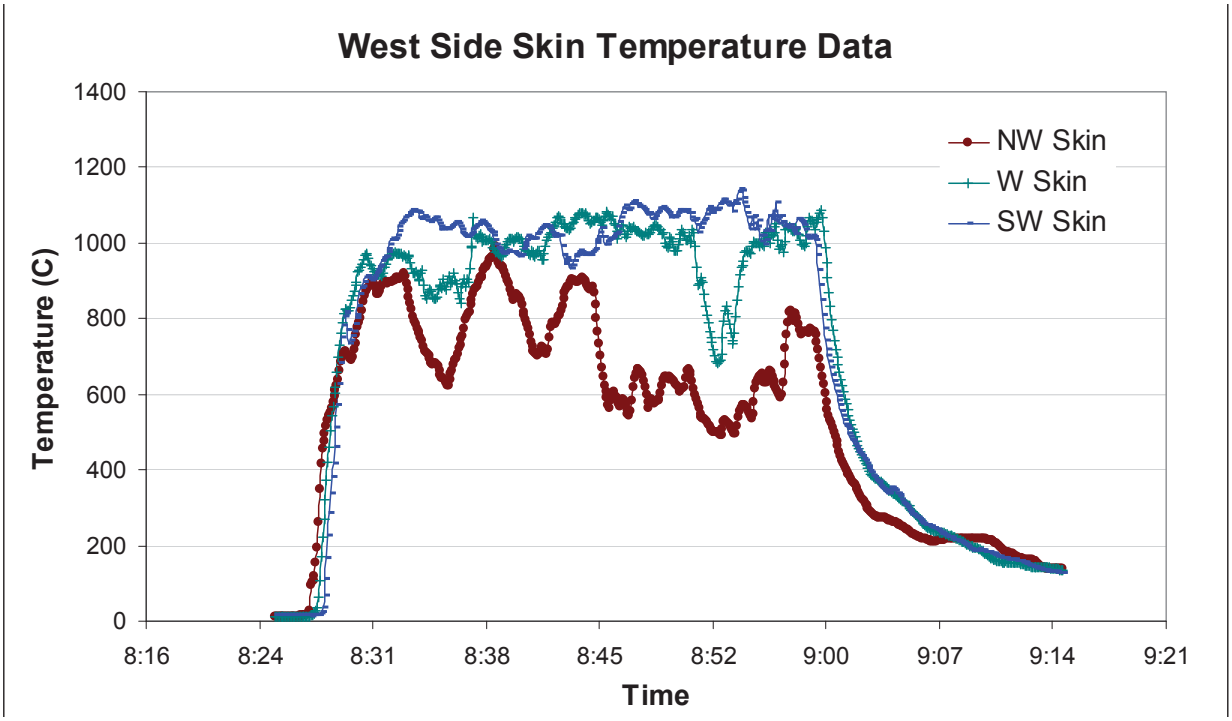

Figure 3-40 Skin Temperature Data from West Side of CTU

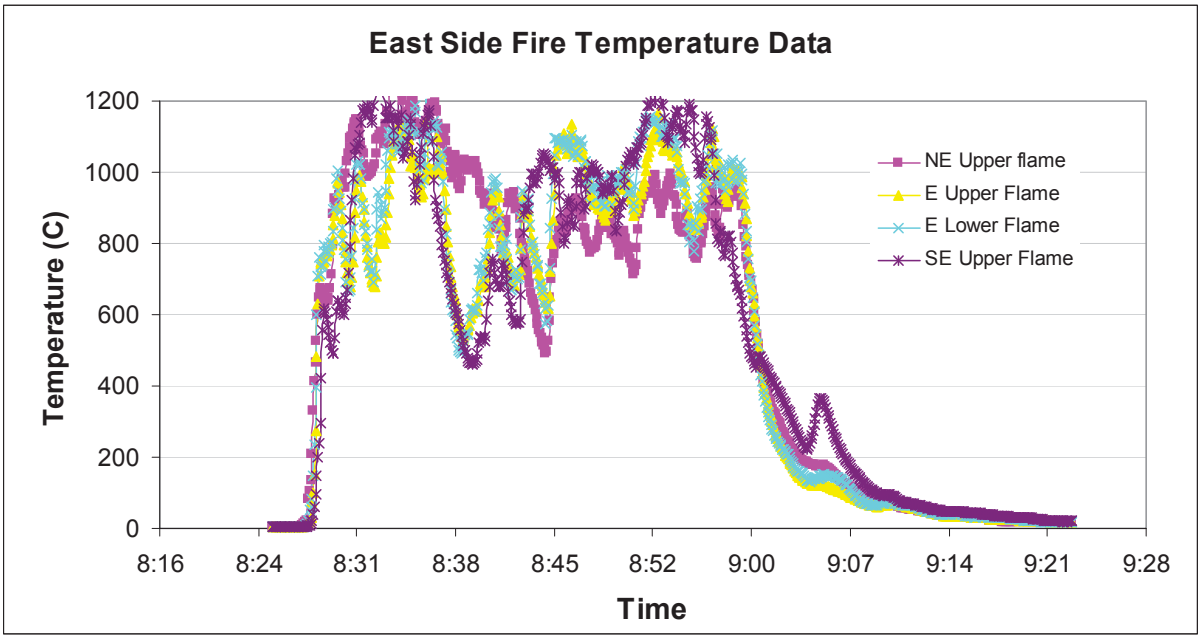

Figure 3-41 Fire Temperature Data from East Side of CTU

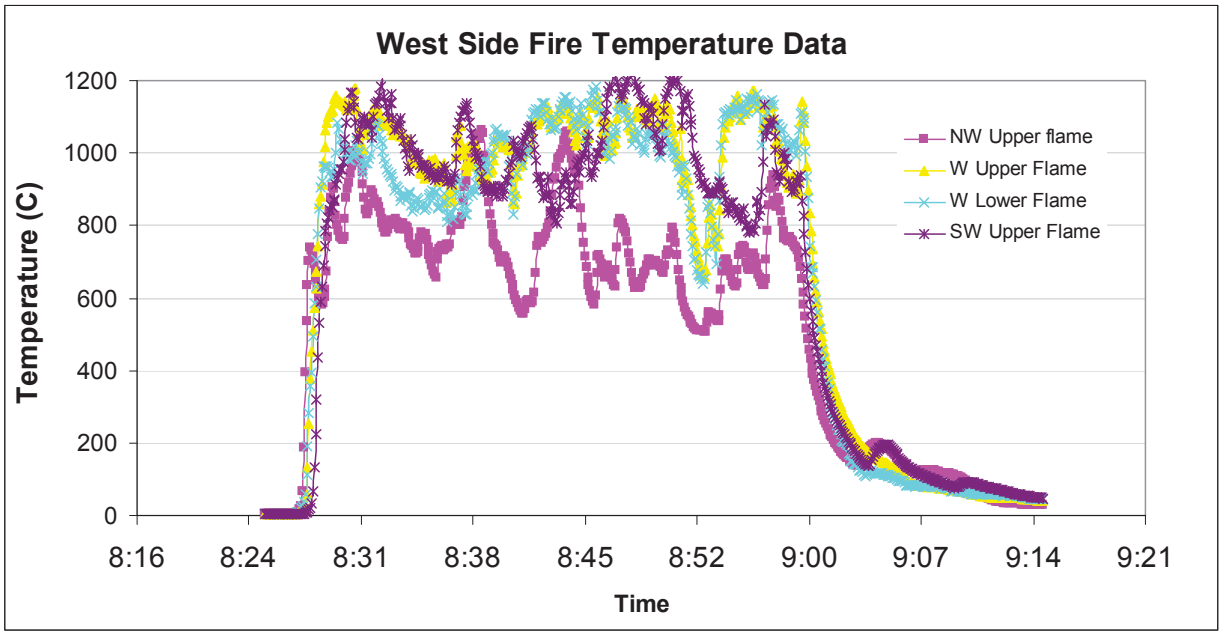

Figure 3-42 Fire Temperature Data from West Side of CTU

Temperature data was also collected using two portable, single wavelength optical thermometers. One was located on a raised platform on the west side of the package. The second was located on the east side of the package. Temperature data was recorded by hand. This data is shown in Tables 3-5 and 3-6.

Table 3-5 Optical Thermometer Data Sheet (West Side, Degrees C)

Time After Pool Fire Ignition	Temperature (North End)	Temperature (Middle)	Temperature (South End)
0 minutes	922	944	874
5 minutes	1047	973	1025
10 minutes	1002	1092	993
15 minutes	937	847	987
20 minutes	1177	982	942
25 minutes	1062	1073	1058
30 minutes	898	1162	968
35 minutes	525	460	484
40 minutes	318	362	294

Table 3-6 Optical Thermometer Data Sheet (East Side, Degrees C)

Time After Pool Fire Ignition	Temperature (North End)	Temperature (Middle)	Temperature (South End)
0 minutes	800	1000	936
5 minutes	978	1062	837
10 minutes	1037	948	932
15 minutes	842	996	835
20 minutes	590	1120	978
25 minutes	552	969	1048
30 minutes	1098	740	980
35 minutes			
40 minutes			

Wind speed measurements were made before, during and after the burn test. Average wind speed during the test was 0.9 miles per hour (0.4 m/s). Peak wind speed measured during the test was 2.2 miles per hour (1.0 m/s). The data was recorded by had at five minute intervals. This data is shown in Table 3-7.

An examination of the moderator blocks after the burn test revealed no significant damage. One small portion of moderator at the bottom end of the package showed signs of combustion, Figure 3-43. The very localized nature of the burn marks (on both the moderator and the refractory fiber felt insulation that covered the moderator) indicates that this was probably caused during the fabrication process. The stainless steel cover sheets are welded into place after the moderator blocks are bolted in and covered with insulation. It appears that the welding torch was applied to the moderator causing a small amount of damage. A brown spot was observed on the back side of one moderator block attached to the Outerpack lid. The polyethylene at this location appears to have been heated to melt temperature, Figure 3-44. A very small amount of flow occurred away from the hot spot. This melt spot was small, affecting only a few cubic centimeters of material. A visual examination of the shock mounts indicated that they were all intact.

Ultra-high molecular weight (UHMW) polyethylene was selected as the neutron moderator for the Traveller package because of its high hydrogen content, its ductility at very low temperatures and its high viscosity at temperatures well above its melt point due to the long molecular chains (MW=3,000,000 to 6,000,000). The relative solution viscosity as measured by ASTM D4020 must be greater than 1.4[1] and is typically found to be 2.3 to 3.5 dl/gm[2] (at 135°C). As a result, UHMW polyethylene does not liquefy above its melt temperature and molded UHMW polyethylene parts are typically made at relatively high temperatures (190°–200°C) and very high pressures (70-100 bar)[3]. Its excellent stability allows it to be used in some applications at temperatures as high as 450°C[4]. Experience in the Traveller test program has shown that the material will soften but not run, even when heated to near vaporization temperature (349°C). However, the Traveller design encapsulates the moderator with stainless steel. This is primarily done to prevent oxygen from reaching the moderator, should it reach vaporization temperature, but it does serve a secondary function of ensuring that the moderator does not significantly distort or flow at high temperatures.

The highest measured temperature inside the package was 171°C which is lower that the typical process temperature used to create the UHMW sheets installed in the Traveller. Unchanged appearance and more importantly, unchanged weight indicate that the plastic did not loose a significant amount of its hydrogen during the test.

1. Stein, H.L., "Ultra High Molecular Weight Polyethylene (UHMWPE)," Engineered Materials Handbook, Vol. 2, Engineering Plastics, 1998.
2. This is a typical value observed in many manufacturers specifications: Crown Plastics (crownplastics.com/properties.htm).
3. Ticona Engineering Polymers information on compression molding, www.ticona.com/index/tech/processing/compression_molding/gur1.htm.
4. Stein, H.L., "Ultra High Molecular Weight Polyethylene (UHMWPE)," Engineered Materials Handbook, Vol. 2, Engineering Plastics, 1998

This page intentionally left blank.

Table 3-7 Wind Data Sheet

Time	Wind Speed (mph)	Wind Direction	Temperature F
8:05	1.7	E	42
8:10	2.0	NE	-
8:15	1.7	E	-
8:20	2.0	E	42
8:25	0.8	E	-
8:30	0.8	E	42
8:35	0.8	E	-
8:40	0.6	E	42
8:45	1.3	E	-
8:50	2.2	N	42
8:55	0	-	-
9:00	1.5	N	-
9:05	0	-	43
9:10	1.3	W	-
9:20	1.7	SW	43
9:30	1.3	SW	44

Wind data was taken every five minutes starting approximately 15 minutes before the burn until 30 minutes after the burn was completed.

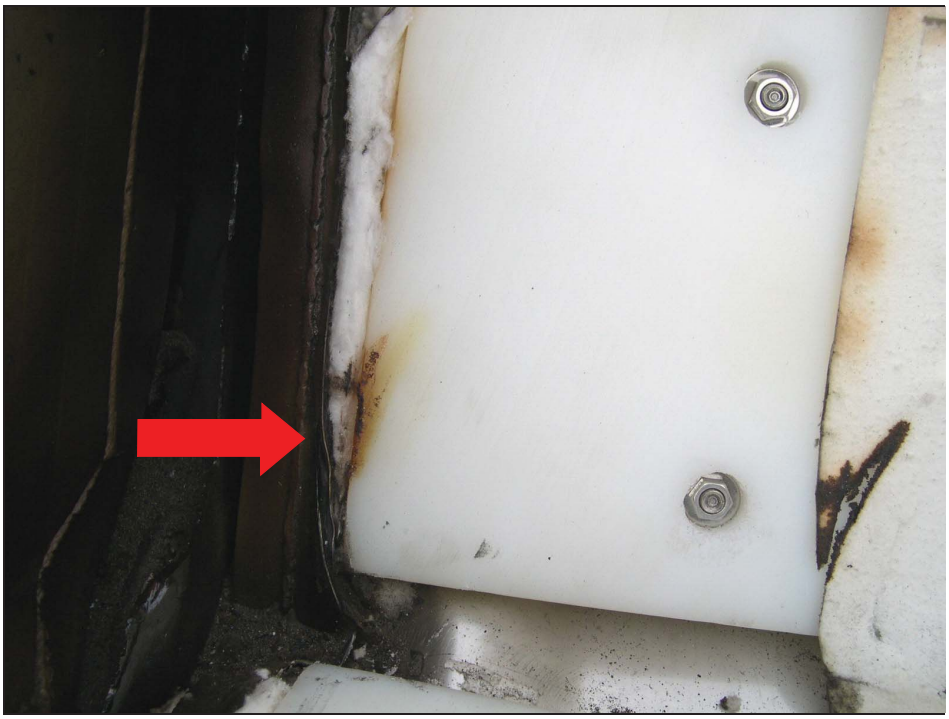

Figure 3-43 Location of Possible Combustion of Moderator

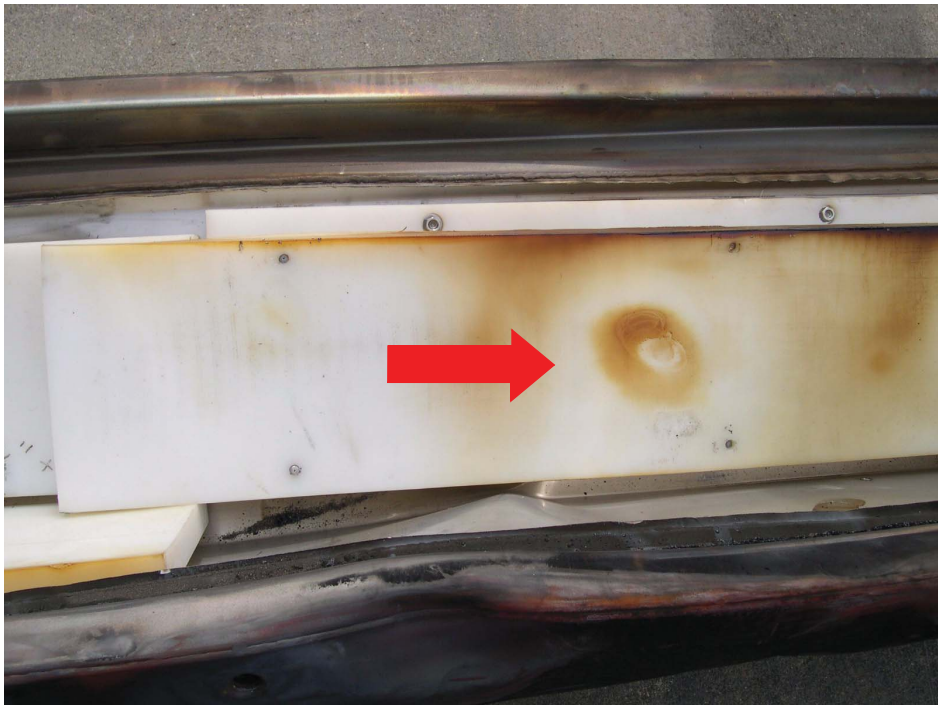

Figure 3-44 Localized Melt Spot in Lid Moderator Block

Twelve sets of non-reversible temperature strips were attached to the CTU. Two were placed on the inside faces of the impact limiters (one at each end), six were placed on the stainless steel covering the moderator in the Outerpack lid, and five were attached to the inside doors of the Clamshell. Except for one set that was unreadable after the test, the peak indicated temperature was 177°C. Locations of the temperature strip sets are shown in Figure 3-45. Readings on one of the Outerpack lid temperature strip sets is shown in Figure 3-46.

Earlier analysis and tests had shown that, if there was no substantial infiltration of hot gas into the package, interior temperatures would remain low during the fire test. This is shown in the results of both the seam burn tests and the impact limiter burn tests (sections 3.6.2 and 3.6.3). In these tests, interior temperatures rose between 50° and 110°C during and after the test. These values are conservative because the tests were performed on a previously burned package where the polyurethane had already turned to char. The primary design concern was hot gas infiltration during the CTU burn test. This would add substantially more heat and cause higher temperatures. This was observed in an earlier burn test (QTU-1). This package was oriented in the same fashion as the CTU, with one Outerpack seam facing the pool surface. Distortion of the Outerpack walls caused hot gasses to enter the package and flow around the clamshell. Because of the geometric arrangement of the Outerpack seam lip, this flow was directed preferentially over the top of the clamshell (as oriented when the package is resting on its feet). Polyurethane ignited at four locations in this region and burned. The moderator under the clamshell was undamaged. Based on this evidence, it seemed best to concentrate the temperature indicating strips on the moderator surface that was expected to be the hottest if significant hot gas infiltration occurred.

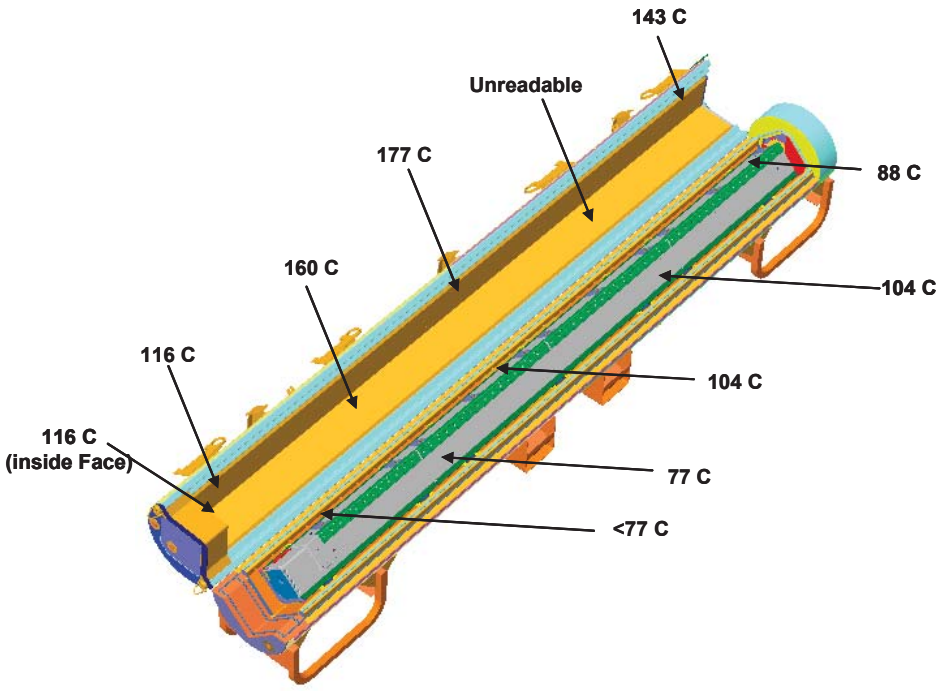

Figure 3-45 Location and Indicated Temperatures of Temperature Strip Sets

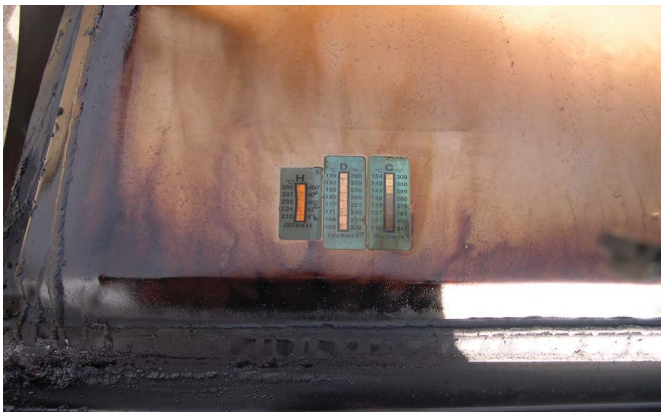

Figure 3-46 Temperature Strip Set After Fire Test

TABLE OF CONTENTS

This page intentionally left blank.

4.0 CONTAINMENT

4.1 DESCRIPTION OF THE CONTAINMENT SYSTEM

4.1.1 Containment Boundary

The Traveller package is limited to transporting unirradiated, low enriched uranium, nuclear fuel assemblies and rods. The radioactive material, bound in sintered pellets having very limited solubility, has minimal propensity to suspend in air. These pellets are sealed in fuel tubes to form the fuel rods portion of each assembly.

Containment System is described in both TSR-1 (§213) and 10CFR71.4 as, "the assembly of components of the packaging intended to retain the radioactive material during transport." The Containment System for the Traveller consists of the fuel rods.

4.2 GENERAL CONSIDERATIONS

4.2.1 Type A Fissile Packages

For type A fissile packages, no loss or dispersal of radioactive material is permitted under normal conditions of transport as specified in 10CFR71.43(f). It has been demonstrated from repeated normal drop scenarios that there is no loss of fissile material from the rods, and therefore no dispersal. Therefore, the containment system remains intact.

4.3 APPENDICES

4.3.1 References

None.

TABLE OF CONTENTS

This page intentionally left blank.

5.0 SHIELDING EVALUATION

The radiation from low enriched uranium in fresh fuel assemblies that affects external dose includes alpha, beta, and gamma radiation. Because of the relatively short range of alpha particles in dense matter, alpha radiation poses little external dose hazard. The most energetic alphas produced by naturally occurring radionuclides will not penetrate the packaging materials.

Several uranium radioactive decay products are beta emitters. A primary radionuclide of concern is protactinium-234 in its metastable state (^{234m}Pa), a daughter of ^{238}U which produces a very high energy beta particle that can travel up to 20 feet in air. Significant beta radiation is also emitted from ^{234}Th (also a daughter of ^{238}U) and ^{231}Th (a daughter of ^{235}U). Typically, these are shielded with ½ inch of plastic, and therefore will be shielded by the packaging materials.

Storage of large quantities of uranium can create low-level gamma radiation fields (less than 0.05 mSv/hr [5 mrem/hr]). In addition to gamma emissions from the uranium decay chains (^{238}U and ^{235}U), recycled fuel materials introduced back into the enrichment process will result in higher gamma radiation fields because of ^{228}Th, a gamma-emitting daughter of ^{232}U with a relatively short half-life (1.9 yr).

The packaging materials of the Traveller effectively limit radiation levels on the external surface of the package. Under conditions of transport normally incident to transportation, the radiation level does not exceed 2 mSv/hour (200 mrem/hour) at any point on the external surface of the package.

5.1 APPENDICES

5.1.1 References

None.

TABLE OF CONTENTS

TABLE OF CONTENTS (cont.)

TABLE OF CONTENTS (cont.)

LIST OF TABLES

LIST OF TABLES (cont.)

LIST OF FIGURES

LIST OF FIGURES (cont.)

This page intentionally left blank.

6.0 CRITICALITY

The following analyses demonstrate that the Traveller complies fully with the requirements of 10CFR71[1] and TS-R-1[2]. The nuclear criticality safety requirements for Type A fissile packages are satisfied for single package and array configurations under normal conditions of transport and hypothetical accident conditions. A comprehensive description of the Traveller packaging is provided in Section 1. This section provides a description of the package (i.e., packaging and contents) that is sufficient for understanding the features of the Traveller that maintain criticality safety.

Specifically, this criticality evaluation presents the following information[3]:

1. Description of the contents and packaging, including maximum and minimum mass of materials, maximum ^{235}U enrichment, physical parameters, type, form, and composition.

2. Description of the calculational models, including sketches with dimensions and materials, pointing out the differences between the models and actual package design, with explanation of how the differences affect the calculations.

3. Justification for the credit assumed for the fixed neutron absorber content, including reference to the acceptance tests that are implemented which verify the presence and uniformity of the absorber.

4. Justification for assuming 90% credit for fixed moderating material.

5. Description of the most reactive content loading and the most reactive configuration of the contents, the packaging, and the package array in the criticality evaluation.

6. Description of the codes and cross-section data used, together with references that provide complete information.

7. Discussion of software capabilities and limitations of importance to the criticality safety evaluations.

1. Title 10, Code of Federal Regulations, Part 71 (10CFR71), Packaging and Transportation of Radioactive Material, edition effective Oct 2004.
2. TS-R-1 1996 (Revised), Regulations for the Safe Transport of Radioactive Material.
3. NUREG/CR-5661, Recommendations for Preparing the Criticality Safety Evaluation of Transport Packages.

8. Description of validation procedures to justify the bias and uncertainties associated with the calculational method, including use of the administrative subcritical margin of 0.05 delta k to set an upper safety limit (USL) of 0.94.

9. Demonstration that the effective neutron multiplication factor (k_{eff}) calculated in the safety analysis is less than the USL after consideration of appropriate bias and uncertainties for the following.

   a. A single package with optimum moderation within the containment (i.e., confinement) system, close water reflection, and the most reactive packaging and content configuration consistent with the effects of either normal conditions of transport or hypothetical accident conditions, whichever is more reactive.

   b. An array of 5N undamaged packages (packages subject to normal conditions of transport) with nothing between the packages and close water reflection of the array.

   c. An array of 2N damaged packages (packages subject to hypothetical accident conditions) if each package were subjected to the tests specified in §71.73, with optimum interspersed moderation and close water reflection of the array.

10. Calculation of the Criticality Safety Index (CSI) based on the value of N determined in the array analyses.

11. Description of the Traveller's Confinement System.

6.1 DESCRIPTION OF CRITICALITY DESIGN

6.1.1 Design Features

This section describes the design features of the Traveller that are important for criticality. The Traveller shipping package carries either a single PWR fuel assembly or a single rod container that holds either PWR or BWR rods. The Traveller is divided into two major systems, Outerpack and Clamshell. The Outerpack consists of a polyurethane foam material sandwiched between concentric stainless steel shells. The Outerpack is a split-shell design with the two halves hinged together. Neutron-moderating high-density polyethylene blocks are affixed to the upper and lower halves of the Outerpack.

The Clamshell is a rectangular aluminum box that completely encloses the contents. It is rotated 45° and mounted in the Outerpack with rubber shock mounts. Neutron absorber panels are slotted into the inner face of each Clamshell side. The Clamshell is designed such that it retains its original dimensions when subjected to the HAC tests. See Figure 6-1 for an exploded view of the Traveller.

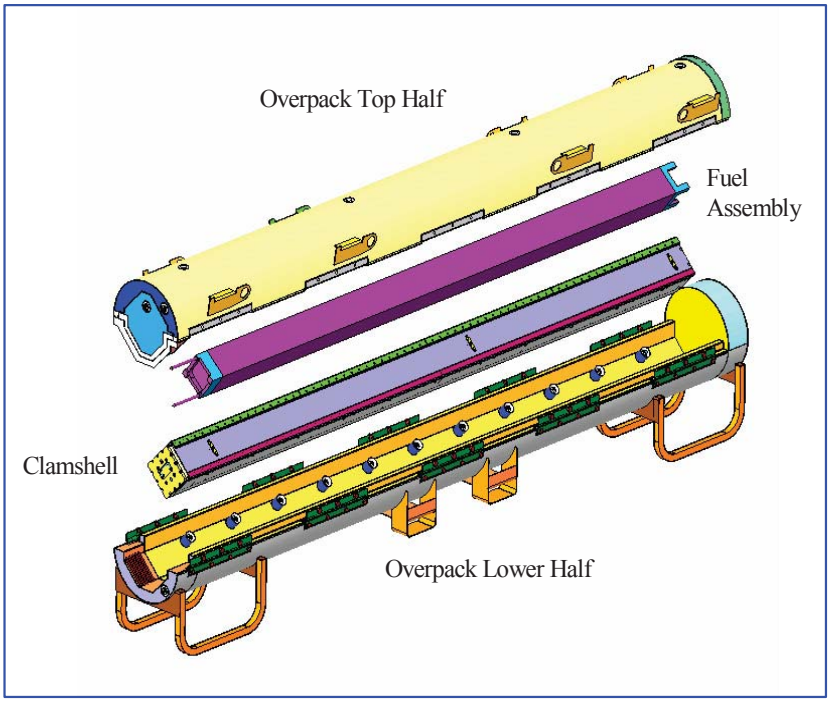

Figure 6-1 Traveller Exploded View

6.1.1.1 Containment System

The Containment System is described in both TSR-1 and 10CFR71 as, “the assembly of components of the packaging intended to retain the radioactive material during transport.” The Containment System for the

Traveller consists of the fuel rods, regardless of whether the Traveller is carrying a fuel assembly or rods in a rod container.

6.1.1.2 Confinement System

The Confinement System is defined in TS-R-1 as "the assembly of fissile material and packaging components specified by the designer and agreed to by the competent authority as intended to preserve criticality safety." Note that TS-G-1.1[1] further describes the confinement system as "that part of a package necessary to maintain the fissile material in the configuration that was assumed in the criticality safety assessment for an individual package." NUREG 1609[2] recommends that the analysis include a discussion of the "structural components that maintain the fissile material or neutron poisons in a fixed position within the package or in a fixed position relative to each other." These structural components are intended to maintain criticality safety of the package. These structural components of the packaging actually comprise part of the Confinement System.

The Confinement System for the Traveller consists of those assembly and packaging components that preserve criticality safety of a single package in isolation. Hence, it consists of the fuel rods, the fuel assembly (or rod container), and the Clamshell assembly, including the neutron absorber panels. The Confinement System is shown in Figure 6-2.

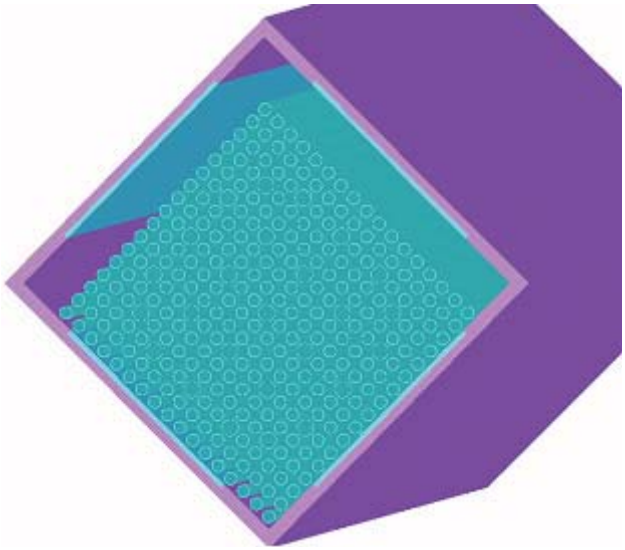

Figure 6-2 Traveller Confinement System

1. IAEA TS-G-1.1, Advisory Material for the IAEA Regulations for the Safe Transport of Radioactive Material.
2. NUREG 1609, Standard Review Plan for Transportation Packages for Radioactive Material

6.1.1.3 Flux Traps

The Traveller package features a unique flux trap system, which does not require an accident condition (i.e., flooding) in order to function. The system was designed to ensure an acceptable subcritical margin for the unlikely but most conservative flooding scenario, described later in this section. The flux trap system consists of neutron absorber panels in the Clamshell immediately adjacent to the contents, and high-density polyethylene (UHMW) blocks affixed to the inside of the Outerpack. Neutrons escaping from one fuel assembly would pass through two moderator blocks prior to passing through the absorber of the neighboring package.

Any flooding outside the Clamshell enhances the performance of the flux trap. The UHMW blocks ensure that there will be neutron moderation, and therefore, flux trap operation, in those array configurations where the contents are moderated inside the Clamshell but where there is no flooding in void spaces outside the Clamshell or between the packages. The flux trap components are further described below. Figure 6-3 shows the flux traps in a seven-package triangular-pitch array of Traveller packages.

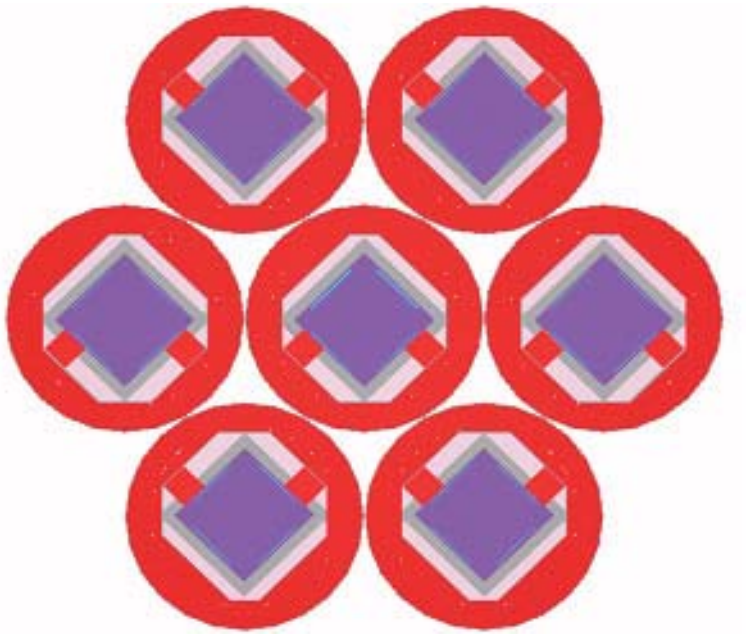

Figure 6-3 Seven Package Array Showing the Flux Trap System

6.1.1.4 Neutron-Absorbing Materials

Neutron absorbing materials are present in the Traveller in two forms: materials of construction and neutron poisons.

6.1.1.4.1 Materials of Construction

Materials of construction include those materials normally present, namely the stainless steel in the Outerpack, the fuel assembly skeleton, and the top nozzle. It also includes the burnable absorbers in the fuel. The evaluation takes credit for approximately 60% of the stainless steel in the inner and outer shells of the Outerpack. See Table 6-11. No credit is taken for the neutron absorbing properties of the fuel assembly skeleton or top nozzle, with the exception of the zirconium thimble tube material. In the criticality model the volumes occupied by skeleton and top nozzle are modeled as water. Water is assumed to increase reactivity more than steel by providing more neutron reflection or moderation than the steel. Finally, the evaluation does not consider the presence of any integral or burnable absorbers.

6.1.1.4.2 Neutron Poisons

Neutron poison has been added to the Traveller specifically to limit reactivity during hypothetical accident conditions. The neutron poison used in the Traveller is in the form of BORAL® panels in the Clamshell. These panels are permanently fixed.

6.1.1.4.3 Deleted

6.1.1.4.4 BORAL

BORAL is a thermal neutron poison material composed of boron carbide and 1100 alloy aluminum. Boron carbide is a compound having a high boron content in a physically stable and chemically inert form. The 1100 alloy aluminum is a light-weight metal with high tensile strength which is protected from corrosion by a highly resistant oxide form. The two materials, boron carbide and aluminum, are chemically compatible and ideally suited for long-term use. BORAL has been licensed by the NRC for use in numerous BWR and PWR spend fuel storage racks and has been used in international reactor installations. Manufacturing QA (i.e., neutronics or chemical testing) ensures that the minimum areal densities are achieved.

The BORAL sheets measure 0.125 inches (0.3175 cm) thick, including cladding and core. The nominal thickness of the cladding and core are as follows: Cladding (0.0179 inches/0.0455 cm), Core (0.0892 inches/ 0.2266 cm), Cladding (0.0179 inches/0.0455 cm). The maximum areal density loading for ^{10}B that corresponds to this thickness is 0.0240 g/cm^2, which equates to a B4C loading of 36.5%. This analysis assumes 75% credit for areal density, which equates to 0.0180 g/cm^2.

6.1.1.5 Neutron-Moderating Materials

Neutron-moderating materials in the Traveller include the polyurethane foam in the Outerpack, the shock mounts, and the high-density polyethylene (UHMW) blocks.

6.1.1.5.1 Polyurethane Foam

Results from the formal thermal test and the numerous scoping burn tests that were conducted indicate that an unpredictable amount of the polyurethane foam burns away. Therefore, no credit is taken for the foam under accident conditions. Rather, the foam is considered to be a floodable void space and will be modeled either as a void or filled with water, depending upon which is the most conservative.

6.1.1.5.2 Shock Mounts

Testing indicates that the shock mounts remain intact and hold the Clamshell in place. However, their contribution as a moderator is insignificant and therefore, they are modeled as full density water in the single package cases and as void spaces in the array cases.

The Traveller STD and Traveller XL have different shock mount configurations, which can be seen in the license drawings. Both configurations are symmetrical about the center of the outerpack. The Traveller STD configuration features four pair of shock mounts at either end of the outerpack, spaced 9.0 inches (22.9 cm) on center, with the end pair about 18 inches (45.7cm) from the end. The Traveller XL configuration has three pair of shock mounts at either end plus a pair in the middle. The pair at the end is about 15 inches (37 cm) from the end. The second pair is 36 inches (91.4 cm) from the first pair, and the third pair is 18 inches (45.7 cm) from the second.

6.1.1.5.3 High-density Polyethylene

High-density polyethylene (UHMW) “poly” is attached to the inside of the upper and lower sections of the Outerpack. The poly configuration is identical for both the Traveller and Traveller XL Outerpacks. The thickness is 1.25 in. [3.18 cm] in the upper section and 1.75 in [4.445 cm] in the lower section. The HPDE is a fixed moderator that together with the fixed neutron absorber installed in the Clamshell forms the flux trap system, which is discussed in Section 6.1.1.3. The UHMW density is 0.92 g/cc. The analysis assumes 90% density, or 0.828 g/cc. Section 6.7.7 discusses the effect of varying the HPDE density on system reactivity.

6.1.1.6 Floodable Void Spaces

The Traveller, including packaging and contents, contains six floodable regions. These regions have been modeled in various flooding combinations, including flooding with partial density water, in order to determine the most conservative accident configuration. The floodable regions are shown in Figure 6-4. (Note that region 1, the pin-gap, is shown in Figure 6-28). Flooding is addressed in Section 6.7.1. The region numbers below correspond to the numbers used in the criticality input decks.

This page intentionally left blank.

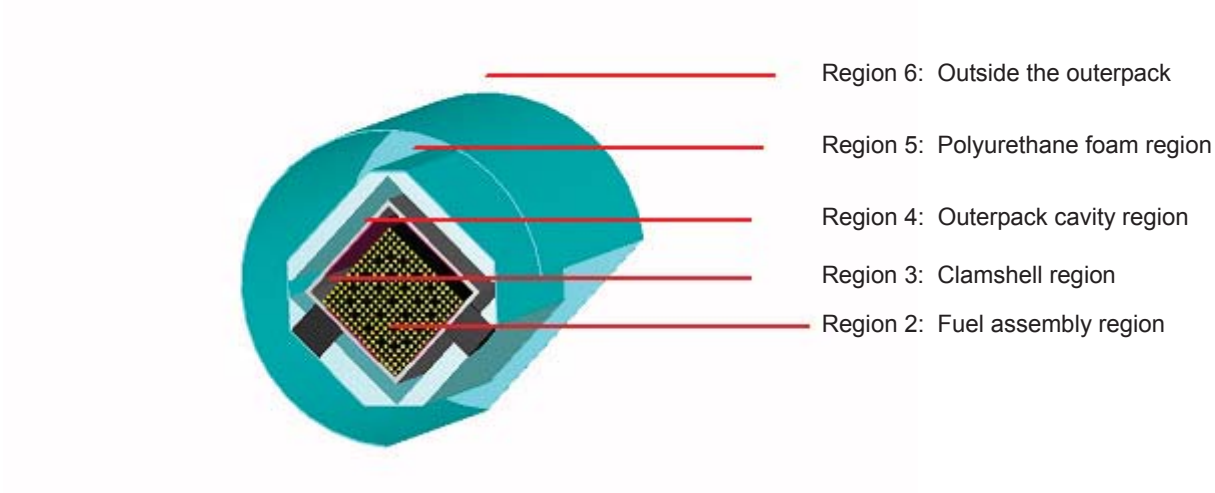

Figure 6-4 Floodable Void Spaces

6.1.1.6.1 Region 1 – Pellet-Cladding Gap (Pin Gap)

The pellet-cladding gap, or pin gap, is the floodable space inside the cladding. It was seen from the testing that some fuel rods may crack. Therefore, it is assumed that all rods have fully flooded pin gaps. The pin-gap is shown in Figure 6-28.

6.1.1.6.2 Region 2 – Fuel Assembly Region

The fuel assembly region is the floodable space in the fuel assembly envelope. It is modeled fully flooded in all configurations. Sensitivity studies were conducted with this area partially flooded to evaluate the effects of differential flooding.

6.1.1.6.3 Region 3 – Clamshell Region

The Clamshell region is the floodable space outside the fuel assembly region and inside the Clamshell. It is modeled both flooded and dry to determine which configuration is most conservative for single package or array. Sensitivity studies were conducted with the Clamshell partially full to evaluate the partial flooding scenario.

6.1.1.6.4 Region 4 – Outerpack Cavity Region

The Outerpack cavity region is the floodable space outside the Clamshell and inside the Outerpack. It was modeled both flooded and dry to determine which configuration is most conservative for single package or array configurations. Sensitivity studies were conducted with the Outerpack cavity region partially full to evaluate the partial flooding scenario.

6.1.1.6.5 Region 5 – Polyurethane Foam Region

The polyurethane foam region is the floodable space that is formed when the polyurethane foam burns away. As mentioned above, since it is difficult to predict how much foam will actually burn away, the entire foam region is modeled as water for the individual package cases and as a void for the array cases. These are the most conservative configurations.

6.1.1.6.6 Region 6 – Outside Outerpack Region

This is the volume outside the Outerpack. It has been modeled both flooded and dry to determine which configuration is most conservative for single package and array.

6.1.1.7 Array Spacing Significant Components

The single component that affects the physical separation of the fissile material contents in package arrays is the Outerpack. The Outerpack outer radius is 12.50 inches ± 1.0 inch (317.50 mm ±25.40 mm). It is a cylindrical annular shell split along the longitudinal axis to form two separate halves. The inner and outer shells are fabricated from 12-gauge [0.104 in. 0.264 cm)] stainless steel sheet, and the space between the shells is filled with polyurethane foam. The foam has a nominal 3.0 in. (7.62 cm) radial thickness and axial thickness of approximately 8.0 in. (20.32 cm). The foam material limits impact forces on the fuel assembly and insulates the fuel assembly from heat generated by a fire. Circumferential stiffeners mounted outside provide significant impact protection to the Outerpack diameter. The Outerpack diameter is not reduced at all following hypothetical accident tests. A sensitivity study was performed to evaluate k_{eff} as a function of Outerpack diameter. This evaluation is described in Section 6.7.11.

6.1.2 Summary Tables of Criticality Evaluation

Sensitivity studies were performed using the Traveller XL to determine the most conservative configurations for the normal and hypothetical accident conditions for an individual package and package arrays. These results, rounded to three decimal places, are shown in Table 6-1. Calculations were also made to show that the Traveller STD is bounded by the Traveller XL. Results for the Traveller STD are given in Table 6-2. Finally, Table 6-3 shows the results for the Rod Pipe in the Traveller XL.

Table 6-1 Summary Table for Traveller XL with PWR Fuel Assembly	
Traveller XL	**K_{eff}**
Single Package	
Normal	0.201
HAC	0.885
Package Array	
Normal	0.272
HAC	0.939

Table 6-2 Summary Table for Traveller STD with PWR Fuel Assembly	
Traveller STD	**K_{eff}**
Single Package	
Normal	n/a
HAC	0.865
Package Array	
Normal	0.256
HAC	0.897

Table 6-3 Summary Table for Traveller XL with the Rod Pipe	
	K_{eff}
Single Package	
Rod Pipe	0.750
Package Array	
Rod Pipe	0.750

6.1.3 Criticality Safety Index (CSI)

6.1.3.1 PWR Fuel Transport Index

The Criticality Safety Index when transporting PWR fuel assemblies is calculated as follows:

2 * N = Array Size
Array Size = 150
N= 150/2 → 75
Therefore, CSI = 50/75 → 0.7

6.1.3.2 Rod Pipe Transport Index

The Criticality Safety Index when transporting rods in either rod container is calculated as follows:

2 * N = Array Size
Array Size = infinite
N= infinity/2 → infinity
Therefore, CSI = 50/infinity → 0.0

6.2 FISSILE MATERIAL CONTENTS

The package will be used to carry heterogeneous uranium compounds in the form of fuel rods. These rods will transported either as PWR fuel assemblies or as loose PWR or BWR fuel rods in a rod container. The uranium enrichment shall not be greater than 5.0 wt% ^{235}U. The uranium isotopic distribution considered in the models in this criticality safety analysis is shown in Table 6-4.

Table 6-4 Uranium Isotope Distribution

Isotope	Modeled Wt%
^{235}U	5.0
^{238}U	95.0

Reactor control cluster (RCC) assemblies, secondary source assemblies, and solid stainless steel rods that may be placed in the PWR fuel assembly are non-fissile material.

6.2.1 PWR Fuel Assemblies

The fuel assembly types to be transported in the Traveller belong to the 14x14, 15x15, 16x16, 17x17, and 18x18 families. Different fuel assembly products in each family may have names not included in this application, but the parameters important to criticality are described in Appendix 6.10.1. The Traveller XL will carry all fuel assembly types while the Traveller will carry the 12-ft. long assemblies.

Calculations were performed to determine which fuel assembly would be the most reactive. Appendix 6.10.2 provides more detail. The analysis compares k_{eff} versus fuel assembly envelope when expanding a 100 cm length of the assembly from nominal to 14 inches (35.56 cm). Figure 6-23 shows the results over the entire range. Figure 6-5 shows regression curve fits over the range of interest, that is, up to 9.6 inches/24.384 cm.

This analysis indicates that the 17x17OFA is the most reactive fuel assembly over the range of interest. However, the difference between the 17x17STD and the 17x17OFA is less significant at the top end of the range (9.6 inches/24.384 cm). The 17x17OFA is the most reactive contents and fuel assembly to use in all calculations. Reactor control cluster (RCC) assemblies, secondary source assemblies, and solid stainless steel that may be placed in the PWR fuel assembly are non-fissile material and lower the water-to-fuel ration in the fuel rod lattice. The fuel rod lattice is under moderated for both nominal and accident conditions; therefore, the displacement of water from the thimble tube locations by the RCC or secondary source assemblies caused k_{eff} to decrease. In addition to adding neutron absorption, the solid stainless steel rod displaces a uranium rod from the fuel lattice which also causes k_{eff} to decrease.

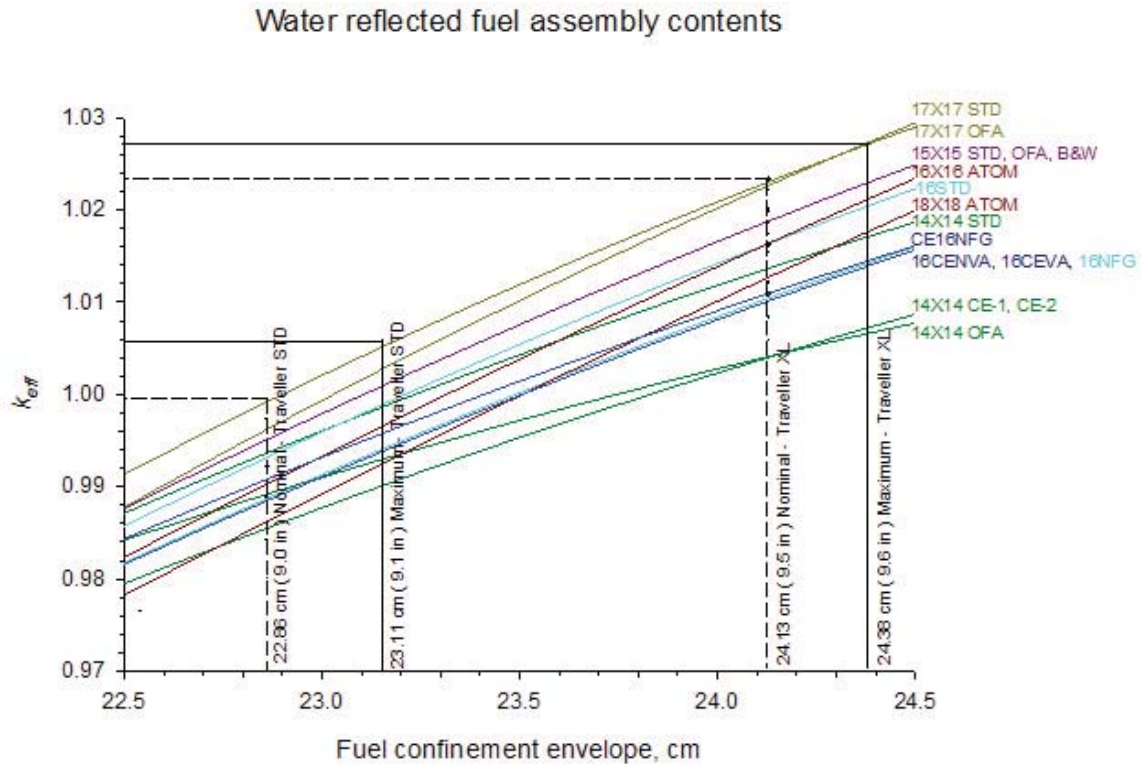

Figure 6-5 Regression Curves of k_{eff} Versus Fuel Assembly Envelope over Range of Interest

6.2.2 PWR and BWR Rods

The Traveller will carry loose rods in a rod pipe. Table 6-5 below gives the nominal parameter ranges for the fuel rods. Analysis for the rod pipe was based solely on pellet diameter and pellet pitch. Therefore, there are no restrictions on the non-fuel components of the rods. Fuel rods that satisfy the criteria of Table 6-5 may be transported. This applies to PWR and BWR fuel rods.

Table 6-5 Fuel Rod Parameters

Parameter	Limit
Maximum Enrichment	5.0 weight percent Uranium-235
Pellet diameter	0.508 – 1.524 cm (0.20 – 0.60 in.)
Maximum stack length	Up to rod container length
Cladding	Zirconium alloy
Integral absorber	Permitted (types include: Gadolinia, Erbia, Boron)
Wrapping or sleeving	Plastic or other material with moderating capability not greater than full density water, except for polyethylene sleeving used to protect fuel rods.
Maximum number of rods per container	Up to rod container capacity

6.3 GENERAL CONSIDERATIONS

The models developed for these calculations are not exact representations of the package, but they do explicitly include all of the physical features that are important to criticality safety. Modeling approximations will be shown to be either conservative or neutral with respect to the criticality safety case. This section describes the packaging and the contents models.

6.3.1 Model Configuration

Geometry input dimensions are taken directly from design drawings and are derived by stacking dimensions from design drawings or calculated using geometric relationships and dimensions shown on design drawings. Longitudinal dimensions in the model are oriented along the z-axis, and latitudinal dimensions are oriented in the x-y plane. The origin of the individual package unit is near the bottom of the package along the z-axis and at the center of the package in the x-y plane. The positive direction is from bottom to top of the package along the z-axis, the positive direction is from left to right along the x-axis when viewed from the top of the package and the positive direction is from lower to upper along the y-axis.

6.3.1.1 Contents Models

The contents models used in support of this analysis include the PWR fuel assembly model, the BWR fuel rod model, and the Rod Pipe.

6.3.1.1.1 PWR Fuel Assembly Model: 17OFA-XL

Section 6.2.1 established that the 17x17OFA would be the fuel assembly used in all calculations. In order to incorporate the maximum fuel assembly length, the 17x17STD-XL, an imaginary fuel assembly, the 17OFA-XL, was modeled in the calculations. The 17OFA-XL model is described in detail in Appendix 6.10.3. It basically consists of concentric cuboids to model the top nozzle assembly, skeleton, and fuel regions. The fuel assembly origin is at the bottom left hand corner of the fuel assembly lower nozzle. The fuel assembly is placed inside the fuel confinement with no translation of the origin. Table 6-6 shows the parameters of the 17OFA-XL and how they compare to the 17x17OFA and 17x17STD.

Table 6-6 17OFA-XL Parameters

Fuel Assembly Type	W-STD/XL	W-OFA	W-OFA/XL
Nominal Pellet Diameter	0.3225 (8.192)	0.3088 (7.843)	0.3088 (7.843)
Annular Pellet Inner Diameter	0.155 (3.937)	0.155 (3.937)	0.155 (3.937)
Nominal Clad Thickness	0.0225 (0.572)	0.0225 (0.572)	0.0225 (0.572)
Clad Material	Zirconium alloy	Zirconium alloy	Zirconium alloy
Nominal Clad Outer Diameter	0.374 (9.499)	0.360 (9.144)	0.360 (9.144)
Maximum Stack Length	169 (4292.6)	145 (3683)	169 (4292.6)
Nominal Assembly Envelope	8.418 (213.817)	8.418 (213.817)	8.418 (213.817)
Kg's ^{235}U Assembly	28	22	28
Nominal Lattice Pitch	0.496 (12.598)	0.496 (12.598)	0.496 (12.598)
GT Diameter	0.482 (12.243)	0.474 (12.040)	0.474 (12.040)
GT Thickness	0.016 (0.406)	0.016 (0.406)	0.016 (0.406)
GT Material	ZIRC	ZIRC	ZIRC
IT Diameter	0.482 (12.243)	0.474 (12.040)	0.474 (12.040)
IT Thickness	0.016 (0.406)	0.016 (0.406)	0.016 (0.406)
IT Material	ZIRC	ZIRC	ZIRC

6.3.1.1.2 Fuel Rod Model

The fuel rods for the rod containers are conservatively modeled in order to bound all PWR and BWR fuel rods that will be transported. The rods are modeled as pellet stacks with no consideration given to cladding or other non-fuel characteristics or properties. The rod container analysis consists of evaluating arrays of pellet stacks inside each container type (Rod Box and Rod Pipe), varying the pellet diameter and pitch to determine the optimum configuration. Actual pellet diameters of fuel to be transported ranges from 0.20 inches to 0.60 inches [0.508 cm to 1.524 cm]. The evaluation modeled the pellets over the range from 0.05 inches to 1.0 inch [0.127 cm to 2.54 cm] at 0.05 inch increments. Pellet pitch in the model ranged from close-packed to 4.0 cm in order to find the optimum water-to-fuel ratios for each pellet diameter.

No credit is taken for integral burnable absorbers. 100% theoretical density is assumed. Parameters are given in Table 6-7. There are no restrictions with respect to the type of neutron absorbers that may be included in the fuel design.

Table 6-7 Fuel Rod Model Dimension Ranges

Element	(cm)	(inch)
Pellet Radius	0.0635 – 1.27	0.025 – 0.50
Pellet Diameter	0.127 – 2.54	0.050 – 1.0
Full Length Rod	448.3862	176.53

6.3.1.1.3 Rod Pipe Model

The Rod Pipe is described in Section 1. It is modeled as a simple cylinder with diameter 6.625 inches/ 16.8275 cm, which equates the nominal outside dimension of a 6.0 inch diameter stainless steel pipe. It is sealed at both ends. No internal padding or cushioning is modeled. Nor is it modeled with any flanges or fittings that enable it to seat inside the Clamshell. It's length is 177 inches/450 cm. The Rod Pipe is positioned at the bottom of the Clamshell.

6.3.1.2 Packaging Model

6.3.1.2.1 Outerpack Model

The actual Traveller STD and Traveller XL outerpacks are identical with the exception that the XL is longer than the STD and the shock mount configurations are different. The shock mount configurations are shown in License Drawing 10001E58. The criticality evaluations will use the same outerpack model for both the STD and XL calculations with the exception of shock mount configuration. The outerpack model is described further in Appendix 6.10.4.

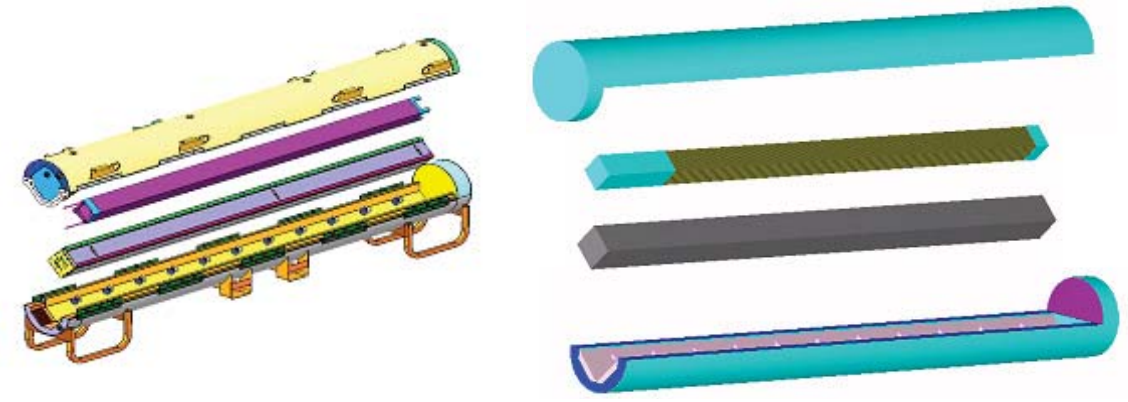

Figure 6-6 Solid Works Model and Keno3D Rendering of Traveller

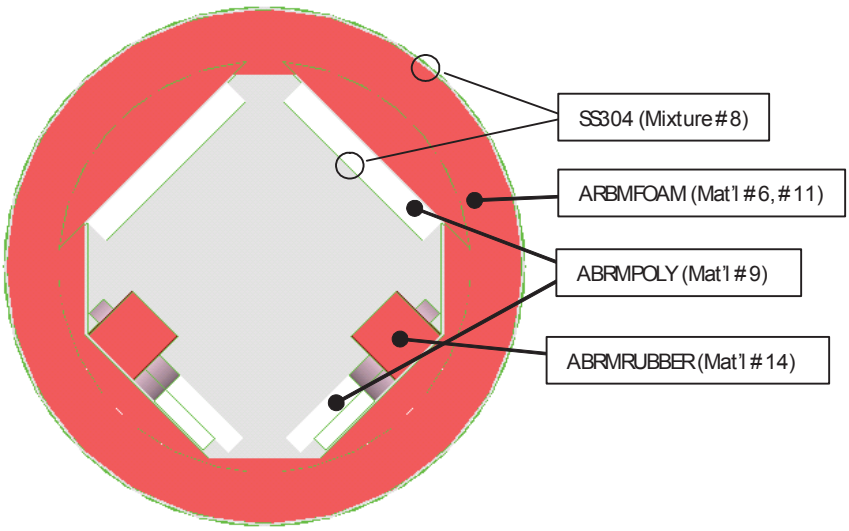

Figure 6-7 Outerpack Model Showing Material

6.3.1.2.2 Clamshell Model

The Clamshell model is described in greater detail in Appendix 6.10.4. It consists of two concentric cuboids to model the outer wall and two intersecting cuboids to model the fixed neutron absorber panels, which are inset into the walls. The Clamshell origin is at the bottom left hand corner of the inside surface. The Clamshell is rotated 45 degrees in the positive direction and the origin is translated in the positive z direction to position the Clamshell inside the Outerpack. The Clamshell can be seen in Figure 6-2 and Figure 6-4.

6.3.2 Material Properties

The Standard Composition Library was used to specify material and mixtures. Those not found in the library are specified using the procedures for arbitrary mixtures described in the SCALE manual. Table 6-8 shows an excerpt from an input deck showing how the material properties are described. The technique used for modeling certain materials as a void (e.g. arbmfoam, arbmrubber) was to change the density by taking it to the 10^{-20} power).

Table 6-8 Sample Input Showing Material Properties

```
TRAVELLER XL,17WOFA,ENV=24.384      cm,L=100      cm,B10=0.018   g/cm2
44groupndf5  latticecell
 uo2 1 1 293 92235 5 92238 95 end
 h2o 2 1 293 end
 zirc4 3 1 293 end
 h2o 4 1 293 end
 h2o 5 1 293 end
 arbmfoam 0.1602e-20  4  0  0  0 6012 70 1001 10 8016 16 7014 4  6 1 293
 end
 al 7 1 293 end
 ss304 8 1 293 end
 polyethylene 9 DEN=0.828 1.0 293 end
 arbmfoam 0.1602e-20  4  0  0  0 6012 70 1001 10 8016 16 7014 4 11 1 293
 end
 b-10 12 0 0.0047781    end
 b-11 12 0 0.019398     end
 c   12 0 0.0060439    end
 al  12 0 0.043223     end
 arbmrubber 1.59e-20  7  0  0  0 8016 46.94 13000 19.92 14000 17.54 6012
 10.79 1001 4.73 11000 0.06 26000 0.02  14 1 293 end
 h2o 15 1 293 end
 uo2 16 1 293 92235 5 92238 95 end
 h2o 17 1 293 end
 zirc4 18 1 293 end
 h2o 19 1 293 end
end comp
squarepitch 1.4669       0.78435      16 19 0.9144       18 0.8001       17 end
more data
res=1  cylinder 0.39218      dan(1)=0.22632       end
```

To more fully document the composition of each compound and/or document the assumptions used in producing the associated cross-section data, a brief description of each material is given in Table 6-9 below:

Table 6-9 Material Descriptions

ZIRC4: Zircaloy - 6.56 g/cc • 98.23 wt % zirconium • 1.45 wt % tin • 0.1 wt % chromium • 0.210 wt % iron • 0.01 wt % hafnium	**SS304:** Stainless steel - 304 - 7.94 g/cc • 68.375 wt % iron • 19 wt % chromium • 9.5 wt % nickel • 2 wt % manganese • 1 wt % silicon • 0.08 wt % carbon • 0.045 wt % phosphorus
UO_2: Uranium dioxide: UO_2 - 10.96 g/cc	**POLYETHYLENE:** Polyethylene: $[C_2H_2]_n$, 0.92 g/cc
H2O: Water: cross sections developed using 1/E weighting everywhere, 0.9982 g/cc	**ARBMFOAM:** • C 50-70 wt % • O14-34 wt % • N 4-12 wt % • H 4-10 wt % • P 0-2 wt % • Si, <1 wt % • Cl <1800 ppm • Other <1 wt %
ARBMRUBBER: Rubber • O 49.94 wt% • Al 19.92 wt% • Si 17.54 wt% • H 4.73 wt% • Na 0.060 wt% • Fe 0.020 wt%	
ARBMBORAL: BORAL • B_4C • ^{10}B loading – 0.024 g/cm^2 • BORAL core thickness – 0.3175cm	

Multiple sets of iron, nickel, and chromium nuclides are available in the Standard Composition Library (FESS, NISS, CRSS). These sets correspond to different weighting functions used in generating the multigroup cross sections. For the 44- and 238-group libraries generated from ENDF/B-V data, there are two special weighting functions. One special weighting function corresponds to 1/E σ_t (E), where σ_t (E) is the total cross section of stainless steel 304. In the other special weighting, σ_t (E) is the cross section for the referenced nuclide.

Table 6-10 Material Compositions

Compound	Density (g/cm^3)	Elt.	Atomic density (atoms/b-cm)	Compound	Density (g/cm^3)	Elt.	Atomic density (atoms/b-cm)
Uranium dioxide	10.9600	U-235	1.23767E-03	BORAL	2.5891	B-10	0.0047781
		U-238	2.32186E-02			B-11	0.019398
		O	4.89126E-02			C	0.0060439
Water	0.9982	O	3.33846E-02			AL-27	0.043223
		H	6.67692E-02	Aluminum	2.7020	AL	6.03066E-02
Zirc 4	6.5600	ZR	4.25413E-02	Stainless steel	7.9400	C	3.18772E-04
		SN-112	4.68065E-06			SI	1.70252E-03
		SN-114	3.13652E-06			P	6.94680E-05
		SN-115	1.73715E-06			CRSS	1.74726E-02
		SN-116	7.01133E-05			MN	1.74071E-03
		SN-117	3.70592E-05			FESS	5.85446E-02
		SN-118	1.16872E-04			NISS	7.74020E-03
		SN-119	4.14021E-05	Polyethylene	0.9200	C	3.95300E-02
		SN-120	1.57260E-04			H	7.90600E-02
		SN-122	2.23417E-05	Silicone Rubber	1.5900	O	2.81077E-02
		SN-124	2.79391E-05			H	4.49402E-02
		FE	1.48557E-04			Fe	3.42922E-06
		CR	7.59779E-05			C	8.60970E-03
		HF	2.21333E-06			Al	7.06913E-03
Foam 11 PCF	0.1602	O	9.65313E-04			Si	5.97996E-03
		H	9.57279E-03			Na	2.49902E-05
		C	5.62769E-03				
		N	2.75581E-04				

6.3.2.1 Package to Model Comparison

A comparison of the mass of materials in the package model to the actual package provides an overall assessment of differences in geometry and material composition. The mass of the materials in the package model is calculated using the volume option in KENO-VI that calculates volumes of each material using the random method. The model volume is multiplied by the material density to obtain the model mass for each material. There are some materials in the actual package that are not included in the package model. Tables 6-11 through Table 6-13 compares the model mass quantities to the actual.

The actual mass of materials is obtained from design drawings for the package. A small quantity of plastic in the Outerpack vent plugs and steel in the shock mount bolts are not included. Also, some of the stainless steel structure in the Outerpack is not included in the model. Over 100 kg (220 lb.) of stainless steel in the components of the package were not included in the model. The cork rubber used as spacer material in the Clamshell, and the stainless steel in the Clamshell hinge pins are not included in the model.

Material No.	Material	Density	Model Mass	Approx. Mass
8	ASTM A240 type 304 SS	7.94 g/cm^3 [494.38 lb/ft^3]	408.7 kg [901 lb.]	488 kg [1866 lb.]
6, 11	Foam	0.10–0.32 g/cm^3 [6.20 lb/ft^3]	130.5 kg [287.7 lb.]	153 kg [339 lb.]
14	Rubber	1.59 g/cm^3 [68.7 lb/ft^3]	3.8 kg [8.3 lb.]	4.5 kg [14 lb.]
9	Polyethylene	0.92 g/cm^3 [57.43 lb/ft^3]	161.5 kg [356 lb.]	187 kg [340 lb.]

Table 6-12 Actual Mass Versus Modeled Mass – Clamshell

Material No.	Material	Density	Model mass	Actual mass
7	6061 Aluminum	2.64 g/cm^3 [164.98 lb/ft^3]	118 kg [260 lb.]	162 kg [357 lb.]
12	BORAL	2.71 g/cm^3 [169.16 lb/ft^3]	25 kg [55 lb.]	25 kg [55 lb.]
NA	Cork/natural rubber	[0.56 g/cm^3] [34.73 lb/ft^3]	0	4.5 kg [9.9 lb.]
NA	Stainless steel	7.94 g/cm^3 [495.68 lb/ft^3]	0	3.72 kg [7.6 lb.]

None of the stainless steel in the bottom and top nozzle is included in the fuel assembly. The uranium dioxide actual mass is less than the model mass because theoretical density is used in the model, but actual density is 96.5 percent the theoretical density. The zirconium mass is less in the model because the spacer grids are not included. Neither the model mass nor the actual mass for the contents includes the mass of the fuel rod bottom and top end plugs, plenum spring. Also, the skeleton stainless steel lock tube and top nozzle insert mass are not included in the comparison.

Table 6-13 Material Specifications for Contents

Material No.	Material	Density	Model mass	Actual mass
1	Uranium dioxide	10.96 g/cm^3 [494.38 lb/ft^3]	575 kg [1268 lb.]	560 kg [1234 lb.]
2, 4	Water	0.9982 g/cm^3 [62.31 lb/ft^3]	Variable	Variable
3	Zircaloy	6.56 g/cm^3 [409.48 lb/ft^3]	126 kg [278 lb.]	148 kg [326 lb.]
NA	Stainless steel	7.94 g/cm^3 [795.63 lb/ft^3]	0 kg [0 lb.]	17 kg [37 lb.]
NA	Inconel		0 kg [0 lb.]	2.60 kg [5.7 lb.]

6.3.3 Computer Codes and Cross-Section Libraries

The 44-group ENDF/B-V library has been developed for use in the analysis of fresh and spent fuel and radioactive waste systems. The library was initially released in version 4.3 of SCALE. Collapsed from the finegroup 238-group ENDF/B-V cross-section library, this broad-group library contains all nuclides (more than 300) from the ENDF/B-V data files. Broad-group boundaries were chosen as a subset of the parent 238-group ENDF/B-V boundaries, emphasizing the key spectral aspects of a typical LWR fuel package.

Specifically, the broad-group structure was designed to accommodate the following features: two windows (where the cross section drops significantly at a particular energy, allowing neutrons at that energy to pass through the material) in the oxygen cross-section spectrum; a window in the cross section of iron; the Maxwellian peak in the thermal range; and the 0.3-eV resonance in 239Pu (which, due to its low energy, cannot be properly modeled via the SCALE Nordheim Integral Treatment module NITAWL-II). The resulting boundaries represent 22 fast and 22 thermal energy groups; the full-group structure is compared with that of the 238-group library. The finegroup 238-group ENDF/B-V cross sections were collapsed into this broad-group structure using a fuel-cell spectrum calculated based on a 17 × 17 Westinghouse pressurized-water reactor (PWR) assembly. Thus, the 44-group library performs well for LWR lattices, but not as well for other types of systems. The 44-group ENDF/B-V library has been tested against its parent library, using a set of 33 benchmark problems in order to demonstrate that the collapsed set was an acceptable representation of 238-group ENDF/B-V, except for intermediate-energy systems.

6.3.4 Demonstration of Maximum Reactivity

This section demonstrates the most reactive configuration of each case presented in sections 6.4, 6.5, and 6.6. Assumptions and approximations are identified and justified. The optimum combinations of internal and interspersed moderation for the different cases are also explained.

6.3.4.1 Evaluation Strategy

It is important to understand the significant differences that exist between the routine transport configuration, the normal condition of transport case, the as-found configuration after hypothetical accident (HAC) testing, and the license-basis case. The Traveller CTU was tested in accordance with U.S. and IAEA regulatory requirements. Mechanical design calculations, finite element analysis calculations, actual drop test data, reasoned engineering analysis, and sound engineering judgment were used to determine worst-case orientations for the mechanical and thermal tests. This is explained in Section 2. The as-found condition of the package represents the most damaging configuration following actual testing. Therefore, it follows that the as-found package configuration combined with the worst-case flooding configuration, conservative material assumptions, and conservative fuel assembly assumptions should form the license-basis case for the safety analysis. (The worst-case flooding condition must be assumed because the Traveller was not actually subjected to an immersion test). The evaluation strategy used to arrive at the license-basis case is presented below. A flow chart showing the evaluation strategy is given in Figure 6-8.

Using the license-basis case as a frame of reference, a series of sensitivity studies were then performed to evaluate certain hypothetical conditions and scenarios. They are listed in Section 6.3.4.9 and discussed in Section 6.7.

6.3.4.2 Baseline Case for Packaging (Routine Condition of Transport)

The baseline case is the routine condition of transport. See Table 6-15. Note that the Routine case was not modeled. It is presented in order to show the conservative differences that exist between it, the normal condition of transport, the as-found condition after testing, and the license-basis case, which are modeled.

The lateral dimensions of the Outerpack for the Traveller STD and Traveller XL are identical and remain the same for all conditions of transport. The Outerpack outer diameter is 25.0 inches (63.5 cm). This diameter does not change throughout the testing. The circumferential stiffeners absorb the impact forces of the 9-meter drop, leaving the packaging diameter unchanged. The lower section polyethylene blocks measure 1.75 inches (4.445 cm). The upper section poly blocks measure 1.25 (3.175) inches. The conditions that vary in the Outerpack model are the condition of the floodable void spaces and the material densities. These items are discussed in the respective sections below.

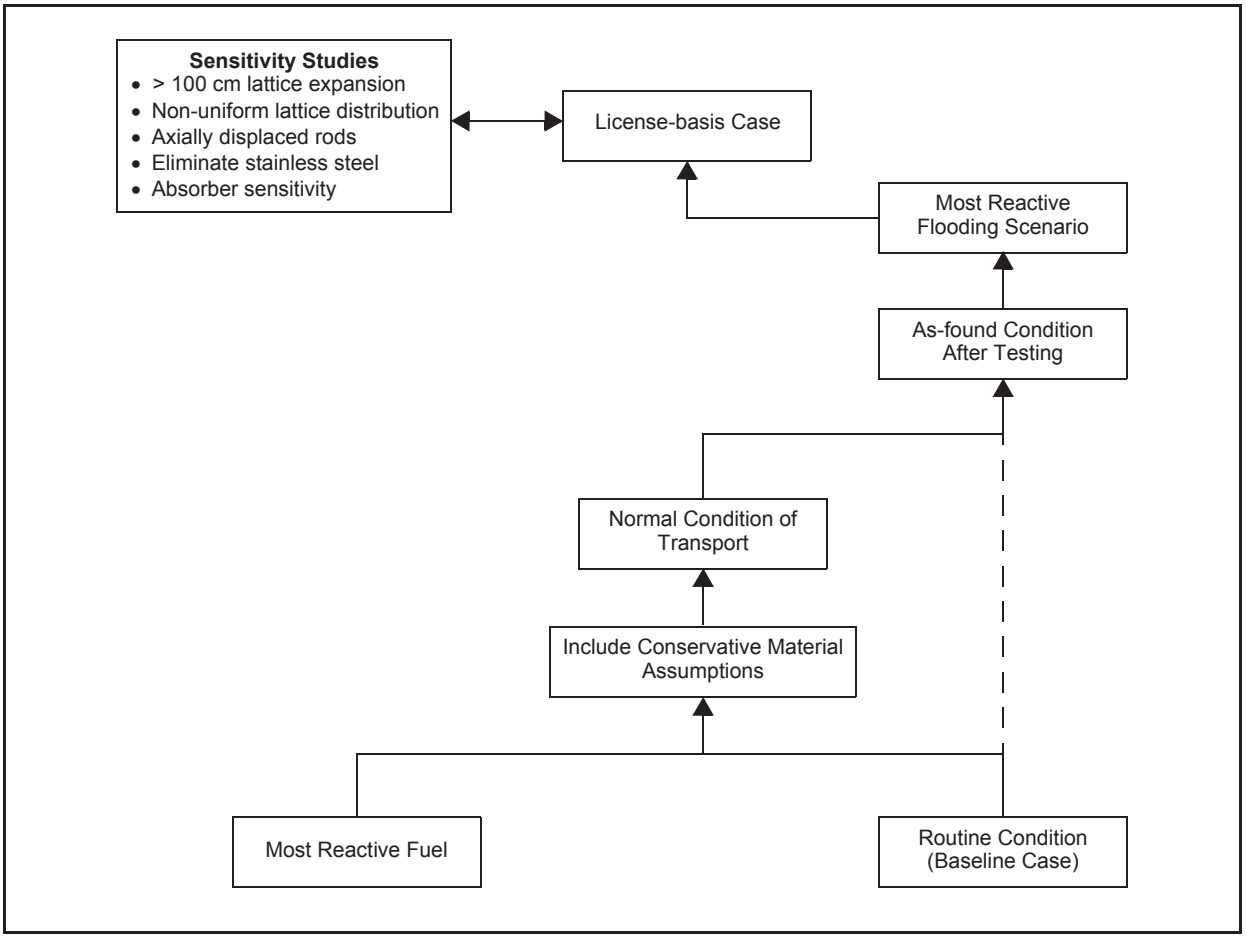

Figure 6-8 Criticality Evaluation Strategy

The internal dimension of the Traveller XL Clamshell measures 9.50±0.05 inches (24.13±0.127 cm), making the maximum dimension 9.55 inches (24.257 cm). The bottom faces of the clamshell are lined with 0.188 inch (0.476 cm) thick cork. The cork lining therefore reduces the effective clamshell dimension to 9.36 inches (23.78 cm).

The internal dimension of the Traveller STD clamshell is 9.00± 0.05 inches (22.86±0.127 cm). The effective volume of the clamshell with the cork lining in place is 8.86 inches (22.51 cm).

For the routine case the polyurethane foam, moderator blocks, and rubber shock mounts are in place.

The ^{10}B content of the neutron absorber plates has a minimum areal density of 0.024 g/cm^2 (BORAL).

All floodable void spaces of the Outerpack are dry for the routine configuration.

The fuel assembly is undamaged. That is, there is no expansion of the lattice pitch and the pin-gap is dry. Nominal cladding thickness is used.

6.3.4.3 Most Reactive Fuel Assembly Type (Contents)

Establishing the most reactive fuel assembly type involved performing a comparison of all PWR fuel assemblies to be transported in the Traveller. The analysis is described in section 6.2.1 and appendix 6.10.2. The following assumptions and conservatisms were included:

- Assumed 100% TD
- Assumed flooded pin-gap
- Ignored dishing, chamfering of pellets
- Ignored burnable poisons (Gd, Erbia, Boron)

6.3.4.4 Most Reactive Flooding Configurations (Flooding Case)

The flooding case takes the license basis case with the most reactive fuel assembly and analyzes for the most reactive flooding scenario for a single package a package array. This was done by modeling the floodable void spaces (see Section 6.1.1.6) in different combinations to determine which combination produces the highest k_{eff}. Included in the combinations were those that replicate total water immersion (full density water) or burial in snow (low density water). The flooding scenarios are discussed in section 6.7.1. The most reactive flooding configuration for a single package is described in section 6.4.1.2. The most reactive flooding configuration for a package array configuration is described in section 6.6.1. The most reactive flooding cases for the individual package and package array cases are summarized in Table 6-15.

Table 6-14 has been deleted.

6.3.4.5 Conservative Material Assumptions

The following conservative material assumptions are incorporated:

- The Traveller XL clamshell is conservatively modeled at 9.60-inches (23.384 cm), neglecting the presence of the cork liner and the manufacturing tolerance. This is a difference of 0.24 inches (0.61 cm).
- The Traveller STD clamshell is conservatively modeled at 9.1 inches (23.114 cm).
- Cork liner in clamshell not considered.
- The polyethylene moderator blocks are modeled 90% actual density, or 0.828g/cc.
- The ^{10}B content is modeled at 75% areal density for BORAL (0.0180 g/cm^2).
- The shock mounts are modeled as a void.
- Shock mount placement is important to criticality because the shock mounts penetrate the moderator through a 6 inch (15.24 cm) cutout. The shock mount configuration for the Traveller STD is modeled according to drawing, relative to either end of the outerpack. The Traveller XL is modeled conservatively in order to maximize the extent to which the 100-cm section of expanded lattice of the fuel assembly is placed over the shock mounts. Hence, the shock mounts are not placed at either end as shown in the license drawing and described in section 6.1.1.5. The first pair is locted 15 inches from the end. The second pair is 18 inches (45.7cm) from the first, and the third is 36 inches from the second. The gap between the first two pair of shock mounts is eliminated in order to maximize the interaction between the expanded sections of fuel.

6.3.4.6 Normal Condition of Transport

The Traveller model under normal condition of transport is described as follows:

- Outerpack dimensions are modeled as in section 6.3.4.2.
- Clamshell is modeled as in section 6.3.4.5.
- Fuel assembly is modeled as in section 6.3.4.2.
- The polyurethane foam and shock mounts are modeled at nominal density. Neither is altered under normal conditions of transport.
- The moderator blocks are modeled as in section 6.3.4.5.
- The neutron absorber is modeled as in section 6.3.4.5.
- All floodable void spaces of the Outerpack are modeled dry.
- The package is close reflected by 20 cm water.

As required by 10CFR71 and TS-R-1, the Traveller shipping package has been designed and constructed such that under the tests specified for normal conditions of transport, the following pertains:

- The contents are subcritical.
- The geometric forms of the package contents are not altered.
- There is no inleakage of water.

This page intentionally left blank.

- There was no reduction in effectiveness of the packaging. Section 2.12.4.2.3 describes the Certification Test Unit (CTU) following the hypothetical accident tests. From that inspection, the following can be concluded:

  — There was no reduction in the total effective volume of the packaging on which nuclear safety is assessed. Because there was no reduction in volume following the hypothetical accident condition testing, it follows that there is none during normal conditions of transport.

  — There was no reduction in the effective spacing between the fissile contents and the outer surface of the packaging. Test results report that the clamshell held the contents in place.

  — There were no breeches in the Outerpack. Hence, there is no occurrence of an aperture in the outer surface of the packaging large enough to allow the entry of a 10 cm (4 in) cube.

- The loss of efficiency of built-in neutron absorbers is addressed. The calculations assume less than 100% ^{10}B for the neutron absorber.

- The loss of efficiency of built-in moderators is addressed. The calculations assume 90% actual moderator density.

- The rearrangement of the contents within the package is addressed. There was no loss of contents from the package.

- There was no reduction of space within the package.

- There was no reduction of spacing between packages.

- The effect of temperature changes is addressed below.

6.3.4.7 Actual As-found Condition After HAC Testing

The actual condition of the Traveller XL package after HAC testing is described in Table 2-5 and section 2.12.4.2.3. It is important to note the actual as-found condition so comparisons can be made between it and the more conservative license-basis condition. The actual as-found condition was analyzed to determine the relative k_{eff} between it and the license-basis case. Results are found under section 6.7.

The Outerpack diameter was unchanged. A good portion, but not all, of the polyurethane foam had burned away. The moderator blocks were in place and not damaged. All shock mounts were in place, holding the clamshell in place. The cork liner was in place.

The bottom nozzle end drop is believed to be the worst-case drop orientation for the fuel assembly because it directly challenges the criticality safety of the package in ways that other drop angles do not. The bottom nozzle impact has been shown to produce the most severe localized damage to the bottom end of the fuel assembly. Further, it is the angle most likely to produce lattice expansion.

As can be seen from above, the as-found condition of the fuel assembly showed 20 cracked rods. Due to the nature of the end impact, the fuel rod array is tightly packed and forced into the bottom nozzle. As the bottom nozzle buckles, the rods located nearest the corners of the adapter plate experience a side loading due to the deforming movement of the plate. This momentum is sufficient to crack the weld but not to break off the bottom end plug because the rods are so tightly packed.

The average magnitude of the crack-widths was 0.03 inches (0.76 mm). The largest crack encompassed about ½ a rod diameter, meaning that none of the end plugs was completely broken off. This cracking is considered insignificant since a 17OFA fuel pellet diameter is 10 times larger than the visible crack widths. Furthermore, localized inward buckling of the rods at the end plug weld zone would tend to reduce the inner diameter of the fuel rod bottom end and preclude the pellet stack from axial movement.

As stated above, the end drop is most likely to produce fuel lattice expansion. In the several prototype and qualification tests conducted prior to the certification test unit testing, (see section 2), it was found that all drop angles other than the end drop compress the fuel assembly lattice. Only the end drop resulted in lattice expansion.

At no point did the lattice pitch expand to fill the clamshell. From the bottom nozzle to the first grid, a 4.0 inch (10.16 cm) span, the fuel envelope measured 9.0 inches (22.86 cm) on one side and 8.75 inches (22.1 cm) on the other. Between grids #1 and #2, about 20 inches (50 cm), the fuel envelope measured 8.32 inches (21.13 cm) on both sides. Between grids #2 and #3, also 20 inches (50 cm), the fuel envelope measured 8.5 inches (21.59 cm) and 8.0 inches (20.32 cm). Between grids #3 and #4 the envelope measured 8.5 inches (21.59 cm) and 8.44 inches (21.44 cm). For the rest of the assembly, the envelope measured no greater than 8.375 inches (21.27 cm). Close examination of the rod arrangement showed that throughout the assembly there was a combination of compressed, nominal, and slightly expanded rod pitches. Several rows of rods were actually touching, some were at nominal pitch, and one or two rods had larger pitch.

Therefore, confinement held because the fissile material remained in the fuel rods and the fuel rods remained inside the clamshell. Neutron absorber and neutron moderator material remained in place.

6.3.4.8 License-Basis Case

The License-Basis Case bounds the as-found condition of the Traveller XL by combining the most reactive flooding configuration of section 6.3.4.4, the conservative material assumptions of section 6.3.4.5, and the conservative assumptions for the fuel assembly which are described in this section. The License-Basis Case is shown in Table 6-15 and described below:

- Outerpack dimensions are modeled as in section 6.3.4.2.
- Clamshell is modeled as in section 6.3.4.5.
- Moderator is modeled as in section 6.3.4.5.
- Neutron absorber is modeled as in section 6.3.4.5.
- Shock mounts are modeled as a void.
- Shock mount placement is modeled as in section 6.3.4.5.
- Foam density, which differs for individual package and package array calculations, is modeled as in Table 6-15.
- Floodable void spaces are modeled as in Table 6-15.
- The fuel assembly is modeled so that it bounds the as-found condition. The model assumes lattice pitch expansion to 9.1 inches (23.114 cm) for the Traveller STD and 9.6 inches (23.384 cm) for the Traveller XL. The lattice expansion is uniformly distributed and extends 100 cm of fuel length.

6.3.4.9 Sensitivity Studies

Sensitivity studies were performed for the following conditions, starting from the license-basis case.

- Partial flooding
- Preferential flooding
- Lattice pitch expansion for full length of fuel assembly
- Non-uniform distribution in lattice expansion
- Axial rod displacement
- ^{10}B areal density
- Moderator density
- Outerpack shell thickness
- Array size
- Annular pellet
- Outerpack diameter
- Actual As-found condition after HAC testing

Table 6-15 Parameters for the Different Traveller Conditions

Parameter	Routine Condition (Not Modeled)	Conservative Material Assumptions (Not Modeled)	Normal Condition of Transport (Modeled)	HAC License-basis Case (Modeled)
SAR Section	6.3.4.2	6.3.4.5	6.3.4.6	6.3.4.8
Outerpack dimension	25.0 inches (63.5 cm)		25.0 inches (63.5 cm)	25.0 inches (63.5 cm)
Polyurethane foam density	Nominal Density		Nominal Density	Water/Void
Shock mount density	Nominal Density		Nominal Density	Void
Clamshell dimension: Traveller	9.0± 0.05 inches (22.86±0.127 cm)			
Clamshell dimension: Traveller XL	9.5±0.05 inches (24.13±0.127 cm)			
Cork liner in place on bottom faces	0.188 inches (0.476 cm)	Not in place	Not in place	Not in place
Effective Clamshell dimension: Traveller	8.86 inches (22.51 cm)	9.1 inches (23.114 cm)	9.1 inches (23.114 cm)	9.1 inches (23.114 cm)
Effective Clamshell dimension: Traveller XL	9.36 inches (23.78 cm)	9.6 inches (24.384 cm)	9.6 inches (24.384 cm)	9.6 inches (24.384 cm)
Neutron absorber density (B-Al/BORAL)	Nominal Density	75%	75%	75%
Moderator density	Nominal Density	90%	90%	90%
Flooding condition (single/array)				
Region 1 – Pin Gap	Dry/Dry		Dry/Dry	Flooded/Flooded
Region 2 – Fuel Assembly Envelope	Dry/Dry		Dry/Dry	Flooded/Flooded
Region 3 - Clamshell	Dry/Dry		Dry/Dry	Flooded/Dry
Region 4 - Outerpack	Dry/Dry		Dry/Dry	Flooded/Dry
Region 5 - Polyurethane Foam	Dry/Dry		Foam/Foam	H_2O/Void
Region 6 - Outside Outerpack	Dry/Dry		H_2O Reflected/Dry	H_2O Reflected/Dry
Fuel Assembly Lattice Pitch Expansion	None	None	None	100 cm

6.4 SINGLE PACKAGE EVALUATION

Calculations were performed to determine the most reactive configuration for a single package in isolation under normal and hypothetical accident conditions of transport. The configurations are described below. These descriptions hold for the Traveller STD and Traveller XL. Discussion for the rod containers is included in section 6.10.7.

6.4.1 Configuration for Fuel Assemblies

6.4.1.1 Configuration Under Normal Conditions of Transport

10CFR71 and TS-R-1 require that the contents be subcritical under normal conditions of transport. TS-R-1 indicates that when it can be demonstrated that the confinement system remains within the packaging following the prescribed tests, close reflection of the package by at least 20-cm water may be assumed. Since this is the case for the Traveller, the individual package evaluation includes the close-reflection around the Outerpack.

The parameters for the normal condition of transport are described in section 6.3.4.6 and shown in Table 6-15.

6.4.1.2 Configuration Under Hypothetical Accident Conditions

The hypothetical accident condition requires that the most reactive flooding configuration be considered. It is generally true that the most reactive configuration for an individual package would be that in which the neutrons are moderated as close to the fuel as possible and reflected back into the fuel assembly region. They should not be allowed to escape or to reach the neutron poison where they would be absorbed.

Calculations have shown that this is the case for the Traveller. Therefore, all floodable void spaces in the package are modeled as fully flooded, and the package is close reflected by 20-cm full density water.

The remaining parameters for the hypothetical accident condition (i.e., the license-basis case) for the Traveller are described in section 6.3.4.8 and shown in Table 6-15.

6.4.2 Results for Fuel Assemblies

The results for single package in isolation calculations are presented in Table 6-16. They include results for normal conditions of transport and hypothetical accident conditions. Included are results for both neutron absorber types.

Table 6-16 Most Reactive Configuration for a Single Package in Isolation

Configuration	Run No.	k_s	Uncert.	Calculated k_{eff}
Traveller STD – Fuel Assembly				
Normal	Bounded by XL			
HAC	STD-HAC-IND	0.8621	0.0012	0.8645
Traveller XL– Fuel Assembly				
Normal	XL-NOR-IND	0.2000	0.0006	0.2012
HAC	XL-HAC-IND	0.8833	0.0009	0.8851
Rod Container				
Normal	Bounded by HAC calculation			
HAC	P-IND-15-6	0.7462	0.0014	0.7490

Figure 6-9 has been deleted.

6.4.3 Configuration for Rod Containers

The discussion on the rod container is found in appendix 6.10.7.

6.5 EVALUATION OF PACKAGE ARRAYS UNDER NORMAL CONDITIONS OF TRANSPORT

6.5.1 Configuration for Fuel Assemblies

The package model for the normal condition of transport is described in section 6.3.4.6. In this analysis it was modeled in an infinite array.

6.5.2 Results for Fuel Assemblies

Table 6-17 Normal Conditions of Transport for Package Array

Configuration	Run No.	k_s	Uncert.	Calculated k_{eff}
Traveller STD – Fuel Assembly				
Package Array – Infinite Package Array				
Normal	STD-NOR-ARRAY-INF	0.2546	0.0005	0.2556
Traveller XL– Fuel Assembly				
Package Array – Infinite Package Array				
Normal	XL-NOR-ARRAY	0.2709	0.0006	0.2721

6.6 PACKAGE ARRAYS UNDER HYPOTHETICAL ACCIDENT CONDITIONS

6.6.1 Configuration for Fuel Assemblies

The most reactive configuration for a package array, in contrast to the individual case, is the one that allows maximum thermal neutron interaction between packages. Section 6.7.1 discusses this in detail. This model assumes a flooding configuration that maximizes neutron interaction. Region 1 (pin-gap) and region 2 (fuel assembly) are flooded to maximize reactivity inside the fuel assembly. Region 3 (Clamshell) is modeled as a void to increase the probability that neutrons escaping the fuel assembly envelope will pass through the neutron poison. The remaining floodable void spaces (region 4 – Outerpack cavity; region 5 – foam; region 6 – outside Outerpack) are modeled as a void to allow maximum interaction between packages in the array.

The configuration of the Outerpack, Clamshell, and contents for the hypothetical accident condition for the Traveller are described in section 6.3.4.8 and shown in Table 6-15. Table 6-18 gives results. Figure 6-10 shows curves for the Traveller XL in a fixed package array as a function of k_{eff} versus length of fuel assembly with lattice expansion.

6.6.2 Results for Fuel Assemblies

Table 6-18 Hypothetical Accident Condition Results for a Package Array

Configuration	Run No.	k_s	Uncert.	Calculated k_{eff}
Traveller STD				
HAC	STD-HAC-ARRAY-100	0.8954	0.0009	0.8972
Traveller XL				
HAC	XL-HAC-ARRAY-100	0.9377	0.0008	0.9393

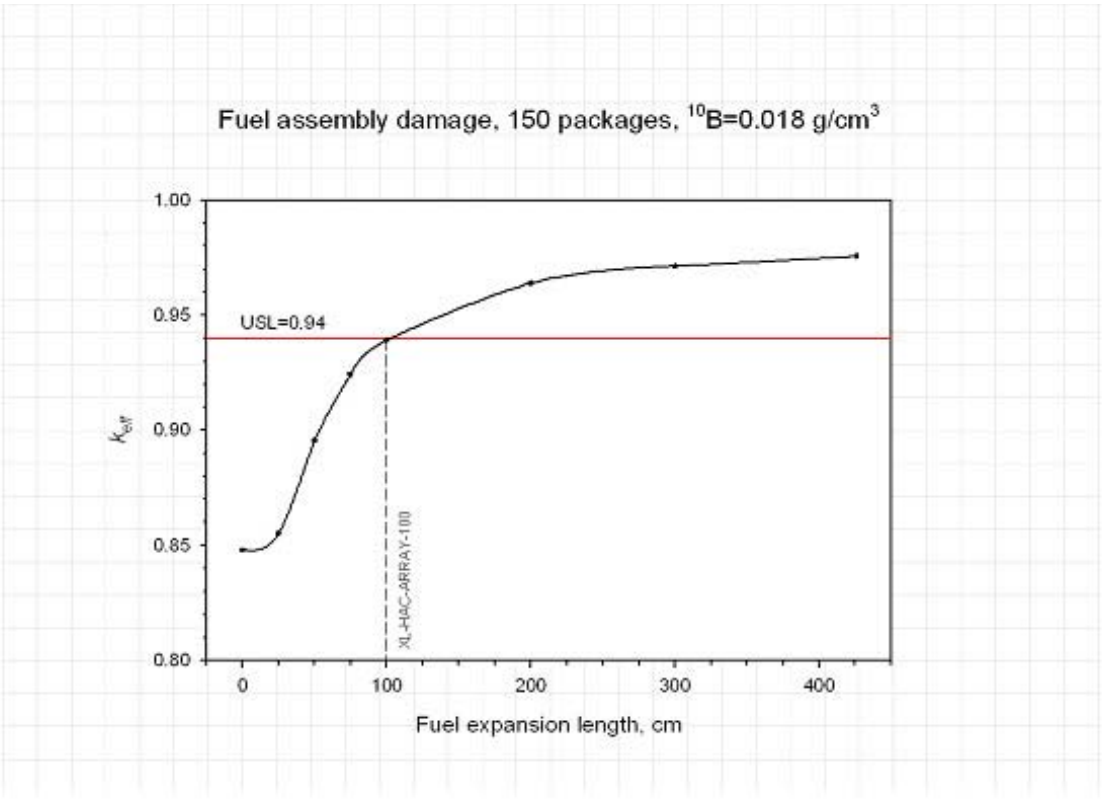

Figure 6-10 Package Array HAC Curve for Traveller XL

6.6.3 Results for Rod Containers

The discussion on the rod container results is found in appendix 6.10.7.

Table 6-19 Hypothetical Accident Condition Results for Rod Container – Package Array

Configuration	Run No.	k_s	Uncert.	Calculated k_{eff}
Rod Box	B-ARR-12-5	0.5367	0.0013	0.5393
Rod Pipe	P-ARR-15-6	0.6518	0.0016	0.6550

6.7 SENSITIVITY STUDIES

6.7.1 Flooding

During transport the package may be subjected to moderation provided by immersion of the package in naturally occurring sources of water (lakes, rivers, ocean, snow, rain) or fire extinguishing agents (water, foams, dry chemicals). Moderator ingress provides varying degrees of moderation inside and outside of the package. The analysis of variance for moderation that is provided by packaging components is evaluated assuming the fuel assembly is moderated with full density water. The greatest interaction between packages, that results in the highest k_{eff} for a package array, occurs when the transport condition causes moderation of the pin-cladding gap and the fuel region, and keeps all other void spaces inside and between the packages dry.

The criticality evaluation considered the Traveller under various flooding schemes to determine the most reactive flooding combination for both the individual package and the array. Note that because the Traveller was not subjected to the immersion test, it is necessary to consider all plausible flooding combinations.

6.7.1.1 Pin-Cladding Gap Flooding

Test results demonstrated that it is possible that rods will crack. Therefore, the evaluation assumes that the pin-gap is flooded for accident conditions. Therefore, the criticality evaluation modeled region 1 as full density water.

6.7.1.2 Most Reactive For Individual Package – Fully Flooded

It is generally true from a criticality perspective that the most reactive configuration for an individual package would be that in which the neutrons are moderated and reflected back into the fuel region before they escape or are absorbed by the neutron poison. Therefore, the most reactive flooding scenario for the individual package assumes that all floodable regions are fully flooded.

6.7.1.3 Most Reactive For Package Array – Preferential Flooding

Preferential flooding (also called differential or sequential flooding) is defined as that scenario in which one cavity of the package remains flooded while one or more of the other cavities drain completely. Referring to section 6.1.1.6 (Floodable Void Spaces) and Figure 6-4, the most reactive configuration for a package array is one in which the neutrons are fully moderated within the fuel region (regions #1 and #2) but where the remaining floodable spaces are modeled as a void to allow neutrons that escape one fuel assembly to have maximum interaction with surrounding packages. Modeling region #3 (Clamshell region) as a void maximizes the probability that neutrons escaping the fuel assembly region will pass out of the Clamshell through the neutron poison. Modeling regions #4 – #6 as voids gives the highest probability of neutron interaction among packages. The array is fully reflected by 20 cm full density water.

The preferential flooding scenario modeled here is unlikely but not impossible. It assumes that the Clamshell drains everywhere except inside the fuel envelope. This scenario does however bound the more likely scenario where the Clamshell drains leaving a water film on the fuel rods.

The preferential flooding scenario also presumes that the entire Outerpack drains leaving water only around the fuel region. The Clamshell is not watertight. Hinge knuckles will allow drainage. As the Outerpack drains, the Clamshell level would drop also.

6.7.1.4 Partial Flooding

Partial flooding differs from preferential flooding in that it is defined as changing water levels in the void spaces of the package. Calculations were performed to evaluate two partial flooding scenarios.

Both involve rotating the package 45° and then changing the water levels in regions #2, #3, and #4. Recall that region #2 is the fuel assembly envelope, region #3 is the area inside the clamshell around the non-expanded fuel assembly, and region #4 is the area inside the outerpack outside the clamshell.

The first scenario involves first keeping regions #2 and #3 flooded (i.e., the areas inside the clamshell) and varying the level in region #4. It can be seen that k_{eff} for the array case drops as region #4 fills because the packages are becoming more isolated. The bounding case here is the preferential flooding scenario described in the previous section. Figure 6-11 shows a rendering of this flooding scenario. Figure 6-12A shows the plot of k_{eff} versus water height in the outerpack. Results are shown in Table 6-37A and a sample input deck is found in Table 6-37C

The second scenario evaluates k_{eff} as a function of varying the water levels in regions #2, #3, and #4 together. That is, this scenario assumes that the water level inside the clamshell rises and falls with the water level in the outerpack. As expected, k_{eff} begins to drop as soon as the fuel is uncovered. Figure 6-12 shows a rendering of this flooding scenario. Figure 6-12B shows the plot of k_{eff} versus water height. Results are shown in Table 6-37B and a sample input deck is found in Table 6-37D.

Figure 6-11 Partial Flooding Scenario #1

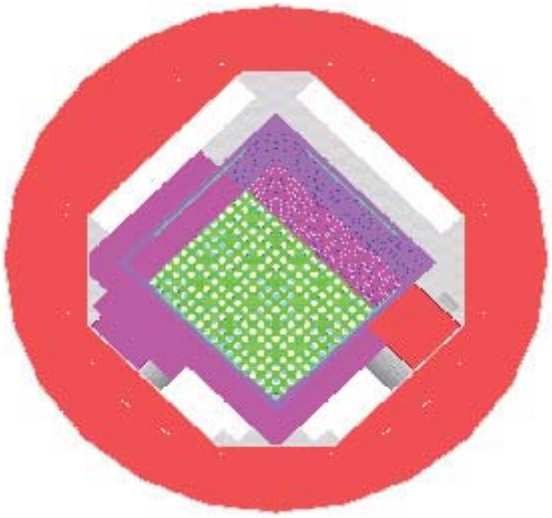

Figure 6-12 Partial Flooding Scenario #2

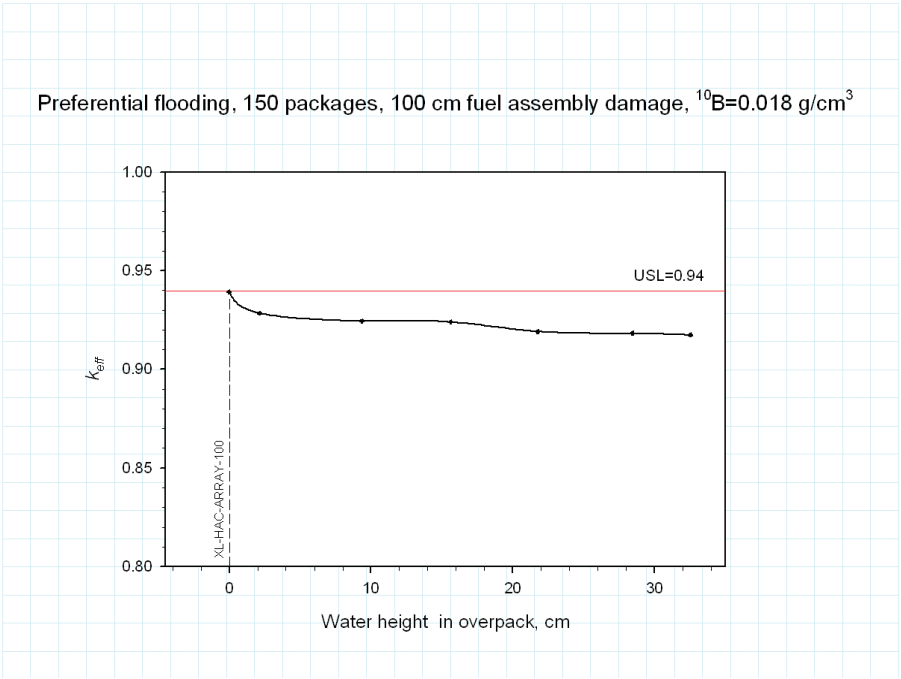

Figure 6-12A Partial Flooding Scenario #1

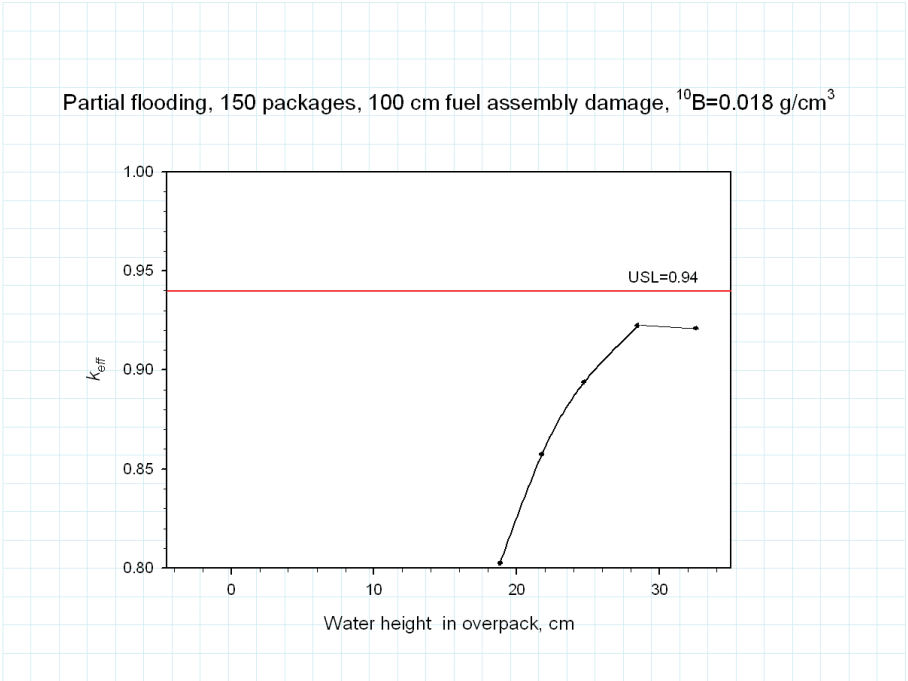

Figure 6-12B Partial Flooding Scenario #2

This page intentionally left blank.

6.7.1.5 Partial Density Interspersed Moderation

Spacing maintains void regions between the packages where environmental factors (snow, rain, ice, and immersion) may provide moderation. Also, materials of construction may scatter or moderate neutrons. The spacing is assumed to be no less than 25 inches provided by the nominal diameter of the Outerpack outer shell. Figure 6-13 shows that the package is overmoderated with respect to interspersed moderation for fuel lattice expansion along a partial length with 2 wt. % Boron where the number of packages in the array is 150.

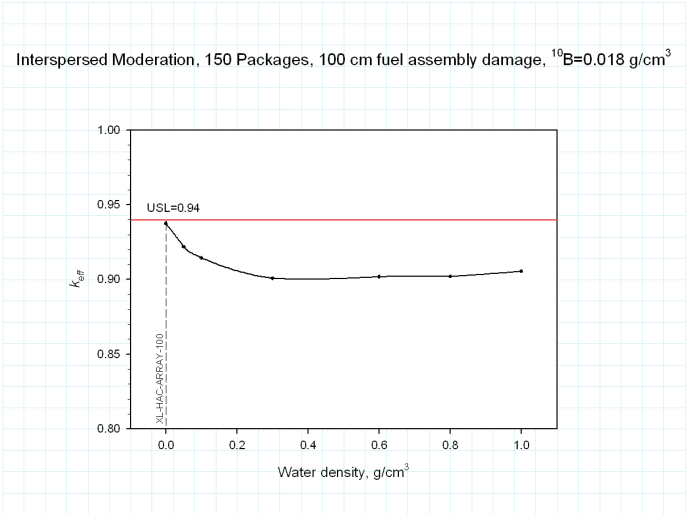

Figure 6-13 Interspersed Moderation Density Curve

6.7.2 Lattice Expansion

From calculations done in support of the Traveller package licensing effort, and from other literature available, it is clear that the factor that has the greatest effect on k_{eff} for a moderated system is lattice pitch expansion. Expanding the lattice pitch of undermoderated fuel assemblies increases the water-fuel ratio. K_{eff} will increase until the water-fuel ratio reaches optimum

This evaluation considered the effect of lattice expansion for all accident configurations. The fuel lattice was expanded to the Clamshell (9.6 inches in Traveller XL and 9.1 inches for Traveller STD) in incremental lengths of 25 cm, 50 cm, 75 cm, 100 cm, 150 cm, 200 cm, 300 cm, and full length (426 cm). It must be noted that analyzing these scenarios does not imply that full-length expansion becomes the license-basis case. Figure 6-10 shows k_{eff} versus length of expanded section for the Traveller XL. Results are given in Table 6-32.

It has been seen from numerous 9-meter drops at different drop angles that any horizontal or shallow angle drop will compress the fuel assembly envelope rather than expand it. Similarly, center-of-gravity drops on the end will cause local crumpling on the end but will not expand the lattice pitch.

Results from a bottom nozzle end drop shows fuel rod lattice pitch expansion at the bottom 20 inches (50 cm). The expansion was not uniformly distributed. There was a combination of rods touching or at compressed pitch, rods at nominal pitch, and rods with expanded pitch.

6.7.2.1 Non-uniform Lattice Expansion

Non-uniform lattice expansion is defined as a fuel envelope with rods at different pitches, such as was found in the tested fuel assemblies. There will be some rods touching, some compressed, some at nominal pitch, and some at expanded pitch. An analysis was performed to determine how non-uniform lattice expansion compared to uniform expansion.

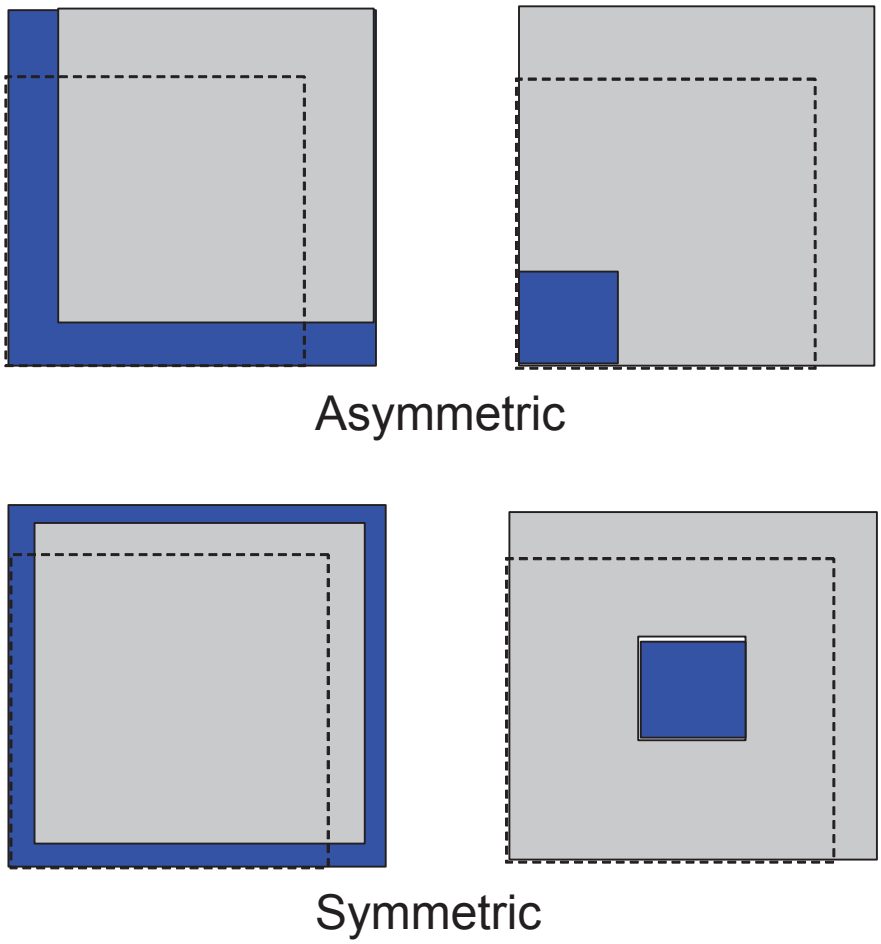

Figure 6-14 Symmetric and Asymmetric Non-uniform Distribution

The analysis assumed a fixed number of rods, namely 289 in a 17x17 array. It then looked at four types of expansion/compression combinations, which can be seen in Figure 6-14. The combinations included compressed rods around the edge of the assembly or in a cluster, in both a symmetric and asymmetric arrangement. The small grid in the figure represents the nominal or close packed rods, and the large grid

represents the remaining rods expanded to the space available for expansion within the confinement of the Clamshell 9.5 inch by 9.5 inch cross section. There are no thimble tubes. These configurations are confined to 100 cm of fuel length.

The graph in Figure 6-15 shows two curves: k_{eff} as a function of the number of rods in the expansion zone {x} and the remaining rods {289-x} either at (1) nominal pitch or (2) close packed. The area between the curves is expected to bound all the rod rearrangements possible within the confinement of the Clamshell. The results show that any compaction of the lattice suppresses the reactivity increase due to rod expansion up until the expansion includes about 100 rods (~1/3 of the assembly). The results also show the importance of the confinement dimension in limiting the possible rearrangements without rods leaving the confines of the Clamshell. These results support the assumption that the most reactive rearrangement is uniform expansion.

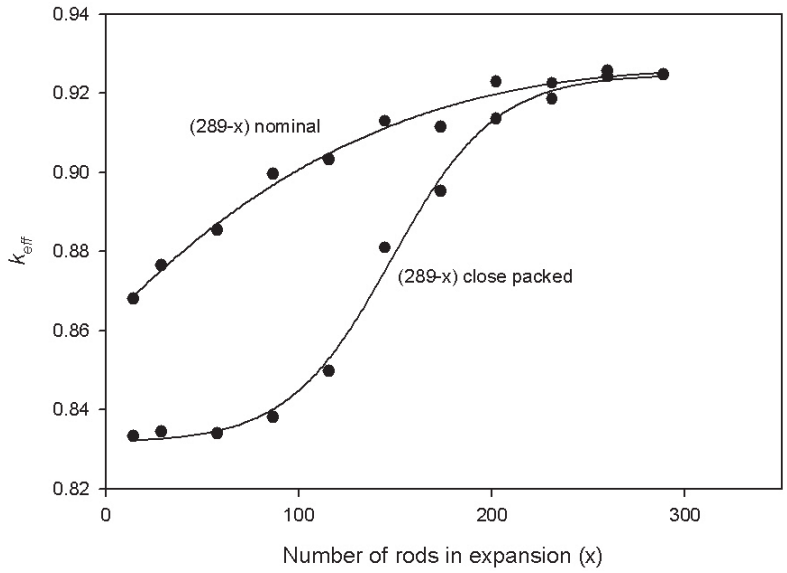

Figure 6-15 Non-uniform Expansion k_{eff} Plot

6.7.3 Annular Pellets

Analysis has determined that annular pellets in the fuel assembly do not increase k_{eff}. Therefore, the fuel assemblies and rods that are allowed to be carried in the Traveller may container annular pellets. Results are given in Table 6-37E. A sample input deck is provided in Table 6-37F. The study was conducted using an earlier version of the Traveller XL model. The most reactive k_{eff} for this model was 0.9332 including the uncertainty. The same model with the annular pellets yielded a result of 0.9290; hence, irrespective of the outerpack used, the study demonstrates that annular pellets are bounded by solid pellets.

6.7.4 Axially Displaced Rods

An axial rod displacement study was conducted using as the baseline model an earlier version of the HAC license-basis case model using a Traveller XL. A sample input deck is included in Table 6-37H. It can be seen that this model includes the appropriate positioning of the neutron absorber plates inside the clamshell such that it bounds the actual package. Likewise the moderator blocks are properly positioned inside the outerpack with the shock mount positions conservatively located. This model is acceptable for use in this analysis because it is looking at the relative importance of displacing rods. The analysis looked at the displacement of 0, 4, 8, 12, 20, 28, 56, 92, and 132 rods. The rods are displaced until they reach the top of the Clamshell. Results showed that k_{eff} remains constant for a few displaced rods (N12) and then drops as N increases. The reason is that the displaced rods effectively displace fissile material from high reactivity region (i.e., the region with the expanded lattice) and put them into a region of low reactivity (the region of the top, which is always overmoderated). Taking into account that the expanded lattice is already close to the optimum pitch value (which, for that assembly size, occurs at P≈1.54 cm or 12 displaced rods), not too much advantage is taken from the fact that "holes" appear in the bottom of the fuel lattice. Figure 6-16 shows the model with 92 axially displaced rods. Results are given in Table 6-37G. A sample input deck is provided in Table 6-37H.

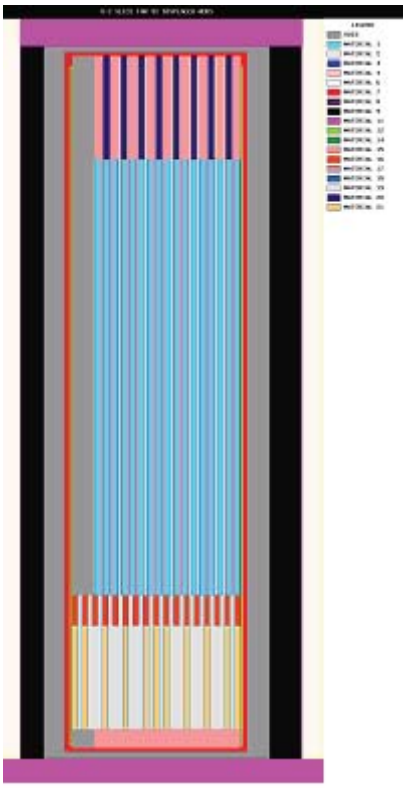

Figure 6-16 Axial Slice Showing 92 Displaced Rods

6.7.5 Polyurethane Foam Moderating Effect

Foam is used as both a thermal insulator and impact absorbing material in the Outerpack. The hydrogen content in the polyurethane foam moderates neutrons outside the confinement system boundary of the individual package. Change to the foam composition can significantly affect the interaction between packages in an array. The polyurethane foam starts to burn when the temperature exceeds 600°F (315°C) leaving a low-density char residual material.

Calculations were not specifically run to determine the effect of removing the foam from the package. However the sensitivity study that was done to evaluate interspersed moderation included modeling the foam region with varying water densities. This analysis bounds the effects of varying foam density.

This page intentionally left blank.

Calculations were run to determine the effect of removing the foam from the package. The configuration evaluated is an infinite array of packages with the fuel assembly moderated and the remainder of the package regions dry. This configuration results in the maximum interaction between individual packages in a package array and emphasizes the effect of eliminating the moderating effect of the foam. Removal of the foam to a lesser extent may be considered equivalent evaluation of interspersed moderation discussed in Section 6.7.1.5. Results showed that eliminating the foam for the configuration that results in maximum interaction results in an increase in k_{eff} of 0.025.

6.7.6 Deleted

6.7.7 Polyethylene Density

Moderator blocks are a packaging component that provide moderation control by maintaining a fixed amount of moderation between the contents in the individual packages. The polyethylene moderator blocks provide moderation that in combination with a neutron poison effectively reduces the interaction between packages. The fixed moderator and a neutron poison are arranged to function as a neutron flux trap.

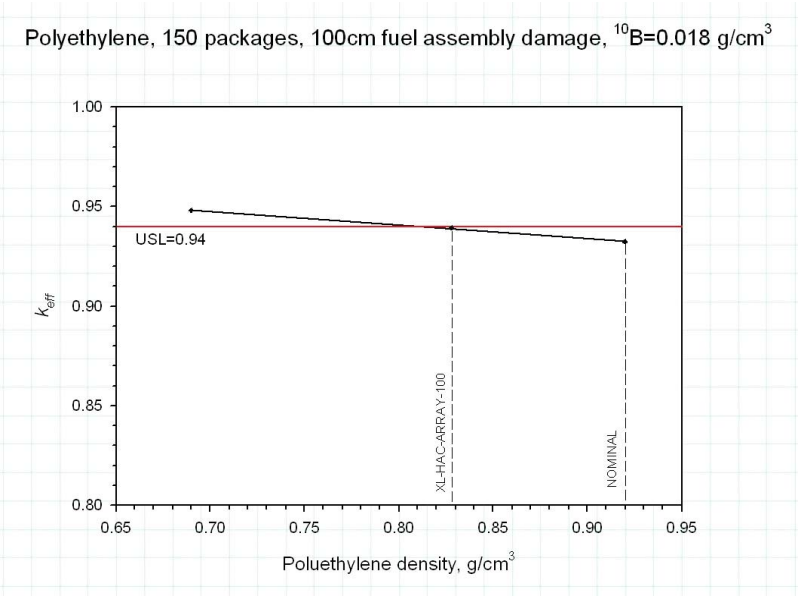

Figure 6-17 Effect of Varying Polyethylene Density

The HAC License-Basis case for the polyethylene was evaluated at densities equating to 100% (ρ = 0.92 gm/cc), 90% (ρ = 0.83 gm/cc), and 75% (ρ = 0.69 gm/cm^3) to determine effect. The configuration is an infinite array of packages with the fuel assembly moderated and the remainder of the package regions dry results in the maximum interaction between individual packages in a package array. The polyurethane foam in the outer pack shell is eliminated and replaced with void to maximize the interaction and emphasize the effect of changes in the polyethylene moderator. Figure 6-17 shows the effect of reducing the polyethylene density for a range of boron content from 2.0 wt% boron to 4.5 wt% boron in the poison plates. The average effect of reducing polyethylene density by 10% increased k_{eff} approximately 1%, and reducing

density to 75% increases k_{eff} approximately 2%. This effect of reducing the polyethylene density blocks is not strongly dependent on the neutron poison content within the range of parameters evaluated. Results are given in Table 6-39B. A sample input deck is provided in Table 6-38.

6.7.8 Reduction of Boron Content in Neutron Absorber

The analysis included a sensitivity study of boron content in the neutron absorber. The sensitivity to ^{10}B areal density is evaluated for a package array with 100 cm fuel lattice expansion. Figure 6-18 shows k_{eff} versus ^{10}B content for BORAL. The ^{10}B effectiveness does not diminish significantly until the areal density decreases to approximately 0.010 gm/cm^2. As can be seen in the curves,

This page intentionally left blank.

the boron content in the Traveller neutron absorbers is well beyond the "knee" on the curve. Results are given in Table 6-39. Number densities used in the boron content analysis are given in Table 6-39A.

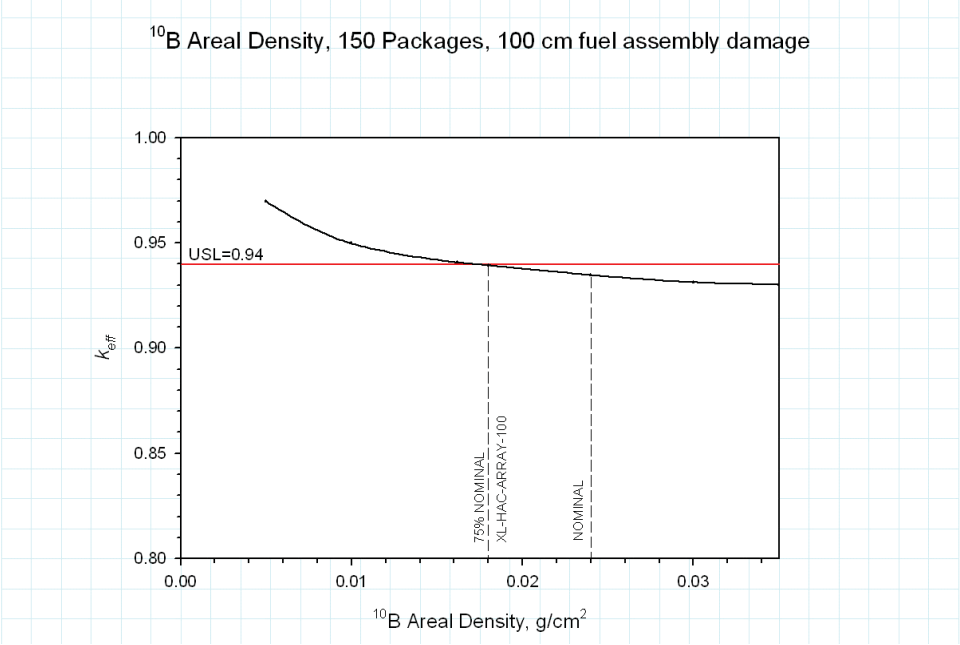

Figure 6-18 Sensitivity Study of Boron Content for Traveller XL Package Array

6.7.9 Elimination of Structural Stainless Steel

Neutron absorption occurs in the stainless steel of the package due to its chromium content. Note that the model takes credit for only about 60% of the stainless steel in the package. Calculations were performed to determine the effect on k_{eff} of variations in stainless steel thickness due to manufacturing tolerances. Figure 6-18A shows the effect. Results are given in Table 6-39C.

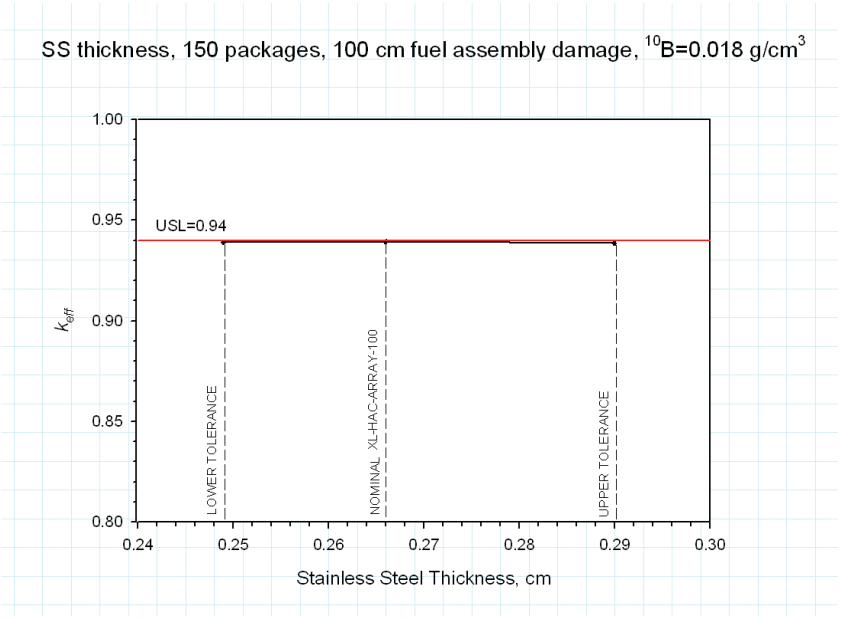

Figure 6-18A Sensitivity Study of Stainless Steel Thickness

6.7.10 Zirconium Reduction

In the accident configurations, the cladding and guide tubes were modeled with nominal dimensions. Cases were run with thinner tubes, dimensioned to reflect the manufacturing tolerance band. The effect of reducing the tube thickness of the zirconium fuel rod and guide thimble tubes by 5 percent is evaluated. The cladding material includes Zirconium-40 that is a resonance absorber within the fuel envelope. Results indicate that a small reduction in absorption in the Zirconium is offset by the increase in moderation when the zirconium is replaced with full density water in the model. There is a net change in k_{eff} that is less than 0.005 for a small reduction in cladding thickness.

6.7.11 Outerpack Diameter

An analysis was performed to evaluate the effect that varying the outerpack diameter has on k_{eff}. Cases were run to bound the manufacturing tolerance band. Results indicate that a change in package diameter equivalent to manufacturing tolerance has virtually no affect on system k_{eff}. Results are given in Table 6-39B. A sample input deck is provided in Table 6-39C.

6.7.12 Actual As-found Condition After HAC Testing

An analysis was performed to determine k_{eff} for the Traveller XL in the actual condition in which it was found following HAC testing. The fuel assembly was modeled in the same way as for the license-basis case, with lattice expansion to 100 cm and 100% theoretical density. The flooding configuration was also modeled the same as for the license-basis case. The packaging was modified in the following ways:

- Moderator blocks modeled at 100% nominal density.
- Neutron absorbers modeled at 100% B-10 content.
- Shock mounts modeled in place at nominal density.

Results from this analysis showed that keff was reduced by approximately 1%.

6.7.13 Package Array Size

An analysis was performed to evaluate the effect that varying the package array size for the Traveller XL under HAC license-basis-conditions. Results indicate that an array of 150 packages will satisfy the USL requirements. Results are given in Table 6-39D. The data are plotted in Figure 6-18B.

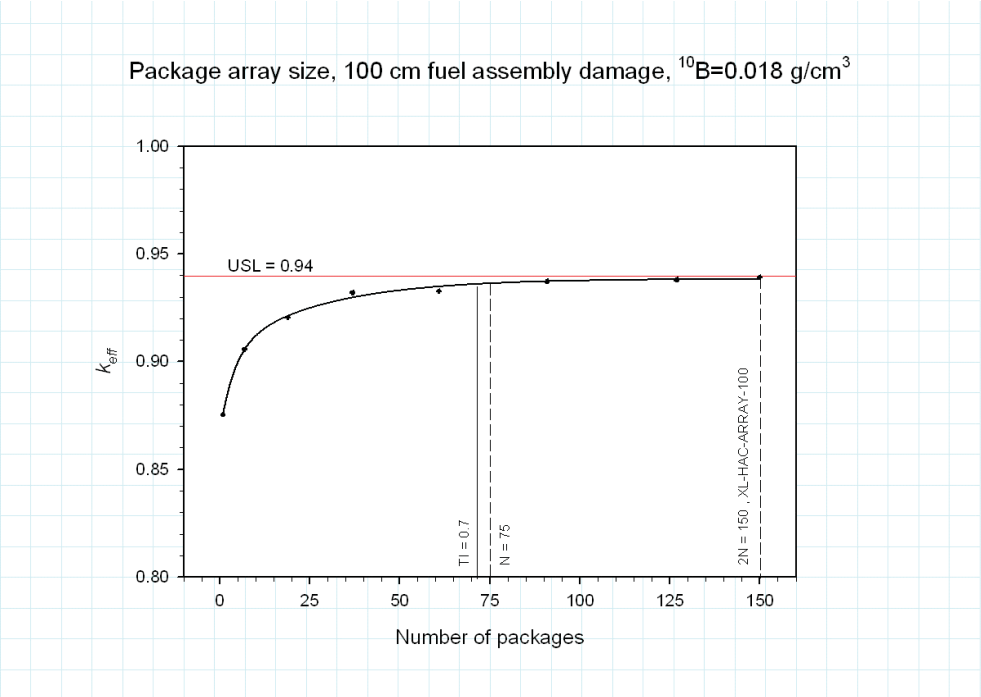

Figure 6-18B Sensitivity Study of Package Array

6.7.14 Clamshell Position Inside Outerpack

An analysis was performed to evaluate the effect of the clamshell coming loose from the shock mounts and coming to rest on the moderator blocks. The study assumes that all of the shock mounts burn away. The two calculations consider the license basis case (XL-HAC-ARRAY-100 model) with the clamshell resting on the moderator blocks either in the lower half of the outerpack (clamshell down model) or, assuming the packages were upside down, with the clamshell resting on the moderator blocks in the upper half of the outerpack. For the clamshell-up model, the clamshell is rotated 180 degrees so the fuel assembly makes contact with the clamshell at the outerpack edge.

The likelihood of this event occurring is very small for numerous reasons. First, even though the shock mounts are not safety related items, actual testing showed that all of the shock mounts survived the drop and fire tests, and remain connected to the clamshell. Second, engineering scoping analysis estimates that if only one pair of shock mounts at each end survives the drop and fire, they are sufficient to hold the clamshell suspended in the outerpack. If all the shock mounts at one end were to be destroyed, then the clamshell may come into contact with the outerpack at that end only.

Nevertheless, calculations were performed to show the effect on keff if all shock mounts were destroyed. The results show no change in keff for the clamshell down model, and a slight increase for the clamshell up and rotated model. Table 6-19A below gives the results. Figure 6-18C shows the clamshell up and rotated model. Table 6-39F gives the input deck for the clamshell up and rotated model.

Figure 6-18C Clamshell Up and Rotated Model

Table 6-19A Clamshell Position Inside Outerpack

Configuration	ks	Uncert.	Calculated keff
Clamshell Up-Rotated	0.9392	0.0009	0.9410
Clamshell Down	0.9377	0.0008	0.9393

6.8 FISSILE MATERIAL PACKAGES FOR AIR TRANSPORT

Application for air transport for the Traveller will be made at a later date.

6.9 BENCHMARK EVALUATIONS

The computer code used for these criticality calculations has been benchmarked against applicable criticality experiments.

6.9.1 Applicability of Benchmark Experiments

There are approximately 180 experiments that are applicable to transport.[1] Of these, 55 were selected based on their structural, material, poison, geometry, and spectral similarities to the Traveller. Table 6-40 in Appendix 6.10.10 gives a summary of available LWR critical experiments and indicates how many of each type were selected. The selected experiments were grouped into four classifications: Simple Lattice, Separator Plate, Flux Trap, and Water Hole experiments. Table 6-41 shows the breakdown of the experiments into the four classifications. In general, there were 15 Simple Lattice experiments, 26 Separator Plate experiments, 8 Flux Trap experiments, and 6 Water Hole experiments.

In determining which experiments were not applicable, criteria were established by which experiments would be rejected. These criteria include:

- No separator plates made of hafnium, copper, cadmium, zirconium, or depleted uranium (include only separator plates made of stainless steel, aluminum or boron),
- No thick wall lead, steel, or uranium reflector material,
- No hexagonal fuel rod lattices,
- No burnable poison rods (Ag-In-Cd rods, B_4C rods, UO_2-Gd_2O_3 rods)
- No soluble boron

The 55 experiments were analyzed for their applicability to the Traveller package. Table 6-42 shows a summary comparison of the benchmark critical experiment properties to the Traveller package. The range of properties for the critical experiment includes range of values for the Traveller package.

In addition, a qualitative evaluation of the neutron event probabilities is also done to compare the importance of the contents and packaging materials relative to neutron absorption. Comparing the absorption probabilities for the critical experiments and package indicates that the importance of neutron absorption is similar between the critical experiments and package model.

1. NUREG/CR-6361 (ORNL/TM-13211): Criticality Benchmark Guide for Light-Water-Reactor Fuel in Transportation and Storage Packages.

The input decks for the 55 experiments were run locally using Keno V.a. The results compared favorably to published results. The input decks were then converted to Keno-VI using the C5TOC6 utility program and run again. These results were used to determine the USL for the Traveller calculations.

The analysis concluded that no single group of critical benchmark experiments (simple lattice, separator plate, flux trap, or water hole) contains all the characteristics of the Traveller shipping package. However, the four groups each represent different aspects of the package model that are important to understanding the bias associated with the package modeling. The simple lattice and water hole experiments represent the fuel region modeling (i.e., fuel enrichment, lattice pitch, water-to-fuel ratio), and the separator plate and flux trap experiments represent additional characteristics of the package modeling (i.e., moderator, neutron absorbers).

6.9.2 Bias Determination

After comparison of critical experiments, USLSTATS was used to assist with the statistical analysis of the benchmark experiments. It provides two methods of determining a USL, and a comparison of these two methods is shown in Figure 6-19.

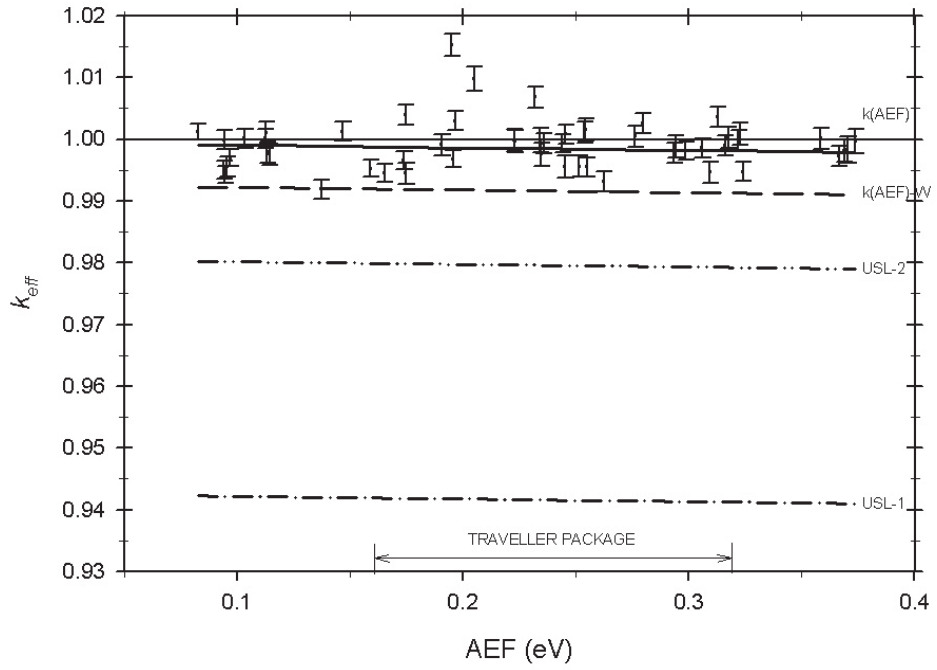

Figure 6-19 Upper Safety Limits (USLs) for 55 LWR Fuel Critical Experiments

The first (referred to as USL-1) uses a confidence band calculated using a linear regression fit based on the results from the selected benchmarks, and places an additional administrative margin on the lower band, which is then used as the USL.

The second method (referred to as USL-2) is a single-sided closed interval approach, using a uniform width. The purpose of this method is to determine a uniform tolerance band over a specified closed interval, based on a linear least squares model. This method uses a statistically calculated subcritical margin (with a confidence level of 0.95 in this case), and is used to determine whether the USL-1 method is sufficiently conservative.

The trending parameter chosen for the two methods was the AEF. The AEF range in the benchmark cases provides ample coverage for the calculated average energy of fission (AEF) values of the various Traveller configurations (individual vs. package array, normal transport vs. HAC, etc). Ample coverage means that no extrapolation is required in order to determine the USL. The end result of this is shown graphically in Figure 6-19.

The results shown in Figure 6-19 indicate that a USL of 0.94 is acceptable including an administrative margin, $\Delta k_m = 0.05$, and a bias of negative 0.01 ($\beta + \Delta\beta = -0.01$). The administrative margin is acceptable because for all grouping of experiments the minimum subcritical margin is positive, USL2-USL1≥ 0. The largest statistical bias (USL-2) is associated with the flux trap group. The application of the statistically based subcritical margin indicates the administrative margin is adequate by a margin of at least 0.015 (USL-2 minus USL-1) even for groups were there is a limited number of data points (i.e., flux trap, water hole). Therefore, the bias determination is made by including all 55 experiments in the USLSTAT calculation.

6.10 APPENDICES

The following appendices are included to provide additional information on material contained elsewhere in Section 6.

6.10.1: References

6.10.2: PWR Fuel Assembly Parameters

6.10.3: Fuel Assembly Comparison

6.10.4: 17OFA-XL Model

6.10.5: Traveller Packaging Model

6.10.6: Single Package Evaluation Calculations

6.10.7: Package Array Evaluation Calculations

6.10.8: Rod Container Calculations

6.10.9: Calculations for Sensitivity Studies

6.10.10: Benchmark Critical Experiments

6.10.1 References

None

This page intentionally left blank.

6.10.2 PWR Fuel Assembly Parameters

The following tables and figures provide the fuel assembly parameters important to criticality safety for the 14x14, 15x15, 16x16, 17x17, and 18x18 fuel types to be transported in the Traveller. Fuel assemblies with other product names, but which satisfy the parameters found in this section may be transported in the Traveller.

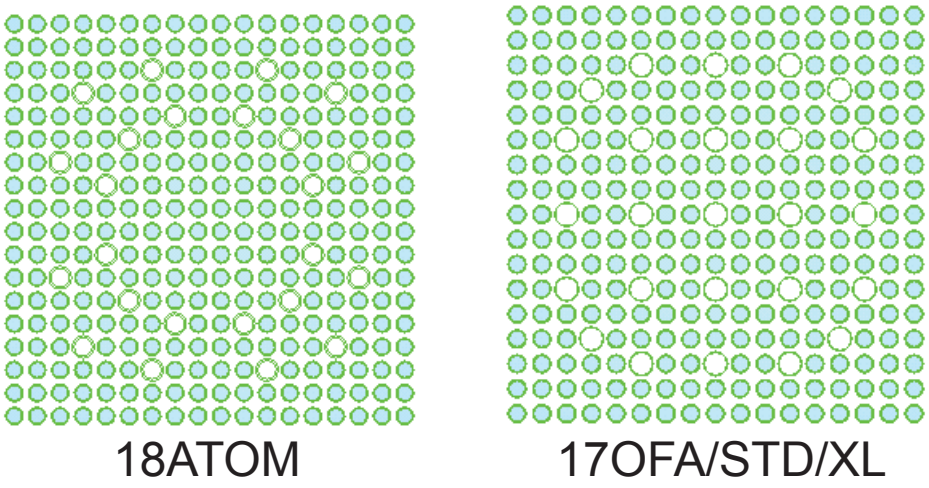

Figure 6-20 Cross Section for 18x18 and 17x17 Assemblies

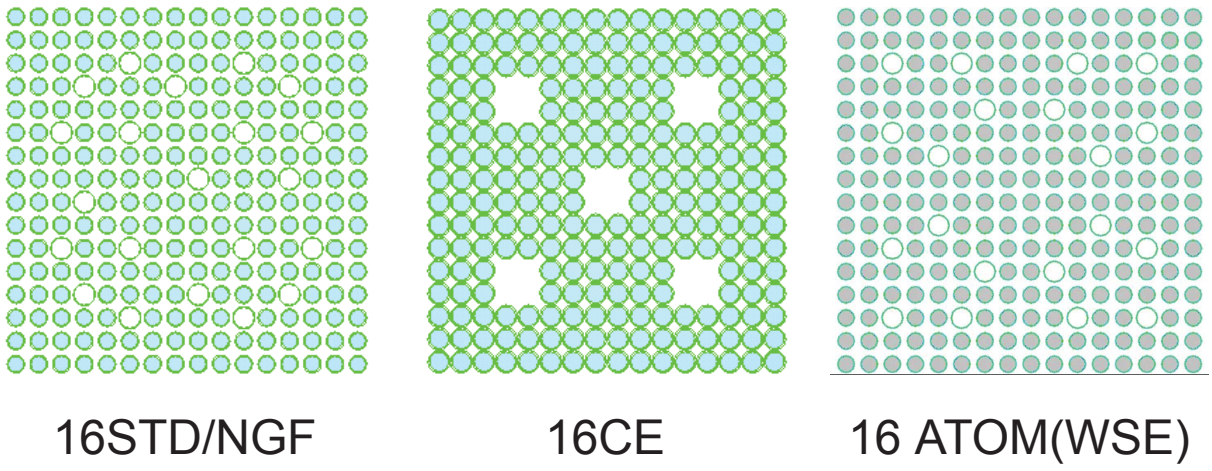

Figure 6-21 Cross Sections for 16x16 Assemblies

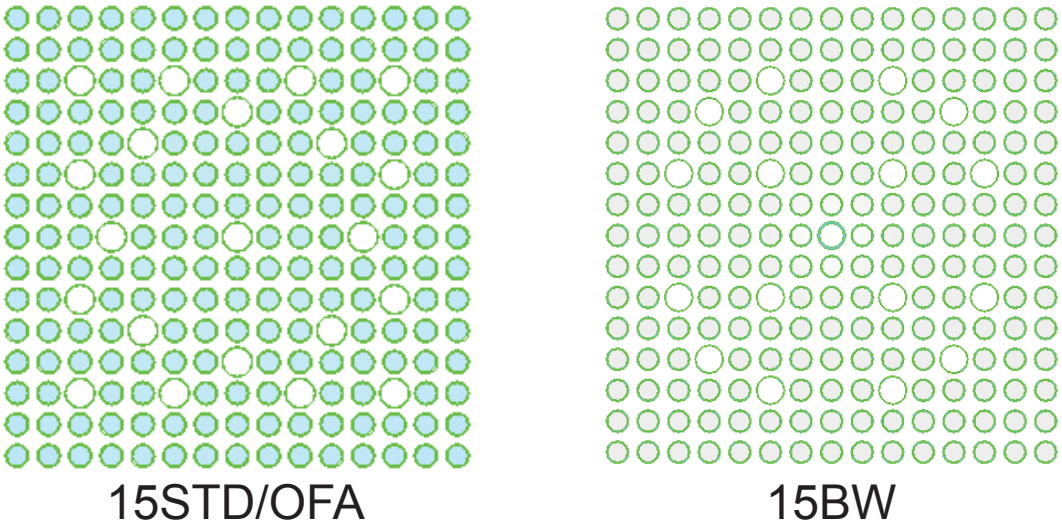

Figure 6-22 Cross Sections for 15x15 Assemblies

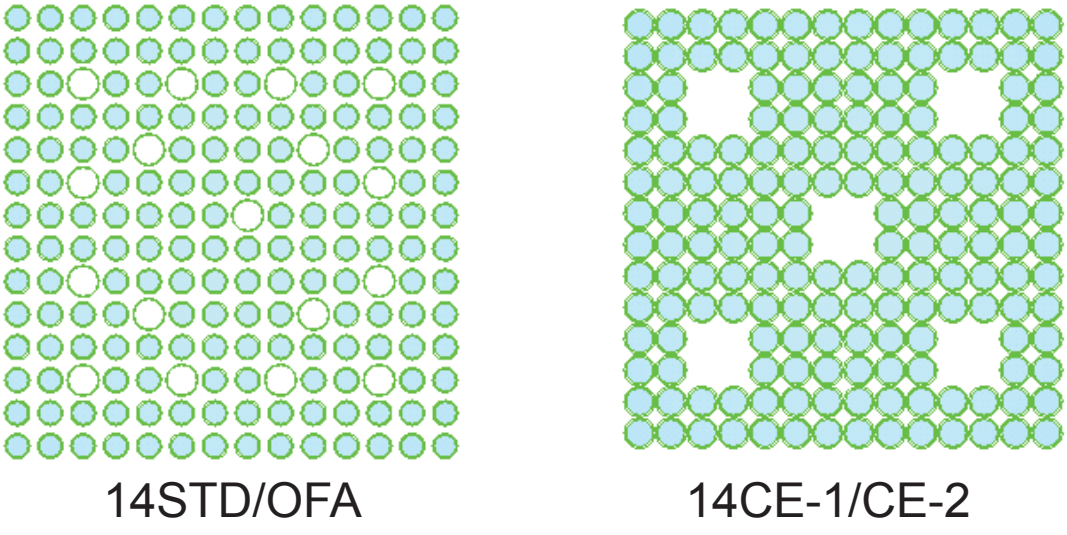

Figure 6-22A Cross Sections for 14x14 Assemblies

This page intentionally left blank.

Table 6-20 Parameters for 14x14 Fuel Assemblies

Fuel Assembly Description	14 X 14	14 X 14	14 X 14
Fuel Assembly Type	W-STD	W-OFA	CE-1/CE-2
No. Fuel Rods per assembly	179	179	176
No. Non-Fuel Rods	17	17	20
Nominal Guide Tube Wall Thickness	0.043 cm (0.017 in.)	0.043 cm (0.017 in.)	0.097 cm (0.038 in.)
Nominal Guide Tube Outer Diameter	1.369 cm (0.539 in.)	1.336 cm (0.526 in.)	2.822 cm (1.111 in.)
Nominal Pellet Diameter	0.929 cm (0.366 in.)	0.875 cm (0.344 in.)	0.956/0.966 cm (0.376/0.381 in.)
Nominal Clad Outer Diameter	1.072 cm (0.422 in.)	1.016 cm (0.400 in.)	1.016 cm (0.440 in.)
Nominal Clad Thickness	0.062 cm (0.024 in.)	0.062 cm (0.024 in.)	0.071/0.066 cm (0.028/0.026 in.)
Clad Material	Zirconium alloy	Zirconium alloy	Zirconium alloy
Nominal Assembly Envelope	19.70 cm (7.76 in.)	19.70 cm (7.76 in.)	20.60 cm (8.11 in.)
Nominal Lattice Pitch	1.412 cm (0.556 in.)	1.412 cm (0.556 in.)	1.473 cm (0.580 in.)

Table 6-21 Parameters for 15x15 Fuel Assemblies

Fuel Assembly Description	15 X 15	15 X 15
Fuel Assembly Type	STD/OFA	B&W
No. Fuel Rods per Assembly	204	208
No. Non-Fuel Rods	21	17
Nominal Guide Tube Wall Thickness	0.043/0.043 cm (0.017/0.017 in.)	0.043 cm (0.017 in.)
Nominal Guide Tube Outer Diameter	1.387/1.354 cm (0.546/0.533 in.)	1.354 cm (0.533 in.)
Nominal Pellet Diameter	0.929 cm (0.366 in.)	0.929 cm (0.366 in.)
Nominal Clad Outer Diameter	1.072 cm (0.422 in.)	1.072 cm (0.422 in.)
Nominal Clad Thickness	0.062 cm (0.024 in.)	0.062 cm (0.024 in.)
Clad Material	Zirconium alloy	Zirconium alloy
Nominal Assembly Envelope	21.39 cm (8.42 in.)	21.66 cm (8.53 in.)
Nominal Lattice Pitch	1.430 cm (0.563 in.)	1.443 cm (0.568 in.)

Table 6-22 Parameters for 16x16 Fuel Assemblies

Fuel Assembly Description	16 X 16	16 X 16	16 X 16	16 X 16
Fuel Assembly Type	16STD	16NGF	ATOM	
No. Fuel Rods per Assembly	235	235	236	
No. Non-Fuel Rods	21	21	20	
Nominal Guide Tube Wall Thickness	0.046 cm (0.018 in.)	0.041 cm (0.016 in.)	0.070 cm (0.028 in.)	
Nominal Guide Tube Outer Diameter	1.196 cm (0.471 in.)	1.204 cm (0.474 in.)	1.380 cm (0.543 in.)	
Nominal Pellet Diameter	0.819 cm (0.3225 in.)	0.784 cm (0.3088 in.)	0.911 cm (0.359 in.)	
Nominal Clad Outer Diameter	0.950 cm (0.3740 in.)	0.914 cm (0.3600 in.)	1.075 cm (0.423 in.)	
Nominal Clad Thickness	0.057 cm (0.0225 in.)	0.057 cm (0.0225 in.)	0.072 cm (0.029 in.)	
Clad Material	Zirconium alloy	Zirconium alloy	Zirconium alloy	
Nominal Assembly Envelope	19.72 cm (7.76 in.)	19.72 cm (7.76 in.)	22.95 cm (9.03 in.)	
Nominal Lattice Pitch	1.232 cm (0.485 in.)	1.232 cm (0.485 in.)	1.430 cm (0.563 in.)	

Table 6-22 Parameters for 16x16 Fuel Assemblies (cont)

Fuel Assembly Description	16 X 16	16 X 16	16 X 16	16 X 16
Fuel Assembly Type	CE16NVA	CE16VA	CE16NFG	
No. Fuel Rods per Assembly	236	236	236	
No. Non-Fuel Rods	20	20	20	
Nominal Guide Tube Wall Thickness	0.102 cm (0.040 in.)	0.102 cm (0.040 in.)	0.102 cm (0.040 in.)	
Nominal Guide Tube Outer Diameter	2.489 cm (0.980 in.)	2.489 cm (0.980 in.)	2.489 cm (0.980 in.)	
Nominal Pellet Diameter	0.8255 cm (0.3250 in.)	0.8268 cm (0.3255 in.)	0.8192 cm (0.3225 in.)	
Nominal Clad Outer Diameter	0.970 cm (0.382 in.)	0.970 cm (0.382 in.)	0.9500 cm (0.3740 in.)	
Nominal Clad Thickness	0.064 cm (0.025 in.)	0.064 cm (0.025 in.)	0.057 cm (0.0225 in.)	
Clad Material	Zirconium alloy	Zirconium alloy	Zirconium alloy	
Nominal Assembly Envelope	20.63 cm (8.12 in.)	20.63 cm (8.12 in.)	20.63 cm (8.12 in.)	
Nominal Lattice Pitch	1.285 cm (0.506 in.)	1.285 cm (0.506 in.)	1.285 cm (0.506 in.)	

Table 6-23 Parameters for 17x17 and 18x18 Fuel Assemblies

Fuel Assembly Description	17 X 17	17 X 17	18 X 18
Fuel Assembly Type	W-STD or XL	W-OFA	ATOM
No. Fuel Rods per Assembly	264	264	300
No. Non-Fuel Rods	25	25	24
Nominal Guide Tube Wall Thickness	0.041/0.051 cm (0.016/0.020 in.)	0.041 cm (0.016 in.)	0.065 cm (0.026 in.)
Nominal Guide Tube Outer Diameter	1.204/1.224/1.24 cm (0.474/0.482/0.488 in.)	1.204 cm (0.474 in.)	1.240 cm (0.488 in.)
Nominal Pellet Diameter	0.819 cm (0.323 in.)	0.784 cm (0.309 in.)	0.805 cm (0.317 in.)
Nominal Clad Outer Diameter	0.950 cm (0.374 in.)	0.914 cm (0.360 in.)	0.950 cm (0.374 in.)
Nominal Clad Thickness	0.057 cm (0.023 in.)	0.057 cm (0.023 in.)	0.064 cm (0.025 in.)
Clad Material	Zirconium alloy	Zirconium alloy	Zirconium alloy
Nominal Assembly Envelope	21.39 cm (8.42 in.)	21.39 cm (8.42 in.)	22.94 cm (9.03 in.)
Nominal Lattice Pitch	1.260 cm (0.496 in.)	1.260 cm (0.496 in.)	1.270 cm (0.500 in.)

This page intentionally left blank.

6.10.3 Fuel Assembly Comparison

Comparison of the fuel assembly k_{eff} values to determine the most reactive contents is done on basis of the fuel confinement envelope. A fuel rod pitch is calculated for each fuel assembly that corresponds to each fuel envelope dimension [nominal, 22.86 cm (9.0 inch), 24.13 cm (9.5 inch), 25.40 cm (10.0 inch), 27.94 cm (11.0 inch), 30.48 cm (12.0 inch), 33.02 cm (13.0 inch), 35.56 cm (14.0 inch)]. A range of fuel envelope dimensions were evaluated to evaluate the sensitivity of keff to the fuel envelope confinement system dimension. Table 6-24 summarizes the k_{eff} values calculated for each fuel assembly with the 100 cm section of expanded lattice where the pitch corresponds to each of the fuel envelope dimensions. A summary ranking of fuel assemblies from most to least reactive is provided in Table 6-24A and shows that the ranking depends on the fuel envelope dimension. As such, no single fuel assembly can be shown to represent the contents with the maximum reactivity for a given fuel envelope confinement dimension. Figure 6-23 shows these k_{eff} values as a function of the fuel envelope confinement dimension, where the accident condition inset is also shown is Figure 6-5. The trendlines represent an equation that provides a reasonable best fit to each series of data points. The ranking of the trendlines does not necessarily match the ranking of the individual data points, but reflect the trends as influenced by the overall fit of the equation to the individual data points. The 17X17 OFA consistently ranks as one of more reactive of the fuel assemblies and the difference between the highest k_{eff} value and the value calculated for the 17X17 OFA is less than 0.005 Δk_{eff} within the range of dimensions for the clamshell confinement (22.86 cm (9.0 in) to 24.13 cm (9.5 in)). The 17X17 OFA is selected to represent the fuel assembly contents for the accident transport condition. Figure 6-24 is a sample input deck used to calculate the k_{eff} values for the individual fuel assembly.

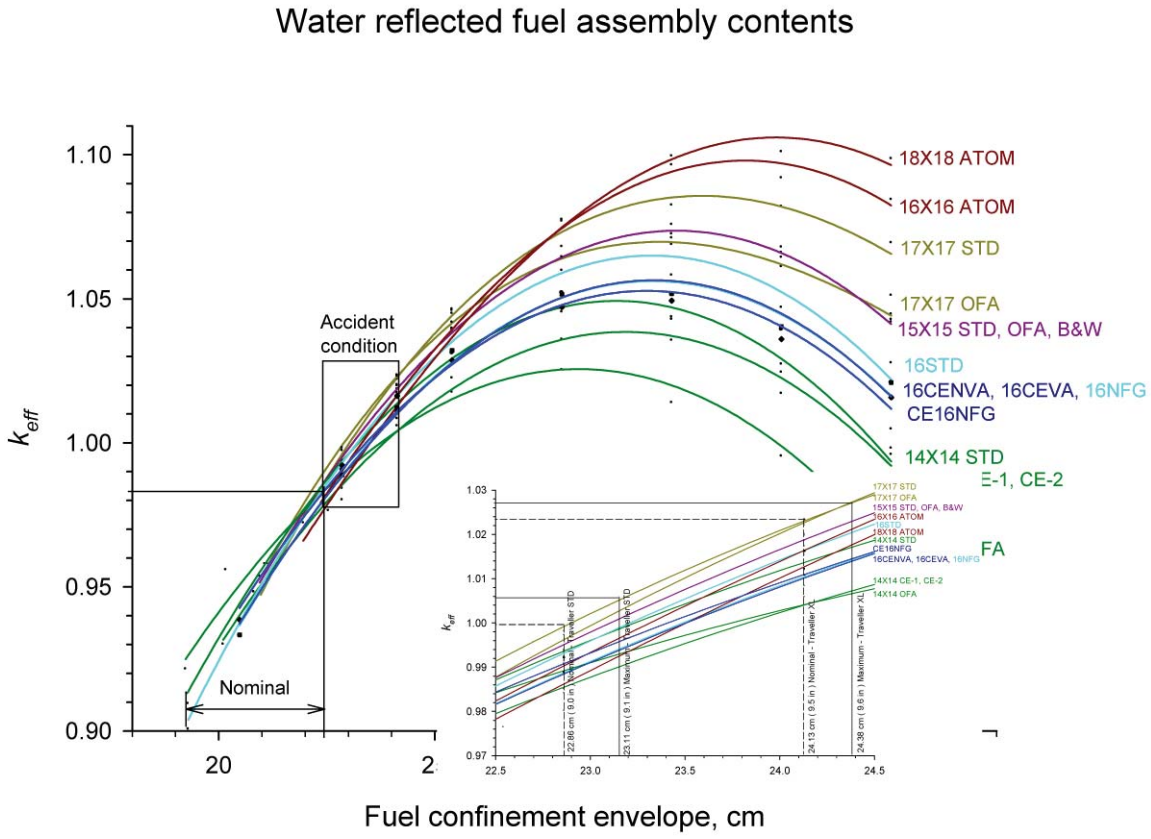

Figure 6-23 Comparison of Fuel Assemblies – Individual Fuel Assembly, 20 cm Water Reflection, 100 cm Lattice Expansion

This page intentionally left blank.

Table 6-24A Summary and Ranking Results in Table 6-24

	Fuel envelope confinement dimension							
		Traveller STD	Traveller XL					
Fuel Assembly	Nominal	22.86 cm (9.0 in)	24.13 cm (9.5 in)	25.40 cm (10.0 in)	27.94 cm (11.0 in)	30.48 cm (12.0 in)	33.02 cm (13.0 in)	35.56 cm (14.0 in)
18X18 ATOM	2	16	12	8	1	8	8	1
	0.9765	0.9802	1.0120	1.0385	1.0775	1.0995	1.101	1.0986
17X17 STD	7	9	1	3	3	9	12	3
	0.9527	0.9915	1.0235	1.0449	1.0769	1.0825	1.082	1.0694
17X17 OFA	4	3	3	2	6	4	2	5
	0.9580	0.9940	1.0221	1.0459	1.0644	1.0688	1.0611	1.0447
16STD	16	4	5	6	8	5	10	8
	0.9006	0.9937	1.0201	1.0394	1.0598	1.0582	1.047	1.0277
16NFG	14	2	7	11	13	13	9	12
	0.9129	0.9973	1.0186	1.031	1.0454	1.0428	1.0273	1.0048
16ATOM	1	14	10	7	2	7	11	2
	0.9841	0.9851	1.0154	1.0387	1.0771	1.0964	1.0919	1.0844
CE16NVA	10	11	11	10	9	10	3	9
	0.9331	0.9906	1.0122	1.0312	1.0520	1.0515	1.0394	1.0209
CE16VA	9	12	14	9	10	6	1	10
	0.9334	0.9889	1.0109	1.0321	1.0516	1.0518	1.0404	1.0209
CE16NFG	8	8	9	13	11	11	7	11
	0.9386	0.9922	1.0163	1.0287	1.0471	1.0493	1.036	1.0158
15X15 STD	6	7	6	4	7	3	5	7
	0.9529	0.9925	1.0198	1.0418	1.064	1.0711	1.066	1.0419
15X15 OFA	5	5	4	5	5	2	6	6
	0.9537	0.9933	1.0209	1.0397	1.0645	1.0725	1.0644	1.0428
15X15 BW	3	6	2	1	4	1	4	4
	0.9581	0.9933	1.0231	1.0464	1.0681	1.0758	1.0679	1.0512
14X14 STD	15	1	8	12	12	12	13	14
	0.9095	0.9982	1.0174	1.0288	1.0465	1.0437	1.0245	0.9981
14X14 OFA	13	10	15	16	16	15	16	16
	0.9215	0.9909	1.0084	1.0176	1.0253	1.0139	0.9954	0.9666
14X14 CE-1	12	13	13	14	14	14	15	13
	0.9301	0.9842	1.0059	1.0225	1.0359	1.0356	1.0171	0.9959
14X14 CE-2	11	15	16	15	15	16	14	15
	0.9276	0.9861	1.0111	1.0264	1.0382	1.0384	1.0245	1.0022

Table 6-24 Individual Fuel Assembly, 20 cm water reflection, 100 cm fuel lattice expansion

Fuel envelope	Pitch (cm)	p/d ratio	k_s	σ_s	$k_s + 2\sigma_s$
18x18 ATOM					
Nominal	1.2700	1.5778	0.9731	1.7000e-3	0.9765
22.86 cm (9.0 inch)	1.2888	1.6011	0.9774	1.4000e-3	0.9802
24.13 cm (9.5 inch)	1.3635	1.6939	1.0088	1.6000e-3	1.0120
25.40 cm (10.0 inch)	1.4382	1.7867	1.0353	1.6000e-3	1.0385
27.94 cm (11.0 inch)	1.5876	1.9723	1.0739	1.8000e-3	1.0775
30.48 cm (12.0 inch)	1.7371	2.1581	1.0963	1.6000e-3	1.0995
33.02 cm (13.0 inch)	1.8865	2.3437	1.0980	1.5000e-3	1.1010
35.56 cm (14.0 inch)	2.0359	2.5293	1.0958	1.4000e-3	1.0986
17x17 STD					
Nominal	1.2598	1.5379	0.9497	1.5000e-3	0.9527
22.86 cm (9.0 inch)	1.3694	1.6717	0.9885	1.5000e-3	0.9915
24.13 cm (9.5 inch)	1.4488	1.7687	1.0201	1.7000e-3	1.0235
25.40 cm (10.0 inch)	1.5281	1.8655	1.0419	1.5000e-3	1.0449
27.94 cm (11.0 inch)	1.6869	2.0593	1.0735	1.7000e-3	1.0769
30.48 cm (12.0 inch)	1.8456	2.2531	1.0793	1.6000e-3	1.0825
33.02 cm (13.0 inch)	2.0044	2.4469	1.0792	1.4000e-3	1.0820
35.56 cm (14.0 inch)	2.1613	2.6385	1.0666	1.4000e-3	1.0694
17x17 OFA					
Nominal	1.2598	1.6062	0.9550	1.5000e-3	0.9580
22.86 cm (9.0 inch)	1.3716	1.7487	0.9910	1.5000e-3	0.9940
24.13 cm (9.5 inch)	1.4510	1.8499	1.0191	1.5000e-3	1.0221
25.40 cm (10.0 inch)	1.5303	1.9510	1.0427	1.6000e-3	1.0459
27.94 cm (11.0 inch)	1.6891	2.1535	1.0616	1.4000e-3	1.0644
30.48 cm (12.0 inch)	1.8479	2.3560	1.0656	1.6000e-3	1.0688
33.02 cm (13.0 inch)	2.0066	2.5583	1.0579	1.6000e-3	1.0611
35.56 cm (14.0 inch)	2.1654	2.7608	1.0419	1.4000e-3	1.0447

Table 6-24 Individual Fuel Assembly, 20 cm water reflection, 100 cm fuel lattice expansion (cont.)					
Fuel envelope	**Pitch (cm)**	**p/d ratio**	**k_s**	**σ_s**	**$k_s + 2\sigma_s$**
16STD					
Nominal	1.2319	1.5039	0.8978	1.4000e-3	0.9006
22.86 cm (9.0 inch)	1.4607	1.7832	0.9909	1.4000e-3	0.9937
24.13 cm (9.5 inch)	1.5453	1.8865	1.0167	1.7000e-3	1.0201
25.40 cm (10.0 inch)	1.6300	1.9899	1.0364	1.5000e-3	1.0394
27.94 cm (11.0 inch)	1.7993	2.1965	1.0564	1.7000e-3	1.0598
30.48 cm (12.0 inch)	1.9687	2.4033	1.0556	1.3000e-3	1.0582
33.02 cm (13.0 inch)	2.1380	2.6100	1.0442	1.4000e-3	1.0470
35.56 cm (14.0 inch)	2.3073	2.8167	1.0245	1.6000e-3	1.0277
16NFG					
Nominal	1.2319	1.5706	0.9097	1.6000e-3	0.9129
22.86 cm (9.0 inch)	1.4630	1.8652	0.9943	1.5000e-3	0.9973
24.13 cm (9.5 inch)	1.5477	1.9732	1.0154	1.6000e-3	1.0186
25.40 cm (10.0 inch)	1.6324	2.0812	1.0278	1.6000e-3	1.0310
27.94 cm (11.0 inch)	1.8017	2.2971	1.0424	1.5000e-3	1.0454
30.48 cm (12.0 inch)	1.9710	2.5129	1.0394	1.7000e-3	1.0428
33.02 cm (13.0 inch)	2.1404	2.7289	1.0245	1.4000e-3	1.0273
35.56 cm (14.0 inch)	2.3097	2.9447	1.0016	1.6000e-3	1.0048
16ATOM					
Nominal	1.4300	1.5682	0.9811	1.5000e-3	0.9841
22.86 cm (9.0 inch)	1.4523	1.5927	0.9821	1.5000e-3	0.9851
24.13 cm (9.5 inch)	1.5370	1.6856	1.0120	1.7000e-3	1.0154
25.40 cm (10.0 inch)	1.6217	1.7785	1.0355	1.6000e-3	1.0387
27.94 cm (11.0 inch)	1.7910	1.9641	1.0739	1.6000e-3	1.0771
30.48 cm (12.0 inch)	1.9603	2.1498	1.0932	1.6000e-3	1.0964
33.02 cm (13.0 inch)	2.1297	2.3356	1.0889	1.5000e-3	1.0919
35.56 cm (14.0 inch)	2.2990	2.5212	1.0816	1.4000e-3	1.0844

Table 6-24 Individual Fuel Assembly, 20 cm water reflection, 100 cm fuel lattice expansion (cont.)					
Fuel envelope	**Pitch (cm)**	**p/d ratio**	**k_s**	**σ_s**	**$k_s + 2\sigma_s$**
CE16NVA					
Nominal	1.3106	1.5876	0.9301	1.5000e-3	0.9331
22.86 cm (9.0 inch)	1.4593	1.7678	0.9876	1.5000e-3	0.9906
24.13 cm (9.5 inch)	1.5440	1.8704	1.0088	1.7000e-3	1.0122
25.40 cm (10.0 inch)	1.6286	1.9729	1.0276	1.8000e-3	1.0312
27.94 cm (11.0 inch)	1.7980	2.1781	1.0492	1.4000e-3	1.0520
30.48 cm (12.0 inch)	1.9673	2.3832	1.0483	1.6000e-3	1.0515
33.02 cm (13.0 inch)	2.1366	2.5882	1.0368	1.3000e-3	1.0394
35.56 cm (14.0 inch)	2.3060	2.7935	1.0179	1.5000e-3	1.0209
CE16VA					
Nominal	1.3106	1.5851	0.9302	1.6000e-3	0.9334
22.86 cm (9.0 inch)	1.4593	1.7650	0.9857	1.6000e-3	0.9889
24.13 cm (9.5 inch)	1.5440	1.8674	1.0079	1.5000e-3	1.0109
25.40 cm (10.0 inch)	1.6286	1.9698	1.0287	1.7000e-3	1.0321
27.94 cm (11.0 inch)	1.7980	2.1746	1.0486	1.5000e-3	1.0516
30.48 cm (12.0 inch)	1.9673	2.3794	1.0490	1.4000e-3	1.0518
33.02 cm (13.0 inch)	2.1366	2.5842	1.0376	1.4000e-3	1.0404
35.56 cm (14.0 inch)	2.3060	2.7891	1.0177	1.6000e-3	1.0209
CE16NFG					
Nominal	1.3120	1.6016	0.9354	1.6000e-3	0.9386
22.86 cm (9.0 inch)	1.4607	1.7831	0.9886	1.8000e-3	0.9922
24.13 cm (9.5 inch)	1.5453	1.8864	1.0133	1.5000e-3	1.0163
25.40 cm (10.0 inch)	1.6300	1.9897	1.0251	1.8000e-3	1.0287
27.94 cm (11.0 inch)	1.7993	2.1964	1.0437	1.7000e-3	1.0471
30.48 cm (12.0 inch)	1.9687	2.4032	1.0463	1.5000e-3	1.0493
33.02 cm (13.0 inch)	2.1380	2.6099	1.0334	1.3000e-3	1.0360
35.56 cm (14.0 inch)	2.3073	2.8165	1.0132	1.3000e-3	1.0158

Table 6-24 Individual Fuel Assembly, 20 cm water reflection, 100 cm fuel lattice expansion (cont.)

Fuel envelope	Pitch (cm)	p/d ratio	k_s	σ_s	$k_s + 2\sigma_s$
15X15 STD					
Nominal	1.4300	1.5386	0.9501	1.4000e-3	0.9529
22.86 cm (9.0 inch)	1.5563	1.6745	0.9891	1.7000e-3	0.9925
24.13 cm (9.5 inch)	1.6470	1.7721	1.0168	1.5000e-3	1.0198
25.40 cm (10.0 inch)	1.7377	1.8697	1.0386	1.6000e-3	1.0418
27.94 cm (11.0 inch)	1.9192	2.0650	1.0608	1.6000e-3	1.0640
30.48 cm (12.0 inch)	2.1006	2.2602	1.0677	1.7000e-3	1.0711
33.02 cm (13.0 inch)	2.2820	2.4554	1.0626	1.7000e-3	1.0660
35.56 cm (14.0 inch)	2.4634	2.6506	1.0393	1.3000e-3	1.0419
15X15 OFA					
Nominal	1.4300	1.5386	0.9507	1.5000e-3	0.9537
22.86 cm (9.0 inch)	1.5563	1.6745	0.9903	1.5000e-3	0.9933
24.13 cm (9.5 inch	1.6470	1.7721	1.0177	1.6000e-3	1.0209
25.40 cm (10.0 inch)	1.7377	1.8697	1.0359	1.9000e-3	1.0397
27.94 cm (11.0 inch)	1.9192	2.0650	1.0617	1.4000e-3	1.0645
30.48 cm (12.0 inch)	2.1006	2.2602	1.0693	1.6000e-3	1.0725
33.02 cm (13.0 inch)	2.2820	2.4554	1.0616	1.4000e-3	1.0644
35.56 cm (14.0 inch)	2.4634	2.6506	1.0400	1.4000e-3	1.0428
15X15 BW					
Nominal	1.4427	1.5523	0.9551	1.5000e-3	0.9581
22.86 cm (9.0 inch)	1.5563	1.6745	0.9899	1.7000e-3	0.9933
24.13 cm (9.5 inch)	1.6470	1.7721	1.0201	1.5000e-3	1.0231
25.40 cm (10.0 inch)	1.7377	1.8697	1.0430	1.7000e-3	1.0464
27.94 cm (11.0 inch)	1.9192	2.0650	1.0649	1.6000e-3	1.0681
30.48 cm (12.0 inch)	2.1006	2.2602	1.0730	1.4000e-3	1.0758
33.02 cm (13.0 inch)	2.2820	2.4554	1.0643	1.8000e-3	1.0679
35.56 cm (14.0 inch)	2.4634	2.6506	1.0482	1.5000e-3	1.0512

Table 6-24 Individual Fuel Assembly, 20 cm water reflection, 100 cm fuel lattice expansion (cont.)					
Fuel envelope	**Pitch (cm)**	**p/d ratio**	**k_s**	**σ_s**	**$k_s + 2\sigma_s$**
14X14 STD					
Nominal	1.4122	1.5195	0.9067	1.4000e-3	0.9095
22.86 cm (9.0 inch)	1.6760	1.8033	0.9950	1.6000e-3	0.9982
24.13 cm (9.5 inch)	1.7737	1.9085	1.0146	1.4000e-3	1.0174
25.40 cm (10.0 inch)	1.8714	2.0136	1.0258	1.5000e-3	1.0288
27.94 cm (11.0 inch)	2.0668	2.2238	1.0429	1.8000e-3	1.0465
30.48 cm (12.0 inch)	2.2622	2.4341	1.0405	1.6000e-3	1.0437
33.02 cm (13.0 inch)	2.4575	2.6442	1.0219	1.3000e-3	1.0245
35.56 cm (14.0 inch)	2.6529	2.8545	0.9955	1.3000e-3	0.9981
14X14 OFA					
Nominal	1.4122	1.6143	0.9183	1.6000e-3	0.9215
22.86 cm (9.0 inch)	1.6803	1.9208	0.9879	1.5000e-3	0.9909
24.13 cm (9.5 inch)	1.7780	2.0325	1.0054	1.5000e-3	1.0084
25.40 cm (10.0 inch)	1.8757	2.1442	1.0144	1.6000e-3	1.0176
27.94 cm (11.0 inch)	2.0711	2.3676	1.0223	1.5000e-3	1.0253
30.48 cm (12.0 inch)	2.2665	2.5909	1.0111	1.4000e-3	1.0139
33.02 cm (13.0 inch)	2.4618	2.8142	0.9924	1.5000e-3	0.9954
35.56 cm (14.0 inch)	2.6572	3.0376	0.9634	1.6000e-3	0.9666
14X14 BW					
Nominal	1.4732	1.5405	0.9271	1.5000e-3	0.9301
22.86 cm (9.0 inch)	1.6725	1.7489	0.9812	1.5000e-3	0.9842
24.13 cm (9.5 inch)	1.7702	1.8511	1.0029	1.5000e-3	1.0059
25.40 cm (10.0 inch)	1.8679	1.9532	1.0189	1.8000e-3	1.0225
27.94 cm (11.0 inch)	2.0633	2.1576	1.0331	1.4000e-3	1.0359
30.48 cm (12.0 inch)	2.2586	2.3618	1.0326	1.5000e-3	1.0356
33.02 cm (13.0 inch)	2.4540	2.5661	1.0143	1.4000e-3	1.0171
35.56 cm (14.0 inch)	2.6494	2.7704	0.9931	1.4000e-3	0.9959

Table 6-24 Individual Fuel Assembly, 20 cm water reflection, 100 cm fuel lattice expansion (cont.)					
Fuel envelope	**Pitch (cm)**	**p/d ratio**	**k_s**	**σ_s**	**$k_s + 2\sigma_s$**
14X14 CE-2					
Nominal	1.4732	1.5243	0.9246	1.5000e-3	0.9276
22.86 cm (9.0 inch)	1.6725	1.7305	0.9829	1.6000e-3	0.9861
24.13 cm (9.5 inch)	1.7702	1.8316	1.0081	1.5000e-3	1.0111
25.40 cm (10.0 inch)	1.8679	1.9327	1.0232	1.6000e-3	1.0264
27.94 cm (11.0 inch)	2.0633	2.1349	1.0350	1.6000e-3	1.0382
30.48 cm (12.0 inch)	2.2586	2.3370	1.0352	1.6000e-3	1.0384
33.02 cm (13.0 inch)	2.4540	2.5391	1.0217	1.4000e-3	1.0245
35.56 cm (14.0 inch)	2.6494	2.7413	0.9990	1.6000e-3	1.0022

```
17x17w-ofa_4_1.451_24.13_in

=csas26     parm=size=300000
17X17W-OFA Fuel envelope=24.13 cm,  HAC length=100
cm
44groupndf5  latticecell
 uo2 1 1 293 92235 5 92238 95 end
 h2o 2 1 293 end
 zirc4 3 1 293 end
 h2o 4 1 293 end
 h2o  5 1 293 end
 h2o 15 1 293 end
 uo2 16 1 293 92235 5 92238 95 end
 h2o 17 1 293 end
 zirc4 18 1 293 end
 h2o 19 1 293 end
end comp
squarepitch 1.451   0.78435  16 19 0.9144   18 0.8001   17 end
more data
res=1  cylinder 0.39218      dan(1)=0.22842       end
read parameter
gen=303
wrs=1
end parameter
read geometry

global
unit 20
com='fuel assembly'
cuboid 1 24.13        0 24.13        0 368.3        0
cuboid 2 44.13       -20          44.13       -20          368.3       -20
hole 31 origin  x=0    y=0       z=0       rotate  a1=0  a2=0 a3=0
hole 21 origin  x=0    y=0       z=100     rotate  a1=0  a2=0 a3=0
media   0 1  1
media  15 1 -1   2
boundary 2

unit 21
com='fuel rods - nominal pitch'
cuboid 1  21.072       0 21.072       0 268.3        0.0000
cuboid 2  21.382       0 21.382       0 268.3        0.0000
array 1 1 place 1 1 1 0.4572       0.4572       0
media 0 1  -1  2
boundary 2

unit 22
com='solid fuel rod - nominal pitch'
cylinder 1  0.39218       368.3            0
cylinder 2  0.40005       368.3            0
cylinder 3  0.4572        368.3            0
cuboid 4  4P0.62992       368.3            0
media 1 1  1
media 2 1  2 -1
media 3 1  3 -2 -1
media 4 1  4 -3 -2 -1
boundary 4

unit 23
com='thimble tube - nominal pitch'
cylinder 1  0.56134       368.3            0
cylinder 2  0.60198       368.3            0
cuboid 3    4P0.62992     368.3            0
media 4 1 1
media 3 1 2 -1
media 4 1 3 -2 -1
boundary 3

unit 31
com='fuel rods - expanded pitch'
cuboid 1  24.13        0 24.13        0 100          0
array 2 1 place 1 1 1 0.4572       0.4572       0
boundary 1

unit 32
com='solid fuel rod - expanded pitch'
cylinder 1  0.39218       368.3            0
cylinder 2  0.40005       368.3            0
cylinder 3  0.4572        368.3            0
cuboid 4  4P0.72549       368.3            0
media 16  1 1
media 17  1 2 -1
media 18  1 3 -2 -1
media 19  1 4 -3 -2 -1
boundary 4

unit 33
com='thimble tube - expanded pitch'
cylinder 1  0.56134       368.3            0
cylinder 2  0.60198       368.3            0
cuboid 3  4P0.72549       368.3            0
media 19 1 1
media 18 1 2 -1
media 19 1 3 -2 -1
boundary 3

end geometry

read array
ara=1 typ=square nux=17 nuy=17 nuz=1
fill 39*22 23 2*22 23 2*22 23 8*22 23 9*22 23 22*22 23
2*22 23 2*22 23
 2*22 23 2*22 23 38*22 23 2*22 23 2*22 23 2*22 23 2*22 23 2*22 23
38*22 23
 2*22 23 2*22 23 2*22 23 2*22 23 22*22 23 9*22 23 8*22 23
2*22 23 2*22
 23 39*22
end fill
ara=2 typ=square nux=17 nuy=17 nuz=1
fill 39*32 33 2*32 33 2*32 33 8*32 33 9*32 33 22*32 33
2*32 33 2*32 33
 2*32 33 2*32 33 38*32 33 2*32 33 2*32 33 2*32 33 2*32 33 2*32 33
38*32 33
 2*32 33 2*32 33 2*32 33 2*32 33 22*32 33 9*32 33 8*32 33
2*32 33 2*32
 33 39*32
end fill

end array

read bnds
+xb=vacuum
-xb=vacuum
+yb=vacuum
-yb=vacuum
+zb=mirror
-zb=vacuum
end bnds

end data
end
```

Figure 6-24 Input Deck for 17x17 OFA

6.10.4 17x17OFA-XL Model

6.10.4.1 Introduction

The same general fuel assembly input deck is used for the several Traveller and Traveller XL criticality calculations. The primary differences are the length and the extent to which the lattice pitch expands in the expanded section. The fuel is expanded to 9.1 inches in the Traveller and 9.6 inches in the Traveller XL.

6.10.4.2 Fuel Assembly Model

The fuel assembly is typically designated as unit 20 in the input decks. Figure 6-25 shows a sample of the unit 20 input lines for the Traveller. Fuel assembly input consists of concentric cuboids to model the top nozzle assembly, skeleton and fuel regions. The fuel assembly origin is at the bottom left hand corner of the fuel assembly lower nozzle. Units #21 (nominal pitch fuel rod array), #31 (expanded pitch fuel rod array), and #40 (top nozzle assembly) are dropped into unit #20 as hole #21 and hole #31. Figure 6-26 shows the different parts that make up unit #20.

```
unit 20
com='fuel assembly'
cuboid 1 21.4122 0 21.4122  0    0       -14.0208
cuboid 2 23.1140 0 23.1140  0  504.1392  -14.0208
hole 31 origin x=0 y=0 z= 0.      rotate  a1=0  a2=0 a3=0
hole 21 origin x=0 y=0 z=100.0000 rotate  a1=0  a2=0 a3=0
hole 40 origin x=0 y=0 z=426.7200 rotate  a1=0  a2=0 a3=0
media  15 1  1
media   0 1 -1 2
boundary 2
```

Figure 6-25 Sample Input Lines for Traveller Fuel Assembly

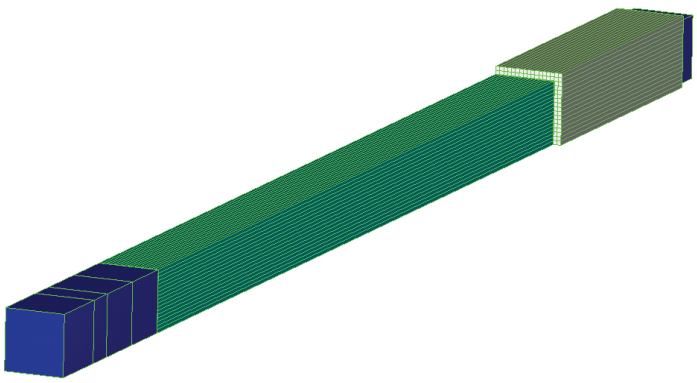

Figure 6-26 Keno 3D Image of Fuel Assembly

6.10.4.3 Fuel Rod Arrays

Units #21 and #31 are the fuel rod arrays. The arrays are identical except that cuboid #4 is sized according to the nominal pitch (unit #21) or expanded pitch (unit #31).

Unit #21 is made up of nominal pitch fuel rods (unit #22) and thimble tubes (unit #23). Unit #31 similarly is made up of expanded pitch fuel rods (unit #32) and thimble tubes (unit #33). Sample input deck lines for these units are found in Figure 6-27.

```
unit 21
com='fuel rods - nominal pitch'
cuboid 1  21.4166  0  21.4166  0  326.7200 0.0000
array 2 1 place 1 1 1 0.6299 0.6299 0
boundary 1

unit 22
com='solid fuel rod - nominal pitch'
cylinder 1  0.3922  448.3862     0
cylinder 2  0.4  448.3862     0
cylinder 3  0.4572  448.3862     0
cuboid 4 0.6299 -0.6299 0.6299 -0.6299 448.3862 0
media 1   1 1
media 2   1 2 -1
media 3   1 3 -2 -1
media 4   1 4 -3 -2 -1
boundary 4

unit 23
com='thimble tube - nominal pitch'
cylinder 1  0.5613  448.3862     0
cylinder 2  0.6020 448.3862     0
cuboid 3 0.6299 -0.6299 0.6299 -0.6299 448.3862 0
media 4 1 1
media 3 1 2 -1
media 4 1 3 -2 -1
boundary 3
```

```
unit 31
com='fuel rods - expanded pitch'
cuboid 1  23.1140   0  23.1140   0  100.0000 0
array 3 1 place 1 1 1 0.4572 0.4572 0
boundary 1

unit 32
com='solid fuel rod - expanded pitch'
cylinder 1  0.3922  448.3862     0
cylinder 2  0.4  448.3862     0
cylinder 3  0.4572  448.3862     0
cuboid 4  0.6937 -0.6937 0.6937 -0.6937 448.3862 0
media 16  1 1
media 17  1 2 -1
media 18  1 3 -2 -1
media 19  1 4 -3 -2 -1
boundary 4

unit 33
com='thimble tube - expanded pitch'
cylinder 1  0.5613  448.3862     0
cylinder 2  0.6020 448.3862     0
cuboid 3 0.6937 -0.6937 0.6937 -0.6937 448.3862 0
media 19 1 1
media 18 1 2 -1
media 19 1 3 -2 -1
boundary 3
```

Figure 6-27 Sample Input Lines for Fuel Rod Cells

6.10.4.4 Fuel Rod Cell

Fuel rod cells (units #22 and #32) are modeled as concentric cylinders for the pellet, gap, and cladding. The cells are bounded by a cuboid whose dimension is determined by lattice pitch. Thimble tubes (units #23 and 33) are similarly structured. Sample input lines for the rod cell units are shown in Figure 6-27. A fuel cell is shown in Figure 6-28.

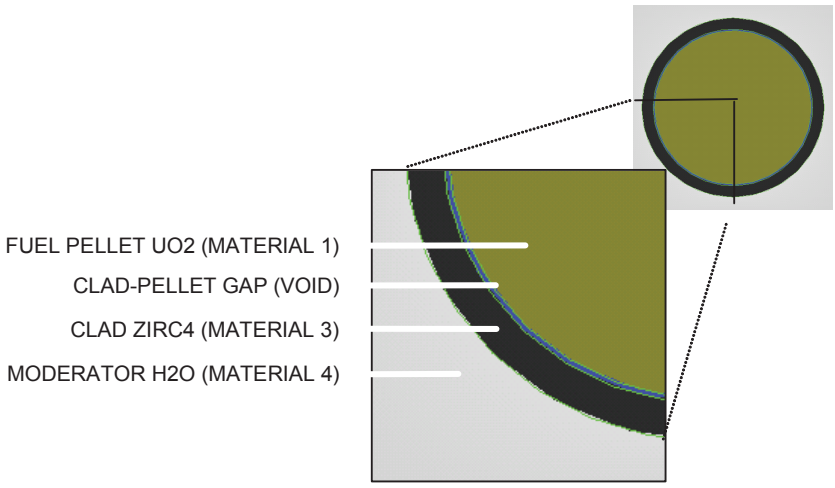

Figure 6-28 Fuel Rod Cell

6.10.5 Traveller Packaging Model

6.10.5.1 Introduction

The Traveller packaging model consists of the Outerpack (unit 10) and clamshell (unit 11). The same Outerpack input deck is used for the Traveller STD and Traveller XL calculations. The axial dimensions for the Traveller XL are used for the Traveller STD because axial differences do not affect results. The shock mount configuration used in the model is a conservative arrangement that bounds both the STD and XL configurations.

The primary difference between the STD and XL models is the lateral dimension of the clamshell where the face-to-face dimensions are different. The STD clamshell is modeled at 9.1 inches and the XL clamshell is modeled at 9.6 inches.

6.10.5.2 Outerpack Model

The Outerpack is defined in unit 10. Figure 6-29 gives a sample of the unit 10 input lines for the Traveller. Some features of the outerpack model are: the shock mounts and shock mount cutouts are defined using cylinders; and the six moderator blocks are defined with cuboids. Figure 6-30 through Figure 6-32 show various renderings of the outerpack. The shock mount configuration for the Traveller XL is a conservative arrangement of the actual configuration. As seen in figure 6-32, there are two pair of shock mounts at the end spaced 18 inches center-to-center. The second set was moved to be 18 inches from the first pair in order that the expanded section of fuel would “see” two pair of shock mounts.

```
unit 10
com='individual package'
cuboid 1   16.904     -15.634     16.904     -15.634     533.1330 0
rotate  a1=45 a2=0 a3=0 origin x=0  y=-1.460 z=0
cuboid 2    21.5900   -21.5900    1.5720   -1.0310   533.1330    0
cuboid 3    20.0790   -20.0790   20.0790   -20.0790   533.1330    0
rotate  a1=45 a2=0 a3=0 origin x=0  y=-1.460 z=0
cuboid 4    20.3450   -20.3450   20.3450   -20.3450   533.3990   -
0.2660
rotate  a1=45 a2=0 a3=0 origin x=0  y=-1.460 z=0
cuboid 5    21.5900   -21.590    23.1498   -23.1498   533.1330    0
cuboid 6    21.8560   -21.8560   23.4158   -23.4158   533.3990   -
0.2660
cuboid 7    20.3840   -20.3840   20.3840   -20.3840   553.8922   -
19.8448
rotate  a1=45 a2=0 a3=0 origin x=0  y=-1.460 z=0
cuboid 8    21.8950   -21.895    23.4548   -23.4548   553.8922   -
19.8448
cylinder  9    25.1050    533.4380    -0.2660
cylinder 10    25.1050    553.9312   -19.8448
cylinder 11    31.4840    533.4380    -0.2660
cylinder 12    31.4840    553.9312   -19.8448
cylinder 13    31.4840    533.4380   -19.8448
cylinder 14    31.7500    554.1972   -20.1100
plane 15  zpl=1  con= -10.0000
cylinder 16 7.62   0 -4.5
 rotate  a1=45 a2=90 a3=0 origin x=18.7310 y=-11.1270
z=494.4364
cylinder 17 3.962  0 -7.60
 rotate  a1=45 a2=90 a3=0 origin x=18.7310 y=-11.1270
z=494.4364
cylinder 18 7.62   0 -4.5
 rotate  a1=-45 a2=90 a3=0 origin x=-18.7310 y=-11.1270
z=494.4364
cylinder 19 3.962  0 -7.60
 rotate  a1=-45 a2=90 a3=0 origin x=-18.7310 y=-11.1270
z=494.4364
cylinder 20 7.62   0 -4.5
 rotate  a1=45 a2=90 a3=0 origin x=18.7310 y=-11.1270
z=448.7164
cylinder 21 3.962  0 -7.60
 rotate  a1=45 a2=90 a3=0 origin x=18.7310 y=-11.1270
z=448.7164
cylinder 22 7.62   0 -4.5
 rotate  a1=-45 a2=90 a3=0 origin x=-18.7310 y=-11.1270
z=448.7164
cylinder 23 3.962  0 -7.60
 rotate  a1=-45 a2=90 a3=0 origin x=-18.7310 y=-11.1270
z=448.7164
cylinder 24 7.62   0 -4.5
 rotate  a1=45 a2=90 a3=0 origin x=18.7310 y=-11.1270
z=402.9964
cylinder 25 3.962  0 -7.60
 rotate  a1=45 a2=90 a3=0 origin x=18.7310 y=-11.1270
z=402.9964
cylinder 26 7.62   0 -4.5
 rotate  a1=-45 a2=90 a3=0 origin x=-18.7310 y=-11.1270
z=402.9964
cylinder 27 3.962  0 -7.60
 rotate  a1=-45 a2=90 a3=0 origin x=-18.7310 y=-11.1270
z=402.9964
cylinder 28 7.62   0 -4.5
 rotate  a1=45 a2=90 a3=0 origin x=18.7310 y=-11.1270
z=357.2764
cylinder 29 3.962  0 -7.60
 rotate  a1=45 a2=90 a3=0 origin x=18.7310 y=-11.1270
z=357.2764
cylinder 30 7.62   0 -4.5
 rotate  a1=-45 a2=90 a3=0 origin x=-18.7310 y=-11.1270
z=357.2764
cylinder 31 3.962  0 -7.60
 rotate  a1=-45 a2=90 a3=0 origin x=-18.7310 y=-11.1270
z=357.2764
cylinder 54 7.62   0 -4.5
 rotate  a1=45 a2=90 a3=0 origin x=18.7310 y=-11.1270
z=265.8364
cylinder 55 3.962  0 -7.60
 rotate  a1=45 a2=90 a3=0 origin x=18.7310 y=-11.1270
z=265.8364
cylinder 56 7.62   0 -4.5
 rotate  a1=-45 a2=90 a3=0 origin x=-18.7310 y=-11.1270
z=265.8364
cylinder 57 3.962  0 -7.60
 rotate  a1=-45 a2=90 a3=0 origin x=-18.7310 y=-11.1270
z=265.8364
cylinder 32 7.62   0 -4.5
 rotate  a1=45 a2=90 a3=0 origin x=18.7310 y=-11.1270
z=174.3964
cylinder 33 3.962  0 -7.60
 rotate  a1=45 a2=90 a3=0 origin x=18.7310 y=-11.1270
z=174.3964
cylinder 34 7.62   0 -4.5
 rotate  a1=-45 a2=90 a3=0 origin x=-18.7310 y=-11.1270
z=174.3964
cylinder 35 3.962  0 -7.60
 rotate  a1=-45 a2=90 a3=0 origin x=-18.7310 y=-11.1270
z=174.3964
cylinder 36 7.62   0 -4.5
 rotate  a1=45 a2=90 a3=0 origin x=18.7310 y=-11.1270
z=128.6764
cylinder 37 3.962  0 -7.60
 rotate  a1=45 a2=90 a3=0 origin x=18.7310 y=-11.1270
z=128.6764
cylinder 38 7.62   0 -4.5
 rotate  a1=-45 a2=90 a3=0 origin x=-18.7310 y=-11.1270
z=128.6764
cylinder 39 3.962  0 -7.60
 rotate  a1=-45 a2=90 a3=0 origin x=-18.7310 y=-11.1270
z=128.6764
cylinder 40 7.62   0 -4.5
 rotate  a1=45 a2=90 a3=0 origin x=18.7310 y=-11.1270 z=82.9564
cylinder 41 3.962  0 -7.60
 rotate  a1=45 a2=90 a3=0 origin x=18.7310 y=-11.1270 z=82.9564
cylinder 42 7.62   0 -4.5
 rotate  a1=-45 a2=90 a3=0 origin x=-18.7310 y=-11.1270
z=82.9564
```

Figure 6-29 Sample Input Deck for Traveller Outerpack (Sheet 1 of 2)

```
cylinder 43 3.962  0 -7.60
 rotate  a1=-45 a2=90 a3=0 origin x=-18.7310 y=-11.1270
z=82.9564cylinder 44 7.62   0 -4.5
 rotate  a1=45 a2=90 a3=0 origin x=18.7310 y=-11.1270
z=37.2364
cylinder 45 3.962  0 -7.60
 rotate  a1=45 a2=90 a3=0 origin x=18.7310 y=-11.1270
 z=37.2364
cylinder 46 7.62   0 -4.5
 rotate  a1=-45 a2=90 a3=0 origin x=-18.7310 y=-11.1270
z=37.2364
cylinder 47 3.962  0 -7.60
 rotate  a1=-45 a2=90 a3=0 origin x=-18.7310 y=-11.1270
z=37.2364
hole 11 rotate  a1=45 a2=0 a3=0  origin  x=0 y=-17.700 z=5.240
cuboid 48    18.174    20.079   10.4238  -9.5152    533.3990    -
0.2660
rotate  a1=-45 a2=0 a3=0 origin x=0  y=-1.460 z=0
cuboid 49    13.6554  -10.4238  16.904    20.079    533.3990    -
0.2660
rotate  a1=45 a2=0 a3=0 origin x=0  y=-1.460 z=0
cuboid 50    16.904    20.079   13.6554  -10.4238   533.3990    -
0.2660
rotate  a1=45 a2=0 a3=0 origin x=0  y=-1.460 z=0
cuboid 51     9.5152  -10.4238 -18.174   -20.079    533.3990    -
0.2660
rotate  a1=-45 a2=0 a3=0 origin x=0  y=-1.460 z=0
cuboid 52    15.634    18.174   12.0238 -11.9197    533.3990    -
0.2660
rotate  a1=-45 a2=0 a3=0 origin x=0  y=-1.460 z=0
cuboid 53    11.9197  -12.0238 -15.634   -18.174    533.3990    -
0.2660
rotate  a1=-45 a2=0 a3=0 origin x=0  y=-1.460 z=0
media  0 1   1   3  5 -17 -19 -21 -23 -29 -31 -55 -57 -33 -35
-41 -43 -45 -47
media  0 1  -1   3  5 -48 -49 -50 -51 -52 -53
media  9 1   3  -16  -17 -20 -21 -28 -29 -54 -55 -32 -33
-40 -41 -44 -45 48
media  9 1   3  -18  -19 -22 -23 -30 -31 -56 -57 -34 -35
-42 -43 -46 -47 51
media  9 1   3  -18  -22  -30  -56  -34  -42  -46  53
media  9 1   3  -16  -20  -28  -54  -32  -40  -44  52
media  9 1   3  49
media  9 1   3  50
media  8 1  -3   4   6
media  8 1   3  -5   6
media  6 1  -4   9
media  6 1   4  -6   9
media  6 1  -9  11
```

```
media  6 1  -7  10 -13
media  6 1   7  -8  10 -13  12
media  6 1 -10 -13  12
media 11 1 -11  13
media 11 1   7   8 -13  12
media  8 1 -12  14
media  0 1 16  -17 3 48
media  0 1 18  -19 3 51
media  0 1 20  -21 3 48
media  0 1 22  -23 3 51
media  0 1 28  -29 3 48
media  0 1 30  -31 3 51
media  0 1 54  -55 3 48
media  0 1 56  -57 3 51
media  0 1 32  -33 3 48
media  0 1 34  -35 3 51
media  0 1 40  -41 3 48
media  0 1 42  -43 3 51
media  0 1 44  -45 3 48
media  0 1 46  -47 3 51
media  0 1 16  -17 3 52
media  0 1 18  -19 3 53
media  0 1 20  -21 3 52
media  0 1 22  -23 3 53
media  0 1 28  -29 3 52
media  0 1 30  -31 3 53
media  0 1 54  -55 3 52
media  0 1 56  -57 3 53
media  0 1 32  -33 3 52
media  0 1 34  -35 3 53
media  0 1 40  -41 3 52
media  0 1 42  -43 3 53
media  0 1 44  -45 3 52
media  0 1 46  -47 3 53
media 14 1 17  3
media 14 1 19  3
media 14 1 21  3
media 14 1 23  3
media 14 1 29  3
media 14 1 31  3
media 14 1 55  3
media 14 1 57  3
media 14 1 33  3
media 14 1 35  3
media 14 1 41  3
media 14 1 43  3
media 14 1 45  3
media 14 1 47  3
boundary 14
```

Figure 6-29 Sample Input Deck for Traveller Outerpack (Sheet 2 of 2)

This page intentionally left blank.

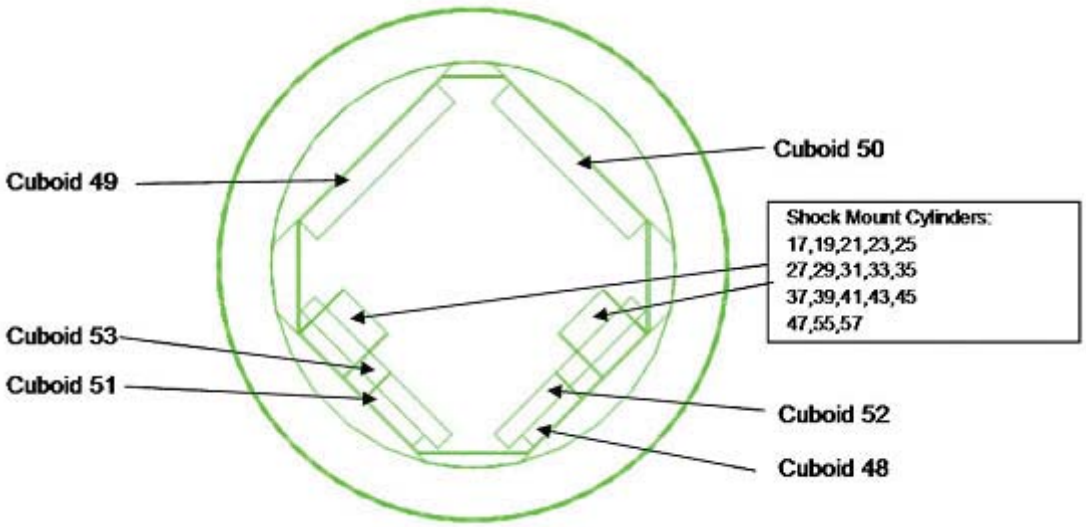

Figure 6-30 Keno 3D Line Schematic of Outerpack Cuboids

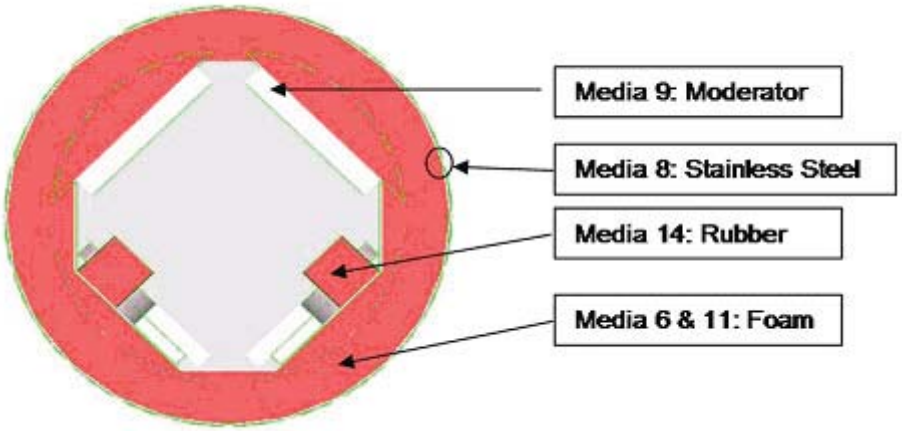

Figure 6-31 Keno 3D Rendering of Outerpack

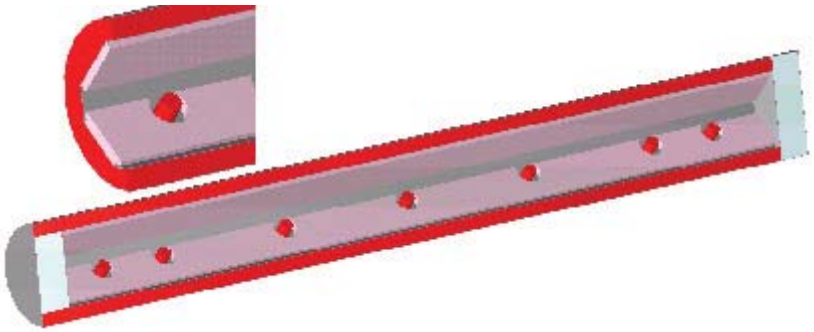

Figure 6-32 Keno 3D Rendering of XL Outerpack

6.10.5.3 Clamshell Model

The Clamshell is defined in unit 11. Figure 6-33 shows a sample of the unit 11 input lines for the Clamshell. Figure 6-34 is a schematic drawing of the Clamshell model.

```
unit 11
com='fuel assembly confinement system'
cuboid 1    24.384       0 24.384       0 520.7000 2.5400
cuboid 2    25.337       -0.9525 25.337        -0.9525
 523.2400  0.0000
cuboid 3    19.812       4.572        24.429       -0.04545
 513.0800  3.81
cuboid 4    19.812       4.572        24.656       -0.27205
 513.0800  3.81
cuboid 5    19.812       4.572        24.702       -0.3175
 513.0800  3.81
cuboid 6    24.429       -0.04545      19.812       4.572
 513.0800  3.81
cuboid 7    24.656       -0.27205      19.812       4.572
 513.0800  3.81
cuboid 8    24.702       -0.3175       19.812       4.572
 513.0800  3.81
hole 20  origin  x=0  y=0  z=16.56  rotate  a1=0 a2=0 a3=0
media  0 1   1
media  7 1  -1   2  -5  -8
media  7 1  -1   3
media 12 1  -3   4
media  7 1  -4   5
media  7 1  -1   6
media 12 1  -6   7
media  7 1  -7   8
boundary 2
```

Figure 6-33 Sample Input Lines for Clamshell

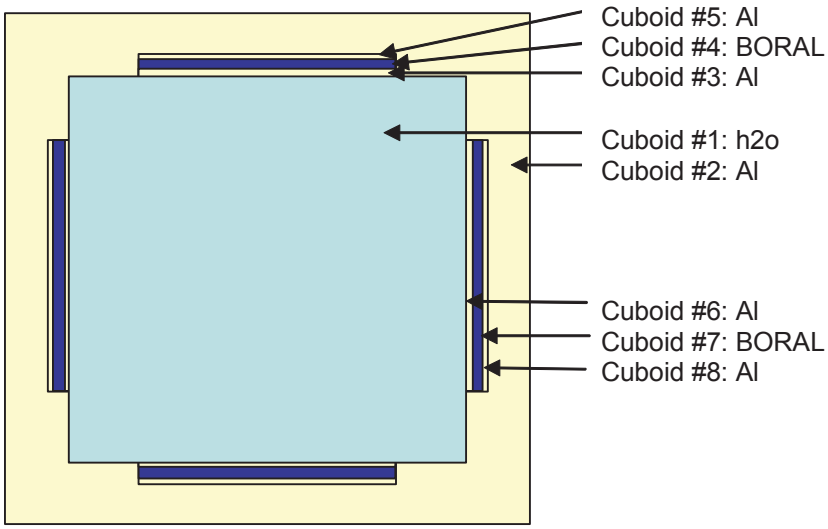

Figure 6-34 Clamshell

6.10.6 Single Package Evaluation Calculations

Results for the single package in isolation calculations are presented below. Table 6-25 shows the results for normal conditions analyzed for Traveller XL only. Table 6-26 presents results for hypothetical accident conditions for the Traveller STD. Table 6-27 gives similar results for the Traveller XL.

Table 6-25 Results for Traveller XL – Normal Conditions of Transport – Individual Package

Run #	ks	σks	ks+2×σks
XL-NOR-IND	0.2000	0.0006	0.2012

Table 6-26 Results for Traveller XL – Hypothetical Accident Conditions – Individual Package

Run #	ks	σks	ks+2×σks
STD-HAC-IND	0.8621	0.0012	0.8645

Table 6-27 Results for Traveller XL – Hypothetical Accident Conditions – Individual Package

Run #	ks	σks	ks+2×σks
XL-HAC-IND-100	0.8833	0.0009	0.8851

Table 6-28 has been deleted.

Pages 6-72 through 6-76 intentionally left blank.

Table 6-29 Sample Input Deck for Traveller XL Single Package – Normal Condition of Transport

```
=csas26     parm=size=300000
TRAVELLER XL,17WOFA,ENV=24.384      cm,L=100      cm,B10=0.018   g/cm2
44groupndf5  latticecell
 uo2 1 1 293 92235 5 92238 95 end
 h2o 2 1 293 end
 zirc4 3 1 293 end
 h2o 4 1 293 end
 h2o 5 1 293 end
 arbmfoam 0.1602  4  0  0  0 6012 70 1001 10 8016 16 7014 4  6 1 293
 end
 al 7 1 293 end
 ss304 8 1 293 end
 polyethylene 9 DEN=0.828 1.0 293 end
 arbmfoam 0.1602  4  0  0  0 6012 70 1001 10 8016 16 7014 4 11 1 293
 end
 b-10 12 0 0.0047781    end
 b-11 12 0 0.019398     end
 c   12 0 0.0060439    end
 al  12 0 0.043223     end
 arbmrubber 1.59  7  0  0  0 8016 46.94 13000 19.92 14000 17.54 6012
 10.79 1001 4.73 11000 0.06 26000 0.02  14 1 293 end
 h2o 15 1 293 end
 uo2 16 1 293 92235 5 92238 95 end
 h2o 17 1 293 end
 zirc4 18 1 293 end
 h2o 19 1 293 end
end comp
squarepitch 1.4669       0.78435      16 19 0.9144       18 0.8001       17 end
more data
res=1  cylinder 0.39218      dan(1)=0.22632       end

read parameter
gen=450
npg=2500
nsk=50
wrs=1
tme=240
end parameter
```

Table 6-29 Sample Input Deck for Traveller XL Single Package – Normal Condition of Transport (cont.)

```
read geometry
unit 10
com='individual package'
cuboid 1    16.904      -15.634      16.904      -15.634      533.1330 0
rotate  a1=45 a2=0 a3=0 origin x=0  y=-1.460 z=0
cuboid 2    21.5900   -21.5900    1.5720    -1.0310   533.1330    0
cuboid 3    20.0790   -20.0790    20.0790   -20.0790   533.1330    0
rotate  a1=45 a2=0 a3=0 origin x=0  y=-1.460 z=0
cuboid 4    20.3450   -20.3450    20.3450   -20.3450   533.3990    -0.2660
rotate  a1=45 a2=0 a3=0 origin x=0  y=-1.460 z=0
cuboid 5    21.5900   -21.590     23.1498   -23.1498   533.1330    0
cuboid 6    21.8560   -21.8560    23.4158   -23.4158   533.3990    -0.2660
cuboid 7    20.3840   -20.3840    20.3840   -20.3840   553.8922   -19.8448
rotate  a1=45 a2=0 a3=0 origin x=0  y=-1.460 z=0
cuboid 8    21.8950   -21.895     23.4548   -23.4548   553.8922   -19.8448
cylinder  9    25.1050    533.4380    -0.2660
cylinder 10    25.1050    553.9312   -19.8448
cylinder 11    31.4840    533.4380    -0.2660
cylinder 12    31.4840    553.9312   -19.8448
cylinder 13    31.4840    533.4380   -19.8448
cylinder 14    31.7500    554.1972   -20.1100
plane 15  zpl=1  con= -10.0000
cylinder 16 7.62   0 -4.5
 rotate  a1=45 a2=90 a3=0 origin x=18.7310 y=-11.1270 z=494.4364
cylinder 17 3.962  0 -7.60
 rotate  a1=45 a2=90 a3=0 origin x=18.7310 y=-11.1270 z=494.4364
cylinder 18 7.62   0 -4.5
 rotate  a1=-45 a2=90 a3=0 origin x=-18.7310 y=-11.1270 z=494.4364
cylinder 19 3.962  0 -7.60
 rotate  a1=-45 a2=90 a3=0 origin x=-18.7310 y=-11.1270 z=494.4364
cylinder 20 7.62   0 -4.5
 rotate  a1=45 a2=90 a3=0 origin x=18.7310 y=-11.1270 z=448.7164
cylinder 21 3.962  0 -7.60
 rotate  a1=45 a2=90 a3=0 origin x=18.7310 y=-11.1270 z=448.7164
cylinder 22 7.62   0 -4.5
 rotate  a1=-45 a2=90 a3=0 origin x=-18.7310 y=-11.1270 z=448.7164
cylinder 23 3.962  0 -7.60
 rotate  a1=-45 a2=90 a3=0 origin x=-18.7310 y=-11.1270 z=448.7164
cylinder 24 7.62   0 -4.5
 rotate  a1=45 a2=90 a3=0 origin x=18.7310 y=-11.1270 z=402.9964
cylinder 25 3.962  0 -7.60
 rotate  a1=45 a2=90 a3=0 origin x=18.7310 y=-11.1270 z=402.9964
cylinder 26 7.62   0 -4.5
 rotate  a1=-45 a2=90 a3=0 origin x=-18.7310 y=-11.1270 z=402.9964
cylinder 27 3.962  0 -7.60
 rotate  a1=-45 a2=90 a3=0 origin x=-18.7310 y=-11.1270 z=402.9964
cylinder 28 7.62   0 -4.5
 rotate  a1=45 a2=90 a3=0 origin x=18.7310 y=-11.1270 z=357.2764
cylinder 29 3.962  0 -7.60
 rotate  a1=45 a2=90 a3=0 origin x=18.7310 y=-11.1270 z=357.2764
```

Table 6-29 Sample Input Deck for Traveller XL Single Package – Normal Condition of Transport (cont.)

```
cylinder 30 7.62   0 -4.5
 rotate  a1=-45 a2=90 a3=0 origin x=-18.7310 y=-11.1270 z=357.2764
cylinder 31 3.962  0 -7.60
 rotate  a1=-45 a2=90 a3=0 origin x=-18.7310 y=-11.1270 z=357.2764
cylinder 54 7.62   0 -4.5
 rotate  a1=45 a2=90 a3=0 origin x=18.7310 y=-11.1270 z=265.8364
cylinder 55 3.962  0 -7.60
 rotate  a1=45 a2=90 a3=0 origin x=18.7310 y=-11.1270 z=265.8364
cylinder 56 7.62   0 -4.5
 rotate  a1=-45 a2=90 a3=0 origin x=-18.7310 y=-11.1270 z=265.8364
cylinder 57 3.962  0 -7.60
 rotate  a1=-45 a2=90 a3=0 origin x=-18.7310 y=-11.1270 z=265.8364
cylinder 32 7.62   0 -4.5
 rotate  a1=45 a2=90 a3=0 origin x=18.7310 y=-11.1270 z=174.3964
cylinder 33 3.962  0 -7.60
 rotate  a1=45 a2=90 a3=0 origin x=18.7310 y=-11.1270 z=174.3964
cylinder 34 7.62   0 -4.5
 rotate  a1=-45 a2=90 a3=0 origin x=-18.7310 y=-11.1270 z=174.3964
cylinder 35 3.962  0 -7.60
 rotate  a1=-45 a2=90 a3=0 origin x=-18.7310 y=-11.1270 z=174.3964
cylinder 36 7.62   0 -4.5
 rotate  a1=45 a2=90 a3=0 origin x=18.7310 y=-11.1270 z=128.6764
cylinder 37 3.962  0 -7.60
 rotate  a1=45 a2=90 a3=0 origin x=18.7310 y=-11.1270 z=128.6764
cylinder 38 7.62   0 -4.5
 rotate  a1=-45 a2=90 a3=0 origin x=-18.7310 y=-11.1270 z=128.6764
cylinder 39 3.962  0 -7.60
 rotate  a1=-45 a2=90 a3=0 origin x=-18.7310 y=-11.1270 z=128.6764
cylinder 40 7.62   0 -4.5
 rotate  a1=45 a2=90 a3=0 origin x=18.7310 y=-11.1270 z=82.9564
cylinder 41 3.962  0 -7.60
 rotate  a1=45 a2=90 a3=0 origin x=18.7310 y=-11.1270 z=82.9564
cylinder 42 7.62   0 -4.5
 rotate  a1=-45 a2=90 a3=0 origin x=-18.7310 y=-11.1270 z=82.9564
cylinder 43 3.962  0 -7.60
 rotate  a1=-45 a2=90 a3=0 origin x=-18.7310 y=-11.1270 z=82.9564
cylinder 44 7.62   0 -4.5
rotate  a1=45 a2=90 a3=0 origin x=18.7310 y=-11.1270 z=37.2364
cylinder 45 3.962  0 -7.60
 rotate  a1=45 a2=90 a3=0 origin x=18.7310 y=-11.1270 z=37.2364
cylinder 46 7.62   0 -4.5
  rotate  a1=-45 a2=90 a3=0 origin x=-18.7310 y=-11.1270 z=37.2364
cylinder 47 3.962  0 -7.60
 rotate  a1=-45 a2=90 a3=0 origin x=-18.7310 y=-11.1270 z=37.2364
hole 11 rotate  a1=45 a2=0 a3=0  origin  x=0 y=-17.700 z=5.240
cuboid 48    18.174    20.079   10.4238  -9.5152    533.3990    -0.2660
rotate  a1=-45 a2=0 a3=0 origin x=0  y=-1.460 z=0
cuboid 49    13.6554  -10.4238  16.904    20.079    533.3990    -0.2660
rotate  a1=45 a2=0 a3=0 origin x=0  y=-1.460 z=0
cuboid 50    16.904    20.079   13.6554  -10.4238   533.3990    -0.2660
rotate  a1=45 a2=0 a3=0 origin x=0  y=-1.460 z=0
```

Table 6-29 Sample Input Deck for Traveller XL Single Package – Normal Condition of Transport (cont.)

```
cuboid 51     9.5152  -10.4238 -18.174   -20.079    533.3990    -0.2660
rotate  a1=-45 a2=0 a3=0 origin x=0  y=-1.460 z=0
cuboid 52    15.634    18.174   12.0238 -11.9197    533.3990    -0.2660
rotate  a1=-45 a2=0 a3=0 origin x=0  y=-1.460 z=0
cuboid 53    11.9197  -12.0238 -15.634   -18.174    533.3990    -0.2660
rotate  a1=-45 a2=0 a3=0 origin x=0  y=-1.460 z=0
media  0 1   1   3  5 -17 -19 -21 -23 -29 -31 -55 -57 -33 -35
-41 -43 -45 -47
media  0 1  -1   3  5 -48 -49 -50 -51 -52 -53
media  9 1   3  -16  -17 -20 -21 -28 -29 -54 -55 -32 -33
-40 -41 -44 -45 48
media  9 1   3  -18  -19 -22 -23 -30 -31 -56 -57 -34 -35
-42 -43 -46 -47 51
media  9 1   3  -18  -22  -30  -56  -34  -42  -46  53
media  9 1   3  -16  -20  -28  -54  -32  -40  -44  52
media  9 1   3  49
media  9 1   3  50
media  8 1  -3   4   6
media  8 1   3  -5   6
media 15 1  -4   9
media 15 1   4  -6   9
media 15 1  -9  11
media 15 1  -7  10 -13
media 15 1   7  -8  10 -13  12
media 15 1 -10 -13  12
media 15 1 -11  13
media 15 1   7   8 -13  12
media  8 1 -12  14
media 15 1 16  -17 3 48
media 15 1 18  -19 3 51
media 15 1 20  -21 3 48
media 15 1 22  -23 3 51
media 15 1 28  -29 3 48
media 15 1 30  -31 3 51
media 15 1 54  -55 3 48
media 15 1 56  -57 3 51
media 15 1 32  -33 3 48
media 15 1 34  -35 3 51
media 15 1 40  -41 3 48
media 15 1 42  -43 3 51
media 15 1 44  -45 3 48
media 15 1 46  -47 3 51
media 15 1 16  -17 3 52
media 15 1 18  -19 3 53
media 15 1 20  -21 3 52
media 15 1 22  -23 3 53
media 15 1 28  -29 3 52
media 15 1 30  -31 3 53
media 15 1 54  -55 3 52
media 15 1 56  -57 3 53
media 15 1 32  -33 3 52
```

Table 6-29 Sample Input Deck for Traveller XL Single Package – Normal Condition of Transport (cont.)

```
media 15 1 34  -35 3 53
media 15 1 40  -41 3 52
media 15 1 42  -43 3 53
media 15 1 44  -45 3 52
media 15 1 46  -47 3 53
media 15 1 17  3
media 15 1 19  3
media 15 1 21  3
media 15 1 23  3
media 15 1 29  3
media 15 1 31  3
media 15 1 55  3
media 15 1 57  3
media 15 1 33  3
media 15 1 35  3
media 15 1 41  3
media 15 1 43  3
media 15 1 45  3
media 15 1 47  3
boundary 14

unit 11
com='fuel assembly confinement system'
cuboid 1    24.384       0 24.384       0 520.7000 2.5400
cuboid 2    25.337       -0.9525 25.337        -0.9525
 523.2400  0.0000
cuboid 3    19.812       4.572        24.429       -0.04545
 513.0800  3.81
cuboid 4    19.812       4.572        24.656       -0.27205
 513.0800  3.81
cuboid 5    19.812       4.572        24.702       -0.3175
 513.0800  3.81
cuboid 6    24.429       -0.04545      19.812       4.572
 513.0800  3.81
cuboid 7    24.656       -0.27205      19.812       4.572
 513.0800  3.81
cuboid 8    24.702       -0.3175       19.812       4.572
 513.0800  3.81
hole 20  origin  x=0  y=0  z=16.56  rotate  a1=0 a2=0 a3=0
media 15 1   1
media  7 1  -1   2  -5  -8
media  7 1  -1   3
media 12 1  -3   4
media  7 1  -4   5
media  7 1  -1   6
media 12 1  -6   7
media  7 1  -7   8
boundary 2

unit 20
```

Table 6-29 Sample Input Deck for Traveller XL Single Package – Normal Condition of Transport (cont.)

```
com='fuel assembly'
cuboid 1 21.072       0 21.072       0   0       -14.0208
cuboid 2 24.384       0 24.384       0 504.1392   -14.0208
hole 21 origin  x=0       y=0       z=0.0001   rotate  a1=0  a2=0 a3=0
hole 40 origin  x=0       y=0       z=426.7201 rotate  a1=0  a2=0 a3=0
media  15 1  1
media   0 1 -1   2
boundary 2

unit 21
com='fuel rods - nominal pitch'
cuboid 1  21.072       0 21.072       0 426.72       0.0000
array 2 1 place 1 1 1 0.4572       0.4572       0
boundary 1

unit 22
com='solid fuel rod - nominal pitch'
cylinder 1  0.39218       426.72          0
cylinder 2  0.40005      426.72          0
cylinder 3  0.4572       426.72          0
cuboid 4  4P0.62992       426.72          0
media 1 1  1
media 0 1  2 -1
media 3 1  3 -2 -1
media 0 1  4 -3 -2 -1
boundary 4

unit 23
com='thimble tube - nominal pitch'
cylinder 1  0.56134       426.72          0
cylinder 2  0.60198       426.72          0
cuboid 3    4P0.62992      426.72          0
media 0 1 1
media 3 1 2 -1
media 0 1 3 -2 -1
boundary 3

unit 31
com='fuel rods - expanded pitch'
cuboid 1  24.384       0 24.384       0 100          0
array 3 1 place 1 1 1 0.4572       0.4572       0
boundary 1
```

Table 6-29 Sample Input Deck for Traveller XL Single Package – Normal Condition of Transport (cont.)

```
unit 32
com='solid fuel rod - expanded pitch'
cylinder 1  0.39218       426.72          0
cylinder 2  0.40005      426.72          0
cylinder 3  0.4572       426.72          0
cuboid 4  4P0.73342       426.72          0
media 16  1 1
media 17  1 2 -1
media 18  1 3 -2 -1
media 19  1 4 -3 -2 -1
boundary 4

unit 33
com='thimble tube - expanded pitch'
cylinder 1  0.56134      426.72          0
cylinder 2  0.60198      426.72          0
cuboid 3  4P0.73342       426.72          0
media 19 1 1
media 18 1 2 -1
media 19 1 3 -2 -1
boundary 3

unit 40
com='top nozzle assembly'
cuboid 1     21.072       0 21.072       0       21.2090     0.0000
cuboid 2     21.072       0 21.072       0      41.8846     0.0000
cuboid 3     21.072       0 21.072       0       52.8193     0.0000
cuboid 4     21.072       0 21.072       0       77.4192     0.0000
cuboid 5     24.384       0 24.384       0       77.4192     0.0008
media  15 1   1
media  15 1  -1   2
media  15 1  -2   3
media  15 1  -3   4
media  15 1  -4   5
boundary 5

global
unit 66
com='individual package 0-deg rotation'
hexprism 1  31.75    554.1972  -20.1498
hole 10  origin  x=0 y=0  z=0  rotate  a1=0 a2=0 a3=0
cylinder 2  51.75    574.1972  -40.1498
cuboid 3  4P51.75   574.1972  -40.1498
media  15 1   1
media  15 1  -1   2
media   0 1  -2   3
boundary  3
```

Table 6-29 Sample Input Deck for Traveller XL Single Package – Normal Condition of Transport (cont.)

```
unit 77
com='individual package 180-deg rotation'
hexprism 1  31.75    554.1972  -20.1498
hole 10  origin  x=0 y=0  z=0  rotate  a1=0 a2=0 a3=180
media   0 1   1
boundary 1

unit 88
com='dummy cell'
hexprism 1  31.75    554.1972  -20.1498
media  15 1   1
boundary 1

unit 99
com='package array'
cylinder 1  31.75    554.1972  -20.1498
cylinder 2  51.75    574.1972  -40.1498
cuboid 3  4P51.75   574.1972  -40.1498
array 1 1  place 9 9 1 0 0 0
media  15 1  -1   2
media   0 1  -2   3
boundary 3

end geometry

read array
ara=1 typ=triangular nux=17 nuy=17 nuz=1 gbl=1
fill
88 88 88 88 88 88 88 88 88 88 88 88 88 88 88 88 88
  88 88 88 88 88 88 88 88 88 88 77 77 77 88 88 88 88
    88 88 88 88 88 88 88 88 66 66 66 66 66 66 66 88 88
      88 88 88 88 88 88 77 77 77 77 77 77 77 77 77 77 88
        88 88 88 88 88 66 66 66 66 66 66 66 66 66 66 66 88
          88 88 88 88 77 77 77 77 77 77 77 77 77 77 77 88
            88 88 88 66 66 66 66 66 66 66 66 66 66 66 66 88
              88 88 88 77 77 77 77 77 88 88 77 77 77 77 77 88 88
                88 88 66 66 66 66 66 88 66 88 66 66 66 66 66 88 88
                  88 88 77 77 77 77 77 88 88 77 77 77 77 77 88 88 88
                    88 66 66 66 66 66 66 66 66 66 66 66 66 66 66 88 88 88
                      88 77 77 77 77 77 77 77 77 77 77 77 77 88 88 88 88
                        88 66 66 66 66 66 88 88 66 66 66 66 88 88 88 88 88
                          88 77 77 77 77 77 77 77 77 77 77 88 88 88 88 88 88
                            88 88 66 66 66 66 66 66 66 88 88 88 88 88 88 88 88
                              88 88 88 77 77 77 77 88 88 88 88 88 88 88 88 88
                              88 88 88 88 88 88 88 88 88 88 88 88 88 88 88 88
end fill
```

Table 6-29 Sample Input Deck for Traveller XL Single Package – Normal Condition of Transport (cont.)

```
ara=2 typ=square nux=17 nuy=17 nuz=1
fill 39*22 23 2*22 23 2*22 23 8*22 23 9*22 23 22*22 23 2*22 23 2*22 23
 2*22 23 2*22 23 38*22 23 2*22 23 2*22 23 2*22 23 2*22 23 38*22 23
 2*22 23 2*22 23 2*22 23 2*22 23 22*22 23 9*22 23 8*22 23 2*22 23 2*22
 23 39*22
end fill
ara=3 typ=square nux=17 nuy=17 nuz=1
fill 39*32 33 2*32 33 2*32 33 8*32 33 9*32 33 22*32 33 2*32 33 2*32 33
 2*32 33 2*32 33 38*32 33 2*32 33 2*32 33 2*32 33 2*32 33 38*32 33
 2*32 33 2*32 33 2*32 33 2*32 33 22*32 33 9*32 33 8*32 33 2*32 33 2*32
 33 39*32
end fill

end array

read bnds
+xb=vacuum
-xb=vacuum
+yb=vacuum
-yb=vacuum
+zb=vacuum
-zb=vacuum
end bnds

end data
end
```

This page intentionally left blank.

6.10.7 Package Array Evaluation Calculations

Results for the package array calculations are presented below. Table 6-30 shows the results for normal conditions for the Traveller XL. Tables 6-31 and 6-32 show results for hypothetical accident conditions for the Traveller STD and Traveller XL, respectively. Table 6-34 shows a sample input deck for the Traveller XL calculations.

Table 6-30 Results for Traveller XL – Normal Conditions of Transport – Package Array

Run #	ks	σks	ks+2×σks
XL-NOR-ARRAY	0.2709	0.0006	0.2721

Table 6-31 Results for Traveller STD – Hypothetical Accident Conditions – Package Array

Run #	Length of Exp. (cm)	ks	σks	ks+2×σks
STD-HAC-ARRAY-100	100.0000	0.8954	0.0009	0.8972

Table 6-32 Package Array Calculations for Traveller XL – HAC

Run #	Length of Exp.(cm)	ks	σks	ks+2×σks
XL-HAC-ARRAY-000	0	0.8466	0.0007	0.8480
XL-HAC-ARRAY-025	25	0.8537	0.0008	0.8553
XL-HAC-ARRAY-050	50	0.8939	0.0009	0.8957
XL-HAC-ARRAY-075	75	0.9223	0.0011	0.9245
XL-HAC-ARRAY-100	100	0.9377	0.0008	0.9393
XL-HAC-ARRAY-200	200	0.9623	0. 0009	0.9641
XL-HAC-ARRAY-300	300	0.9694	0. 0010	0.9714
XL-HAC-ARRAY-426	426	0.9742	8.0000e-4	0.9758

Table 6-33 has been deleted.

Pages 6-87 – 6-91 intentionally left blank.

Table 6-34 Input Deck for Traveller XL Package Array – HAC

```
PA_HAC_BORAL_5_5_100_0.19630.out
=csas26     parm=size=300000
TRAVELLER XL,17WOFA,ENV=24.384      cm,L=100      cm,B10=0.018   g/cm2
44groupndf5  latticecell
 uo2 1 1 293 92235 5 92238 95 end
 h2o 2 1 293 end
 zirc4 3 1 293 end
 h2o 4 1 293 end
 h2o 5 1 293 end
 arbmfoam 0.1602e-20  4  0  0  0 6012 70 1001 10 8016 16 7014 4  6 1 293
 end
 al 7 1 293 end
 ss304 8 1 293 end
 polyethylene 9 DEN=0.828 1.0 293 end
 arbmfoam 0.1602e-20  4  0  0  0 6012 70 1001 10 8016 16 7014 4 11 1 293
 end
 b-10 12 0 0.0047781    end
 b-11 12 0 0.019398     end
 c   12 0 0.0060439    end
 al  12 0 0.043223     end
 arbmrubber 1.59e-20  7  0  0  0 8016 46.94 13000 19.92 14000 17.54 6012
 10.79 1001 4.73 11000 0.06 26000 0.02  14 1 293 end
 h2o 15 1 293 end
 uo2 16 1 293 92235 5 92238 95 end
 h2o 17 1 293 end
 zirc4 18 1 293 end
 h2o 19 1 293 end
end comp
squarepitch 1.4669       0.78435      16 19 0.9144       18 0.8001       17 end
more data
res=1  cylinder 0.39218      dan(1)=0.22632       end

read parameter
gen=450
npg=2500
nsk=50
wrs=1
tme=240
end parameter

read geometry
unit 10
com='individual package'
cuboid 1    16.904       -15.634       16.904       -15.634       533.1330 0
rotate  a1=45 a2=0 a3=0 origin x=0  y=-1.460 z=0
cuboid 2     21.5900   -21.5900     1.5720    -1.0310   533.1330     0
cuboid 3     20.0790   -20.0790    20.0790   -20.0790   533.1330     0
rotate  a1=45 a2=0 a3=0 origin x=0  y=-1.460 z=0
cuboid 4     20.3450   -20.3450    20.3450   -20.3450   533.3990    -0.2660
rotate  a1=45 a2=0 a3=0 origin x=0  y=-1.460 z=0
cuboid 5     21.5900   -21.590     23.1498   -23.1498   533.1330     0
```

Table 6-34 Input Deck for Traveller XL Package Array – HAC (cont.)

```
PA_HAC_BORAL_5_5_100_0.19630.out
cuboid 6    21.8560   -21.8560    23.4158   -23.4158   533.3990    -0.2660
cuboid 7    20.3840   -20.3840    20.3840   -20.3840   553.8922   -19.8448
rotate  a1=45 a2=0 a3=0 origin x=0  y=-1.460 z=0
cuboid 8    21.8950   -21.895     23.4548   -23.4548   553.8922   -19.8448
cylinder  9    25.1050    533.4380    -0.2660
cylinder 10    25.1050    553.9312   -19.8448
cylinder 11    31.4840    533.4380    -0.2660
cylinder 12    31.4840    553.9312   -19.8448
cylinder 13    31.4840    533.4380   -19.8448
cylinder 14    31.7500    554.1972   -20.1100
plane 15  zpl=1  con= -10.0000
cylinder 16 7.62   0 -4.5
 rotate  a1=45 a2=90 a3=0 origin x=18.7310 y=-11.1270 z=494.4364
cylinder 17 3.962  0 -7.60
 rotate  a1=45 a2=90 a3=0 origin x=18.7310 y=-11.1270 z=494.4364
cylinder 18 7.62   0 -4.5
 rotate  a1=-45 a2=90 a3=0 origin x=-18.7310 y=-11.1270 z=494.4364
cylinder 19 3.962  0 -7.60
 rotate  a1=-45 a2=90 a3=0 origin x=-18.7310 y=-11.1270 z=494.4364
cylinder 20 7.62   0 -4.5
 rotate  a1=45 a2=90 a3=0 origin x=18.7310 y=-11.1270 z=448.7164
cylinder 21 3.962  0 -7.60
 rotate  a1=45 a2=90 a3=0 origin x=18.7310 y=-11.1270 z=448.7164
cylinder 22 7.62   0 -4.5
 rotate  a1=-45 a2=90 a3=0 origin x=-18.7310 y=-11.1270 z=448.7164
cylinder 23 3.962  0 -7.60
 rotate  a1=-45 a2=90 a3=0 origin x=-18.7310 y=-11.1270 z=448.7164
cylinder 24 7.62   0 -4.5
 rotate  a1=45 a2=90 a3=0 origin x=18.7310 y=-11.1270 z=402.9964
cylinder 25 3.962  0 -7.60
 rotate  a1=45 a2=90 a3=0 origin x=18.7310 y=-11.1270 z=402.9964
cylinder 26 7.62   0 -4.5
 rotate  a1=-45 a2=90 a3=0 origin x=-18.7310 y=-11.1270 z=402.9964
cylinder 27 3.962  0 -7.60
 rotate  a1=-45 a2=90 a3=0 origin x=-18.7310 y=-11.1270 z=402.9964
cylinder 28 7.62   0 -4.5
 rotate  a1=45 a2=90 a3=0 origin x=18.7310 y=-11.1270 z=357.2764
cylinder 29 3.962  0 -7.60
 rotate  a1=45 a2=90 a3=0 origin x=18.7310 y=-11.1270 z=357.2764
cylinder 30 7.62   0 -4.5
 rotate  a1=-45 a2=90 a3=0 origin x=-18.7310 y=-11.1270 z=357.2764
cylinder 31 3.962  0 -7.60
 rotate  a1=-45 a2=90 a3=0 origin x=-18.7310 y=-11.1270 z=357.2764
cylinder 54 7.62   0 -4.5
 rotate  a1=45 a2=90 a3=0 origin x=18.7310 y=-11.1270 z=265.8364
cylinder 55 3.962  0 -7.60
 rotate  a1=45 a2=90 a3=0 origin x=18.7310 y=-11.1270 z=265.8364
cylinder 56 7.62   0 -4.5
 rotate  a1=-45 a2=90 a3=0 origin x=-18.7310 y=-11.1270 z=265.8364
cylinder 57 3.962  0 -7.60
```

Table 6-34 Input Deck for Traveller XL Package Array – HAC (cont.)

```
 PA_HAC_BORAL_5_5_100_0.19630.out
rotate  a1=-45 a2=90 a3=0 origin x=-18.7310 y=-11.1270 z=265.8364
cylinder 32 7.62   0 -4.5
 rotate  a1=45 a2=90 a3=0 origin x=18.7310 y=-11.1270 z=174.3964
cylinder 33 3.962  0 -7.60
 rotate  a1=45 a2=90 a3=0 origin x=18.7310 y=-11.1270 z=174.3964
cylinder 34 7.62   0 -4.5
 rotate  a1=-45 a2=90 a3=0 origin x=-18.7310 y=-11.1270 z=174.3964
cylinder 35 3.962  0 -7.60
 rotate  a1=-45 a2=90 a3=0 origin x=-18.7310 y=-11.1270 z=174.3964
cylinder 36 7.62   0 -4.5
 rotate  a1=45 a2=90 a3=0 origin x=18.7310 y=-11.1270 z=128.6764
cylinder 37 3.962  0 -7.60
 rotate  a1=45 a2=90 a3=0 origin x=18.7310 y=-11.1270 z=128.6764
cylinder 38 7.62   0 -4.5
 rotate  a1=-45 a2=90 a3=0 origin x=-18.7310 y=-11.1270 z=128.6764
cylinder 39 3.962  0 -7.60
 rotate  a1=-45 a2=90 a3=0 origin x=-18.7310 y=-11.1270 z=128.6764
cylinder 40 7.62   0 -4.5
 rotate  a1=45 a2=90 a3=0 origin x=18.7310 y=-11.1270 z=82.9564
cylinder 41 3.962  0 -7.60
 rotate  a1=45 a2=90 a3=0 origin x=18.7310 y=-11.1270 z=82.9564
cylinder 42 7.62   0 -4.5
 rotate  a1=-45 a2=90 a3=0 origin x=-18.7310 y=-11.1270 z=82.9564
cylinder 43 3.962  0 -7.60
 rotate  a1=-45 a2=90 a3=0 origin x=-18.7310 y=-11.1270 z=82.9564
cylinder 44 7.62   0 -4.5
 rotate  a1=45 a2=90 a3=0 origin x=18.7310 y=-11.1270 z=37.2364
cylinder 45 3.962  0 -7.60
 rotate  a1=45 a2=90 a3=0 origin x=18.7310 y=-11.1270 z=37.2364
cylinder 46 7.62   0 -4.5
 rotate  a1=-45 a2=90 a3=0 origin x=-18.7310 y=-11.1270 z=37.2364
cylinder 47 3.962  0 -7.60
rotate  a1=-45 a2=90 a3=0 origin x=-18.7310 y=-11.1270 z=37.2364
hole 11 rotate  a1=45 a2=0 a3=0  origin  x=0 y=-17.700 z=5.240
cuboid 48    18.174    20.079   10.4238  -9.5152    533.3990    -0.2660
rotate  a1=-45 a2=0 a3=0 origin x=0  y=-1.460 z=0
cuboid 49    13.6554  -10.4238  16.904    20.079    533.3990    -0.2660
rotate  a1=45 a2=0 a3=0 origin x=0  y=-1.460 z=0
cuboid 50    16.904    20.079   13.6554  -10.4238   533.3990    -0.2660
rotate  a1=45 a2=0 a3=0 origin x=0  y=-1.460 z=0
cuboid 51     9.5152  -10.4238 -18.174   -20.079    533.3990    -0.2660
rotate  a1=-45 a2=0 a3=0 origin x=0  y=-1.460 z=0
cuboid 52    15.634    18.174   12.0238 -11.9197    533.3990    -0.2660
rotate  a1=-45 a2=0 a3=0 origin x=0  y=-1.460 z=0
cuboid 53    11.9197  -12.0238 -15.634   -18.174    533.3990    -0.2660
rotate  a1=-45 a2=0 a3=0 origin x=0  y=-1.460 z=0
media  0 1   1   3  5 -17 -19 -21 -23 -29 -31 -55 -57 -33 -35
-41 -43 -45 -47
media  0 1  -1   3  5 -48 -49 -50 -51 -52 -53
media  9 1   3  -16  -17 -20 -21 -28 -29 -54 -55 -32 -33
```

Table 6-34 Input Deck for Traveller XL Package Array – HAC (cont.)

```
PA_HAC_BORAL_5_5_100_0.19630.out
-40 -41 -44 -45 48
media  9 1   3  -18  -19 -22 -23 -30 -31 -56 -57 -34 -35
-42 -43 -46 -47 51
media  9 1   3  -18  -22  -30  -56  -34  -42  -46  53
media  9 1   3  -16  -20  -28  -54  -32  -40  -44  52
media  9 1   3  49
media  9 1   3  50
media  8 1  -3   4   6
media  8 1   3  -5   6
media  6 1  -4   9
media  6 1   4  -6   9
media  6 1  -9  11
media  6 1  -7  10 -13
media  6 1   7  -8  10 -13  12
media  6 1 -10 -13  12
media 11 1 -11  13
media 11 1   7   8 -13  12
media  8 1 -12  14
media  0 1 16  -17 3 48
media  0 1 18  -19 3 51
media  0 1 20  -21 3 48
media  0 1 22  -23 3 51
media  0 1 28  -29 3 48
media  0 1 30  -31 3 51
media  0 1 54  -55 3 48
media  0 1 56  -57 3 51
media  0 1 32  -33 3 48
media  0 1 34  -35 3 51
media  0 1 40  -41 3 48
media  0 1 42  -43 3 51
media  0 1 44  -45 3 48
media  0 1 46  -47 3 51
media  0 1 16  -17 3 52
media  0 1 18  -19 3 53
media  0 1 20  -21 3 52
media  0 1 22  -23 3 53
media  0 1 28  -29 3 52
media  0 1 30  -31 3 53
media  0 1 54  -55 3 52
media  0 1 56  -57 3 53
media  0 1 32  -33 3 52
media  0 1 34  -35 3 53
media  0 1 40  -41 3 52
media  0 1 42  -43 3 53
media  0 1 44  -45 3 52
media  0 1 46  -47 3 53
media 14 1 17  3
media 14 1 19  3
media 14 1 21  3
media 14 1 23  3
```

Table 6-34 Input Deck for Traveller XL Package Array – HAC (cont.)

```
 PA_HAC_BORAL_5_5_100_0.19630.out
media 14 1 29  3
media 14 1 31  3
media 14 1 55  3
media 14 1 57  3
media 14 1 33  3
media 14 1 35  3
media 14 1 41  3
media 14 1 43  3
media 14 1 45  3
media 14 1 47  3
boundary 14

unit 11
com='fuel assembly confinement system'
cuboid 1    24.384       0 24.384       0 520.7000 2.5400
cuboid 2    25.337       -0.9525 25.337        -0.9525
 523.2400  0.0000
cuboid 3    19.812       4.572        24.429       -0.04545
513.0800  3.81
cuboid 4    19.812       4.572        24.656       -0.27205
 513.0800  3.81
cuboid 5    19.812       4.572        24.702       -0.3175
 513.0800  3.81
cuboid 6    24.429       -0.04545      19.812       4.572
  513.0800  3.81
cuboid 7    24.656       -0.27205      19.812       4.572
 513.0800  3.81
cuboid 8    24.702       -0.3175       19.812       4.572
 513.0800  3.81
hole 20  origin  x=0  y=0  z=16.56  rotate  a1=0 a2=0 a3=0
media  0 1   1
media  7 1  -1   2  -5  -8
media  7 1  -1   3
media 12 1  -3   4
media  7 1  -4   5
media  7 1  -1   6
media 12 1  -6   7
media  7 1  -7   8
boundary 2

unit 20
com='fuel assembly'
cuboid 1 21.072       0 21.072       0   0        -14.0208
cuboid 2 24.384       0 24.384       0 504.1392   -14.0208
hole 31 origin  x=0       y=0       z=0.0001   rotate  a1=0  a2=0 a3=0
hole 21 origin  x=0       y=0       z=100.0001 rotate  a1=0  a2=0 a3=0
hole 40 origin  x=0       y=0       z=426.7201 rotate  a1=0  a2=0 a3=0
media  15 1  1
media   0 1 -1   2
boundary 2
```

Table 6-34 Input Deck for Traveller XL Package Array – HAC (cont.)

```
 PA_HAC_BORAL_5_5_100_0.19630.out
unit 21
com='fuel rods - nominal pitch'
cuboid 1  21.072       0 21.072       0 326.72       0.0000
array 2 1 place 1 1 1 0.4572       0.4572       0
boundary 1

unit 22
com='solid fuel rod - nominal pitch'
cylinder 1  0.39218       426.72          0
cylinder 2  0.40005      426.72          0
cylinder 3  0.4572       426.72          0
cuboid 4  4P0.62992       426.72          0
media 1 1  1
media 2 1  2 -1
media 3 1  3 -2 -1
media 4 1  4 -3 -2 -1
boundary 4

unit 23
com='thimble tube - nominal pitch'
cylinder 1  0.56134       426.72          0
cylinder 2  0.60198       426.72          0
cuboid 3    4P0.62992      426.72          0
media 4 1 1
media 3 1 2 -1
media 4 1 3 -2 -1
boundary 3

unit 31
com='fuel rods - expanded pitch'
cuboid 1  24.384       0 24.384       0 100          0
array 3 1 place 1 1 1 0.4572       0.4572       0
boundary 1

unit 32
com='solid fuel rod - expanded pitch'
cylinder 1  0.39218       426.72          0
cylinder 2  0.40005      426.72          0
cylinder 3  0.4572       426.72          0
cuboid 4  4P0.73342       426.72          0
media 16  1 1
media 17  1 2 -1
media 18  1 3 -2 -1
media 19  1 4 -3 -2 -1
boundary 4

unit 33
com='thimble tube - expanded pitch'
cylinder 1  0.56134      426.72          0
cylinder 2  0.60198      426.72          0
```

Table 6-34 Input Deck for Traveller XL Package Array – HAC (cont.)

```
 PA_HAC_BORAL_5_5_100_0.19630.out
cuboid 3  4P0.73342       426.72          0
media 19 1 1
media 18 1 2 -1
media 19 1 3 -2 -1
boundary 3

unit 40
com='top nozzle assembly'
cuboid 1     21.072       0 21.072       0       21.2090     0.0000
cuboid 2     21.072       0 21.072       0      41.8846     0.0000
cuboid 3     21.072       0 21.072       0       52.8193     0.0000
cuboid 4     21.072       0 21.072       0       77.4192     0.0000
cuboid 5     24.384       0 24.384       0       77.4192     0.0008
media  15 1   1
media  15 1  -1   2
media  15 1  -2   3
media  15 1  -3   4
media  15 1  -4   5
boundary 5

unit 66
com='individual package 0-deg rotation'
hexprism 1  31.75    554.1972  -20.1498
hole 10  origin  x=0 y=0  z=0  rotate  a1=0 a2=0 a3=0
media   0 1   1
boundary 1

unit 77
com='individual package 180-deg rotation'
hexprism 1  31.75    554.1972  -20.1498
hole 10  origin  x=0 y=0  z=0  rotate  a1=0 a2=0 a3=180
media   0 1   1
boundary 1

unit 88
com='dummy cell'
hexprism 1  31.75    554.1972  -20.1498
media  15 1   1
boundary 1

global
unit 99
com='package array'
cylinder 1  432.2355   554.1972  -20.1498
cylinder 2  452.2355   574.1972  -40.1498
cuboid 3  452.2355  -452.2355  452.2355  -452.2355   574.1972  -40.1498
array 1 1  place 9 9 1 0 0 0
media  15 1  -1   2
media   0 1  -2   3
boundary 3

end geometry
```

Table 6-34 Input Deck for Traveller XL Package Array – HAC (cont.)

```
 PA_HAC_BORAL_5_5_100_0.19630.out
read array
ara=1 typ=triangular nux=17 nuy=17 nuz=1 gbl=1
fill
88 88 88 88 88 88 88 88 88 88 88 88 88 88 88 88 88
  88 88 88 88 88 88 88 88 88 88 77 77 77 88 88 88 88
    88 88 88 88 88 88 88 88 66 66 66 66 66 66 66 88 88
      88 88 88 88 88 88 77 77 77 77 77 77 77 77 77 77 88
        88 88 88 88 88 66 66 66 66 66 66 66 66 66 66 66 88
          88 88 88 77 77 77 77 77 77 77 77 77 77 77 77 88
            88 88 88 66 66 66 66 66 66 66 66 66 66 66 66 88
              88 88 88 77 77 77 77 77 77 77 77 77 77 77 88 88
                88 88 66 66 66 66 66 66 66 66 66 66 66 66 88 88
                  88 88 77 77 77 77 77 77 77 77 77 77 77 88 88 88
                    88 66 66 66 66 66 66 66 66 66 66 66 66 88 88 88
                      88 77 77 77 77 77 77 77 77 77 77 77 88 88 88 88
                        88 66 66 66 66 66 66 66 66 66 66 66 88 88 88 88 88
                          88 77 77 77 77 77 77 77 77 77 77 88 88 88 88 88
                            88 88 66 66 66 66 66 66 66 88 88 88 88 88 88 88
                              88 88 88 77 77 77 77 88 88 88 88 88 88 88 88 88
                              88 88 88 88 88 88 88 88 88 88 88 88 88 88 88 88
end fill

ara=2 typ=square nux=17 nuy=17 nuz=1
fill 39*22 23 2*22 23 2*22 23 8*22 23 9*22 23 22*22 23 2*22 23 2*22 23
 2*22 23 2*22 23 38*22 23 2*22 23 2*22 23 2*22 23 2*22 23 38*22 23
 2*22 23 2*22 23 2*22 23 2*22 23 22*22 23 9*22 23 8*22 23 2*22 23 2*22
 23 39*22
end fill
ara=3 typ=square nux=17 nuy=17 nuz=1
fill 39*32 33 2*32 33 2*32 33 8*32 33 9*32 33 22*32 33 2*32 33 2*32 33
 2*32 33 2*32 33 38*32 33 2*32 33 2*32 33 2*32 33 2*32 33 38*32 33
 2*32 33 2*32 33 2*32 33 2*32 33 22*32 33 9*32 33 8*32 33 2*32 33 2*32
 33 39*32
end fill

end array
read bnds
+xb=vacuum
-xb=vacuum
+yb=vacuum
-yb=vacuum
+zb=vacuum
-zb=vacuum
end bnds

end data
end
```

Table 6-35 has been deleted.

Pages 6-99 – 6-103 intentionally left blank

6.10.8 Rod Container Calculations

6.10.8.1 Introduction

The calculations involved two separate analyses, one for the Rod Pipe, and another for the Rod Box. The approach used was the same for both. First, each container was modeled using the Traveller XL outerpack model for the hypothetical accident conditions for individual package and package array cases. Second, the analyses consisted of modeling pellet stacks inside the container and varying the pitch to determine the optimum pellet pitch-to-diameter ratio. The following pellet diameters were used with corresponding pitches in order to find the optimum values. Note that not all pitch/diameter runs were completed. However, sufficient data were obtained to define curves.

Pitch Value (cm)	Pellet Diameters (cm)
Close Packed (pitch = diameter)	0.25/ 0.30/0.35/0.40/0.45/0.50/0.60/0.80/0.90/1.00
1.2	0.05/0.10/0.15/0.20/0.25/0.30/0.35/0.40/0.45/0.50
1.5	0.05/0.10/0.15/0.20/0.25/0.30/0.35/0.40/0.45/0.50
1.8	0.05/0.10/0.15/0.20/0.25/0.30/0.35/0.40/0.45/0.50
2.0	0.05/0.10/0.15/0.20/0.25/0.30/0.35/0.40/0.45/0.50
2.5	0.25/ 0.30/0.35/0.40/0.45/0.50/0.60/0.80/0.90/1.00
3.0	0.25/ 0.30/0.35/0.40/0.45/0.50/0.60/0.80/0.90/1.00
4.0	0.25/ 0.30/0.35/0.40/0.45/0.50/0.60/0.80/0.90/1.00

After plotting curves to find approximate maximum k_{eff} values for the pitch/diameter combinations, two array cases were selected, one each for the rod box and rod pipe. These were analyzed to determine the effect on k_{eff} of varying the interspersed moderation water density. These results are shown in Figure 6-39.

6.10.8.2 Models

The fuel rod model is described in Section 6.3.1.1.2. The container models, which consist of a simple cylinder and cube, are described in Section 6.3.1.1.3 and Section 6.3.1.1.4. The box and pipe materials were not included in the models. The dimensions equate to the outside dimensions of the particular container. Figure 6-40 shows the rod box and rod pipe models inside the Traveller XL.

6.10.8.3 Individual Package Configuration

The analysis assumes the most conservative flooding configuration for the individual package, which is the fully flooded condition. This is discussed in Section 6.7.1.

6.10.8.4 Package Array Configuration

The analysis uses the same flooding configuration for the package array case under hypothetical accident conditions, namely the XL-HAC-ARRAY-100 model. This is discussed in Section 6.7.1.

6.10.8.5 Results

The results indicate that both rod container types are geometry limiting with respect to criticality. Calculated k_{eff} results were found to be less than 0.75 for all cases. The rod pipe appears to be the bounding container, and that the individual case results were higher than the infinite planar array cases that were modeled. Note that the infinite planar array cases assumed full water density inside the rod container and void in all interstitial spaces. That is, referring to Figure 6-4 (Floodable Void Spaces), regions 3 through 6 were modeled as a void. While this flooding configuration is most conservative for a fuel assembly, an interspersed moderation density sensitivity study demonstrated that full density water in all interstitial spaces results in the highest k_{eff}. The infinite planar array case with full density interstitial moderation is essentially equivalent to an individual package in isolation. Therefore, the highest k_{eff} for an package array for rod containers will be equal to the highest k_{eff} for an individual package in isolation.

Plots are provided that to show k_{eff} versus pellet diameter for the pitch values, for each of the four groups. These are presented as Figures 6-35 (Rod Pipe Individual Package), 6-36 (Rod Pipe Package Array), 6-37 (Rod Box Individual Package), and 6-38 (Rod Box Package Array).

Results are given in Tables 6-36 (Rod Pipe Individual Package), 6-36A (Rod Pipe Package Array), 6-36B (Rod Box Individual), and 6-36C (Rod Box Package Array). The highest k_{eff} values from the four tables are shown below.

Table	Run #	ks	sigma	Ks+2s	Pell. Diam. (inch)	Pell. Diam. (cm)	Rod Pitch (inch)	Rod Pitch (cm)	p/d
6-36	P-IP-15-6	0.7425	0.0015	0.7455	0.25	0.762	0.591	1.50	1.97
6-36A	P-ARR-15-6	0.6622	0.0016	0.6654	0.30	0.762	0.591	1.50	1.97
6-36B	B-IP-15-6	0.7008	0.0015	0.7038	0.30	0.762	0.591	1.50	1.97
6-36C	B-ARR-15-6	0.5512	0.0014	0.5540	0.30	0.762	0.591	1.50	1.97

The interspersed moderation density study was performed using the P-ARR-15-6 and B-ARR-15-6 array cases. Results are shown in Table 6-36D. It can be seen that there is good agreement between the zero density interspersed case (B-INTER-000, P-INTER-000) and the package array case (B-ARR-15-6, P-ARR-15-6), and between the full density interspersed case (B-INTER-100, P-INTER-100) and the individual package case (B-IP-15-6, P-IP-15-6). The data are plotted in Figure 6-39. This analysis demonstrates that the full density water interspersed case is the optimum infinite planar array case. A final calculation was made to show that the infinite 3-D array case compares well with the infinite planar array case. The 3D array case was modeled by replacing the water boundary condition on the +/- z axis with a mirror boundary condition. These results are also shown in Table 6-36D.

Sample input decks for Rod Box Individual Package, Rod Pipe Package Array, and Rod Pipe Interspersed Moderation are provided in Tables 6-36E, 6-36F, and 6-36G, respectively.

This page intentionally left blank.

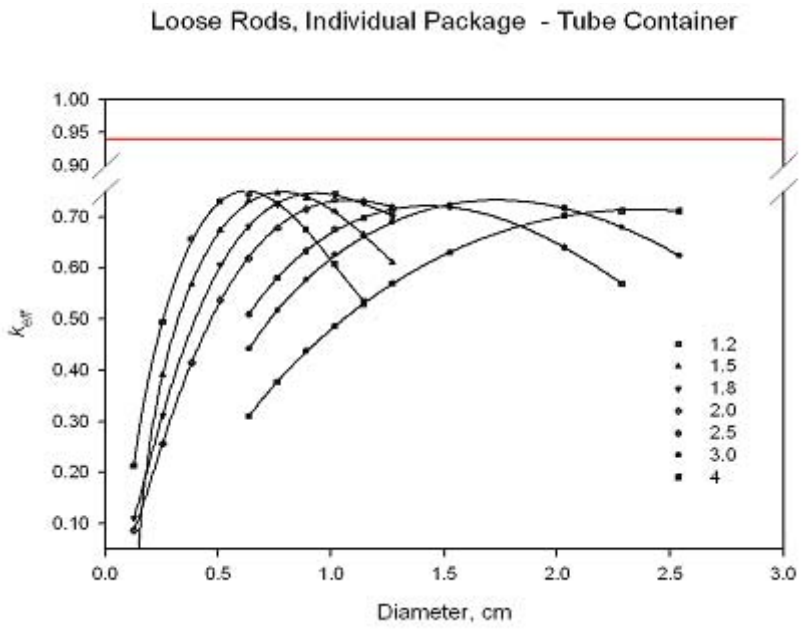

Figure 6-35 Rod Pipe – k_{eff} vs. Pellet Diameter for Individual Package

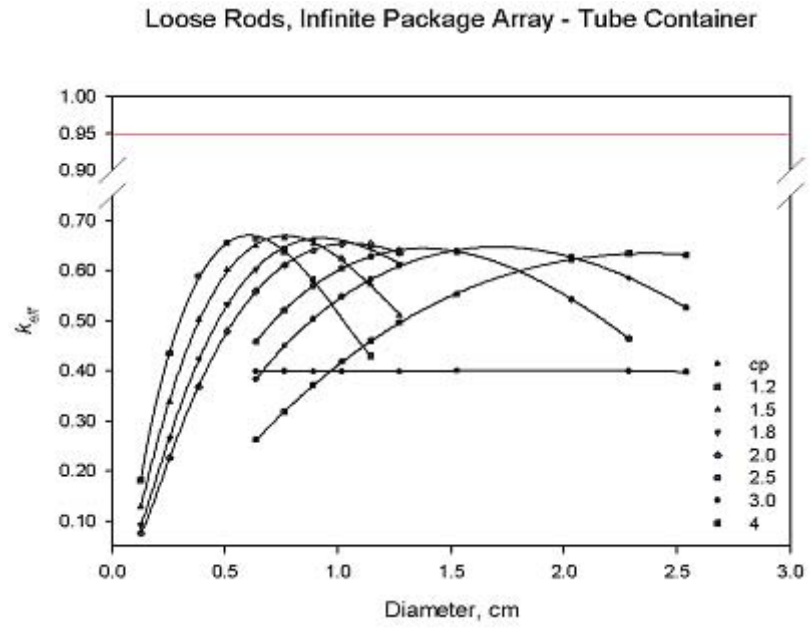

Figure 6-36 Rod Pipe – k_{eff} vs. Pellet Diameter for Infinite Array

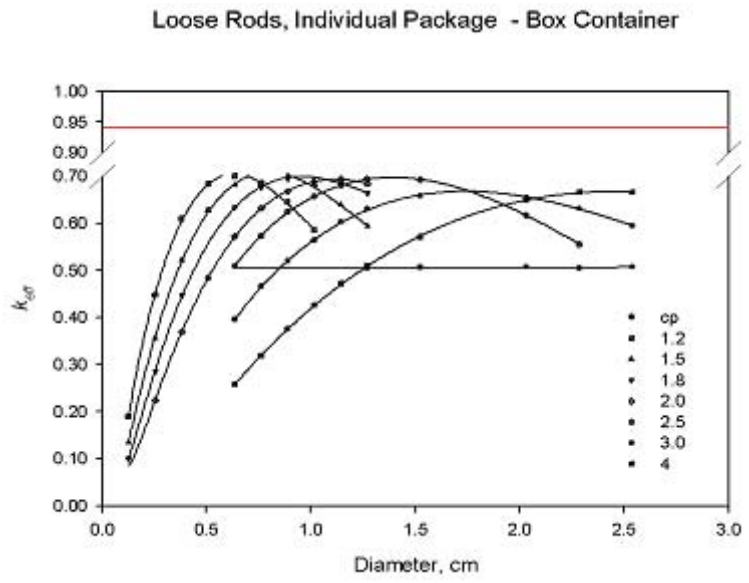

Figure 6-37 Rod Box – k_{eff} vs. Pellet Diameter for Individual Package

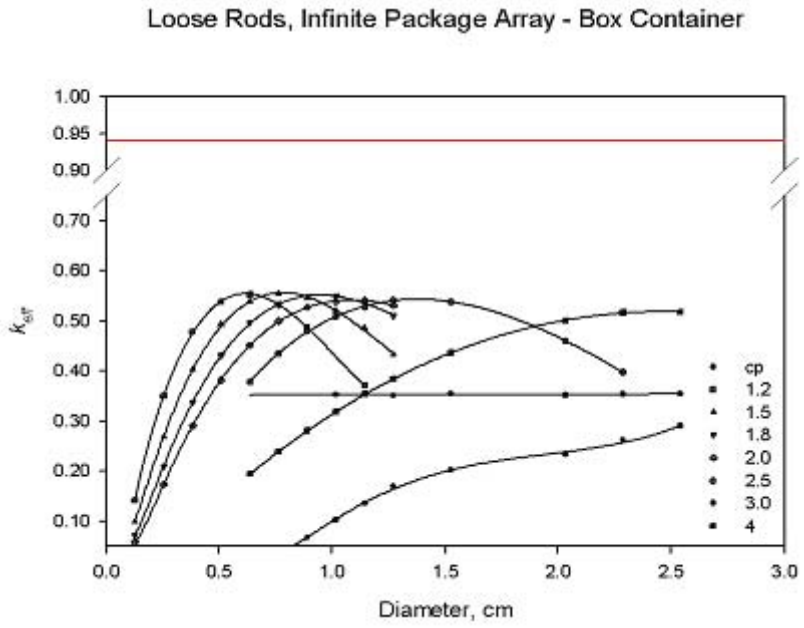

Figure 6-38 Rod Box – k_{eff} vs. Pellet Diameter for Package Array

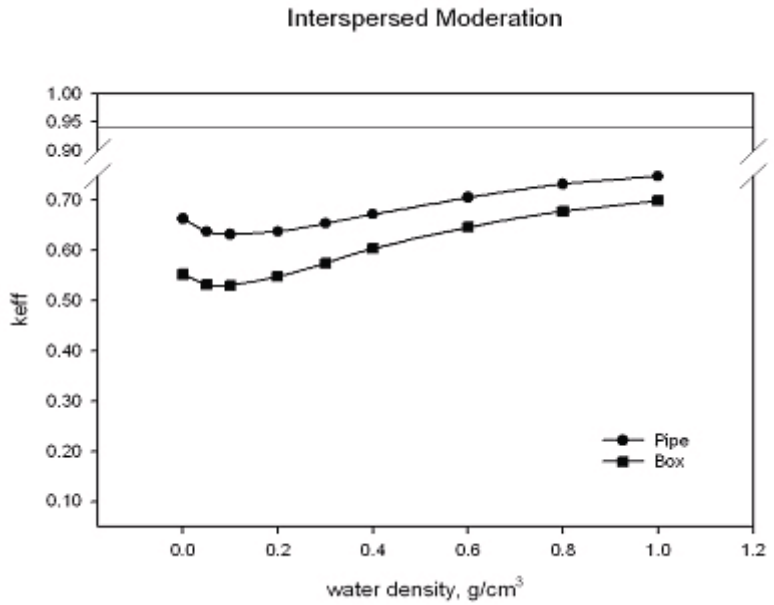

Figure 6-39 Interspersed Moderation Curves for Rod Box and Rod Pipe

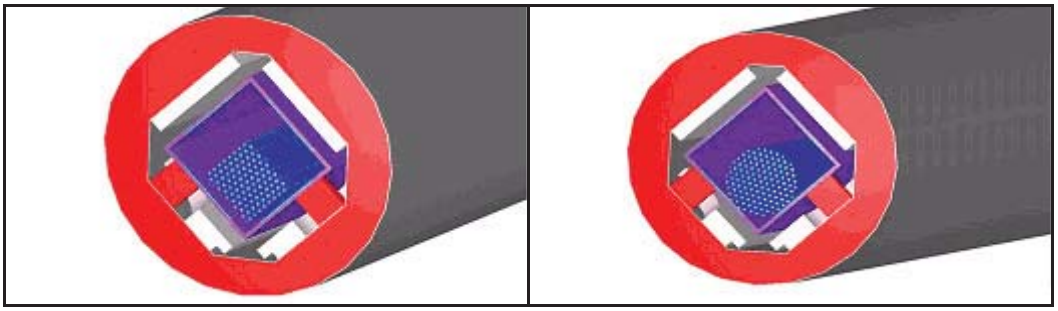

Figure 6-40 Rod Box and Rod Pipe in Traveller XL

Table 6-36 Results for Rod Pipe Individual Package HAC

Run #	ks	sigma	Ks+2s	No. Fuel Rods	Pell. Diam. (inch)	Pell. Diam. (cm)	Rod Pitch (inch)	Rod Pitch (cm)	p/d
1.2 cm Pitch									
P-IP-12-1	0.2118	0.0008	0.2134	187	0.05	0.127	0.472	1.20	9.45
P-IP-12-2	0.4917	0.0012	0.4941	187	0.10	0.254	0.472	1.20	4.72
P-IP-12-3	0.6545	0.0013	0.6571	187	0.15	0.381	0.472	1.20	3.15
P-IP-12-4	0.7281	0.0014	0.7309	187	0.20	0.508	0.472	1.20	2.36
P-IP-12-5	0.7416	0.0013	0.7442	187	0.25	0.635	0.472	1.20	1.89
P-IP-12-6	0.7233	0.0014	0.7261	187	0.30	0.762	0.472	1.20	1.57
P-IP-12-7	0.6731	0.0014	0.6759	187	0.35	0.889	0.472	1.20	1.35
P-IP-12-8	0.6049	0.0011	0.6071	187	0.40	1.016	0.472	1.20	1.18
P-IP-12-9	0.5329	0.0011	0.6071	187	0.45	1.143	0.472	1.20	1.05
P-IP-12-10				187	0.50	1.270	0.472	1.20	0.94
1.5 cm Pitch									
P-IP-15-2	0.3893	0.0011	0.3915	121	0.05	0.127	0.591	1.50	11.81
P-IP-15-3	0.5654	0.0013	0.5680	121	0.10	0.254	0.591	1.50	5.91
P-IP-15-4	0.6706	0.0015	0.6736	121	0.15	0.381	0.591	1.50	3.94
P-IP-15-5	0.7285	0.0015	0.7315	121	0.20	0.508	0.591	1.50	2.95
P-IP-15-6	0.7425	0.0015	0.7455	121	0.25	0.635	0.591	1.50	2.36
P-IP-15-7	0.7339	0.0014	0.7367	121	0.30	0.762	0.591	1.50	1.97
P-IP-15-8	0.7073	0.0015	0.7103	121	0.35	0.889	0.591	1.50	1.69
P-IP-15-9	0.6639	0.0013	0.6665	121	0.40	1.016	0.591	1.50	1.48
P-IP-15-10	0.6081	0.0014	0.6109	121	0.45	1.143	0.591	1.50	1.31
1.8 cm Pitch									
P-IP-18-1	0.1097	0.0005	0.1107	85	0.05	0.127	0.709	1.80	14.17
P-IP-18-2	0.3104	0.0009	0.3122	85	0.10	0.254	0.709	1.80	7.09
P-IP-18-3				85	0.15	0.381	0.709	1.80	4.72
P-IP-18-4	0.6039	0.0015	0.6069	85	0.20	0.508	0.709	1.80	3.54
P-IP-18-5	0.6776	0.0016	0.6808	85	0.25	0.635	0.709	1.80	2.83
P-IP-18-6	0.7225	0.0013	0.7251	85	0.30	0.762	0.709	1.80	2.36
P-IP-18-7	0.7384	0.0015	0.7414	85	0.35	0.889	0.709	1.80	2.02
P-IP-18-8	0.7425	0.0015	0.7455	85	0.40	1.016	0.709	1.80	1.77
P-IP-18-9	0.7246	0.0015	0.7276	85	0.45	1.143	0.709	1.80	1.57
P-IP-18-10	0.6977	0.0013	0.7003	85	0.50	1.270	0.709	1.80	1.42

Table 6-36 Results for Rod Pipe Individual Package HAC (cont.)

Run #	ks	sigma	Ks+2s	No. Fuel Rods	Pell. Diam. (inch)	Pell. Diam. (cm)	Rod Pitch (inch)	Rod Pitch (cm)	p/d
2.0 cm Pitch									
P-IP-20-1	0.0858	0.0005	0.0868	61	0.05	0.127	0.787	2.00	15.75
P-IP-20-2	0.2548	0.0008	0.2564	61	0.10	0.254	0.787	2.00	7.87
P-IP-20-3	0.4130	0.0010	0.4150	61	0.15	0.381	0.787	2.00	5.25
P-IP-20-4	0.5349	0.0012	0.5373	61	0.20	0.508	0.787	2.00	3.94
P-IP-20-5	0.6165	0.0013	0.6191	61	0.25	0.635	0.787	2.00	3.15
P-IP-20-6	0.6754	0.0015	0.6784	61	0.30	0.762	0.787	2.00	2.62
P-IP-20-7	0.7118	0.0014	0.7146	61	0.35	0.889	0.787	2.00	2.25
P-IP-20-8	0.7310	0.0014	0.7338	61	0.40	1.016	0.787	2.00	1.97
P-IP-20-9	0.7274	0.0015	0.7304	61	0.45	1.143	0.787	2.00	1.75
P-IP-20-10	0.7159	0.0014	0.7187	61	0.50	1.270	0.787	2.00	1.57
2.5 cm Pitch									
P-IP-25-1	0.5069	0.0014	0.5097	37	0.25	0.635	0.984	2.50	3.94
P-IP-25-2	0.5780	0.0013	0.5806	37	0.30	0.762	0.984	2.50	3.28
P-IP-25-3	0.6304	0.0015	0.6334	37	0.35	0.889	0.984	2.50	2.81
P-IP-25-4	0.6730	0.0015	0.6760	37	0.40	1.016	0.984	2.50	2.46
P-IP-25-5	0.6953	0.0014	0.6981	37	0.45	1.143	0.984	2.50	2.19
P-IP-25-6	0.7094	0.0015	0.7124	37	0.50	1.270	0.984	2.50	1.97
P-IP-25-7	0.7169	0.0015	0.7199	37	0.60	1.524	0.984	2.50	1.64
P-IP-25-8	0.6371	0.0014	0.6399	37	0.80	2.032	0.984	2.50	1.23
P-IP-25-9				37	0.90	2.286	0.984	2.50	1.09
P-IP-25-10				37	1.00	2.540	0.984	2.50	0.98
3.0 cm Pitch									
P-IP-30-1				31	0.25	0.635	1.181	3.00	4.72
P-IP-30-2				31	0.30	0.762	1.181	3.00	3.94
P-IP-30-3	0.5740	0.0014	0.5768	31	0.35	0.889	1.181	3.00	3.37
P-IP-30-4	0.6234	0.0013	0.6260	31	0.40	1.016	1.181	3.00	2.95
P-IP-30-5	0.6578	0.0015	0.6608	31	0.45	1.143	1.181	3.00	2.62
P-IP-30-6	0.6873	0.0014	0.6901	31	0.50	1.270	1.181	3.00	2.36
P-IP-30-7	0.7198	0.0014	0.7226	31	0.60	1.524	1.181	3.00	1.97
P-IP-30-8	0.7132	0.0018	0.7168	31	0.80	2.032	1.181	3.00	1.48
P-IP-30-9	0.6765	0.0016	0.6797	31	0.90	2.286	1.181	3.00	1.31
P-IP-30-10	0.6212	0.0013	0.6238	31	1.00	2.540	1.181	3.00	1.18

Table 6-36 Results for Rod Pipe Individual Package HAC (cont.)

Run #	ks	sigma	Ks+2s	No. Fuel Rods	Pell. Diam. (inch)	Pell. Diam. (cm)	Rod Pitch (inch)	Rod Pitch (cm)	p/d
4.0 cm Pitch									
P-IP-40-1	0.3085	0.0010	0.3105	19	0.25	0.635	1.575	4.00	6.30
P-IP-40-2	0.3754	0.0011	0.3776	19	0.30	0.762	1.575	4.00	5.25
P-IP-40-3	0.4356	0.0012	0.4380	19	0.35	0.889	1.575	4.00	4.50
P-IP-40-4	0.4837	0.0013	0.4863	19	0.40	1.016	1.575	4.00	3.94
P-IP-40-5	0.5266	0.0013	0.5292	19	0.45	1.143	1.575	4.00	3.50
P-IP-40-6	0.5676	0.0013	0.5702	19	0.50	1.270	1.575	4.00	3.15
P-IP-40-7	0.6280	0.0013	0.6306	19	0.60	1.524	1.575	4.00	2.62
P-IP-40-8	0.6999	0.0014	0.7027	19	0.80	2.032	1.575	4.00	1.97
P-IP-40-9				19	0.90	2.286	1.575	4.00	1.75
P-IP-40-10	0.7081	0.0015	0.7111	19	1.00	2.540	1.575	4.00	1.57

Table 6-36A Results for Rod Pipe Package Array HAC

Run #	ks	sigma	Ks+2s	No. Fuel Rods	Pell. Diam. (inch)	Pell. Diam. (cm)	Rod Pitch (inch)	Rod Pitch (cm)	p/d
Close Packed									
P-ARR-CP-1	0.3961	0.0009	0.3979		0.25	0.635	0.25	0.64	1.0
P-ARR-CP-2	0.3972	0.0009	0.3990		0.30	0.762	0.30	0.76	1.0
P-ARR-CP-3	0.3962	0.0009	0.3980		0.35	0.889	0.35	0.89	1.0
P-ARR-CP-4	0.3967	0.0008	0.3983	253	0.40	1.016	0.40	1.02	1.0
P-ARR-CP-5				200	0.45	1.143	0.45	1.14	1.0
P-ARR-CP-6	0.3967	0.0009	0.3985	163	0.50	1.270	0.50	1.27	1.0
P-ARR-CP-7	0.3981	0.0008	0.3997	109	0.60	1.524	0.60	1.52	1.0
P-ARR-CP-8				64	0.80	2.032	0.80	2.03	1.0
P-ARR-CP-9	0.3975	0.0008	0.3991	54	0.90	2.286	0.90	2.29	1.0
P-ARR-CP-10	0.3950	0.0009	0.3968	41	1.00	2.540	1.00	2.54	1.0
1.2 cm Pitch									
P-ARR-12-1	0.1800	0.0007	0.1814	187	0.05	0.127	0.472	1.20	9.45
P-ARR-12-2	0.4332	0.0012	0.4356	187	0.10	0.254	0.472	1.20	4.72
P-ARR-12-3	0.5860	0.0013	0.5886	187	0.15	0.381	0.472	1.20	3.15
P-ARR-12-4	0.6532	0.0014	0.6560	187	0.20	0.508	0.472	1.20	2.36
P-ARR-12-5	0.6604	0.0017	0.6638	187	0.25	0.635	0.472	1.20	1.89
P-ARR-12-6	0.6351	0.0014	0.6379	187	0.30	0.762	0.472	1.20	1.57
P-ARR-12-7	0.5792	0.0016	0.5824	187	0.35	0.889	0.472	1.20	1.35
P-ARR-12-8				187	0.40	1.016	0.472	1.20	1.18
P-ARR-12-9	0.4271	0.0010	0.4291		0.45	1.143	0.472	1.20	1.05
P-ARR-12-10					0.50	1.270	0.472	1.20	0.94
1.5 cm Pitch									
P-ARR-15-1	0.1271	0.0006	0.1283	121	0.05	0.127	0.591	1.50	11.81
P-ARR-15-2	0.3364	0.0011	0.3386	121	0.10	0.254	0.591	1.50	5.91
P-ARR-15-3	0.4993	0.0013	0.5019	121	0.15	0.381	0.591	1.50	3.94
P-ARR-15-4	0.5984	0.0014	0.6012	121	0.20	0.508	0.591	1.50	2.95
P-ARR-15-5	0.6463	0.0015	0.6493	121	0.25	0.635	0.591	1.50	2.36
P-ARR-15-6	0.6622	0.0016	0.6654	121	0.30	0.762	0.591	1.50	1.97
P-ARR-15-7	0.6511	0.0016	0.6543	121	0.35	0.889	0.591	1.50	1.69
P-ARR-15-8	0.6218	0.0014	0.6246	121	0.40	1.016	0.591	1.50	1.48
P-ARR-15-9	0.5706	0.0013	0.5732	121	0.45	1.143	0.591	1.50	1.31
P-ARR-15-10	0.5090	0.0011	0.5112	121	0.50	1.270	0.591	1.50	1.18

Table 6-36A Results for Rod Pipe Package Array HAC (cont.)

Run #	ks	sigma	Ks+2s	No. Fuel Rods	Pell. Diam. (inch)	Pell. Diam. (cm)	Rod Pitch (inch)	Rod Pitch (cm)	p/d
1.8 cm Pitch									
P-ARR-18-1	0.0919	0.0005	0.0929	85	0.05	0.127	0.709	1.80	14.17
P-ARR-18-2	0.2645	0.0009	0.2663	85	0.10	0.254	0.709	1.80	7.09
P-ARR-18-3	0.4208	0.0012	0.4232	85	0.15	0.381	0.709	1.80	4.72
P-ARR-18-4	0.5298	0.0013	0.5324	85	0.20	0.508	0.709	1.80	3.54
P-ARR-18-5	0.6002	0.0014	0.6030	85	0.25	0.635	0.709	1.80	2.83
P-ARR-18-6	0.6426	0.0014	0.6454	85	0.30	0.762	0.709	1.80	2.36
P-ARR-18-7	0.6598	0.0015	0.6628	85	0.35	0.889	0.709	1.80	2.02
P-ARR-18-8				85	0.40	1.016	0.709	1.80	1.77
P-ARR-18-9	0.6430	0.0014	0.6458	85	0.45	1.143	0.709	1.80	1.57
P-ARR-18-10	0.6098	0.0010	0.6118	85	0.50	1.270	0.709	1.80	1.42
2.0 cm Pitch									
P-ARR-20-1	0.0751	0.0004	0.0759	61	0.05	0.127	0.787	2.00	15.75
P-ARR-20-2	0.2248	0.0009	0.2266	61	0.10	0.254	0.787	2.00	7.87
P-ARR-20-3	0.3662	0.0010	0.3682	61	0.15	0.381	0.787	2.00	5.25
P-ARR-20-4	0.4765	0.0012	0.4789	61	0.20	0.508	0.787	2.00	3.94
P-ARR-20-5	0.5565	0.0014	0.5593	61	0.25	0.635	0.787	2.00	3.15
P-ARR-20-6	0.6077	0.0016	0.6109	61	0.30	0.762	0.787	2.00	2.62
P-ARR-20-7	0.6371	0.0014	0.6399	61	0.35	0.889	0.787	2.00	2.25
P-ARR-20-8	0.6505	0.0015	0.6535	61	0.40	1.016	0.787	2.00	1.97
P-ARR-20-9	0.6497	0.0017	0.6531	61	0.45	1.143	0.787	2.00	1.75
P-ARR-20-10	0.6317	0.0010	0.6337	61	0.50	1.270	0.787	2.00	1.57
2.5 cm Pitch									
P-ARR-25-1	0.4558	0.0013	0.4584	37	0.25	0.635	0.984	2.50	3.94
P-ARR-25-2	0.5188	0.0013	0.5214	37	0.30	0.762	0.984	2.50	3.28
P-ARR-25-3	0.5679	0.0013	0.5705	37	0.35	0.889	0.984	2.50	2.81
P-ARR-25-4	0.6022	0.0014	0.6050	37	0.40	1.016	0.984	2.50	2.46
P-ARR-25-5	0.6257	0.0013	0.6283	37	0.45	1.143	0.984	2.50	2.19
P-ARR-25-6	0.6373	0.0015	0.6403	37	0.50	1.270	0.984	2.50	1.97
P-ARR-25-7	0.6351	0.0014	0.6379	37	0.60	1.524	0.984	2.50	1.64
P-ARR-25-8	0.5410	0.0012	0.5434	37	0.80	2.032	0.984	2.50	1.23
P-ARR-25-9	0.4619	0.0011	0.4641	37	0.90	2.286	0.984	2.50	1.09
P-ARR-25-10					1.00	2.540	0.984	2.50	0.98

Table 6-36A Results for Rod Pipe Package Array HAC (cont.)

Run #	ks	sigma	Ks+2s	No. Fuel Rods	Pell. Diam. (inch)	Pell. Diam. (cm)	Rod Pitch (inch)	Rod Pitch (cm)	p/d
3.0 cm Pitch									
P-ARR-30-1	0.3806	0.0012	0.3830	31	0.25	0.635	1.181	3.00	4.72
P-ARR-30-2	0.4473	0.0012	0.4497	31	0.30	0.762	1.181	3.00	3.94
P-ARR-30-3	0.5012	0.0012	0.5036	31	0.35	0.889	1.181	3.00	3.37
P-ARR-30-4	0.5451	0.0015	0.5481	31	0.40	1.016	1.181	3.00	2.95
P-ARR-30-5	0.5806	0.0013	0.5832	31	0.45	1.143	1.181	3.00	2.62
P-ARR-30-6	0.6066	0.0013	0.6092	31	0.50	1.270	1.181	3.00	2.36
P-ARR-30-7	0.6367	0.0015	0.6397	31	0.60	1.524	1.181	3.00	1.97
P-ARR-30-8	0.6246	0.0015	0.6276	31	0.80	2.032	1.181	3.00	1.48
P-ARR-30-9	0.5822	0.0014	0.5850	31	0.90	2.286	1.181	3.00	1.31
P-ARR-30-10	0.5232	0.0013	0.5258	31	1.00	2.540	1.181	3.00	1.18
4.0 cm Pitch									
P-ARR-40-1	0.2606	0.0009	0.2624	19	0.25	0.635	1.575	4.00	6.30
P-ARR-40-2	0.3157	0.0011	0.3179	19	0.30	0.762	1.575	4.00	5.25
P-ARR-40-3	0.3690	0.0011	0.3712	19	0.35	0.889	1.575	4.00	4.50
P-ARR-40-4	0.4158	0.0011	0.4180	19	0.40	1.016	1.575	4.00	3.94
P-ARR-40-5	0.4577	0.0012	0.4601	19	0.45	1.143	1.575	4.00	3.50
P-ARR-40-6	0.4942	0.0013	0.4968	19	0.50	1.270	1.575	4.00	3.15
P-ARR-40-7	0.5506	0.0013	0.5532	19	0.60	1.524	1.575	4.00	2.62
P-ARR-40-8	0.6191	0.0014	0.6219	19	0.80	2.032	1.575	4.00	1.97
P-ARR-40-9	0.6309	0.0015	0.6339	19	0.90	2.286	1.575	4.00	1.75
P-ARR-40-10	0.6280	0.0014	0.6308	19	1.00	2.540	1.575	4.00	1.57

Table 6-36B Results for Rod Box Individual Package HAC

Run #	ks	sigma	Ks+2s	No. Fuel Rods	Pell. Diam. (inch)	Pell. Diam. (cm)	Rod Pitch (inch)	Rod Pitch (cm)	p/d
Close Packed									
B-IP-CP-1					0.25	0.635	0.25	0.64	1.0
B-IP-CP-2					0.30	0.762	0.30	0.76	1.0
B-IP-CP-3					0.35	0.889	0.35	0.89	1.0
B-IP-CP-4				196	0.40	1.016	0.40	1.02	1.0
B-IP-CP-5	0.5025	0.0011	0.5047	155	0.45	1.143	0.45	1.14	1.0
B-IP-CP-6	0.5044	0.0011	0.5066	120	0.50	1.270	0.50	1.27	1.0
B-IP-CP-7				85	0.60	1.524	0.60	1.52	1.0
B-IP-CP-8	0.5048	0.0011	0.5070	51	0.80	2.032	0.80	2.03	1.0
B-IP-CP-9	0.5028	0.0010	0.5048	42	0.90	2.286	0.90	2.29	1.0
B-IP-CP-10	0.5044	0.0012	0.5068	32	1.00	2.540	1.00	2.54	1.0
1.2 cm Pitch									
B-IP-12-1	0.188	0.0007	0.1894	143	0.05	0.127	0.472	1.20	9.45
B-IP-12-2	0.4459	0.0012	0.4483	143	0.10	0.254	0.472	1.20	4.72
B-IP-12-3	0.6061	0.0015	0.6091	143	0.15	0.381	0.472	1.20	3.15
B-IP-12-4	0.6798	0.0015	0.6828	143	0.20	0.508	0.472	1.20	2.36
B-IP-12-5	0.6967	0.0014	0.6995	143	0.25	0.635	0.472	1.20	1.89
B-IP-12-6	0.6819	0.0014	0.6847	143	0.30	0.762	0.472	1.20	1.57
B-IP-12-7	0.6430	0.0013	0.6456	143	0.35	0.889	0.472	1.20	1.35
B-IP-12-8	0.5829	0.0012	0.5853		0.40	1.016	0.472	1.20	1.18
B-IP-12-9					0.45	1.143	0.472	1.20	1.05
B-IP-12-10				143	0.50	1.270	0.472	1.20	0.94
1.5 cm Pitch									
B-IP-15-1	0.1333	0.0006	0.1345	93	0.05	0.127	0.591	1.50	11.81
B-IP-15-2	0.3543	0.0010	0.3563	93	0.10	0.254	0.591	1.50	5.91
B-IP-15-3	0.5198	0.0012	0.5222	93	0.15	0.381	0.591	1.50	3.94
B-IP-15-4	0.6254	0.0013	0.6280	93	0.20	0.508	0.591	1.50	2.95
B-IP-15-5	0.6774	0.0015	0.6804	93	0.25	0.635	0.591	1.50	2.36
B-IP-15-6	0.7008	0.0015	0.7038	93	0.30	0.762	0.591	1.50	1.97
B-IP-15-7	0.6964	0.0016	0.6996	93	0.35	0.889	0.591	1.50	1.69
B-IP-15-8	0.6780	0.0014	0.6808	93	0.40	1.016	0.591	1.50	1.48
B-IP-15-9	0.6363	0.0014	0.6391	93	0.45	1.143	0.591	1.50	1.31
B-IP-15-10	0.5906	0.0014	0.5934	93	0.50	1.270	0.591	1.50	1.18

Table 6-36B Results for Rod Box Individual Package HAC (cont.)

Run #	ks	sigma	Ks+2s	No. Fuel Rods	Pell. Diam. (inch)	Pell. Diam. (cm)	Rod Pitch (inch)	Rod Pitch (cm)	p/d
1.8 cm Pitch									
B-IP-18-1	0.0994	0.0005	0.1004	67	0.05	0.127	0.709	1.80	14.17
B-IP-18-2	0.2836	0.0009	0.2854	67	0.10	0.254	0.709	1.80	7.09
B-IP-18-3	0.4446	0.0012	0.4470	67	0.15	0.381	0.709	1.80	4.72
B-IP-18-4				67	0.20	0.508	0.709	1.80	3.54
B-IP-18-5	0.6307	0.0013	0.6333	67	0.25	0.635	0.709	1.80	2.83
B-IP-18-6	0.6733	0.0014	0.6761	67	0.30	0.762	0.709	1.80	2.36
B-IP-18-7	0.6912	0.0016	0.6944	67	0.35	0.889	0.709	1.80	2.02
B-IP-18-8	0.6972	0.0015	0.7002	67	0.40	1.016	0.709	1.80	1.77
B-IP-18-9	0.6822	0.0015	0.6852	67	0.45	1.143	0.709	1.80	1.57
B-IP-18-10	0.6606	0.0014	0.6634	67	0.50	1.270	0.709	1.80	1.42
2.0 cm Pitch									
B-IP-20-1				45	0.05	0.127	0.787	2.00	15.75
B-IP-20-2	0.2234	0.0008	0.2250	45	0.10	0.254	0.787	2.00	7.87
B-IP-20-3	0.3674	0.0010	0.3694	45	0.15	0.381	0.787	2.00	5.25
B-IP-20-4	0.4817	0.0013	0.4843	45	0.20	0.508	0.787	2.00	3.94
B-IP-20-5	0.5695	0.0013	0.5721	45	0.25	0.635	0.787	2.00	3.15
B-IP-20-6	0.6295	0.0013	0.6321	45	0.30	0.762	0.787	2.00	2.62
B-IP-20-7	0.6645	0.0014	0.6673	45	0.35	0.889	0.787	2.00	2.25
B-IP-20-8	0.6854	0.0017	0.6888	45	0.40	1.016	0.787	2.00	1.97
B-IP-20-9	0.6895	0.0017	0.6929	45	0.45	1.143	0.787	2.00	1.75
B-IP-20-10	0.6807	0.0016	0.6839	45	0.50	1.270	0.787	2.00	1.57
2.5 cm Pitch									
B-IP-25-1	0.5067	0.0013	0.5093	39	0.25	0.635	0.984	2.50	3.94
B-IP-25-2	0.5712	0.0012	0.5736	39	0.30	0.762	0.984	2.50	3.28
B-IP-25-3	0.6216	0.0014	0.6244	39	0.35	0.889	0.984	2.50	2.81
B-IP-25-4	0.6539	0.0014	0.6567	39	0.40	1.016	0.984	2.50	2.46
B-IP-25-5	0.6775	0.0014	0.6803	39	0.45	1.143	0.984	2.50	2.19
B-IP-25-6	0.6910	0.0015	0.6940	39	0.50	1.270	0.984	2.50	1.97
B-IP-25-7	0.6890	0.0014	0.6918	39	0.60	1.524	0.984	2.50	1.64
B-IP-25-8	0.6143	0.0014	0.6171	39	0.80	2.032	0.984	2.50	1.23
B-IP-25-9	0.5528	0.0012	0.5552	39	0.90	2.286	0.984	2.50	1.09
B-IP-25-10				39	1.00	2.540	0.984	2.50	0.98

Table 6-36B Results for Rod Box Individual Package HAC (cont.)

Run #	ks	sigma	Ks+2s	No. Fuel Rods	Pell. Diam. (inch)	Pell. Diam. (cm)	Rod Pitch (inch)	Rod Pitch (cm)	p/d
3.0 cm Pitch									
B-IP-30-1	0.3935	0.0011	0.3957	23	0.25	0.635	1.181	3.00	4.72
B-IP-30-2	0.4641	0.0011	0.4663	23	0.30	0.762	1.181	3.00	3.94
B-IP-30-3	0.5174	0.0013	0.5200	23	0.35	0.889	1.181	3.00	3.37
B-IP-30-4	0.5609	0.0013	0.5635	23	0.40	1.016	1.181	3.00	2.95
B-IP-30-5	0.5996	0.0014	0.6024	23	0.45	1.143	1.181	3.00	2.62
B-IP-30-6	0.6279	0.0013	0.6305	23	0.50	1.270	1.181	3.00	2.36
B-IP-30-7	0.6551	0.0014	0.6579	23	0.60	1.524	1.181	3.00	1.97
B-IP-30-8	0.6522	0.0014	0.6550	23	0.80	2.032	1.181	3.00	1.48
B-IP-30-9	0.6275	0.0016	0.6307	23	0.90	2.286	1.181	3.00	1.31
B-IP-30-10	0.5917	0.0014	0.5945	23	1.00	2.540	1.181	3.00	1.18
4.0 cm Pitch									
B-IP-40-1	0.2573	0.0009	0.2591	14	0.25	0.635	1.575	4.00	6.30
B-IP-40-2	0.3168	0.0009	0.3186	14	0.30	0.762	1.575	4.00	5.25
B-IP-40-3	0.3734	0.0011	0.3756	14	0.35	0.889	1.575	4.00	4.50
B-IP-40-4	0.4227	0.0014	0.4255	14	0.40	1.016	1.575	4.00	3.94
B-IP-40-5	0.4695	0.0012	0.4719	14	0.45	1.143	1.575	4.00	3.50
B-IP-40-6	0.5075	0.0014	0.5103	14	0.50	1.270	1.575	4.00	3.15
B-IP-40-7	0.5683	0.0012	0.5707	14	0.60	1.524	1.575	4.00	2.62
B-IP-40-8	0.6459	0.0015	0.6489	14	0.80	2.032	1.575	4.00	1.97
B-IP-40-9	0.6631	0.0014	0.6659	14	0.90	2.286	1.575	4.00	1.75
B-IP-40-10	0.6620	0.0010	0.6640	14	1.00	2.540	1.575	4.00	1.57

Table 6-36C Results for Rod Box Package Array HAC

Run #	ks	sigma	Ks+2s	No. Fuel Rods	Pell. Diam. (inch)	Pell. Diam. (cm)	Rod Pitch (inch)	Rod Pitch (cm)	p/d
Close Packed									
B-ARR-CP-1					0.25	0.635	0.25	0.64	1.0
B-ARR-CP-2					0.30	0.762	0.30	0.76	1.0
B-ARR-CP-3					0.35	0.889	0.35	0.89	1.0
B-ARR-CP-4	0.3506	0.0009	0.3524	196	0.40	1.016	0.40	1.02	1.0
B-ARR-CP-5	0.3502	0.0008	0.3518	155	0.45	1.143	0.45	1.14	1.0
B-ARR-CP-6	0.3493	0.0008	0.3509	120	0.50	1.270	0.50	1.27	1.0
B-ARR-CP-7	0.3523	0.0008	0.3539	85	0.60	1.524	0.60	1.52	1.0
B-ARR-CP-8	0.3496	0.0009	0.3514	51	0.80	2.032	0.80	2.03	1.0
B-ARR-CP-9	0.3513	0.0008	0.3529	42	0.90	2.286	0.90	2.29	1.0
B-ARR-CP-10	0.3526	0.0008	0.3542	32	1.00	2.540	1.00	2.54	1.0
1.2 cm Pitch									
B-ARR-12-1	0.1397	0.0007	0.1411	143	0.05	0.127	0.472	1.20	9.45
B-ARR-12-2	0.3478	0.0011	0.3500	143	0.10	0.254	0.472	1.20	4.72
B-ARR-12-3	0.4753	0.0014	0.4781	143	0.15	0.381	0.472	1.20	3.15
B-ARR-12-4	0.5352	0.0013	0.5378	143	0.20	0.508	0.472	1.20	2.36
B-ARR-12-5	0.5492	0.0014	0.5520	143	0.25	0.635	0.472	1.20	1.89
B-ARR-12-6	0.5301	0.0014	0.5329	143	0.30	0.762	0.472	1.20	1.57
B-ARR-12-7	0.4843	0.0012	0.4867	143	0.35	0.889	0.472	1.20	1.35
B-ARR-12-8				143	0.40	1.016	0.472	1.20	1.18
B-ARR-12-9	0.3689	0.0009	0.3707	143	0.45	1.143	0.472	1.20	1.05
B-ARR-12-10				143	0.50	1.270	0.472	1.20	0.94
1.5 cm Pitch									
B-ARR-15-1	0.0977	0.0006	0.0989	93	0.05	0.127	0.591	1.50	11.81
B-ARR-15-2	0.2661	0.0008	0.2677	93	0.10	0.254	0.591	1.50	5.91
B-ARR-15-3	0.4009	0.0011	0.4031	93	0.15	0.381	0.591	1.50	3.94
B-ARR-15-4	0.4894	0.0014	0.4922	93	0.20	0.508	0.591	1.50	2.95
B-ARR-15-5	0.5343	0.0017	0.5377	93	0.25	0.635	0.591	1.50	2.36
B-ARR-15-6	0.5512	0.0014	0.5540	93	0.30	0.762	0.591	1.50	1.97
B-ARR-15-7	0.5427	0.0014	0.5455	93	0.35	0.889	0.591	1.50	1.69
B-ARR-15-8	0.5175	0.0013	0.5201	93	0.40	1.016	0.591	1.50	1.48
B-ARR-15-9	0.4835	0.0012	0.4859	93	0.45	1.143	0.591	1.50	1.31
B-ARR-15-10	0.4301	0.0010	0.4321	93	0.50	1.270	0.591	1.50	1.18

Table 6-36C Results for Rod Box Package Array HAC (cont.)

Run #	ks	sigma	Ks+2s	No. Fuel Rods	Pell. Diam. (inch)	Pell. Diam. (cm)	Rod Pitch (inch)	Rod Pitch (cm)	p/d
1.8 cm Pitch									
B-ARR-18-1	0.0714	0.0005	0.0724	67	0.05	0.127	0.709	1.80	14.17
B-ARR-18-2	0.2078	0.0008	0.2094	67	0.10	0.254	0.709	1.80	7.09
B-ARR-18-3	0.3349	0.0011	0.3371	67	0.15	0.381	0.709	1.80	4.72
B-ARR-18-4	0.4284	0.0013	0.4310	67	0.20	0.508	0.709	1.80	3.54
B-ARR-18-5	0.4928	0.0014	0.4956	67	0.25	0.635	0.709	1.80	2.83
B-ARR-18-6	0.5290	0.0014	0.5318	67	0.30	0.762	0.709	1.80	2.36
B-ARR-18-7	0.5450	0.0014	0.5478	67	0.35	0.889	0.709	1.80	2.02
B-ARR-18-8	0.5458	0.0015	0.5488	67	0.40	1.016	0.709	1.80	1.77
B-ARR-18-9	0.5351	0.0012	0.5375	67	0.45	1.143	0.709	1.80	1.57
B-ARR-18-10	0.5075	0.0012	0.5099	67	0.50	1.270	0.709	1.80	1.42
2.0 cm Pitch									
B-ARR-20-1	0.0573	0.0004	0.0581	45	0.05	0.127	0.787	2.00	15.75
B-ARR-20-2	0.1719	0.0008	0.1735	45	0.10	0.254	0.787	2.00	7.87
B-ARR-20-3	0.2884	0.0010	0.2904	45	0.15	0.381	0.787	2.00	5.25
B-ARR-20-4	0.3791	0.0013	0.3817	45	0.20	0.508	0.787	2.00	3.94
B-ARR-20-5	0.4485	0.0012	0.4509	45	0.25	0.635	0.787	2.00	3.15
B-ARR-20-6	0.4957	0.0016	0.4989	45	0.30	0.762	0.787	2.00	2.62
B-ARR-20-7	0.5245	0.0014	0.5273	45	0.35	0.889	0.787	2.00	2.25
B-ARR-20-8	0.5354	0.0014	0.5382	45	0.40	1.016	0.787	2.00	1.97
B-ARR-20-9	0.5369	0.0015	0.5399	45	0.45	1.143	0.787	2.00	1.75
B-ARR-20-10	0.5281	0.0013	0.5307	45	0.50	1.270	0.787	2.00	1.57
2.5 cm Pitch									
B-ARR-25-1	0.3757	0.0011	0.3779	39	0.25	0.635	0.984	2.50	3.94
B-ARR-25-2	0.4322	0.0012	0.4346	39	0.30	0.762	0.984	2.50	3.28
B-ARR-25-3	0.4771	0.0013	0.4797	39	0.35	0.889	0.984	2.50	2.81
B-ARR-25-4	0.5060	0.0013	0.5086	39	0.40	1.016	0.984	2.50	2.46
B-ARR-25-5	0.5241	0.0015	0.5271	39	0.45	1.143	0.984	2.50	2.19
B-ARR-25-6	0.5388	0.0013	0.5414	39	0.50	1.270	0.984	2.50	1.97
B-ARR-25-7	0.5344	0.0015	0.5374	39	0.60	1.524	0.984	2.50	1.64
B-ARR-25-8	0.4577	0.0012	0.4601	39	0.80	2.032	0.984	2.50	1.23
B-ARR-25-9	0.3956	0.0009	0.3974	39	0.90	2.286	0.984	2.50	1.09
B-ARR-25-10				39	1.00	2.540	0.984	2.50	0.98

Table 6-36C Results for Rod Box Package Array HAC (cont.)

Run #	ks	sigma	Ks+2s	No. Fuel Rods	Pell. Diam. (inch)	Pell. Diam. (cm)	Rod Pitch (inch)	Rod Pitch (cm)	p/d
3.0 cm Pitch									
B-ARR-30-1	0.3011	0.0010	0.3031	23	0.25	0.635	1.181	3.00	4.72
B-ARR-30-2	0.3604	0.0011	0.3626	23	0.30	0.762	1.181	3.00	3.94
B-ARR-30-3	0.4042	0.0012	0.4066	23	0.35	0.889	1.181	3.00	3.37
B-ARR-30-4	0.4404	0.0012	0.4428	23	0.40	1.016	1.181	3.00	2.95
B-ARR-30-5	0.4714	0.0013	0.4740	23	0.45	1.143	1.181	3.00	2.62
B-ARR-30-6	0.4946	0.0013	0.4972	23	0.50	1.270	1.181	3.00	2.36
B-ARR-30-7	0.5184	0.0013	0.5210	23	0.60	1.524	1.181	3.00	1.97
B-ARR-30-8	0.5063	0.0012	0.5087	23	0.80	2.032	1.181	3.00	1.48
B-ARR-30-9	0.4758	0.0012	0.4782	23	0.90	2.286	1.181	3.00	1.31
B-ARR-30-10	0.4345	0.0011	0.4367	23	1.00	2.540	1.181	3.00	1.18
4.0 cm Pitch									
B-ARR-40-1	0.1926	0.0008	0.1942	14	0.25	0.635	1.575	4.00	6.30
B-ARR-40-2	0.2364	0.0009	0.2382	14	0.30	0.762	1.575	4.00	5.25
B-ARR-40-3	0.2784	0.0010	0.2804	14	0.35	0.889	1.575	4.00	4.50
B-ARR-40-4	0.3159	0.0013	0.3185	14	0.40	1.016	1.575	4.00	3.94
B-ARR-40-5	0.3522	0.0011	0.3544	14	0.45	1.143	1.575	4.00	3.50
B-ARR-40-6	0.3814	0.0011	0.3836	14	0.50	1.270	1.575	4.00	3.15
B-ARR-40-7	0.4332	0.0014	0.4360	14	0.60	1.524	1.575	4.00	2.62
B-ARR-40-8	0.4976	0.0013	0.5002	14	0.80	2.032	1.575	4.00	1.97
B-ARR-40-9	0.5137	0.0014	0.5165	14	0.90	2.286	1.575	4.00	1.75
B-ARR-40-10	0.5140	0.0014	0.5168	14	1.00	2.540	1.575	4.00	1.57

Table 6-36D Rod Box and Rod Pipe Interspersed Moderation Results			
Run #	**ks**	**sigma**	**Ks+2s**
Rod Box Interspersed Moderation Cases			
B-INTER-000	0.5501	0.0013	0.5527
B-INTER-005	0.5296	0.0014	0.5324
B-INTER-010	0.5284	0.0014	0.5312
B-INTER-020	0.5457	0.0014	0.5485
B-INTER-030	0.5731	0.0013	0.5757
B-INTER-040	0.6013	0.0015	0.6043
B-INTER-060	0.6443	0.0014	0.6471
B-INTER-080	0.6755	0.0015	0.6785
B-INTER-100	0.6962	0.0016	0.6994
Corresponding Rod Box Individual Package and Infinite Planar Array Cases			
B-ARR-15-6	0.5512	0.0014	0.5540
B-IP-15-6	0.7008	0.0015	0.7038
Rod Box Infinite Three Dimensional Array Cases			
B-ARR-15-6-3D	0.6962	0.0016	0.6994
Rod Pipe Interspersed Moderation Cases			
P-INTER-000	0.6611	0.0015	0.6641
P-INTER-005	0.6347	0.0016	0.6379
P-INTER-010	0.6299	0.0014	0.6327
P-INTER-020	0.6350	0.0015	0.6380
P-INTER-030	0.6514	0.0015	0.6544
P-INTER-040	0.6696	0.0014	0.6724
P-INTER-060	0.7028	0.0015	0.7058
P-INTER-080	0.7296	0.0016	0.7328
P-INTER-100	0.7455	0.0013	0.7481
Corresponding Rod Pipe Individual Package and Infinite Planar Array Cases			
P-ARR-15-6	0.6622	0.0016	0.6654
P-IP-15-6	0.7425	0.0015	0.7455
Rod Pipe Infinite Three Dimensional Array Cases			
P-ARR-15-6-3D	0.7455	0.0013	0.7481

Table 6-36E Input Deck for Rod Box Individual Package – 1.5 cm Pitch; 0.35 inch Diameter

```
PA_HAC_BORAL_6_3_1.5_7_0.889_in
=csas26     parm=size=300000
TRAVELLER XL,ROD TUBE,PA,NPD=0.889       ,PITCH=1.5
44groupndf5  latticecell
 uo2 1 1 293 92235 5 92238 95 end
 h2o 2 1 293 end
 zirc4 3 1 293 end
 h2o 4 1 293 end
 h2o 5 1 293 end
 arbmfoam 0.1602e-20  4  0  0  0 6012 70 1001 10 8016 16 7014 4  6 1 293
 end
 al 7 1 293 end
 ss304 8 1 293 end
 polyethylene 9 DEN=0.828 1.0 293 end
 arbmfoam 0.1602e-20  4  0  0  0 6012 70 1001 10 8016 16 7014 4 11 1 293
 end
 b-10 12 0 0.0047781    end
 b-11 12 0 0.019398     end
 c   12 0 0.0060439    end
 al  12 0 0.043223     end
 arbmrubber 1.59  7  0  0  0 8016 46.94 13000 19.92 14000 17.54 6012
 10.79 1001 4.73 11000 0.06 26000 0.02  14 1 293 end
 h2o 15 1 293 end
 uo2 16 1 293 92235 5 92238 95 end
 h2o 17 1 293 end
 zirc4 18 1 293 end
 h2o 19 1 293 end
end comp
triangpitch 1.5          0.889      16 19 end
more data
res=1  cylinder 0.39218      dan(1)=0.22632       end

read parameter
gen=303
wrs=1
end parameter
read geometry
unit 10
com='individual package'
cuboid 1    16.904       -15.634       16.904       -15.634       533.1330 0
rotate  a1=45 a2=0 a3=0 origin x=0  y=-1.460 z=0
cuboid 2     21.5900   -21.5900     1.5720    -1.0310   533.1330     0
cuboid 3     20.0790   -20.0790    20.0790   -20.0790   533.1330     0
rotate  a1=45 a2=0 a3=0 origin x=0  y=-1.460 z=0
cuboid 4     20.3450   -20.3450    20.3450   -20.3450   533.3990    -0.2660
rotate  a1=45 a2=0 a3=0 origin x=0  y=-1.460 z=0
cuboid 5     21.5900   -21.590     23.1498   -23.1498   533.1330     0
cuboid 6     21.8560   -21.8560    23.4158   -23.4158   533.3990    -0.2660
cuboid 7     20.3840   -20.3840    20.3840   -20.3840   553.8922   -19.8448
rotate  a1=45 a2=0 a3=0 origin x=0  y=-1.460 z=0
cuboid 8     21.8950   -21.895     23.4548   -23.4548   553.8922   -19.8448
```

Table 6-36E Input Deck for Rod Box Individual Package – 1.5 cm Pitch; 0.35 inch Diameter (cont.)

```
PA_HAC_BORAL_6_3_1.5_7_0.889_in
cylinder  9    25.1050    533.4380    -0.2660
cylinder 10    25.1050    553.9312   -19.8448
cylinder 11    31.4840    533.4380    -0.2660
cylinder 12    31.4840    553.9312   -19.8448
cylinder 13    31.4840    533.4380   -19.8448
cylinder 14    31.7500    554.1972   -20.1100

plane 15  zpl=1  con= -10.0000
cylinder 16 7.62   0 -4.5
 rotate  a1=45 a2=90 a3=0 origin x=18.7310 y=-11.1270 z=494.4364
cylinder 17 3.962  0 -7.60
 rotate  a1=45 a2=90 a3=0 origin x=18.7310 y=-11.1270 z=494.4364
cylinder 18 7.62   0 -4.5
 rotate  a1=-45 a2=90 a3=0 origin x=-18.7310 y=-11.1270 z=494.4364
cylinder 19 3.962  0 -7.60
 rotate  a1=-45 a2=90 a3=0 origin x=-18.7310 y=-11.1270 z=494.4364
cylinder 20 7.62   0 -4.5
 rotate  a1=45 a2=90 a3=0 origin x=18.7310 y=-11.1270 z=448.7164
cylinder 21 3.962  0 -7.60
 rotate  a1=45 a2=90 a3=0 origin x=18.7310 y=-11.1270 z=448.7164
cylinder 22 7.62   0 -4.5
 rotate  a1=-45 a2=90 a3=0 origin x=-18.7310 y=-11.1270 z=448.7164
cylinder 23 3.962  0 -7.60
 rotate  a1=-45 a2=90 a3=0 origin x=-18.7310 y=-11.1270 z=448.7164
cylinder 24 7.62   0 -4.5
 rotate  a1=45 a2=90 a3=0 origin x=18.7310 y=-11.1270 z=402.9964
cylinder 25 3.962  0 -7.60
 rotate  a1=45 a2=90 a3=0 origin x=18.7310 y=-11.1270 z=402.9964
cylinder 26 7.62   0 -4.5
rotate  a1=-45 a2=90 a3=0 origin x=-18.7310 y=-11.1270 z=402.9964
cylinder 27 3.962  0 -7.60
 rotate  a1=-45 a2=90 a3=0 origin x=-18.7310 y=-11.1270 z=402.9964
cylinder 28 7.62   0 -4.5
 rotate  a1=45 a2=90 a3=0 origin x=18.7310 y=-11.1270 z=357.2764
cylinder 29 3.962  0 -7.60
 rotate  a1=45 a2=90 a3=0 origin x=18.7310 y=-11.1270 z=357.2764
cylinder 30 7.62   0 -4.5
 rotate  a1=-45 a2=90 a3=0 origin x=-18.7310 y=-11.1270 z=357.2764
cylinder 31 3.962  0 -7.60
 rotate  a1=-45 a2=90 a3=0 origin x=-18.7310 y=-11.1270 z=357.2764
cylinder 54 7.62   0 -4.5
 rotate  a1=45 a2=90 a3=0 origin x=18.7310 y=-11.1270 z=265.8364
cylinder 55 3.962  0 -7.60
 rotate  a1=45 a2=90 a3=0 origin x=18.7310 y=-11.1270 z=265.8364
cylinder 56 7.62   0 -4.5
 rotate  a1=-45 a2=90 a3=0 origin x=-18.7310 y=-11.1270 z=265.8364
cylinder 57 3.962  0 -7.60
 rotate  a1=-45 a2=90 a3=0 origin x=-18.7310 y=-11.1270 z=265.8364
```

Table 6-36E Input Deck for Rod Box Individual Package – 1.5 cm Pitch; 0.35 inch Diameter (cont.)

```
PA_HAC_BORAL_6_3_1.5_7_0.889_in
cylinder 32 7.62   0 -4.5
 rotate  a1=45 a2=90 a3=0 origin x=18.7310 y=-11.1270 z=174.3964
cylinder 33 3.962  0 -7.60
 rotate  a1=45 a2=90 a3=0 origin x=18.7310 y=-11.1270 z=174.3964
cylinder 34 7.62   0 -4.5
 rotate  a1=-45 a2=90 a3=0 origin x=-18.7310 y=-11.1270 z=174.3964
cylinder 35 3.962  0 -7.60
 rotate  a1=-45 a2=90 a3=0 origin x=-18.7310 y=-11.1270 z=174.3964
cylinder 36 7.62   0 -4.5
 rotate  a1=45 a2=90 a3=0 origin x=18.7310 y=-11.1270 z=128.6764
cylinder 37 3.962  0 -7.60
 rotate  a1=45 a2=90 a3=0 origin x=18.7310 y=-11.1270 z=128.6764
cylinder 38 7.62   0 -4.5
 rotate  a1=-45 a2=90 a3=0 origin x=-18.7310 y=-11.1270 z=128.6764
cylinder 39 3.962  0 -7.60
 rotate  a1=-45 a2=90 a3=0 origin x=-18.7310 y=-11.1270 z=128.6764
cylinder 40 7.62   0 -4.5
 rotate  a1=45 a2=90 a3=0 origin x=18.7310 y=-11.1270 z=82.9564
cylinder 41 3.962  0 -7.60
 rotate  a1=45 a2=90 a3=0 origin x=18.7310 y=-11.1270 z=82.9564
cylinder 42 7.62   0 -4.5
 rotate  a1=-45 a2=90 a3=0 origin x=-18.7310 y=-11.1270 z=82.9564
cylinder 43 3.962  0 -7.60
 rotate  a1=-45 a2=90 a3=0 origin x=-18.7310 y=-11.1270 z=82.9564
cylinder 44 7.62   0 -4.5
 rotate  a1=45 a2=90 a3=0 origin x=18.7310 y=-11.1270 z=37.2364
cylinder 45 3.962  0 -7.60
 rotate  a1=45 a2=90 a3=0 origin x=18.7310 y=-11.1270 z=37.2364
cylinder 46 7.62   0 -4.5
 rotate  a1=-45 a2=90 a3=0 origin x=-18.7310 y=-11.1270 z=37.2364
cylinder 47 3.962  0 -7.60
 rotate  a1=-45 a2=90 a3=0 origin x=-18.7310 y=-11.1270 z=37.2364
hole 11 rotate  a1=45 a2=0 a3=0  origin  x=0 y=-17.700 z=5.240
cuboid 48    18.174    20.079   10.4238  -9.5152    533.3990    -0.2660
rotate  a1=-45 a2=0 a3=0 origin x=0  y=-1.460 z=0
cuboid 49    13.6554  -10.4238  16.904    20.079    533.3990    -0.2660
rotate  a1=45 a2=0 a3=0 origin x=0  y=-1.460 z=0
cuboid 50    16.904    20.079   13.6554  -10.4238   533.3990    -0.2660
rotate  a1=45 a2=0 a3=0 origin x=0  y=-1.460 z=0
cuboid 51     9.5152  -10.4238 -18.174   -20.079    533.3990    -0.2660
rotate  a1=-45 a2=0 a3=0 origin x=0  y=-1.460 z=0
cuboid 52    15.634    18.174   12.0238 -11.9197    533.3990    -0.2660
rotate  a1=-45 a2=0 a3=0 origin x=0  y=-1.460 z=0
cuboid 53    11.9197  -12.0238 -15.634   -18.174    533.3990    -0.2660
rotate  a1=-45 a2=0 a3=0 origin x=0  y=-1.460 z=0
media 15 1   1   3  5 -17 -19 -21 -23 -29 -31 -55 -57 -33 -35
-41 -43 -45 -47
media 15 1  -1   3  5 -48 -49 -50 -51 -52 -53
```

Table 6-36E Input Deck for Rod Box Individual Package – 1.5 cm Pitch; 0.35 inch Diameter (cont.)

```
PA_HAC_BORAL_6_3_1.5_7_0.889_in
media  9 1   3  -16  -17 -20 -21 -28 -29 -54 -55 -32 -33
-40 -41 -44 -45 48
media  9 1   3  -18  -19 -22 -23 -30 -31 -56 -57 -34 -35
-42 -43 -46 -47 51
media  9 1   3  -18  -22  -30  -56  -34  -42  -46  53
media  9 1   3  -16  -20  -28  -54  -32  -40  -44  52
media  9 1   3  49
media  9 1   3  50
media  8 1  -3   4   6
media  8 1   3  -5   6
media 15 1  -4   9
media 15 1   4  -6   9
media 15 1  -9  11
media 15 1  -7  10 -13
media 15 1   7  -8  10 -13  12
media 15 1 -10 -13  12
media 15 1 -11  13
media 15 1   7   8 -13  12
media  8 1 -12  14
media 15 1 16  -17 3 48
media 15 1 18  -19 3 51
media 15 1 20  -21 3 48
media 15 1 22  -23 3 51
media 15 1 28  -29 3 48
media 15 1 30  -31 3 51
media 15 1 54  -55 3 48
media 15 1 56  -57 3 51
media 15 1 32  -33 3 48
media 15 1 34  -35 3 51
media 15 1 40  -41 3 48
media 15 1 42  -43 3 51
media 15 1 44  -45 3 48
media 15 1 46  -47 3 51
media 15 1 16  -17 3 52
media 15 1 18  -19 3 53
media 15 1 20  -21 3 52
media 15 1 22  -23 3 53
media 15 1 28  -29 3 52
media 15 1 30  -31 3 53
media 15 1 54  -55 3 52
media 15 1 56  -57 3 53
media 15 1 32  -33 3 52
media 15 1 34  -35 3 53
media 15 1 40  -41 3 52
media 15 1 42  -43 3 53
media 15 1 44  -45 3 52
media 15 1 46  -47 3 53
media 14 1 17  3
media 14 1 19  3
```

Table 6-36E Input Deck for Rod Box Individual Package – 1.5 cm Pitch; 0.35 inch Diameter (cont.)

```
PA_HAC_BORAL_6_3_1.5_7_0.889_in
media 14 1 21  3
media 14 1 23  3
media 14 1 29  3
media 14 1 31  3
media 14 1 55  3
media 14 1 57  3
media 14 1 33  3
media 14 1 35  3
media 14 1 41  3
media 14 1 43  3
media 14 1 45  3
media 14 1 47  3
boundary 14

unit 11
com='fuel assembly confinement system'
cuboid 1    24.384       0 24.384       0 520.7000 2.5400
cuboid 2    25.337       -0.9525 25.337        -0.9525
 523.2400  0.0000
cuboid 3    19.812       4.572        24.429       -0.04545
 513.0800  3.81
cuboid 4    19.812       4.572        24.656       -0.27205
 513.0800  3.81
cuboid 5    19.812       4.572        24.702       -0.3175
 513.0800  3.81
cuboid 6    24.429       -0.04545      19.812       4.572
 513.0800  3.81
cuboid 7    24.656       -0.27205      19.812       4.572
 513.0800  3.81
cuboid 8    24.702       -0.3175       19.812       4.572
 513.0800  3.81
hole 13  origin  x=8.4138       y=8.4138       z=16.5600  rotate  a1=0 a2=0 a3=0
media 15 1   1
media  7 1  -1   2  -5  -8
media  7 1  -1   3
media 12 1  -3   4
media  7 1  -4   5
media  7 1  -1   6
media 12 1  -6   7
media  7 1  -7   8
boundary 2

unit 13
com='rod box with tri pitch rod array'
cuboid  1   2P6.5          2P6.75          450.0  -0.0
array 10           1  place 12 12 1 0 0 0
boundary 1
```

Table 6-36E Input Deck for Rod Box Individual Package – 1.5 cm Pitch; 0.35 inch Diameter (cont.)

```
PA_HAC_BORAL_6_3_1.5_7_0.889_in
unit 67
com='solid fuel rod'
cylinder 1 0.4445       448.3862     0
hexprism 2 0.75             450.0       -0.0
media 16  1 1
media 19  2 2 -1
boundary 2
global
unit 55
com='single package unit'
cylinder 1    51.75    574.1972 -40.1498
hole 10  origin  x=0 y=0  z=0  rotate  a1=0 a2=0 a3=0
cuboid   2 4p51.75 574.1972 -40.1498
media  15 1   1
media   0 1  -1 2
boundary 2

unit 66
com='individual package 0-deg rotation'
hexprism 1  31.75    554.1972  -20.1498
hole 10  origin  x=0 y=0  z=0  rotate  a1=0 a2=0 a3=0
media   0 1   1
boundary 1
unit 68
com='individual rod dummy cell'
hexprism 1  0.75         450.0  -0.0
media   19 1   1
boundary 1
unit 77
com='individual package 180-deg rotation'
hexprism 1  31.75    554.1972  -20.1498
hole 10  origin  x=0 y=0  z=0  rotate  a1=0 a2=0 a3=180
media   0 1   1
boundary 1
unit 88
com='dummy cell'
hexprism 1  31.75    554.1972  -20.1498
media  0 1   1
boundary 1

unit 99
com='package array'
cylinder 1  372.0761   554.1972  -20.1498
cylinder 2  392.0761   574.1972  -40.1498
cuboid 3  392.0761  -392.0761  392.0761  -392.0761   574.1972  -40.1498
array 1 1  place 8 8 1 0 0 0
media   0 1  -1   2
media   0 1  -2   3
boundary 3
```

Table 6-36E Input Deck for Rod Box Individual Package – 1.5 cm Pitch; 0.35 inch Diameter (cont.)

```
PA_HAC_BORAL_6_3_1.5_7_0.889_in
end geometry
read array
ara=1 typ=triangular nux=15 nuy=15 nuz=1 gbl=1
fill
88 88 88 88 88 88 88 88 88 88 88 88 88 88 88
  88 88 88 88 88 88 88 88 88 66 66 66 88 88 88
    88 88 88 88 88 88 88 77 77 77 77 77 77 88 88
     88 88 88 88 88 88 66 66 66 66 66 66 66 88 88
       88 88 88 88 88 77 77 77 77 77 77 77 77 88 88
         88 88 88 88 66 66 66 66 66 66 66 66 66 88 88
           88 88 88 77 77 77 77 77 77 77 77 77 88 88
             88 88 66 66 66 66 66 66 66 66 66 66 66 88 88
               88 88 77 77 77 77 77 77 77 77 77 77 88 88 88
                 88 88 66 66 66 66 66 66 66 66 66 88 88 88 88
                   88 77 77 77 77 77 77 77 77 77 77 88 88 88 88
                     88 66 66 66 66 66 66 66 66 66 88 88 88 88 88
                       88 88 77 77 77 77 77 77 88 88 88 88 88 88 88
                         88 88 88 88 88 88 88 88 88 88 88 88 88 88 88
                           88 88 88 88 88 88 88 88 88 88 88 88 88 88 88
end fill
ara=10 typ=triangular nux=30 nuy=30 nuz=1
com='rodbox filled'
fill 900*67 end fill
end array
read bnds
+xb=vacuum
-xb=vacuum
+yb=vacuum
-yb=vacuum
+zb=vacuum
-zb=vacuum
end bnds
end data
end
```

Table 6-36F Input Deck for Rod Pipe Package Array – 1.5 cm Pitch; 0.30 inch Diameter

```
PA_HAC_BORAL_6_3_1.5_7_0.889_in
=csas26     parm=size=300000
TRAVELLER XL,ROD TUBE,PA,NPD=0.762       ,PITCH=1.5
44groupndf5  latticecell
 uo2 1 1 293 92235 5 92238 95 end
 h2o 2 1 293 end
 zirc4 3 1 293 end
 h2o 4 1 293 end
 h2o 5 1 293 end
 arbmfoam 0.1602e-20  4  0  0  0 6012 70 1001 10 8016 16 7014 4  6 1 293
 end
 al 7 1 293 end
 ss304 8 1 293 end
 polyethylene 9 DEN=0.828 1.0 293 end
 arbmfoam 0.1602e-20  4  0  0  0 6012 70 1001 10 8016 16 7014 4 11 1 293
 end
 b-10 12 0 0.0047781    end
 b-11 12 0 0.019398     end
 c   12 0 0.0060439    end
 al  12 0 0.043223     end
 arbmrubber 1.59e-20  7  0  0  0 8016 46.94 13000 19.92 14000 17.54 6012
 10.79 1001 4.73 11000 0.06 26000 0.02  14 1 293 end
 h2o 15 1 293 end
 uo2 16 1 293 92235 5 92238 95 end
 h2o 17 1 293 end
 zirc4 18 1 293 end
 h2o 19 1 293 end
end comp
triangpitch 1.5          0.762      16 19 end
more data
res=1  cylinder 0.39218      dan(1)=0.22632       end

read parameter
gen=303
wrs=1
end parameter

read geometry
unit 10
com='individual package'
cuboid 1    16.904       -15.634       16.904       -15.634       533.1330 0
rotate  a1=45 a2=0 a3=0 origin x=0  y=-1.460 z=0
cuboid 2     21.5900   -21.5900     1.5720    -1.0310   533.1330     0
cuboid 3     20.0790   -20.0790    20.0790   -20.0790   533.1330     0
rotate  a1=45 a2=0 a3=0 origin x=0  y=-1.460 z=0
cuboid 4     20.3450   -20.3450    20.3450   -20.3450   533.3990    -0.2660
rotate  a1=45 a2=0 a3=0 origin x=0  y=-1.460 z=0
cuboid 5     21.5900   -21.590     23.1498   -23.1498   533.1330     0
cuboid 6     21.8560   -21.8560    23.4158   -23.4158   533.3990    -0.2660
cuboid 7     20.3840   -20.3840    20.3840   -20.3840   553.8922   -19.8448
rotate  a1=45 a2=0 a3=0 origin x=0  y=-1.460 z=0
```

Table 6-36F Input Deck for Rod Pipe Package Array – 1.5 cm Pitch; 0.30 inch Diameter (cont.)

```
PA_HAC_BORAL_6_3_1.5_7_0.889_in
cuboid 8    21.8950   -21.895    23.4548   -23.4548   553.8922   -19.8448
cylinder  9    25.1050    533.4380    -0.2660
cylinder 10    25.1050    553.9312   -19.8448
cylinder 11    31.4840    533.4380    -0.2660
cylinder 12    31.4840    553.9312   -19.8448
cylinder 13    31.4840    533.4380   -19.8448
cylinder 14    31.7500    554.1972   -20.1100

plane 15  zpl=1  con= -10.0000
cylinder 16 7.62   0 -4.5
 rotate  a1=45 a2=90 a3=0 origin x=18.7310 y=-11.1270 z=494.4364
cylinder 17 3.962  0 -7.60
 rotate  a1=45 a2=90 a3=0 origin x=18.7310 y=-11.1270 z=494.4364
cylinder 18 7.62   0 -4.5
 rotate  a1=-45 a2=90 a3=0 origin x=-18.7310 y=-11.1270 z=494.4364
cylinder 19 3.962  0 -7.60
 rotate  a1=-45 a2=90 a3=0 origin x=-18.7310 y=-11.1270 z=494.4364
cylinder 20 7.62   0 -4.5
 rotate  a1=45 a2=90 a3=0 origin x=18.7310 y=-11.1270 z=448.7164
cylinder 21 3.962  0 -7.60
 rotate  a1=45 a2=90 a3=0 origin x=18.7310 y=-11.1270 z=448.7164
cylinder 22 7.62   0 -4.5
 rotate  a1=-45 a2=90 a3=0 origin x=-18.7310 y=-11.1270 z=448.7164
cylinder 23 3.962  0 -7.60
 rotate  a1=-45 a2=90 a3=0 origin x=-18.7310 y=-11.1270 z=448.7164
cylinder 24 7.62   0 -4.5
 rotate  a1=45 a2=90 a3=0 origin x=18.7310 y=-11.1270 z=402.9964
cylinder 25 3.962  0 -7.60
 rotate  a1=45 a2=90 a3=0 origin x=18.7310 y=-11.1270 z=402.9964
cylinder 26 7.62   0 -4.5
 rotate  a1=-45 a2=90 a3=0 origin x=-18.7310 y=-11.1270 z=402.9964
cylinder 27 3.962  0 -7.60
 rotate  a1=-45 a2=90 a3=0 origin x=-18.7310 y=-11.1270 z=402.9964
cylinder 28 7.62   0 -4.5
 rotate  a1=45 a2=90 a3=0 origin x=18.7310 y=-11.1270 z=357.2764
cylinder 29 3.962  0 -7.60
 rotate  a1=45 a2=90 a3=0 origin x=18.7310 y=-11.1270 z=357.2764
cylinder 30 7.62   0 -4.5
 rotate  a1=-45 a2=90 a3=0 origin x=-18.7310 y=-11.1270 z=357.2764
cylinder 31 3.962  0 -7.60
 rotate  a1=-45 a2=90 a3=0 origin x=-18.7310 y=-11.1270 z=357.2764
cylinder 54 7.62   0 -4.5
 rotate  a1=45 a2=90 a3=0 origin x=18.7310 y=-11.1270 z=265.8364
cylinder 55 3.962  0 -7.60
 rotate  a1=45 a2=90 a3=0 origin x=18.7310 y=-11.1270 z=265.8364
cylinder 56 7.62   0 -4.5
 rotate  a1=-45 a2=90 a3=0 origin x=-18.7310 y=-11.1270 z=265.8364
cylinder 57 3.962  0 -7.60
 rotate  a1=-45 a2=90 a3=0 origin x=-18.7310 y=-11.1270 z=265.8364
```

Table 6-36F Input Deck for Rod Pipe Package Array – 1.5 cm Pitch; 0.30 inch Diameter (cont.)

```
PA_HAC_BORAL_6_3_1.5_7_0.889_in
cylinder 32 7.62   0 -4.5
 rotate  a1=45 a2=90 a3=0 origin x=18.7310 y=-11.1270 z=174.3964
cylinder 33 3.962  0 -7.60
 rotate  a1=45 a2=90 a3=0 origin x=18.7310 y=-11.1270 z=174.3964
cylinder 34 7.62   0 -4.5
 rotate  a1=-45 a2=90 a3=0 origin x=-18.7310 y=-11.1270 z=174.3964
cylinder 35 3.962  0 -7.60
 rotate  a1=-45 a2=90 a3=0 origin x=-18.7310 y=-11.1270 z=174.3964
cylinder 36 7.62   0 -4.5
 rotate  a1=45 a2=90 a3=0 origin x=18.7310 y=-11.1270 z=128.6764
cylinder 37 3.962  0 -7.60
 rotate  a1=45 a2=90 a3=0 origin x=18.7310 y=-11.1270 z=128.6764
cylinder 38 7.62   0 -4.5
 rotate  a1=-45 a2=90 a3=0 origin x=-18.7310 y=-11.1270 z=128.6764
cylinder 39 3.962  0 -7.60
 rotate  a1=-45 a2=90 a3=0 origin x=-18.7310 y=-11.1270 z=128.6764
cylinder 40 7.62   0 -4.5
 rotate  a1=45 a2=90 a3=0 origin x=18.7310 y=-11.1270 z=82.9564
cylinder 41 3.962  0 -7.60
 rotate  a1=45 a2=90 a3=0 origin x=18.7310 y=-11.1270 z=82.9564
cylinder 42 7.62   0 -4.5
 rotate  a1=-45 a2=90 a3=0 origin x=-18.7310 y=-11.1270 z=82.9564
cylinder 43 3.962  0 -7.60
 rotate  a1=-45 a2=90 a3=0 origin x=-18.7310 y=-11.1270 z=82.9564
cylinder 44 7.62   0 -4.5
 rotate  a1=45 a2=90 a3=0 origin x=18.7310 y=-11.1270 z=37.2364
cylinder 45 3.962  0 -7.60
 rotate  a1=45 a2=90 a3=0 origin x=18.7310 y=-11.1270 z=37.2364
cylinder 46 7.62   0 -4.5
 rotate  a1=-45 a2=90 a3=0 origin x=-18.7310 y=-11.1270 z=37.2364
cylinder 47 3.962  0 -7.60
 rotate  a1=-45 a2=90 a3=0 origin x=-18.7310 y=-11.1270 z=37.2364
hole 11 rotate  a1=45 a2=0 a3=0  origin  x=0 y=-17.700 z=5.240
cuboid 48    18.174    20.079   10.4238  -9.5152    533.3990    -0.2660
rotate  a1=-45 a2=0 a3=0 origin x=0  y=-1.460 z=0
cuboid 49    13.6554  -10.4238  16.904    20.079    533.3990    -0.2660
rotate  a1=45 a2=0 a3=0 origin x=0  y=-1.460 z=0
cuboid 50    16.904    20.079   13.6554  -10.4238   533.3990    -0.2660
rotate  a1=45 a2=0 a3=0 origin x=0  y=-1.460 z=0
cuboid 51     9.5152  -10.4238 -18.174   -20.079    533.3990    -0.2660
rotate  a1=-45 a2=0 a3=0 origin x=0  y=-1.460 z=0
cuboid 52    15.634    18.174   12.0238 -11.9197    533.3990    -0.2660
rotate  a1=-45 a2=0 a3=0 origin x=0  y=-1.460 z=0
cuboid 53    11.9197  -12.0238 -15.634   -18.174    533.3990    -0.2660
rotate  a1=-45 a2=0 a3=0 origin x=0  y=-1.460 z=0
media  0 1   1   3  5 -17 -19 -21 -23 -29 -31 -55 -57 -33 -35
-41 -43 -45 -47
media  0 1  -1   3  5 -48 -49 -50 -51 -52 -53
```

Table 6-36F Input Deck for Rod Pipe Package Array – 1.5 cm Pitch; 0.30 inch Diameter (cont.)

```
PA_HAC_BORAL_6_3_1.5_7_0.889_in
media  9 1   3  -16  -17 -20 -21 -28 -29 -54 -55 -32 -33
-40 -41 -44 -45 48
media  9 1   3  -18  -19 -22 -23 -30 -31 -56 -57 -34 -35
-42 -43 -46 -47 51
media  9 1   3  -18  -22  -30  -56  -34  -42  -46  53
media  9 1   3  -16  -20  -28  -54  -32  -40  -44  52
media  9 1   3  49
media  9 1   3  50
media  8 1  -3   4   6
media  8 1   3  -5   6
media  6 1  -4   9
media  6 1   4  -6   9
media  6 1  -9  11
media  6 1  -7  10 -13
media  6 1   7  -8  10 -13  12
media  6 1 -10 -13  12
media 11 1 -11  13
media 11 1   7   8 -13  12
media  8 1 -12  14
media  0 1 16  -17 3 48
media  0 1 18  -19 3 51
media  0 1 20  -21 3 48
media  0 1 22  -23 3 51
media  0 1 28  -29 3 48
media  0 1 30  -31 3 51
media  0 1 54  -55 3 48
media  0 1 56  -57 3 51
media  0 1 32  -33 3 48
media  0 1 34  -35 3 51
media  0 1 40  -41 3 48
media  0 1 42  -43 3 51
media  0 1 44  -45 3 48
media  0 1 46  -47 3 51
media  0 1 16  -17 3 52
media  0 1 18  -19 3 53
media  0 1 20  -21 3 52
media  0 1 22  -23 3 53
media  0 1 28  -29 3 52
media  0 1 30  -31 3 53
media  0 1 54  -55 3 52
media  0 1 56  -57 3 53
media  0 1 32  -33 3 52
media  0 1 34  -35 3 53
media  0 1 40  -41 3 52
media  0 1 42  -43 3 53
media  0 1 44  -45 3 52
media  0 1 46  -47 3 53
media 14 1 17  3
```

Table 6-36F Input Deck for Rod Pipe Package Array – 1.5 cm Pitch; 0.30 inch Diameter (cont.)

```
PA_HAC_BORAL_6_3_1.5_7_0.889_in
media 14 1 19  3
media 14 1 21  3
media 14 1 23  3
media 14 1 29  3
media 14 1 31  3
media 14 1 55  3
media 14 1 57  3
media 14 1 33  3
media 14 1 35  3
media 14 1 41  3
media 14 1 43  3
media 14 1 45  3
media 14 1 47  3
boundary 14

unit 11
com='fuel assembly confinement system'
cuboid 1    24.384       0 24.384       0 520.7000 2.5400
cuboid 2    25.337       -0.9525 25.337        -0.9525
 523.2400  0.0000
cuboid 3    19.812       4.572        24.429       -0.04545
 513.0800  3.81
cuboid 4    19.812       4.572        24.656       -0.27205
 513.0800  3.81
cuboid 5    19.812       4.572        24.702       -0.3175
 513.0800  3.81
cuboid 6    24.429       -0.04545      19.812       4.572
 513.0800  3.81
cuboid 7    24.656       -0.27205      19.812       4.572
 513.0800  3.81
cuboid 8    24.702       -0.3175       19.812       4.572
 513.0800  3.81
hole 13  origin  x=8.4138       y=8.4138       z=16.5600  rotate  a1=0 a2=0 a3=0
media  0 1   1
media  7 1  -1   2  -5  -8
media  7 1  -1   3
media 12 1  -3   4
media  7 1  -4   5
media  7 1  -1   6
media 12 1  -6   7
media  7 1  -7   8
boundary 2

unit 13
com='rod box with tri pitch rod array'
cylinder 1  8.4138          450.0  -0.0
cuboid  2  4p8.4138         450.0  -0.0
array 10           1  place 15 15 1 0 0 0
```

Table 6-36F Input Deck for Rod Pipe Package Array – 1.5 cm Pitch; 0.30 inch Diameter (cont.)

```
PA_HAC_BORAL_6_3_1.5_7_0.889_in
media   0 1  -1  2
boundary 2

unit 67
com='solid fuel rod'
cylinder 1 0.381        448.3862     0
hexprism 2 0.75             450.0       -0.0
media 16  1 1
media 19  2 2 -1
boundary 2
global
unit 55
com='single package unit'
cylinder 1    31.7500    554.1972   -20.1498
hole 10  origin  x=0 y=0  z=0  rotate  a1=0 a2=0 a3=0
cuboid   2 4p31.75 554.1972 -20.1498
media   0 1   1
media   0 1  -1 2
boundary 2

unit 66
com='individual package 0-deg rotation'
hexprism 1  31.75    554.1972  -20.1498
hole 10  origin  x=0 y=0  z=0  rotate  a1=0 a2=0 a3=0
media   0 1   1
boundary 1

unit 68
com='individual rod dummy cell'
hexprism 1  0.75         450.0  -0.0
media   19 1   1
boundary 1

unit 77
com='individual package 180-deg rotation'
hexprism 1  31.75    554.1972  -20.1498
hole 10  origin  x=0 y=0  z=0  rotate  a1=0 a2=0 a3=180
media   0 1   1
boundary 1

unit 88
com='dummy cell'
hexprism 1  31.75    554.1972  -20.1498
media  0 1   1
boundary 1

unit 99
com='package array'
cylinder 1  372.0761   554.1972  -20.1498
```

Table 6-36F Input Deck for Rod Pipe Package Array – 1.5 cm Pitch; 0.30 inch Diameter (cont.)

```
PA_HAC_BORAL_6_3_1.5_7_0.889_in
cylinder 2  392.0761   574.1972  -40.1498
cuboid 3  392.0761  -392.0761  392.0761  -392.0761   574.1972  -40.1498
array 1 1  place 8 8 1 0 0 0
media   0 1  -1   2
media   0 1  -2   3
boundary 3

end geometry

read array
ara=1 typ=triangular nux=15 nuy=15 nuz=1 gbl=1
fill
88 88 88 88 88 88 88 88 88 88 88 88 88 88 88
  88 88 88 88 88 88 88 88 88 66 66 66 88 88 88
    88 88 88 88 88 88 88 77 77 77 77 77 77 88 88
     88 88 88 88 88 88 66 66 66 66 66 66 66 88 88
       88 88 88 88 88 77 77 77 77 77 77 77 88 88
         88 88 88 88 66 66 66 66 66 66 66 66 66 88 88
           88 88 88 77 77 77 77 77 77 77 77 77 88 88
             88 88 66 66 66 66 66 66 66 66 66 66 66 88 88
               88 88 77 77 77 77 77 77 77 77 77 88 88 88
                 88 88 66 66 66 66 66 66 66 66 66 88 88 88 88
                   88 77 77 77 77 77 77 77 77 77 88 88 88 88
                     88 66 66 66 66 66 66 66 66 66 88 88 88 88 88
                       88 88 77 77 77 77 77 77 88 88 88 88 88 88 88
                         88 88 88 88 88 88 88 88 88 88 88 88 88 88 88
                           88 88 88 88 88 88 88 88 88 88 88 88 88 88 88
end fill
ara=10 typ=triangular nux=30 nuy=30 nuz=1
com='rodbox filled'
fill 900*67 end fill
end array
read bnds
+xb=mirror
-xb=mirror
+yb=mirror
-yb=mirror
+zb=h2o
-zb=h2o
end bnds
end data
end
```

Table 6-36G Input Deck for Rod Pipe Interspersed Moderation – 60% H2O Density

```
PA_HAC_BORAL_6_3_INTER060_in
=csas26     parm=size=300000
TRAVELLER XL,ROD TUBE,PA,NPD=0.762       ,PITCH=1.5
44groupndf5  latticecell
 uo2 1 1 293 92235 5 92238 95 end
 h2o 2 1 293 end
 zirc4 3 1 293 end
 h2o 4 1 293 end
 h2o 5 1 293 end
 arbmfoam 0.1602e-20  4  0  0  0 6012 70 1001 10 8016 16 7014 4  6 1 293
 end
 al 7 1 293 end
 ss304 8 1 293 end
 polyethylene 9 DEN=0.828 1.0 293 end
 arbmfoam 0.1602e-20  4  0  0  0 6012 70 1001 10 8016 16 7014 4 11 1 293
 end
 b-10 12 0 0.0047781    end
 b-11 12 0 0.019398     end
 c   12 0 0.0060439    end
 al  12 0 0.043223     end
 arbmrubber 1.59  7  0  0  0 8016 46.94 13000 19.92 14000 17.54 6012
 10.79 1001 4.73 11000 0.06 26000 0.02  14 1 293 end
 h2o 15 DEN=0.60 1.0 293 end
 uo2 16 1 293 92235 5 92238 95 end
 h2o 17 1 293 end
 zirc4 18 1 293 end
 h2o 19 1 293 end
end comp
triangpitch 1.5          0.762      16 19 end
more data
res=1  cylinder 0.39218      dan(1)=0.22632       end

read parameter
gen=303
wrs=1
end parameter

read geometry
unit 10
com='individual package'
cuboid 1    16.904       -15.634       16.904       -15.634       533.1330 0
rotate  a1=45 a2=0 a3=0 origin x=0  y=-1.460 z=0
cuboid 2     21.5900   -21.5900     1.5720    -1.0310   533.1330     0
cuboid 3     20.0790   -20.0790    20.0790   -20.0790   533.1330     0
rotate  a1=45 a2=0 a3=0 origin x=0  y=-1.460 z=0
cuboid 4     20.3450   -20.3450    20.3450   -20.3450   533.3990    -0.2660
rotate  a1=45 a2=0 a3=0 origin x=0  y=-1.460 z=0
cuboid 5     21.5900   -21.590     23.1498   -23.1498   533.1330     0
cuboid 6     21.8560   -21.8560    23.4158   -23.4158   533.3990    -0.2660
cuboid 7     20.3840   -20.3840    20.3840   -20.3840   553.8922   -19.8448
rotate  a1=45 a2=0 a3=0 origin x=0  y=-1.460 z=0
```

Table 6-36G Input Deck for Rod Pipe Interspersed Moderation – 60% H2O Density (cont.)

```
PA_HAC_BORAL_6_3_INTER060_in
cuboid 8    21.8950   -21.895    23.4548   -23.4548   553.8922   -19.8448
cylinder  9    25.1050    533.4380    -0.2660
cylinder 10    25.1050    553.9312   -19.8448
cylinder 11    31.4840    533.4380    -0.2660
cylinder 12    31.4840    553.9312   -19.8448
cylinder 13    31.4840    533.4380   -19.8448
cylinder 14    31.7500    554.1972   -20.1100
plane 15  zpl=1  con= -10.0000
cylinder 16 7.62   0 -4.5
 rotate  a1=45 a2=90 a3=0 origin x=18.7310 y=-11.1270 z=494.4364
cylinder 17 3.962  0 -7.60
 rotate  a1=45 a2=90 a3=0 origin x=18.7310 y=-11.1270 z=494.4364
cylinder 18 7.62   0 -4.5
 rotate  a1=-45 a2=90 a3=0 origin x=-18.7310 y=-11.1270 z=494.4364
cylinder 19 3.962  0 -7.60
 rotate  a1=-45 a2=90 a3=0 origin x=-18.7310 y=-11.1270 z=494.4364
cylinder 20 7.62   0 -4.5
 rotate  a1=45 a2=90 a3=0 origin x=18.7310 y=-11.1270 z=448.7164
cylinder 21 3.962  0 -7.60
 rotate  a1=45 a2=90 a3=0 origin x=18.7310 y=-11.1270 z=448.7164
cylinder 22 7.62   0 -4.5
 rotate  a1=-45 a2=90 a3=0 origin x=-18.7310 y=-11.1270 z=448.7164
cylinder 23 3.962  0 -7.60
 rotate  a1=-45 a2=90 a3=0 origin x=-18.7310 y=-11.1270 z=448.7164
cylinder 24 7.62   0 -4.5
 rotate  a1=45 a2=90 a3=0 origin x=18.7310 y=-11.1270 z=402.9964
cylinder 25 3.962  0 -7.60
 rotate  a1=45 a2=90 a3=0 origin x=18.7310 y=-11.1270 z=402.9964
cylinder 26 7.62   0 -4.5
 rotate  a1=-45 a2=90 a3=0 origin x=-18.7310 y=-11.1270 z=402.9964
cylinder 27 3.962  0 -7.60
 rotate  a1=-45 a2=90 a3=0 origin x=-18.7310 y=-11.1270 z=402.9964
cylinder 28 7.62   0 -4.5
 rotate  a1=45 a2=90 a3=0 origin x=18.7310 y=-11.1270 z=357.2764
cylinder 29 3.962  0 -7.60
 rotate  a1=45 a2=90 a3=0 origin x=18.7310 y=-11.1270 z=357.2764
cylinder 30 7.62   0 -4.5
 rotate  a1=-45 a2=90 a3=0 origin x=-18.7310 y=-11.1270 z=357.2764
cylinder 31 3.962  0 -7.60
 rotate  a1=-45 a2=90 a3=0 origin x=-18.7310 y=-11.1270 z=357.2764
cylinder 54 7.62   0 -4.5
 rotate  a1=45 a2=90 a3=0 origin x=18.7310 y=-11.1270 z=265.8364
cylinder 55 3.962  0 -7.60
 rotate  a1=45 a2=90 a3=0 origin x=18.7310 y=-11.1270 z=265.8364
cylinder 56 7.62   0 -4.5
 rotate  a1=-45 a2=90 a3=0 origin x=-18.7310 y=-11.1270 z=265.8364
cylinder 57 3.962  0 -7.60
 rotate  a1=-45 a2=90 a3=0 origin x=-18.7310 y=-11.1270 z=265.8364
```

Table 6-36G Input Deck for Rod Pipe Interspersed Moderation – 60% H2O Density (cont.)

```
PA_HAC_BORAL_6_3_INTER060_in
cylinder 32 7.62   0 -4.5
 rotate  a1=45 a2=90 a3=0 origin x=18.7310 y=-11.1270 z=174.3964
cylinder 33 3.962  0 -7.60
 rotate  a1=45 a2=90 a3=0 origin x=18.7310 y=-11.1270 z=174.3964
cylinder 34 7.62   0 -4.5
 rotate  a1=-45 a2=90 a3=0 origin x=-18.7310 y=-11.1270 z=174.3964
cylinder 35 3.962  0 -7.60
 rotate  a1=-45 a2=90 a3=0 origin x=-18.7310 y=-11.1270 z=174.3964
cylinder 36 7.62   0 -4.5
 rotate  a1=45 a2=90 a3=0 origin x=18.7310 y=-11.1270 z=128.6764
cylinder 37 3.962  0 -7.60
 rotate  a1=45 a2=90 a3=0 origin x=18.7310 y=-11.1270 z=128.6764
cylinder 38 7.62   0 -4.5
 rotate  a1=-45 a2=90 a3=0 origin x=-18.7310 y=-11.1270 z=128.6764
cylinder 39 3.962  0 -7.60
 rotate  a1=-45 a2=90 a3=0 origin x=-18.7310 y=-11.1270 z=128.6764
cylinder 40 7.62   0 -4.5
 rotate  a1=45 a2=90 a3=0 origin x=18.7310 y=-11.1270 z=82.9564
cylinder 41 3.962  0 -7.60
 rotate  a1=45 a2=90 a3=0 origin x=18.7310 y=-11.1270 z=82.9564
cylinder 42 7.62   0 -4.5
 rotate  a1=-45 a2=90 a3=0 origin x=-18.7310 y=-11.1270 z=82.9564
cylinder 43 3.962  0 -7.60
 rotate  a1=-45 a2=90 a3=0 origin x=-18.7310 y=-11.1270 z=82.9564
cylinder 44 7.62   0 -4.5
 rotate  a1=45 a2=90 a3=0 origin x=18.7310 y=-11.1270 z=37.2364
cylinder 45 3.962  0 -7.60
 rotate  a1=45 a2=90 a3=0 origin x=18.7310 y=-11.1270 z=37.2364
cylinder 46 7.62   0 -4.5
 rotate  a1=-45 a2=90 a3=0 origin x=-18.7310 y=-11.1270 z=37.2364
cylinder 47 3.962  0 -7.60
 rotate  a1=-45 a2=90 a3=0 origin x=-18.7310 y=-11.1270 z=37.2364
hole 11 rotate  a1=45 a2=0 a3=0  origin  x=0 y=-17.700 z=5.240
cuboid 48    18.174    20.079   10.4238  -9.5152    533.3990    -0.2660
rotate  a1=-45 a2=0 a3=0 origin x=0  y=-1.460 z=0
cuboid 49    13.6554  -10.4238  16.904    20.079    533.3990    -0.2660
rotate  a1=45 a2=0 a3=0 origin x=0  y=-1.460 z=0
cuboid 50    16.904    20.079   13.6554  -10.4238   533.3990    -0.2660
rotate  a1=45 a2=0 a3=0 origin x=0  y=-1.460 z=0
cuboid 51     9.5152  -10.4238 -18.174   -20.079    533.3990    -0.2660
rotate  a1=-45 a2=0 a3=0 origin x=0  y=-1.460 z=0
cuboid 52    15.634    18.174   12.0238 -11.9197    533.3990    -0.2660
rotate  a1=-45 a2=0 a3=0 origin x=0  y=-1.460 z=0
cuboid 53    11.9197  -12.0238 -15.634   -18.174    533.3990    -0.2660
rotate  a1=-45 a2=0 a3=0 origin x=0  y=-1.460 z=0
media 15 1   1   3  5 -17 -19 -21 -23 -29 -31 -55 -57 -33 -35
-41 -43 -45 -47
media 15 1  -1   3  5 -48 -49 -50 -51 -52 -53
```

Table 6-36G Input Deck for Rod Pipe Interspersed Moderation – 60% H2O Density (cont.)

```
PA_HAC_BORAL_6_3_INTER060_in
media  9 1   3  -16  -17 -20 -21 -28 -29 -54 -55 -32 -33
-40 -41 -44 -45 48
media  9 1   3  -18  -19 -22 -23 -30 -31 -56 -57 -34 -35
-42 -43 -46 -47 51
media  9 1   3  -18  -22  -30  -56  -34  -42  -46  53
media  9 1   3  -16  -20  -28  -54  -32  -40  -44  52
media  9 1   3  49
media  9 1   3  50
media  8 1  -3   4   6
media  8 1   3  -5   6
media 15 1  -4   9
media 15 1   4  -6   9
media 15 1  -9  11
media 15 1  -7  10 -13
media 15 1   7  -8  10 -13  12
media 15 1 -10 -13  12
media 15 1 -11  13
media 15 1   7   8 -13  12
media  8 1 -12  14
media 15 1 16  -17 3 48
media 15 1 18  -19 3 51
media 15 1 20  -21 3 48
media 15 1 22  -23 3 51
media 15 1 28  -29 3 48
media 15 1 30  -31 3 51
media 15 1 54  -55 3 48
media 15 1 56  -57 3 51
media 15 1 32  -33 3 48
media 15 1 34  -35 3 51
media 15 1 40  -41 3 48
media 15 1 42  -43 3 51
media 15 1 44  -45 3 48
media 15 1 46  -47 3 51
media 15 1 16  -17 3 52
media 15 1 18  -19 3 53
media 15 1 20  -21 3 52
media 15 1 22  -23 3 53
media 15 1 28  -29 3 52
media 15 1 30  -31 3 53
media 15 1 54  -55 3 52
media 15 1 56  -57 3 53
media 15 1 32  -33 3 52
media 15 1 34  -35 3 53
media 15 1 40  -41 3 52
media 15 1 42  -43 3 53
media 15 1 44  -45 3 52
media 15 1 46  -47 3 53
media 14 1 17  3
```

Table 6-36G Input Deck for Rod Pipe Interspersed Moderation – 60% H2O Density (cont.)

```
PA_HAC_BORAL_6_3_INTER060_in
media 14 1 19  3
media 14 1 21  3
media 14 1 23  3
media 14 1 29  3
media 14 1 31  3
media 14 1 55  3
media 14 1 57  3
media 14 1 33  3
media 14 1 35  3
media 14 1 41  3
media 14 1 43  3
media 14 1 45  3
media 14 1 47  3
boundary 14

unit 11
com='fuel assembly confinement system'
cuboid 1    24.384       0 24.384       0 520.7000 2.5400
cuboid 2    25.337       -0.9525 25.337        -0.9525
 523.2400  0.0000
cuboid 3    19.812       4.572        24.429       -0.04545
 513.0800  3.81
cuboid 4    19.812       4.572        24.656       -0.27205
 513.0800  3.81
cuboid 5    19.812       4.572        24.702       -0.3175
 513.0800  3.81
cuboid 6    24.429       -0.04545      19.812       4.572
 513.0800  3.81
cuboid 7    24.656       -0.27205      19.812       4.572
 513.0800  3.81
cuboid 8    24.702       -0.3175       19.812       4.572
 513.0800  3.81
hole 13  origin  x=8.4138       y=8.4138       z=16.5600  rotate  a1=0 a2=0 a3=0
media 15 1   1
media  7 1  -1   2  -5  -8
media  7 1  -1   3
media 12 1  -3   4
media  7 1  -4   5
media  7 1  -1   6
media 12 1  -6   7
media  7 1  -7   8
boundary 2
unit 13
com='rod box with tri pitch rod array'
cylinder 1  8.4138          450.0  -0.0
cuboid  2  4p8.4138         450.0  -0.0
array 10           1  place 15 15 1 0 0 0
media  15 1  -1  2
boundary 2
```

Table 6-36G Input Deck for Rod Pipe Interspersed Moderation – 60% H2O Density (cont.)

```
PA_HAC_BORAL_6_3_INTER060_in
unit 67
com='solid fuel rod'
cylinder 1 0.381        448.3862     0
hexprism 2 0.75             450.0       -0.0
media 16  1 1
media 19  2 2 -1
boundary 2
global
unit 55
com='single package unit'
cylinder 1    31.75    554.1972 -20.1498
hole 10  origin  x=0 y=0  z=0  rotate  a1=0 a2=0 a3=0
cuboid   2 4p31.75 554.1972 -20.1498
media  15 1   1
media  15 1  -1 2
boundary 2

unit 66
com='individual package 0-deg rotation'
hexprism 1  31.75    554.1972  -20.1498
hole 10  origin  x=0 y=0  z=0  rotate  a1=0 a2=0 a3=0
media   0 1   1
boundary 1

unit 68
com='individual rod dummy cell'
hexprism 1  0.75         450.0  -0.0
media   19 1   1
boundary 1

unit 77
com='individual package 180-deg rotation'
hexprism 1  31.75    554.1972  -20.1498
hole 10  origin  x=0 y=0  z=0  rotate  a1=0 a2=0 a3=180
media   0 1   1
boundary 1

unit 88
com='dummy cell'
hexprism 1  31.75    554.1972  -20.1498
media  0 1   1
boundary 1

unit 99
com='package array'
cylinder 1  372.0761   554.1972  -20.1498
cylinder 2  392.0761   574.1972  -40.1498
cuboid 3  392.0761  -392.0761  392.0761  -392.0761   574.1972  -40.1498
```

Table 6-36G Input Deck for Rod Pipe Interspersed Moderation – 60% H2O Density (cont.)

```
PA_HAC_BORAL_6_3_INTER060_in
array 1 1  place 8 8 1 0 0 0
media   0 1  -1   2
media   0 1  -2   3
boundary 3

end geometry

read array
ara=1 typ=triangular nux=15 nuy=15 nuz=1 gbl=1
fill

88 88 88 88 88 88 88 88 88 88 88 88 88 88 88
  88 88 88 88 88 88 88 88 88 66 66 66 88 88 88
    88 88 88 88 88 88 88 77 77 77 77 77 77 88 88
     88 88 88 88 88 88 66 66 66 66 66 66 66 88 88
       88 88 88 88 88 77 77 77 77 77 77 77 77 88 88
         88 88 88 88 66 66 66 66 66 66 66 66 66 88 88
           88 88 88 77 77 77 77 77 77 77 77 77 77 88 88
             88 88 66 66 66 66 66 66 66 66 66 66 66 88 88
               88 88 77 77 77 77 77 77 77 77 77 77 88 88 88
                 88 88 66 66 66 66 66 66 66 66 66 88 88 88 88
                   88 77 77 77 77 77 77 77 77 77 77 88 88 88 88
                     88 66 66 66 66 66 66 66 66 66 88 88 88 88 88
                       88 88 77 77 77 77 77 77 88 88 88 88 88 88 88
                         88 88 88 88 88 88 88 88 88 88 88 88 88 88 88
                           88 88 88 88 88 88 88 88 88 88 88 88 88 88 88

end fill


ara=10 typ=triangular nux=30 nuy=30 nuz=1
com='rodbox filled'
fill 900*67 end fill

end array

read bnds
+xb=mirror
-xb=mirror
+yb=mirror
-yb=mirror
+zb=h2o
-zb=h2o
end bnds

end data
end
```

6.10.9 Calculations for Sensitivity Studies

6.10.9.1 Partial Density Interspersed Moderation Data

The data below reports the results of one of the interspersed moderation studies. The Traveller STD package accident condition model was run with different moderation densities. Table 6-37 shows the results for the graph in section 6.7.1.5. Table 6-38 shows a sample input deck.

Table 6-37 Partial Density Interspersed Moderation Results for Traveller XL

Run No.	Interspersed Water Density (g/cc)	ks	σks	ks+2×σks
XL-HAC-ARRAY-100	0.0000	0.9377	0.0008	0.9393
INTER-005	0.0500	0.9203	0.0008	0.9219
INTER-010	0.1000	0.9127	0.0009	0.9145
INTER-030	0.3000	0.8991	0.0009	0.9009
INTER-060	0.6000	0.8998	0.0010	0.9018
INTER-080	0.8000	0.9003	0.0009	0.9021
INTER-100	1.0000	0.9035	0.0010	0.9055

6.10.9.2 Partial Flooding Data

Table 6-37A Results for Partial Flooding Scenario #1

Run #	Level	ks	σks	ks+2×σks
XL-HAC-ARRAY-100	0.0000	0.9377	0.0008	0.9393
PREF-LVL1	2.1657	0.9268	0.0008	0.9284
PREF-LVL2	9.3761	0.9229	0.0008	0.9245
PREF-LVL3	15.6340	0.9220	0.0010	0.9240
PREF-LVL4	21.7746	0.9176	0.0008	0.9192
PREF-LVL5	28.4553	0.9162	0.0010	0.9182
PREF-LVL6	32.5380	0.9158	0.0008	0.9174

Table 6-37B Results for Partial Flooding Scenario #2

Run #	Level	ks	σks	ks+2×σks
PART-LVL1	0.0000	0.3043	0.0006	0.3055
PART-LVL1	2.1657	0.2967	0.0007	0.2981
PART-LVL2	18.8297	0.8010	0.0008	0.8026
PART-LVL3	21.7634	0.8555	0.0010	0.8575
PART-LVL4	24.6971	0.8920	0.0009	0.8938
PART-LVL5	28.4553	0.9204	0.0010	0.9224
PART-LVL6	32.5380	0.9193	0.0009	0.9211

Table 6-37C Input Deck for Partial Flooding Scenario #1

```
=csas26     parm=size=300000
TRAVELLER XL,17WOFA,ENV=24.384      cm,L=100      cm,B10=0.018   g/cm2
44groupndf5  latticecell
 uo2 1 1 293 92235 5 92238 95 end
 h2o 2 1 293 end
 zirc4 3 1 293 end
 h2o 4 1 293 end
 h2o 5 1 293 end
 arbmfoam 0.1602e-20  4  0  0  0 6012 70 1001 10 8016 16 7014 4  6 1 293
 end
 al 7 1 293 end
 ss304 8 1 293 end
 polyethylene 9 DEN=0.828 1.0 293 end
 arbmfoam 0.1602e-20  4  0  0  0 6012 70 1001 10 8016 16 7014 4 11 1 293
 end
 b-10 12 0 0.0047781    end
 b-11 12 0 0.019398     end
 c   12 0 0.0060439    end
 al  12 0 0.043223     end
 arbmrubber 1.59e-20  7  0  0  0 8016 46.94 13000 19.92 14000 17.54 6012
 10.79 1001 4.73 11000 0.06 26000 0.02  14 1 293 end
 h2o 15 1 293 end
 uo2 16 1 293 92235 5 92238 95 end
 h2o 17 1 293 end
 zirc4 18 1 293 end
 h2o 19 1 293 end
end comp
squarepitch 1.4669       0.78435      16 19 0.9144       18 0.8001       17 end
more data
res=1  cylinder 0.39218      dan(1)=0.22632       end

read parameter
gen=450
npg=2500
nsk=50
wrs=1
tme=240
end parameter
```

Table 6-37C Input Deck for Partial Flooding Scenario #1 (cont.)

```
read geometry
unit 10
com='individual package'
cuboid 1    16.904      -15.634      16.904      -15.634      533.1330 0
rotate  a1=45 a2=0 a3=0 origin x=0  y=-1.460 z=0
cuboid 2    21.5900   -21.5900    1.5720   -1.0310   533.1330    0
cuboid 3    20.0790   -20.0790   20.0790   -20.0790   533.1330    0
rotate  a1=45 a2=0 a3=0 origin x=0  y=-1.460 z=0
cuboid 4    20.3450   -20.3450   20.3450   -20.3450   533.3990   -0.2660
rotate  a1=45 a2=0 a3=0 origin x=0  y=-1.460 z=0
cuboid 5    21.5900   -21.590    23.1498   -23.1498   533.1330    0
cuboid 6    21.8560   -21.8560   23.4158   -23.4158   533.3990   -0.2660
cuboid 7    20.3840   -20.3840   20.3840   -20.3840   553.8922   -19.8448
rotate  a1=45 a2=0 a3=0 origin x=0  y=-1.460 z=0
cuboid 8    21.8950   -21.895    23.4548   -23.4548   553.8922   -19.8448
cylinder  9   25.1050   533.4380   -0.2660
cylinder 10   25.1050   553.9312   -19.8448
cylinder 11   31.4840   533.4380   -0.2660
cylinder 12   31.4840   553.9312   -19.8448
cylinder 13   31.4840   533.4380   -19.8448
cylinder 14   31.7500   554.1972   -20.1100
plane 15  xpl=1 ypl=1  con= 0.0
cylinder 16 7.62   0 -4.5
 rotate  a1=45 a2=90 a3=0 origin x=18.7310 y=-11.1270 z=494.4364
cylinder 17 3.962  0 -7.60
 rotate  a1=45 a2=90 a3=0 origin x=18.7310 y=-11.1270 z=494.4364
cylinder 18 7.62   0 -4.5
 rotate  a1=-45 a2=90 a3=0 origin x=-18.7310 y=-11.1270 z=494.4364
cylinder 19 3.962  0 -7.60
 rotate  a1=-45 a2=90 a3=0 origin x=-18.7310 y=-11.1270 z=494.4364
cylinder 20 7.62   0 -4.5
 rotate  a1=45 a2=90 a3=0 origin x=18.7310 y=-11.1270 z=448.7164
cylinder 21 3.962  0 -7.60
 rotate  a1=45 a2=90 a3=0 origin x=18.7310 y=-11.1270 z=448.7164
cylinder 22 7.62   0 -4.5
 rotate  a1=-45 a2=90 a3=0 origin x=-18.7310 y=-11.1270 z=448.7164
cylinder 23 3.962  0 -7.60
 rotate  a1=-45 a2=90 a3=0 origin x=-18.7310 y=-11.1270 z=448.7164
cylinder 24 7.62   0 -4.5
 rotate  a1=45 a2=90 a3=0 origin x=18.7310 y=-11.1270 z=402.9964
cylinder 25 3.962  0 -7.60
 rotate  a1=45 a2=90 a3=0 origin x=18.7310 y=-11.1270 z=402.9964
cylinder 26 7.62   0 -4.5
 rotate  a1=-45 a2=90 a3=0 origin x=-18.7310 y=-11.1270 z=402.9964
cylinder 27 3.962  0 -7.60
 rotate  a1=-45 a2=90 a3=0 origin x=-18.7310 y=-11.1270 z=402.9964
cylinder 28 7.62   0 -4.5
 rotate  a1=45 a2=90 a3=0 origin x=18.7310 y=-11.1270 z=357.2764
cylinder 29 3.962  0 -7.60
 rotate  a1=45 a2=90 a3=0 origin x=18.7310 y=-11.1270 z=357.2764
cylinder 30 7.62   0 -4.5
```

Table 6-37C Input Deck for Partial Flooding Scenario #1 (cont.)

```
rotate  a1=-45 a2=90 a3=0 origin x=-18.7310 y=-11.1270 z=357.2764
cylinder 31 3.962  0 -7.60
 rotate  a1=-45 a2=90 a3=0 origin x=-18.7310 y=-11.1270 z=357.2764
cylinder 54 7.62   0 -4.5
 rotate  a1=45 a2=90 a3=0 origin x=18.7310 y=-11.1270 z=265.8364
cylinder 55 3.962  0 -7.60
 rotate  a1=45 a2=90 a3=0 origin x=18.7310 y=-11.1270 z=265.8364
cylinder 56 7.62   0 -4.5
 rotate  a1=-45 a2=90 a3=0 origin x=-18.7310 y=-11.1270 z=265.8364
cylinder 57 3.962  0 -7.60
 rotate  a1=-45 a2=90 a3=0 origin x=-18.7310 y=-11.1270 z=265.8364
cylinder 32 7.62   0 -4.5
 rotate  a1=45 a2=90 a3=0 origin x=18.7310 y=-11.1270 z=174.3964
cylinder 33 3.962  0 -7.60
 rotate  a1=45 a2=90 a3=0 origin x=18.7310 y=-11.1270 z=174.3964
cylinder 34 7.62   0 -4.5
 rotate  a1=-45 a2=90 a3=0 origin x=-18.7310 y=-11.1270 z=174.3964
cylinder 35 3.962  0 -7.60
 rotate  a1=-45 a2=90 a3=0 origin x=-18.7310 y=-11.1270 z=174.3964
cylinder 36 7.62   0 -4.5
 rotate  a1=45 a2=90 a3=0 origin x=18.7310 y=-11.1270 z=128.6764
cylinder 37 3.962  0 -7.60
 rotate  a1=45 a2=90 a3=0 origin x=18.7310 y=-11.1270 z=128.6764
cylinder 38 7.62   0 -4.5
 rotate  a1=-45 a2=90 a3=0 origin x=-18.7310 y=-11.1270 z=128.6764
cylinder 39 3.962  0 -7.60
 rotate  a1=-45 a2=90 a3=0 origin x=-18.7310 y=-11.1270 z=128.6764
cylinder 40 7.62   0 -4.5
 rotate  a1=45 a2=90 a3=0 origin x=18.7310 y=-11.1270 z=82.9564
cylinder 41 3.962  0 -7.60
 rotate  a1=45 a2=90 a3=0 origin x=18.7310 y=-11.1270 z=82.9564
cylinder 42 7.62   0 -4.5
 rotate  a1=-45 a2=90 a3=0 origin x=-18.7310 y=-11.1270 z=82.9564
cylinder 43 3.962  0 -7.60
 rotate  a1=-45 a2=90 a3=0 origin x=-18.7310 y=-11.1270 z=82.9564
cylinder 44 7.62   0 -4.5
 rotate  a1=45 a2=90 a3=0 origin x=18.7310 y=-11.1270 z=37.2364
cylinder 45 3.962  0 -7.60
 rotate  a1=45 a2=90 a3=0 origin x=18.7310 y=-11.1270 z=37.2364
cylinder 46 7.62   0 -4.5
 rotate  a1=-45 a2=90 a3=0 origin x=-18.7310 y=-11.1270 z=37.2364
cylinder 47 3.962  0 -7.60
 rotate  a1=-45 a2=90 a3=0 origin x=-18.7310 y=-11.1270 z=37.2364
hole 11 rotate  a1=45 a2=0 a3=0  origin  x=0 y=-17.700 z=5.240
cuboid 48    18.174    20.079   10.4238  -9.5152    533.3990    -0.2660
rotate  a1=-45 a2=0 a3=0 origin x=0  y=-1.460 z=0
cuboid 49    13.6554  -10.4238  16.904    20.079    533.3990    -0.2660
rotate  a1=45 a2=0 a3=0 origin x=0  y=-1.460 z=0
cuboid 50    16.904    20.079   13.6554  -10.4238   533.3990    -0.2660
rotate  a1=45 a2=0 a3=0 origin x=0  y=-1.460 z=0
cuboid 51     9.5152  -10.4238 -18.174   -20.079    533.3990    -0.2660
```

Table 6-37C Input Deck for Partial Flooding Scenario #1 (cont.)

```
rotate  a1=-45 a2=0 a3=0 origin x=0  y=-1.460 z=0
cuboid 52    15.634    18.174   12.0238 -11.9197    533.3990    -0.2660
rotate  a1=-45 a2=0 a3=0 origin x=0  y=-1.460 z=0
cuboid 53    11.9197  -12.0238 -15.634   -18.174    533.3990    -0.2660
rotate  a1=-45 a2=0 a3=0 origin x=0  y=-1.460 z=0
media  0 1   1  15  3  5 -17 -19 -21 -23 -29 -31 -55 -57 -33 -35
-41 -43 -45 -47
media 15 1   1 -15  3  5 -17 -19 -21 -23 -29 -31 -55 -57 -33 -35
-41 -43 -45 -47
media  0 1  -1   3  5 -48 -49 -50 -51 -52 -53
media  9 1   3  -16  -17 -20 -21 -28 -29 -54 -55 -32 -33
-40 -41 -44 -45 48
media  9 1   3  -18  -19 -22 -23 -30 -31 -56 -57 -34 -35
-42 -43 -46 -47 51
media  9 1   3  -18  -22  -30  -56  -34  -42  -46  53
media  9 1   3  -16  -20  -28  -54  -32  -40  -44  52
media  9 1   3  49
media  9 1   3  50
media  8 1  -3   4   6
media  8 1   3  -5   6
media  6 1  -4   9
media  6 1   4  -6   9
media  6 1  -9  11
media  6 1  -7  10 -13
media  6 1   7  -8  10 -13  12
media  6 1 -10 -13  12
media 11 1 -11  13
media 11 1   7   8 -13  12
media  8 1 -12  14
media  0 1 16  -17 3 48
media  0 1 18  -19 3 51
media  0 1 20  -21 3 48
media  0 1 22  -23 3 51
media  0 1 28  -29 3 48
media  0 1 30  -31 3 51
media  0 1 54  -55 3 48
media  0 1 56  -57 3 51
media  0 1 32  -33 3 48
media  0 1 34  -35 3 51
media  0 1 40  -41 3 48
media  0 1 42  -43 3 51
media  0 1 44  -45 3 48
media  0 1 46  -47 3 51
media  0 1 16  -17 3 52
media 15 1 18  -19 3 53
media  0 1 20  -21 3 52
media 15 1 22  -23 3 53
media  0 1 28  -29 3 52
media 15 1 30  -31 3 53
media  0 1 54  -55 3 52
media 15 1 56  -57 3 53
```

Table 6-37C Input Deck for Partial Flooding Scenario #1 (cont.)

```
media  0 1 32  -33 3 52
media 15 1 34  -35 3 53
media  0 1 40  -41 3 52
media 15 1 42  -43 3 53
media  0 1 44  -45 3 52
media 15 1 46  -47 3 53
media 14 1 17  3
media 15 1 19  3
media 14 1 21  3
media 15 1 23  3
media 14 1 29  3
media 15 1 31  3
media 14 1 55  3
media 15 1 57  3
media 14 1 33  3
media 15 1 35  3
media 14 1 41  3
media 15 1 43  3
media 14 1 45  3
media 15 1 47  3
boundary 14

unit 11
com='fuel assembly confinement system'
cuboid 1    24.384       0 24.384       0 520.7000 2.5400
cuboid 2    25.337       -0.9525 25.337        -0.9525
 523.2400  0.0000
cuboid 3    19.812       4.572        24.429       -0.04545
 513.0800  3.81
cuboid 4    19.812       4.572        24.656       -0.27205
 513.0800  3.81
cuboid 5    19.812       4.572        24.702       -0.3175
 513.0800  3.81
cuboid 6    24.429       -0.04545      19.812       4.572
 513.0800  3.81
cuboid 7    24.656       -0.27205      19.812       4.572
 513.0800  3.81
cuboid 8    24.702       -0.3175       19.812       4.572
 513.0800  3.81
hole 20  origin  x=0  y=0  z=16.56  rotate  a1=0 a2=0 a3=0
media  0 1   1
media  7 1  -1   2  -5  -8
media  7 1  -1   3
media 12 1  -3   4
media  7 1  -4   5
media  7 1  -1   6
media 12 1  -6   7
media  7 1  -7   8
boundary 2
```

Table 6-37C Input Deck for Partial Flooding Scenario #1 (cont.)

```
unit 20
com='fuel assembly'
cuboid 1 21.072       0 21.072       0   0       -14.0208
cuboid 2 24.384       0 24.384       0 504.1392   -14.0208
hole 31 origin  x=0       y=0       z=0.0001   rotate  a1=0  a2=0 a3=0
hole 21 origin  x=0       y=0       z=100.0001 rotate  a1=0  a2=0 a3=0
hole 40 origin  x=0       y=0       z=426.7201 rotate  a1=0  a2=0 a3=0
media  15 1  1
media   0 1 -1   2
boundary 2

unit 21
com='fuel rods - nominal pitch'
cuboid 1  21.072       0 21.072       0 326.72       0.0000
array 2 1 place 1 1 1 0.4572       0.4572       0
boundary 1

unit 22
com='solid fuel rod - nominal pitch'
cylinder 1  0.39218       426.72          0
cylinder 2  0.40005      426.72          0
cylinder 3  0.4572       426.72          0
cuboid 4  4P0.62992       426.72          0
media 1 1  1
media 2 1  2 -1
media 3 1  3 -2 -1
media 4 1  4 -3 -2 -1
boundary 4

unit 23
com='thimble tube - nominal pitch'
cylinder 1  0.56134       426.72          0
cylinder 2  0.60198       426.72          0
cuboid 3    4P0.62992      426.72          0
media 4 1 1
media 3 1 2 -1
media 4 1 3 -2 -1
boundary 3

unit 31
com='fuel rods - expanded pitch'
cuboid 1  24.384       0 24.384       0 100          0
array 3 1 place 1 1 1 0.4572       0.4572       0
boundary 1

unit 32
com='solid fuel rod - expanded pitch'
cylinder 1  0.39218       426.72          0
cylinder 2  0.40005      426.72          0
cylinder 3  0.4572       426.72          0
cuboid 4  4P0.73342       426.72          0
media 16  1 1
```

Table 6-37C Input Deck for Partial Flooding Scenario #1 (cont.)

```
media 17  1 2 -1
media 18  1 3 -2 -1
media 19  1 4 -3 -2 -1
boundary 4

unit 33
com='thimble tube - expanded pitch'
cylinder 1  0.56134      426.72          0
cylinder 2  0.60198      426.72          0
cuboid 3  4P0.73342       426.72          0
media 19 1 1
media 18 1 2 -1
media 19 1 3 -2 -1
boundary 3

unit 40
com='top nozzle assembly'
cuboid 1     21.072       0 21.072       0       21.2090     0.0000
cuboid 2     21.072       0 21.072       0      41.8846     0.0000
cuboid 3     21.072       0 21.072       0       52.8193     0.0000
cuboid 4     21.072       0 21.072       0       77.4192     0.0000
cuboid 5     24.384       0 24.384       0       77.4192     0.0008
media  15 1   1
media  15 1  -1   2
media  15 1  -2   3
media  15 1  -3   4
media  15 1  -4   5
boundary 5

unit 66
com='individual package 0-deg rotation'
hexprism 1  31.75    554.1972  -20.1498
hole 10  origin  x=0 y=0  z=0  rotate  a1=0 a2=0 a3=0
media   0 1   1
boundary 1

unit 77
com='individual package 180-deg rotation'
hexprism 1  31.75    554.1972  -20.1498
hole 10  origin  x=0 y=0  z=0  rotate  a1=0 a2=0 a3=180
media   0 1   1
boundary 1

unit 88
com='dummy cell'
hexprism 1  31.75    554.1972  -20.1498
media  15 1   1
boundary 1

global
unit 99
```

Table 6-37C Input Deck for Partial Flooding Scenario #1 (cont.)

```
com='package array'
cylinder 1  432.2355   554.1972  -20.1498
cylinder 2  452.2355   574.1972  -40.1498
cuboid 3  452.2355  -452.2355  452.2355  -452.2355   574.1972  -40.1498
array 1 1  place 9 9 1 0 0 0
media  15 1  -1   2
media   0 1  -2   3
boundary 3

end geometry

read array
ara=1 typ=triangular nux=17 nuy=17 nuz=1 gbl=1
fill
88 88 88 88 88 88 88 88 88 88 88 88 88 88 88 88 88
  88 88 88 88 88 88 88 88 88 88 77 77 77 88 88 88 88
    88 88 88 88 88 88 88 88 66 66 66 66 66 66 66 88 88
      88 88 88 88 88 88 77 77 77 77 77 77 77 77 77 77 88
        88 88 88 88 88 66 66 66 66 66 66 66 66 66 66 66 88
          88 88 88 88 77 77 77 77 77 77 77 77 77 77 77 88
            88 88 88 66 66 66 66 66 66 66 66 66 66 66 66 88
              88 88 88 77 77 77 77 77 77 77 77 77 77 77 88 88
                88 88 66 66 66 66 66 66 66 66 66 66 66 66 88 88
                  88 88 77 77 77 77 77 77 77 77 77 77 77 88 88 88
                    88 66 66 66 66 66 66 66 66 66 66 66 66 88 88 88
                      88 77 77 77 77 77 77 77 77 77 77 77 88 88 88 88
                        88 66 66 66 66 66 66 66 66 66 66 66 88 88 88 88 88
                          88 77 77 77 77 77 77 77 77 77 77 88 88 88 88 88
                            88 88 66 66 66 66 66 66 66 88 88 88 88 88 88 88
                              88 88 88 77 77 77 77 88 88 88 88 88 88 88 88 88
                              88 88 88 88 88 88 88 88 88 88 88 88 88 88 88 88
end fill

ara=2 typ=square nux=17 nuy=17 nuz=1
fill 39*22 23 2*22 23 2*22 23 8*22 23 9*22 23 22*22 23 2*22 23 2*22 23
 2*22 23 2*22 23 38*22 23 2*22 23 2*22 23 2*22 23 2*22 23 38*22 23
 2*22 23 2*22 23 2*22 23 2*22 23 22*22 23 9*22 23 8*22 23 2*22 23 2*22
 23 39*22
end fill
ara=3 typ=square nux=17 nuy=17 nuz=1
fill 39*32 33 2*32 33 2*32 33 8*32 33 9*32 33 22*32 33 2*32 33 2*32 33
 2*32 33 2*32 33 38*32 33 2*32 33 2*32 33 2*32 33 2*32 33 38*32 33
 2*32 33 2*32 33 2*32 33 2*32 33 22*32 33 9*32 33 8*32 33 2*32 33 2*32
 33 39*32
end fill

end array

read bnds
+xb=vacuum
-xb=vacuum
```

Table 6-37C Input Deck for Partial Flooding Scenario #1 (cont.)

```
+yb=vacuum
-yb=vacuum
+zb=vacuum
-zb=vacuum
end bnds

end data
end
```

Table 6-37D Input Deck for Partial Flooding Scenario #2

```
=csas26     parm=size=300000
TRAVELLER XL,17WOFA,ENV=24.384      cm,L=100      cm,B10=0.018   g/cm2
44groupndf5  latticecell
 uo2 1 1 293 92235 5 92238 95 end
 h2o 2 1 293 end
 zirc4 3 1 293 end
 h2o 4 1 293 end
 h2o 5 1 293 end
 arbmfoam 0.1602e-20  4  0  0  0 6012 70 1001 10 8016 16 7014 4  6 1 293
 end
 al 7 1 293 end
 ss304 8 1 293 end
 polyethylene 9 DEN=0.828 1.0 293 end
 arbmfoam 0.1602e-20  4  0  0  0 6012 70 1001 10 8016 16 7014 4 11 1 293
 end
 b-10 12 0 0.0047781    end
 b-11 12 0 0.019398     end
 c   12 0 0.0060439    end
 al  12 0 0.043223     end
 arbmrubber 1.59e-20  7  0  0  0 8016 46.94 13000 19.92 14000 17.54 6012
 10.79 1001 4.73 11000 0.06 26000 0.02  14 1 293 end
 h2o 15 1 293 end
 uo2 16 1 293 92235 5 92238 95 end
 h2o 17 1 293 end
 zirc4 18 1 293 end
 h2o 19 1 293 end
uo2 20 1 293 92235 5 92238 95 end
 zirc4 21 1 293 end
 uo2 22 1 293 92235 5 92238 95 end
 zirc4 23 1 293 end
end comp
squarepitch 1.4669       0.78435      16 19 0.9144       18 0.8001       17 end
more data
res=1  cylinder 0.39218      dan(1)=0.22632
res=20 cylinder 0.39218      dan(20)=9.6506941E-01
res=22 cylinder 0.39218      dan(22)=9.7027081E-01 end

read parameter
gen=450
npg=2500
nsk=50
wrs=1
tme=240
end parameter
```

Table 6-37D Input Deck for Partial Flooding Scenario #2 (cont.)

```
read geometry
unit 10
com='individual package'
cuboid 1    16.904       -15.634       16.904       -15.634       533.1330 0
rotate  a1=45 a2=0 a3=0 origin x=0  y=-1.460 z=0
cuboid 2     21.5900   -21.5900     1.5720    -1.0310   533.1330     0
cuboid 3     20.0790   -20.0790    20.0790   -20.0790   533.1330     0
rotate  a1=45 a2=0 a3=0 origin x=0  y=-1.460 z=0
cuboid 4     20.3450   -20.3450    20.3450   -20.3450   533.3990    -0.2660
rotate  a1=45 a2=0 a3=0 origin x=0  y=-1.460 z=0
cuboid 5     21.5900   -21.590     23.1498   -23.1498   533.1330     0
cuboid 6     21.8560   -21.8560    23.4158   -23.4158   533.3990    -0.2660
cuboid 7     20.3840   -20.3840    20.3840   -20.3840   553.8922   -19.8448
rotate  a1=45 a2=0 a3=0 origin x=0  y=-1.460 z=0
cuboid 8     21.8950   -21.895     23.4548   -23.4548   553.8922   -19.8448
cylinder  9    25.1050    533.4380    -0.2660
cylinder 10    25.1050    553.9312   -19.8448
cylinder 11    31.4840    533.4380    -0.2660
cylinder 12    31.4840    553.9312   -19.8448
cylinder 13    31.4840    533.4380   -19.8448
cylinder 14    31.7500    554.1972   -20.1100
plane 15  xpl=1 ypl=1  con=-13.02668
cylinder 16 7.62   0 -4.5
 rotate  a1=45 a2=90 a3=0 origin x=18.7310 y=-11.1270 z=494.4364
cylinder 17 3.962  0 -7.60
 rotate  a1=45 a2=90 a3=0 origin x=18.7310 y=-11.1270 z=494.4364
cylinder 18 7.62   0 -4.5
 rotate  a1=-45 a2=90 a3=0 origin x=-18.7310 y=-11.1270 z=494.4364
cylinder 19 3.962  0 -7.60
 rotate  a1=-45 a2=90 a3=0 origin x=-18.7310 y=-11.1270 z=494.4364
cylinder 20 7.62   0 -4.5
 rotate  a1=45 a2=90 a3=0 origin x=18.7310 y=-11.1270 z=448.7164
cylinder 21 3.962  0 -7.60
 rotate  a1=45 a2=90 a3=0 origin x=18.7310 y=-11.1270 z=448.7164
cylinder 22 7.62   0 -4.5
 rotate  a1=-45 a2=90 a3=0 origin x=-18.7310 y=-11.1270 z=448.7164
cylinder 23 3.962  0 -7.60
 rotate  a1=-45 a2=90 a3=0 origin x=-18.7310 y=-11.1270 z=448.7164
cylinder 24 7.62   0 -4.5
 rotate  a1=45 a2=90 a3=0 origin x=18.7310 y=-11.1270 z=402.9964
cylinder 25 3.962  0 -7.60
 rotate  a1=45 a2=90 a3=0 origin x=18.7310 y=-11.1270 z=402.9964
cylinder 26 7.62   0 -4.5
 rotate  a1=-45 a2=90 a3=0 origin x=-18.7310 y=-11.1270 z=402.9964
cylinder 27 3.962  0 -7.60
 rotate  a1=-45 a2=90 a3=0 origin x=-18.7310 y=-11.1270 z=402.9964
cylinder 28 7.62   0 -4.5
 rotate  a1=45 a2=90 a3=0 origin x=18.7310 y=-11.1270 z=357.2764
cylinder 29 3.962  0 -7.60
 rotate  a1=45 a2=90 a3=0 origin x=18.7310 y=-11.1270 z=357.2764
cylinder 30 7.62   0 -4.5
```

Table 6-37D Input Deck for Partial Flooding Scenario #2 (cont.)

```
 rotate  a1=-45 a2=90 a3=0 origin x=-18.7310 y=-11.1270 z=357.2764
cylinder 31 3.962  0 -7.60
 rotate  a1=-45 a2=90 a3=0 origin x=-18.7310 y=-11.1270 z=357.2764
cylinder 54 7.62   0 -4.5
 rotate  a1=45 a2=90 a3=0 origin x=18.7310 y=-11.1270 z=265.8364
cylinder 55 3.962  0 -7.60
 rotate  a1=45 a2=90 a3=0 origin x=18.7310 y=-11.1270 z=265.8364
cylinder 56 7.62   0 -4.5
 rotate  a1=-45 a2=90 a3=0 origin x=-18.7310 y=-11.1270 z=265.8364
cylinder 57 3.962  0 -7.60
 rotate  a1=-45 a2=90 a3=0 origin x=-18.7310 y=-11.1270 z=265.8364
cylinder 32 7.62   0 -4.5
 rotate  a1=45 a2=90 a3=0 origin x=18.7310 y=-11.1270 z=174.3964
cylinder 33 3.962  0 -7.60
 rotate  a1=45 a2=90 a3=0 origin x=18.7310 y=-11.1270 z=174.3964
cylinder 34 7.62   0 -4.5
 rotate  a1=-45 a2=90 a3=0 origin x=-18.7310 y=-11.1270 z=174.3964
cylinder 35 3.962  0 -7.60
 rotate  a1=-45 a2=90 a3=0 origin x=-18.7310 y=-11.1270 z=174.3964
cylinder 36 7.62   0 -4.5
 rotate  a1=45 a2=90 a3=0 origin x=18.7310 y=-11.1270 z=128.6764
cylinder 37 3.962  0 -7.60
 rotate  a1=45 a2=90 a3=0 origin x=18.7310 y=-11.1270 z=128.6764
cylinder 38 7.62   0 -4.5
 rotate  a1=-45 a2=90 a3=0 origin x=-18.7310 y=-11.1270 z=128.6764
cylinder 39 3.962  0 -7.60
 rotate  a1=-45 a2=90 a3=0 origin x=-18.7310 y=-11.1270 z=128.6764
cylinder 40 7.62   0 -4.5
 rotate  a1=45 a2=90 a3=0 origin x=18.7310 y=-11.1270 z=82.9564
cylinder 41 3.962  0 -7.60
 rotate  a1=45 a2=90 a3=0 origin x=18.7310 y=-11.1270 z=82.9564
cylinder 42 7.62   0 -4.5
 rotate  a1=-45 a2=90 a3=0 origin x=-18.7310 y=-11.1270 z=82.9564
cylinder 43 3.962  0 -7.60
 rotate  a1=-45 a2=90 a3=0 origin x=-18.7310 y=-11.1270 z=82.9564
cylinder 44 7.62   0 -4.5
 rotate  a1=45 a2=90 a3=0 origin x=18.7310 y=-11.1270 z=37.2364
cylinder 45 3.962  0 -7.60
 rotate  a1=45 a2=90 a3=0 origin x=18.7310 y=-11.1270 z=37.2364
cylinder 46 7.62   0 -4.5
 rotate  a1=-45 a2=90 a3=0 origin x=-18.7310 y=-11.1270 z=37.2364
cylinder 47 3.962  0 -7.60
 rotate  a1=-45 a2=90 a3=0 origin x=-18.7310 y=-11.1270 z=37.2364
hole 11 rotate  a1=45 a2=0 a3=0  origin  x=0 y=-17.700 z=5.240
cuboid 48    18.174    20.079   10.4238  -9.5152    533.3990    -0.2660
rotate  a1=-45 a2=0 a3=0 origin x=0  y=-1.460 z=0
cuboid 49    13.6554  -10.4238  16.904    20.079    533.3990    -0.2660
rotate  a1=45 a2=0 a3=0 origin x=0  y=-1.460 z=0
cuboid 50    16.904    20.079   13.6554  -10.4238   533.3990    -0.2660
rotate  a1=45 a2=0 a3=0 origin x=0  y=-1.460 z=0
cuboid 51     9.5152  -10.4238 -18.174   -20.079    533.3990    -0.2660
```

Table 6-37D Input Deck for Partial Flooding Scenario #2 (cont.)

```
rotate  a1=-45 a2=0 a3=0 origin x=0  y=-1.460 z=0
cuboid 52    15.634    18.174   12.0238 -11.9197    533.3990    -0.2660
rotate  a1=-45 a2=0 a3=0 origin x=0  y=-1.460 z=0
cuboid 53    11.9197  -12.0238 -15.634   -18.174    533.3990    -0.2660
rotate  a1=-45 a2=0 a3=0 origin x=0  y=-1.460 z=0
media  0 1   1  15  3  5 -17 -19 -21 -23 -29 -31 -55 -57 -33 -35
-41 -43 -45 -47
media 15 1   1 -15  3  5 -17 -19 -21 -23 -29 -31 -55 -57 -33 -35
-41 -43 -45 -47
media  0 1  -1   3  5 -48 -49 -50 -51 -52 -53
media  9 1   3  -16  -17 -20 -21 -28 -29 -54 -55 -32 -33
-40 -41 -44 -45 48
media  9 1   3  -18  -19 -22 -23 -30 -31 -56 -57 -34 -35
-42 -43 -46 -47 51
media  9 1   3  -18  -22  -30  -56  -34  -42  -46  53
media  9 1   3  -16  -20  -28  -54  -32  -40  -44  52
media  9 1   3  49
media  9 1   3  50
media  8 1  -3   4   6
media  8 1   3  -5   6
media  6 1  -4   9
media  6 1   4  -6   9
media  6 1  -9  11
media  6 1  -7  10 -13
media  6 1   7  -8  10 -13  12
media  6 1 -10 -13  12
media 11 1 -11  13
media 11 1   7   8 -13  12
media  8 1 -12  14
media  0 1 16  -17 3 48
media  0 1 18  -19 3 51
media  0 1 20  -21 3 48
media  0 1 22  -23 3 51
media  0 1 28  -29 3 48
media  0 1 30  -31 3 51
media  0 1 54  -55 3 48
media  0 1 56  -57 3 51
media  0 1 32  -33 3 48
media  0 1 34  -35 3 51
media  0 1 40  -41 3 48
media  0 1 42  -43 3 51
media  0 1 44  -45 3 48
media  0 1 46  -47 3 51
media  0 1 16  -17 3 52
media 15 1 18  -19 3 53
media 15 1 20  -21 3 52
media 15 1 22  -23 3 53
media 15 1 28  -29 3 52
media 15 1 30  -31 3 53
media 15 1 54  -55 3 52
media 15 1 56  -57 3 53
```

Table 6-37D Input Deck for Partial Flooding Scenario #2 (cont.)

```
media 15 1 32  -33 3 52
media 15 1 34  -35 3 53
media 15 1 40  -41 3 52
media 15 1 42  -43 3 53
media 15 1 44  -45 3 52
media 15 1 46  -47 3 53
media 15 1 17  3
media 15 1 19  3
media 15 1 21  3
media 15 1 23  3
media 15 1 29  3
media 15 1 31  3
media 15 1 55  3
media 15 1 57  3
media 15 1 33  3
media 15 1 35  3
media 15 1 41  3
media 15 1 43  3
media 15 1 45  3
media 15 1 47  3
boundary 14

unit 11
com='fuel assembly confinement system'
cuboid 1    24.384       0 24.384       0 520.7000 2.5400
cuboid 2    25.337       -0.9525 25.337        -0.9525
 523.2400  0.0000
cuboid 3    19.812       4.572        24.429       -0.04545
 513.0800  3.81
cuboid 4    19.812       4.572        24.656       -0.27205
 513.0800  3.81
cuboid 5    19.812       4.572        24.702       -0.3175
 513.0800  3.81
cuboid 6    24.429       -0.04545      19.812       4.572
 513.0800  3.81
cuboid 7    24.656       -0.27205      19.812       4.572
 513.0800  3.81
cuboid 8    24.702       -0.3175       19.812       4.572
 513.0800  3.81
hole 20  origin  x=0  y=0  z=16.56  rotate  a1=0 a2=0 a3=0
media  0 1   1
media  7 1  -1   2  -5  -8
media  7 1  -1   3
media 12 1  -3   4
media  7 1  -4   5
media  7 1  -1   6
media 12 1  -6   7
media  7 1  -7   8
boundary 2
```

Table 6-37D Input Deck for Partial Flooding Scenario #2 (cont.)

```
unit 20
com='fuel assembly'
cuboid 1 21.072       0 21.072       0   0       -14.0208
cuboid 2 24.384       0 24.384       0   0       -14.0208
cuboid 3 24.384       0 24.384       0 504.1392   -14.0208
cuboid 4 21.072       0 21.072       0 504.1392   100.0002
cuboid 5 24.384       0 24.384       0 504.1392   100.0002
plane  6 xpl=1  con=-21.72638
hole 31 origin  x=0       y=0       z=0.0001   rotate  a1=0  a2=0 a3=0
hole 21 origin  x=0       y=0       z=100.0001 rotate  a1=0  a2=0 a3=0
hole 40 origin  x=0       y=0       z=426.7201 rotate  a1=0  a2=0 a3=0
media  15 1  1
media  15 1 -1   2  -6
media   0 1 -1   2   6
media   0 1  4
media  15 1 -4   5  -6
media   0 1 -4   5   6
media   0 1 -2  -5   3
boundary 3

unit 21
com='fuel rods - nominal pitch'
cuboid 1  21.072       0 21.072       0 326.72       0.0000
array 2 1 place 1 1 1 0.4572       0.4572       0
boundary 1

unit 22
com='solid fuel rod - nominal pitch'
cylinder 1  0.39218       426.72          0
cylinder 2  0.40005      426.72          0
cylinder 3  0.4572       426.72          0
cuboid 4  4P0.62992       426.72          0
media 1 1  1
media 2 1  2 -1
media 3 1  3 -2 -1
media 4 1  4 -3 -2 -1
boundary 4

unit 23
com='thimble tube - nominal pitch'
cylinder 1  0.56134       426.72          0
cylinder 2  0.60198       426.72          0
cuboid 3    4P0.62992      426.72          0
media 4 1 1
media 3 1 2 -1
media 4 1 3 -2 -1
boundary 3

unit 24
com='solid fuel rod - nominal pitch - dry'
cylinder 1  0.39218       426.72          0
cylinder 2  0.40005      426.72          0
```

Table 6-37D Input Deck for Partial Flooding Scenario #2 (cont.)

```
cylinder 3  0.4572       426.72          0
cuboid 4  4P0.62992       426.72          0
media 20 1  1
media 0 1  2 -1
media 21 1  3 -2 -1
media 0 1  4 -3 -2 -1
boundary 4

unit 25
com='thimble tube - nominal pitch - dry'
cylinder 1  0.56134       426.72          0
cylinder 2  0.60198       426.72          0
cuboid 3    4P0.62992      426.72          0
media 0 1 1
media 21 1 2 -1
media 0 1 3 -2 -1
boundary 3

unit 31
com='fuel rods - expanded pitch'
cuboid 1  24.384       0 24.384       0 100          0
array 3 1 place 1 1 1 0.4572       0.4572       0
boundary 1

unit 32
com='solid fuel rod - expanded pitch'
cylinder 1  0.39218       426.72          0
cylinder 2  0.40005      426.72          0
cylinder 3  0.4572       426.72          0
cuboid 4  4P0.73342       426.72          0
media 16  1 1
media 17  1 2 -1
media 18  1 3 -2 -1
media 19  1 4 -3 -2 -1
boundary 4

unit 33
com='thimble tube - expanded pitch'
cylinder 1  0.56134      426.72          0
cylinder 2  0.60198      426.72          0
cuboid 3  4P0.73342       426.72          0
media 19 1 1
media 18 1 2 -1
media 19 1 3 -2 -1
boundary 3

unit 34
com='solid fuel rod - expanded pitch - dry'
cylinder 1  0.39218       426.72          0
cylinder 2  0.40005      426.72          0
cylinder 3  0.4572       426.72          0
```

Table 6-37D Input Deck for Partial Flooding Scenario #2 (cont.)

```
cuboid 4  4P0.73342       426.72          0
media 22  1 1
media  0  1 2 -1
media 23  1 3 -2 -1
media  0  1 4 -3 -2 -1
boundary 4

unit 35
com='thimble tube - expanded pitch - dry'
cylinder 1  0.56134      426.72          0
cylinder 2  0.60198      426.72          0
cuboid 3  4P0.73342       426.72          0
media  0 1 1
media 23 1 2 -1
media  0 1 3 -2 -1
boundary 3

unit 40
com='top nozzle assembly'
cuboid 1     21.072       0 21.072       0       21.2090     0.0000
cuboid 2     21.072       0 21.072       0      41.8846     0.0000
cuboid 3     21.072       0 21.072       0       52.8193     0.0000
cuboid 4     21.072       0 21.072       0       77.4192     0.0000
cuboid 5     24.384       0 24.384       0       77.4192     0.0008
media  15 1   1
media  15 1  -1   2
media  15 1  -2   3
media  15 1  -3   4
media  15 1  -4   5
boundary 5

unit 66
com='individual package 0-deg rotation'
hexprism 1  31.75    554.1972  -20.1498
hole 10  origin  x=0 y=0  z=0  rotate  a1=0 a2=0 a3=0
media   0 1   1
boundary 1

unit 77
com='individual package 180-deg rotation'
hexprism 1  31.75    554.1972  -20.1498
hole 10  origin  x=0 y=0  z=0  rotate  a1=0 a2=0 a3=180
media   0 1   1
boundary 1

unit 88
com='dummy cell'
hexprism 1  31.75    554.1972  -20.1498
media  15 1   1
boundary 1
```

Table 6-37D Input Deck for Partial Flooding Scenario #2 (cont.)

```
global
unit 99
com='package array'
cylinder 1  432.2355   554.1972  -20.1498
cylinder 2  452.2355   574.1972  -40.1498
cuboid 3  452.2355  -452.2355  452.2355  -452.2355   574.1972  -40.1498
array 1 1  place 9 9 1 0 0 0
media  15 1  -1   2
media   0 1  -2   3
boundary 3

end geometry

read array
ara=1 typ=triangular nux=17 nuy=17 nuz=1 gbl=1
fill
88 88 88 88 88 88 88 88 88 88 88 88 88 88 88 88 88
  88 88 88 88 88 88 88 88 88 88 77 77 77 88 88 88 88
    88 88 88 88 88 88 88 88 66 66 66 66 66 66 66 88 88
      88 88 88 88 88 88 77 77 77 77 77 77 77 77 77 77 88
        88 88 88 88 88 66 66 66 66 66 66 66 66 66 66 66 88
          88 88 88 88 77 77 77 77 77 77 77 77 77 77 77 77 88
            88 88 88 66 66 66 66 66 66 66 66 66 66 66 66 66 88
              88 88 88 77 77 77 77 77 77 77 77 77 77 77 77 88 88
                88 88 66 66 66 66 66 66 66 66 66 66 66 66 66 88 88
                  88 88 77 77 77 77 77 77 77 77 77 77 77 77 88 88 88
                    88 66 66 66 66 66 66 66 66 66 66 66 66 66 88 88 88
                      88 77 77 77 77 77 77 77 77 77 77 77 77 88 88 88 88
                        88 66 66 66 66 66 66 66 66 66 66 66 88 88 88 88 88
                          88 77 77 77 77 77 77 77 77 77 77 88 88 88 88 88 88
                            88 88 66 66 66 66 66 66 66 88 88 88 88 88 88 88 88
                             88 88 88 77 77 77 77 88 88 88 88 88 88 88 88 88 88
                             88 88 88 88 88 88 88 88 88 88 88 88 88 88 88 88 88
end fill

ara=2 typ=square nux=17 nuy=17 nuz=1
fill
22 22 22 22 22 22 22 22 22 22 22 22 22 22 22 22 22
22 22 22 22 22 22 22 22 22 22 22 22 22 22 22 22 22
22 22 22 22 22 23 22 22 23 22 22 23 22 22 22 22 22
22 22 22 23 22 22 22 22 22 22 22 22 22 23 22 22 22
22 22 22 22 22 22 22 22 22 22 22 22 22 22 22 22 22
22 22 23 22 22 23 22 22 23 22 22 23 22 22 23 22 22
22 22 22 22 22 22 22 22 22 22 22 22 22 22 22 22 22
22 22 22 22 22 22 22 22 22 22 22 22 22 22 22 22 22
22 22 23 22 22 23 22 22 23 22 22 23 22 22 23 22 22
22 22 22 22 22 22 22 22 22 22 22 22 22 22 22 22 22
22 22 22 22 22 22 22 22 22 22 22 22 22 22 22 22 22
22 22 23 22 22 23 22 22 23 22 22 23 22 22 23 22 22
22 22 22 22 22 22 22 22 22 22 22 22 22 22 22 22 22
22 22 22 23 22 22 22 22 22 22 22 22 22 23 22 22 22
```

Table 6-37D Input Deck for Partial Flooding Scenario #2 (cont.)

```
22 22 22 22 22 23 22 22 23 22 22 23 22 22 22 22 22
22 22 22 22 22 22 22 22 22 22 22 22 22 22 22 22 22
22 22 22 22 22 22 22 22 22 22 22 22 22 22 22 22 22
end fill
ara=3 typ=square nux=17 nuy=17 nuz=1
fill
32 32 32 32 32 32 32 32 32 32 32 32 32 32 32 34 34
32 32 32 32 32 32 32 32 32 32 32 32 32 32 32 34 34
32 32 32 32 32 33 32 32 33 32 32 33 32 32 32 34 34
32 32 32 33 32 32 32 32 32 32 32 32 32 33 32 34 34
32 32 32 32 32 32 32 32 32 32 32 32 32 32 32 34 34
32 32 33 32 32 33 32 32 33 32 32 33 32 32 33 34 34
32 32 32 32 32 32 32 32 32 32 32 32 32 32 32 34 34
32 32 32 32 32 32 32 32 32 32 32 32 32 32 32 34 34
32 32 33 32 32 33 32 32 33 32 32 33 32 32 33 34 34
32 32 32 32 32 32 32 32 32 32 32 32 32 32 32 34 34
32 32 32 32 32 32 32 32 32 32 32 32 32 32 32 34 34
32 32 33 32 32 33 32 32 33 32 32 33 32 32 33 34 34
32 32 32 32 32 32 32 32 32 32 32 32 32 32 32 34 34
32 32 32 33 32 32 32 32 32 32 32 32 32 33 32 34 34
32 32 32 32 32 33 32 32 33 32 32 33 32 32 32 34 34
32 32 32 32 32 32 32 32 32 32 32 32 32 32 32 34 34
32 32 32 32 32 32 32 32 32 32 32 32 32 32 32 34 34
end fill

end array

read bnds
+xb=vacuum
-xb=vacuum
+yb=vacuum
-yb=vacuum
+zb=vacuum
-zb=vacuum
end bnds

end data
end
```

6.10.9.3 Annular Pellet Study Data

Table 6-37E Results for Annular Pellet Study

Run #	ks	σks	σks
PA-HAC-ANNULAR	0.9274	0.0008	0.9290

Table 6-37F Input Deck for Annular Pellet Study

```
=csas26     parm=size=300000
TRAVELLER XL,17WOFA,ENV=24.384      cm,L=100      cm,B10=0.018   g/cm2
44groupndf5  latticecell
 uo2 1 1 293 92235 5 92238 95 end
 h2o 2 1 293 end
 zirc4 3 1 293 end
 h2o 4 1 293 end
 h2o 5 1 293 end
 arbmfoam 0.1602e-20  4  0  0  0 6012 70 1001 10 8016 16 7014 4  6 1 293
 end
 al 7 1 293 end
 ss304 8 1 293 end
 polyethylene 9 DEN=0.828 1.0 293 end
 arbmfoam 0.1602e-20  4  0  0  0 6012 70 1001 10 8016 16 7014 4 11 1 293
 end
 b-10 12 0 0.0047781    end
 b-11 12 0 0.019398     end
 c   12 0 0.0060439    end
 al  12 0 0.043223     end
 arbmrubber 1.59e-20  7  0  0  0 8016 46.94 13000 19.92 14000 17.54 6012
 10.79 1001 4.73 11000 0.06 26000 0.02  14 1 293 end
 h2o 15 1 293 end
 uo2 16 1 293 92235 5 92238 95 end
 h2o 17 1 293 end
 zirc4 18 1 293 end
 h2o 19 1 293 end
 uo2 20 1 293 92235 5 92238 95 end
 zirc4 21 1 293 end
 uo2 22 1 293 92235 5 92238 95 end
 zirc4 23 1 293 end
end comp
squarepitch 1.4669       0.78435      16 19 0.9144       18 0.8001       17 end
more data
res=1  cylinder 0.39218      dan(1)=0.22632
RES=21 CYLINDER 0.39218 0.19685
DAN(21)=0.28016729
RES=22 CYLINDER 0.4572 0.40005
DAN(22)=0.37575367
RES=23 CYLINDER 0.39218 0.19685
DAN(23)=0.34480012
RES=24 CYLINDER 0.4572 0.40005
DAN(24)=0.43692386 end
```

Table 6-37F Input Deck for Annular Pellet Study (cont.)

```
read parameter
gen=450
npg=2500
nsk=50
wrs=1
end parameter

read geometry
unit 10
com='individual package'
cuboid 1    16.904      -15.634      16.904      -15.634      533.1330 0
rotate  a1=45 a2=0 a3=0 origin x=0  y=-1.460 z=0
cuboid 2    21.5900   -21.5900    1.5720    -1.0310   533.1330    0
cuboid 3    20.0790   -20.0790    20.0790   -20.0790   533.1330    0
rotate  a1=45 a2=0 a3=0 origin x=0  y=-1.460 z=0
cuboid 4    20.3450   -20.3450    20.3450   -20.3450   533.3990    -0.2660
rotate  a1=45 a2=0 a3=0 origin x=0  y=-1.460 z=0
cuboid 5    21.5900   -21.590     23.1498   -23.1498   533.1330    0
cuboid 6    21.8560   -21.8560    23.4158   -23.4158   533.3990    -0.2660
cuboid 7    20.3840   -20.3840    20.3840   -20.3840   553.8922   -19.8448
rotate  a1=45 a2=0 a3=0 origin x=0  y=-1.460 z=0
cuboid 8    21.8950   -21.895     23.4548   -23.4548   553.8922   -19.8448
cylinder  9    25.1050    533.4380    -0.2660
cylinder 10    25.1050    553.9312   -19.8448
cylinder 11    31.4840    533.4380    -0.2660
cylinder 12    31.4840    553.9312   -19.8448
cylinder 13    31.4840    533.4380   -19.8448
cylinder 14    31.7500    554.1972   -20.1100
plane 15  zpl=1  con= -10.0000
cylinder 16 7.62   0 -4.5
 rotate  a1=45 a2=90 a3=0 origin x=18.7310 y=-11.1270 z=494.4364
cylinder 17 3.962  0 -7.60
 rotate  a1=45 a2=90 a3=0 origin x=18.7310 y=-11.1270 z=494.4364
cylinder 18 7.62   0 -4.5
 rotate  a1=-45 a2=90 a3=0 origin x=-18.7310 y=-11.1270 z=494.4364
cylinder 19 3.962  0 -7.60
 rotate  a1=-45 a2=90 a3=0 origin x=-18.7310 y=-11.1270 z=494.4364
cylinder 20 7.62   0 -4.5
 rotate  a1=45 a2=90 a3=0 origin x=18.7310 y=-11.1270 z=448.7164
cylinder 21 3.962  0 -7.60
 rotate  a1=45 a2=90 a3=0 origin x=18.7310 y=-11.1270 z=448.7164
cylinder 22 7.62   0 -4.5
 rotate  a1=-45 a2=90 a3=0 origin x=-18.7310 y=-11.1270 z=448.7164
cylinder 23 3.962  0 -7.60
 rotate  a1=-45 a2=90 a3=0 origin x=-18.7310 y=-11.1270 z=448.7164
cylinder 24 7.62   0 -4.5
 rotate  a1=45 a2=90 a3=0 origin x=18.7310 y=-11.1270 z=402.9964
cylinder 25 3.962  0 -7.60
 rotate  a1=45 a2=90 a3=0 origin x=18.7310 y=-11.1270 z=402.9964
cylinder 26 7.62   0 -4.5
```

Table 6-37F Input Deck for Annular Pellet Study (cont.)

```
 rotate  a1=-45 a2=90 a3=0 origin x=-18.7310 y=-11.1270 z=402.9964
cylinder 27 3.962  0 -7.60
 rotate  a1=-45 a2=90 a3=0 origin x=-18.7310 y=-11.1270 z=402.9964
cylinder 28 7.62   0 -4.5
 rotate  a1=45 a2=90 a3=0 origin x=18.7310 y=-11.1270 z=357.2764
cylinder 29 3.962  0 -7.60
 rotate  a1=45 a2=90 a3=0 origin x=18.7310 y=-11.1270 z=357.2764
cylinder 30 7.62   0 -4.5
 rotate  a1=-45 a2=90 a3=0 origin x=-18.7310 y=-11.1270 z=357.2764
cylinder 31 3.962  0 -7.60
 rotate  a1=-45 a2=90 a3=0 origin x=-18.7310 y=-11.1270 z=357.2764
cylinder 32 7.62   0 -4.5
 rotate  a1=45 a2=90 a3=0 origin x=18.7310 y=-11.1270 z=174.3964
cylinder 33 3.962  0 -7.60
 rotate  a1=45 a2=90 a3=0 origin x=18.7310 y=-11.1270 z=174.3964
cylinder 34 7.62   0 -4.5
 rotate  a1=-45 a2=90 a3=0 origin x=-18.7310 y=-11.1270 z=174.3964
cylinder 35 3.962  0 -7.60
 rotate  a1=-45 a2=90 a3=0 origin x=-18.7310 y=-11.1270 z=174.3964
cylinder 36 7.62   0 -4.5
 rotate  a1=45 a2=90 a3=0 origin x=18.7310 y=-11.1270 z=128.6764
cylinder 37 3.962  0 -7.60
 rotate  a1=45 a2=90 a3=0 origin x=18.7310 y=-11.1270 z=128.6764
cylinder 38 7.62   0 -4.5
 rotate  a1=-45 a2=90 a3=0 origin x=-18.7310 y=-11.1270 z=128.6764
cylinder 39 3.962  0 -7.60
 rotate  a1=-45 a2=90 a3=0 origin x=-18.7310 y=-11.1270 z=128.6764
cylinder 40 7.62   0 -4.5
 rotate  a1=45 a2=90 a3=0 origin x=18.7310 y=-11.1270 z=82.9564
cylinder 41 3.962  0 -7.60
 rotate  a1=45 a2=90 a3=0 origin x=18.7310 y=-11.1270 z=82.9564
cylinder 42 7.62   0 -4.5
 rotate  a1=-45 a2=90 a3=0 origin x=-18.7310 y=-11.1270 z=82.9564
cylinder 43 3.962  0 -7.60
 rotate  a1=-45 a2=90 a3=0 origin x=-18.7310 y=-11.1270 z=82.9564
cylinder 44 7.62   0 -4.5
 rotate  a1=45 a2=90 a3=0 origin x=18.7310 y=-11.1270 z=37.2364
cylinder 45 3.962  0 -7.60
 rotate  a1=45 a2=90 a3=0 origin x=18.7310 y=-11.1270 z=37.2364
cylinder 46 7.62   0 -4.5
 rotate  a1=-45 a2=90 a3=0 origin x=-18.7310 y=-11.1270 z=37.2364
cylinder 47 3.962  0 -7.60
 rotate  a1=-45 a2=90 a3=0 origin x=-18.7310 y=-11.1270 z=37.2364
hole 11 rotate  a1=45 a2=0 a3=0  origin  x=0 y=-17.700 z=5.240
media  0 1   2
media  0 1  -2   1   5  -17 -19 -21 -23 -25 -27 -29 -31 -33 -35 -37
-39 -41 -43 -45 -47
media  9 1  -1   3   5  -2 -16 -18 -20 -22 -24 -26 -28 -30 -32 -34 -36
-38 -40 -42 -44 -46 -17 -19 -21 -23 -25 -27 -29 -31 -33 -35 -37
-39 -41 -43 -45 -47
media  8 1  -3   4   6
```

Table 6-37F Input Deck for Annular Pellet Study (cont.)

```
media  8 1   3  -5   6
media  6 1  -4   9
media  6 1   4  -6   9
media  6 1  -9  11
media  6 1  -7  10 -13
media  6 1   7  -8  10 -13  12
media  6 1 -10 -13  12
media 11 1 -11  13
media 11 1   7   8 -13  12
media  8 1  -12 14
media  0 1 16  -17  5  -1  3
media  0 1 18  -19  5  -1  3
media  0 1 20  -21  5  -1  3
media  0 1 22  -23  5  -1  3
media  0 1 24  -25  5  -1  3
media  0 1 26  -27  5  -1  3
media  0 1 28  -29  5  -1  3
media  0 1 30  -31  5  -1  3
media  0 1 32  -33  5  -1  3
media  0 1 34  -35  5  -1  3
media  0 1 36  -37  5  -1  3
media  0 1 38  -39  5  -1  3
media  0 1 40  -41  5  -1  3
media  0 1 42  -43  5  -1  3
media  0 1 44  -45  5  -1  3
media  0 1 46  -47  5  -1  3
media 14 1 17  3
media 14 1 19  3
media 14 1 21  3
media 14 1 23  3
media 14 1 25  3
media 14 1 27  3
media 14 1 29  3
media 14 1 31  3
media 14 1 33  3
media 14 1 35  3
media 14 1 37  3
media 14 1 39  3
media 14 1 41  3
media 14 1 43  3
media 14 1 45  3
media 14 1 47  3
boundary 14

unit 11
com='fuel assembly confinement system'
cuboid 1    24.384       0 24.384       0 520.7000 2.5400
cuboid 2    25.337       -0.9525 25.337        -0.9525
 523.2400  0.0000
cuboid 3    19.812       4.572        24.429       -0.04545
 513.0800  3.81
```

Table 6-37F Input Deck for Annular Pellet Study (cont.)

```
cuboid 4    19.812      4.572       24.656      -0.27205
 513.0800  3.81
cuboid 5    19.812      4.572       24.702      -0.3175
 513.0800  3.81
cuboid 6    24.429      -0.04545     19.812      4.572
 513.0800  3.81
cuboid 7    24.656      -0.27205     19.812      4.572
 513.0800  3.81
cuboid 8    24.702      -0.3175      19.812      4.572
 513.0800  3.81
hole 20  origin  x=0  y=0  z=16.56  rotate  a1=0 a2=0 a3=0
media  0 1   1
media  7 1  -1   2  -5  -8
media  7 1  -1   3
media 12 1  -3   4
media  7 1  -4   5
media  7 1  -1   6
media 12 1  -6   7
media  7 1  -7   8
boundary 2

unit 20
com='fuel assembly'
cuboid 1 21.072       0 21.072       0   0       -14.0208
cuboid 2 24.384       0 24.384       0 504.1392   -14.0208
hole 34 origin  x=0       y=0       z=0.0001   rotate  a1=0  a2=0 a3=0
hole 31 origin  x=0       y=0       z=30.4802  rotate  a1=0  a2=0 a3=0
hole 21 origin  x=0       y=0       z=100.0003 rotate  a1=0  a2=0 a3=0
hole 24 origin  x=0       y=0       z=396.2404 rotate  a1=0  a2=0 a3=0
hole 40 origin  x=0       y=0       z=426.7205 rotate  a1=0  a2=0 a3=0
media  15 1  1
media   0 1 -1   2
boundary 2

unit 21
com='fuel rods - nominal pitch'
cuboid 1  21.072       0 21.072       0 296.28       0.0000
array 2 1 place 1 1 1 0.4572       0.4572       0
boundary 1

unit 22
com='solid fuel rod - nominal pitch'
cylinder 1  0.39218       426.72           0
cylinder 2  0.40005       426.72           0
cylinder 3  0.4572        426.72           0
cuboid 4  4P0.62992       426.72           0
media 1 1  1
media 2 1  2 -1
media 3 1  3 -2 -1
media 4 1  4 -3 -2 -1
boundary 4
```

Table 6-37F Input Deck for Annular Pellet Study (cont.)

```
unit 23
com='thimble tube - nominal pitch'
cylinder 1  0.56134       426.72          0
cylinder 2  0.60198       426.72          0
cuboid 3    4P0.62992     426.72          0
media 4 1 1
media 3 1 2 -1
media 4 1 3 -2 -1
boundary 3

unit 24
com='fuel rods annular - nominal pitch'
cuboid 1  21.072       0 21.072       0 30.48       0.0000
array 4 1 place 1 1 1 0.4572       0.4572       0
boundary 1

UNIT 25
COM='annular fuel rod - nominal pitch'
CYLINDER 1  0.19685 426.72  0
CYLINDER 2  0.39218  426.72  0
CYLINDER 3  0.40005  426.72  0
CYLINDER 4  0.4572  426.72  0
CUBOID 5    4P0.62992 426.72  0
media 2  1 1
media 20 1 2 -1
media 2  1 3 -2 -1
media 21 1 4 -3 -2 -1
media 4  1 5 -4 -3 -2 -1
boundary 5

unit 31
com='fuel rods - expanded pitch'
cuboid 1  24.384       0 24.384       0 69.52          0
array 3 1 place 1 1 1 0.4572       0.4572       0
boundary 1

unit 32
com='solid fuel rod - expanded pitch'
cylinder 1  0.39218       426.72          0
cylinder 2  0.40005      426.72          0
cylinder 3  0.4572       426.72          0
cuboid 4  4P0.73342       426.72          0
media 16  1 1
media 17  1 2 -1
media 18  1 3 -2 -1
media 19  1 4 -3 -2 -1
boundary 4

unit 33
com='thimble tube - expanded pitch'
```

Table 6-37F Input Deck for Annular Pellet Study (cont.)

```
cylinder 1  0.56134      426.72          0
cylinder 2  0.60198      426.72          0
cuboid 3  4P0.73342       426.72          0
media 19 1 1
media 18 1 2 -1
media 19 1 3 -2 -1
boundary 3

unit 34
com='fuel rods annular - expanded pitch'
cuboid 1  24.384       0 24.384       0 30.48          0
array 5 1 place 1 1 1 0.4572       0.4572       0
boundary 1

UNIT 35
COM='annular fuel rod - expanded pitch'
CYLINDER 1  0.19685 426.72  0
CYLINDER 2  0.39218  426.72  0
CYLINDER 3  0.40005  426.72  0
CYLINDER 4  0.4572  426.72  0
CUBOID 5    4P0.73342 426.72  0
media 17  1 1
media 22  1 2 -1
media 17  1 3 -2 -1
media 23  1 4 -3 -2 -1
media 19  1 5 -4 -3 -2 -1
boundary 5

unit 40
com='top nozzle assembly'
cuboid 1     21.072       0 21.072       0       21.2090     0.0000
cuboid 2     21.072       0 21.072       0      41.8846     0.0000
cuboid 3     21.072       0 21.072       0       52.8193     0.0000
cuboid 4     21.072       0 21.072       0       77.4192     0.0000
cuboid 5     24.384       0 24.384       0       77.4192     0.0008
media  15 1   1
media  15 1  -1   2
media  15 1  -2   3
media  15 1  -3   4
media  15 1  -4   5
boundary 5

unit 66
com='individual package 0-deg rotation'
hexprism 1  31.75    554.1972  -20.1498
hole 10  origin  x=0 y=0  z=0  rotate  a1=0 a2=0 a3=0
media   0 1   1
boundary 1

unit 77
com='individual package 180-deg rotation'
```

Table 6-37F Input Deck for Annular Pellet Study (cont.)

```
hexprism 1  31.75    554.1972  -20.1498
hole 10  origin  x=0 y=0  z=0  rotate  a1=0 a2=0 a3=180
media   0 1   1
boundary 1

unit 88
com='dummy cell'
hexprism 1  31.75    554.1972  -20.1498
media  15 1   1
boundary 1

global
unit 99
com='package array'
cylinder 1  432.2355   554.1972  -20.1498
cylinder 2  452.2355   574.1972  -40.1498
cuboid 3  452.2355  -452.2355  452.2355  -452.2355   574.1972  -40.1498
array 1 1  place 9 9 1 0 0 0
media  15 1  -1   2
media   0 1  -2   3
boundary 3

end geometry

read array
ara=1 typ=triangular nux=17 nuy=17 nuz=1 gbl=1
fill
88 88 88 88 88 88 88 88 88 88 88 88 88 88 88 88 88
  88 88 88 88 88 88 88 88 88 88 77 77 77 88 88 88 88
    88 88 88 88 88 88 88 88 66 66 66 66 66 66 66 88 88
      88 88 88 88 88 88 77 77 77 77 77 77 77 77 77 77 88
        88 88 88 88 88 66 66 66 66 66 66 66 66 66 66 66 88
          88 88 88 88 77 77 77 77 77 77 77 77 77 77 77 88
            88 88 88 66 66 66 66 66 66 66 66 66 66 66 66 88
              88 88 88 77 77 77 77 77 77 77 77 77 77 77 88 88
                88 88 66 66 66 66 66 66 66 66 66 66 66 66 88 88
                  88 88 77 77 77 77 77 77 77 77 77 77 77 88 88 88
                    88 66 66 66 66 66 66 66 66 66 66 66 66 88 88 88
                      88 77 77 77 77 77 77 77 77 77 77 77 88 88 88 88
                        88 88 66 66 66 66 66 66 66 66 88 88 88 88 88 88
                          88 88 88 77 77 77 77 88 88 88 88 88 88 88 88 88
                          88 88 88 88 88 88 88 88 88 88 88 88 88 88 88 88

end fill

ara=2 typ=square nux=17 nuy=17 nuz=1
fill 39*22 23 2*22 23 2*22 23 8*22 23 9*22 23 22*22 23 2*22 23 2*22 23
 2*22 23 2*22 23 38*22 23 2*22 23 2*22 23 2*22 23 2*22 23 2*22 23 38*22 23
 2*22 23 2*22 23 2*22 23 2*22 23 2*22 23 22*22 23 9*22 23 8*22 23 2*22 23 2*22
```

Table 6-37F Input Deck for Annular Pellet Study (cont.)

```
23 39*22
end fill
ara=3 typ=square nux=17 nuy=17 nuz=1
fill 39*32 33 2*32 33 2*32 33 8*32 33 9*32 33 22*32 33 2*32 33 2*32 33
 2*32 33 2*32 33 38*32 33 2*32 33 2*32 33 2*32 33 2*32 33 38*32 33
 2*32 33 2*32 33 2*32 33 2*32 33 22*32 33 9*32 33 8*32 33 2*32 33 2*32
 33 39*32
end fill
ara=4 typ=square nux=17 nuy=17 nuz=1
fill 39*25 23 2*25 23 2*25 23 8*25 23 9*25 23 22*25 23 2*25 23 2*25 23
 2*25 23 2*25 23 38*25 23 2*25 23 2*25 23 2*25 23 2*25 23 38*25 23
 2*25 23 2*25 23 2*25 23 2*25 23 22*25 23 9*25 23 8*25 23 2*25 23 2*25
 23 39*25
end fill
ara=5 typ=square nux=17 nuy=17 nuz=1
fill 39*35 33 2*35 33 2*35 33 8*35 33 9*35 33 22*35 33 2*35 33 2*35 33
 2*35 33 2*35 33 38*35 33 2*35 33 2*35 33 2*35 33 2*35 33 38*35 33
 2*35 33 2*35 33 2*35 33 2*35 33 22*35 33 9*35 33 8*35 33 2*35 33 2*35
 33 39*35
end fill

end array

read bnds
+xb=vacuum
-xb=vacuum
+yb=vacuum
-yb=vacuum
+zb=vacuum
-zb=vacuum
end bnds

end data
end
```

6.10.9.4 Axial Displacement Study Data

Table 6-37G Results for Axial Displacement Study

Run #	No. Rods Displaced	ks	σks	ks+2×σks
DISPLACE-0	0	0.9304	0.0008	0.9320
DISPLACE-4	4	0.9311	0.0010	0.9331
DISPLACE-8	8	0.9304	0.0008	0.9320
DISPLACE-12	12	0.9292	0.0008	0.9309
DISPLACE-20	20	0.9259	0.0009	0.9278
DISPLACE-28	28	0.9267	0.0010	0.9286
DISPLACE-56	56	0.9152	0.0009	0.9170
DISPLACE-92	92	0.8915	0.0009	0.8933
DISPLACE-132	132	0.8733	0.0008	0.8749

Table 6-37H Input Deck for Axial Displacement Study

Example of input deck for 92 displaced rods

```
=csas26     parm=size=300000
TRAVELLER XL,17WOFA,ENV=24.384      cm,L=100      cm,B10=0.018   g/cm2
44groupndf5  latticecell
 uo2 1 1 293 92235 5 92238 95 end
 h2o 2 1 293 end
 zirc4 3 1 293 end
 h2o 4 1 293 end
 h2o 5 1 293 end
 arbmfoam 0.1602e-20  4  0  0  0 6012 70 1001 10 8016 16 7014 4  6 1 293
 end
 al 7 1 293 end
 ss304 8 1 293 end
 polyethylene 9 DEN=0.828 1.0 293 end
 arbmfoam 0.1602e-20  4  0  0  0 6012 70 1001 10 8016 16 7014 4 11 1 293
 end
 b-10 12 0 0.0047781    end
 b-11 12 0 0.019398     end
 c   12 0 0.0060439    end
 al  12 0 0.043223     end
 arbmrubber 1.59e-20  7  0  0  0 8016 46.94 13000 19.92 14000 17.54 6012
 10.79 1001 4.73 11000 0.06 26000 0.02  14 1 293 end
 h2o 15 1 293 end
 uo2 16 1 293 92235 5 92238 95 end
 h2o 17 1 293 end
 zirc4 18 1 293 end
 h2o 19 1 293 end
 uo2 20 1 293 92235 5 92238 95 end
 uo2 21 1 293 92235 5 92238 95 end
end comp
squarepitch 1.4669       0.78435      16 19 0.9144       18 0.8001       17 end
more data
res=1  cylinder 0.39218      dan(1)=0.22632
res=20  cylinder 0.39218     dan(20)=0.0212
res=21  cylinder 0.39218     dan(21)=0.04987       end

read parameter   TME=360.   gen=450  npg=2500   nsk=50
wrs=1     run=NO
end parameter
```

Table 6-37H Input Deck for Axial Displacement Study (cont.)

```
read geometry
unit 10
com='individual package'
cuboid 1    16.904       -15.634       16.904       -15.634       533.1330 0
rotate  a1=45 a2=0 a3=0 origin x=0  y=-1.460 z=0
cuboid 2     21.5900   -21.5900     1.5720    -1.0310   533.1330     0
cuboid 3     20.0790   -20.0790    20.0790   -20.0790   533.1330     0
rotate  a1=45 a2=0 a3=0 origin x=0  y=-1.460 z=0
cuboid 4     20.3450   -20.3450    20.3450   -20.3450   533.3990    -0.2660
rotate  a1=45 a2=0 a3=0 origin x=0  y=-1.460 z=0
cuboid 5     21.5900   -21.590     23.1498   -23.1498   533.1330     0
cuboid 6     21.8560   -21.8560    23.4158   -23.4158   533.3990    -0.2660
cuboid 7     20.3840   -20.3840    20.3840   -20.3840   553.8922   -19.8448
rotate  a1=45 a2=0 a3=0 origin x=0  y=-1.460 z=0
cuboid 8     21.8950   -21.895     23.4548   -23.4548   553.8922   -19.8448
cylinder  9    25.1050    533.4380    -0.2660
cylinder 10    25.1050    553.9312   -19.8448
cylinder 11    31.4840    533.4380    -0.2660
cylinder 12    31.4840    553.9312   -19.8448
cylinder 13    31.4840    533.4380   -19.8448
cylinder 14    31.7500    554.1972   -20.1100
plane 15  zpl=1  con= -10.0000
cylinder 16 7.62   0 -4.5
 rotate  a1=45 a2=90 a3=0 origin x=18.7310 y=-11.1270 z=494.4364
cylinder 17 3.962  0 -7.60
 rotate  a1=45 a2=90 a3=0 origin x=18.7310 y=-11.1270 z=494.4364
cylinder 18 7.62   0 -4.5
 rotate  a1=-45 a2=90 a3=0 origin x=-18.7310 y=-11.1270 z=494.4364
cylinder 19 3.962  0 -7.60
 rotate  a1=-45 a2=90 a3=0 origin x=-18.7310 y=-11.1270 z=494.4364
cylinder 20 7.62   0 -4.5
 rotate  a1=45 a2=90 a3=0 origin x=18.7310 y=-11.1270 z=448.7164
cylinder 21 3.962  0 -7.60
 rotate  a1=45 a2=90 a3=0 origin x=18.7310 y=-11.1270 z=448.7164
cylinder 22 7.62   0 -4.5
 rotate  a1=-45 a2=90 a3=0 origin x=-18.7310 y=-11.1270 z=448.7164
cylinder 23 3.962  0 -7.60
 rotate  a1=-45 a2=90 a3=0 origin x=-18.7310 y=-11.1270 z=448.7164
cylinder 24 7.62   0 -4.5
 rotate  a1=45 a2=90 a3=0 origin x=18.7310 y=-11.1270 z=402.9964
cylinder 25 3.962  0 -7.60
 rotate  a1=45 a2=90 a3=0 origin x=18.7310 y=-11.1270 z=402.9964
cylinder 26 7.62   0 -4.5
 rotate  a1=-45 a2=90 a3=0 origin x=-18.7310 y=-11.1270 z=402.9964
cylinder 27 3.962  0 -7.60
 rotate  a1=-45 a2=90 a3=0 origin x=-18.7310 y=-11.1270 z=402.9964
cylinder 28 7.62   0 -4.5
 rotate  a1=45 a2=90 a3=0 origin x=18.7310 y=-11.1270 z=357.2764
cylinder 29 3.962  0 -7.60
 rotate  a1=45 a2=90 a3=0 origin x=18.7310 y=-11.1270 z=357.2764
cylinder 30 7.62   0 -4.5
```

Table 6-37H Input Deck for Axial Displacement Study (cont.)

```
 rotate  a1=-45 a2=90 a3=0 origin x=-18.7310 y=-11.1270 z=357.2764
cylinder 31 3.962  0 -7.60
 rotate  a1=-45 a2=90 a3=0 origin x=-18.7310 y=-11.1270 z=357.2764
cylinder 32 7.62   0 -4.5
 rotate  a1=45 a2=90 a3=0 origin x=18.7310 y=-11.1270 z=174.3964
cylinder 33 3.962  0 -7.60
 rotate  a1=45 a2=90 a3=0 origin x=18.7310 y=-11.1270 z=174.3964
cylinder 34 7.62   0 -4.5
 rotate  a1=-45 a2=90 a3=0 origin x=-18.7310 y=-11.1270 z=174.3964
cylinder 35 3.962  0 -7.60
 rotate  a1=-45 a2=90 a3=0 origin x=-18.7310 y=-11.1270 z=174.3964
cylinder 36 7.62   0 -4.5
 rotate  a1=45 a2=90 a3=0 origin x=18.7310 y=-11.1270 z=128.6764
cylinder 37 3.962  0 -7.60
 rotate  a1=45 a2=90 a3=0 origin x=18.7310 y=-11.1270 z=128.6764
cylinder 38 7.62   0 -4.5
 rotate  a1=-45 a2=90 a3=0 origin x=-18.7310 y=-11.1270 z=128.6764
cylinder 39 3.962  0 -7.60
 rotate  a1=-45 a2=90 a3=0 origin x=-18.7310 y=-11.1270 z=128.6764
cylinder 40 7.62   0 -4.5
 rotate  a1=45 a2=90 a3=0 origin x=18.7310 y=-11.1270 z=82.9564
cylinder 41 3.962  0 -7.60
 rotate  a1=45 a2=90 a3=0 origin x=18.7310 y=-11.1270 z=82.9564
cylinder 42 7.62   0 -4.5
 rotate  a1=-45 a2=90 a3=0 origin x=-18.7310 y=-11.1270 z=82.9564
cylinder 43 3.962  0 -7.60
 rotate  a1=-45 a2=90 a3=0 origin x=-18.7310 y=-11.1270 z=82.9564
cylinder 44 7.62   0 -4.5
 rotate  a1=45 a2=90 a3=0 origin x=18.7310 y=-11.1270 z=37.2364
cylinder 45 3.962  0 -7.60
 rotate  a1=45 a2=90 a3=0 origin x=18.7310 y=-11.1270 z=37.2364
cylinder 46 7.62   0 -4.5
 rotate  a1=-45 a2=90 a3=0 origin x=-18.7310 y=-11.1270 z=37.2364
cylinder 47 3.962  0 -7.60
 rotate  a1=-45 a2=90 a3=0 origin x=-18.7310 y=-11.1270 z=37.2364
hole 11 rotate  a1=45 a2=0 a3=0  origin  x=0 y=-17.700 z=5.240
media  0 1   2
media  0 1  -2   1   5  -17 -19 -21 -23 -25 -27 -29 -31 -33 -35 -37
-39 -41 -43 -45 -47
media  9 1  -1   3   5  -2 -16 -18 -20 -22 -24 -26 -28 -30 -32 -34 -36
-38 -40 -42 -44 -46 -17 -19 -21 -23 -25 -27 -29 -31 -33 -35 -37
-39 -41 -43 -45 -47
media  8 1  -3   4   6
media  8 1   3  -5   6
media  6 1  -4   9
media  6 1   4  -6   9
media  6 1  -9  11
media  6 1  -7  10 -13
media  6 1   7  -8  10 -13  12
media  6 1 -10 -13  12
media 11 1 -11  13
```

Table 6-37H Input Deck for Axial Displacement Study (cont.)

```
media 11 1   7   8 -13  12
media  8 1  -12 14
media  0 1 16  -17  5  -1  3
media  0 1 18  -19  5  -1  3
media  0 1 20  -21  5  -1  3
media  0 1 22  -23  5  -1  3
media  0 1 24  -25  5  -1  3
media  0 1 26  -27  5  -1  3
media  0 1 28  -29  5  -1  3
media  0 1 30  -31  5  -1  3
media  0 1 32  -33  5  -1  3
media  0 1 34  -35  5  -1  3
media  0 1 36  -37  5  -1  3
media  0 1 38  -39  5  -1  3
media  0 1 40  -41  5  -1  3
media  0 1 42  -43  5  -1  3
media  0 1 44  -45  5  -1  3
media  0 1 46  -47  5  -1  3
media 14 1 17  3
media 14 1 19  3
media 14 1 21  3
media 14 1 23  3
media 14 1 25  3
media 14 1 27  3
media 14 1 29  3
media 14 1 31  3
media 14 1 33  3
media 14 1 35  3
media 14 1 37  3
media 14 1 39  3
media 14 1 41  3
media 14 1 43  3
media 14 1 45  3
media 14 1 47  3
boundary 14

unit 11
com='fuel assembly confinement system'
cuboid 1    24.384       0 24.384       0 520.7000 2.5400
cuboid 2    25.337       -0.9525 25.337        -0.9525
 523.2400  0.0000
cuboid 3    19.812       4.572        24.429       -0.04545
 513.0800  3.81
cuboid 4    19.812       4.572        24.656       -0.27205
 513.0800  3.81
cuboid 5    19.812       4.572        24.702       -0.3175
 513.0800  3.81
cuboid 6    24.429       -0.04545      19.812       4.572
 513.0800  3.81
cuboid 7    24.656       -0.27205      19.812       4.572
 513.0800  3.81
```

Table 6-37H Input Deck for Axial Displacement Study (cont.)

```
cuboid 8    24.702       -0.3175       19.812       4.572
 513.0800  3.81
hole 20  origin  x=0  y=0  z=16.56  rotate  a1=0 a2=0 a3=0
media  0 1   1
media  7 1  -1   2  -5  -8
media  7 1  -1   3
media 12 1  -3   4
media  7 1  -4   5
media  7 1  -1   6
media 12 1  -6   7
media  7 1  -7   8
boundary 2

unit 20
com='fuel assembly'
cuboid 1 21.072       0 21.072       0   0        -14.0208
cuboid 2 24.384       0 24.384       0 504.1392   -14.0208
hole 31 origin  x=0       y=0       z=0.0001   rotate  a1=0  a2=0 a3=0
hole 21 origin  x=0       y=0       z=100.0001 rotate  a1=0  a2=0 a3=0
media  15 1  1
media   0 1 -1   2
boundary 2

unit 21
com='fuel rods - nominal pitch'
cuboid 1  21.072       0 21.072       0 404.1392       0.0000
array 2 1 place 1 1 1 0.4572       0.4572       0
boundary 1

unit 22
com='solid fuel rod - nominal pitch'
cylinder 1  0.39218       326.72           0
cylinder 2  0.40005      326.72           0
cylinder 3  0.4572       326.72           0
cuboid 4  4P0.62992       326.72           0
cuboid 5  4P0.62992       404.1392         0
media 1 1  1
media 2 1  2 -1
media 3 1  3 -2 -1
media 4 1  4 -3 -2 -1
media 15  1  5  -4 -3 -2 -1
boundary 5

unit 23
com='thimble tube - nominal pitch'
cylinder 1  0.56134       326.72           0
cylinder 2  0.60198        326.72           0
cuboid 3    4P0.62992      326.72           0
cuboid 4    4P0.62992      404.1392         0
media 4 1 1
media 3 1 2 -1
```

Table 6-37H Input Deck for Axial Displacement Study (cont.)

```
media 4 1 3 -2 -1
media 15  1  4  -3 -2 -1
boundary 4

unit 44
com='solid fuel rod - displaced rod at top of clamshell'

cylinder 1  0.39218       326.72          0
cylinder 2  0.39218       404.1392        0
cylinder 3  0.40005       404.1392        0
cylinder 4  0.4572        404.1392        0
cuboid 5  4P0.62992       404.1392        0
media 1 1  1
media 20 1  2 -1
media 2  1  3 -2 -1
media 3 1  4 -3 -2 -1
media 4 1  5 -4 -3 -2 -1
boundary 5

unit 31
com='fuel rods - expanded pitch'
cuboid 1  24.384       0 24.384       0 100          0
array 3 1 place 1 1 1 0.4572       0.4572       0
boundary 1

unit 32
com='solid fuel rod - expanded pitch'
cylinder 1  0.39218       77.4192          0
cylinder 2  0.39218       426.72           0
cylinder 3  0.40005      426.72           0
cylinder 4  0.4572       426.72           0
cuboid 5  4P0.73342       426.72           0
media 21  1 1
media 16  1 2 -1
media 17  1 3 -2 -1
media 18  1 4 -3 -2 -1
media 19  1 5 -4 -3 -2 -1
boundary 5

unit 33
com='thimble tube - expanded pitch'
cylinder 1  0.56134      426.72           0
cylinder 2  0.60198      426.72           0
cuboid 3  4P0.73342       426.72           0
media 19 1 1
media 18 1 2 -1
media 19 1 3 -2 -1
boundary 3

unit 45
com='solid fuel rod - expanded pitch'
```

Table 6-37H Input Deck for Axial Displacement Study (cont.)

```
cylinder 1  0.39218       426.72        77.4192
cylinder 2  0.40005      426.72         77.4192
cylinder 3  0.4572       426.72         77.4192
cuboid 4  4P0.73342       426.72           0
media 16  1 1
media 17  1 2 -1
media 18  1 3 -2 -1
media 19  1 4 -3 -2 -1
boundary 4

unit 66
com='individual package 0-deg rotation'
hexprism 1  31.75    554.1972  -20.1498
hole 10  origin  x=0 y=0  z=0  rotate  a1=0 a2=0 a3=0
media   0 1   1
boundary 1

unit 77
com='individual package 180-deg rotation'
hexprism 1  31.75    554.1972  -20.1498
hole 10  origin  x=0 y=0  z=0  rotate  a1=0 a2=0 a3=180
media   0 1   1
boundary 1

unit 88
com='dummy cell'
hexprism 1  31.75    554.1972  -20.1498
media  15 1   1
boundary 1

global
unit 99
com='package array'
cylinder 1  432.2355   554.1972  -20.1498
cylinder 2  452.2355   574.1972  -40.1498
cuboid 3  452.2355  -452.2355  452.2355  -452.2355   574.1972  -40.1498
array 1 1  place 9 9 1 0 0 0
media  15 1  -1   2
media   0 1  -2   3
boundary 3

end geometry

read array
ara=1 typ=triangular nux=17 nuy=17 nuz=1 gbl=1
fill

88 88 88 88 88 88 88 88 88 88 88 88 88 88 88 88 88
  88 88 88 88 88 88 88 88 88 88 77 77 77 88 88 88 88
    88 88 88 88 88 88 88 88 66 66 66 66 66 66 66 88 88
```

Table 6-37H Input Deck for Axial Displacement Study (cont.)

```
      88 88 88 88 88 88 77 77 77 77 77 77 77 77 77 77 88
        88 88 88 88 88 66 66 66 66 66 66 66 66 66 66 66 88
          88 88 88 88 77 77 77 77 77 77 77 77 77 77 77 88
            88 88 88 66 66 66 66 66 66 66 66 66 66 66 66 88
              88 88 88 77 77 77 77 77 77 77 77 77 77 77 88 88
                88 88 66 66 66 66 66 66 66 66 66 66 66 66 88 88
                  88 88 77 77 77 77 77 77 77 77 77 77 77 88 88 88
                    88 66 66 66 66 66 66 66 66 66 66 66 66 88 88 88
                      88 77 77 77 77 77 77 77 77 77 77 77 88 88 88 88
                        88 66 66 66 66 66 66 66 66 66 66 66 88 88 88 88 88
                          88 77 77 77 77 77 77 77 77 77 77 88 88 88 88 88 88
                           88 88 66 66 66 66 66 66 66 88 88 88 88 88 88 88 88
                            88 88 88 77 77 77 77 88 88 88 88 88 88 88 88 88 88
                            88 88 88 88 88 88 88 88 88 88 88 88 88 88 88 88 88
        end fill


ara=2 typ=square nux=17 nuy=17 nuz=1
 fill

 22 22 22 22 22 22 22 22  22  22 22 22 22 22 22 22 22
 22 44 22 44 22 44 22 44  22  44 22 44 22 44 22 44 22
 22 22 44 22 44 23 44 22  23  22 44 23 44 22 44 22 22
 22 44 22 23 22 44 22 44  22  44 22 44 22 23 22 44 22
 22 22 44 22 44 22 44 22  22  22 44 22 44 22 44 22 22
 22 44 23 44 22 23 22 44  23  44 22 23 22 44 23 44 22
 22 22 44 22 44 22 44 22  22  22 44 22 44 22 44 22 22
 22 44 22 44 22 44 22 44  22  44 22 44 22 44 22 44 22

 22 22 23 22 22 23 22 22  23  22 22 23 22 22 23 22 22

 22 44 22 44 22 44 22 44  22  44 22 44 22 44 22 44 22
 22 22 44 22 44 22 44 22  22  22 44 22 44 22 44 22 22
 22 44 23 44 22 23 22 44  23  44 22 23 22 44 23 44 22
 22 22 44 22 44 22 44 22  22  22 44 22 44 22 44 22 22
 22 44 22 23 22 44 22 44  22  44 22 44 22 23 22 44 22
 22 22 44 22 44 23 44 22  23  22 44 23 44 22 44 22 22
 22 44 22 44 22 44 22 44  22  44 22 44 22 44 22 44 22
 22 22 22 22 22 22 22 22  22  22 22 22 22 22 22 22 22
end fill
ara=3 typ=square nux=17 nuy=17 nuz=1
 fill
 32 32 32 32 32 32 32 32  32  32 32 32 32 32 32 32 32
 32 45 32 45 32 45 32 45  32  45 32 45 32 45 32 45 32
 32 32 45 32 45 33 45 32  33  32 45 33 45 32 45 32 32
 32 45 32 33 32 45 32 45  32  45 32 45 32 33 32 45 32
 32 32 45 32 45 32 45 32  32  32 45 32 45 32 45 32 32
 32 45 33 45 32 33 32 45  33  45 32 33 32 45 33 45 32
 32 32 45 32 45 32 45 32  32  32 45 32 45 32 45 32 32
```

Displaced rods location

Table 6-37H Input Deck for Axial Displacement Study (cont.)

```
 32 45 32 45 32 45 32 45  32  45 32 45 32 45 32 45 32

 32 32 33 32 32 33 32 32  33  32 32 33 32 32 33 32 32

 32 45 32 45 32 45 32 45  32  45 32 45 32 45 32 45 32
 32 32 45 32 45 32 45 32  32  32 45 32 45 32 45 32 32
 32 45 33 45 32 33 32 45  33  45 32 33 32 45 33 45 32
 32 32 45 32 45 32 45 32  32  32 45 32 45 32 45 32 32
 32 45 32 33 32 45 32 45  32  45 32 45 32 33 32 45 32
 32 32 45 32 45 33 45 32  33  32 45 33 45 32 45 32 32
 32 45 32 45 32 45 32 45  32  45 32 45 32 45 32 45 32
 32 32 32 32 32 32 32 32  32  32 32 32 32 32 32 32 32
end fill
end array

read bnds
+xb=vacuum
-xb=vacuum
+yb=vacuum
-yb=vacuum
+zb=vacuum
-zb=vacuum
end bnds
READ PLOT
clr=0  150  150  150
    1    0  229  238
    2  255  225  225
    3    0    0  205
    4  238  182  193
    5  255  255  224
    6  238   10    0
    7   90   40   90
    8   10    0    0
    9  255    0  255
   10  127  255    0
   11   50  130   10
   12  238  153  153
   13  255   69    0
   14  190  140  140
   15    0  100  180
   16  214  236  238
   17   25    0  100
  end color
    PIC=MAT
 TTL=' X-Z slice for 92 displaced rods'
    XUL=-17.7    YUL=13.22  ZUL=554.0
    XLR=15.02    YLR=-19.6  ZLR=-20.0
    UAX=0.70711  VAX=-0.70711  WDN=-1.0  NAX=800 NDN=2000  end
 TTL='X-Y slice  for 92  displaced rods at Z=40.'
    XUL=-17.7    YUL=15.6    ZUL=+40.
    XLR=+17.7    YLR=-19.6     ZLR=+40.
```

Coordinates for Figure 1

Coordinates for Figure 2.b

Table 6-37H Input Deck for Axial Displacement Study (cont.)

```
    UAX=1.0     VDN=-1.0  NAX=2000            end
 TTL='X-Y slice  for 92  displaced rods at Z=450.'
    XUL=-17.7    YUL=15.6    ZUL=+450.
    XLR=+17.7    YLR=-19.6     ZLR=+450.
    UAX=1.0     VDN=-1.0  NAX=2000
END PLOT
end data
end
```

Coordinates for Figure 2.a

Table 6-38 Input Deck for Moderator Density Study

```
=csas26     parm=size=300000
TRAVELLER XL,17WOFA,ENV=24.384      cm,L=100      cm,B10=0.018   g/cm2
44groupndf5  latticecell
uo2 1 1 293 92235 5 92238 95 end
h2o 2 1 293 end
zirc4 3 1 293 end
h2o 4 1 293 end
h2o 5 1 293 end
arbmfoam 0.1602e-20  4  0  0  0 6012 70 1001 10 8016 16 7014 4  6 1 293
end
al 7 1 293 end
ss304 8 1 293 end
polyethylene 9 DEN=0.828 1.0 293 end
arbmfoam 0.1602e-20  4  0  0  0 6012 70 1001 10 8016 16 7014 4 11 1 293
end
b-10 12 0 0.0047781    end
b-11 12 0 0.019398     end
c   12 0 0.0060439    end
al  12 0 0.043223     end
arbmrubber 1.59e-20  7  0  0  0 8016 46.94 13000 19.92 14000 17.54 6012
10.79 1001 4.73 11000 0.06 26000 0.02  14 1 293 end
h2o 15 DEN=0.4 1.0 293 end
uo2 16 1 293 92235 5 92238 95 end
h2o 17 1 293 end
zirc4 18 1 293 end
h2o 19 1 293 end
h2o 20 1 293 end
end comp
squarepitch 1.4669       0.78435      16 19 0.9144       18 0.8001       17 end
more data
res=1  cylinder 0.39218      dan(1)=0.22632       end

read parameter
gen=450
npg=2500
nsk=50
wrs=1
tme=240
end parameter
```

Table 6-38 Input Deck for Moderator Density Study (cont.)

```
read geometry
unit 10
com='individual package'
cuboid 1    16.904      -15.634      16.904      -15.634      533.1330 0
rotate  a1=45 a2=0 a3=0 origin x=0  y=-1.460 z=0
cuboid 2    21.5900   -21.5900    1.5720   -1.0310   533.1330    0
cuboid 3    20.0790   -20.0790   20.0790   -20.0790   533.1330    0
rotate  a1=45 a2=0 a3=0 origin x=0  y=-1.460 z=0
cuboid 4    20.3450   -20.3450   20.3450   -20.3450   533.3990   -0.2660
rotate  a1=45 a2=0 a3=0 origin x=0  y=-1.460 z=0
cuboid 5    21.5900   -21.590    23.1498   -23.1498   533.1330    0
cuboid 6    21.8560   -21.8560   23.4158   -23.4158   533.3990   -0.2660
cuboid 7    20.3840   -20.3840   20.3840   -20.3840   553.8922   -19.8448
rotate  a1=45 a2=0 a3=0 origin x=0  y=-1.460 z=0
cuboid 8    21.8950   -21.895    23.4548   -23.4548   553.8922   -19.8448
cylinder  9   25.1050   533.4380   -0.2660
cylinder 10   25.1050   553.9312   -19.8448
cylinder 11   31.4840   533.4380   -0.2660
cylinder 12   31.4840   553.9312   -19.8448
cylinder 13   31.4840   533.4380   -19.8448
cylinder 14   31.7500   554.1972   -20.1100
plane 15  zpl=1  con= -10.0000
cylinder 16 7.62   0 -4.5
rotate  a1=45 a2=90 a3=0 origin x=18.7310 y=-11.1270 z=494.4364
cylinder 17 3.962  0 -7.60
rotate  a1=45 a2=90 a3=0 origin x=18.7310 y=-11.1270 z=494.4364
cylinder 18 7.62   0 -4.5
rotate  a1=-45 a2=90 a3=0 origin x=-18.7310 y=-11.1270 z=494.4364
cylinder 19 3.962  0 -7.60
rotate  a1=-45 a2=90 a3=0 origin x=-18.7310 y=-11.1270 z=494.4364
cylinder 20 7.62   0 -4.5
rotate  a1=45 a2=90 a3=0 origin x=18.7310 y=-11.1270 z=448.7164
cylinder 21 3.962  0 -7.60
rotate  a1=45 a2=90 a3=0 origin x=18.7310 y=-11.1270 z=448.7164
cylinder 22 7.62   0 -4.5
rotate  a1=-45 a2=90 a3=0 origin x=-18.7310 y=-11.1270 z=448.7164
cylinder 23 3.962  0 -7.60
rotate  a1=-45 a2=90 a3=0 origin x=-18.7310 y=-11.1270 z=448.7164
cylinder 24 7.62   0 -4.5
rotate  a1=45 a2=90 a3=0 origin x=18.7310 y=-11.1270 z=402.9964
cylinder 25 3.962  0 -7.60
rotate  a1=45 a2=90 a3=0 origin x=18.7310 y=-11.1270 z=402.9964
cylinder 26 7.62   0 -4.5
rotate  a1=-45 a2=90 a3=0 origin x=-18.7310 y=-11.1270 z=402.9964
cylinder 27 3.962  0 -7.60
rotate  a1=-45 a2=90 a3=0 origin x=-18.7310 y=-11.1270 z=402.9964
cylinder 28 7.62   0 -4.5
rotate  a1=45 a2=90 a3=0 origin x=18.7310 y=-11.1270 z=357.2764
cylinder 29 3.962  0 -7.60
rotate  a1=45 a2=90 a3=0 origin x=18.7310 y=-11.1270 z=357.2764
```

Table 6-38 Input Deck for Moderator Density Study (cont.)

```
cylinder 30 7.62   0 -4.5
rotate  a1=-45 a2=90 a3=0 origin x=-18.7310 y=-11.1270 z=357.2764
cylinder 31 3.962  0 -7.60
rotate  a1=-45 a2=90 a3=0 origin x=-18.7310 y=-11.1270 z=357.2764
cylinder 54 7.62   0 -4.5
rotate  a1=45 a2=90 a3=0 origin x=18.7310 y=-11.1270 z=265.8364
cylinder 55 3.962  0 -7.60
rotate  a1=45 a2=90 a3=0 origin x=18.7310 y=-11.1270 z=265.8364
cylinder 56 7.62   0 -4.5
rotate  a1=-45 a2=90 a3=0 origin x=-18.7310 y=-11.1270 z=265.8364
cylinder 57 3.962  0 -7.60
rotate  a1=-45 a2=90 a3=0 origin x=-18.7310 y=-11.1270 z=265.8364
cylinder 32 7.62   0 -4.5
rotate  a1=45 a2=90 a3=0 origin x=18.7310 y=-11.1270 z=174.3964
cylinder 33 3.962  0 -7.60
rotate  a1=45 a2=90 a3=0 origin x=18.7310 y=-11.1270 z=174.3964
cylinder 34 7.62   0 -4.5
rotate  a1=-45 a2=90 a3=0 origin x=-18.7310 y=-11.1270 z=174.3964
cylinder 35 3.962  0 -7.60
rotate  a1=-45 a2=90 a3=0 origin x=-18.7310 y=-11.1270 z=174.3964
cylinder 36 7.62   0 -4.5
rotate  a1=45 a2=90 a3=0 origin x=18.7310 y=-11.1270 z=128.6764
cylinder 37 3.962  0 -7.60
rotate  a1=45 a2=90 a3=0 origin x=18.7310 y=-11.1270 z=128.6764
cylinder 38 7.62   0 -4.5
rotate  a1=-45 a2=90 a3=0 origin x=-18.7310 y=-11.1270 z=128.6764
cylinder 39 3.962  0 -7.60
rotate  a1=-45 a2=90 a3=0 origin x=-18.7310 y=-11.1270 z=128.6764
cylinder 40 7.62   0 -4.5
rotate  a1=45 a2=90 a3=0 origin x=18.7310 y=-11.1270 z=82.9564
cylinder 41 3.962  0 -7.60
rotate  a1=45 a2=90 a3=0 origin x=18.7310 y=-11.1270 z=82.9564
cylinder 42 7.62   0 -4.5
rotate  a1=-45 a2=90 a3=0 origin x=-18.7310 y=-11.1270 z=82.9564
cylinder 43 3.962  0 -7.60
rotate  a1=-45 a2=90 a3=0 origin x=-18.7310 y=-11.1270 z=82.9564
cylinder 44 7.62   0 -4.5
rotate  a1=45 a2=90 a3=0 origin x=18.7310 y=-11.1270 z=37.2364
cylinder 45 3.962  0 -7.60
rotate  a1=45 a2=90 a3=0 origin x=18.7310 y=-11.1270 z=37.2364
cylinder 46 7.62   0 -4.5
rotate  a1=-45 a2=90 a3=0 origin x=-18.7310 y=-11.1270 z=37.2364
cylinder 47 3.962  0 -7.60
rotate  a1=-45 a2=90 a3=0 origin x=-18.7310 y=-11.1270 z=37.2364
hole 11 rotate  a1=45 a2=0 a3=0  origin  x=0 y=-17.700 z=5.240
cuboid 48    18.174    20.079   10.4238  -9.5152    533.3990    -0.2660
rotate  a1=-45 a2=0 a3=0 origin x=0  y=-1.460 z=0
cuboid 49    13.6554  -10.4238  16.904    20.079    533.3990    -0.2660
rotate  a1=45 a2=0 a3=0 origin x=0  y=-1.460 z=0
cuboid 50    16.904    20.079   13.6554  -10.4238   533.3990    -0.2660
rotate  a1=45 a2=0 a3=0 origin x=0  y=-1.460 z=0
```

Table 6-38 Input Deck for Moderator Density Study (cont.)

```
cuboid 51     9.5152  -10.4238 -18.174   -20.079    533.3990    -0.2660
rotate  a1=-45 a2=0 a3=0 origin x=0  y=-1.460 z=0
cuboid 52    15.634    18.174   12.0238 -11.9197    533.3990    -0.2660
rotate  a1=-45 a2=0 a3=0 origin x=0  y=-1.460 z=0
cuboid 53    11.9197  -12.0238 -15.634   -18.174    533.3990    -0.2660
rotate  a1=-45 a2=0 a3=0 origin x=0  y=-1.460 z=0
media 15 1   1   3  5 -17 -19 -21 -23 -29 -31 -55 -57 -33 -35
-41 -43 -45 -47
media 15 1  -1   3  5 -48 -49 -50 -51 -52 -53
media  9 1   3  -16  -17 -20 -21 -28 -29 -54 -55 -32 -33
-40 -41 -44 -45 48
media  9 1   3  -18  -19 -22 -23 -30 -31 -56 -57 -34 -35
-42 -43 -46 -47 51
media  9 1   3  -18  -22  -30  -56  -34  -42  -46  53
media  9 1   3  -16  -20  -28  -54  -32  -40  -44  52
media  9 1   3  49
media  9 1   3  50
media  8 1  -3   4   6
media  8 1   3  -5   6
media 15 1  -4   9
media 15 1   4  -6   9
media 15 1  -9  11
media 15 1  -7  10 -13
media 15 1   7  -8  10 -13  12
media 15 1 -10 -13  12
media 15 1 -11  13
media 15 1   7   8 -13  12
media  8 1 -12  14
media 15 1 16  -17 3 48
media 15 1 18  -19 3 51
media 15 1 20  -21 3 48
media 15 1 22  -23 3 51
media 15 1 28  -29 3 48
media 15 1 30  -31 3 51
media 15 1 54  -55 3 48
media 15 1 56  -57 3 51
media 15 1 32  -33 3 48
media 15 1 34  -35 3 51
media 15 1 40  -41 3 48
media 15 1 42  -43 3 51
media 15 1 44  -45 3 48
media 15 1 46  -47 3 51
media 15 1 16  -17 3 52
media 15 1 18  -19 3 53
media 15 1 20  -21 3 52
media 15 1 22  -23 3 53
media 15 1 28  -29 3 52
media 15 1 30  -31 3 53
media 15 1 54  -55 3 52
media 15 1 56  -57 3 53
media 15 1 32  -33 3 52
```

Table 6-38 Input Deck for Moderator Density Study (cont.)

```
media 15 1 34  -35 3 53
media 15 1 40  -41 3 52
media 15 1 42  -43 3 53
media 15 1 44  -45 3 52
media 15 1 46  -47 3 53
media 15 1 17  3
media 15 1 19  3
media 15 1 21  3
media 15 1 23  3
media 15 1 29  3
media 15 1 31  3
media 15 1 55  3
media 15 1 57  3
media 15 1 33  3
media 15 1 35  3
media 15 1 41  3
media 15 1 43  3
media 15 1 45  3
media 15 1 47  3
boundary 14

unit 11
com='fuel assembly confinement system'
cuboid 1    24.384      0 24.384      0 520.7000 2.5400
cuboid 2    25.337      -0.9525 25.337       -0.9525
0.0000
cuboid 3    19.812      4.572       24.429      -0.04545
3.81
cuboid 4    19.812      4.572       24.656      -0.27205
3.81
cuboid 5    19.812      4.572       24.702      -0.3175
3.81
cuboid 6    24.429      -0.04545     19.812      4.572
3.81
cuboid 7    24.656      -0.27205     19.812      4.572
3.81
cuboid 8    24.702      -0.3175      19.812      4.572
3.81
hole 20  origin  x=0  y=0  z=16.56  rotate  a1=0 a2=0 a3=0
media 15 1   1
media  7 1  -1   2  -5  -8
media  7 1  -1   3
media 12 1  -3   4
media  7 1  -4   5
media  7 1  -1   6
media 12 1  -6   7
media  7 1  -7   8
boundary 2

unit 20
com='fuel assembly'
```

Table 6-38 Input Deck for Moderator Density Study (cont.)

```
cuboid 1 21.072       0 21.072       0   0        -14.0208
cuboid 2 24.384       0 24.384       0 504.1392   -14.0208
hole 31 origin  x=0       y=0       z=0.0001   rotate  a1=0  a2=0 a3=0
hole 21 origin  x=0       y=0       z=100.0001 rotate  a1=0  a2=0 a3=0
hole 40 origin  x=0       y=0       z=426.7201 rotate  a1=0  a2=0 a3=0
media  15 1  1
media  15 1 -1   2
boundary 2

unit 21
com='fuel rods - nominal pitch'
cuboid 1  21.072       0 21.072       0 326.72       0.0000
array 2 1 place 1 1 1 0.4572       0.4572       0
boundary 1

unit 22
com='solid fuel rod - nominal pitch'
cylinder 1  0.39218       426.72          0
cylinder 2  0.40005      426.72          0
cylinder 3  0.4572       426.72          0
cuboid 4  4P0.62992       426.72          0
media 1 1  1
media 2 1  2 -1
media 3 1  3 -2 -1
media 4 1  4 -3 -2 -1
boundary 4

unit 23
com='thimble tube - nominal pitch'
cylinder 1  0.56134       426.72          0
cylinder 2  0.60198       426.72          0
cuboid 3    4P0.62992      426.72          0
media 4 1 1
media 3 1 2 -1
media 4 1 3 -2 -1
boundary 3

unit 31
com='fuel rods - expanded pitch'
cuboid 1  24.384       0 24.384       0 100          0
array 3 1 place 1 1 1 0.4572       0.4572       0
boundary 1

unit 32
com='solid fuel rod - expanded pitch'
cylinder 1  0.39218       426.72          0
cylinder 2  0.40005      426.72          0
cylinder 3  0.4572       426.72          0
cuboid 4  4P0.73342       426.72          0
media 16  1 1
media 17  1 2 -1
```

Table 6-38 Input Deck for Moderator Density Study (cont.)

```
media 18  1 3 -2 -1
media 19  1 4 -3 -2 -1
boundary 4

unit 33
com='thimble tube - expanded pitch'
cylinder 1  0.56134     426.72          0
cylinder 2  0.60198     426.72          0
cuboid 3  4P0.73342      426.72          0
media 19 1 1
media 18 1 2 -1
media 19 1 3 -2 -1
boundary 3

unit 40
com='top nozzle assembly'
cuboid 1     21.072      0 21.072      0       21.2090     0.0000
cuboid 2     21.072      0 21.072      0      41.8846     0.0000
cuboid 3     21.072      0 21.072      0       52.8193     0.0000
cuboid 4     21.072      0 21.072      0       77.4192     0.0000
cuboid 5     24.384      0 24.384      0       77.4192     0.0008
media  15 1   1
media  15 1  -1   2
media  15 1  -2   3
media  15 1  -3   4
media  15 1  -4   5
boundary 5

unit 66
com='individual package 0-deg rotation'
hexprism 1  31.75    554.1972  -20.1498
hole 10  origin  x=0 y=0  z=0  rotate  a1=0 a2=0 a3=0
media  15 1   1
boundary 1

unit 77
com='individual package 180-deg rotation'
hexprism 1  31.75    554.1972  -20.1498
hole 10  origin  x=0 y=0  z=0  rotate  a1=0 a2=0 a3=180
media  15 1   1
boundary 1

unit 88
com='dummy cell'
hexprism 1  31.75    554.1972  -20.1498
media  20 1   1
boundary 1

global
unit 99
com='package array'
```

Table 6-38 Input Deck for Moderator Density Study (cont.)

```
cylinder 1  432.2355   554.1972  -20.1498
cylinder 2  452.2355   574.1972  -40.1498
cuboid 3  452.2355  -452.2355  452.2355  -452.2355   574.1972  -40.1498
array 1 1  place 9 9 1 0 0 0
media  20 1  -1   2
media   0 1  -2   3
boundary 3

end geometry

read array
ara=1 typ=triangular nux=17 nuy=17 nuz=1 gbl=1
fill

88 88 88 88 88 88 88 88 88 88 88 88 88 88 88 88 88
88 88 88 88 88 88 88 88 88 88 77 77 77 88 88 88 88
88 88 88 88 88 88 88 88 66 66 66 66 66 66 66 88 88
88 88 88 88 88 88 77 77 77 77 77 77 77 77 77 77 88
88 88 88 88 88 66 66 66 66 66 66 66 66 66 66 66 88
88 88 88 88 77 77 77 77 77 77 77 77 77 77 77 77 88
88 88 88 66 66 66 66 66 66 66 66 66 66 66 66 66 88
88 88 88 77 77 77 77 77 77 77 77 77 77 77 88 88 88
88 88 66 66 66 66 66 66 66 66 66 66 66 66 66 88 88
88 88 77 77 77 77 77 77 77 77 77 77 77 77 88 88 88
88 66 66 66 66 66 66 66 66 66 66 66 66 66 66 88 88 88
88 77 77 77 77 77 77 77 77 77 77 77 77 88 88 88 88
88 66 66 66 66 66 66 66 66 66 66 66 66 88 88 88 88 88
88 77 77 77 77 77 77 77 77 77 77 88 88 88 88 88 88
88 88 66 66 66 66 66 66 66 88 88 88 88 88 88 88 88
88 88 88 77 77 77 77 88 88 88 88 88 88 88 88 88 88
88 88 88 88 88 88 88 88 88 88 88 88 88 88 88 88 88
end fill

ara=2 typ=square nux=17 nuy=17 nuz=1
fill 39*22 23 2*22 23 2*22 23 8*22 23 9*22 23 22*22 23 2*22 23 2*22 23
2*22 23 2*22 23 38*22 23 2*22 23 2*22 23 2*22 23 2*22 23 38*22 23
2*22 23 2*22 23 2*22 23 2*22 23 22*22 23 9*22 23 8*22 23 2*22 23 2*22
23 39*22
end fill
ara=3 typ=square nux=17 nuy=17 nuz=1
fill 39*32 33 2*32 33 2*32 33 8*32 33 9*32 33 22*32 33 2*32 33 2*32 33
2*32 33 2*32 33 38*32 33 2*32 33 2*32 33 2*32 33 2*32 33 38*32 33
2*32 33 2*32 33 2*32 33 2*32 33 22*32 33 9*32 33 8*32 33 2*32 33 2*32
33 39*32
end fill

end array

read bnds
+xb=vacuum
-xb=vacuum
```

Table 6-38 Input Deck for Moderator Density Study (cont.)

```
+yb=vacuum
-yb=vacuum
+zb=vacuum
-zb=vacuum
end bnds

end data
end
```

6.10.9.5 Boron Content Sensitivity Study

The Traveller XL was evaluated for sensitivity to varying the boron content in the absorber. Table 6-39 below gives the output data that was used to derive the curve in Section 6.7.8.

Table 6-39 Results of Boron Sensitivity Study

Run #	^{10}B Areal Density (g/cm^2)	ks	σks	ks+2×σks
B10--0050	0.0050	0.9682	0.0008	0.9698
B10-0100	0.0100	0.9478	0.0010	0.9498
B10-0162	0.0160	0.9389	0.0009	0.9405
B10-0180	0.0180	0.9377	0.0008	0.9393
B10-0240	0.0240	0.9329	0.0009	0.9347
B10-0300	0.0300	0.9295	0.0009	0.9313
B10-0350	0.0350	0.9284	0.0009	0.9302

Table 6-39A Number Densities for Boron Sensitivity Study

Run #	^{10}B Areal Density (g/cm^2)	B-10	B-11	C	Al
B10-0050	0.0050	0.0013272	0.0053882	0.0016789	0.05203
B10-0100	0.0100	0.002655	0.010776	0.003358	0.048643
B10-0162	0.0160	0.0043003	0.017458	0.0054396	0.044443
B10-0180	0.0180	0.0047781	0.019398	0.0060439	0.043223
B10-0240	0.0240	0.0063708	0.025864	0.0080586	0.039158
B10-0300	0.0300	0.0079635	0.032329	0.010073	0.035094
B10-0350	0.0350	0.0092907	0.037718	0.011752	0.031706

Table 6-39B Results of Polyethylene Sensitivity Study

Run #	Density (g/cc)	ks	σks	ks+2×σks
POLY-069	0.690	0.9465	0.0008	0.9481
POLY-090	0.828	0.9377	0.0008	0.9393
POLY-100	0.920	0.9306	0.0009	0.9324

Table 6-39C Results of Stainless Steel Sensitivity Study

Run #	Thickness (cm)	ks	σks	ks+2×σks
SS-MINUS	0.2490	0.9372	0.0009	0.9390
XL-HAC-ARRAY-100	0.2660	0.9377	0.0008	0.9393
SS-PLUS	0.2900	0.9368	0.0009	0.9386

Table 6-39D Results of Array Study

Run #	Array Size	ks	σks	ks+2×σks
XL-HAC-ARR1-100	1	0.8738	0.0008	0.8754
XL-HAC-ARR7-100	7	0.9040	0.0009	0.9058
XL-HAC-ARR19-100	19	0.9187	0.0009	0.9205
XL-HAC-ARR37-100	37	0.9303	0.0009	0.9321
XL-HAC-ARR61-100	61	0.9307	0.0013	0.9327
XL-HAC-ARR91-100	91	0.9354	0.0009	0.9372
XL-HAC-ARR127-100	127	0.9362	0.0009	0.9380
XL-HAC-ARRAY-100	150	0.9377	0.0008	0.9393

Table 6-39E Results of Outerpack Diameter Study

Run #	Outerpack Diameter (inch)	ks	σks	ks+2×σks
XL-HAC-ARRD24-100	24	0.9387	0.0009	0.9405
XL-HAC-ARRAY-100	25	0.9377	0.0008	0.9393
XL-HAC-ARRD26-100	26	0.9357	0.0008	0.9373

Table 6-39F Input Deck for Clamshell Up-Rotated Configuration

```
=csas26     parm=size=300000
TRAVELLER XL,17WOFA,ENV=24.384      cm,L=100      cm,B10=0.018   g/cm2
44groupndf5  latticecell
 uo2 1 1 293 92235 5 92238 95 end
 h2o 2 1 293 end
 zirc4 3 1 293 end
 h2o 4 1 293 end
 h2o 5 1 293 end
 arbmfoam 0.1602e-20  4  0  0  0 6012 70 1001 10 8016 16 7014 4  6 1 293
 end
 al 7 1 293 end
 ss304 8 1 293 end
 polyethylene 9 DEN=0.828 1.0 293 end
 arbmfoam 0.1602e-20  4  0  0  0 6012 70 1001 10 8016 16 7014 4 11 1 293
 end
 b-10 12 0 0.0047781    end
 b-11 12 0 0.019398     end
 c   12 0 0.0060439    end
 al  12 0 0.043223     end
 arbmrubber 1.59e-20  7  0  0  0 8016 46.94 13000 19.92 14000 17.54 6012
 10.79 1001 4.73 11000 0.06 26000 0.02  14 1 293 end
 h2o 15 1 293 end
 uo2 16 1 293 92235 5 92238 95 end
 h2o 17 1 293 end
 zirc4 18 1 293 end
 h2o 19 1 293 end
end comp
squarepitch 1.4669       0.78435      16 19 0.9144       18 0.8001       17 end
more data
res=1  cylinder 0.39218      dan(1)=0.22632       end

read parameter
gen=450
npg=2500
nsk=50  rnd=3BA304463B68
wrs=1
tme=240
end parameter

read geometry
unit 10
com='individual package'
cuboid 1    16.904       -15.634       16.904       -15.634       533.1330 0
rotate  a1=45 a2=0 a3=0 origin x=0  y=-1.460 z=0
cuboid 2     21.5900   -21.5900     1.5720    -1.0310   533.1330     0
cuboid 3     20.0790   -20.0790    20.0790   -20.0790   533.1330     0
rotate  a1=45 a2=0 a3=0 origin x=0  y=-1.460 z=0
cuboid 4     20.3450   -20.3450    20.3450   -20.3450   533.3990    -0.2660
rotate  a1=45 a2=0 a3=0 origin x=0  y=-1.460 z=0
```

Table 6-39F Input Deck for Clamshell Up-Rotated Configuration (cont.)

```
cuboid 5     21.5900   -21.590     23.1498   -23.1498   533.1330     0
cuboid 6     21.8560   -21.8560    23.4158   -23.4158   533.3990    -0.2660
cuboid 7     20.3840   -20.3840    20.3840   -20.3840   553.8922   -19.8448
rotate  a1=45 a2=0 a3=0 origin x=0  y=-1.460 z=0
cuboid 8     21.8950   -21.895     23.4548   -23.4548   553.8922   -19.8448
cylinder  9    25.1050    533.4380    -0.2660
cylinder 10    25.1050    553.9312   -19.8448
cylinder 11    31.4840    533.4380    -0.2660
cylinder 12    31.4840    553.9312   -19.8448
cylinder 13    31.4840    533.4380   -19.8448
cylinder 14    31.7500    554.1972   -20.1100
plane 15  zpl=1  con= -10.0000
cylinder 16 7.62   0 -4.5
 rotate  a1=45 a2=90 a3=0 origin x=18.7310 y=-11.1270 z=494.4364
cylinder 17 3.962  0 -7.60
 rotate  a1=45 a2=90 a3=0 origin x=18.7310 y=-11.1270 z=494.4364
cylinder 18 7.62   0 -4.5
 rotate  a1=-45 a2=90 a3=0 origin x=-18.7310 y=-11.1270 z=494.4364
cylinder 19 3.962  0 -7.60
 rotate  a1=-45 a2=90 a3=0 origin x=-18.7310 y=-11.1270 z=494.4364
cylinder 20 7.62   0 -4.5
 rotate  a1=45 a2=90 a3=0 origin x=18.7310 y=-11.1270 z=448.7164
cylinder 21 3.962  0 -7.60
 rotate  a1=45 a2=90 a3=0 origin x=18.7310 y=-11.1270 z=448.7164
cylinder 22 7.62   0 -4.5
 rotate  a1=-45 a2=90 a3=0 origin x=-18.7310 y=-11.1270 z=448.7164
cylinder 23 3.962  0 -7.60
 rotate  a1=-45 a2=90 a3=0 origin x=-18.7310 y=-11.1270 z=448.7164
cylinder 24 7.62   0 -4.5
 rotate  a1=45 a2=90 a3=0 origin x=18.7310 y=-11.1270 z=402.9964
cylinder 25 3.962  0 -7.60
 rotate  a1=45 a2=90 a3=0 origin x=18.7310 y=-11.1270 z=402.9964
cylinder 26 7.62   0 -4.5
 rotate  a1=-45 a2=90 a3=0 origin x=-18.7310 y=-11.1270 z=402.9964
cylinder 27 3.962  0 -7.60
 rotate  a1=-45 a2=90 a3=0 origin x=-18.7310 y=-11.1270 z=402.9964
cylinder 28 7.62   0 -4.5
 rotate  a1=45 a2=90 a3=0 origin x=18.7310 y=-11.1270 z=357.2764
cylinder 29 3.962  0 -7.60
 rotate  a1=45 a2=90 a3=0 origin x=18.7310 y=-11.1270 z=357.2764
cylinder 30 7.62   0 -4.5
 rotate  a1=-45 a2=90 a3=0 origin x=-18.7310 y=-11.1270 z=357.2764
cylinder 31 3.962  0 -7.60
 rotate  a1=-45 a2=90 a3=0 origin x=-18.7310 y=-11.1270 z=357.2764
cylinder 54 7.62   0 -4.5
 rotate  a1=45 a2=90 a3=0 origin x=18.7310 y=-11.1270 z=265.8364
cylinder 55 3.962  0 -7.60
 rotate  a1=45 a2=90 a3=0 origin x=18.7310 y=-11.1270 z=265.8364
```

Table 6-39F Input Deck for Clamshell Up-Rotated Configuration (cont.)

```
cylinder 56 7.62   0 -4.5
 rotate  a1=-45 a2=90 a3=0 origin x=-18.7310 y=-11.1270 z=265.8364
cylinder 57 3.962  0 -7.60
 rotate  a1=-45 a2=90 a3=0 origin x=-18.7310 y=-11.1270 z=265.8364
cylinder 32 7.62   0 -4.5
 rotate  a1=45 a2=90 a3=0 origin x=18.7310 y=-11.1270 z=174.3964
cylinder 33 3.962  0 -7.60
 rotate  a1=45 a2=90 a3=0 origin x=18.7310 y=-11.1270 z=174.3964
cylinder 34 7.62   0 -4.5
 rotate  a1=-45 a2=90 a3=0 origin x=-18.7310 y=-11.1270 z=174.3964
cylinder 35 3.962  0 -7.60
 rotate  a1=-45 a2=90 a3=0 origin x=-18.7310 y=-11.1270 z=174.3964
cylinder 36 7.62   0 -4.5
 rotate  a1=45 a2=90 a3=0 origin x=18.7310 y=-11.1270 z=128.6764
cylinder 37 3.962  0 -7.60
 rotate  a1=45 a2=90 a3=0 origin x=18.7310 y=-11.1270 z=128.6764
cylinder 38 7.62   0 -4.5
 rotate  a1=-45 a2=90 a3=0 origin x=-18.7310 y=-11.1270 z=128.6764
cylinder 39 3.962  0 -7.60
 rotate  a1=-45 a2=90 a3=0 origin x=-18.7310 y=-11.1270 z=128.6764
cylinder 40 7.62   0 -4.5
 rotate  a1=45 a2=90 a3=0 origin x=18.7310 y=-11.1270 z=82.9564
cylinder 41 3.962  0 -7.60
 rotate  a1=45 a2=90 a3=0 origin x=18.7310 y=-11.1270 z=82.9564
cylinder 42 7.62   0 -4.5
 rotate  a1=-45 a2=90 a3=0 origin x=-18.7310 y=-11.1270 z=82.9564
cylinder 43 3.962  0 -7.60
 rotate  a1=-45 a2=90 a3=0 origin x=-18.7310 y=-11.1270 z=82.9564
cylinder 44 7.62   0 -4.5
 rotate  a1=45 a2=90 a3=0 origin x=18.7310 y=-11.1270 z=37.2364
cylinder 45 3.962  0 -7.60
 rotate  a1=45 a2=90 a3=0 origin x=18.7310 y=-11.1270 z=37.2364
cylinder 46 7.62   0 -4.5
 rotate  a1=-45 a2=90 a3=0 origin x=-18.7310 y=-11.1270 z=37.2364
cylinder 47 3.962  0 -7.60
 rotate  a1=-45 a2=90 a3=0 origin x=-18.7310 y=-11.1270 z=37.2364
hole 11 rotate  a1=225 a2=0 a3=0  origin  x=0 y=21.01625 z=5.240
cuboid 48    18.174    20.079   10.4238  -9.5152    533.3990    -0.2660
rotate  a1=-45 a2=0 a3=0 origin x=0  y=-1.460 z=0
cuboid 49    13.6554  -10.4238  16.904    20.079    533.3990    -0.2660
rotate  a1=45 a2=0 a3=0 origin x=0  y=-1.460 z=0
cuboid 50    16.904    20.079   13.6554  -10.4238   533.3990    -0.2660
rotate  a1=45 a2=0 a3=0 origin x=0  y=-1.460 z=0
cuboid 51     9.5152  -10.4238 -18.174   -20.079    533.3990    -0.2660
rotate  a1=-45 a2=0 a3=0 origin x=0  y=-1.460 z=0
cuboid 52    15.634    18.174   12.0238 -11.9197    533.3990    -0.2660
rotate  a1=-45 a2=0 a3=0 origin x=0  y=-1.460 z=0
cuboid 53    11.9197  -12.0238 -15.634   -18.174    533.3990    -0.2660
rotate  a1=-45 a2=0 a3=0 origin x=0  y=-1.460 z=0
```

Table 6-39F Input Deck for Clamshell Up-Rotated Configuration (cont.)

```
media  0 1   1   3  5 -17 -19 -21 -23 -29 -31 -55 -57 -33 -35
-41 -43 -45 -47
media  0 1  -1   3  5 -48 -49 -50 -51 -52 -53
media  9 1   3  -16  -17 -20 -21 -28 -29 -54 -55 -32 -33
-40 -41 -44 -45 48
media  9 1   3  -18  -19 -22 -23 -30 -31 -56 -57 -34 -35
-42 -43 -46 -47 51
media  9 1   3  -18  -22  -30  -56  -34  -42  -46  53
media  9 1   3  -16  -20  -28  -54  -32  -40  -44  52
media  9 1   3  49
media  9 1   3  50
media  8 1  -3   4   6
media  8 1   3  -5   6
media  6 1  -4   9
media  6 1   4  -6   9
media  6 1  -9  11
media  6 1  -7  10 -13
media  6 1   7  -8  10 -13  12
media  6 1 -10 -13  12
media 11 1 -11  13
media 11 1   7   8 -13  12
media  8 1 -12  14
media  0 1 16  -17 3 48
media  0 1 18  -19 3 51
media  0 1 20  -21 3 48
media  0 1 22  -23 3 51
media  0 1 28  -29 3 48
media  0 1 30  -31 3 51
media  0 1 54  -55 3 48
media  0 1 56  -57 3 51
media  0 1 32  -33 3 48
media  0 1 34  -35 3 51
media  0 1 40  -41 3 48
media  0 1 42  -43 3 51
media  0 1 44  -45 3 48
media  0 1 46  -47 3 51
media  0 1 16  -17 3 52
media  0 1 18  -19 3 53
media  0 1 20  -21 3 52
media  0 1 22  -23 3 53
media  0 1 28  -29 3 52
media  0 1 30  -31 3 53
media  0 1 54  -55 3 52
media  0 1 56  -57 3 53
media  0 1 32  -33 3 52
media  0 1 34  -35 3 53
media  0 1 40  -41 3 52
media  0 1 42  -43 3 53
```

Table 6-39F Input Deck for Clamshell Up-Rotated Configuration (cont.)

```
media  0 1 44  -45 3 52
media  0 1 46  -47 3 53
media 14 1 17  3
media 14 1 19  3
media 14 1 21  3
media 14 1 23  3
media 14 1 29  3
media 14 1 31  3
media 14 1 55  3
media 14 1 57  3
media 14 1 33  3
media 14 1 35  3
media 14 1 41  3
media 14 1 43  3
media 14 1 45  3
media 14 1 47  3
boundary 14

unit 11
com='fuel assembly confinement system'
cuboid 1    24.384      0 24.384      0 520.7000 2.5400
cuboid 2    25.337      -0.9525 25.337       -0.9525
 523.2400  0.0000
cuboid 3    19.812      4.572       24.429      -0.04545
 513.0800  3.81
cuboid 4    19.812      4.572       24.656      -0.27205
 513.0800  3.81
cuboid 5    19.812      4.572       24.702      -0.3175
 513.0800  3.81
cuboid 6    24.429      -0.04545     19.812      4.572
 513.0800  3.81
cuboid 7    24.656      -0.27205     19.812      4.572
 513.0800  3.81
cuboid 8    24.702      -0.3175      19.812      4.572
 513.0800  3.81
hole 20  origin  x=0  y=0  z=16.56  rotate  a1=0 a2=0 a3=0
media  0 1   1
media  7 1  -1   2  -5  -8
media  7 1  -1   3
media 12 1  -3   4
media  7 1  -4   5
media  7 1  -1   6
media 12 1  -6   7
media  7 1  -7   8
boundary 2

unit 20
com='fuel assembly'
cuboid 1 21.072       0 21.072       0   0       -14.0208
```

Table 6-39F Input Deck for Clamshell Up-Rotated Configuration (cont.)

```
cuboid 2 24.384       0 24.384       0 504.1392   -14.0208
hole 31 origin  x=0       y=0       z=0.0001   rotate  a1=0  a2=0 a3=0
hole 21 origin  x=0       y=0       z=100.0001 rotate  a1=0  a2=0 a3=0
hole 40 origin  x=0       y=0       z=426.7201 rotate  a1=0  a2=0 a3=0
media  15 1  1
media   0 1 -1   2
boundary 2

unit 21
com='fuel rods - nominal pitch'
cuboid 1  21.072       0 21.072       0 326.72       0.0000
array 2 1 place 1 1 1 0.4572       0.4572       0
boundary 1

unit 22
com='solid fuel rod - nominal pitch'
cylinder 1  0.39218       426.72          0
cylinder 2  0.40005      426.72          0
cylinder 3  0.4572       426.72          0
cuboid 4  4P0.62992       426.72          0
media 1 1  1
media 2 1  2 -1
media 3 1  3 -2 -1
media 4 1  4 -3 -2 -1
boundary 4

unit 23
com='thimble tube - nominal pitch'
cylinder 1  0.56134       426.72          0
cylinder 2  0.60198       426.72          0
cuboid 3    4P0.62992      426.72          0
media 4 1 1
media 3 1 2 -1
media 4 1 3 -2 -1
boundary 3

unit 31
com='fuel rods - expanded pitch'
cuboid 1  24.384       0 24.384       0 100          0
array 3 1 place 1 1 1 0.4572       0.4572       0
boundary 1

unit 32
com='solid fuel rod - expanded pitch'
cylinder 1  0.39218       426.72          0
cylinder 2  0.40005      426.72          0
cylinder 3  0.4572       426.72          0
cuboid 4  4P0.73342       426.72          0
media 16  1 1
```

Table 6-39F Input Deck for Clamshell Up-Rotated Configuration (cont.)

```
media 17  1 2 -1
media 18  1 3 -2 -1
media 19  1 4 -3 -2 -1
boundary 4

unit 33
com='thimble tube - expanded pitch'
cylinder 1  0.56134     426.72          0
cylinder 2  0.60198     426.72          0
cuboid 3  4P0.73342      426.72          0
media 19 1 1
media 18 1 2 -1
media 19 1 3 -2 -1
boundary 3

unit 40
com='top nozzle assembly'
cuboid 1     21.072      0 21.072      0       21.2090     0.0000
cuboid 2     21.072      0 21.072      0      41.8846     0.0000
cuboid 3     21.072      0 21.072      0       52.8193     0.0000
cuboid 4     21.072      0 21.072      0       77.4192     0.0000
cuboid 5     24.384      0 24.384      0       77.4192     0.0008
media  15 1   1
media  15 1  -1   2
media  15 1  -2   3
media  15 1  -3   4
media  15 1  -4   5
boundary 5

unit 66
com='individual package 0-deg rotation'
hexprism 1  31.75    554.1972  -20.1498
hole 10  origin  x=0 y=0  z=0  rotate  a1=0 a2=0 a3=0
media   0 1   1
boundary 1

unit 77
com='individual package 180-deg rotation'
hexprism 1  31.75    554.1972  -20.1498
hole 10  origin  x=0 y=0  z=0  rotate  a1=0 a2=0 a3=180
media   0 1   1
boundary 1

unit 88
com='dummy cell'
hexprism 1  31.75    554.1972  -20.1498
media  15 1   1
boundary 1
```

Table 6-39F Input Deck for Clamshell Up-Rotated Configuration (cont.)

```
global
unit 99
com='package array'
cylinder 1  432.2355   554.1972  -20.1498
cylinder 2  452.2355   574.1972  -40.1498
cuboid 3  452.2355  -452.2355  452.2355  -452.2355   574.1972  -40.1498
array 1 1  place 9 9 1 0 0 0
media  15 1  -1   2
media   0 1  -2   3
boundary 3

end geometry

read array
ara=1 typ=triangular nux=17 nuy=17 nuz=1 gbl=1
fill
88 88 88 88 88 88 88 88 88 88 88 88 88 88 88 88 88
  88 88 88 88 88 88 88 88 88 88 77 77 77 88 88 88 88
    88 88 88 88 88 88 88 88 66 66 66 66 66 66 66 88 88
      88 88 88 88 88 88 77 77 77 77 77 77 77 77 77 77 88
        88 88 88 88 88 66 66 66 66 66 66 66 66 66 66 66 88
          88 88 88 88 77 77 77 77 77 77 77 77 77 77 77 88
            88 88 88 66 66 66 66 66 66 66 66 66 66 66 66 88
              88 88 88 77 77 77 77 77 77 77 77 77 77 77 88 88
                88 88 66 66 66 66 66 66 66 66 66 66 66 66 88 88
                  88 88 77 77 77 77 77 77 77 77 77 77 77 88 88 88
                    88 66 66 66 66 66 66 66 66 66 66 66 66 88 88 88
                      88 77 77 77 77 77 77 77 77 77 77 77 88 88 88 88
                        88 66 66 66 66 66 66 66 66 66 66 66 88 88 88 88 88
                          88 77 77 77 77 77 77 77 77 77 77 88 88 88 88 88
                            88 88 66 66 66 66 66 66 66 88 88 88 88 88 88 88
                              88 88 88 77 77 77 77 88 88 88 88 88 88 88 88
                              88 88 88 88 88 88 88 88 88 88 88 88 88 88 88
end fill

ara=2 typ=square nux=17 nuy=17 nuz=1
fill 39*22 23 2*22 23 2*22 23 8*22 23 9*22 23 22*22 23 2*22 23 2*22 23
 2*22 23 2*22 23 38*22 23 2*22 23 2*22 23 2*22 23 2*22 23 38*22 23
 2*22 23 2*22 23 2*22 23 2*22 23 22*22 23 9*22 23 8*22 23 2*22 23 2*22
 23 39*22
end fill
ara=3 typ=square nux=17 nuy=17 nuz=1
fill 39*32 33 2*32 33 2*32 33 8*32 33 9*32 33 22*32 33 2*32 33 2*32 33
 2*32 33 2*32 33 38*32 33 2*32 33 2*32 33 2*32 33 2*32 33 38*32 33
 2*32 33 2*32 33 2*32 33 2*32 33 22*32 33 9*32 33 8*32 33 2*32 33 2*32
 33 39*32
end fill
```

Table 6-39F Input Deck for Clamshell Up-Rotated Configuration (cont.)

```
end array

read bnds
+xb=vacuum
-xb=vacuum
+yb=vacuum
-yb=vacuum
+zb=vacuum
-zb=vacuum
end bnds

end data
end
```

This page intentionally left blank.

6.10.10 Benchmark Critical Experiments

Table 6-40 Summary of Available LWR Critical Experiments

Report	No. of available experiments	No. of selected experiments	Description of criticality experiments
ANS Transactions, Vol. 33, p. 362 (Ref. 5)	25	9/9	4.74 wt % ^{235}U UO_2 fuel rods in square lattices of 1.35 cm pitch; fuel 235 clusters separated by air, polystyrene, polyethylene, or water; fuel clusters submersed in aqueous $NaNO_3$ solution
BAW-1484 (Ref. 6)	37	1/10	2.46 wt % ^{235}U UO_2 fuel rods in square lattices of 1.636 cm pitch; the spacing between 3 × 3 array of LWR-type fuel assemblies is filled with water and B4C pins, stainless steel sheets, or borated stainless steel sheets; lattices with borated moderator
EPRI-NP-196 (Ref. 7)	6	3/6	2.35 wt % ^{235}U UO_2 fuel rods in square lattices of 1.562, 1.905, 235 and 2.210 cm pitch; lattices with borated moderator
NS&E, Vol. 71 (Ref. 8)	26	3/6	4.74 wt % ^{235}U UO_2 fuel rods in square lattices of 1.26 cm, 1.60 cm, 2.10 cm, and 2.52 cm pitch; triangular and triangular with pseudo-cylindrical shape lattices of 1.35, 1.72, and 2.26 cm pitch; irregular hexagonal lattices of 1.35 cm pitch; lattices with water holes
PNL-2438 (Ref. 9)	48	4/6	2.35 wt % ^{235}U UO_2 fuel rods in square lattices of 2.032 cm pitch; Cd, Al, Cu, stainless steel, borated stainless steel, Boral, and Zircaloy separator plates between assemblies
PNL-2827 (Ref. 10)	23	1/9	2.35 and 4.31 wt % ^{235}U UO_2 fuel rods in square lattices of 2.032, 235 and 2.540 cm pitch; reflecting walls of Pb or depleted uranium
PNL-3314 (Ref. 11)	142	18/27	2.35 and 4.31 wt % ^{235}U UO_2 fuel rods in square lattices of 1.684 and 1.892 cm pitch; stainless steel, borated stainless steel, Cd, Al, Cu, Boral, Boroflex, and Zircaloy separator plates between assemblies; lattices with water holes and voids
PNL-3926 (Ref. 12)	22	2/14	2.35 and 4.31 wt % ^{235}U UO_2 fuel rods in square lattices of 1.684, 235 and 1.892 cm pitch; reflecting walls of Pb or depleted uranium
WCAP-3269 (Ref. 15)	157	3/9	2.7, 3.7, and 5.7 wt % ^{235}U UO_2 fuel rods in square lattices of 1.029, 1.105, and 1.422 cm pitch; lattices with Ag-In-Cd absorber rods, water holes, void tubes

Table 6-40 Summary of Available LWR Critical Experiments (cont.)

Report	No. of available experiments	No. of selected experiments	Description of criticality experiments
WCAP-3385 (Ref. 16)	3	2/2	5.74 wt % ^{235}U UO_2 fuel rods in square lattices of 1.321, 1.422, and 2.012 cm pitch
BAW-1645 (Ref. 17)	21	2/8	2.46 wt % ^{235}U UO_2 fuel rods in close-packed triangular lattices of 1.209 cm pitch, close-packed square lattices of 1.209 cm pitch, and square lattices of 1.410 cm pitch
PNL-6205 (Ref. 20)	19	1/1	4.31 wt % ^{235}U UO_2 fuel rods in square lattices of 1.891 cm pitch; Boral flux traps
PNL-7167 (Ref. 21)	9	4/4	4.31 wt % ^{235}U UO_2 fuel rods in square lattices of 1.891 cm pitch; Boral flux traps containing voids filled with Al plates, Al rods, or UO_2 fuel rods.

Table 6-41 Critical Benchmark Experiment Classification

Report	Critical Benchmark Experiment Groups			
	Simple lattice	**Separator plate**	**Flux trap**	**Water hole**
ANS Transactions, Vol. 33, p. 362	ANS33SLG (8)	ANS33AL1 (1) ANS33AL2 (2) ANS33AL3 (3)	ANS33EB1 (4) ANS33EB2 (5) ANS33EP1 (6) ANS33EP2 (7) ANS33STY(9)	
BAW-1484	BW1484SL (24)			
EPRI-NP-196	EPRU65 (45) EPRU75 (47) EPRU87 (44)			
NS&E, Vol. 71, p. 154	NS&E71SQ (54)			NS&E71W1 (55) NS&E71W2 (56)
PNL-2438	P2438SLG (60)	P2438AL (57) P2438BA (58) P2438SS (61)		
PNL-2615		P2615AL (63) P2615BA (64) P2615SS (68)		
PNL-2827	P2827SLG (74)			
PNL-3314	P3314SLG (96)	P3314AL (79) P3314BA (80) P3314BC (81) P3314BF1 (82) P3314BF2 (83) P3314BS1 (84) P3314BS2 (85) P3314BS3 (86) P3314BS4 (87) P3314SS1 (97) P3314SS2 (98) P3314SS3 (99) P3314SS4 (100) P3314SS5 (101) P3314SS6 (102)		P3314W1 (103) P3314W2 (104)
PNL-3926	P3926SL1 (138) P3926SL2 (139)			
PNL-6205		P62FT231 (154)		
PNL-7167		P71F214R (158)	P71F14F3 (155) P71 F14V3 (156) P71 F14V53 (157)	
WCAP-3269	W3269SL1 (168) W3269SL2 (169)			W3269W1 (170) W3269W2 (171)
WCAP-3385	W3385SL1 (172) W3385SL2 (173)			
Total	**15**	**26**	**8**	**6**

Table 6-42 Summary Comparison of Benchmark Critical Experiment Properties to Traveller

	Critical Benchmark Experiments					
	All	**Simple lattice**	**Separator**	**Flux Trap**	**Water Hole**	**Traveller Package**
Number of cases	55	15	26	8	6	19
Properties of Lattice						
Water-to-fuel volume ratio	1.196-5.067	1.196-5.067	1.6-3.883	1.6-2.302	1.495-1.932	2.21-3.49
Hydrogen-to-fissile ratio	97.6-504.2	97.6-504.2	105-398.	105-138.4	98.3-218.6	120.5-190.4
Lattice pitch	1.26-2.540	1.26-2.21	1.35-2.54	1.35-1.891	1.26-1.892	1.26-1.467
Dancoff factor	0.03889-0.3772	0.05727-0.3772	0.03889-0.20179	0.17388-0.20096	0.17284-0.25719	0.13137-0.22632
Water hole/No. pins	0.051-0.152	NA	NA	NA	0.051-0.152	0.095
Properties of UO_2 fuel rods						
Outside diameter, cm	0.86-1.4147	0.86-1.206	0.94-1.4147	0.94-1.4147	0.94-1.4147	0.9144
Wall thickness, cm	0.038-0.081	0.038-0.081	0.06-0.0762	0.06-0.0762	0.038-0.0795	0.05715
Wall material	Al Zircaloy-4 304SS	Al Zircaloy-4 304SS	Al	Al	Zircaloy-4 304SS	Zircaloy-4
Pellet diameter, cm	0.7544-1.2649	0.7544-1.2649	0.79-1.2649	0.79-1.2649	0.79-1.2649	0.7844
Total fuel length, cm	97.155-156.44	97.155-156.44	97.155-156.44	97.155-156.44	97.155-156.44	426.72
Active fuel length, cm	90.0-153.44	90.0-153.44	90.0-153.44	90.0-153.44	90.0-153.44	426.72
Enrichment, $^{235}U/U$ wt%	2.35-5.74	2.35-5.74	2.35-4.74	4.31-4.74	2.35-5.70	5.00
Fuel density, g/cm^3	9.20-10.412	9.20-10.412	9.20-10.412	10.38-10.412	9.20-10.412	10.96

Table 6-42 Summary Comparison of Benchmark Critical Experiment Properties to Traveller (cont.)

	Critical Benchmark Experiments					
	All	**Simple lattice**	**Separator**	**Flux Trap**	**Water Hole**	**Traveller Package**
Neutron Interaction Characteristics						
^{10}B areal densities, g/cm^2	0.026 -0.090	NA	0.026-0.090	0-0.073	NA	0.0203
Plate thickness, cm	0.231-0.772	NA	0.231-0.772	0.300-0.673	NA	0.3175
AGF	32.82-36.61	33.1-36.61	32.85-36.28	32.82-34.29	33.18-35.25	33.49-34.98
AEF, eV	0.0828-0.3738	0.0828-0.3240	0.0948-0.3703	0.2050-0.3738	0.1468-0.3095	0.1944-0.2759
Separation, cm	2.5-12.97	5-12.97	2.5-11.55	2.5-5.19	NA	9.5-12.54
Geometry						
Moderator height, Hc (cm)	25.54-129.65	38.61-129.65	25.54-64.2	NA	NA	NA

This page intentionally left blank.

TABLE OF CONTENTS

This page intentionally left blank.

7.0 PACKAGE OPERATIONS

The following information contains the significant events relating to the routine use of fuel assembly shipping packages. Complete detailed instructions are outlined within the individual plant operating procedures and quality control instructions pertinent to each specific operation.

7.1 PACKAGE LOADING

7.1.1 Preparation for Loading

7.1.1.1 Receive Shipping Package

- Unload the shipping package from the truck.
- Report any obvious damage to the package engineer.
- Prepare a package identification route card.

7.1.1.2 Clean Shipping Package

- Use soap or a suitable detergent and water to clean the package.
- Hose down the package and direct a high pressure water stream.
- Move the package to the refurbishing or lay down areas.

7.1.1.3 Refurbish Shipping Package

- Check package upper and lower outerpack exterior for damage.
- Open outerpack and check for internal damage or excessive wear.
- Repair/rework as required.
- Check clamshell for loose parts, and if found, secure per specifications and drawings.
- Vacuum package to collect foreign debris.

7.1.1.4 Configure Package for Fuel Assembly Loading

- Configure (install) top axial restraint and axial spacers for specific fuel assembly type.
- Check accelerometers for QC seal, calibration, and tripped condition. Install or replace as necessary.

7.1.1.5 Inspection

- Verify that the package interior/exterior outerpack and clamshell are clean, and in good condition.
- Verify that the top axial restraint, axial spacers and grids pads are present and in good working condition.
- Verify that outstanding package ECN’s have been cleared prior to release for loading.

7.1.2 Loading Contents and Closing Package

- Raise shipping package to vertical position and lockout support arms.
- Loosen upper outerpack swing bolts.
- Remove upper outerpack bolts on one side of the package.
- Swing open upper outerpack door.
- Remove the hinge pin and open clamshell top access door.
- Loosen and remove clamshell top head and axial restraint.
- Open lower clamshell doors by turning latches to open position.
- Install clamshell door stops.
- Check upper and lower accelerometers are not tripped.
- Install fuel assembly by resting on clamshell bottom head.
- Check grid pads are positioned at fuel assembly grids and nozzles.
- Remove door stops.
- Close lower clamshell doors and secure latches by turning to lock position.
- Remove fuel tool.
- Install clamshell top head and tighten axial restraint.
- Close clamshell top access door and install hinge pin.
- Close the upper outerpack.
- Rotate outerpack swings bolts into bracket and torque to 20 ± 1 foot pounds.
- Install outerpack bolts and torque to 60 ± 5 foot pounds.
- Unlock upper support arm and lower package to horizontal position.

7.1.2.1 Inspection

- Verify that the fuel assembly has been released.
- Verify that the fuel assembly is properly oriented in the package.
- Verify that the grids pads are located at the grids and nozzles.
- Verify the accelerometers are sealed, calibrated and not tripped.
- Verify general cleanliness and absence of debris inside the package prior to closing the upper outerpack door.
- Verify that the swing bolts are torqued to 20 ± 1 foot pounds and the outerpack bolts to 60 ± 5 foot pounds.
- Verify one approved tamper proof security seal is installed on opposite side of the package.
- Verify that the required decals, license plates, labels, stencil markings, etc. are present and legible.

7.1.3 Preparation for Transport

7.1.3.1 Truck Loading of Shipping Packages

- Place shipping package on trailer equipped to permit chaining down of package.
- Center and place package lengthwise on trailer.
- Install spacer bars, if required, and install quick release lockout pin.
- Secure packages to trailer bed with stops.
- Chain packages to trailer using "come along" tighteners and chains of 3/8 inch minimum diameter.
- Place webbing swings over spacer bars, if required, and secure to trailer.

7.1.3.2 Regulatory

- Conduct direct alpha surveys on both the packages and the accessible areas of the flatbed.
- Perform the removable alpha and beta-gamma external smear surveys on both the packages and the accessible areas of the flatbed. If any single alpha measurement exceeds 220 dpm/100 cm^2 or beta-gamma measurement exceeds 2200 dpm/100 cm^2, notify Regulatory Engineering for instructions on decontamination.

7.1.3.3 Inspection

- Verify that packages are properly stacked and secured.
- Verify that required Health Physics, Radioactive and any other placards or labels have been properly placed.
- Verify that two tamper proof security seals have been properly placed on each package.

7.2 PACKAGE UNLOADING

7.2.1 Receipt of Package from Carrier

- Perform an external inspection of the unopened package and record any significant observations.
- Verify that two tamper proof security seals have been properly placed on each package. If either seal is missing or damaged, record the damage and follow site procedures for possible security issues.

7.2.2 Removal of Contents

- Install package into the upender.
- Remove all but one of the upper outerpack bolts on one side of the package. (All other hinge bolts remain in place).
- Raise the package to full vertical position and lockout upender support arms.
- Remove the remaining hinge bolt from the one side.
- Loosen upper outerpack swings bolts and rotate away.
- Open upper outerpack door a full 180 degrees.
- Check upper and lower accelerometers for tripped condition.
- Remove the clamshell top hinge pin and open clamshell access door.
- Loosen and remove clamshell top head and top axial restraint assembly.
- Install and latch the plant fuel tool.
- Tension crane cable between 300 to 500 pounds.
- Turn lower clamshell door latches to open position and open doors.
- Install clamshell door stops.
- Lift fuel assembly at least 1.5 inches above clamshell bottom head.
- Carefully remove fuel assembly from clamshell.
- Move fuel assembly to dry storage.
- Prepare to close clamshell by removing clamshell door stops.
- Close lower clamshell doors and secure latches.
- Install clamshell top head and axial restraint.
- Close clamshell top access door and install hinge pin.
- Rotate outerpack swing bolts into bracket and torque to 20 ± 1 foot pounds.
- Install outerpack bolts and torque to 60 ± 5 foot pounds.
- Unlock upender support arms and lower package to horizontal position.

7.3 PREPARATION OF EMPTY PACKAGE FOR TRANSPORT

- Verify the package is empty of contents.
- Verify radiation levels do not exceed limits prescribed in 49 CFR 173.421 (a) (2).
- Verify non-fixed radioactive surface contamination does not exceed limits prescribed in 49 CFR 173.421 (a) (3).
- Verify the package does not contain more than 15 grams of uranium-235.
- Verify the packaging is in unimpaired condition and is securely closed.
- Verify the internal contamination does not exceed 100 times limits prescribed in 49 CFR 173.428 (c).
- Remove any previously applied labels affixed for fuel shipments.
- Affix an “Empty” label.

7.4 APPENDICES

7.4.1 References

None.

TABLE OF CONTENTS

This page intentionally left blank.

8.0 ACCEPTANCE TESTS AND MAINTENANCE PROGRAM

8.1 ACCEPTANCE TESTS

Per the requirements of 10 CFR §71.85(c), this section discusses the inspections and acceptance tests to be performed prior to first use of the Traveller package.

8.1.1 Visual Inspections and Measurements

All Traveller packaging materials of construction and welds shall be examined in accordance with the requirements delineated in Table 2-2 of Section 2.

The Traveller STD and Traveller XL packages have manufacturing drawings that are controlled within a quality assurance program. The drawings have quality control characteristics that must be inspected during the process. Source inspection and final release of the package will be performed by Westinghouse to verify the quality characteristics were inspected and that the package is acceptable. Any characteristic that is out of specification must be reported. It will then be dispositioned according to Westinghouse procedure.

8.1.2 Weld Examinations

All Traveller welds shall be examined to verify conformance with all applicable codes, and standards and notes on each applicable drawing or specification.

8.1.3 Structural Tests

The Traveller packaging contains hoist rings which require acceptance inspection.

8.1.4 Pressure Leak Tests

The Traveller packaging does not have any requirements for leak or pressure testing.

8.1.5 Component and Material Tests

8.1.5.1 Polyurethane Foam

The Traveller packaging utilizes a closed-cell, polyurethane foam and must certified to meet the requirements and acceptance criteria for installation, inspection, and testing as defined in this section.

The finished foam product shall be greater than 85% closed cell polyurethane plastic foam of the self-extinguishing variety of the density specified. The closed cell configuration will ensure that the foam will not be susceptible to significant water absorption.

8.1.5.1.1 Density

Rigid polyurethane foam shall have a density per the following table:

Part	Lb/ft^3
End Caps	20.0 +/- 2.0
Package body	10.0 +/- 1.0
Inner Limiter	6.0 +/- 1.0

Density shall be determined in accordance with ASTM D-1622 with the following exceptions:

a) A minimum of one specimen per pour shall be taken, distributed regularly throughout the batch.

b) Conditioning shall be 70°F to 80°F and 40% – 60% relative humidity for 12 hours minimum.

c) Test conditions shall be 70°F to 80°F and 30% – 70% relative humidity.

d) Length, width and thickness measurements shall be made with a 6-inch digital or dial caliper.

e) Measurements shall be made and reported to the nearest 0.001 inches.

f) Density shall be reported in pounds per cubic foot and no correction made for the (negligible) buoyant effect of air.

g) The standard deviation of the three density determinations need not be calculated or reported.

8.1.5.1.2 Mechanical Properties

Exhibited foam compressive strength for 10% strain parallel to foam rise shall be determined in accordance with ASTM D-1621, with the exceptions noted below, and shall fall within the following range of values:

Part	Density	Min	Max
End	20.0 +/- 2.0	888 psi	1332 psi
Body	10.0 +/- 1.0	262 psi	393 psi
Inner	6.0 +/- 1.0	132 psi	198 psi

a) Specimen shall be right rectangular prisms 1.0+/-0.1 inches thick x 2.0+/-0.1 inches x 2.0+/-0.1 inches with the 1.0+/-0.1 inch dimension parallel to the direction of foam rise.

b) A specimen from each batch shall be tested.

c) Conditioning shall be 70°F to 80°F and 40% – 60% relative humidity for 12 hours minimum.

d) Test conditions shall be 70°F to 80°F and 30% – 70% relative humidity.

e) Length, width and thickness measurements shall be made with a 6-inch digital or dial caliper.

f) Measurements shall be made and reported to the nearest 0.001 inches.

g) Strain rate shall be 0.1 +/- 0.05 in/in – min.

h) Only actual values (not averages or standard deviations) need be reported.

8.1.5.1.3 Flame Retardant Characteristics

Flame retardant characteristics shall be qualified by demonstrating compliance with the following requirements. The requirements shall be demonstrated by flame testing described in FAA Powerplant Engineering Report No. 3A. Additional certification testing to validate the flame-retardant characteristics shall also be performed in accordance with ASTM F-501-93. The test described in b) below is not applicable to the 6 pcf foam.

a) Foam shall not be capable of sustaining a flame for a period greater than five (5) minutes, following the removal of the heat source and after being exposed to temperatures up to 1,500°F. A heat source with a flame temperature of at least 1,500°F is applied until the foam is ignited. The heat source is removed after ignition of the foam and the time until self-extinguishment of the flame (absence of flame) will be monitored and compared against the 5-minute acceptance criteria.

b) Prepare a representative sample of the foam material and test in accordance with the following:

   1) Cut two pieces of sheet metal (16 gauge maximum/25 gauge minimum) to a size sufficient to cover a 10 inch diameter test sample.

   2) Attach a thermocouple at the approximate center of one side of each piece of sheet metal.

   3) Prepare a representative sample of the foam material inside a 10-inch inner diameter by 6-inch long steel cylinder. Foam to fill the entire length of the cylinder and the full 10-inch diameter.

4) Sandwich the sample between the two pieces of sheet metal, with the thermocouples in contact with the foam.

5) Expose one end of the foam sample (sheet metal) to a heat source. Apply enough heat to cause the indicated thermocouple temperature to increase from ambient temperature to 1,475°F minimum on the exposed side.

6) Hold the sample at a minimum of 1,475°F for a minimum period of thirty (30) minutes.

Acceptance criteria shall be as follows:

During the period that heat is applied, the thermocouple on the non-exposed end of the sample shall not exceed 180°F. The thermocouple on the back side (away from the flame) shall be isolated from the sheet metal to prevent heat from radiating from the metal instead of traversing the foam core. The thermocouple can be isolated using a piece of Nomex cloth or approved equivalent.

8.1.5.1.4 Thermal Properties

The foam shall exhibit the following thermal characteristics for the 6 pcf, 10 pcf and 20 pcf nominal density pours, minimum of three specimens per qualification:

a) Thermal Conductivity

Thermal conductivity (Test Method – ASTM C-177 at 75°F mean temperature)	**k-factor** (BTU/Hr-ft^2-F/inch)
LAST-A-FOAM® FR-3706	0.240
LAST-A-FOAM® FR-3710	0.279
LAST-A-FOAM® FR-3720	0.376

b) Specific Heat

0.353 BTU/lb-°F (Test Method – ASTM E-1269)

8.1.5.1.5 Water Absorption

The average water absorption by the foam observed by testing using ASTM D-2842, with the following exceptions, shall not be more than 5% by volume. The construction of the Traveller will further ensure that in actual operation, significantly lower water absorption rate would be observed.

a) Length, width and thickness measurements shall be made with a digital or dial caliper.

b) Measurements shall be made and reported to the nearest 0.001 inches.

c) A single specimen of the qualifying material shall be molded to the density range as stated in the density chart above.

d) The specimen shall consist of a single 3.0 inches x 6.0 inches x 6.0 inches (tolerance on dimension is 0.5 inches) block of foam.

e) No correction shall be made for cut or open cells in the specimen's volume calculations.

8.1.5.1.6 Chemical Composition

The chemical composition of the foam shall be as follows:

C – 50 – 70%
O – 14 – 34%
N – 4 – 12%
H – 4 – 10%
P – 0 – 2%
Si – < 1%
Cl – < 1800 PPM
Leachable Chlorides < 1 PPM
Other < 1%

The foam will be a rigid polyether polyurethane formed as reaction product of the primary chemicals: polyphenylene, polymethylene, polyisocyanate (polymeric isocyanate) and polyoxypropylene glycols (polyether polyols). These materials react to produce a rigid, polyether, polyurethane foam. The foam will not contain halogen containing flame retardant or trichloromonoflouromethane (Freon 11).

Leachable chloride testing is required when using stainless steel as the container structure because free chloride ions in contact with the container sides have been faulted as a contributor to stress corrosion cracking. Leachable chlorides will not be greater than 1 ppm when tested in accordance with GP-TM9510: Method for Sample Preparation and Determination of Leachable Chlorides in Rigid Polyurethane Foam or EPA 300.0: Determination of Inorganic Anions by Ion Chromatography.

8.1.5.2 Neutron Absorber Plates

Neutron absorber plates are installed along the four faces of the Clamshell to meet the requirements specified in Section 6 of this document. The Traveller packaging has two options for this material.

a) Deleted.

b) BORAL – a hot-rolled composite aluminum sheet consisting of a core of uniformly distributed boron carbide and aluminum particles which is enclosed within layers of pure aluminum forming a solid barrier against the environment.

The plates are used to ensure subcriticality during transportation as a neutron absorber and are not relied upon for the conductivity or mechanical properties. The service conditions are not so severe as to promote significant alterations of these plates. Therefore, durability of these neutron absorbing materials is regarded to meet or exceed the service requirements of this application.

To ensure the BORAL meets the drawing requirements, the plates will be inspected on a periodic basis not to exceed five years per Section 8.2.5. This will ensure that the BORAL maintains its durability throughout its service lifetime. The visual inspection will verify that the plates are present and in good condition. This includes inspection of the BORAL core for chipping or flaking resulting from brittleness. There are no significant loads applied to the BORAL plates, therefore no durability problems should arise during normal conditions of transport.

No processing changes are anticipated for the production of BORAL since the established process will be used to produce the packages.

8.1.5.2.1 Deleted

8.1.5.2.2A BORAL

Boron-10 Areal Density

The BORAL neutron absorber plate minimum ^{10}B areal density for the final thickness of 0.125 ±0.006" is 0.024 gm/cm^2. Acceptance testing to ensure that the manufacturing process is operating in a satisfactory manner may be conducted using neutronics transmission or chemical analysis to ensure an effective minimum ^{10}B areal density of 0.018 gm/cm^2 (75% credit of Boron-10).

Neutron Transmittance is a neutron counting testing technique performed to determine the concentration of an isotope in a material. Testing involves placement of test coupons in a calibrated neutron source beam and measuring the number of neutrons allowed to pass through the test material. Based on the number of neutron count, the areal density of the coupon can be calculated and compared to certified standards. Chemical analysis is assay testing performed on a sample taken from test coupons to determine the boron content.

Neutronics Absorption Testing Requirements

Neutron Transmittance testing shall be performed at thermal neutron energies per approved test method to verify the minimum required ^{10}B concentration. Test coupons are considered acceptable when the transmittance data indicates a ^{10}B areal density equal to or greater than 0.024 gm/cm^2. Statistical data on transmissivity may be coupled with luminescence test data to demonstrate uniformity of the boron material.

Neutron Radiograph testing shall be performed for each selected sample with a luminance test or approved equivalent to verify the uniformity of the ^{10}B distribution in the sheet at thermal neutron energies. Neutron Radiograph (luminance) testing is a non-destructive imaging technique for the internal evaluation of materials. It involves attenuation of a neutron beam by an object to be radiographed, and registration of the attenuation process (as an image) on film or video. Inspection results shall be recorded using the appropriate data recording method by the testing facility.

Chemical Testing Requirements

Chemical testing may be employed as an acceptable substitute to the neutronics testing to verify the minimum areal density of ^{10}B is present in the neutron absorber plate. Prior to ^{10}B verification by chemical testing, the process shall be demonstrated to be equivalent to the neutronics testing described with respect to ^{10}B uniformity and isotopic composition. Test coupons are considered acceptable when the calculated ^{10}B areal density is equal to or greater than is 0.024 gm/cm^2.

Sampling Rates and Test Methods

The inspection levels shall be as stipulated in the supplier submitted process specification(s). Test methods, when not referenced herein, shall be reviewed by Westinghouse Columbia engineering. Sample coupons shall be randomly selected and be representative of the configuration, material, and lot being evaluated.

Requirement	Number of Tests Per Lot	Test Method
Aluminum Alloy Composition	1 per Heat	ASTM B209 and Approved Procedure
Neutron Radiograph	100%(1)	NFD Approved Procedure
Neutron Transmittance for ^{10}B Areal Density	100%(1)	NFD Approved Procedure
Chemical Testing	100%(2)	NFD Approved Procedure

Notes:

(1) For every lot, initial sampling of coupons for neutron transmission measurements and radiograph/radioscopy shall be 100%, which shall be considered normal sampling. Rejection of a given coupon shall result in rejection of any contiguous plate(s). Reduced sampling (50%) may be introduced based upon acceptance of all coupons in the first 25% of the lot. The approved process specification shall reflect the use of reduced sampling, as applicable. A rejection during reduced inspection will require a return to 100% inspection of the lot.

(2) For every lot, initial sampling of coupons for chemical testing shall be 100%, which shall be considered normal sampling. Rejection of a given coupon shall result in rejection of any contiguous plate(s). Reduced sampling of the lot to 95/95 confidence sampling is acceptable based upon acceptance of all coupons in the first 25% of the lot. The approved process specification shall reflect the use of reduced sampling, as applicable. A rejection during reduced inspection will require a return to 100% inspection of the lot.

This page intentionally left blank.

8.1.5.2.3 Mechanical Tests

The neutron absorber plates perform a neutronic function in the Traveller packages. Thus, no mechanical testing is required.

8.1.5.2.4 Moved to Sections 8.1.5.2.1 and 8.1.5.2.1A.

8.1.5.2.5 Moved to Sections 8.1.5.2.1 and 8.1.5.2.1A.

8.1.5.2.6 Visual Inspection

For all plates, the finished plate shall be free of visual surface cracks, blisters, pores, or foreign inclusions.

BORAL

Evidence of foreign material shall be cause for rejection (embedded pieces of B_4C matrix are not considered foreign material). Creases or other surface discontinuities are acceptable on the cladding of the BORAL provided the core is not exposed. If necessary, the plate shall be examined with a 5X glass to determine if a surface indication is a crease or a crack. Surface roughness shall not exceed 125 RMS roughness maximum.

8.1.5.2.7 Tests

a) Lot Definition – A lot shall consist of all plate of the same nominal size, condition and finish that is produced from the same heat, processed in the same manner, and presented for inspection at the same time.

b) Heat Definition – A heat shall consist of the total molten metal output from a single heating in a batch melting process or the total metal output from essentially a single heating in a continuous melting operation and targeted at a fixed metal chemistry at the furnace spout.

c) Deleted.

d) Coupon (BORAL) – A selected sample of the thinnest section of a lot of the neutron absorber used for acceptance testing of the candidate material.

8.1.5.3 Polyethylene Sheeting

This section establishes the requirements and acceptance criteria for inspection and testing of Ultra High Molecular Weight (UHMW) Polyethylene sheeting utilized within the Traveller packaging.

8.1.5.3.1 Polyethylene Composition

The supplier shall certify that the polyethylene is Ultra High Molecular Weight (UHMW).

8.1.6 Shielding Tests

The Traveller package does not contain any biological shielding.

8.1.7 Thermal Tests

The material properties utilized in Chapter 3, Thermal Evaluation, are consistently conservative for the Normal Conditions of Transport (NCT) thermal analysis performed. The Hypothetical Accident Condition (HAC) fire certification testing of the Traveller package (see Section 3.6.5, Traveller Certification Test Unit Burn Test) served to verify material performance in the HAC thermal environment. As such, with the exception of the tests required for specific packaging components, as discussed in Section 8.1.5, Component and Material Tests, specific acceptance tests for material thermal properties are not required or performed.

8.2 MAINTENANCE PROGRAM

This section describes the maintenance program used to ensure continued performance of the Traveller package.

Visual inspection for damage of all exposed surfaces will be performed before each use. Individual components will also be inspected as described in the sections below. If any defects are found during inspection, the package will be segregated and dispositioned by standard site procedure before its next use.

8.2.1 Structural Tests

The Traveller packaging does not contain any structural or lifting/tiedown devices that require testing. There is also no pressure testing requirement.

8.2.2 Pressure Leak Tests

The Traveller packaging does not have any requirements for leak testing.

8.2.3 Component and Material Tests

8.2.3.1 Fasteners

Threaded components shall be inspected prior to each use for deformed or stripped threads. Damaged components shall be repaired or replaced prior to further use.

8.2.3.2 Weather Seal

Prior to each use, visual inspection of the braided fiberglass sleaving or silicon weather seal shall be performed for tears, damage, or deterioration. Unacceptable sleaving or seals shall be replaced.

8.2.3.3 Shock Mounts

Prior to first use and at an interval not to exceed five years or 50 cycles, whichever is more limiting, each Lord Sandwich Shock Mount (Part Number J-5425-275 or engineering approved equivalent) shall be visually inspected. The inspection shall verify the condition of the shock mount for tears, missing material or deterioration from aging. A load shall be placed on the clamshell to tension the shock mounts to visual inspect. A light source and with a videoscope is used to inspect the full circumference of each shock mount. Damaged or suspect shock mounts shall be replaced with Lord Sandwich Shock Mount Part Number J-5425-275 or engineering approved equivalent.

8.2.4 Thermal

No thermal tests are necessary to ensure continued performance of the Traveller packaging.

8.2.5 Neutron Absorber Plates

On a periodic basis (not to exceed five years or 50 cycles, whichever is more limiting), packages will be inspected to verify the neutron absorber plate configuration complies with the drawing requirements. Quality Control Instructions and Mechanical Operating Procedures will define the specific inspection requirements. In accordance with established company procedures, a visual inspection will be conducted of the visible side of the neutron absorber plates. Personnel will visually verify that the plates are present and in good condition. Any neutron absorber plate with deep scratches or gouges, which expose the inner boron carbide center, shall be replaced. Neutron absorber plates covered with cork rubber shall be visually inspected at each screw location and the cork rubber inspected for signs of tampering. Documentation relating to these inspections, repairs, part replacements, etc. will be produced and maintained.

8.3 APPENDICES

8.3.1 References

None.

This page intentionally left blank.